

GEOLOGICAL FIELDWORK 2007

A Summary of Field Activities and Current Research



GEOLOGICAL FIELDWORK 2007

A Summary of Field Activities and Current Research

**Ministry of Energy, Mines
and Petroleum Resources**
British Columbia Geological Survey

Paper 2008-1

Ministry of Energy, Mines and Petroleum Resources Mining and Minerals Division British Columbia Geological Survey

Parts of this publication may be quoted or reproduced if source and authorship is acknowledged.
The following is the recommended format for referencing individual works contained in this publication:

Diakow, L.J. (2008): Spences Bridge Bedrock Mapping Project: preliminary results from the Merritt region, south-central British Columbia (parts of NTS 092H/14, 15; 092I/02); in *Geological Fieldwork 2007, BC Ministry of Energy Mines and Petroleum Resources*, Paper 2008-1, pages 1-4.

COVER PHOTO: *Brian Grant examines core from the Lac La Hache property of GWR Resources Inc during a fieldtrip visiting alkaline porphyry occurrences. Mineralization at the property displays many of the characteristics of the alkalic copper-gold porphyry deposits, which are an important source of copper within British Columbia. Brian was Director of Geosciences Initiatives, BC Geological Survey, before he retired from public service in January, 2008.*

This publication is also available, free of charge, as colour digital files, in Adobe Acrobat PDF format, from the BC Ministry of Energy, Mines and Petroleum Resources internet website at:

http://www.em.gov.bc.ca/Mining/Geosurv/Publications/catalog/cat_fldwk.htm

British Columbia Cataloguing in Publication Data

Main entry under title:

Geological Fieldwork: - 1974 -

Annual.

Issuing body varies

Vols. For 1978-1996 issued in series: Paper / British Columbia. Ministry of Energy, Mines and Petroleum Resources; vols for 1997- 1998, Paper / British Columbia. Ministry of Employment and Investment; vols for 1999-2004, Paper / British Columbia Ministry of Energy and Mines; vols for 2005- , Paper / British Columbia Ministry of Energy, Mines and Petroleum Resources.

Includes Bibliographical references.

ISSN 0381-243X=Geological Fieldwork

1. Geology - British Columbia - Periodicals. 2. Mines and mineral resources - British Columbia - Periodicals. 3. Geology - Fieldwork - Periodicals. 4. Geology, Economic - British Columbia - Periodicals. 5. British Columbia. Geological Survey Branch - Periodicals. I. British Columbia. Geological Division. II. British Columbia. Geological Survey Branch. III. British Columbia. Geological Survey Branch. IV. British Columbia. Dept. of Mines and Petroleum Resources. V. British Columbia. Ministry of Energy, Mines and Petroleum Resources. VI. British Columbia. Ministry of Employment and Investment. VII. British Columbia Ministry of Energy and Mines. VIII. Series: Paper (British Columbia. Ministry of Energy, Mines and Petroleum Resources). IX. Series: Paper (British Columbia. Ministry of Employment and Investment). X. Series: Paper (British Columbia Ministry of Energy and Mines). XI. Series: Paper (British Columbia Ministry of Energy, Mines and Petroleum Resources).

VICTORIA
BRITISH COLUMBIA
CANADA

JANUARY 2008

FOREWORD

Geological Fieldwork 2007

The **British Columbia Geological Survey** (BCGS) presents the results of 2007 geoscience surveys and studies in this thirty-third edition of *Geological Fieldwork*. Most of the articles within this volume are contributions from Survey staff who have worked extensively throughout the province on its geology, geochemistry and mineral deposits. Many BCGS projects include important contributions from researchers and contractors from other organizations. As well, the Survey includes quality submissions in this publication from any professional geoscientist which may add to the province's geoscience database.

The results of the 2007 field surveys and the provision of new geoscience data will lead to tenure acquisition and increased mineral exploration expenditures as it has in previous years. These activities are the first steps towards the development of new mines, which benefit British Columbians, particularly those living in regional communities.

BC Geological Survey Successes

- Survey staff have made significant new mineral discoveries or redefined the mineral potential during their mapping programs in the Chezacut, Merritt, northern Vancouver Island and Terrace areas which should attract mineral tenure acquisition and highlight the under-explored mineral potential of these areas.
- More than 28 300 industry assessment reports have now been published as PDF files to the Survey website, improving access to this critical exploration database. This is part of the Survey's ongoing responsibility to be the custodian for the province's mineral and coal geoscience data.
- Survey staff have created a Drainage Geochemical Atlas for British Columbia which incorporates data collected over 25 years. The Atlas presents a leveled dataset which will be invaluable for regional studies across the Province.
- MapPlace is used by the exploration community around the world and continues to attract exploration investment to the province. The British Columbia Geological Survey geological database and MapPlace have been ranked as a top geoscience database globally by the Fraser Institute Survey for 2006-07.
- Mapping in the Interior Plateau shows that Quaternary volcanic cover rocks are thinner and less extensive than previously shown on geological maps, which encourages more exploration in the region.
- Survey staff, including those based in the Vancouver and Ministry regional offices, contributed their expertise to assist in government decisions, respond to client inquiries in confidence, and report on industry activity in the province.

- The Survey was funded by government to start a three year Cooperative Geological Student Mapping Program to train and mentor geology students as they prepare for their careers. In 2006-07 the Survey hired more than 35 geoscience assistants and provided training and guidance to undergraduate and graduate research projects.
- Field trips led by Survey staff in 2007 included a Porphyry Deposits Tour to Northwestern British Columbia and a visit to the Myra Falls mine.

2007 BCGS Field Surveys, Database Activities and Publications

Articles in this volume include reports on British Columbia Geological Survey programs in the Boundary district, Chilcotin, Merritt, northern Vancouver Island, Peace River coalfield, Quesnel, Terrace and 100 Mile House areas. Three articles highlight some of the many opportunities for economic development related to the province's industrial minerals. New geochemical data from the Quesnel Trough and the Drainage Geochemical Atlas are also discussed in the volume.

The Survey has recognized the impact of the Mountain Pine Beetle infestation in the central interior of the province by expanding its 2006 and 2007 programs in this region. Despite excellent mineral potential, the central interior has been under-explored due to widespread glacial till blankets and young volcanic cover rocks. The objective is to diversify local economies by attracting mineral exploration which could lead to the discovery of new mines. In other parts of the province both mineral exploration and mining contribute to local jobs and taxes and support regional infrastructure.

Many BCGS programs involved cooperative partnerships with universities, other government agencies, Geoscience BC, First Nations, communities and industry. The Survey continued its tradition of working with the Geological Survey of Canada on British Columbia projects providing technical and financial assistance to the Targeted Geoscience Initiative in southern and central British Columbia.

All geoscience publications are routinely posted to the BC Ministry of Energy, Mines and Petroleum Resources website. MapPlace, one of the world's premier geoscience internet-map systems, continues to improve with the addition of more data layers and improved tools. Clients can now freely access 100% of the company mineral assessment reports from the ARIS database over the web. Survey staff played active roles as presenters and organizers at numerous conferences and events to market British Columbia's mineral potential, including a trade mission to Asia, international conferences in Toronto and Vancouver, and numerous meetings and workshops around the province.

Over the past year the BCGS published *Geological Fieldwork 2006*, 10 Open File maps and reports, 1 Geoscience Map, 11 GeoFile maps, reports and data files and 5 Information Circulars. In addition to these traditional publications, Survey geologists provided expertise to companys carrying out exploration and mine development

work in the Province. As well, the Survey processed about 550 assessment reports submitted for tenure maintenance.

Working with the regional geologists as key authors, the Survey also published *Exploration and Mining in British Columbia 2006* and *British Columbia Mines and Mineral Exploration Overview 2006* and coordinated the submission of articles on provincial industry activities published by the Canadian Institute of Mining, in the *Mineral Exploration* magazine by AMEBC and Northern Miner.

This Fieldwork volume is made possible by the hard work and expertise of numerous authors who have contributed their insight to improve our understanding of British Columbia's geology and mineral deposits. The articles have been improved by peer and supervisor review and Tania Demchuk's steady hand in coordinating the articles

and providing feedback to the authors. The quality services of RnD Technical are acknowledged for helping to put the volume together. Brian Grant, the editor, deserves special commendation for being the key person in so many ways in producing *Geological Fieldwork*. This is his 20th, and last year, at the helm as he is returning to the private sector.

*D.V. Lefebure
Chief Geologist
British Columbia Geological Survey*

www.empr.gov.bc.ca/Geology

(see following pages for a photo of BC Geological Survey staff and a location map of 2007 field projects.)

Geoscience BC Reports

Geoscience BC's project reports for 2007 are available in their volume, *Geoscience BC Summary of Activities 2007, Geoscience BC Report 2008-1*. This report is available in hardcopy or as a download from Geoscience BC's website, www.geosciencebc.com.

Previous Geoscience BC project reports were included in *Geological Fieldwork 2005* and *2006*.

CONTENTS

- Diakow, L.J.:** Spences Bridge Bedrock Mapping Project: preliminary results from the Merritt region, south-central British Columbia 1
- Enkin, R.J., Vidal, B.S., Baker, J. and Struyk, N.M.:** Physical properties and paleomagnetic database for south-central British Columbia. 5
- Hartlaub, R.P. and Paradis, S.:** Evaluation of the geology and stratabound base metal potential of the middle and upper Purcell Supergroup, southeastern British Columbia 9
- Hora, Z.D., Langrová, A., and Pivec, E.:** Eaglet property revisited: fluorite-molybdenite porphyry-like hydrothermal system, east-central British Columbia 17
- Hora, Z.D.:** Diatomite resource assessment in the Quesnel area, central British Columbia 31
- Legun, A.S.:** Thickness trends of J seam, and its split at the Falher D shoreline, Wolverine River area, Peace River coalfield, northeastern British Columbia. 39
- Lett, R.E. and Sandwith, Z.:** Geochemical orientation surveys in the Quesnel Terrane between Quesnel and Williams Lake, central British Columbia 49
- Lett, R.E., Man, E.C. and Mihalynuk, M.G.:** Towards a drainage geochemical atlas for British Columbia 61
- Logan, J.:** Geology and mineral occurrences of the Quesnel Terrane, Cottonwood map sheet, central British Columbia 69
- Massey, N.W.D. and Duffy, A.:** Boundary Project: McKinney Creek and Beavertell areas, south-central British Columbia 87
- McKeown, M., Nelson, J. and Friedman, R.:** Newly discovered volcanic-hosted massive sulphide potential within Paleozoic volcanic rocks of the Stikine assemblage, Terrace area, northwestern British Columbia 103
- Mihalynuk, M.G., Peat, C.R., Terhune, K. and Orovan, E.A.:** Regional geology and resource potential of the Chezacut map area, central British Columbia 117
- Mihalynuk, M.G., Friedman, R.M. and Ullrich, T.D.:** Geochronological results from reconnaissance investigations in the Beetle Infested Zone, south-central British Columbia 135
- Moynihan, D.P. and Pattison, D.R.M.:** Origin of the Kootenay Lake metamorphic high, southeastern British Columbia. 147
- Nelson, J., Kyba, J., McKeown, M. and Angen, J.:** Terrace Regional Mapping Project, year 3: contributions to stratigraphic, structural and exploration concepts, Zymoetz River to Kitimat River, east-central British Columbia 159
- Nixon, G.T., Larocque, J., Pals, A., Styán, J., Greene, A.R. and Scoates, J.S.:** High-Mg lavas in the Karmutsen flood basalts, northern Vancouver Island: stratigraphic setting and metallogenic significance 175
- Schiarizza, P. and Bligh, J.S.:** Geology and mineral occurrences of the Timothy Lake area, south-central British Columbia 191
- Simandl, G.J.:** Newly recognized white talc-carbonate filler potential of the Greenwood – Bridesville area, British Columbia and brief talc market review 213
- Wojdak, P.J.:** Fireside deposit: diagenetic barite in strata of the Kechika Group, and vein barite related to rifting of the Kechika Trough, northwestern British Columbia . 219



British Columbia Geological Survey staff; December 17, 2007

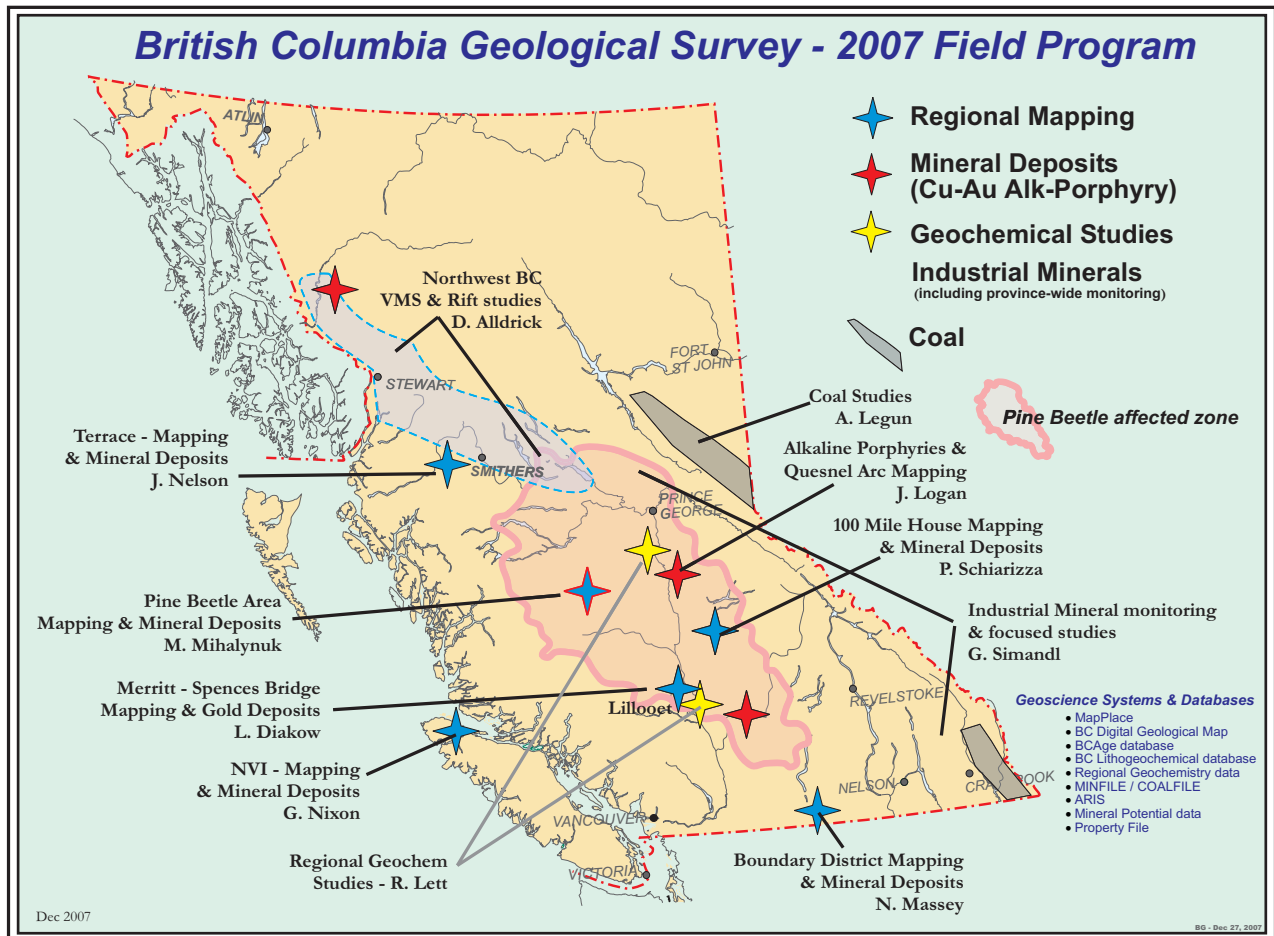
Back row: Mitch Mihalyuk, Alan Duffy, John Bligh, Andrew Legun, Pat Desjardins, Kirk Hancock, Andrew Cuthbert, Geoff Laroque, George Simandl, Margo McKeown, Dani Alldrick;

3rd row: Brian Grant, Rachel Kerr, Dave Frankl, Nick Massey, Ray Lett, Tania Demchuk, Larry Diakow, Taira Nakanishi;

2nd row: Gib McArthur, Larry Jones, JoAnne Nelson, Paul Scott, Graham Nixon, Mandy Desautels, Bruce Northcote, Dave Lefebure;

Front row: Laura de Groot, Martin Lin, Travis Ferbey, Jim Logan, Paul Schiarizza;

Missing: Alan Wilcox, Tim Hewett, Caoimhe Peat.



Spences Bridge Bedrock Mapping Project: Preliminary Results from the Merritt Region, South-Central British Columbia (Parts of NTS 092H/14, 15; 092I/02)

by L.J. Diakow

KEYWORDS: Merritt, Ashcroft map area, Nicola Group, Spences Bridge Group, epithermal mineralization

INTRODUCTION

The Spences Bridge Project is a multiyear bedrock mapping – mineral deposits exploration project. It focuses on two major rock successions: island arc rocks of the Late Triassic Nicola Group, specifically the western belt (facies) and a superimposed mid-Cretaceous continent-margin arc succession, the Spences Bridge Group, in selected areas between Princeton in the south and Pavilion in the north (Fig 1). The project objectives are to upgrade the geological understanding and evaluate the economic mineral potential for these contrasting arc regimes.

This brief report presents preliminary geological observations made during the inaugural field season conducted near Merritt in the fall of 2007. No analytical results from the project are yet available. A more in-depth report, incorporating detailed lithological descriptions, stratigraphic relationships and various analyses and age determinations, will be included in future work.

2007 FIELD PROGRAM

During September and October, more than 50 traverses were conducted, providing detailed 1:20 000 scale geological coverage over a 300 km² area (Fig 1). The shape of the study area resembles an inverted 'L', the southwest-trending segment informally designated the Iron Mountain – Selish Mountain transect and the shorter, northwest-oriented segment, the Gillis Lake – Maka Creek transect.

This mapping overlaps geographically and, moreover, supplements and refines parts of a solid geological foundation constructed from earlier mapping-based studies. These studies include: Preto's (1979) tripartite time-stratigraphic subdivision of the Nicola Group into lithostratigraphic belts or facies, McMillan's (1981) mapping of the western

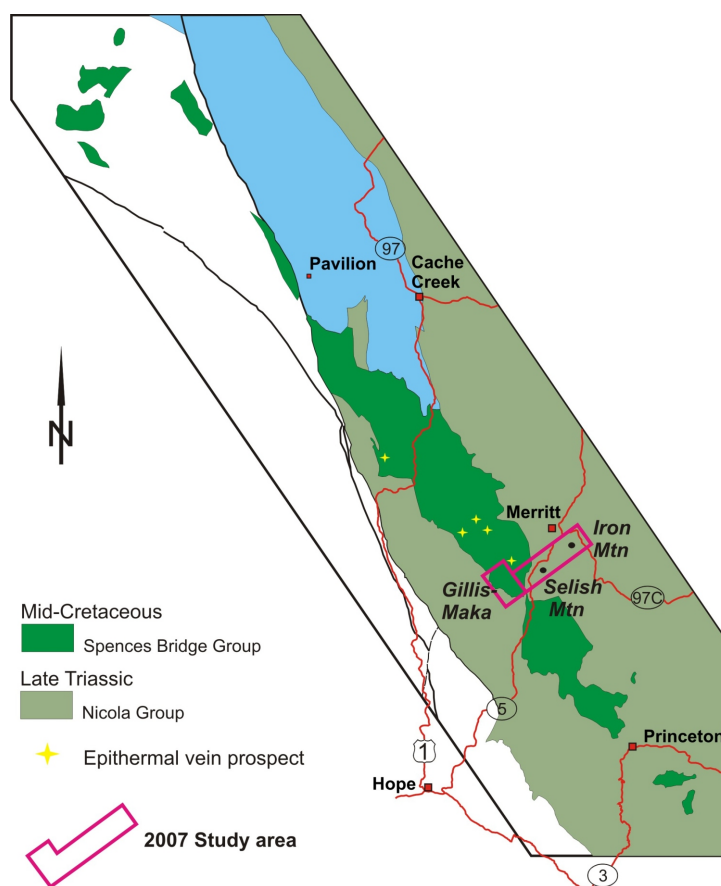


Figure 1. Location of the 1:20 000 scale mapping project covering the Iron Mountain – Selish Mountain and Gillis Lake – Maka Creek transects, and distribution of recently discovered epithermal vein prospects hosted by mid-Cretaceous Spences Bridge Group.

belt of the Nicola Group at Iron Mountain, and Thor-kelson's (1986) mapping of the Spences Bridge Group.

GENERALIZED STRATIGRAPHY

Iron Mountain – Selish Mountain Transect

This area comprises two mountains that make up a north-trending ridge, with the Coquihalla Highway lying at lower elevation along the western margin. Iron Mountain is located at the north end of the ridge, immediately south of Merritt. Situated farther south, Selish Mountain marks a

This publication is also available, free of charge, as colour digital files in Adobe Acrobat® PDF format from the BC Ministry of Energy, Mines and Petroleum Resources website at http://www.em.gov.bc.ca/Mining/Geosurv/Publications/catalog/cat_fldwk.htm

geological division between older layered rocks cropping out to the north and a crosscutting, stock-size granitoid cropping out to the south.

Layered rocks throughout this transect represent the oldest stratigraphy in the study area. A persistent trend in bedding attitudes, from topographically lowest to highest exposures between Iron and Selish mountains, defines a moderately southeast-inclined homocline that is internally disrupted by steep, mainly west-northwest-striking faults, oriented roughly orthogonal to the general north-northeast strike of beds.

The bottom of the homoclinal succession consists of a largely indivisible, monotonous sequence composed of variably red-oxidized dark green basaltic lava flows. They exhibit a variety of textures, from aphyric and aphanitic to pyroxene plagioclase porphyries, and contain weak to moderately pervasive replacement by secondary chlorite, epidote and calcite.

Based on the absence of features indicative of submarine deposition, these mafic rocks are interpreted to have been deposited in a subaerial environment. An exception, however, occurs at the locally gradational upper contact, as indicated by the presence of relatively thin, massive pyroxene-phyric lavas alternating with marine sedimentary strata.

The mafic unit is replaced upsection by an extensive subaerial volcanic succession that contains locally interspersed fine clastic and carbonate beds. This volcanic succession is dominated by dark maroon and green andesitic tuffs, particularly in the vicinity of Selish Mountain. Felsic eruptives, however, constitute the most distinctive rocks in the succession, Dacitic flows and some associated tuffs make up a relatively small component of the Selish Mountain section, although at Iron Mountain the felsic rocks are volumetrically significant and include lava flows, associated airfall tuffs containing sparse quartz crystals and abundant felsic fragments. Minor beds of epiclastic sandstone derived from volcanic rocks and composed of abundant felsic fragments and quartz grains are interlayered with felsic rocks and, up section, alternate with limestone.

Felsic volcanic units at Iron Mountain grade upwards into limestone beds and intercalated calcareous sandstones and granule conglomerates. These sedimentary rocks have an aggregate thickness in excess of 60 m and provide a local stratigraphic marker. They contain a diverse shallow-marine fossil assemblage including belemnoids, crinoids, corals, bivalves and ammonoids.

Carbonates have also been mapped at several widely spaced localities in the Selish Mountain section, although generally as minor beds. They differ from those at Iron Mountain in the nature of bounding rocks, thickness, appearance and fossil content, thereby making direct correlation impossible. Within the Iron Mountain – Selish Mountain transect it appears that significant carbonate deposition recurred during at least three relatively short-lived, marine transgressive events, each carbonate deposit apparently corresponding in time with hiatuses or at least with substantially diminished subaerial volcanic activity.

AGE OF ROCK UNITS

McMillan (1981) assigned volcanic and sedimentary rocks in the Iron Mountain – Selish Mountain transect to the western belt of the Nicola Group. Despite a number of fossil sites found at Iron Mountain (McMillan, 1981), none

of the fossils appear to have been definitively identified and they are hence excluded from a compilation of fossil collections for the Ashcroft map area (Monger, 1989a, b). Based on this compilation, fossil-bearing sedimentary rocks interbedded with volcanic rocks found elsewhere in the western Nicola Belt are late Carnian to early Norian in age. However, the age of the Nicola Group in the Iron Mountain – Selish Mountain transect remains to be determined. Isotopic age and fossil samples collected during this study aim to test the possibility that the felsic volcanic unit and overlying carbonates may represent a younger, perhaps Early Jurassic arc sequence that unconformably overlies the mafic volcanic unit.

Three dacitic-rhyolitic volcanic samples were collected for uranium-lead (U-Pb) dating. The stratigraphically lowest felsic rock collected, west of Selish Mountain, is derived from a 20 cm thick waterlain ash interlayered with siltstone. It sharply overlies pyroxene-bearing lavas that are presumed to mark the top of the mafic volcanic unit. A second sample collected from the summit of Selish Mountain is a flow-laminated dacite. The stratigraphic position of this sample is uncertain; however, it provides an inferred age for a thick assemblage of associated airfall volcanic rocks dominated by oxidized maroon lapilli and finer tuffs that occupy much of the apparent lower and middle parts of the unit. A date from the upper part of the dacitic volcanic succession can be determined from quartz-bearing dacitic tuffs collected from Iron Mountain. The dacite in this location is interbedded with limestone and grades upwards into a sedimentary marker composed of several limestones interbedded with calcareous sandstones. Two fossil collections, containing a diverse bivalve assemblage locally coexisting with ammonoids, were extracted from the sandstone.

Gillis Lake – Maka Creek Transect

Mid-Cretaceous rocks of the Spences Bridge Group form a narrow, northwest-trending belt regionally covering nearly 3200 km², and unconformably overlie the Late Triassic Nicola Group and associated intrusions (Fig 1; Monger, 1989a, b; Monger and McMillan, 1989). Cretaceous stratigraphy underlying much of the Gillis Lake – Maka Creek transect forms part of a contiguous mapping project, roughly 250 km² in extent, conducted for an MSc thesis (Thorkelson, 1986) that subsequently led to subdivision and formal definition of the Spences Bridge Group (Thorkelson and Rouse, 1989).

Remapping the geology in the Gillis Lake – Maka Creek transect during this study revealed a crudely layered, subaerial volcano-sedimentary stratigraphy. This bedded succession forms a northeast-inclined homocline and rests nonconformably on granitic rocks of probable Late Triassic to Early Jurassic age. The homocline is made up of a number of distinctive volcanic and intervolcanic sedimentary units that are readily traceable along strike. The continuity of rock units, however, is disrupted by numerous steep faults trending north to northeast, which probably developed during regional Eocene extensional tectonic episodes.

A representative stratigraphic section for the Spences Bridge Group in the Gillis Lake – Maka Creek transect, in which all mappable units are stacked successively and no faults were recognized, is at least 1600 m thick. The underlying basement consists of an intrusive complex composed of pyroxene diorite that, in many places, is intruded by

younger dikes and small apophysis composed generally of granodiorite and quartz monzonite. White aphanitic felsite dikes, in turn, crosscut the older phases.

Initial deposits of the Spences Bridge Group consist of pyroxene-phyric andesite. Nearly identical lava flows recur in at least two intervals well above this basal flow member. Resistant, lithic-rich, dacitic ash-flow tuff occurs immediately above the lowest andesite, and a similar deposit is found near the top of the section. Differentiating sequentially younger volcanic strata from lithologically similar older strata is facilitated by three distinctive conglomeratic beds dispersed at successively higher levels in the stratigraphy. The lowest, enclosed as a thick bulbous-shaped body within the lowest andesite unit, is distinguished by the preponderance of intrusive clasts derived from nearby plutonic basement rocks. The next highest conglomerate occurs at the interface marking the top of the lowest pyroxene andesite with overlying dacitic ash-flow tuff. This conglomerate is thinner than the lower conglomerate and composed exclusively of metavolcanic, metaplutonic and vein quartz clasts, which indicates it is derived from a metamorphosed terrain. The stratigraphically highest conglomerate crops out close to the top of the section and contains a variety of clasts that resemble underlying volcanic units of the Spences Bridge Group. It is the thickest of the three conglomerate units and also contains significant interbedded sandstone units, some of which display large-scale planar crossbeds. The uppermost conglomeratic unit passes into a thick, mixed unit composed of reworked and primary fragmental rocks that constitute the top of the stratigraphic section.

In addition to the three distinctive conglomerates, sedimentary rocks, including finer granule conglomerate and sandstone, are interspersed at several other levels, consistently at the contact of several specific volcanic units. These finer clastic beds commonly contain rock clasts and crystals derived locally from underlying volcanic or plutonic units, such as pyroxene, quartz or sometimes biotite. Without exception, sandstone units encountered throughout the section all contain plant debris, which indicates that the volcano-sedimentary sequence was deposited in a terrestrial setting.

Thorkelson and Rouse (1989) reported a U-Pb date of 104.5 ± 0.3 Ma on rhyolite from the lower part of the Spences Bridge Group. This Early Cretaceous, Albian date is corroborated by identification of fossil leaves and palynomorphs that extends deposition of the Spences Bridge Group into the Cenomanian stage of the Late Cretaceous (Thorkelson and Rouse, 1989). Ash-flow tuff forming the lower of two lithologically similar pyroclastic flows recognized in the Gillis Lake – Maka Creek section was sampled to determine when felsic volcanism began.

MINERALIZATION

The study area contains relatively few recorded MINFILE (2007) prospects, consisting mainly of small copper and lead-zinc-barite prospects hosted by mafic and felsic volcanic rocks of the Nicola Group. Mining exploration in the Merritt region currently focuses on precious-metal-bearing epithermal quartz veins hosted in subaerial volcanic rocks of the Spences Bridge Group. Epithermal vein deposits constitute an important new exploration tar-

get throughout the belt of Spences Bridge Group rocks. They became evident after 2001, during follow-up of geochemical anomalies detected in selected stream sediments samples, coupled with diligent prospecting by E. Balon, all of which subsequently led to a number of significant vein discoveries.

In this first year of bedrock mapping, field efforts focussed on determining stratigraphy and structure, with only minor work conducted on the mineral deposits. As mapping expands north and south next season, epithermal prospects, including those at Prospect Valley, Sullivan Ridge and Ponderosa, shown in Figure 1, will be incorporated into the developing geological framework. The character of epithermal mineralization, geological controls and time-space relationship with major magmatic events are integral components of the regional mapping project focussing on the Spences Bridge Group.

During the course of fieldwork, zones of rusty altered rocks were routinely sampled for assay. Of the 28 samples collected from 12 widely separated sites exhibiting varying intensities of hydrothermal alteration, 10 sites can be categorized as epithermal-type, one as porphyry-type and one as a base-metal-bearing vein. Interestingly, all but one of these alteration sites occur within rocks mapped as part of the western belt of the Nicola Group. Since the assay results were not available when this report was written, they will be presented in a table accompanying the open file map scheduled for release in spring 2008.

ACKNOWLEDGMENTS

Tim Hewitt is thanked for assembling essential orthophoto and topographic base maps, for building the databases and for his enthusiastic field assistance.

REFERENCES

- McMillan, W.J. (1981): Nicola Project – Merritt Area; *BC Ministry of Energy, Mines and Petroleum Resources*, Preliminary Map 47, 2 sheets at 1:25 000 scale.
- MINFILE (2007): MINFILE BC mineral deposits database; *BC Ministry of Energy, Mines and Petroleum Resources*, URL <<http://www.em.gov.bc.ca/Mining/Geolsurv/Minfile/>> [November 2007].
- Monger, J.W.H. (1989a): Geology, Hope, British Columbia; *Geological Survey of Canada*, Map 41-1989, sheet 1, scale 1:250 000.
- Monger, J.W.H. (1989b): Fossil locations, Ashcroft, British Columbia; *Geological Survey of Canada*, Map 42-1989, sheet 2, scale 1:250 000.
- Monger, J.W.H. and McMillan, W.J. (1989): Geology, Ashcroft, British Columbia; *Geological Survey of Canada*, Map 42-1989, sheet 2, scale 1:250 000.
- Preto, V.A. (1979): Geology of the Nicola Group between Merritt and Princeton; *BC Ministry of Energy, Mines and Petroleum Resources*, Bulletin 69, 90 pages.
- Thorkelson, D.J.: (1986): Geology of the mid-Cretaceous volcanic units near Kingsvale, southwestern British Columbia; in Current Research, Part B, *Geological Survey of Canada*, Paper 85-1B, pages 333–339.
- Thorkelson, D.J. and Rouse, G.E. (1989): Revised stratigraphic nomenclature and age determinations for mid-Cretaceous volcanic rocks in southwestern British Columbia; *Canadian Journal of Earth Sciences*, Volume 26, pages 2016–2031.

Physical Properties and Paleomagnetic Database for South-Central British Columbia

by R.J. Enkin¹, B.S. Vidal², J. Baker¹, and N.M. Struyk³

KEYWORDS: geophysical surveys, physical properties, magnetic susceptibility, density, TGI-3 – Cordillera Project, Geoscience for Mountain Pine Beetle Response Project, south-central British Columbia

South-central British Columbia has become the focus of renewed mineral exploration activity. In response to the devastation facing the region's forests due to the mountain pine beetle infestation, governments are supporting economic diversification with a series of programs. This region is one of the areas identified for the current Targeted Geoscience Initiative III (TGI-3), and both federal and provincial geological surveys have created projects to promote mineral and energy exploration in the Mountain Pine Beetle Infested Zone (BIZ).

Mihalynuk (2007) demonstrated that the BIZ (defined using data from the BC Ministry of Forests and Range, 2005) has significant mineral inventory and mineral exploration deficits. The region has been largely avoided by mineral exploration geologists because of poor outcrop and apparent cover by Cenozoic volcanic rocks. The metallogenic geological provinces surrounding the BIZ almost certainly underlie the BIZ itself, and economic deposits should be available for exploitation. "Perhaps the greatest impediment to attracting significant mineral exploration investment in the BIZ is the geological uncertainty posed by the extent and thickness of cover successions" (Mihalynuk, 2007, p. 141). However traditional exploration strategies are not sufficient and must therefore be complemented with greater use of geochemical and geophysical surveys.

Gravity, magnetic, electromagnetic, radiometric and seismic surveys all provide methods both to image the cover and to recognize exploration targets underneath. To identify the lithological sources of geophysical anomalies, it is necessary to identify the physical property fingerprints of each rock type and each formation. What are the spatial variations of both mean values and their dispersions? Where are geophysically imageable contrasts found, and what techniques should be applied to optimize geophysical surveys and their interpretation? It is necessary to compile a physical properties database to answer these questions.

At present we have collected data from 2932 sites from the TGI-3 – Cordillera and Beetle Infested Zone (Fig 1).

The work is still in progress, and we expect the database will increase in size significantly over the coming months.

The goals of the projects that procured these data varied considerably and, accordingly, each employed different methods and strategies. These are grouped into three types of data:

- **In-situ measurement:** Magnetic susceptibility was measured at the outcrop, either with an Exploranium KT9 or with the more sensitive GF Instruments SM-20 susceptibility meter. Typically five to ten measurements were recorded from an outcrop over a distance of several metres and the average was reported.
- **Laboratory measurement of hand samples:** Several mappers have submitted hand samples collected during geological mapping to the physical properties laboratory at the Geological Survey of Canada – Pacific in Sidney. Density was measured using the 'weight-in-air – weight-in-water' method (Muller, 1967). Magnetic susceptibility of the hand samples was measured using the SM-20. Samples that were large enough to subsample and had magnetic susceptibility greater than about 1×10^{-3} SI were cored with a 2.5 cm diamond-drill bit. The magnetic remanence was measured with an Agico Inc. JR5-A magnetometer, and accurate magnetic susceptibility was measured using a Sapphire SI2B susceptibility meter. The value of magnetic remanence over susceptibility provides a Koenigsberger ratio, which is the relative strength of remanent to induced magnetism.
- **Sampling for paleomagnetic study:** Lithological formations, which potentially hold strong and stable magnetic remanence, were drilled in the field and oriented using a magnetic or solar compass. This is particularly important for interpreting aeromagnetic maps of the Chilcotin basalts, as the Koenigsberger ratios for these rocks are high (i.e., magnetic remanence dominates over induced magnetism), and they can produce either strong positive anomalies if the magnetic polarity is normal or negative anomalies for reverse polarity flows.

The pooled results for magnetic susceptibility (2932 sites) and density (2387 sites) are shown in Figures 2 and 3. Publication of the database and its analysis are in preparation. For the purpose at hand, it is important to note the distribution of samples. Some regions have excellent coverage due to the availability of suitable outcrops and recent geological activity that led to the sampling. The sampling, however, is never uniform. Mappers do not collect samples on the basis of the area they represent, but rather attempt to sample the range of rock types. Exotic occurrences will be selected while the common hostrocks will only occasionally induce additional sampling. This is particularly the case for altered or mineralized rocks, which are the main

¹ Geological Survey of Canada – Pacific, Sidney, BC

² Department of Geography, University of Victoria, Victoria, BC

³ Hunter Dickinson Inc., Vancouver, BC

This publication is also available, free of charge, as colour digital files in Adobe Acrobat® PDF format from the BC Ministry of Energy, Mines and Petroleum Resources website at http://www.em.gov.bc.ca/Mining/Geosurv/Publications/catalog/cat_fldwk.htm

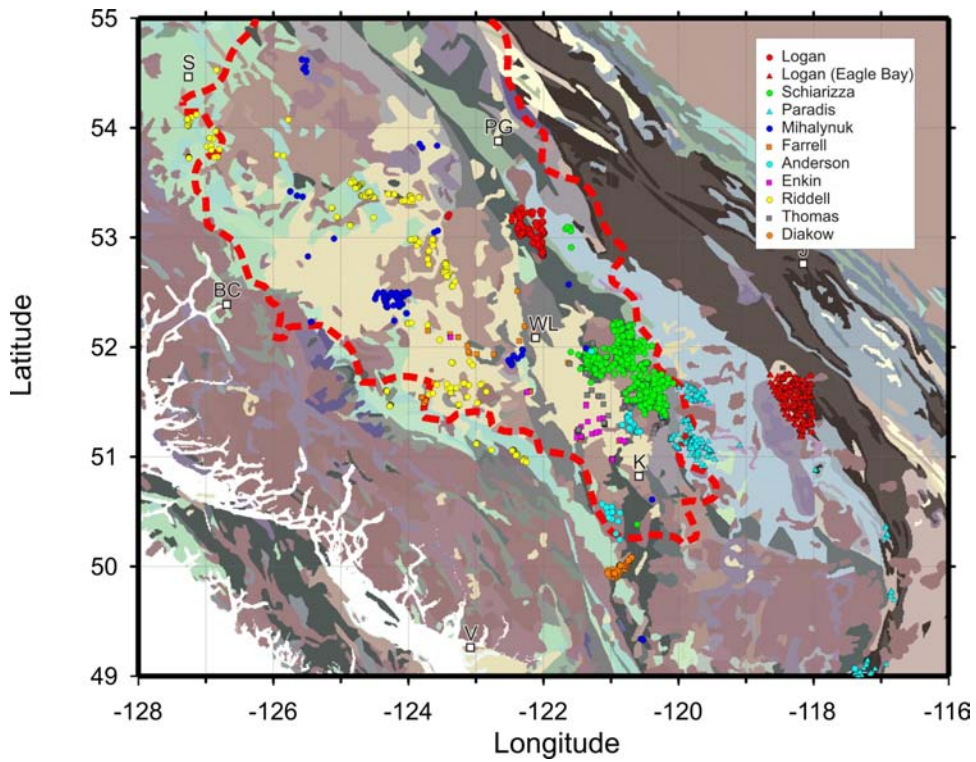


Figure 1. Locations of physical properties data from the Targeted Geoscience Initiative III – Cordillera and Beetle Infested Zone of south-central British Columbia, coded by collection. The base map is adapted from Journeay and Williams' (1995) version of Wheeler and McFeely's (1991) Tectonic Assemblage Map of the Canadian Cordillera. Abbreviations: V, Vancouver; K, Kamloops; WL, Williams Lake; BC, Bella Coola; PG, Prince George; S, Smithers. The Beetle-Infested Zone (BIZ) as defined by Mihalynuk (2007) is outlined with the red dashed line.

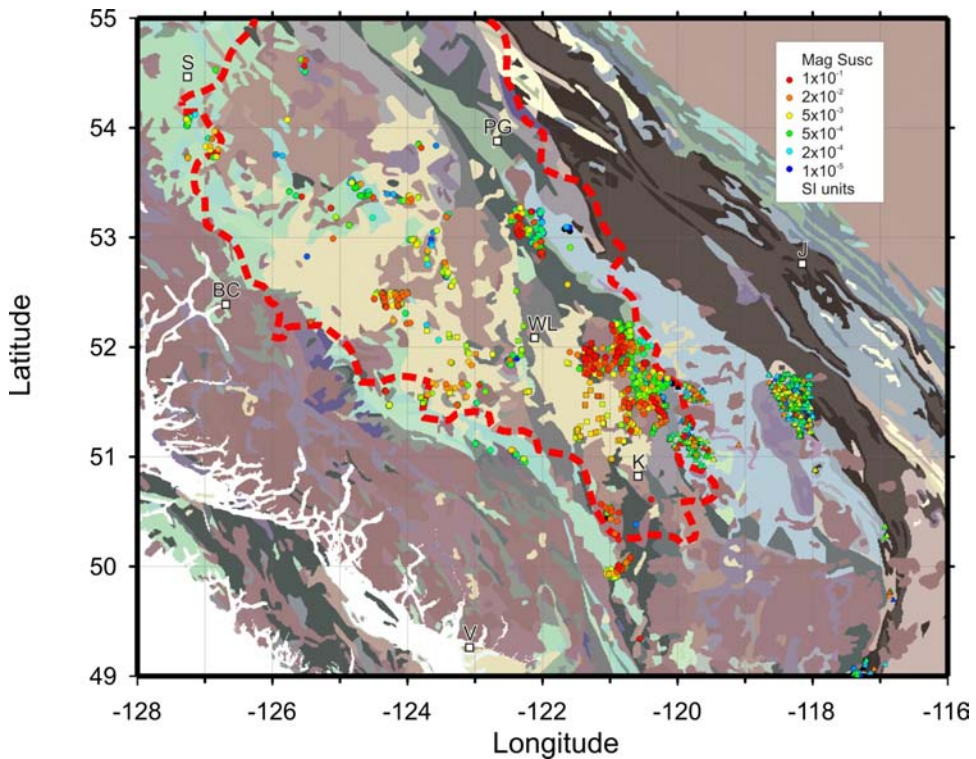


Figure 2. Magnetic susceptibility (SI/volume units) of 2932 sites, coded with a spectrum of colours from blue to red. See Figure 1 for legend of the base map.

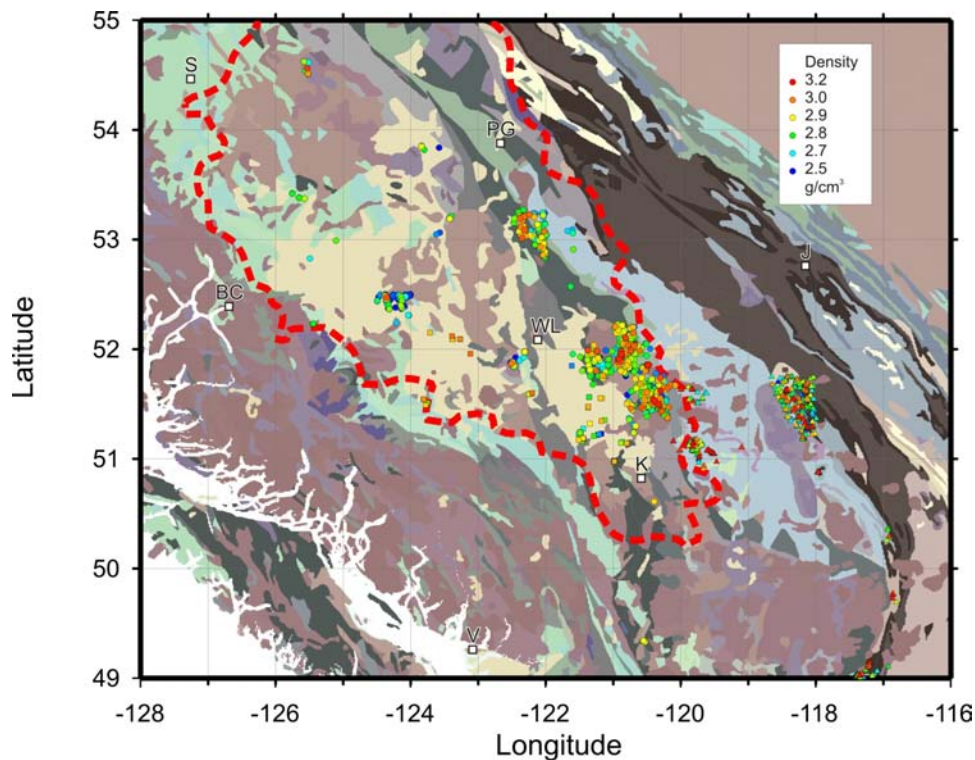


Figure 3. Density (g/cm^3) of 2387 sites, coded with a spectrum of colours from blue to red. See Figure 1 for legend of the base map.

target for geophysical surveys precisely because of their rarity. Furthermore, the three-dimensional nature of stratigraphy means that spatial averaging over two dimensions will necessarily lead to misleading interpretations. It is thus essential, when compiling spatial and lithological means, to give the correct weighting to each sample and, furthermore, to group them correctly together.

That being said, certain patterns are apparent even at the large scale illustrated in Figures 2 and 3. The Thuya and Takomkane plutons north of Kamloops stand out as rocks of high magnetic susceptibility and density that should be easily visible in geophysical surveys, even under glacial or possibly volcanic cover. There are significant variations in the physical properties of the Chilcotin basalts. In the northwest, densities are high while the susceptibility is low. The highest susceptibilities are found in young volcanic rocks north of Kamloops, which are apparently younger than the Chilcotin Group, *sensu stricto*.

The major paleomagnetic contrast we have noted within the Chilcotin Group is that southern Chilcotin sections, such as at Chasm and Deadman River, show multiple polarity reversals, allowing the possibility to map out regional isochron surfaces. In contrast, sections in the northwest, such as Bull Canyon and Dog Creek, show one polarity with little paleomagnetic directional dispersion, which suggests very rapid effusion.

There are certainly legacy datasets and sample collections that could be measured to add to the physical properties database under compilation. Preferably, all samples

should be greater than 250 ml in volume. Sampling location, lithology and formation name must accompany the submission of samples. Readers are invited to notify the authors if they know of sources of samples or spreadsheets of previously measured samples for inclusion in this physical properties database.

REFERENCES

- BC Ministry of Forests and Range (2005): BC forest health survey data 2004; *BC Ministry of Forests and Range*, URL <http://www.for.gov.bc.ca/ftp/HFP/external/!publish/Aerial_Overview/2004/> [November 2007].
- Journey, J.M. and Williams, S.P. (1995): GIS map library: a window on Cordilleran geology (version 1.0); *Geological Survey of Canada*, Open File 2948, digital version of Wheeler and McFeeley (1991).
- Mihalynuk, M.G. (2007): Evaluation of mineral inventories and mineral exploration deficit of the Interior Plateau Beetle Infested Zone (BIZ), south-central British Columbia; in *Geological Fieldwork 2006, BC Ministry of Energy, Mines and Petroleum Resources*, Paper 2007-1 and *Geoscience BC*, Report 2007-1, pages 137–141.
- Muller, L.D. (1967): Density determinations; in *Physical Methods in Determinative Mineralogy*, Zuaaman, J., Editor, *Academic Press*, pages 459–466.
- Wheeler, J.O. and McFeeley, P. (1991): Tectonic assemblage map of the Canadian Cordillera and adjacent part of the United States of America; *Geological Survey of Canada*, Map 1712A, scale 1:2 000 000.

Evaluation of the Geology and Stratabound Base Metal Potential of the Middle and Upper Purcell Supergroup, Southeastern British Columbia (NTS 082G/03, 04, 05, 06)

by R.P. Hartlaub¹ and S. Paradis²

KEYWORDS: Middle Proterozoic, Purcell Supergroup, Nicol Creek Formation, Creston Formation, sediment-hosted copper, mineral exploration

INTRODUCTION

The Middle Proterozoic Purcell Supergroup of southeastern British Columbia hosts the Sullivan deposit, one of the world's largest SEDEX Zn-Pb deposits. The Sullivan is hosted in the Aldridge Formation of the lower Purcell Supergroup, near Kimberly, BC. The discovery of this deposit led to extensive exploration of the Aldridge Formation, and these exploration activities continue to this day. Younger rocks of the middle and upper Purcell Supergroup, those rocks lying above the Aldridge/Prichard formation, have received much less attention in BC, even though they host numerous sediment-hosted Cu (\pm Ag \pm Co) deposits and polymetallic veins (Fig 1, 2).

Sediment-hosted Cu deposits are the second most important global source of Cu, following only porphyry Cu deposits in total resource. The majority of sediment-hosted Cu deposits are formed within continental rift basins (Brown, 1992) due to fluid mixing within permeable, shallow-water sedimentary and, more rarely, volcanic rocks (Cox et al., 2003). Major deposits lie within the Kupferschiefer belt of Europe and the Zambian Copperbelt of Africa. Proterozoic sedimentary rocks of the middle Belt Supergroup in Montana also contain important sediment-hosted Cu-Ag deposits, including Troy, Rock Creek and Montanore (Fig 1; Hayes and Einaudi, 1986; Boleneus et al., 2005).

This paper reviews the stratabound base metal potential of the middle and upper Purcell Supergroup in the area south and east of Cranbrook, BC in NTS sheets 082G/03, 04, 05 and 06. This area was previously mapped by Höy and Carter (1988), with detailed unit descriptions reported in Höy (1993). Five weeks of reconnaissance mapping were conducted across the area and some detailed work was carried out within areas of known mineral occurrences (Fig 2). Important contributions from this work include the discovery of a new sediment-hosted Cu occurrence and recogni-

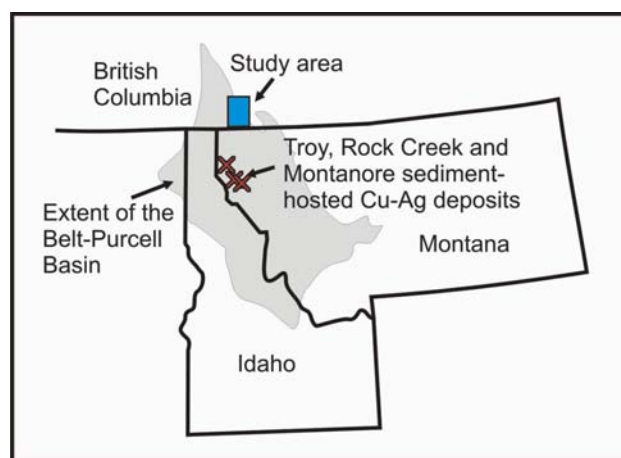


Figure 1. Approximate extent of the exposed Belt-Purcell Basin in British Columbia, Montana, Idaho and Washington. The location of the study area is shown in relation to known sediment-hosted Cu deposits.

tion of volcanic-hosted massive sulphide (VHMS) potential.

REGIONAL GEOLOGY

The Mesoproterozoic Belt-Purcell Basin is believed to represent an intracontinental rift system that has been filled by both marine and fluvial sediments (Lydon, 2007). The basin, which is termed the 'Belt Basin' or the 'Belt Supergroup' in the United States and the Purcell Supergroup in Canada, extends from southeastern British Columbia into Idaho, western Montana and eastern Washington. The basin developed as a branching system of sub-basins along basement structures that were later shortened and folded (Price and Sears, 2000). In southeastern BC, the oldest rocks of the Purcell Supergroup are exposed along the core and western margin of a large-scale anticlinorium. Mesoproterozoic rocks of the Purcell Basin in Canada have been stratigraphically subdivided in different ways by different authors working in different locations. Readers are directed to Höy (1993), Lydon (2007) and Gardner and Johnston (2007) for a complete discussion of stratigraphic changes within the basin.

The Canadian portion of the basin, south and east of Cranbrook, contains up to 12 km thicknesses of rift-fill turbidite rocks at the base. These 'rift-fill' rocks, termed the 'Aldridge Formation', host the world-class Sullivan SEDEX Zn-Pb deposit (Lydon, 2007). Above the Aldridge Formation, the Creston, Kitchener and Van Creek forma-

¹ Department of Mining and Mineral Exploration, British Columbia Institute of Technology, Burnaby, BC

² Geological Survey of Canada – Pacific, Sidney, BC

This publication is also available, free of charge, as colour digital files in Adobe Acrobat® PDF format from the BC Ministry of Energy, Mines and Petroleum Resources website at http://www.em.gov.bc.ca/Mining/Geolsurv/Publications/catalog/cat_fldwk.htm

tions, taken together, can be considered the middle succession of the Purcell Supergroup (Fig 3). They represent the beginning of the ‘rift-cover’ sequence (Lydon, 2007), but they predate the eruption of a thick package of flood basalts termed the ‘Purcell lavas’, also known as the Nicol Creek Formation. The upper Purcell Supergroup consists of shallow-water, fine-grained clastic rocks of the Van Creek, Gateway, Phillips and Roosville formations (Höy, 1993), which are overlain by flood basalts and volcaniclastic rocks of the Nicol Creek Formation. Directly overlying the Nicol Creek Formation are coarse clastic and stromatolitic carbonate rocks of the Sheppard Formation.

An extremely thick overburden blanket covers much of the Purcell Mountains south of Cranbrook. This glacial overburden has placed a severe limitation on mapping and prospecting activities in the region. Outcrops are limited to steep cliff faces, roadcuts and local ridges. Although this lack of outcrop may have limited the success of prospecting and soil sampling, other methods can now be applied to the region in order to ‘see through’ this cover. In addition, forestry roads provide excellent access to most parts of the region.

UNIT DESCRIPTIONS

The following descriptions of stratigraphic units are based on five weeks of reconnaissance mapping in the southern Purcell Mountains, within NTS sheets 082G/03, 04 and 05. As such, the following unit descriptions and stratigraphy (Fig 3) are specific to this area and do not account

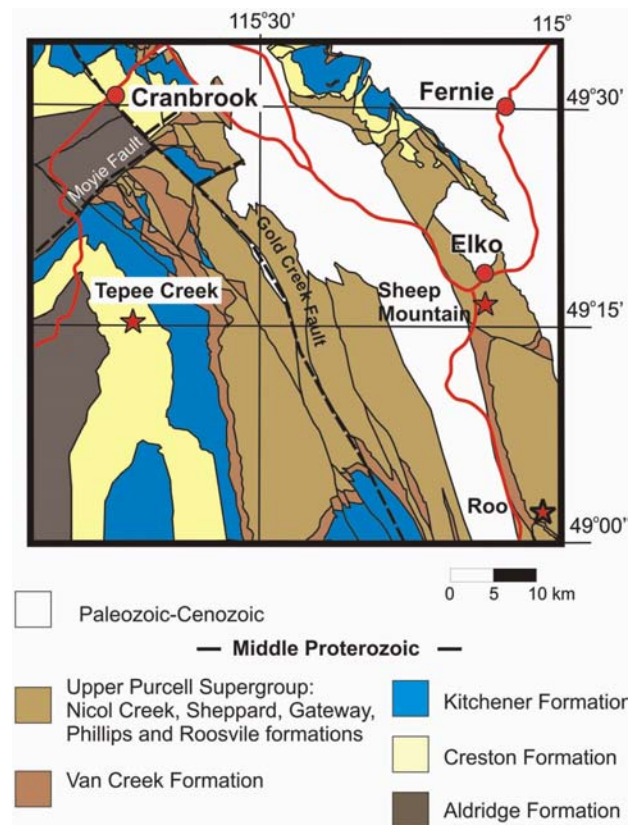


Figure 2. Simplified geology of the study area (modified from Höy et al., 1995). Mineral occurrences discussed in the text are indicated with red stars.

for regional differences within the basin. Höy (1993) and Gardner and Johnston (2007) can be consulted for additional information on unit thicknesses and regional variations. The middle and upper Purcell Supergroup was examined both regionally and in detail around known mineral occurrences.

Creston Formation

The Creston Formation has been divided into three units based on lithology and environment of deposition (Höy, 1993). The lowermost unit is dominated by siltstone and argillite, the middle unit is dominated by quartz arenite with lesser siltstone, and the upper unit is predominantly siltstone. It is the middle sandstone-dominated unit, termed the ‘Revett Formation’ in Montana, that hosts the Troy, Rock Creek and Montanore Cu-Ag deposits. The Creston Formation was examined east of Moyie Lake along several forestry roads that parallel Tepee Creek. The lower Creston (i.e., Burke Formation) in this area contains a distinctive dark grey to black fissile siltstone. Above this unit, mauve and green siltstone and argillite predominate, becoming interlayered with quartz arenite of the middle Creston. Crossbedding and ripple marks are common within the quartz-rich sandstone, consistent with deposition in a relatively shallow, high-energy environment (Fig 4). Both siltstone and sandstone are variably bleached and contain epigenetic euhedral crystals of either pyrite or magnetite.

Kitchener and Van Creek Formations

The Kitchener Formation is a distinctive horizon of carbonate rocks that include oolitic limestone and dolomitic siltstone (Höy, 1993). This unit is commonly pyritic, but no stratabound mineral occurrences have been recorded within it. The overlying Van Creek Formation consists of maroon or green interlayered siltstone and argillite. The unit is thinly bedded to laminated and locally fissile. Mud-chip breccias, ripple marks and desiccation cracks indicate that this unit was deposited in shallow water. Gabbro

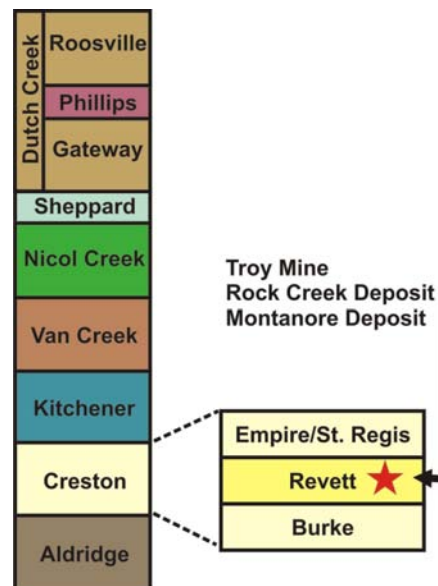


Figure 3. Simplified stratigraphy of the Purcell Supergroup, south-east of Cranbrook, British Columbia.

dikes and sills are relatively common near the top of the Van Creek Formation.

Nicol Creek Formation

The Nicol Creek Formation consists of a distinctive flood basalt unit within the dominantly siliciclastic Belt-Purcell Supergroup. In the United States, the Nicol Creek Formation is termed the 'Purcell lavas' and is best exposed in Glacier National Park, Montana. The Purcell lavas are commonly used as a marker horizon within the basin due to their distinctive nature and relatively widespread occurrence. The Nicol Creek basalts have not been dated, in large part due to a general lack of zircon in mafic extrusive rocks. However, a regionally restricted rhyolite to quartz latite flow yielded a 1443 ± 7 Ma age from the Purcell lavas in Montana (Evans et al., 2000). Within the study area, the Nicol Creek Formation is dominated by vesicular and amygdaloidal flows. Vesicles and gas chambers locally provide well-defined top indicators to the flows (Fig 5a, b). Plagioclase-porphyrific flows are also relatively common and are typically interlayered with the vesicular lavas (Fig 6). No sign of pillow structures was noted, consistent with subaerial lava eruption. Höy (1993) produced several measured sections of the Nicol Creek Formation and reported that thin pillowed horizons do exist. Volcaniclastic rocks and layered tuffs occur, but are relatively thin horizons compared to the massive basalts (Fig 7). McGimsey (1985) provided a detailed account of volcanic flow and vent facies from the Purcell lavas within Glacier National Park in Montana. The Nicol Creek basalts are reported to have a subalkaline to alkaline, within-plate geochemical signature (Höy, 1993). A full suite of volcanic samples was collected in 2007 for detailed petrographic, geochemical and geochronological analysis.

Sheppard Formation

The Sheppard Formation directly overlies volcanic rocks of the Nicol Creek Formation, but is thin and rarely exposed within the mapping area. Where exposed, the formation is extremely distinctive due to the presence of well-developed stromatolitic rocks at the top of the section. The



Figure 4. Fine crossbedding, quartz veining and bleaching in a quartz arenite from the middle Creston Formation (07RH-222, UTM Zone 11, 5451375N, 593089E, NAD 83).

growth of stromatolites within the Sheppard Formation may have been aided by hydrothermal activity within the basin (e.g., Canet et al., 2005), initiated by the emplacement of Nicol Creek magmas. Interlayered siltstone, quartz arenite and oolitic carbonate rocks were all identified in the Gold Creek area south of Cranbrook. An unconformable relationship between the Sheppard and Nicol Creek formations has been suggested due to locally missing (eroded?) Nicol Creek strata and the local presence of conglomerate at the base of the Sheppard (Höy, 1993). An angular unconformity appears to be present locally at the contact between these two formations at the Roo mineral occurrence (Fig 2).

Gateway, Phillips and Roosville Formations (Dutch Creek)

The Gateway Formation is a relatively thick unit that is well exposed south of Cranbrook, especially on the slopes of Mount Baker and along the Gold Creek forestry road. The unit comprises maroon or green siltstone and argillite. The shallow-water nature of this unit is clearly indicated by an abundance of ripple marks, desiccation cracks and salt casts (Fig 8). The presence of salt casts has been considered distinctive of the stratigraphically equivalent unit in

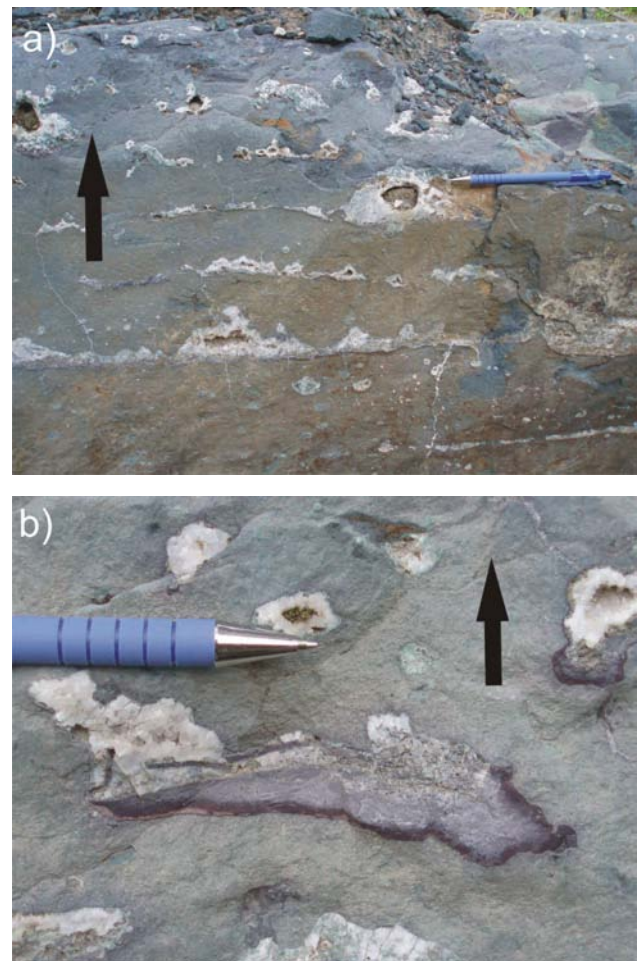


Figure 5. a) and b) Quartz and chalcedony (agate)-filled vesicles and gas chambers indicating way-up direction in Nicol Creek basalts, with arrow indicating top direction (07RH-022; UTM Zone 11, 5471929N, 600783E, NAD 83).



Figure 6. Plagioclase-porphyritic basalt flow (bottom), overlain by aphyric basalt (top; 07RH-246; UTM Zone 11, 5431970N, 646320E, NAD 83).



Figure 7. Volcanic breccia interpreted to be pyroclastic in nature. Clast types are heterogeneous, including those interpreted to be basalt (top right) and aphanitic tan ones that may be tuffaceous (07RH-237; UTM Zone 11, 5492107N, 593798E, NAD 83).



Figure 8. Well-developed salt casts in siltstone from the Gateway Formation (07RH-055; UTM Zone 11, 5471044N, 602185E, NAD 83).

Montana (O'Brien, 1968). The Gateway ranges from thin to thick bedded, and a strong cleavage is locally developed. The Gateway is separated from the overlying Roosville Formation by a distinctive maroon sandstone rich in muscovite, termed the 'Phillips Formation'. Without this marker formation, it is impossible to identify the contact between the upper Gateway and the lower Roosville (Gardner and Johnston, 2007).

INTRUSIVE ROCKS

Intrusive rocks are extremely rare within the study area. A coarse-grained gabbro dike, exposed near Eager hill north of Cranbrook, cuts the Kitchener Formation and includes numerous thin veins containing chalcopyrite (Fig 9). This gabbro may represent a feeder dike to the overlying Nicol Creek basalts. A geochemical comparison will be undertaken to explore this possibility. The presence of Cu in this dike is also consistent with local Cu mineralization in the Nicol Creek Formation. Additional gabbro dikes were identified within the Van Creek Formation, west of the satellite towers near the top of Mount Baker. The margins of these dikes locally display contact metamorphism and quartz veining.

Several K-feldspar porphyritic syenite sills are exposed on the steep east slope of Sheep Mountain (Fig 2). At this location, they cut siltstone and dolomitic rocks of the Dutch Creek Formation. The matrix of the sills is extremely fine grained, suggesting a very shallow level of emplacement. Sheep Mountain also hosts a large zone of alteration and sporadic Cu mineralization that could be related to the emplacement of the syenite magmas. A suite of poorly exposed lamprophyre, minette dikes is also found on the northwest side of Sheep Mountain.

EXPLORATION HISTORY AND ECONOMIC GEOLOGY

Within BC, the Purcell Supergroup has a relatively limited mineral exploration history south and east of Cranbrook. This is especially apparent when compared to the portion of the basin north and west of Cranbrook. Despite this, a couple exploration programs have focused on sporadic Cu (Gold Creek, MINFILE 082GSW022; MIN-



Figure 9. Gabbro dike containing numerous chalcopyrite-bearing veins (07RH-225; UTM Zone 11, 5492533N, 592837E, NAD 83).

FILE, 2007) and mercury showings (Frankie, MINFILE 082GSW034) within the upper Purcell Supergroup along Gold Creek south of Cranbrook. Drilling was concentrated on the Nicol Creek volcanic rocks and the Gateway sedimentary rocks that had geophysical (IP, VLF-EM) anomalies. High Cu values (up to 0.65% over 0.3 m) were noted in several quartz veins near the upper contact of the Nicol Creek basalts (Klewchuk et al., 1990, DH#90-1). Although the first author was unable to locate any surface occurrences associated with this work, a new Cu occurrence was discovered in older strata of the middle Creston Formation. Two other areas with significant exploration histories were also examined. The first is the Sheep Mountain region, near Elko. This area contains a large group of vein and sediment-hosted Cu occurrences (Silver King, Ramshorn, Leah, Jennie, and Sweet May). Secondly, a group of mineral occurrences is located in the Galton Range just north of the Canada – United States border (Roo, Wilda, Green, Wolf and Cabin).

Sediment-Hosted Copper Potential of the Middle Creston Formation

As noted above, a new Cu occurrence was discovered within the Creston Formation along the Tepee Creek forestry road (UTM 593577E, 5454607N). The new showing, termed here ‘Tepee Creek’, consists of green argillite containing fine bornite and chalcopyrite along the bedding planes (Fig 10). Minor amounts of green Cu oxidation mark the discovery outcrop. Two grab samples returned assay results with elevated Cu (564 and 2086 ppm) and Ag (2 and 6 ppm). The showing is about 1.5 km southeast of the Silver Pipe occurrence, a gossanous vein system with elevated Pb, Ag and Cu values (MINFILE 82GSW058). The Silver Pipe occurrence is also hosted in interbedded siltstone and quartzite of the middle Creston Formation. Grab samples from the gossan yielded high Pb, Ag and Cu values (Yeager and Ikona, 1982). It is interesting to note that the Troy mine in Montana contains significant Ag (i.e., 32.3 g/t; Revett Minerals Inc., 2007), has an outer mineralization zone of galena-calcite and contains veins that crosscut stratigraphy (Mauk and White, 2004).



Figure 10: Finely disseminated chalcopyrite-bornite±chalcocite in a green argillite layer within the middle Creston Formation (07RH-142; UTM Zone 11, 5454607N, 593577E, NAD 83).

A significant alteration zone is exposed about 1 km south of the Tepee Creek Cu occurrence. In this area, spectacular purple and red hematite mottling is indicative of oxidized fluid movement along bedding planes and fractures (Fig 11a, b). A similar style of alteration occurs at the Kupferschiefer sediment-hosted Cu deposit in Poland (Cox et al., 2003). The alteration may mark the location of a localized redox front. Identifying such redox fronts is important for tracing the movement of ore-bearing fluids. The presence of magnetite or pyrite may be helpful in identifying reduced units that are prospective for Cu deposition.

Intrusions, Copper Mineralization and Alteration Zones of the Sheep Mountain Area

Numerous small mineral showings occur on and adjacent to Sheep Mountain, directly south of Elko near the intersection of the Wigwam and Elk rivers (Fig 2). Showings in this area include the Ramshorn, Jennie, Sweet May, Silver King, and Leah (MINFILE 82GSW010, 011, 012, 028 and 029). Although the recorded locations of these showings are vague, there can be no doubt that numerous miner-

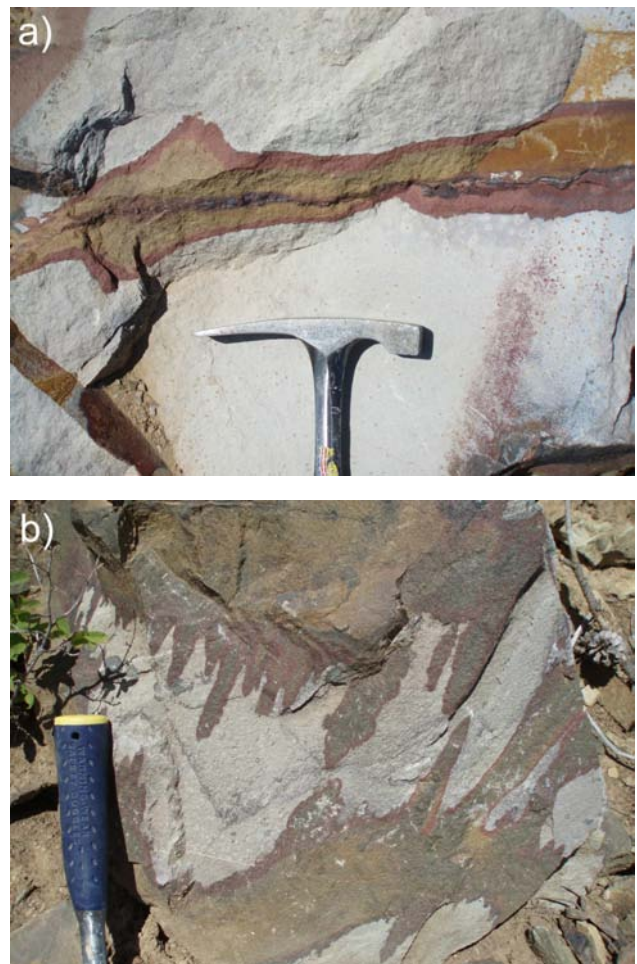


Figure 11. a) and b) Red and purple iron-oxide alteration patterns within sandstone from the middle Creston Formation. This alteration is especially striking due to the white bleaching (argillic alteration) of the rock. The alteration is exposed approximately 1 km south of the newly discovered Tepee Creek Cu occurrence (07RH-220; UTM Zone 11, 5453395N, 594044E, NAD 83).

alized exploration trenches and adits exist on Sheep Mountain. A thick apron (>50 m) of glacial till covers much of the area, and the west side of Sheep Mountain has minimal bedrock exposure. The steep east side of the mountain has numerous small exposures, as well as at least one adit. Steep cliffs along west shore of the Elk River also have exposed outcrop, but they were not investigated due to the difficulty of access. The Roosville Formation is the main unit exposed on Sheep Mountain, but the limited outcrop prevents a complete stratigraphic description. A 10 m thick syenite sill with large, well-developed K-feldspar phenocrysts intrudes siltstone and dolostone of the Roosville Formation along the eastern face of the mountain. Quartz arenite, which may be part of the Mount Nelson Formation, is exposed along the top of the slope as well as in several exploration pits.

A huge zone of alteration is coincident with the exposed syenite sill, but it is unclear whether the alteration zone is related to the sill or other intrusions. Intense argillic and sericitic alteration occurs for several kilometres along the Elk River (Fig 12). Although sedimentary layering is still identifiable, most original minerals have been replaced by clay, sericite, quartz and pyrite. Quartz stockwork (Fig 13) and thick quartz-carbonate veins occur throughout the area. Copper mineralization is typically found within these veins and coating fractures in sedimentary rocks (Fig 14). One major Cu-bearing vein trends approximately 060° and dips steeply southeast. Copper minerals include chalcopyrite, bornite, malachite and azurite. A significant amount of iron-oxide alteration also occurs in angular float on the west side of mountain.

VHMS Potential of the Nicol Creek Volcanic Rocks (Roo Property)

The Roo property (Fig 2) is located within the Galton Range east of Roosville, north of the border with the United States and within the Phillips Creek drainage basin. The Nicol Creek Formation is well exposed on the property and is directly overlain by sandstone, conglomerate, and stromatolitic carbonate rocks of the Sheppard Formation.



Figure 12. Well-developed argillic and sericitic alteration exposed on the east side of the Elk River near Sheep Mountain. An anastomosing array of near-vertical faults cut through the outcrop and were probable pathways for hydrothermal fluid (07RH-075; UTM Zone 11, 5458239N, 638624E, NAD 83).

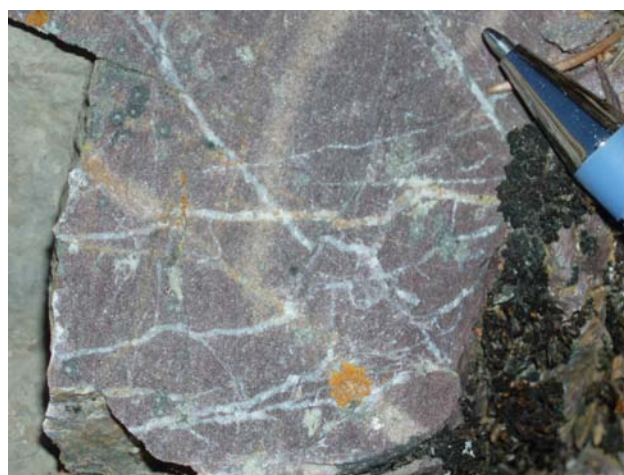


Figure 13. Fine quartz stockwork cutting the Phillips Formation on the east shore of the Elk River near Sheep Mountain (07RH-076; UTM Zone 11, 5457834N, 638848E, NAD 83).

The volcanic rocks of the Nicol Creek include a series of amygdaloidal and porphyritic basalt flows, as well as pyroclastic rocks. Thin-section analysis of the pyroclastic rock indicates that the angular to slightly flattened clasts are porphyritic and/or amygdaloidal, and range in composition from felsic to mafic. A trachyte sill has also been reported in the area (Thomson, 1990a). Initial discoveries of mineralization were reported from 1902, but more recent work was completed by Cominco Ltd. in 1967, Teck Corporation in 1989 and Noranda Inc. in 1993. Previous work included prospecting, trenching, geological mapping, drilling and geochemistry. Drilling by Teck Exploration Ltd. recorded numerous 1 to 5 m thick mineralized intersections with Cu grades up to 1.8% (Thomson, 1990a). The majority of Cu mineralization was hosted in coarse clastic rocks of the Sheppard Formation (Thomson, 1990a, b), possibly related to a synsedimentary growth fault (Kemp, 1992). Recent discoveries, however, indicate that mineralization occurs in both the sedimentary and underlying volcanic rocks (C.

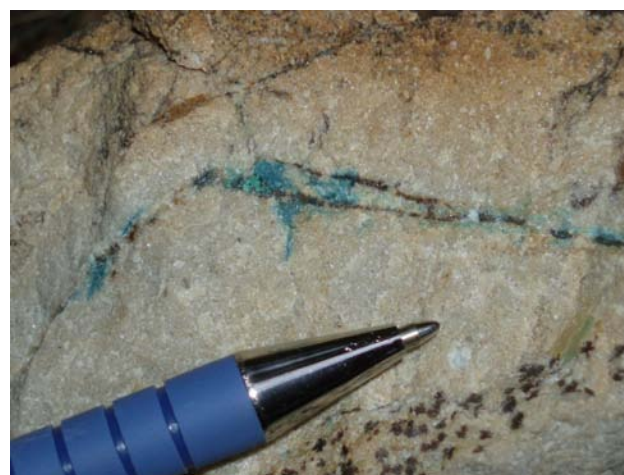


Figure 14. Fine Cu mineralization (chalcopyrite-bornite) and alteration coating fractures within a quartz arenite. This mineralization is exposed within exploration pits on Sheep Mountain (07RH-111; UTM Zone 11, 5457246N 637820E, NAD 83).

Kennedy, Ruby Red Resources Inc., pers comm, 2007). It has been suggested that Cu from Nicol Creek magmas was remobilized into the sedimentary rocks (Thomson, 1990b), but it is possible that all mineralization on the property is directly associated with volcanic activity (VHMS-type). Propylitic and sericitic alteration of the volcanic rocks was locally noted, and barite veins occur throughout the area. A vein up to 1.5 m wide at the Phillips Creek occurrence (MINFILE 082GSE001) was mined for barite in 1940. Barite veining, alteration and elevated cobalt values are all consistent with the presence of a volcanic vent in the area. An angular unconformity locally exists between the Nicol Creek and Sheppard formations; however, this contact may represent the rapid build-up, tilting and erosion of a volcanic pile surrounding a vent complex. Wave-washed sandstone and conglomerate could have been deposited along the flanks of the volcanic pile, while stromatolites developed as the pile stabilized.



Figure 15: Exposure on the west side of the Elk River, south of Elko. The thick layer of glacial drift that is exposed at the top of the cliff is typical of much of the study area. The underlying Purcell Supergroup rocks have undergone significant argillic alteration. Height of the cliff face is approximately 100 m (photo taken from 07RH-075; UTM Zone 11, 5458239N, 638624E, NAD 83).

FUTURE DIRECTIONS FOR MINERAL EXPLORATION

A fairly thick blanket of glacial drift covers much of the bedrock south of Cranbrook and southwest of Fernie (Fig 15). Despite the limited bedrock exposure, a large network of forestry roads provides excellent access and several Cu occurrences have been noted. The high potential of the region is reinforced by the existence of large Cu-Ag deposits in Montana. To capitalize on this potential, targeted exploration methods are required. The following list includes some methods that may prove successful:

- Focus exploration on strata of the middle Creston and Nicol Creek formations.
- Acquire high-resolution geophysics to trace prospective horizons and redox fronts.
- Determine mineral alteration assemblages in order to target drill programs.
- Develop a geochemical database of units to better track geochemical anomalies.
- Utilize remote (spectral?) imaging to determine outcrop locations.
- Obtain basal till samples for geochemical and heavy mineral studies.
- utilize new methods, such as Mobile Metal Ion (MMI)SM geochemistry.

A final consideration for exploration activities is the prospective size of target mineralization. The Troy orebody in Montana is approximately 2300 m (7500 ft.) long, 550 m (1800 ft.) wide and 25 m (80 ft.) thick (Revett Minerals Inc., 2007). Therefore, the surface expression of a similar sediment-hosted Cu deposit is likely to be relatively thin, but should be traceable for a reasonable distance along strike.

ACKNOWLEDGMENTS

Research funding for this project was provided to the first author by the Targeted Geoscience Initiative III (TGI-3) of Natural Resources Canada. Craig and Sean Kennedy are deeply thanked for their informative discussions and for providing access to some of the properties discussed in this text. Dave Grieve and David Gardner are thanked for their continued interest and for insightful discussions. Dave Pigkin provided interesting background information and access to his core-logging facilities. Finally, Tanweer Razi is thanked for his cheerful and reliable assistance in the field.

REFERENCES

- Boleneus, D.E., Appelgate, L.M., Stewart, J.H. and Zientek, M.L. (2005): Stratabound copper-silver deposits of the Mesoproterozoic Revett Formation, Montana and Idaho; *United States Geological Survey, Scientific Investigations Report 2005-5231*, 66 pages.
- Brown, A.C. (1992): Sediment-hosted stratiform copper deposits; *Geoscience Canada*, Volume 19, Number 3, pages 125–141.
- Canet, C., Prol-Ledesma, R.M., Torres-Alvarado, I., Gilg, H.A., Villanueva, R.E. and Cruz, R. (2005): Silica-carbonate stromatolites related to coastal hydrothermal venting in Bahia Concepcion, Baja California Sur, Mexico; *Sedimentary Geology*, Volume 174, pages 97–113.
- Cox, D.P., Lindsey, D.A., Singer, D.A. and Diggles, M.F. (2003): Sediment-hosted copper deposits of the world: deposit models and database; *United States Geological Survey, Open-File Report 03-107*.
- Evans, K.V., Aleinikoff, J.N., Obradovich, J.D. and Fanning, C.M. (2000): SHRIMP U-Pb geochronology of volcanic rocks, Belt Supergroup, western Montana: evidence for rapid de-

- position of sedimentary strata; *Canadian Journal of Earth Sciences*, Volume 37, pages 1287–1300.
- Gardner, D.W. and Johnston, S.T. (2007): Sedimentology, correlation, and depositional environment of the upper Purcell Supergroup, northern Purcell Basin, southeastern British Columbia; *Geological Survey of Canada*, Current Research 2007-A6, 13 pages.
- Hayes, T.S. and Einaudi, M.T. (1986): Genesis of the Spar Lake strata-bound copper-silver deposit, Montana: part I, controls inherited from sedimentation and pre-ore diagenesis; *Economic Geology*; Volume 81, pages 1899–1931.
- Höy, T. (1993): Geology of the Purcell Supergroup in the Fernie west-half map area, southeastern British Columbia; *BC Ministry of Energy, Mines and Petroleum Resources*, Bulletin 84, 157 pages.
- Höy, T., Price, R.A., Legun, A., Grant, B., and Brown, D. (1995): Purcell Supergroup, geological compilation map; *BC Ministry of Energy, Mines and Petroleum Resources*, Geoscience Map 1995-1, scale 1:250 000.
- Höy, T. and Carter, G. (1988): Geology of the Fernie west half map sheet (and part of Nelson east half) (082G/W half, 082F/E half); *BC Ministry of Energy, Mines, and Petroleum Resources*, Open File 1988-14, scale 1:100 000.
- Kemp, R. (1992): Geological and geochemical report on the Roo 1–7 claim group; *BC Ministry of Energy, Mines and Petroleum Resources*, Assessment Report 22644, 33 pages.
- Klewchuk, P., Bapty, M. and Ryley, J.K. (1990): Geochemical, geophysical and diamond drill report on the Gold Creek Project; *BC Ministry of Energy, Mines and Petroleum Resources*, Assessment Report 19965, 349 pages.
- Lydon, J.W. (2007): Geology and metallogeny of the Belt-Purcell Basin; in *Mineral Deposits of Canada: A Synthesis of Major Deposit Types, District Metallogeny, the Evolution of Geological Provinces, and Exploration Methods*, Goodfellow, W.D., editor, *Geological Association of Canada*, Mineral Deposits Division, Special Publication 5, pages 581–607.
- Mauk, J.L. and White, B.G. (2004): Stratigraphy of the Proterozoic Revett Formation and its control on Ag-Pb-Zn vein mineralization in the Coeur d’Alene district, Idaho; *Economic Geology*, Volume 99, pages 295–312.
- McGimsey, R.G. (1985): The Purcell lava, Glacial National Park, Montana; *United States Geological Survey*, Open File Report 85-0543, 191 pages.
- MINFILE (2007): MINFILE BC mineral deposits database; *BC Ministry of Energy, Mines and Petroleum Resources*, URL <<http://www.em.gov.bc.ca/Mining/GeolSurv/Minfile/>> [November 2007].
- O’Brien, D.C. (1968): Cubic casts as indicators of ‘top and bottom’ in the Shields Formation (Precambrian Belt Supergroup); *Journal of Sedimentary Petrology*, Volume 38, pages 685–687.
- Price, R.A. and Sears, J.W. (2000): A preliminary palinspastic map of the Mesoproterozoic Belt-Purcell Supergroup, Canada and USA: implications for the tectonic setting and structural evolution of the Purcell anticlinorium and the Sullivan deposit; in *The Geological Environment of the Sullivan Deposit*, British Columbia, Lydon, J.W., Höy, T., Slack, J.F., and Knapp, M.E., editors, *Geological Association of Canada*, Mineral Deposits Division, Special Publication 1, pages 61–81.
- Revett Minerals Inc. (2007): Troy mine project; *Revett Minerals Inc.*, URL <<http://www.revettminerals.com/revOpTroy.php>> [November 30, 2007].
- Thomson, G.R. (1990a): Diamond drilling report on the Roo 1–3 claims; *BC Ministry of Energy, Mines and Petroleum Resources*, Assessment Report 20700, 71 pages.
- Thomson, G.R. (1990b): Geological and trenching report on the Roo claims; *BC Ministry of Energy, Mines and Petroleum Resources*, Assessment Report 19898, 45 pages.
- Yeager, D.A. and Ikona C.K. (1982): Geological and geochemical report on the Silver Pipe 1–16 mineral claims; *BC Ministry of Energy, Mines and Petroleum Resources*, Assessment Report 10907.

Eaglet Property Revisited: Fluorite-Molybdenite Porphyry-Like Hydrothermal System, East-Central British Columbia (NTS 093A/10W)

by Z.D. Hora¹, A. Langrová² and E. Pivec³

KEYWORDS: Eaglet deposit, MINFILE 093A 046, fluorite, fluorspar, celestite, celestine, molybdenite, potassic alteration, pyrochlore, niobium

INTRODUCTION

The Eaglet property is located on the northern side of Quesnel Lake, 2.5 km east of the North Arm (Fig 1) in NTS area 093A/10W. The identified mineralized zones are located north of Wasko Creek and west of Barrett Creek. Freeport Resources Inc. of Vancouver has owned the property since 1994 when they restaked it as the 'Q claims'.

Exploration of the Eaglet deposit began in 1946 with the discovery of fluorite in Barrett Creek canyon. The property was briefly examined by Canex Aerial Exploration in 1966. Between 1971 and 1985, Eaglet Mines Ltd. conducted a systematic program of trenching and diamond-drilling, and developed two adits.

Exploration activities ceased at Eaglet when international fluorspar prices suddenly dropped from US\$130–210/tonne in 1984 to US\$72–115 in 1985, following a fall in molybdenum prices from US\$25/kilogram in 1980 to below US\$10 in 1983. Fluorspar and fluorite are synonymous terms, with fluorite used more in scientific terminology and fluorspar being a rather technical term in industrial applications.

Given the current strength of commodity prices, with fluorspar at US\$180–280/tonne (*Industrial Minerals*, No. 481, October 2007) and molybdenum at US\$32.75–34.00/lb of Mo oxide (*The Northern Miner*, November 26–December 2, 2007), an update to the public-domain geoscience knowledge of the Eaglet deposit was warranted.

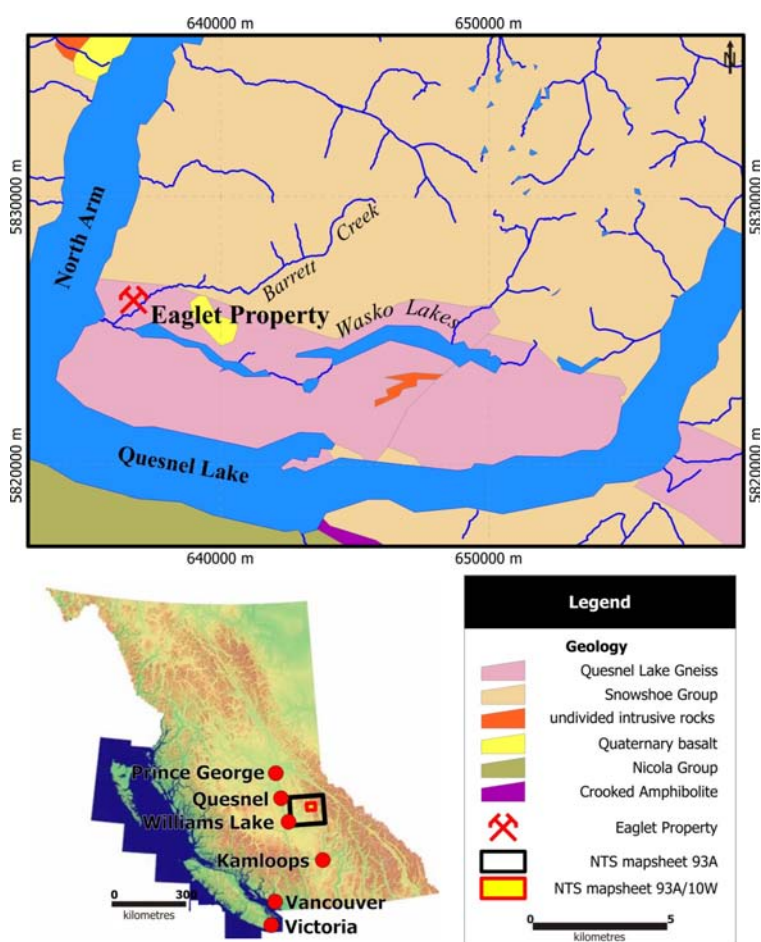


Figure 1. Location of study area, east of the North Arm of Quesnel Lake.

EXPLORATION OVERVIEW

Mineralization discovered in Barrett Creek canyon was disseminated fluorite and minor celestite, pyrite, galena, sphalerite and molybdenite. In a 1966 report, J.M. McCammon described the discovery zone hostrocks as quartz-feldspar-mica gneiss injected with pegmatite, aplite and granitic rock.

Exploration between 1971 and 1985 included 126 surface diamond-drill holes totalling 19 687 m, together with 9 underground horizontal diamond-drill holes (from adit 1) totalling 1525 m (Fig 2). In addition, two adits, no 1 of 292 m and no 2 of 373 m were driven to test the mineraliza-

¹ Consultant, Victoria, BC

² Institute of Geology, Academy of Sciences of the Czech Republic, Prague, Czech Republic

³ Institute of Geology, Academy of Sciences of the Czech Republic, Prague, Czech Republic (retired)

This publication is also available, free of charge, as colour digital files in Adobe Acrobat® PDF format from the BC Ministry of Energy, Mines and Petroleum Resources website at http://www.em.gov.bc.ca/Mining/Geosurv/Publications/catalog/cat_fldwk.htm

tion underground (Fig 3, 4). This program covered an area 1500 m long and 900 m wide on a south-facing forested slope between elevations of 760 and 915 m. Unfortunately, only a small part of the exploration work was documented and is publicly available in Assessment Reports 5639, 9515 and 10447 filed by Eaglet Mines Ltd. The only geochemical data available from the exploration campaign are incomplete CaF₂ assays for 120 of drillholes, 9 of which also have Ag values. The presence of molybdenite has been only briefly mentioned in the *George Cross Newsletter* (1983) and *The Northern Miner* (1984). According to internal Eaglet Mines Ltd. reports, a “good quality fluorspar concentrate” and a saleable MoS₂ concentrate were obtained in pilot tests by Kamloops Research and Assay Laboratory Ltd. In 1985, Eaglet Mines Ltd. contracted Peter Read to map adit 2 and relog the on-site core with the objective of conducting a structural analysis of the deposit. Unfortunately, the project was not completed, although 60 manuscript drillcore logs and a map of adit 2 were purchased by Freeport Resources Inc. (Hora, 2005). Preliminary conclusions of this incomplete structural study indicate that the Eaglet mineral zones are folded by late, broad, open upright folds and are locally truncated by faults (P. Read, pers. comm., in Pell, 1992).

When Freeport took control of the deposit in 1994, a variety of pulp samples were stored inside a shed on the property. These included 189 samples from the 1983 diamond-drilling program (holes 83 to 104) and 632 samples of ‘ribs’ and ‘rounds’ from adit 2. The diamond-drill hole samples were sent by Freeport for reanalysis of 31 elements by inductively coupled plasma – mass spectrometry (ICP-MS) and CaF₂ by wet chemistry (Hora, 2005), and the samples from adit 2 for 34 elements by ICP-MS. In 2005, Freeport also tested samples containing visible molybdenite, collected from the adit 2 muck piles (Fig 5) to document processing suitability of this mineralization type (B. Clark, pers comm, 2005).

GEOLOGICAL SETTING

The Eaglet deposit is located within Early Mississippian Quesnel Lake granitic orthogneiss (Okulitch, 1985) at its contact with Late Proterozoic biotite-garnet metapelite of the Snowshoe Group (Struik, 1983). Along its structurally modified intrusive northern contact are abundant xenoliths of garnet-biotite metapelite and garnet amphibolite. The deposit area is covered by a continuous blanket of overburden, which varies in thickness from 1.2 to 33.2 m (averaging 11.3 m), as documented from 63 drillhole logs (Hora, 2005). However, contact relationships exposed in the Barrett Creek canyon show an easterly strike and shallow northerly dip (Pell, 1992).

Orthogneiss composition ranges from diorite to granite to syenite (Ferri et al., 1999). The U-Pb zircon geochronometry indicates an age between 375 and 335 Ma (Mortensen et al., 1987). Eaglet mineralization is within the East Quesnel Lake gneiss facies (Fig 4, 6, 7). This facies displays I-type attributes with indications of some assimilation of continental material. Most geochemical characteristics of the East facies point to magma genesis within an arc setting, but its origins are not fully understood (Ferri et al., 1999). Some authors have argued that characteristics of at least parts of the East Quesnel Lake gneiss are consistent with a within-plate or anorogenic setting (Montgomery and Ross, 1989).



Figure 2. Eaglet core storage facility in 2007.

Any geochemical discrimination of Quesnel Lake gneiss near the Eaglet deposit must consider the affects of alteration. The salmon pink colour of gneiss blocks found on muck piles from adits 1 and 2 and in most of the drillcore points to widespread potassic alteration and major-element mobility. In particular, any tectonic discrimination based upon the highly mobile large-ion lithophile elements, such as K, Rb, Sr and Ba, is suspect.

PETROGRAPHY, MINERALOGY AND CHEMISTRY

Mineralogy was investigated using optical microscopy, X-ray powder diffractometry and electron microprobe microanalytical techniques at the Institute of Geology, Academy of Sciences of the Czech Republic in Prague. Unless specifically noted, analytical data and tables are part of this study.

Microanalytical and X-Ray Diffraction Methods

Microanalytical analyses were made on polished sections with a CAMECA SX-100 electron microprobe using the wavelength dispersive technique. The beam diameter was 2µm with an accelerating potential of 15 kV. A beam current of 10 nA was measured on a Faraday cup. A counting time of 10 s was used for all elements. The standards employed were synthetic SiO₂, TiO₂, Al₂O₃, Fe₂O₃ and MgO, and natural jadeite, leucite, apatite, diopside, spinel and barite. The data were reduced using the $\Phi(\rho z)$ Merlet correction.

Mineral phases were also identified by X-ray powder diffraction (XRD), using a Phillips X’Pert APD that employs CuK α radiation and graphite monochromator. Scanning speed was set to 1°/min, generator voltage to 40 kV and current to 40 mA.

The ICP-MS analytical results were provided by Vancouver laboratories Min En Labs, Assayers Canada and ACME Analytical Laboratories Ltd.

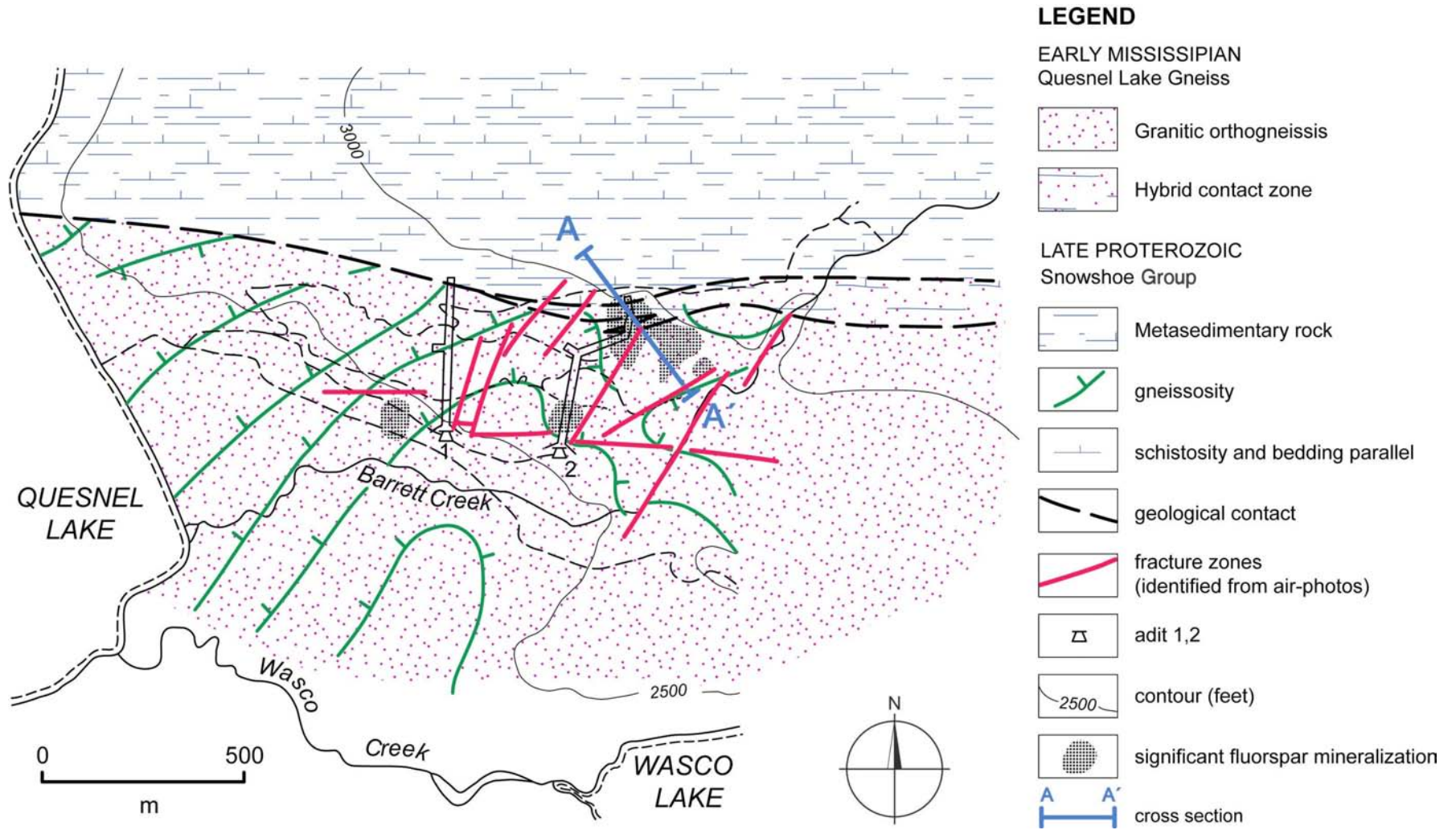


Figure 4. Geology of the property area (modified after Pell, 1992), with faults identified from airphotos.



Figure 5. Aerial view of muck piles from adit 2 as they appeared in 2007.

Petrography

The dominant rock types are salmon pink and light grey gneisses, locally displaying a yellow overprint (Fig 7). They are fine to medium grained and composed of a sucrosic mixture of K-feldspar, albite, quartz and kaolinite group minerals. The rocks are frequently so heavily altered and recrystallized that their gneissic fabric is partially or entirely obscured. Samples of the Quesnel Lake gneiss collected in 2007 present a broader range of rock types than previously recognized: alkaline pyroxenite to leucogranite, aplite and gradations into metapelitic xenoliths.

Mineralogy includes potentially economic minerals fluorite, molybdenite and celestite; dominant rock-forming minerals microcline, albite and quartz; and accessory minerals rutile, pyrite, zircon, sphene, fluorapatite, magnetite and pyrochlore. Secondary minerals resulting from low-temperature hydrothermal alteration are siderite, disseminated very fine grained hematite, calcite, dickite, nakrite, kaolinite 1T with 1Md, and fluorapophyllite.

Figures 8 to 11 document three main stages of physical and chemical changes affecting the orthogneiss:

- 1) Following silicification and regional metamorphism, the rocks were subjected to albitization and then K-feldspar alteration (microcline) and silicification.
- 2) Introduction of sulphide minerals (MoS_2 , PbS and ZnS) may have occurred next, then addition of fluorine and deposition of the oldest generation of fluorite.

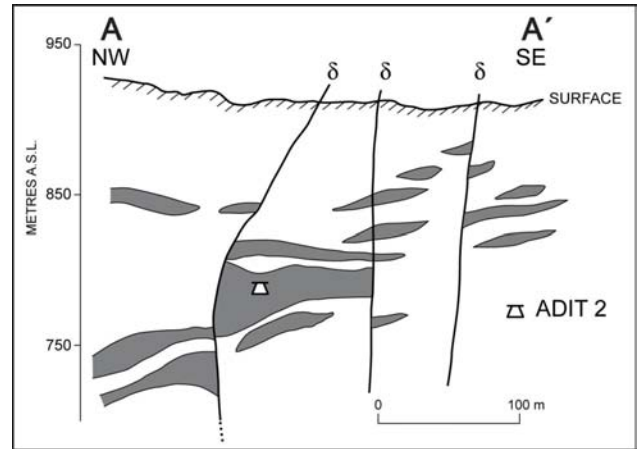


Figure 6. Northwest-southeast section across the mineralized zone, constructed using data projected from drillholes 33, 67, 58, 1, 45, 93, 50, 51, 57, 77 and 80 (adapted from Ball and Boggaram, 1985). Faults (δ) interpreted from airphotos.

- 3) A period of cataclasis ensued, followed by carbonate alteration and addition of multiple generations of fluorite and celestite. Growth of these minerals was accompanied by the alteration products kaolinite, sericite, chlorite and zeolite minerals. Secondary fluorapophyllite was identified by XRD analysis.

Demonstrating that some minerals are remnants of an original protolith is difficult. Only in a few thin sections are the outlines of the original minerals visible where they have been replaced by microcline and their boundaries enhanced by the presence of quartz (Fig 9d). Identification of residual minerals incorporated from the original protolith is less ambiguous (Fig 8b, 10c, 10d). The chemical composition of dominant minerals, identified by XRD as microcline and low albite, is consistent in the samples analyzed (Fig 12; Table 1). Therefore, we interpret these minerals as a product of the same large-scale replacement process. The intensity of feldspar alteration makes distinctions between original rock types uncertain.

A mica sample recovered from aplitic granite intersected in drillhole 43-81 provided an age of 127 ± 4 Ma



Figure 7. Sample of East Quesnel Lake gneiss showing pervasive alteration, adit 2.

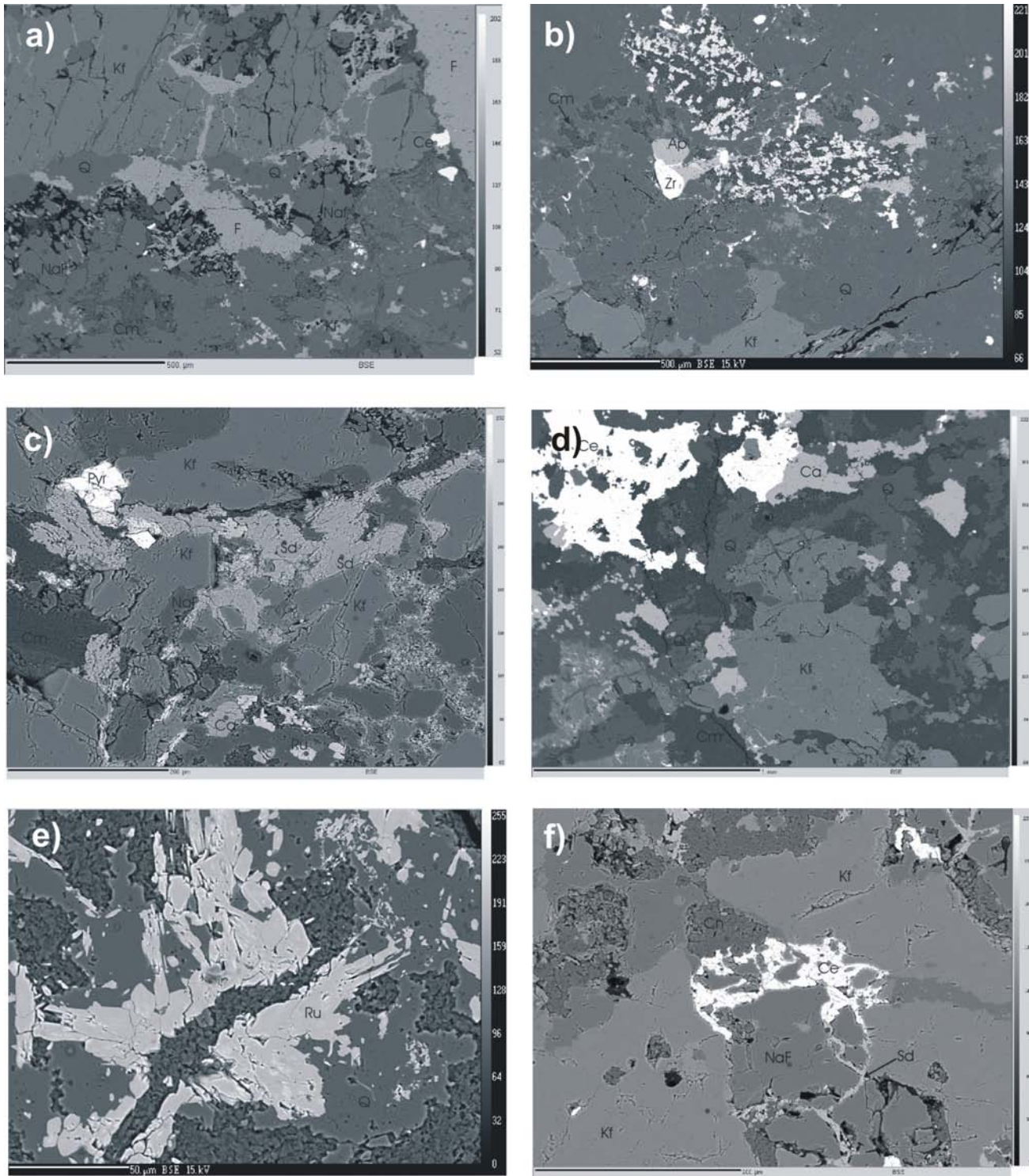


Figure 8. Scanning electron microscope (SEM) photomicrographs showing a) brecciated microcline (Kf) replacing albite (NaF), with fractures in microcline filled by quartz (Q) and fluorite (F); youngest minerals are celestite (Cs) and a clay mineral of the kaolinite group (Cm); b) hydrothermal quartz (Q) replacing microcline (Kf) and enclosing apatite (Ap) and zircon (Zr) with, to the right and up from them, original titanium mineral crystals altered to a mixture of rutile and clay mineral; c) cataclasis of microcline (Kf), which is replacing albite (NaF); intergranular space is filled by siderite (Sd) with pyrite (Pyr) grains; albite contains disseminated grains of calcite (Ca); d) microcline (Kf) cut by microveinlets of quartz (Q) and calcite (Ca); the calcite is partly engulfed by celestite, perhaps indicating replacement of calcite by celestite; in this sample, extensive mats of kaolinite (Cm; type IT) indicate advanced alteration; e) rutile crystals (Ru) enclosed by quartz (Q), with kaolinite (type IT) penetrating both; f) microcline (Kf) replacing albite (NaF), and celestite (Ce), siderite (Sd) and a clay mineral of the kaolinite group (Cn) replacing both feldspars along fractures and grain boundaries.

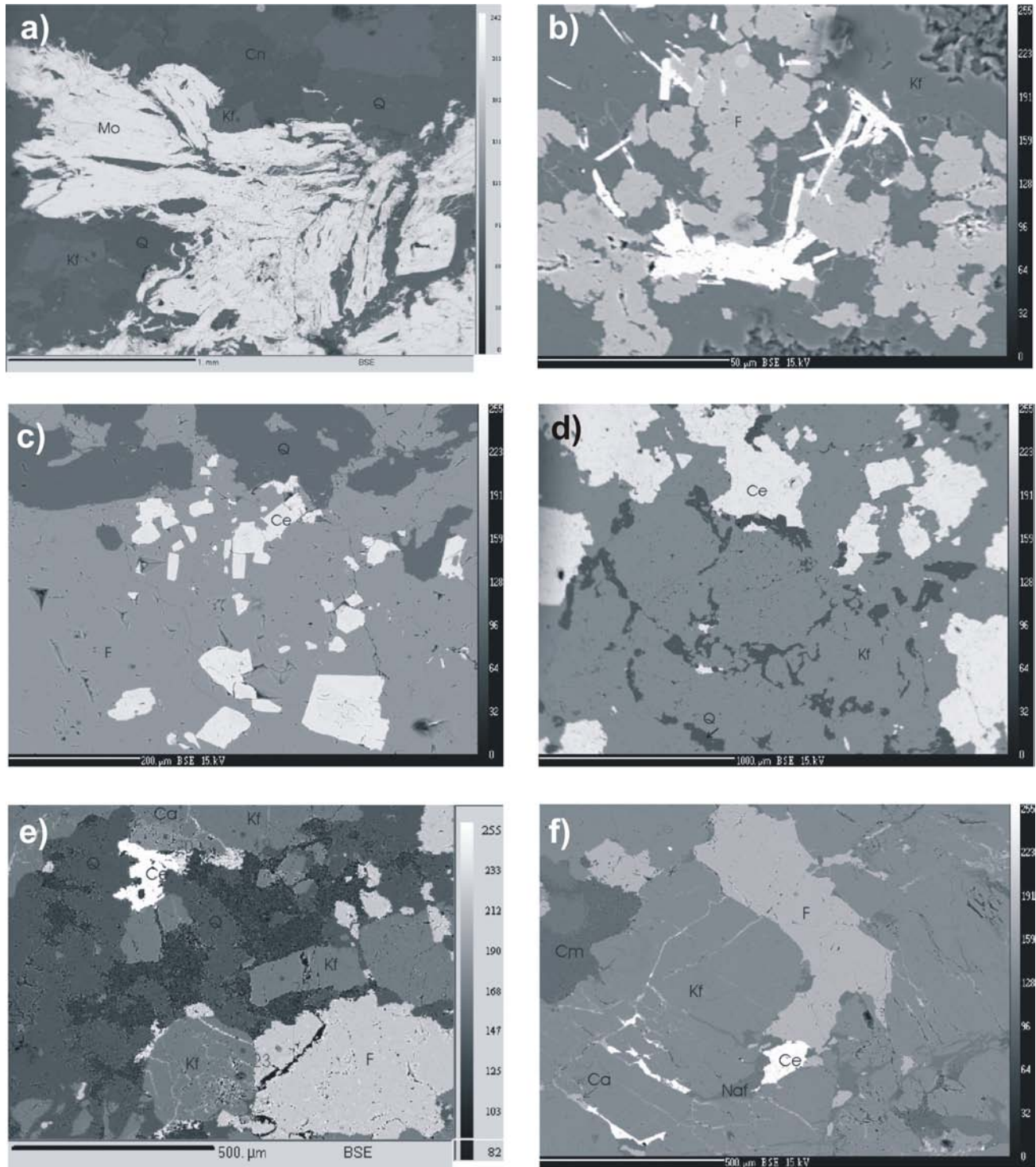


Figure 9. Scanning electron microscope (SEM) photomicrographs showing a) hydrothermal quartz (Q) with an aggregate of molybdenite (Mo) flakes; K-feldspar enclosed in quartz is structurally disordered and is probably a remnant of the original rock; the rock is highly altered, with nacrite present in addition to kaolinite (Cn); b) crystal aggregates of fluorite (F) formed at the expense of K-feldspar (Kf); elongate, prismatic, highly charged (bright) mineral replacing fluorite is an unidentified mineral with high Y, Ce, La and Nd, probably a carbonate related to bastnaesite; c) idiomorphic celestite (Ce) formed at the expense of fluorite (F) and quartz (Q); d) microcline (Kf) replacing the original rock-forming minerals; patchy quartz (Q) outlines the boundaries of replaced minerals and celestite (Cs) replaces both microcline and quartz; e) a highly clay-altered rock specimen, with the oldest mineral being microcline (Kf) and later minerals, in order of paragenesis, being quartz (Q), fluorite (F) and celestite (Ce), all of them replaced by a dark-coloured clay mineral (Cm); f) cataclastic microcline (Kf) replacing albite (Naf), with both being replaced by calcite (Ca), fluorite (F), celestite (Ce) and a clay mineral (probably kaolinite).

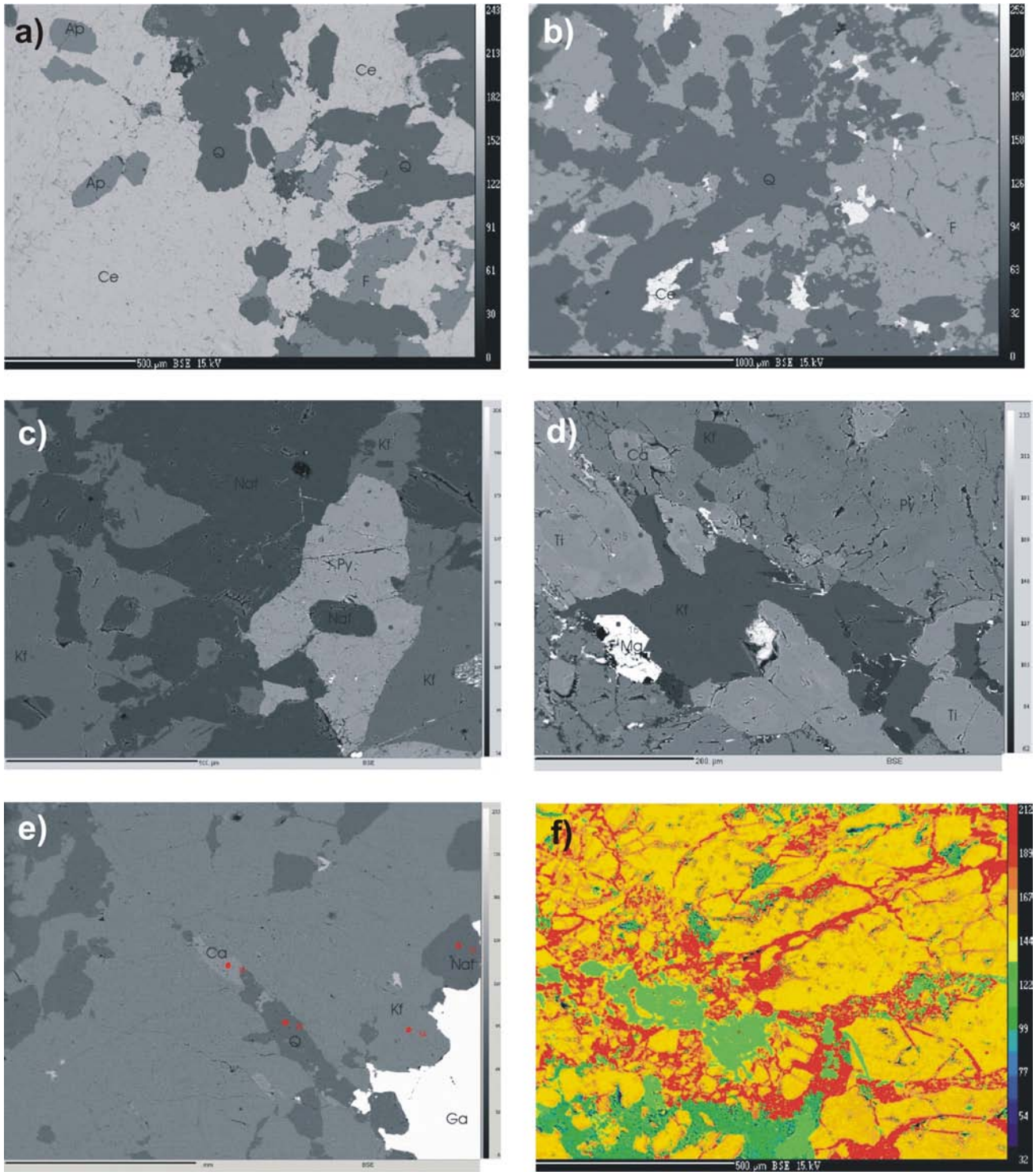


Figure 10. Scanning electron microscope (SEM) photomicrographs showing a) remnants of quartz (Q) and fluorite (F) within celestite (Ce), with apatite (Ap) grains being the only residual minerals from the original protolith; b) quartz (Q) being replaced by fluorite (F), with celestite (Ce) replacing both; c) that the protolith in this sample was probably an alkaline intrusive, as indicated by remnants of original pyroxene (Py) of aegirine-augite composition; albite (Naf) grain is enclosed by the pyroxene and both are replaced by microcline (Kf); d) the same protolith as in 10c; aegirine-augite is associated with magnetite (Mg), sphene (Ti) and calcite (Ca), and late microcline replaces all igneous minerals; e) a quartz (Q) – calcite(Ca) vein with galena (Ga), the galena replacing both microcline (Kf) and albite (Naf); f) colour-enhanced element mapping in a backscatter photomicrograph; microcline is yellow, fluorite is red, siderite is pale green and kaolinite is dark green.

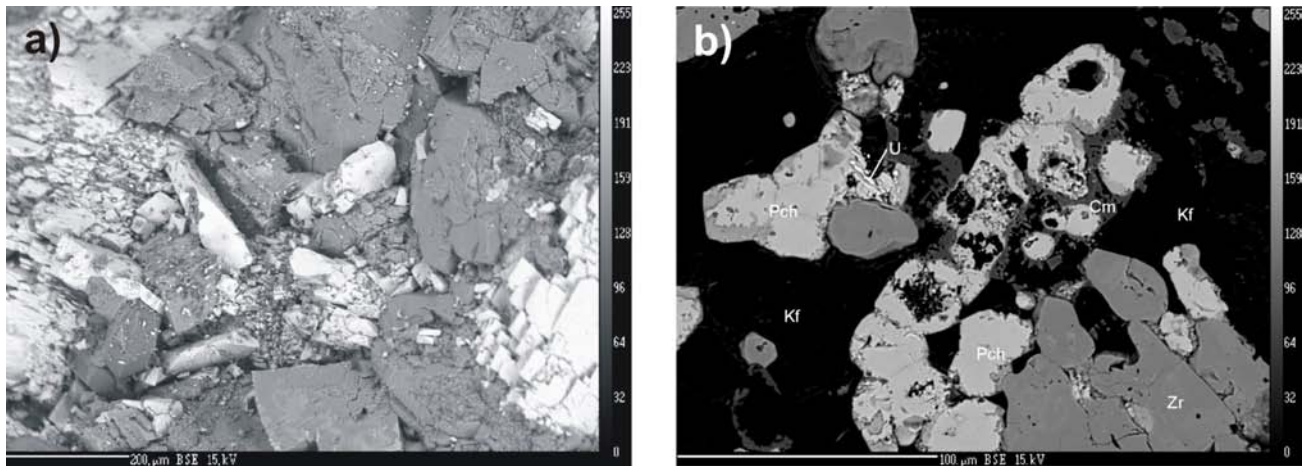


Figure 11. Scanning electron microscope (SEM) photomicrograph showing a) celestite crystals in vugs of carbonate-altered rock; b) aggregates of pyrochlore (Pch) crystals and zircon (Zr) grains enclosed in microcline (Kf) matrix, with the margins of both microcline and pyrochlore corroded and replaced by kaolinite (Cm); bright white inclusions in the pyrochlore are probably uraninite (U).

(Pell, 1992), which is within the range of Cretaceous stocks and dikes with Mo mineralization in the Quesnel and Kootenay terranes elsewhere. A less reliable fission-track date on fluorite from adit 1 suggests an age of formation of 104.6 Ma (Pell, 1992), which is within the same general range.

Alkali feldspars are the dominant minerals of the hostrocks on the Eaglet property. Microcline in anhedral grains with evidence of cataclasis (Fig 8a, 10f) makes up almost 50% of the rocks. It often shows undulatory extinction. Preserved silica rims on original mineral components commonly outline the grain boundaries within the original protolith (Fig 9d). The X-ray diffraction diagrams of microcline confirm its ordered structural state close to the pure theoretical composition. Chemical composition corresponds with very high purity $KAlSi_3O_8$ (orthoclase (Or); Fig 12; Table 1), with only low content of the albite (Ab; max. 4.7%) and celsian (Ca; $BaAl_2Si_2O_8$; max. 0.5%) components.

Albite in samples from the Eaglet property is intergrown with quartz, the second most abundant mineral. Petrographic identification of low albite based on polysynthetic and carlsbad-albite twinning was confirmed by XRD. The crystallization of albite preceded formation of microcline (Fig 8c, 8f). Chemical composition (Table 1; Fig 12) corresponds to very pure albite (Ab; $NaAlSi_3O_8$), with only 1.3% Or component and a negligible (0.4%) An content.

Chondrite-normalized rare earth element (REE) abundance patterns for all four samples analyzed are enriched in light rare earth elements (LREE). The LREE pattern is marked by a high La/Sm_N ratio (up to ~180, average ~140), while the content of heavy rare earth elements (HREE) is low but variable ($Gd/Lu_N = \sim 1$ on average). All of the analyzed samples have distinctly positive Eu anomalies (Fig 13; Table 2). The samples selected for REE analysis are from mineralized zones high in Sr (>10 000 ppm).

Quartz is present in several mineral associations and several generations that are texturally indistinguishable from each other. The dominant is quartz of hydrothermal origin (Fig 14). Other typical products of low-temperature hydrothermal alteration are siderite (Fig 8c), calcite

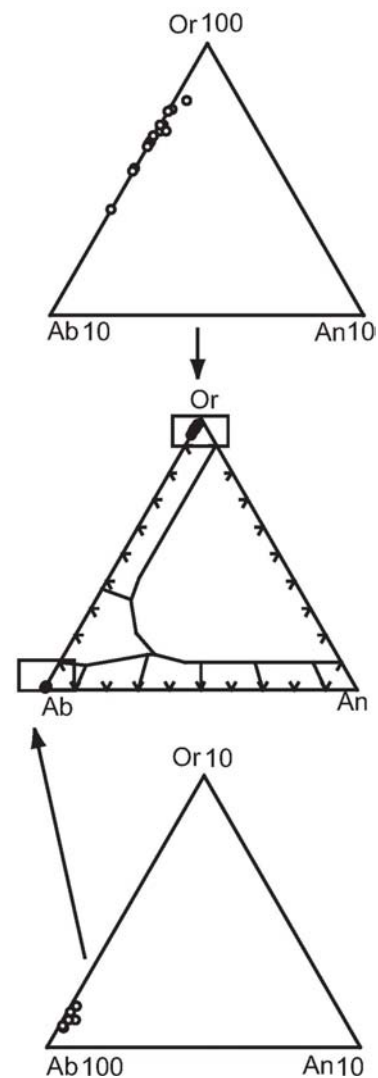


Figure 12. Feldspar minerals from the Eaglet property plotted on an orthoclase-albite-anorthite ternary diagram with expanded orthoclase and albite apices.

TABLE 1. GEOCHEMISTRY OF TYPICAL ROCK-FORMING MINERALS IN EAST QUESNEL LAKE GNEISS FROM THE EAGLET PROPERTY.

	Microcline			Albite			Quartz			Sphe		Rutile
SiO ₂	64.09	64.49	64.88	68.88	68.33	68.36	98.62	98.80	99.77	30.61	30.22	0.41
TiO ₂	0.00	0.01	0.04	0.00	0.06	0.01	0.66	0.80	0.03	31.56	33.71	89.16
Al ₂ O ₃	17.78	18.29	18.06	19.07	19.34	19.66	0.00	0.00	0.92	1.73	1.19	0.00
Cr ₂ O ₃	0.00	0.00	0.00	0.00	0.00	0.00	0.06	0.01	0.00	0.01	0.00	0.00
MnO	0.00	0.00	0.00	0.01	0.00	0.00	0.00	0.12	0.00	0.13	0.26	0.00
FeO	0.23	0.13	0.15	0.16	0.65	0.22	0.00	0.00	0.00	2.01	1.59	2.31
MgO	0.00	0.00	0.00	0.04	0.03	0.00	0.03	0.02	0.00	0.00	0.31	0.00
CaO	0.01	0.01	0.00	0.09	0.04	0.06	0.00	0.03	0.03	26.45	27.13	0.18
BaO	0.23	0.13	0.06	0.00	0.10	0.00	0.04	0.01	0.00	0.00	0.00	0.00
Na ₂ O	0.41	0.54	0.70	11.57	11.73	11.73	0.00	0.00	0.04	0.00	0.31	0.00
K ₂ O	16.65	16.54	16.37	0.17	0.12	0.16	0.00	0.02	0.06	0.04	0.01	0.05
Total	99.42	100.14	100.26	100.00	100.39	100.20	99.41	99.81	99.85	92.54	94.46	92.11

	Magnetite		Aegirine-augite		Siderite		Calcite		Kaolinite		Muscovite	
SiO ₂	1.18	0.06	52.49	51.83	1.11	0.15	0.28	0.03	47.95	45.46	45.33	45.9
TiO ₂	0.11	0.01	0.04	0.05	0.00	0.00	0.01	0.00	0.03	0.16	0.20	0.23
Al ₂ O ₃	1.07	0.00	1.58	0.95	0.57	0.11	0.00	0.00	37.85	32.77	33.43	33.28
Cr ₂ O ₃	0.04	0.00	0.00	0.00	0.00	0.00	0.00	0.00	0.00	0.02	0.04	0.04
MnO	0.00	0.04	2.75	1.77	0.79	1.03	0.15	0.51	0.07	0.13	0.06	0.14
FeO	83.04	89.28	16.08	23.12	50.3	50.44	0.16	1.73	0.19	5.17	5.16	5.12
MgO	0.12	0.00	5.92	4.31	5.05	4.31	0.00	0.04	0.07	0.55	0.44	0.47
CaO	0.45	0.05	14.15	10.91	1.66	1.83	54.48	54.34	0.00	0.00	0.01	0.00
BaO	0.04	0.00	0.02	0.00	0.00	0.00	0.00	0.02	0.00	0.12	0.02	0.00
Na ₂ O	0.08	0.00	5.92	7.79	0.09	0.22	0.17	0.03	0.03	0.35	0.34	0.32
K ₂ O	0.04	0.00	0.01	0.02	0.06	0.01	0.02	0.03	0.00	10.54	10.55	10.38
Total	86.16	89.43	99.13	99.47	59.63	58.13	55.26	56.74	86.19	95.26	95.58	95.89

(Fig 9f) and clay minerals of the kaolinite group: kaolinite, dickite and nacrite (Fig 8a, 8d, 9a, 9e, 11b).

Magnetite is the most common accessory mineral, forming euhedral to anhedral crystals (Fig 10d). The Fe₃O₄ component (87.9–99.0%) is dominant over the ilmenite (Mg₂TiO₄) admixture (up to 10.2%). The geikielite (MgTiO₃) component is minor (up to 1.3%).

Muscovite is another common accessory in rocks on the Eaglet property (Table 1). Its volume is variable, locally

reaching several percent. A genetically important accessory is zinnwaldite, found in centimetre-wide greisen veinlets. Its presence was confirmed by XRD.

Other common accessory minerals are rutile (Fig 8b, 8e), sphene (Table 1; Fig 8b, 8e, 10d), fluorapatite (Fig 8b, 10a), pyrite (Fig 8c) and pyrochlore. Pyrochlore commonly occurs as individual grains and crystal aggregates (Fig 11b; Table 3). Pyrochlore, present locally in amounts up to several volume percent, is found in association with microcline, zircon, pyrite and clay minerals of the kaolinite group. Accessory zircon (Fig 8b, 11b), sphalerite and galena (Fig 10e) are rare.

Irregular zones of dark bands within altered East Quesnel Lake gneiss are highly altered amphibolite, garnet amphibolite and pyroxene-bearing rock. Aegirine-augite can enclose euhedral albite crystals and is found in association with microcline, albite, calcite, sphene and magnetite (Fig 10c, 10d, 15; Table 1).

Economic Minerals

Until now, Eaglet had been considered a fluorspar property. In outcrops along Barrett Creek, fluorite showings have been described as disseminated grains, veinlets and scattered veins up to 15 cm thick, and as pods and irregular masses 15 to 20 cm wide (McCammon, 1966). Fluorspar mineralization also crops out in sparse exposures for a distance of 400 m westward from Barrett Creek canyon and again on the lakeshore, 1600 m further west. After an initial search for massive veins was unsuccessful, exploration work targeted lower grade feldspathic zones with fluorite impregnations and a stockwork character (Fig 6,

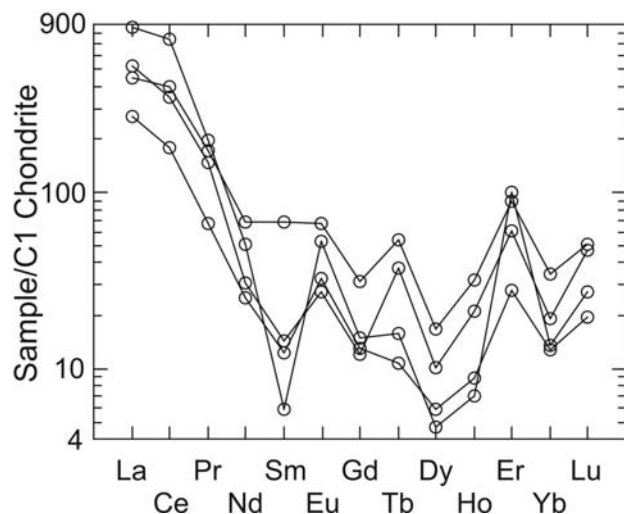


Figure 13. Chondrite-normalized rare earth element pattern of East Quesnel Lake gneiss, Eaglet property.

TABLE 2. RARE EARTH ELEMENT ANALYSES OF EAST QUESNEL LAKE GNEISS HIGHLY ALTERED ZONE, EAGLET PROPERTY. ANALYSES BY ACME ANALYTICAL LABORATORIES LTD.

Sample	Y (ppm)	La (ppm)	Ce (ppm)	Pr (ppm)	Nd (ppm)	Sm (ppm)	Eu (ppm)	Gd (ppm)	Tb (ppm)	Dy (ppm)	Ho (ppm)	Er (ppm)	Tm (ppm)	Yb (ppm)	Lu (ppm)
B 110303	26.3	124.5	212.1	14.0	14.5	2.2	1.6	2.5	1.4	2.6	1.2	10.1		3.3	1.2
B 110313	4.8	45.2	79.9	5.7	5.5	1.6	0.5	1.3	1.0			4.3		0.6	0.3
B 110315	26.4	11.0	22.0	0.5	4.9		0.4	1.3	0.3		0.6			1.4	0.3
B 110316	7.9	41.2	73.8	4.4	7.2	1.6	0.6	1.5	0.6			4.4		0.8	0.2
B 110320	44.5	105.1	243.3	16.3	31.6	10.4	3.9	6.5	2.0	4.3	1.8	14.9		5.9	1.3
S92-502	18.4	35.8	62.5	4.4	5.7		1.2	2.2	0.2			0.8		1.5	0.3
S93-520	21.7	37.3	54.8	5.0	4.6		1.3	2.3				1.3		1.8	0.5
S97-562	27.7	206.3	449.4	18.8	24.0	0.9	3.1	3.1	0.6	1.2	0.4	16.5	0.3	2.3	0.7
S98-585	22.1	103.1	173.4	10.2	12.6		1.5	2.1				2.2		1.9	0.5
S102-854	23.1	64.5	109.5	6.4	11.8	1.9	1.9	2.7	0.4	1.5	0.5	4.6		2.2	0.5

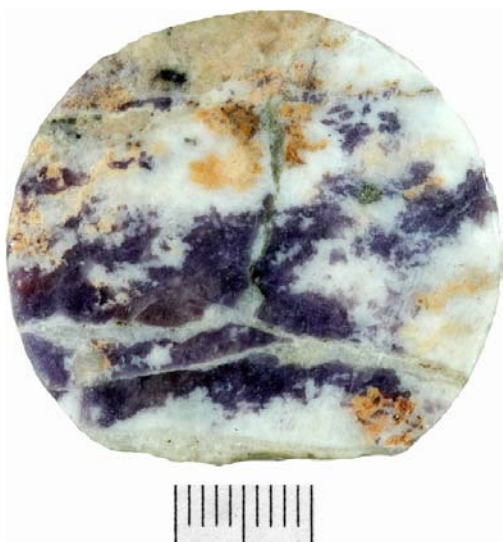


Figure 14. Sample of 'BQ' drillcore showing an early generation of fluorite (Fl) fractured and cemented by quartz (Qtz).

TABLE 3. ANALYSES OF PYROCHLORE, EAGLET PROPERTY.

	QL A6	QL A6	QL C10	QI C10
ThO ₂			0.36	0.31
TiO ₂	8.73	8.49	8.59	8.74
ZrO ₂			0.00	
Nb ₂ O ₅	55.53	56.01	56.18	57.52
Ta ₂ O ₅	1.28	1.25	1.19	1.25
U ₂ O ₅	15.42	15.85	15.45	15.59
Ce ₂ O ₃			0.00	
La ₂ O ₃			0.00	
MnO	0.36	0.06	0.16	0.26
FeO	1.98	2.48	3.14	2.08
CaO	6.58	5.67	3.69	5.34
Total	89.88	89.81	89.04	91.11

14, 16). Late discovery of molybdenite in adit 2 has not been followed up by work to outline its distribution within the deposit. In 2007, the authors also found molybdenite in a rock pile outside adit 1. Molybdenite is frequently but randomly present along slickenside and gneissosity planes as

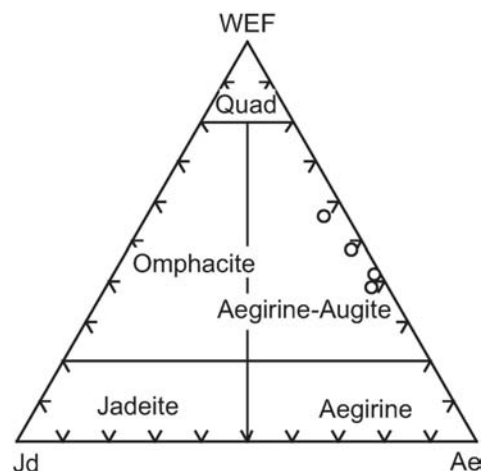


Figure 15. Pyroxene from East Quesnel Lake gneiss on the Eaglet property plotted on wollastonite/enstatite/ferrosilite (WEF) – jadeite (Jd) – aegirine/acmite (Ac) diagram (after Morimoto, 1988).



Figure 16. Mineralized breccia in adit 2 of the Eaglet property, showing patchy purple fluorite, flesh-coloured veins of K-feldspar, white celestite and blue-grey silicified zones.

groups of flakes several centimetres in size (Fig 17). Molybdenite also occurs within quartz veinlets and as grains within crosscutting veinlets of fluorite (Fig 9a). The X-ray diffraction analysis of a laboratory-scale concentration test sample identified two forms of MoS₂, the 3R and 2H, in rel-



Figure 17. Sample of coarse-grained molybdenite from adit 2, Eaglet property.

atively similar amounts (Table 4). The widespread presence of celestite in the deposit is unusual. It is commonly found with fluorite and calcite (Fig 11a) and, in some samples, celestite is more common than fluorite (Fig 9c, 9f, 10a). It replaces both fluorite and calcite (Fig 8d, 10f, 18).

The chemical composition of fluorite and celestite, as determined by electrode microprobe microanalysis, is shown in Table 5. Fluorite is very pure, with only 0.25% SrO, irrespective of which of several generations of fluorite is analyzed. The dark purple colour definitely represents a very early fluorite phase. Celestite exhibits zoning of Sr, with an increase from grain centres to the rims (Ba content decreases). Impurities in molybdenite within the mineral phases analyzed by microprobe are below the detection limits of the instrument.

The widespread association of fluorite with feldspar-altered zones at the Eaglet property may suggest a magmatic source for the fluorine component. Specialized magmas with elevated fluorine are usually 'dry', and fluorine migrates from the protolith into the melt only at higher temperatures in the late stages of protolith melting. It may accumulate in the residual melt, lowering the temperature of the

TABLE 4. MINERAL COMPOSITION OF MOLYBDENITE CONCENTRATE, EAGLET PROPERTY. ANALYSES BY THE MINERAL LAB, INC.

Mineral name	Chemical formula	Approx. wt %
Molybdenite ⁽¹⁾	MoS ₂	33
Molybdenite ⁽²⁾	MoS ₂	22
Quartz	SiO ₂	10
Fluorite	CaF ₂	<5
Calcite	CaCO ₃	<5
K-feldspar	KAlSi ₃ O ₈	<5
Talc	Mg ₃ Si ₄ O ₁₀ (OH) ₂	<10
Kaolinite	Al ₂ Si ₂ O ₅ (OH) ₄	<10
Pyrophyllite	Al ₂ Si ₄ O ₁₀ (OH) ₂	<5?
Sepiolite	Mg ₄ Si ₆ O ₁₅ (OH) ₂ ·6H ₂ O	<10?
Unidentified'	?	<5

⁽¹⁾ '3R' type; also called 'rhombohedral type'

⁽²⁾ '2H' type; also called 'hexagonal type'



Figure 18. Typical fluorite (FI) – celestite (ClS) – quartz (Qtz) mineralization from adit 2, Eaglet property. Sample is 5 cm across.

granite solidus to 600–650°C and gradually developing into postmagmatic fluids. Exsolved fluorine-rich fluids may migrate along steep fracture systems into overlying rocks. In a favourable environment, such as a cataclastically deformed feldspathic host, the fluids may react with the host and result in fluorite flooding. A similar process has been described from tin-bearing metallogenic provinces (Tischendorf and Förster, 1990, 1994; Štemprok, 1993).

Mineralized zones at Eaglet can attain thicknesses of up to 30 m (Fig 6). Past exploration efforts at Eaglet have

TABLE 5. CHEMICAL COMPOSITION OF FLUORITE AND CELESTITE, EAGLET PROPERTY.

	Fluorite				
	gr	v	v	gr	v
SiO ₂	0.03	0.01	0.01	0.00	0.01
Al ₂ O ₃	0.01	0.00	0.00	0.00	0.00
MnO	0.00	0.02	0.06	0.00	0.00
FeO	0.02	0.03	0.01	0.00	0.00
CaO	52.30	51.34	51.61	52.95	51.81
BaO	0.00	0.00	0.01	0.00	0.00
SrO	0.17	0.25	0.02	0.23	0.01
SO ₄	0.00	0.00	0.00	0.00	0.01
F	47.67	47.19	47.40	48.06	47.14
ThO ₂	0.01	0.02	0.06		
Total	100.24	99.02	99.24	101.33	98.98

Abbreviations: gr, individual grains; v, fluorite in veinlets >1 mm

	Celestite				
	gr	gr	lgr core	lgr rim	lgr core
MnO	0.00	0.00	0.06	0.05	0.00
FeO	0.07	0.02	0.07	0.01	0.01
CaO	1.21	1.13	0.05	0.12	0.17
BaO	6.36	6.59	2.75	8.57	3.96
SrO	48.81	48.16	54.08	48.11	51.97
Ce ₂ O ₃	0.38	0.27	0.26	0.22	0.23
F	0.06	0.00	0.00	0.01	0.00
SO ₄	43.42	43.17	43.58	42.41	42.98
Total	100.44	99.36	100.86	99.50	99.35

Abbreviations: gr, small grain <1mm; lgr, larger grain >1 mm

outlined eight such zones, four of them described as 'main zones' (Ball and Boggaram, 1985). The special association of higher grade fluorite accumulations with feldspathic zones should not be considered a genetic affiliation (Pivec, 1973). The source of Sr is disputable; however, it is most likely the result of late to postmagmatic fluids penetrating the Snowshoe Group. Such enrichment is not common, but it has been described at other localities, such as the Beauvoir granite in France (Raimbault and Azencott, 1987) and the Ghost Lake batholith in Ontario (Breaks and Moore, 1992). Five more fissure celestite localities in Canada have been listed by Dawson (1985).

Discussion

A large number of ICP-MS analytical results from drillcore and adit 2 samples can be used to demonstrate element associations (or lack thereof) at Eaglet (Hora, 2005). Some previous reports, such as Ball and Boggaram (1985), mentioned the presence of scheelite and wolframite in the deposit. This was not confirmed by our study, and tungsten is practically absent in all laboratory results. However, under UV light, some varieties of apatite, which is very common at the property, have fluorescence similar to that of scheelite, and the two can easily be confused. Tin is also impoverished within the analytical dataset. Lithium is frequently slightly elevated (in the low tens of ppm range). The widespread presence of Sr, frequently in quantities over 1%, is surprising. Only a small set of five samples was analyzed for Nb; all of them had concentrations ranging from tens of ppm to 857 ppm. Lead and zinc are usually elevated in the same samples, mainly in the tens of ppm and only occasionally in the hundreds of ppm (Hora, 2005).

Approximately 25% of samples collected from 13 drillcores from the 1983 exploration program have Mo concentrations ranging from the high tens of ppm to 270 ppm. The high values were found in samples from drillholes 93, 11, 96, 99, 102 and 103 (Hora, 2005). Samples collected from the walls and roof of adit 2, which was driven into the same general area of mineralization, have considerably higher Mo values: more than 15% of 562 samples contain between 100 ppm and 1143 ppm Mo. In particular, adit sections from 240 to 297 m and from 324 to 369 m have consistently high Mo values within this range (B. Clark, pers comm, 2007). Such a difference leads to the question of whether a large volume of samples from 'ribs' and 'rounds', collected during the driving of the adit, gives a more representative result than a sample of 'BQ' drillcore.

There are similarities in mineralogy and geochemistry, such as the presence of potassic alteration, fluorspar, molybdenite, celestite and REE minerals, between the Eaglet property and the well-known Rexpar property (MINFILE 082M 007; Pell, 1992). The presence of pyrochlore with fluorite in a granitic host is also known from the Upper Cretaceous Horseshoe batholith, south of Golden (Reesor, 1973).

SUMMARY

Mineralization at the Eaglet property is interpreted as the product of two superimposed hydrothermal events. Early, pervasive, alkalic feldspar alteration was the product of an alkali sodium and successive potassium-bearing hydrothermal event. These fluids may have originated from a deep-seated, well-differentiated intrusive body. They in-

vaded structurally prepared East Quesnel Lake orthogneiss, perhaps focused on the north flank of the local structural culmination. Extensive feldspar alteration embrittled the gneissic host rocks. Subsequent deformation of the East Quesnel Lake gneiss resulted in brittle dilatancy within the feldspar alteration zones (versus more ductile, unaltered quartz-rich gneiss), thereby forming zones susceptible to percolation by hydrothermal fluids (Fig 6). Successive hydrothermal activity contributed quartz, molybdenite, fluorite, carbonate minerals, and celestite and other accessory minerals, such as a prismatic REE carbonate mineral (Fig 9b). They are interpreted as products of thermal-metamorphic alteration above a differentiated Early Cretaceous granitic body. The large area covered by this aureole indicates a potentially significant size for this unexposed intrusion. The high differentiation of such a deep source is also indicated by several lamprophyre and feldspar porphyry dikes reported from adit 1 (Ball and Boggaram, 1985). Our identification of greisen veinlets with zinnwaldite also suggests a deeper source of alkaline elements. The suspected faults, interpreted from airphotos (Fig 4, 6), are likely premineral faults with postmineral activity proposed to explain the distribution of mineralized zones intersected by drilling, as well as the conduits for hydrothermal fluids and local displacement.

Eaglet Mines Ltd. reported an outlined resource of 24 Mt with an average grade of 11.5% CaF₂, including 2 Mt grading 15% CaF₂ (Ball and Boggaram, 1985). An estimate of the Mo resource has not yet been attempted.

ACKNOWLEDGMENTS

The authors would like to thank B. Clark and Freeport Resources Inc. for significant help in visiting the property. The company also assisted in accessing the historical Eaglet Mines Ltd. files on the Eaglet property. M. Mihalyuk's constructive comments significantly improved the original manuscript. M. Lang, J. Pávková and Z. Korbelová provided technical help; J. Brožek and V. Šrein helped with photodocumentation; and J. Rajlichová helped with drafting figures. J. Dobrovolný helped with X-ray records and V. Boehm assisted with the electron microprobe work.

SELECTED BIBLIOGRAPHY

- Ball, C.W. and Boggaram, G. (1985): Geological investigation of the Eaglet fluorspar deposits; *Mining Magazine*, June 1985, pages 506–509.
- Breaks, F.W. and Moore, J.M., Jr. (1992): The Ghost Lake Batholith, Superior Province of northwestern Ontario: a fertile, S-type, peraluminous granite – rare earth pegmatite system; *Canadian Mineralogist*, Volume 30, pages 835–875.
- Dawson, K.R. (1985): Geology of barium, strontium, and fluorine deposits in Canada; *Geological Survey of Canada*, Economic Geology Report 34, 136 pages.
- Ferri, F., Hoy, T. and Friedman, R.M. (1999): Description, U-Pb age and tectonic setting of the Quesnel Lake Gneiss, east-central British Columbia; *BC Ministry of Energy, Mines and Petroleum Resources*, Paper 1999-1, pages 69–80.
- George Cross Newsletter (1983): Eaglet Mines Limited; *George Cross Newsletter*, Number 226, November 22, 1983.
- Hora, Z.D. (2005): Assessment report on the Eaglet property; *BC Ministry of Energy, Mines and Petroleum Resources*, Assessment Report 27823, 253 pages.

- McCammon, J.W. (1966): Fluorite: Eaglet group; *BC Minister of Mines*, Annual Report, 1965, pages 263–264.
- McLarty, D. (1982): Diamond drilling report of the Eaglet, and Wasko, east side of the Norm Quesnel Lake; *BC Ministry of Energy, Mines and Petroleum Resources*, Assessment Report 9515, 122 pages.
- Mitchell, J.A. (1975): Diamond drilling report on the Eaglet claim group, Junction Mountain, Quesnel Lake area; *BC Ministry of Energy, Mines and Petroleum Resources*, Assessment Report 5639, 63 pages.
- Montgomery, J.R. and Ross, J.V.(1989): A note on the Quesnel Lake Gneiss, Caribou Mountains, British Columbia; *Canadian Journal of Earth Sciences*, Volume 26, pages 1503–1508.
- Morimoto, N. (1988): Nomenclature of pyroxenes; *Schweitzer Mineralogische Petrologische Mitteilungen*, Volume 68, pages 95–111.
- Mortensen, J.K., Montgomery, J.R. and Phillipone, J. (1987): U-Pb zircon, monazite, and sphene ages for granitic orthogneiss of the Barkerville Terrane, east-central British Columbia; *Canadian Journal of Earth Sciences*, Volume 24, pages 1261–1266.
- Neiva, A.M.R. (1974): Greisenization of muscovite-biotite albite granite of northern Portugal; *Chemical Geology*, Volume 13, pages 295–308.
- Okulitch, A.V. (1985): Paleozoic plutonism in southeastern British Columbia; *Canadian Journal of Earth Sciences*, Volume 22, pages 1409–1424.
- Pearce, J.A., Harris, N.B.W. and Tindle, A.G. (1984): Trace element discrimination diagrams for the tectonic interpretation of granitic rocks; *Journal of Petrology*, Volume 25, pages 956–983.
- Pell, J. (1992): Fluorspar and fluorine in British Columbia; *BC Ministry of Energy, Mines and Petroleum Resources*, Open File 1992-16, 82 pages.
- Pivec, E. (1973): Hydrothermal K-feldspar (adularia) from fluorite bearing veins; *Acta Universitatis Carolinae, Geologica*, Number 3, pages 171–197.
- Raimbault, L. and Azencott, C. (1987); Géochimie des éléments majeurs et trace du granite à métaux Pares de Beauvoir (sondage GPF, Eschassières); BRGM Orléans Cedex 2, Géologie de la France, Volumes 2–3, pages 189–198.
- Reesor, J.E. (1973): Geology of the Lardeau map-area, east-half, British Columbia; *Geological Survey of Canada*, Memoir 369, 129 pages.
- Robertson, A. (1982): Eaglet Mines Limited, drilling report, Quesnel Lake; *BC Ministry of Energy, Mines and Petroleum Resources*, Assessment Report 10447, 137 pages.
- Siedner, G. (1965): Geochemical features of a strongly fractionated alkali igneous suite; *Geochimica et Cosmochimica Acta*, Volume 29, pages 113–137.
- Štemprok, M. (1993): Genetic models for metallogenic specialization of tin and tungsten deposits associated with the Krušné Hory – Erzgebirge granite batholith; *The Society of Resource Geology Tokyo*, Special Issue 15, pages 373–383.
- Struik, L.C. (1983): Quesnel Lake and a part of Mitchell Lake; *Geological Survey of Canada*, Open File Map 962, scale 1:50 000.
- Taylor, R.P. and Fryer, B.J. (1982): Rare earth element geochemistry as an aid to interpreting hydrothermal ore deposits; *in Mineralization Associated with Acid Magmatism*, Evans, A.M., Editor, *John Wiley and Sons*, New York, pages 357–365.
- The Northern Miner (1984): Eaglet able to recover metals at Quesnel; *The Northern Miner*, July 19, 1984, page A15.
- Tischendorf G. and Förster, H.J. (1990): Acid magmatism and related metallogenesis in the Erzgebirge; *Geologisches Jahrbuch*, Volume 25, pages 443–454.
- Tischendorf G. and Förster, H.J. (1994): Hercynian granite magmatism and related metallogenesis in the Erzgebirge; *Monograph Series on Mineral Deposits*, Gebrüder Bornträger, Berlin-Stuttgart, Volume 31, pages 5–23.

Diatomite Resource Assessment in the Quesnel Area, Central British Columbia (NTS 093B/10E; 093G/2E)

by Z.D.Hora¹

KEYWORDS: industrial minerals, Tertiary, Miocene, lacustrine sediments, diatomite

INTRODUCTION

The presence of diatomite in the Quesnel area has been known since 1877 (Dawson, 1877). Over the years, the diatomite deposits have been subjected to a number of examinations by both government agencies and industry. Some examples of work are Reinecke (1920), Eardly-Wilmot (1928), Cummings (1948) and McCammon (1960). In 1963, Godfrey prepared several unpublished geological reports for Pacific Diatomite Ltd. of Edmonton (Godfrey, 1963), and Visman and Picard (1969) focused on a new process for the beneficiation of Quesnel diatomite. In 1994, Hora and Hancock sampled diatomite outcrops in the Quesnel area as part of an industrial minerals assessment (Hora and Hancock, 1995). The analytical results that followed this assessment provide the basis for this paper. In the western United States, similar deposits were subject to extensive processing studies by the United States Bureau of Mines (Skinner et al., 1944) before being developed by the industry into high-value products.

HISTORY OF DIATOMITE DEVELOPMENT IN THE QUESNEL AREA

From 1937 until 1969, Fairey and Cunliff, later Fairey and Co. Ltd. of Vancouver, used the diatomite from Quesnel (Lot 6182 north of Quesnel airport) for insulation, ceramic products and pozzolanic cement admixtures.

Considerable effort was expended between 1938 and 1942 to develop the diatomite from the Buck Ridge area south of Quesnel. Work was initiated by the owner, P.G. Lepetich, with the assistance of the BC Ministry of Energy, Mines and Petroleum Resources with the goal of producing diatomite suitable for mineral fillers and filtration products, but without any success.

In 1963, Crownite Diatoms Ltd. of Calgary began development of a pit on the western edge of Quesnel (Lot 906) and construction of a processing plant near the confluence of the Fraser and Quesnel rivers. Their main products were industrial and domestic absorbents and anti-caking agents

for fertilizer pellets. In 1982, the plant was relocated adjacent to the pit site and operated briefly under the name Microsil Industrial Minerals Ltd. Competition from Western Clay Products of Kamloops and an inadequate marketing strategy were two factors that contributed to the closure of the Quesnel plant and pit in 1984.

During the 1990s, regular shipments of diatomite were made from a pit opened on Lot 1615 in the Buck Ridge area by Clayburn Industries Ltd. (Fig 1). Clayburn, based in

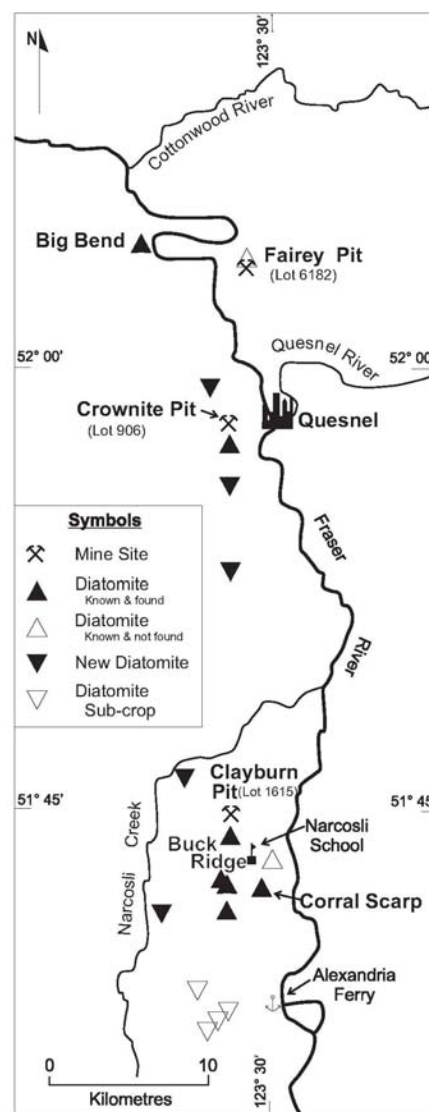


Figure 1. Location map of the study area.

¹Consultant, Victoria, BC

This publication is also available, free of charge, as colour digital files in Adobe Acrobat® PDF format from the BC Ministry of Energy, Mines and Petroleum Resources website at http://www.em.gov.bc.ca/Mining/Geosurv/Publications/catalog/cat_fldwk.htm

Abbotsford, BC, shipped small quantities of diatomite from the pit to its plant to manufacture several grades of insulation bricks for several years between 1990 and 1998. More economical diatomite imports from the United States was one of the factors that contributed to the discontinuation of this small-scale mining operation. At present, both pits on Lots 906 and 1615 are recontoured and reclaimed.

DIATOMITE DEPOSITS

Geology

Quesnel diatomite has been described as the Crownite Formation (Rouse and Mathews, 1979). It is a horizontal layer of diatomaceous earth, approximately 12 m thick, of Middle to Late Miocene age, between 13 and 8 Ma. Diatom species contained within include *Melosira pancipunctata*, *Melosira granulata*, *Melosira undulata*, *Fragilaria virescense*, *Cascinodiscus punctuatus* and *Eurinella sp.*, which were identified by Rouse (1959).

The Crownite Formation is the youngest of the Miocene sedimentary units in the area and is underlain by the Fraser Bend Formation (Rouse and Matthews, 1979). Fraser Bend sedimentary rocks consist of mostly gravel in the lower 50 m and alternating sand, silt, clay and fine gravel in the upper 90 m.

The Crownite Formation is overlain by the Chilcotin basalt of the Late Miocene. The basalt forms a solid cap to many diatomite sections between the town of Quesnel and the Alexandria ferry, ~50 km to the south. Columnar jointing, pillow lava and palagonite breccia are common features of the basalt cap.

Diatomite is found in numerous showings over the entire distance west of the Fraser River between the site of the original diatomite discovery on the Blackwater River (Lot 1469, southeast corner; Dawson, 1877) and the Alexandria ferry (Fig 1). Most are minor exposures in roadcuts, gullies, slide scarps and animal burrows. The best exposures are in the areas of Big Bend, the Crownite pit on Lot 906 and the Clayburn pit on Lot 1615.

Diatomite beds are not uniform in appearance. Some of the layers are massive, while others are broken into small angular fragments 5 to 10 cm in size. The colour is generally pale beige to white, with various darker and lighter shades. Neither fracture density nor colour seem to correlate with chemical composition. There is a rusty weathering, harder and denser bed about 20 cm thick in approximately the middle of the unit, identified by McCammon (1960) as pumicite with some diatoms and silt. This layer has been found in a number of sites in the Quesnel area and may be considered a marker horizon representing a volcanic event that occurred during the deposition of the Crownite Formation.

Reported analytical data from grab samples during previous studies indicate that diatoms constitute some 75 to 80% of unprocessed diatomaceous earth. Between 7 and 11% of the samples is Al_2O_3 , which is due to the presence of clay and volcanic ash (McCammon, 1960). Because of such variability in impurities, selective mining may be necessary. If so, Al_2O_3 distribution must be determined; therefore, available exposures were systematically channel sampled over all accessible thicknesses. Three sites were available for such sampling: natural exposures in the Big Bend area, the Crownite pit and the Clayburn pit. Samples

were collected from hammer and shovel-cut channels in 50 cm segments from beds with uniform appearance, or in shorter segments in the cases of sudden changes in colour or density of the sediment.

The entire Miocene sequence has been subjected to extensive gravitational block sliding that is best observed on the western side of the Fraser River between Big Bend and Alexandria. The diatomite exposures have been mildly disturbed, apparently by motion on extensive fault blocks, many of which affect the whole Miocene sedimentary sequence and are presently active. Some slide blocks, particularly in the area between Narcosli Creek and Fraser River south of Quesnel, are several kilometres in length and up to 300 m wide. The vertical displacement of individual blocks, as observed from recently active scarps, has been from 1 to 2 m, up to more than 10 m. The diatomite has, therefore, been exposed at different elevations, leading to greatly overestimated thicknesses in the past. It is apparent that practically the entire area is encompassed by a massive slide zone parallel to the river. Although the slide blocks show signs of being recently active, many farm buildings and residences constructed on them do not appear to have foundation problems. The slides, which probably developed within the last 10 000 years, are now in equilibrium with the erosive forces of the river and gravity forces of the soil mass within the slide, and with piezometric pressures existing on failure surfaces (Hardy et al., 1978). Mining activities in both the Crownite and the Clayburn pits do not precipitate any noticeable instability.

Big Bend

The Big Bend area has the best natural exposures of the Crownite Formation. Because of steep slopes as a result of the Fraser River undercutting its western bank, the block sliding is advanced and individual blocks are relatively small in size. Some blocks sliding down the steep slope are only a few metres wide and a few tens to hundreds metres in length. Block sliding is active, as can be observed by bent and inclined trees and fresh slumps and scarps. This situation offers fresh (if somewhat hazardous) exposures of diatomite that are accessible for sampling. Samples were collected in two sections representing a 7.5 m thickness of diatomite beds. A volcanic ash layer was used as a marker to correlate beds in two separate blocks. Section 1 was sampled from the surface to the top of a 20 cm rusty, hard, dense volcanic ash layer 5 m from the top (Fig 2). In the second block, section 2 was sampled for 2.5 m below the volcanic marker bed (Fig 3). The marker was not sampled or analyzed. Analytical results are shown in Tables 1 and 2.

Crownite Pit

The Crownite pit has the largest exposure of diatomite beds in the Quesnel area. The pit was developed on Lot 906 at the western edge of the city over an area of approximately 300 by 600 m with four benches each 7 m high (Fig 4). The top bench was developed through diatomite up into an irregular layer of sandy gravel from 10 to 50 cm thick overlain by a basalt cap composed of up to 150 cm of pillow lava interspersed with palagonite breccia. In spite of extensive benching, fresh exposures of diatomite were rather uncommon due to 10 years of abandonment, sloughing and use of the pit by local all-terrain vehicles and dirt bikers. Therefore, the diatomite had to be sampled in five different segments to obtain a complete composite section. Tracing the



Figure 2. Site of Big Bend Section 1, Quesnel area.

marker horizon is difficult. It is probable that sampling of some parts of the section was duplicated, because of one or possibly two slump blocks between the top and bottom benches. Since the sampling followed the rainwater rills across the benches at approximately 45° dip, the 15 m of samples represent approximately 10 m of vertical thickness (Fig 5, Table 2).

Clayburn Pit

The Clayburn pit is located in the Buck Ridge area, Lot 1615, approximately 30 km south of Quesnel (Fig 1). The overburden has been stripped from this pit over an area of 100 by 100 m and two faces were exposed across the north and south part of the stripped area. The north face has exposed the diatomite bed over a thickness of 7 vertical metres (Fig 6). From the overall terrain configuration, it is estimated that the north face is below the marker bed. The marker bed is exposed in the southern face with diatomite for 3 m above and 2.5 m below it (Fig 7). In all Clayburn pit exposures, the diatomite beds exhibit features indicating slumping and displacement, such as bedding plane deformation, fractures filled with debris and soil, and an offset of the marker bed by approximately 1 vertical metre. A minor

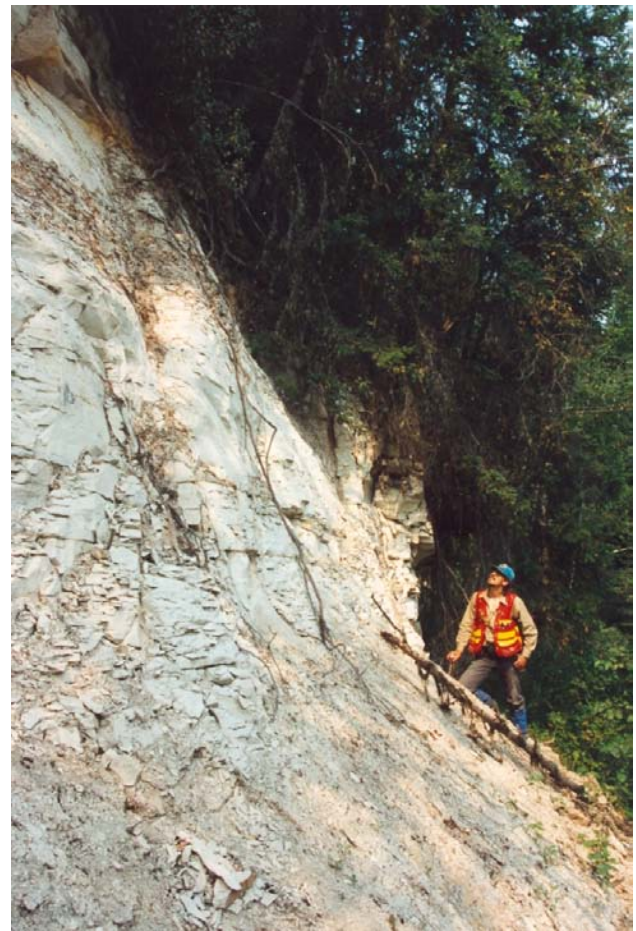


Figure 3. Site of Big Bend Section 2, Quesnel area. A rusty-coloured bed in the upper left corner is the volcanic ash marker bed.

scarp along the western limits of Lot 1615, and displacement of basalt boulders, suggests the presence of a block slide plane. In the middle of the southern face, a shallow, 10 m wide depression in the Crownite Formation is infilled

TABLE 1. CHEMICAL COMPOSITIONS OF BIG BEND SAMPLES, QUESNEL AREA, ANALYZED BY X-RAY FLUORESCENCE (XRF) FROM THE BONDAR AND CLEGG LABORATORY.

Lab No.	Field No.	SiO ₂ (%)	TiO ₂ (%)	Al ₂ O ₃ (%)	Fe ₂ O ₃ * (%)	MnO (%)	MgO (%)	CaO (%)	Na ₂ O (%)	K ₂ O (%)	P ₂ O ₅ (%)	LOI (%)	Total (%)	Ba (ppm)	Cr** (ppm)	
50366	BigBnd-1-0	69.48	0.41	11.74	4.29	0.03	1.06	0.58	0.36	0.88	0.05	10.53	99.47	495	94	Section 1 0.0 5.0 m
50367	BigBnd-1-0.5	70.94	0.4	10.93	3.97	0.02	1.06	0.5	0.33	0.87	0.05	10.24	99.37	466	107	
50368	BigBnd-1-1.0	70.46	0.5	10.45	3.94	0.05	0.97	0.48	0.29	0.75	0.05	10.67	98.66	399	79	
50369	BigBnd-1-1.5	65.41	0.41	12.15	4.35	0.03	1.02	0.59	0.33	0.8	0.05	14.35	99.54	438	105	
50370	BigBnd-1-2.0	68.72	0.58	10.76	3.79	0.05	0.94	0.51	0.28	0.81	0.05	12.04	98.58	417	73	
50372	BigBnd-1-2.5	66.92	0.53	11.55	4.75	0.13	1.02	0.54	0.32	0.91	0.07	12.18	98.97	463	87	
50373	BigBnd-1-3.0	58.68	0.34	9.96	11.58	0.6	1	0.61	0.26	0.79	0.13	16	100	433	72	
50374	BigBnd-1-3.5	65.98	0.52	11.39	3.73	0.03	1.02	0.47	0.39	0.87	0.06	14.62	99.13	447	83	
50375	BigBnd-1-4.0	62.09	0.5	13.32	4.37	0.03	1.06	0.62	0.33	0.89	0.06	15.84	99.16	454	89	
50376	BigBnd-1-4.5	38.63	0.35	7.3	29.2	1.07	0.34	0.74	0.65	1.92	0.28	18.29	98.81	393	-10	
50377	BigBnd-1-5.0	59.19	0.57	15.9	5	0.04	1.21	0.63	0.36	1.04	0.07	15.33	99.4	519	101	
50378	BigBnd-2-0.5	59.95	0.73	16.52	5.22	0.06	1.29	0.53	0.36	1.01	0.07	12.89	98.69	532	104	Section 2 0.0 3.0 m
50379	BigBnd-2-1.0	60.56	0.73	16.47	4.98	0.03	1.33	0.54	0.38	1.06	0.07	12.76	98.97	545	94	
50380	BigBnd-2-1.5	61.52	0.64	15.47	4.94	0.07	1.29	0.55	0.38	1	0.07	13.47	99.5	875	97	
50381	BigBnd-2-2.0	61.03	0.58	16.01	5.46	0.07	1.38	0.57	0.41	1.04	0.07	13.11	99.79	526	118	
50382	BigBnd-2-2.5	60.77	0.68	15.67	5.61	0.12	1.36	0.53	0.39	1.03	0.07	12.86	99.15	517	93	
50383	BigBnd-2-2.5	60.56	0.66	15.48	5.63	0.11	1.38	0.49	0.37	1.02	0.07	13.21	99.04	510	112	

TABLE 2. CHEMICAL COMPOSITIONS OF CROWNITE PIT SAMPLES, QUESNEL AREA, ANALYZED BY X-RAY FLUORESCENCE (XRF) FROM THE BONDAR AND CLEGG LABORATORY.

Lab. No.	Field No.	SiO ₂ (%)	TiO ₂ (%)	Al ₂ O ₃ (%)	Fe ₂ O ₃ ⁺ (%)	MnO (%)	MgO (%)	CaO (%)	Na ₂ O (%)	K ₂ O (%)	P ₂ O ₅ (%)	LOI (%)	Total (%)	Ba (ppm)	Cr ⁺⁺ (ppm)		
50384	CR0-0.5	65.31	0.56	12.04	5.3	0.21	1.55	1.41	0.88	0.96	0.16	11.32	99.77	627	104	Section 1 0.0 8.3 m	
50385	CR0.5-1.0	64.32	0.73	12.33	5.27	0.07	1.6	1.49	1.01	0.99	0.15	10.82	98.85	598	123		
50386	CR1.0-1.5	64.39	0.62	12.56	4.61	0.03	1.47	0.98	0.64	0.87	0.08	12.72	99.03	523	96		
50387	CR1.5-2.0	63.29	0.49	11.84	4.31	0.06	1.34	1.9	0.44	0.75	0.06	14.22	98.76	504	83		
50388	CR2.0-2.5	67.82	0.41	10.59	3.97	0.02	1.2	0.63	0.41	0.69	0.05	13.26	99.1	403	83		
50389	CR2.5-3.0	67.28	0.49	11.14	4.07	0.02	1.3	0.65	0.44	0.73	0.05	12.91	99.13	422	86		
50390	CR3.0-3.5	66.85	0.48	10.61	3.93	0.02	1.23	0.58	0.42	0.78	0.05	14.01	99.03	629	99		
50391	STD SY2	59.91	0.18	12.31	6.18	0.32	2.71	8.03	4.36	4.46	0.42	1.19	100.11	415	-10		
50392	CR3.5-4.0	68.37	0.41	11.3	4.12	0.02	1.33	0.58	0.44	0.85	0.05	12.56	100.09	460	90		
50393	CR4.0-4.5	66.87	0.42	10.69	4.16	0.02	1.29	0.57	0.39	0.81	0.05	13.07	98.41	573	133		
50394	CR4.5-5.0	69.09	0.42	10.47	4	0.02	1.25	0.6	0.42	0.76	0.05	11.86	98.99	442	81		
50395	CR5.0-5.5	67.47	0.4	10.55	4.06	0.03	1.23	0.59	0.43	0.79	0.05	12.89	98.55	484	79		
50396	CR5.5-5.95	68.48	0.37	10.37	3.9	0.06	1.18	0.53	0.35	0.71	0.04	12.79	98.83	399	85		
50397	CR5.95-6.3	68.43	0.35	9.99	3.84	0.03	1.14	0.51	0.35	0.72	0.04	13.44	98.89	396	145		
50398	CR6.3-7.0	66.97	0.41	10.79	4.16	0.05	1.26	0.58	0.43	0.83	0.05	13.17	98.75	437	110		
50399	CR7.0-7.6	67.64	0.4	10.51	4.09	0.02	1.14	0.6	0.44	0.81	0.04	12.99	98.74	485	116		
50400	CR7.6-7.8	68.13	0.39	9.1	7.32	0.02	0.87	0.46	0.35	1.26	0.06	10.99	99.05	855	127		
50401	CR7.67.8(DU)	67.96	0.42	9.39	7	0.02	0.91	0.47	0.38	1.19	0.06	11.24	99.15	980	112		
50402	CR7.8-8.3	68.58	0.41	10.19	3.86	0.02	1.15	0.68	0.47	0.78	0.05	12.86	99.11	468	148		
50403	CR2-0.0-0.3	65.12	0.41	11.53	5.85	0.15	1.33	0.8	0.41	0.86	0.1	12.38	99.2	2524	84		Section 2 0.0 4.0 m
50404	CR2-0.3-0.8	66.23	0.44	12.31	4.71	0.06	1.33	0.67	0.4	0.89	0.06	12.19	99.35	488	97		
50405	CR2-0.8-1.3	65.29	0.46	12.9	4.73	0.04	1.36	0.68	0.42	0.9	0.05	12.73	99.61	445	75		
50406	CR2-1.3-1.9	66.34	0.42	11.4	5.52	0.12	1.34	0.67	0.38	0.87	0.08	12.19	99.39	503	72		
50407	CR2-1.9-2.3	58.16	0.34	9.72	11.92	0.47	1.31	1.86	0.32	0.74	0.9	14.09	99.9	593	68		
50408	CR2-2.3-2.8	67.3	0.43	11.07	4.14	0.05	1.21	0.61	0.38	0.81	0.08	13.15	99.28	419	109		
50409	CR2-2.8-3.2	68.47	0.42	10.57	3.94	0.05	1.15	0.56	0.36	0.78	0.06	12.76	99.17	425	122		
50410	CR2-3.2-3.6	66.88	0.44	11.47	4.15	0.06	1.21	0.79	0.52	0.83	0.09	13.06	99.55	461	85		
50411	Std SY2	59.73	0.13	12.27	6.19	0.32	2.69	8.03	4.36	4.52	0.42	1.79	100.49	406	-10		
50412	CR2-3.6-4.0	66.6	0.4	11.37	4.35	0.05	1.26	0.65	0.38	0.86	0.12	13.22	99.31	436	82		
50413	CR3-0.0-0.5	68.38	0.46	10.76	3.95	0.02	1.13	0.62	0.37	0.8	0.04	12.51	99.09	401	88	Section 3 0.0 8.0 m	
50414	CR3-0.5-1.2	67.53	0.47	10.49	3.89	0.02	1.08	0.62	0.34	0.75	0.04	13.86	99.14	405	76		
50415	CR3-1.2-1.5	71.95	0.44	8.54	2.94	0.01	0.89	0.55	0.28	0.7	0.05	12.51	98.92	488	103		
50416	CR3-1.5-2.0	71.41	0.41	8.5	3	0.01	0.88	0.57	0.28	0.58	0.04	13.06	98.78	321	72		
50417	CR3-2.0-2.5	70.25	0.36	9.96	3.78	0.02	1.01	0.69	0.39	0.7	0.04	12.32	99.57	373	107		
50418	CR3-2.5-3.0	70.08	0.44	9.34	3.33	0.02	0.97	0.57	0.31	0.67	0.04	12.87	98.7	559	76		
50419	CR3-3.0-3.5	70.11	0.48	9.46	3.35	0.02	0.99	0.6	0.33	0.67	0.04	12.5	98.6	421	73		
50420	CR3-3.5-4.0	70.68	0.48	9.21	3.18	0.03	0.95	0.59	0.3	0.65	0.04	12.53	98.69	447	78		
50421	CR33.5-4(DU)	71.04	0.47	9.38	3.3	0.03	0.98	0.61	0.33	0.66	0.04	12.07	98.99	671	105		
50422	CR3-4.0-4.5	71.48	0.33	9.01	3.33	0.06	0.94	0.63	0.35	0.64	0.04	12.64	99.49	378	71		
50423	CR3-4.5-5.0	70.22	0.46	9.58	3.38	0.03	0.98	0.61	0.36	0.67	0.04	12.51	98.89	399	94		
50424	CR3-5.0-5.5	69.73	0.49	9.82	3.54	0.05	1.03	0.67	0.47	0.73	0.05	12.17	98.82	588	71		
50425	CR3-5.5-6.0	65.88	0.48	11.14	3.91	0.21	1.16	0.66	0.47	0.9	0.06	12.84	-9	10000	73		
50426	CR3-6.0-6.5	65.87	0.48	12.08	4.58	0.1	1.27	0.65	0.44	0.94	0.05	12.76	99.27	459	77		
50427	CR3-6.5-7.0	51.75	0.35	8.87	19.04	0.35	1.27	1.1	0.3	0.68	0.43	15.55	99.79	905	57		
50428	CR3-7.0-7.2	53.57	0.39	9.2	16.75	0.26	1.31	1.11	0.31	0.71	0.43	15.45	99.54	405	56		
50429	CR3-7.2-8.0	65.3	0.59	12.34	4.56	0.07	1.23	0.68	0.41	0.89	0.06	12.8	98.98	450	83		
50430	CR4-0.0-0.4	73.53	0.24	6.71	4.56	0.07	0.87	0.38	0.28	0.56	0.06	11.93	99.23	287	75	Section 4 0.0 4.3 m	
50431	STD SY2	59.46	0.28	12.25	6	0.31	2.66	7.97	4.36	4.44	0.42	1.12	99.31	409	12		
50432	CR4-0.4-0.9	68.48	0.3	7.29	4.04	0.14	0.85	4.29	0.43	0.67	2.54	10.79	99.9	682	78		
50433	CR4-0.9-1.5	73.41	0.4	8.13	3.31	0.03	0.98	0.6	0.37	0.7	0.12	11.01	99.11	441	91		
50434	CR4-1.5-2.0	72.28	0.39	8.62	3.41	0.02	1.09	0.46	0.34	0.7	0.04	11.84	99.24	387	76		
50435	CR4-2.0-2.5	72.37	0.39	8.38	3.32	0.02	1.05	0.44	0.33	0.66	0.04	11.94	98.99	392	74		
50436	CR4-2.5-3.0	73.13	0.31	8.24	3.38	0.05	1.05	0.45	0.33	0.68	0.04	11.97	99.67	330	111		
50437	CR4-3.0-3.5	70.64	0.36	9.54	3.75	0.06	1.2	0.53	0.42	0.77	0.04	12.45	99.82	511	82		
50438	CR4-3.5-4.0	71.62	0.36	8.94	3.59	0.06	1.08	0.5	0.34	0.65	0.04	12.26	99.49	376	78		
50439	CR4-4.5-4.3	74.3	0.3	7.41	2.88	0.06	0.9	0.43	0.32	0.56	0.03	12.31	99.54	302	66		
50440	CR5-0.0-0.3	46.95	0.31	8.63	24.74	0.34	1.25	0.88	0.31	0.71	0.38	15.54	100.1	539	89	Section 5 0.0 4.5 m	
50441	CR50-0.3(DU)	47.05	0.3	8.61	25.64	0.45	1.23	0.9	0.32	0.71	0.4	15.11	100.78	552	70		
50442	CR5-0.3-0.8	66.34	0.46	12.12	4.92	0.04	1.27	0.6	0.42	0.91	0.07	12.6	99.81	506	131		
50443	CR5-0.8-1.1	67.16	0.49	11.79	4.34	0.04	1.24	0.6	0.43	0.89	0.06	12.63	99.73	523	99		
50444	CR5-1.1-1.6	52.68	0.38	9.42	19.03	0.35	1.2	0.74	0.37	0.76	0.25	15.01	100.25	523	59		
50445	CR5-1.6-1.9	65.66	0.46	11.79	5.17	0.06	1.27	0.59	0.38	0.89	0.07	13.13	99.55	750	81		
50446	CR5-1.9-2.1	53	0.35	9.48	18.44	0.31	1.18	0.72	0.36	0.78	0.25	15.37	100.3	529	59		
50447	CR5-2.1-2.5	65.01	0.45	12.13	5.11	0.18	1.25	0.75	0.52	1.01	0.07	13.3	99.89	1076	74		
50448	CR5-2.5-3.0	65.89	0.53	11.94	4.81	0.08	1.21	0.97	0.68	1.18	0.08	12.16	99.6	651	75		
50449	CR5-3.0-3.5	68.22	0.46	11.09	4.21	0.03	1.2	0.61	0.48	0.98	0.06	12.39	99.79	547	85		
50450	CR5-3.5-4.0	75.67	0.27	6.15	2.77	0.07	0.74	0.4	0.28	0.48	0.04	12.08	99	391	70		
50451	STD SO2	52.24	1.34	15.16	7.69	0.09	0.88	2.69	2.52	2.88	0.69	14.01	100.28	888	-10		
50452	CR5-4.0-4.5	75.65	0.24	6.33	2.84	0.2	0.74	0.4	0.27	0.52	0.04	11.67	98.94	340	66		

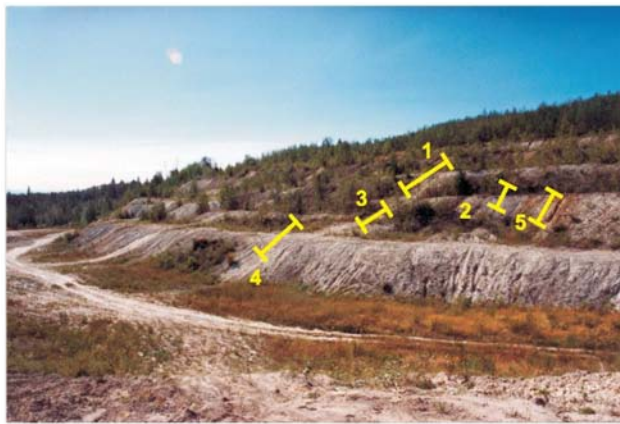


Figure 4. Crownite pit with the benches and section locations.



Figure 5. Exposing the bedrock for channel sampling.



Figure 6. Sampling the south face above the marker bed; Clayburn pit, Quesnel area.

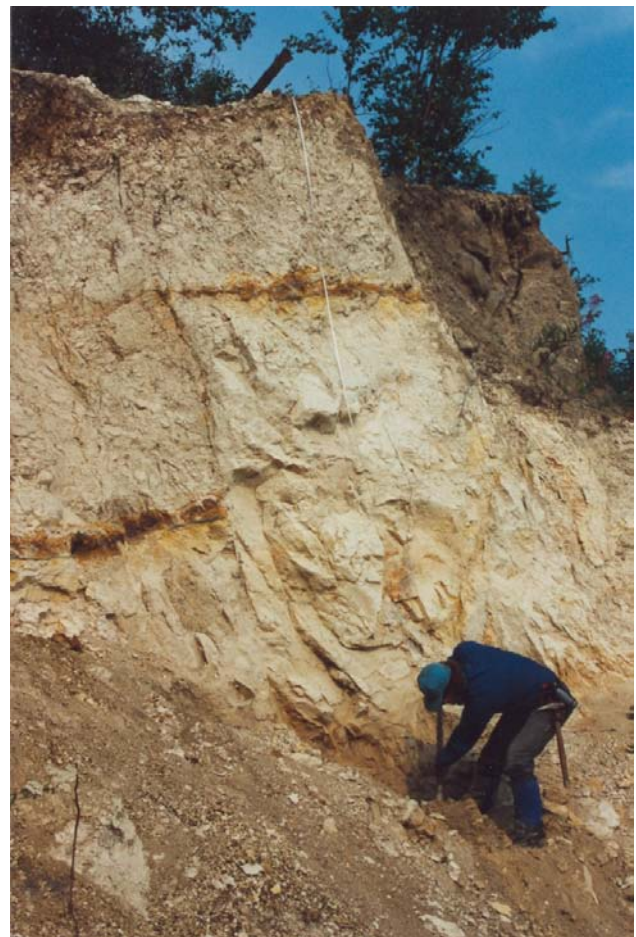


Figure 7. Sampling the south face below the marker bed with 1 m vertical displacement; Clayburn pit, Quesnel area.

with 10 cm of silt, small pebbles, charcoal, diatomite fragments and up to 1 m of palagonite breccia interspersed with pillow basalt (Fig 9). Table 3 presents the analytical results.

Corral Scarp

About 5 km southeast of the Clayburn pit, an exposure of diatomite 15 m wide and 3 m high is located between the road to the Alexandria ferry and the Fraser River, next to a corral on the Lepetich farm. White, massive, blocky diatomite is exposed on a scarp/slump plane (Fig 10). Analysis of the sample taken from this outcrop (Table 4) indicates low clay contamination, comparable to some samples from the Clayburn pit.

DIATOMITE PRODUCTION AND END USES

In 2006, 799 000 tonnes of diatomite was produced from 11 separate mining areas and 9 processing facilities in the western United States (California, Nevada, Oregon and Washington). Of this tonnage, 59% is used for filtration, 22% is used as cement ingredient, 9% is for fillers, 5% for absorbents, 2% for insulation and 3% for a variety of other minor applications (Founie, 2007). Deposits in Nevada, Oregon and Washington are lacustrine in origin and are composed of diatoms like those of the Quesnel deposits.

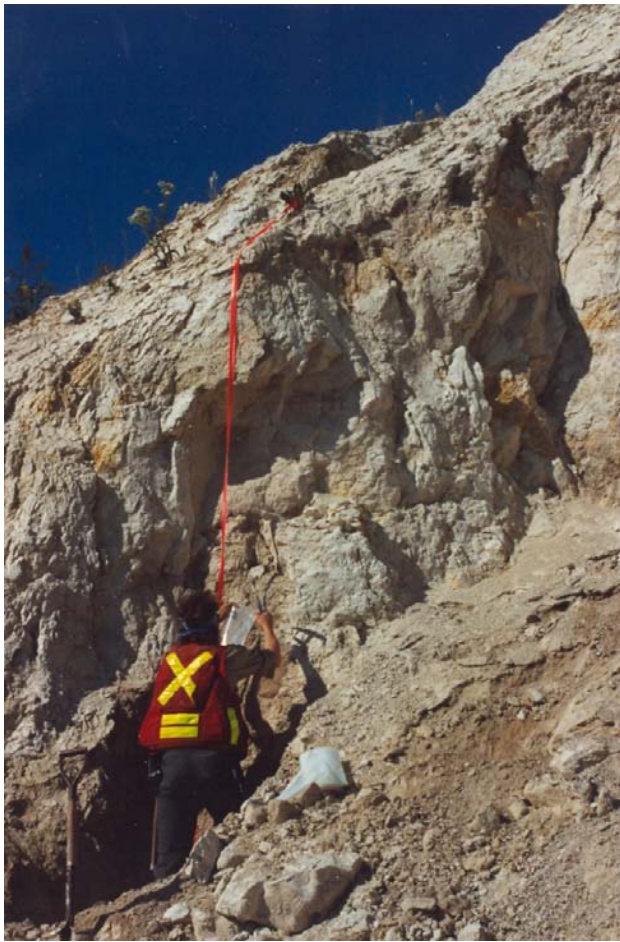


Figure 8. Sampling the north face of the Clayburn pit, Quesnel area.



Figure 9. Basalt flow filling a shallow depression in Crownite Formation top; Clayburn pit, Quesnel area.

Diatomite from these deposits is processed into high-value end products.

Two samples of commercial diatomite — one from Nevada and the other from Oregon — have the following main components: the sample from Lovelock, Nevada has 89.75% SiO₂, 3.08% Al₂O₃, 1.33% Fe₂O₃ and an LOI of 4.70%. The sample from Vale, Oregon has 87.92% SiO₂, 3.66% Al₂O₃, 1.37% Fe₂O₃ and an LOI of 5.15% (Breese and Bodycomb, 2006).

According to Harben (1995), commercial diatomite contains from 85 to 94% SiO₂, from 1 to 7% Al₂O₃ and from 0.4 to 2.5% Fe₂O₃. Different end uses have a number of specific requirements in dry and wet density, sizing, median pore size, oil absorption and permeability.

TABLE 3. CHEMICAL COMPOSITION OF CLAYBURN PIT SAMPLES; ALL ELEMENTS ANALYZED BY X-RAY FLUORESCENCE (XRF) BY THE BONDOR AND CLEGG LABORATORY, EXCEPT FOR TOTAL S, WHICH WAS ANALYZED BY THE LECO INSTRUMENTS METHOD AT THE BONDAR AND CLEGG LABORATORY.

Lab. No.	Field No.	SiO ₂ (%)	TiO ₂ (%)	Al ₂ O ₃ (%)	Fe ₂ O ₃ * (%)	MnO (%)	MgO (%)	Ba (ppm)	CaO (%)	Na ₂ O (%)	K ₂ O (%)	LOI (%)	Cr (%)	P ₂ O ₅ (%)	Total (%)	S Tot (%)	
49059	Clay - M - Min - 0	70.48	0.41	8.4	2.69	0.03	0.89	295	0.35	0.43	0.49	14.46	64	0.03	98.7	0.38	North face upper samples 0.0 3.5 m
49060	Clay - M - Min - 0.5	71.39	0.38	7.62	2.34	0.04	0.83	309	0.29	0.44	0.45	14.22	41	-0.03	98.04	0.37	
49061	Clay - M - Min - 0.5 (Rep.)	71.97	0.32	7.66	2.41	0.04	0.84	291	0.29	0.45	0.46	14.21	55	-0.03	98.69	0.38	
49062	Clay - M-Min - 1.0	72.18	0.37	7.18	2.45	0.01	0.87	276	0.26	0.43	0.44	14.03	41	-0.03	98.25	0.4	
49063	Clay - M-Min - 1.5	73.18	0.34	6.34	2.83	0.02	0.79	267	0.32	0.38	0.38	13.91	34	0.03	98.56	0.37	
49064	Clay - M-Min - 2.0	72.9	0.31	6.11	3.16	0.02	0.72	246	0.32	0.33	0.38	13.58	44	0.03	97.89	0.25	
49065	Clay - M-Min - 2.5	72.09	0.29	6.54	3.48	0.02	0.76	262	0.32	0.33	0.39	13.89	37	0.03	98.17	0.25	
49066	Clay - M-Min - 3.0	70.89	0.3	6.81	3.75	0.04	0.87	265	0.41	0.4	0.42	14.38	41	0.04	98.34	0.41	
49067	Clay - M-Min - 3.5	71.2	0.31	6.42	3.93	0.04	0.84	267	0.31	0.35	0.39	14.64	34	0.04	98.49	0.35	
49068	Clay - M - Plus - 0	67.02	0.5	10.88	3.02	0.03	0.83	333	0.38	0.34	0.55	14.58	58	0.03	98.2	0.13	North face lower samples 0.0 3.5 m
49069	Clay - M-Min - 0.5	66.84	0.53	11.43	3.21	0.02	0.94	381	0.45	0.36	0.59	14.35	70	0.04	98.81	0.21	
49070	Clay - M-Min - 1.0	64.92	0.51	10.72	3.74	0.03	1.15	358	0.65	0.54	0.56	15.58	58	0.04	98.49	0.58	
49071	Std. SO 2	51.83	1.29	14.69	7.4	0.09	0.81	851	2.6	2.37	2.77	14.43	30	0.66	99.02	0.03	
49072	Clay - M-Min - 1.5	63.81	0.54	10.74	4.3	0.03	1.17	392	0.76	0.53	0.57	15.81	62	0.05	98.36	0.58	
49073	Clay - M-Min - 2.0	64.09	0.53	10.38	3.35	0.03	1.24	366	0.8	0.53	0.54	15.89	64	0.04	97.46	0.72	
49074	Clay - M-Min - 2.5	66.01	0.51	10.59	2.97	0.02	1.07	384	0.46	0.46	0.55	15.4	70	0.04	98.13	0.35	
49075	Clay - M-Min - 3.0	65.15	0.52	10.64	2.97	0.02	1.18	311	0.72	0.47	0.52	15.7	57	-0.03	97.92	0.64	
49076	Clay - M-Min - 3.5	63.39	0.47	10.61	4.17	0.02	1.25	308	0.97	0.43	0.48	16.03	58	-0.03	97.86	0.63	
49077	Clay Top 1	65.5	0.41	10.03	4.69	0.04	1.26	386	0.82	0.42	0.58	14.6	64	0.04	98.44	0.24	South face upper samples 0.0 3.0 m
49078	Clay Top 2	64.32	0.44	8.9	6.39	0.1	1.58	379	0.94	0.5	0.53	14.91	61	0.05	98.7	0.34	
49079	Clay Top 3	69.09	0.42	7.84	3.89	0.05	1.3	333	0.67	0.58	0.5	13.99	60	0.04	98.41	0.35	
49080	Clay Top 4	69.07	0.52	9.57	3.71	0.03	0.93	567	0.76	0.79	0.94	12.44	54	0.05	98.88	0.11	
49081	Clay Top 4 (Rep.)	68.89	0.5	9.64	3.74	0.03	0.95	538	0.75	0.79	0.95	12.45	47	0.05	98.8	0.11	
49082	Clay Top 5	71.83	0.42	7.79	2.68	0.01	0.85	371	0.38	0.39	0.55	13.31	53	0.04	98.29	0.08	
49083	Clay Top 6	75.84	0.25	6.07	2.14	0.01	0.68	303	0.36	0.37	0.42	12.84	45	0.03	99.04	0.11	
49084	Clay Low -1	73.24	0.36	7.08	2.35	0.01	0.79	319	0.36	0.35	0.43	13.24	49	0.03	98.27	0.14	South face lower samples 0.0 2.5 m
49085	Clay Low -2	75.35	0.31	6.37	2.18	0.04	0.64	285	0.27	0.25	0.37	12.8	49	-0.03	98.61	0.02	
49086	Clay Low -3	76.56	0.24	5.49	2.01	0.02	0.55	252	0.25	0.22	0.33	12.66	46	-0.03	98.36	0.02	
49087	Clay Low -4	76.42	0.29	5.12	1.96	0.02	0.58	239	0.52	0.27	0.33	12.56	36	-0.03	98.1	0.04	
49088	Clay Low -5	76.51	0.31	5.31	1.91	0.02	0.55	241	0.39	0.23	0.33	12.56	44	-0.03	98.15	0.04	

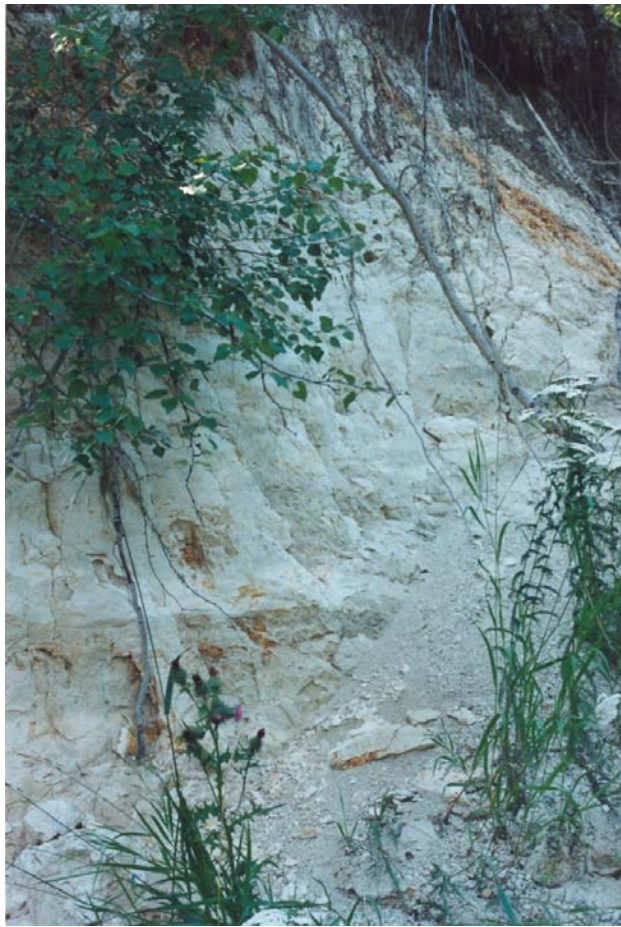


Figure 10. Corral scarp outcrop, Lepetich farm, showing white, massive, blocky diatomite exposed on a scarp/slump plane.

CONCLUSIONS

Proven production records indicate that Quesnel diatomite is suitable for end uses having low purity requirements, such as insulation bricks, pozzolan admixtures and domestic and industrial absorbents. Attempts to develop higher-end value products in the past have not succeeded. It should be mentioned here, though, that the major industry development of lacustrine diatomite deposits in the western United States has taken place in the last 20 to 30 years and was preceded by extensive processing studies by United States Bureau of Mines. There have also been processes developed for the beneficiation of Quesnel diatomite, which reduced the Al_2O_3 content from 12.38 to 4.8% in the intermediate product fraction (Visman and Picard, 1969). Main components of Quesnel diatomite are also not very different from those published for raw product from commercial deposits.

Comparing analytical results from three main sampled sites in our study, there is an apparent decrease in Al_2O_3 content from north to south. A significant number of samples from the Clayburn pit have Al_2O_3 values between 5 and 8%, compared to a few samples from the Crownite pit and only two from the Big Bend. Therefore, the areas of Buck Ridge and the Alexandria ferry probably have the best potential for diatomite with the lowest content of impurities and future industrial development.

ACKNOWLEDGMENTS

The author wishes to thank K. Hancock for capable help in the field and his assistance in finding the data collected years ago. Constructive comments and editorial improvements were provided by M. Mihalynuk. Geotechnical staff of the BC Ministry of Transportation helped to locate the geotechnical report dealing with block slides in Quesnel area.

REFERENCES

- Breese, R.O.Y. and Bodycomb, F.M. (2006): Diatomite; in *Industrial Minerals and Rocks, Society for Mining, Metallurgy, and Exploration, Inc.*, pages 433–450.
- Cummings, J.M. (1948): Diatomite; in *Minister of Mines Annual Report 1947, BC Ministry of Energy, Mines and Petroleum Resources*, pages 209–211.
- Dawson, G.M. (1877): Report on explorations in British Columbia; *Geological Survey of Canada, Reports on Explorations and Surveys of 1875–76*, pages 233–280.
- Eardley-Wilmot, V.L. (1928): Diatomite, its occurrence, preparation and uses; *Canada Mines Branch, Publication 691*, 182 pages.
- Founie, A. (2007): Diatomite; in *Minerals Yearbook 2006, United States Geological Survey*, pages 22.1–22.5.
- Godfrey, J.D. (1963): Diatomaceous earth deposits in the Quesnel district, British Columbia; *BC Ministry of Energy, Mines and Petroleum Resources*, Property File, private report, 24 pages.
- Harben, P. (1995): The Industrial Minerals HandyBook; *Metal Bulletin PLC*, 253 pages.
- Hardy, R.M., Stepanek, M. and Dahlman, A. (1978): Report on geotechnical investigations and recommended mitigative measures (town of Quesnel); *BC Ministry of Highways*, unpublished report for Geotechnical and Materials Branch of the Ministry of Highways and Public Works, 97 pages.
- Hora, Z.D. and Hancock, K.D. (1995): Quesnel area – industrial minerals assessment; in *Geological Fieldwork 1994, BC Ministry of Energy, Mines and Petroleum Resources*, Paper 1995-1, pages 395–404.
- McCammon, J.W. (1960): Diatomite; in *Minister of Mines Annual Report 1959, BC Ministry of Energy, Mines and Petroleum Resources*, pages 156–166.
- Reinecke, L. (1920): Mineral deposits between Lillooet and Prince George, British Columbia; *Geological Survey of Canada, Memoir 118*, 129 pages.

TABLE 4. CHEMICAL COMPOSITION OF LEPETICH FARM CORRAL SAMPLE; ALL ELEMENTS ANALYZED BY X-RAY FLUORESCENCE (XRF) BY THE BONDAR AND CLEGG LABORATORY.

Lab. No.	Field No.	SiO ₂ (%)	TiO ₂ (%)	Al ₂ O ₃ (%)	Fe ₂ O ₃ * (%)	MnO (%)	MgO (%)	CaO (%)	Na ₂ O (%)	K ₂ O (%)	P ₂ O ₅ (%)	LOI (%)	Total (%)	Ba (ppm)	Cr** (ppm)
50359	Lep-coral	78.6	0.31	6.01	2.09	0.01	0.63	0.24	0.59	0.4	0.11	9.55	98.58	285	112

- Rouse, G.E. (1959): Report to J.W. McCammon on a fossil plant collection made from Quesnel area; *BC Ministry of Energy, Mines and Petroleum Resources*, unpublished report, 2 pages.
- Rouse, G.E. and Mathews, W.H. (1979): Tertiary geology and palynology of the Quesnel area, British Columbia; *Bulletin of Canadian Petroleum Geology*, Volume 27, Number 4, pages 418–445.
- Skinner, K.G., Dammann, A.A., Swift, R.E., Eyerly, G.B. and Schuck, G.R., Jr. (1944): Diatomites of the Pacific Northwest as filter-aids; *United States Bureau of Mines*, Bulletin 460, 87 pages.
- Visman, J. and Picard, J.L. (1969): Process for Beneficiation of Diatomite Ore; Canadian Patent Number 890249; *Minister of Mines and Resources*, Canadian Intellectual Property Office, 19 pages.

Thickness Trends of J seam, and Its Split at the Falher D Shoreline, Wolverine River Area, Peace River Coalfield, Northeastern British Columbia (parts of NTS 093I, P)

by A.S. Legun

KEYWORDS: coal geology, middle Gates Formation, Peace River coalfield, NTS 093P, NTS 093I, Wolverine River, Murray River, Perry Creek pit, Falher D, Falher C, J seam, transgression, regression, J conglomerate, E conglomerate, COALFILE

INTRODUCTION

The area of study is located southwest of the town of Tumbler Ridge in northeast BC (Fig 1). It lies in an area of old, new and potential pits (Fig 2) that target coals of the middle Gates Formation of the Cretaceous (early to middle Albian).

Arguably J seam, at the base of the middle Gates Formation, is the important economic coal seam in the area. This report compiles the thickness trends of J seam between Bullmoose Mt. in the north and Babcock Mt. to the south (Fig 2). It details the thinning trend of this seam where it is overlain by nearshore deposits of J conglomerate (Falher D).

J seam is also split by J conglomerate with J1 ply extending over the northward-thickening wedge of nearshore deposits in the Perry Creek deposit area. The development of J seam peat spans a period of shoreline advance and retreat. It may represent a transgressive-regressive coal seam couplet as modelled by Diessel (1992) and Banerjee et al. (1996). Transgressive-regressive couplets explain why paralic coals are thick near the paleocoast (Fig 3).

Accommodation in the paralic environment is defined as the available space between the peat basin floor and sea level. The water table generally coincides with, or is influenced by sea level. A significant accommodation reversal in coastal peat (e.g., a change from a drying-up to a wetting-up trend) is often related to shoreline migrations. Accommodation reversal surfaces in J seam have been identified utilizing maceral analysis and petrographic indices such as tissue preservation and gelification (Lamberson et al., 1991; Diessel et al., 2000). This study provides supporting context to that work.

In the study area, onlap of nearshore J conglomerate involved wave erosion and reworking, sediment winnowing, stacking of nearshore deposits at high stand, loading and compaction of the adjoining coastal mire (J2 ply). A coastal lagoon formed at the margin of a barrier shoal and is

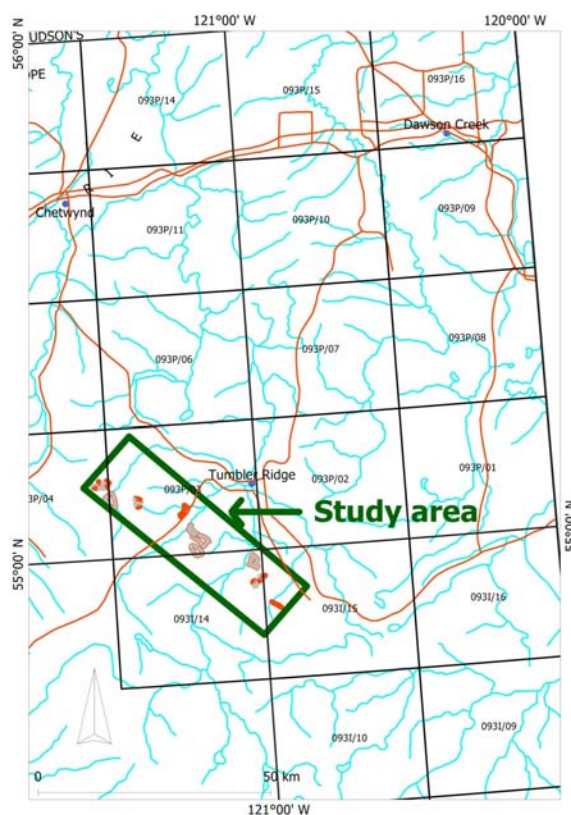


Figure 1. Location of study area, Tumbler Ridge, northeastern BC.

represented by a thickened shale lens onlapping the conglomerate. A tentative model of the transgressive-regressive cycle is presented, drawing on relationships at Perry Creek pit and Mt. Spieker.

Other coal splits by marine tongues may be present in the area. A split in G seam in the Marmot area may be related to Falher C deposits nearby.

Some early aspects of this work are reported in Legun (2006a). Updates to the distribution of clean sandstone and conglomerate of Falher C and D are presented in Legun (2006b).

Wedge-like units of nearshore sedimentary rocks within the middle Gates Formation coal section affect aspects of coal extraction and pit planning in three ways: 1) they increase strip ratios and they include siliceous-rich conglomerate that influences the pH of waste rock drainage; 2) they indicate the probability of higher sulphur content in underlying or adjacent coal; and 3) they make com-

This publication is also available, free of charge, as colour digital files in Adobe Acrobat® PDF format from the BC Ministry of Energy, Mines and Petroleum Resources website at http://www.em.gov.bc.ca/Mining/Geosurv/Publications/catalog/cat_fldwk.htm

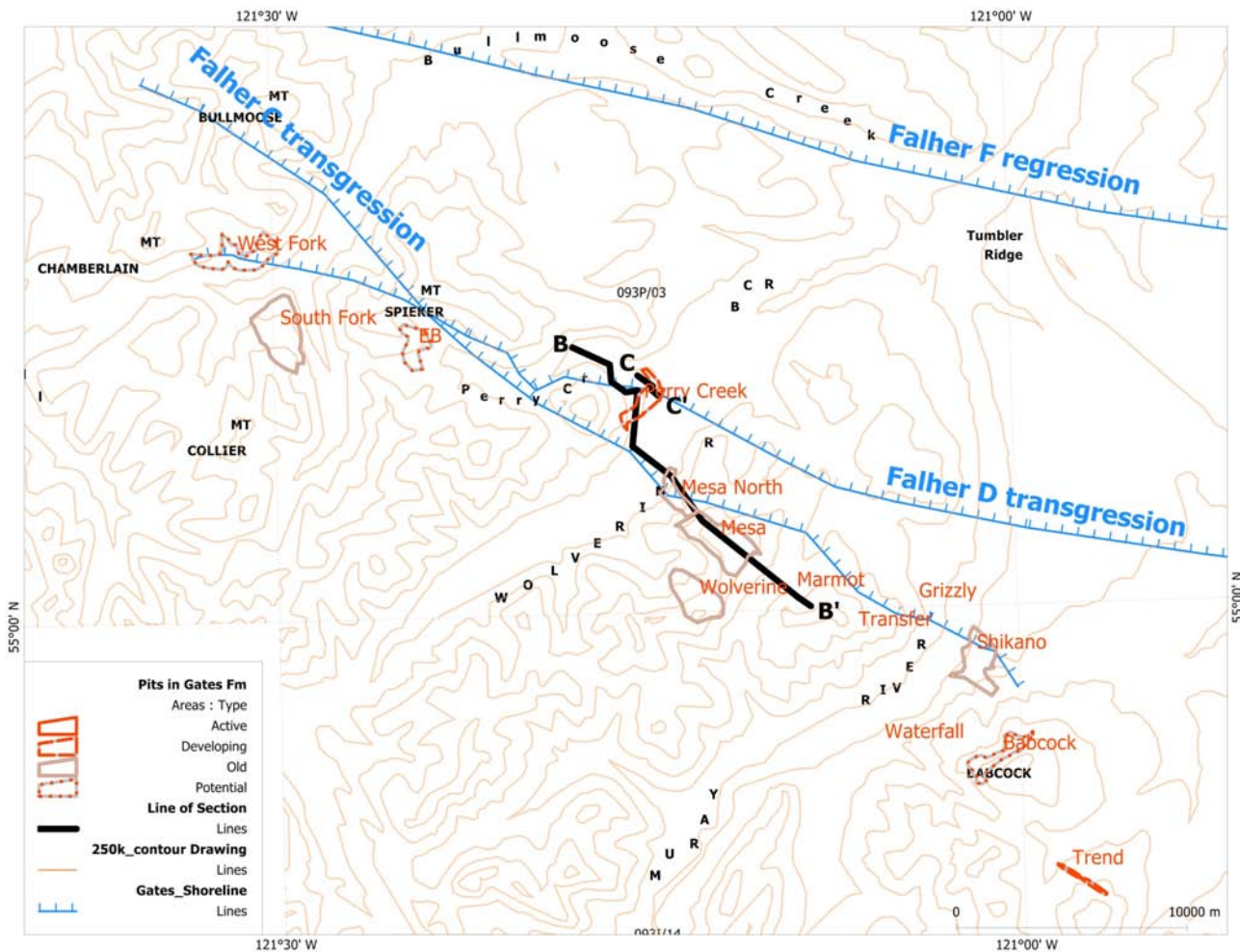


Figure 2. Coal pits, coal exploration areas, middle Gates Formation shoreline positions, and lines of section in the study area, northeastern BC.

petent roof rock for underground mining options or an excellent pit floor.

GATES FORMATION STRATIGRAPHY

The general stratigraphic framework of the Gates Formation is shown in Table 1. The Gates Formation is informally divided into lower, middle and upper members. The lower member is the Quintette sandstone, composed largely of clean sheet sandstone of shoreface and shallow shoal origin. It caps a transitional facies with Moosebar

Formation shale below and underpins the middle Gates Formation coal measures, defined by geologists at Quintette Coal Ltd. as the interval bounded by K (lower) and D (upper) seams. Locally overlying D seam is a cap-rock sandstone and conglomerate unit, known as the Babcock (from extensive exposures on Babcock Mt.). These are estuarine shoal deposits of the upper Gates Formation that abruptly end the major coal-bearing period of the middle Gates Formation. Above the upper Gates Formation and below the overlying Hulcross Formation shale is an unnamed unit of thin coal and shale layers.

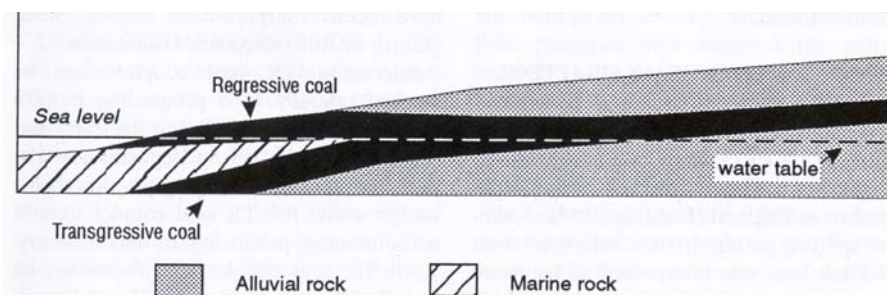


Figure 3. Model of transgressive-regressive coal couplet (after Diessel, 1992).

Middle Gates Formation

The J seam lies at the base of the middle Gates Formation coal section at Wolverine but K seam underpins it to the south at Murray River. The middle Gates Formation may contain up to 18 m of medium to low volatile coal in 60 m of section. Regional-scale correlations of middle Gates Formation coals indicate five to six seams that are laterally continuous and reach economic thickness over a

TABLE 1. STRATIGRAPHIC NOMENCLATURE OF THE GATES FORMATION AND ITS RELATION TO FALHER CYCLES, NORTHEASTERN BC.

	West Fork deposit	Teck Bullmoose pit (reclaimed), EB pit	Mt. Spieker Ridge	Perry Creek pit	Subsurface (oil and gas wells)	Carmichael regional study (1983)	Qunitette Coal Ltd. Mesa pit (reclaimed)
Upper Gates Formation	unit 5 unit 4	upper seams'		Fortress Mt. unit	Notikewan Notikewan	unnamed Babcock member	thin coals and shale Babcock member
Middle Gates Formation	(E seam)	(E seam)		D seam			D seam
	(D seam)	(D seam)		E, F seams Wolverine unit	Falher C		E seam E conglomerate
	(C seam)	(C seam)	C seam	G seam			G seam
	unnamed conglomerate A, B seams	A, B seams	C2 seam? unnamed conglomerate A, B seams	J seam (J1 ply) J conglomerate	Falher D		J seam
Lower Gates Formation	unit 1			J seam (J2,3 plies) Quintette sandstone	Falher F Falher G	Sheriff member Torrens member	Quintette sandstone

Note: () indicate comparable stratigraphic position.

significant area. Of these, J and E seams show the thickest coal development. The J seam may exceed 7 m with low ash and could be mined as a single seam with no subplies and very thin partings. The E seam tends to be composite, formed of several closely spaced plies. Portions of these become very ashy (E1) or develop abundant partings (lower part of E3). The F seam, generally cleaner, is equivalent to E2/E3 where those plies separate from E1 in the Marmot (Hermann North) area, southeast of the reclaimed Mesa pit. Correlation and extents of middle Gates Formation coals are shown in summary figures of Qunitette Coal Ltd. (COALFILE 753; COALFILE, 2007), Carmichael (1983) and Leckie (1983). Although major seams are often shown in a simple ordered sequence in a stratigraphic column, the seam architecture has some complexity. Correlations between pits indicate seams split or amalgamate, or stratigraphically approach each other. Approaches include D and E (Shikano and Mesa pits) and J and K (Babcock pit). The G seam is split in the Marmot area with the upper ply migrating stratigraphically to E4 seam in the Mesa pit area to the northwest. The seam architecture has not been adequately related to the geometry of nearby deltaic lobes and marine tongues.

FALHER CYCLES, MARINE TONGUES AND COAL

Cycles of marine regression, named Falher cycles, are distinguished by gamma log responses that indicate upward-coarsening sequences. The cycles are alphabetically named G (stratigraphically lowest) to A (highest). Ideally they comprise a basal transgressive lag deposit, upward-coarsening shale, sandstone to conglomerate with marine trace fossils followed by evidence of terrestriation (rootings, coal). Upper beds of cycle F correspond to the Quintette sandstone. At the top of the Falher F and C cycles are shoreface deposits that form the widespread floors to the J and E seams. Cycle G lies within the Moosebar transitional facies in the study area but is the Torrens sandstone floor to a major coal seam near the Alberta border.

J and E conglomerate in coalfield terminology correlates to the sandy and conglomeratic (i.e., non-shaly) nearshore deposits of Falher C and D. Wedge-like in geometry, Falher D directly overlies J seam while Falher C is above G seam and below E. Borehole QWD7115 in the Perry Creek pit area is key in tying Falher cycle correlations

to J and E conglomerates in the Wolverine area. The E conglomerate develops and extends from Mesa North pit while J conglomerate develops in the northern half of Western Canada Coal Corp.'s (WCCC) Perry Creek pit, Mt. Spieker ridge and in the undeveloped West Fork deposit.

SHORELINES

Both Leckie (1983) and Carmichael (1983) produced maps of shoreline trends. The maximum regressive limit is the most northerly occurrence of coal or carbonaceous shale, capping a coarsening-upward sequence. The transgressive limit is marked by the southern limit (zero isopach) of clean sandstone and conglomerate of nearshore origin (zero edge of J or E conglomerate). During the Falher F regression, the shoreline migrated to a position north of Bullmoose Mt. (Fig 2). The subsequent transgression (Falher D) brought it to an east-west position near Mt. Spieker. It subsequently retreated well to the north and advanced again (Falher C) with a northwest-southeast shoreline position that lies close to a line from Bullmoose Mt. to Mesa North pit to Shikano pit. A portion of the middle Gates Formation outcrop section at Perry Creek is shown in Figure 4. This section lies south of the Falher D transgression line but north of Falher C.

J SEAM THICKNESS STUDY

Elements of J seam have a wide extent, though regional correlations may correspond to a coal interval rather than a discrete seam. It persists eastward to the Alberta deep basin as the 4th coal seam. Southeast of Wolverine, along the structural trend, it is split by a deltaic lobe at Monkman and continues as seams B4, B5 to the Belcourt area. In the southwest, along the trend of Five Cabin Creek syncline it is locally missing and replaced by fluvial conglomerate (Carmichael, 1983, Fig 6, 25). Some trends north of the Wolverine River are shown in Summary Figure 3.6 of Leckie (1983). Trends to the northeast, immediately outside the coalbelt, are poorly known due to few wells.

In the area of study, J seam has been mined at South Fork pit and a number of Qunitette Coal Ltd. pits including Mesa, Wolverine and Shikano. It is currently mined at the Perry Creek and Trend pits. The J seam forms a significant resource at prospective pits that include EB, West Fork and Hermann North.

Over a large part of the study area, J seam has few and relatively thin (less than 0.5 m) rock splits. Where splits are present the seam is subdivided into local plies named J1, J2 and J3. In the Bullmoose area, J seam equates to two separate seams, locally named A and B. The basal J3 ply is probably equivalent to A seam as they both rest on Quintette sandstone. The B seam corresponds to J2 as both are locally overlain by Falher D conglomerate. The A and B seams are referred as J(A) and J(B) below.

Trends were compiled using group and individual borehole thickness data. Group data includes 'in pit' isopachs or seam averages. Individual thickness data is presented in seam intercept drilling summaries and in correlation charts. Thickness is often quoted as a fraction: coal thickness/seam thickness. Seam thickness and not coal thickness values were used in this study. These thicknesses are derived from picks of high resolution density logs in conjunction with gamma ray logs (and caliper). Additional thickness data is available in logs of petroleum wells though the geophysical logs have a coarser resolution.

The author employed a simple approach to assess trends. Seam thickness averages were used for densely drilled areas and point values where data was sparse. Values of separate plies (J1, J2, J3) were summed. The J(A) and J(B) seams were summed in the Bullmoose area.

Thickness trends are evaluated from data points in the folded terrain of the Rocky Mountain foothills. The data points and trends reflect crustal shortening of perhaps 15% and have not been palinspastically restored to original geographic position.

Results

Results of the thickness study revealed three thickness domains (Areas 1, 2, 3) of J seam (Fig 5). Seam thickness trends are superimposed on isopachs of J conglomerate (in metres). In the Perry Creek area, thicknesses that include J1 ply above the J conglomerate are shown in an inset.

Area 1 is a seaward area where J seam thins rapidly. The boundary follows the partially defined 4 m isopach of J seam. The thinning trend is normal to the linear trend of J conglomerate, and is particularly evident in the more densely drilled areas of West Fork and Perry Creek pit. The thinning trend continues east of the coalbelt in the subsurface and is recognizable in J seam and Falher D signatures in well logs. The J seam is thick south of the Falher D line. A possible exception occurs near well 15372 (Fig 5) where both J seam and J conglomerate are thick.

Area 2 is a large coastal area where J seam exceeds 4 m. Individual pit maps of J seam contours do not display any dominant trends that are normal or parallel to the shore.

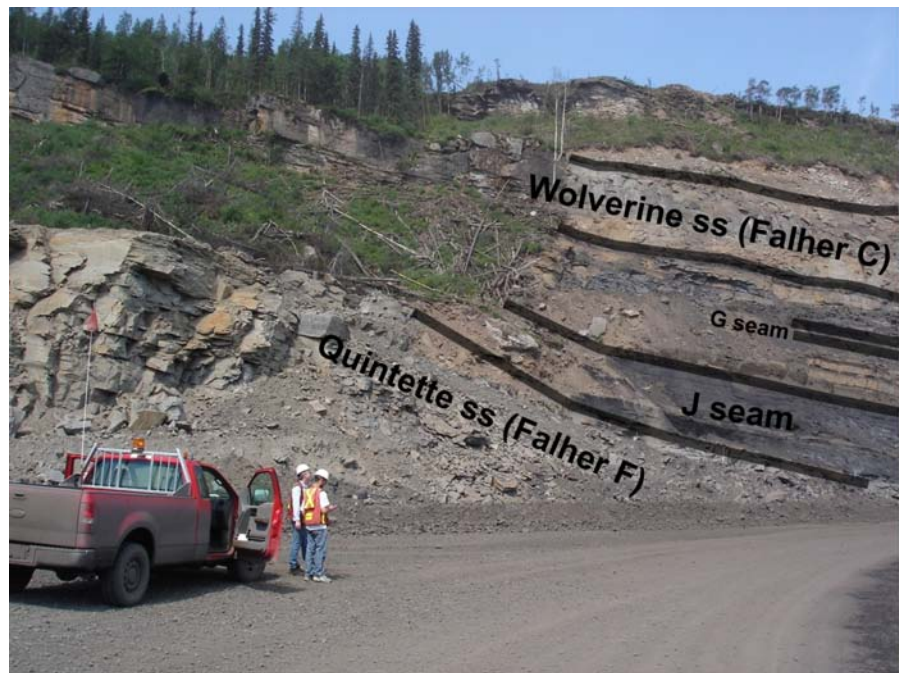


Figure 4. Outcrop section in the Perry Creek pit showing the base of middle Gates Formation (J seam) resting on clean Quintette sandstone (ss), northeastern BC.

This domain extends east of the coalbelt into the subsurface.

Area 3 is an area where J seam is less than 4 m thick. This includes portions of Wolverine pit and Waterfall Creek drill areas. The seam thins due to thick rock splits. This area may border alluvial plains of the upper coast.

DETAILS OF THINNING TREND IN AREA 1 (NEAR FALHER D SHORELINE).

At the Mesa and Perry Creek pits, minor shale partings divide J seam into three coal plies (Fig 6). The partings thicken northward and the upper interseam rock (between J2 and J1 coal) is replaced by conglomerate. The logs from a line of development drillholes (Fig 7) show the separation of J1 ply from the main seam. The J conglomerate rapidly thickens northward to upwards of 40 m with the J1 ply above. Beyond the drillhole line, J1 thins to less than 0.5 m in drillhole QWD 7120 to the northwest (Fig 7 inset).

J2 coal ply has a clean upper contact suggesting it may be locally eroded below the conglomerate. Western Canada Coal Corp. (2003) reports that "Where J conglomerate forms the J2 roof, J2 is cleaner as it lacks the rock and/or high-ash coal bands in its upper part". In the line of section (C' to C), J2 thins from 4 to 2.7 m over 1 km. Further to the northwest, J2 splits into two plies, each of which thins and becomes shaly. The upper ply is not present in the last drillhole of this trend (PR 2006-24, Fig 7 inset).

In the Bullmoose area, both J(A) and J(B) seams thin northward to the West Fork area. In contrast to trends at Perry Creek, the interseam shale does not thicken. J(B) is locally eroded against J conglomerate, the contact is marked by chert pebbles in fine sand with coal fragments, some replaced by pyrite. This is very similar to observations at Mt. Spieker and the Perry Creek pit. Northward J(A) thins to a carbonaceous mudstone and J(B) persists to the northern parts of Bullmoose Mt.

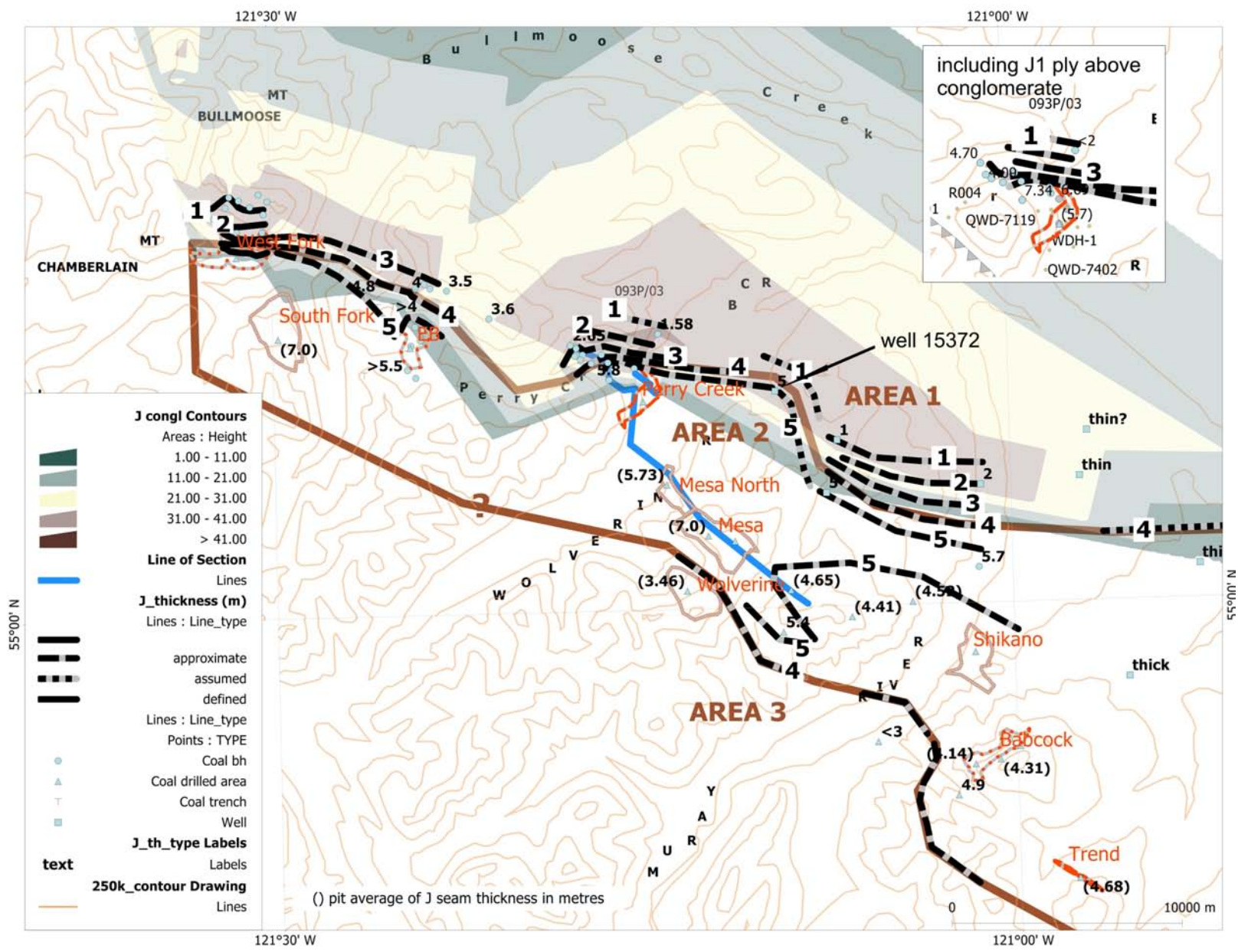


Figure 5. Relation of J (composite) seam thickness to isopach trends of J conglomerate (Falher D).

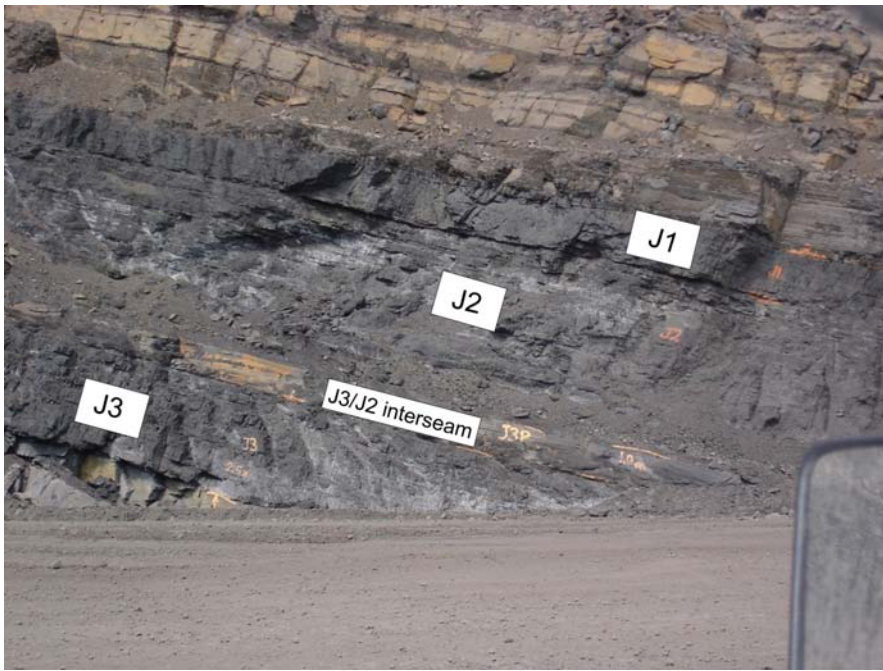


Figure 6. Exposure of J seam plies at Perry Creek pit, northeastern BC. The J2/J1 parting, barely apparent, passes northward to several metres of shale and then J conglomerate.

J(A) and J(B) have a combined thickness exceeding 5.5 m in the EB pit area but are separated by up to 15 m of interseam rock. The seam thickness is reduced to 4 m at the southwestern edge of adjoining Mt. Spieker ridge. On the ridge itself, the thinning trend of each seam continues with the combined thickness dropping to 2 m or less.

INTERPRETATION OF TRENDS AT THE PALEOSHORE

The thinning of the lower coal plies (JA or J3) is depositional as their roof shale is intact. The contact of ply J(B) or J2 with conglomerate marks a surface of marine erosion. The pebble lag on the coal surface is due to wave action (above storm wave base) during southern advance of the Falher D sea. On Mt. Spieker ridge, shale is locally present above B seam, even near the zero edge of the conglomerate (COALFILE 556, trench data). The erosion thus appears to be shallow and the thinning of upper plies is largely depositional.

On Mt. Spieker ridge, it is unclear whether the transgressive lag underpins the conglomerate to its zero edge, that is, whether the edge of the conglomerate coincides with the shoreline. Marine conditions are clearly documented a kilometre to the north with herringbone crossbedding, Rhizocorallium trace fossils and storm sheet facies of swaley cross-stratification (Leckie and Walker, 1982). In the Perry Creek valley, in a comparable position from the zero edge, tens of metres of massive sandstone lie above J2 coal at the creek's edge. It is loaded by sandstone pillows and intervening pockets of pebbly mudstone. The massive sandstone with basal flute casts suggests mass influx of sediment, possibly a baymouth splay below a distributary.

Toward the zero edge on Mt. Spieker ridge, Leckie (1983) suggested a fluvial regime based on the presence of a root horizon, large lateral accretion bedforms and a high proportion of conglomerate. Trench data in the area

(COALFILE 556) suggests B seam thickness is maintained below the channel. The author suggested the accretion bedforms extending over 15 m in height may be the southern (coast facing) slope of a barrier shoal (Legun, 2006a). Well-washed, quartzitic sandstone occurs near the top of J conglomerate with current bedforms parallel to the shore. At Perry Creek, the well log for diamond-drill hole QPR 88003 (Fig 7) has density spikes that suggest the presence of carbonaceous shale lenses in J conglomerate. An estuarine environment with shore-parallel and shore-normal elements may be an inclusive description of sedimentation complexities at the coast/marine interface in both areas.

The source of nearshore sandstone and conglomerate is not readily evident. Channel bodies are not identified landward of the linear trend of J conglomerate — areas that include EB pit, South Fork (Bullmoose mine) and south Perry Creek pit. A thick, blocky gamma profile in a recent drillhole (COALFILE 901, PRC R003) near Fortress Mt. (Fig 7 inset) may represent a channel. It is south of the conglomerate line.

A shale interval between the top of J(B) and base of C2 seam can be traced from Mt. Spieker ridge (drillhole MS23) to the EB pit area (drillhole MS19). At Mt. Spieker, it is only a metre or so thick on top of J conglomerate while it is 16 m at the EB pit where the conglomerate is missing. It suggests the presence of a shale-filled lagoon landward of the coastal shoal or barrier. Overwash during storm events leads to sediment loading and compaction of adjoining mires creating accommodation space (i.e., a lagoon). An example of this in the modern historical record was reconstructed by Long et al. (2006).

Marine influence on coastal peat further south is indicated by fossils immediately above J seam in drillhole QWD 7402 (Fig 7 inset) and the sulphur content of J seam (D. McNeil, pers comm, 2007).

A model for J seam regressive couplet is presented in Figure 8, utilizing relationships at Mt. Spieker and Perry Creek.

PETROGRAPHIC INDICATOR STUDIES AND J SEAM SPLIT

The split of J seam provides improved context for petrographic indicator studies of J seam. Kalkreuth and Leckie (1989) suggested there was considerable transported (drifted) material in the J3 ply, given the high proportion of degraded vitrinite and inertodetrinite. With a falling sea level, a modest gradient was established on the new coastal plain. J3 began in a marsh environment subject to flood pulses that brought in abundant organic debris. The basal peat was part of the shoaling process and reflected a

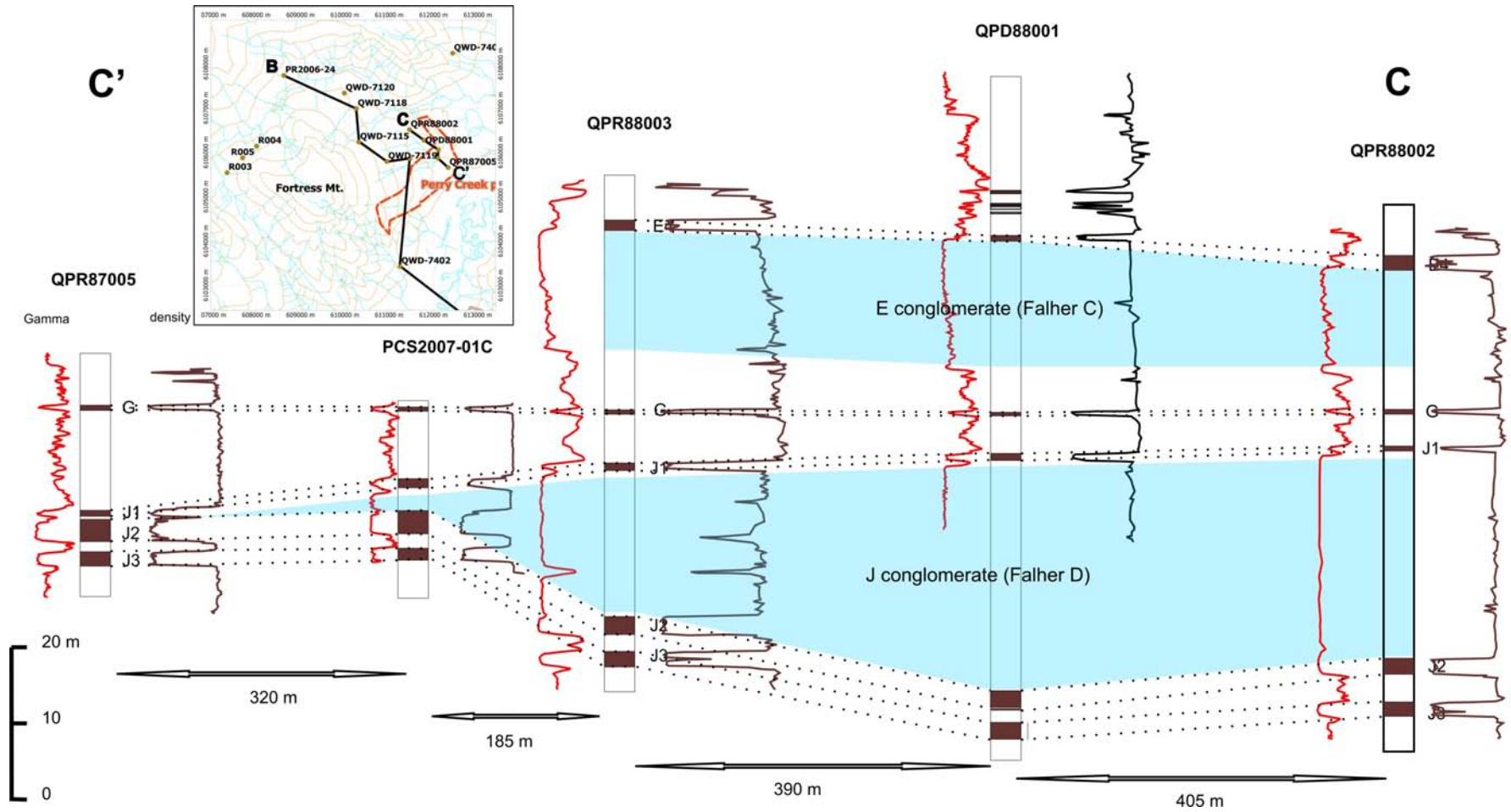


Figure 7. Line of development drillholes showing correlation of J1 ply above J conglomerate, northeastern BC.

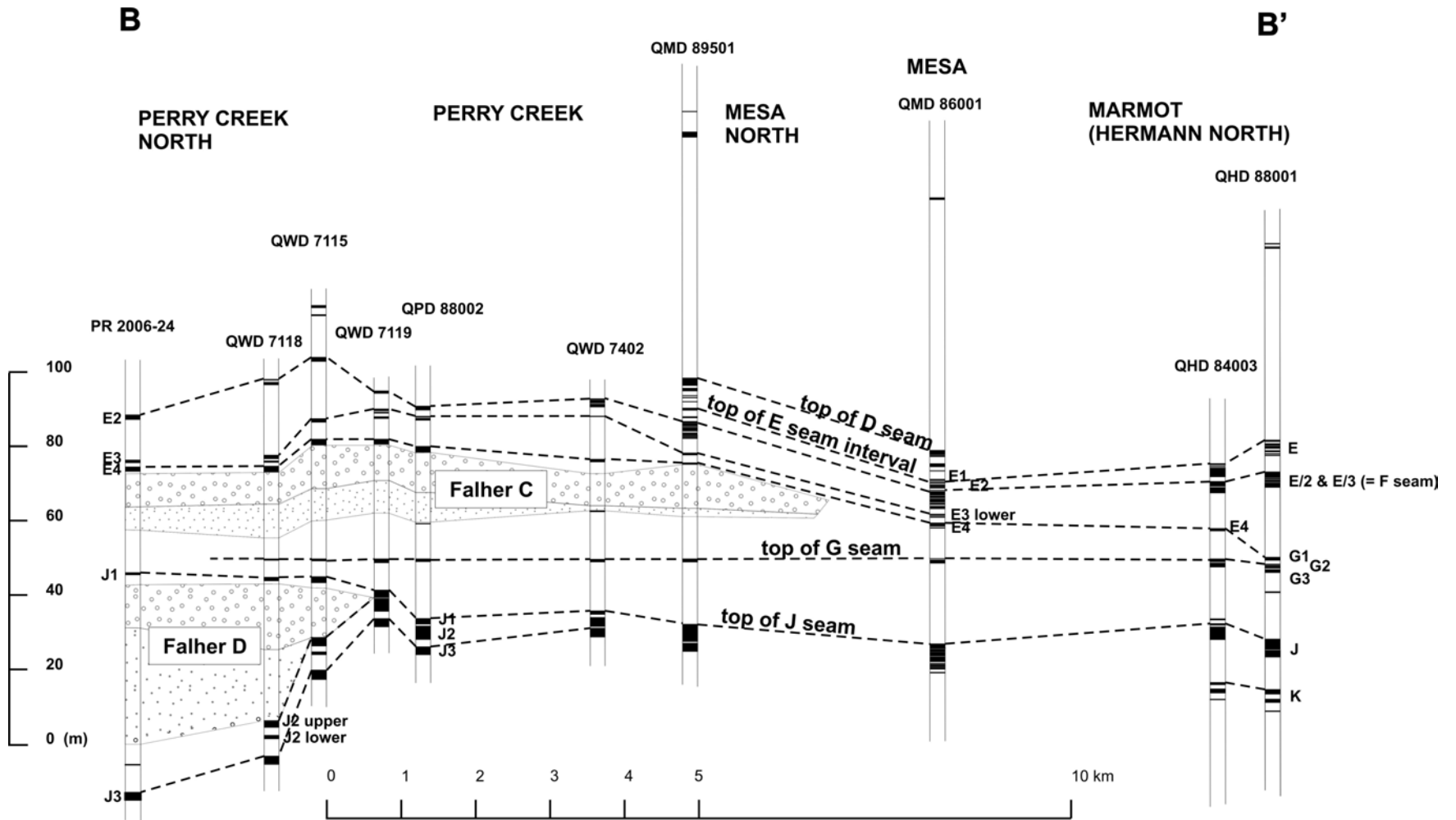


Figure 9. Line of section Perry Creek North pit to Marmot (Hermann North) areas, northeastern BC.

REFERENCES

- Banerjee, I., Kalkreuth, W. and Davies, E.H. (1996): Coal seam splits and transgressive-regressive coal couplets: a key to stratigraphy of high-frequency sequences; *Geology*, Volume 24, Number 11, pages 1001–1004.
- Carmichael, S.M. (1983): Sedimentology of the Lower Cretaceous Gates and Moosebar formations, northeast coalfields, British Columbia; unpublished PhD thesis, *University of British Columbia*, 285 pages.
- COALFILE (2007): COALFILE BC coal data and reports; *BC Ministry of Energy, Mines and Petroleum Resources*, URL <<http://www.em.gov.bc.ca/mining/geolsurv/coal/Coaldatabases/coaldata.htm>> [December 2007].
- Diessel, C.F.K. (1992): Coal-bearing deposition systems; *Springer-Verlag*, Berlin, 721 pages.
- Diessel, C., Boyd, R., Wadsworth, J., Leckie, D. and Chalmers, G. (2000): On balanced and unbalanced accommodation/peat accumulation ratios in the Cretaceous coals from Gates Formation, western Canada, and their sequence-stratigraphic significance; *International Journal of Coal Geology*, Volume 43, pages 143–186.
- Kalkreuth, W. and Leckie, D.A. (1989): Sedimentological and petrographical characteristics of Cretaceous strandplain coals: a model for coal accumulation from the North American western interior seaway; in *Peat and Coal: Origin, Facies and Depositional Models*, Lyons, P.C. and Alpern, B., Editors, *International Journal of Coal Geology*, Volume 12, pages 381–424.
- Lamberson, M.N., Bustin, R.M. and Kalkreuth, W. (1991): Lithotype (maceral) composition and variation as correlated with paleo-wetland environments, Gates Formation, north-eastern British Columbia, Canada; *International Journal of Coal Geology*, Volume 18, pages 87–124.
- Leckie, D.A. and Walker, R.G. (1982): Storm- and tide-dominated shorelines in Cretaceous Moosebar-Lower Gates interval - outcrop equivalents of deep basin gas trap in western Canada; *American Association of Petroleum Geologists, Bulletin*, Volume 66, Number 2, pages 138–157.
- Leckie, D.A. (1983): Sedimentology of the Moosebar and Gates formations (Lower Cretaceous); unpublished PhD thesis, *McMaster University*, 515 pages.
- Legun, A.S. (2006a): The Gates Formation in the Wolverine River area, northeastern BC; in *Geological Fieldwork 2005*, *BC Ministry of Energy, Mines and Petroleum Resources*, Paper 2006-1, pages 73–82.
- Legun, A.S. (2006b): Peace River coalfield, northeast British Columbia (NTS 093P, I, O, 094B); *BC Ministry of Energy, Mines and Petroleum Resources*, Open File 2006-13.
- Long, A.J., Waller, M.P. and Stupples, P. (2006): Driving mechanisms of coastal change: peat compaction and the destruction of late Holocene coastal wetlands; *Marine Geology*, Volume 225, pages 63–84.
- Wadsworth, J., Boyd, R., Diessel, C. and Leckie, D. (2003): Stratigraphic style of coal and non-marine strata in a high accommodation setting: Falher member and Gates Formation (Lower Cretaceous), western Canada; *Bulletin of Canadian Petroleum Geology*, Volume 51, Number 3, pages 275–303.
- Western Canada Coal Corp. (2004): Environmental assessment supplementary information report for the Wolverine project, Volume 1; *BC Environmental Assessment Office*, URL <http://www.eao.gov.bc.ca/epic/output/html/deploy/epic_document_162_18906.html>, Additional Information Report – Main Document [December 2007].

Geochemical Orientation Surveys in the Quesnel Terrane between Quesnel and Williams Lake, central British Columbia (NTS 093A, B, G)

by R.E. Lett and Z. Sandwith¹

KEYWORDS: Quesnel Terrane, soil geochemistry, copper, gold

INTRODUCTION

Orientation surveys are an essential part of any large-scale geochemical program because they serve to establish optimum sampling and analytical techniques. Among variables that need to be determined by a soils orientation are the sample density, soil horizon, sample grain size or mineral fraction, and analytical method. Establishing geochemical background for each element, either by reference to literature values or by calculating statistics from the orientation survey data, is the first stage in defining an anomaly. Closely linked to establishing background is deciding on the combination of sample grain size, sample digestion technique and element detection method that will give the greatest anomaly contrast (signal to noise ratio) for all ore indicator and pathfinder elements.

Selective and sequential metal extractions have long been used in stream sediment and soil surveys to improve geochemical anomaly contrast. For example, Cameron et al. (2004) showed that selective extraction techniques, such as Enzyme LeachSM and Mobile Metal IonSM analysis, are often able to better detect sulphide and other types of mineralization beneath thick surficial deposits by enhancing geochemical anomaly contrast. The factors that govern element transport and migration from source to site of accumulation must be appreciated for correctly interpreting the subtle but often distinct element patterns revealed in selective extraction data. Among the factors influencing element dispersion are lithochemistry, bedrock geology, surficial geology (including stratigraphy and material thickness), glacial erosion and transport of mineralization from a bedrock source, soil drainage, soil-forming processes, soil redox potential and soil pH.

Geochemical models can help estimate the influence of these variables on anomaly formation by visually demonstrating the relationships between a mineral deposit and its geochemical response in the near-surface environment. First proposed by Bradshaw (1975) for the Canadian Cordillera, conceptual geochemical models have most recently been adapted by Butt et al. (2005) in Australia to simplify the interpretation of complex survey data with visual three-dimensional diagrams. Lett and Bradshaw (2002) proposed

developing an atlas of similar geochemical models supported by real analytical and field data from Cordilleran case histories. For example, Hoffman and Perkins (1990) developed a geochemical model for Au-Cu porphyry mineralization, from geology and lithochemical studies, to explain the results of multi-element soil surveys on the Cat Mountain deposit in central British Columbia. Their model proposed concentric lithochemical zones radiating from a W-Ag core into a Mo zone, a Au zone, a Cu-Co-Fe zone and, finally, a peripheral As-Al-V-Mn zone. Depending on the erosion level of the Cu-Au-mineralized bedrock, there was a lateral transition from the peripheral As-Al-V-Mn into a Pb-Zn zone.

Much of the current mineral exploration in British Columbia has focused on Quesnel Terrane rocks because of production from economic Cu-Au deposits such as Mount Polley. Although there have been few specific orientation studies to determine the near-surface geochemical expression of Cu-Au porphyry deposits, the results of recent orientation surveys over epithermal Au mineralization have been published by Cook and Dunn (2007). They demonstrated that the partial extraction of trace elements using Enzyme Leach and Mobile Metal Ion analysis from soil samples collected over the Tommy and Ted Au-mineralized epithermal vein near Vanderhoof, BC could improve geochemical contrast compared to results from more rigorous acid digestion. Many of the elements detected by the partial extraction used by Cook and Dunn (2007) were important pathfinders for base and precious metal mineralization. Hall (1998) described a number of the more recently developed partial extraction methods and assessed the analytical precision for geochemical pathfinders determined by these techniques. Not only is the analytical method (e.g., Enzyme Leach) important for enhancing contrast, but so too is the element suite that best characterizes mineralization. Improved geochemical techniques need to be developed for detecting more deeply buried mineral deposits, since much of central BC has an extensive cover of plateau basalts and glacially transported overburden. Here we report preliminary results of orientation geochemical studies over the Mouse Mountain (MINFILE 093G 003) and Shiko Lake (MINFILE 093A 058) porphyry Cu-Au mineral occurrences, as well as a target for possible Cu mineralization near Soda Creek. The locations of these three areas are shown in Figure 1.

SURVEY TECHNIQUES

Field Sampling

Samples from major soil horizons were taken down vertical profiles at specific intervals in the Mouse Mountain, Shiko Lake and Soda Creek areas. The profiles were

¹ University of Victoria, Victoria, BC

This publication is also available, free of charge, as colour digital files in Adobe Acrobat[®] PDF format from the BC Ministry of Energy, Mines and Petroleum Resources website at http://www.em.gov.bc.ca/Mining/GeolSurv/Publications/catalog/cat_fldwk.htm

located at stations along road and bush traverses that were generally orientated perpendicular to the regional ice-flow direction. Several sampling traverses up and down-ice of a mineralized zone (where known) were completed, although it was often not practical to carry out an extensive or regular sampling pattern. Where possible, the following samples were taken from:

- the decomposed humus (F-H) horizon, just beneath the surface vegetation litter;
- the upper B soil horizon, just beneath the eluviated (Ae) horizon (where visible);
- the lower B soil horizon close to the transition between the B and C soil horizons;
- a depth of 20 to 25 cm for Mobile Metal Ion analysis; and
- the C soil horizon glacial sediment (typically till).

Eighty-eight upper B-horizon, 84 lower B-horizon and 83 C-horizon samples were taken (including quality-control field duplicates). Median midpoint depths of the upper B, lower B and C-horizon samples were 16.0 cm (1st to 3rd quartile ranged from 13 to 18 cm), 26 cm (1st to 3rd quartile ranged from 24 to 26 cm) and 43 cm (1st to 3rd quartile ranged from 36 to 57 cm), respectively. Horizons were identified in the field using the Canadian Soil Classification Working Group (1998) nomenclature. However, distinction between ‘upper’ and ‘lower’ B horizon is often arbitrary because there is commonly only a subtle change in soil colour and texture within a given profile.

The samples were collected from hand-dug pits or from trenches excavated in road cuts. Profile sites were accurately located with a Garmin Map 60 hand-held GPS unit. Duplicate samples were taken at a frequency of one duplicate per twenty routine samples. Depth, soil texture, soil colour (Munsell Classification) and structure were described for each sample taken, with details on the percentage, size and shape of rock clasts and presence (or absence) of clast striations recorded. Still digital photographs were taken of each profile and a short video made to record details of the area surrounding the station. At the end of each day, the B-horizon pH was measured on a 1:1 (by volume) slurry of soil to distilled water with an Extech® Instruments Corporation P110 pH meter calibrated daily with pH 4 and 7 buffers. Multiple samples were collected from each horizon for use in different analytical methods. For example, B-horizon soil and litter samples for aqua regia digestion – inductively coupled plasma – mass spectrometry (ICP-MS) analysis were collected in Hubco Inc. polyester weave bags, and the C-horizon samples (glacial sediment) were collected in large PVC bags. Samples intended for Enzyme LeachSM, Soil Gas HydrocarbonsSM and Mobile Metal IonSM analysis were collected and double-bagged in sealed PVC Ziploc® bags. A number of sediment samples were also collected in Hubco bags from streams in the areas surveyed. A typical soil from the Mouse Mountain area is shown in Figure 2.

Sample Preparation

The F-H, B and C-horizon samples were oven dried at 35 to 40°C and prepared in the British Columbia Geological Survey laboratory, Victoria, BC before being sent for analysis at commercial laboratories. The F-H-horizon samples were milled. Part of the B-horizon sample and stream sediment samples were disaggregated and sieved to –80 mesh

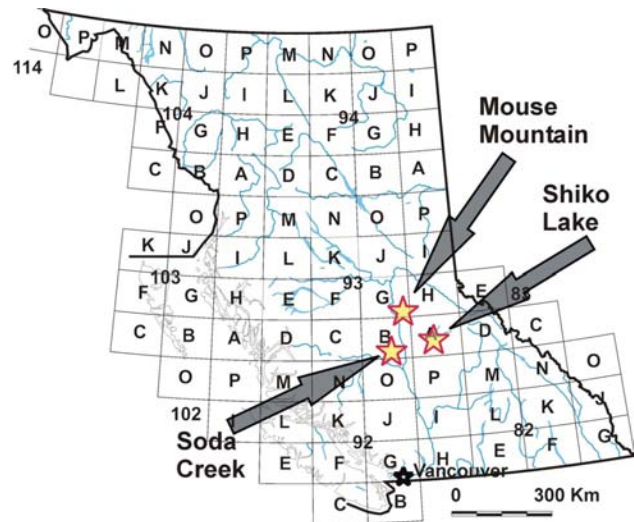


Figure 1. Location of the Mouse Mountain, Shiko Lake and Soda Creek survey areas, central British Columbia.

(<0.180 mm), whereas C-horizon (glacial sediment) samples were sieved to –230 mesh (<0.063 mm). The +2 mm size fraction of the glacial sediment was archived for later identification of clast lithology. Sieved or milled duplicate samples (generally from one of the field replicates) and standard reference materials were inserted into each batch of 20 samples before analysis. No preparation was carried

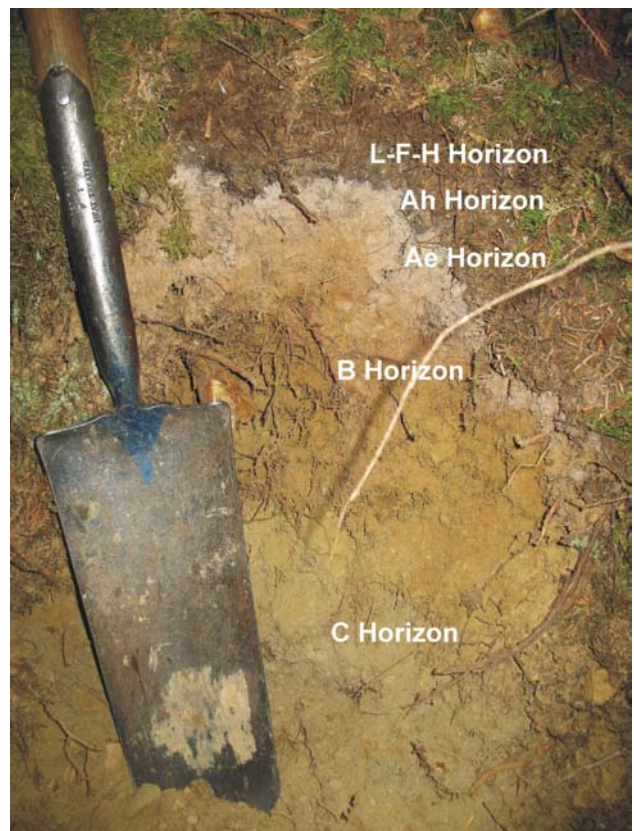


Figure 2. Profile showing Brunisolic soil developed on till, Mouse Mountain area.

TABLE 1. ELEMENTS DETERMINED BY AQUA REGIA – INDUCTIVELY COUPLED PLASMA – MASS SPECTROMETRY (AR-ICP), INSTRUMENTAL NEUTRON ACTIVATION ANALYSIS (INAA), MOBILE METAL IONSM (MMI) AND ENZYME LEACHSM (EL) ANALYSIS, WITH INSTRUMENTAL DETECTION LIMITS. DETECTION LIMITS FOR ALL ELEMENTS BY EL AND MMI ARE IN PARTS PER BILLION (PPB); ELEMENTS DETERMINED BY AR-ICP AND INAA ARE IN PARTS PER MILLION (PPM). EL RESULTS FOR CL, HG, SC AND TI ARE SEMIQUANTITATIVE.

out on the soil samples sent for Enzyme Leach, Soil Gas Hydrocarbons and Mobile Metal Ion analysis.

Sample Analysis

Analysis of samples is currently in progress by the following methods:

- **Aqua regia digestion – ICP-MS:** The <0.18 mm soil and <0.063 mm glacial sediment fractions have been analyzed for 37 elements, including Au and Cu, at Acme Analytical Laboratories, Vancouver, BC by aqua regia digestion (HNO₃-HCl-H₂O 1:1:1 by volume), followed by ICP-MS.
- **Instrumental neutron activation analysis (INAA):** The <0.180 mm soil and <0.063 mm glacial sediment fractions are being analyzed for 33 elements, including Au, at Activation Laboratories Limited, Ancaster, Ontario by INAA. This method involves irradiation of either a 5 or 20 g sample in a high-density neutron flux, followed by counting the gamma-ray emission from elements after a decay period.
- **Enzyme LeachSM analysis:** This technique, developed by Activation Laboratories Limited, Ancaster, Ontario, detects small element variations in B-horizon soils over and around mineral deposits by selectively removing the amorphous manganese dioxide soil-particle coatings with hydrogen peroxide, thereby releasing trapped trace elements (Yeager et al., 1998).
- **Soil Gas Hydrocarbons (SGH)SM:** Developed by Activation Laboratories Limited, Ancaster, Ontario, this is an extractive procedure for C5 to C17 organic compounds that have been absorbed on B-horizon soil samples. The procedure is designed to measure these compounds in the low parts per trillion (ppt) concentration range.
- **Mobile Metal Ion (MMI)SM analysis:** This technique, developed by Mann et al. (1998), utilizes reagents containing strong ligands designed to extract metals such as Cu, Pb, Zn, Ni, Cd, Au, Ag, Co and Pd from soil samples.
- **Loss-on-ignition (LOI):** LOI of soil samples at 500°C was determined on the <0.180 mm fraction of the B-horizon soil samples at Acme Analytical Limited, Vancouver, BC.

Elements analyzed and detection limits for the aqua regia – ICP-MS, INAA, Enzyme Leach, and Mobile Metal Ion analytical methods are listed in Table 1.

Element	AR-ICP (ppm)	INAA (ppm)	MMI (ppb)	EL (ppb)
Ag	0.002	5	1	0.2
Al	100		1	
As	0.1	0.5	10	1
Au	0.002	0.002	0.1	0.05
B	1			
Ba	0.5	50	10	1
Be				2
Bi	0.02		1	0.8
Br		0.5		5
Ca	100	10000	10	
Cd	0.01		1	0.2
Ce		3	5	0.1
Cl				2000
Co	0.1	1	5	1
Cr	0.5	5	100	20
Cs		1		0.1
Cu	0.01		10	3
Dy			1	0.1
Er			0.5	0.1
Eu		0.2	0.5	0.1
Fe	100	100	1	
Ga	0.2			1
Gd			1	0.1
Ge				0.5
Hf		1		0.1
Hg	0.005	1		1SQ
Ho				0.1
I				2
In				0.1
K	100			
Ir		0.005		
La	0.5	0.5	1	0.1
Li			5	2
Lu				0.1
Mg	100		1	
Mn	1			1
Mo	0.01	1	5	1
Na	100	100		
Nb			0.5	1
Nd		5	1	0.1
Ni	0.1	20	5	3
Os				1
P	10			
Pb	0.01		10	1
Pr			1	0.1
Pt			1	1
Pd			1	1
Rb		15	5	1
Re				0.01
Rh				
Ru				1
S	20			
Sb	0.02	0.1	1	0.1
Sc	0.1		5	100SQ
Se	0.1	3		5
Sm		0.1	1	0.1
Sn		200	1	0.8
Sr	0.5	50	10	1
Ta		0.5	1	0.1
Tb		0.5	1	0.1
Te	0.02		10	1
Th	0.1		0.5	0.1
Ti	10		3	100SQ
Tl	0.02		0.5	0.1
Tm				0.1
U	0.1	0.5	1	0.1
V	2			1
W	0.2	1	1	1
Y			5	0.5
Yb		0.5	1	0.1
Zn	0.1	50	20	10
Zr			5	1

SURVEY AREAS

Mouse Mountain

Soil profiles were sampled over part of the Mouse Mountain mineral occurrence (MINFILE 093G 003), a property located 10 km east of Quesnel, BC and currently being developed by Richfield Ventures Corp. Undulating topography around Mouse Mountain is typical of the Fraser River basin, where most of the surface below 1200 m is drift covered (Holland, 1976). Mouse Mountain, a prominent uneven rocky ridge rising to 1020 m, with a steeper northwest-facing slope and a gentler southeast-facing slope, could be interpreted as a *roche moutonnée* formed by regional ice flow from the southeast during the late Wisconsinan. Glaciers advanced into the region from both the Coast and Cariboo mountains, resulting in ice-flow events towards the north and northwest, respectively. These ice-flow events were followed by a later northwest advance from the Cariboo Mountains only. Tipper (1971) described north-trending glacial groves as a common glacial landform in the area east of Quesnel and suggested that these features could reflect erosion by one or more glacial advance(s) (or glaciations) across the region. The extent of the last glacial advance into the Mouse Mountain area is uncertain. Glacial sediments deposited on gentler hillsides are typically sandy till, whereas reworked till and colluvium occur on steeper slopes. During final stages of deglaciation, ice blocked the Fraser River and a large proglacial lake filled much of the Fraser River basin. Thick sand and clay units near Prince George are typical of sediments deposited in this lake. Near Mouse Mountain, however, an intermittent thin veneer of sand and gravel could be evidence of the reworking of the underlying till by proglacial lake water (Tipper, 1971).

Undisturbed soil formed on the better drained glacial sediments is mainly a humo-ferric Podzol that supports Douglas-fir, white spruce, lodgepole pine, trembling aspen and paper birch. These are species typical of the Douglas-fir – white spruce ecological subzone (Lord, 1982). Willow, alder and devils club grow densely along valley floors and in wetlands. The area around Mouse Mountain has been extensively logged and there is presently some damage to timber by the mountain pine beetle.

Regional geology of the Mouse Mountain area consists of Triassic arc-related volcanic and sedimentary rocks and Jurassic intrusive complexes (Panteleyev et al., 1996; Logan, 2008). Jonnes and Logan (2007) described the geology, Cu-Au mineralization and alteration of the Mouse Mountain mineral property in detail, so only a summary will be given here. There are three separate northwest-trending zones of pyrite, chalcopyrite, malachite and azurite mineralization within a carbonate-potassic-altered monzonite stock that has intruded Upper Triassic Nicola Group lapilli tuff. Siltstone and pyroxene basalt also crop out on the property. Soil samples were collected along traverses crossing the poorly exposed Rainbow mineralized zone in the northwestern part of the property. Where visible, Cu-Au mineralization at the Rainbow zone consists of disseminated and vein-hosted pyrite, chalcopyrite, malachite and azurite, with traces of fluorite, sphalerite and bornite within ankerite-fuchsite-altered monzonite. Up to 2500 ppm Cu and 100 ppb Au have been reported in rock samples from this zone (Jonnes and Logan, 2007).

Shiko Lake

The Shiko (Redgold) mineral occurrence (MINFILE 093A 058) is a property owned by R. Durfeld and is currently being developed by NovaGold Resources Inc. Detailed soil sampling on this property, located northwest of Shiko Lake, focused on a partly drift-covered, steep-sided ridge 2 km south of Mitchell Bay on Quesnel Lake. The northwest-trending ridge (1020 m) on which the property is situated is typical of the undulating Fraser Plateau to the west and is in contrast to the more rugged Quesnel Highlands (Holland, 1976). Glaciers advanced from the southeast into the region from the Cariboo Mountains, as suggested by rare striations and crescent-shaped rock gouges, with orientations between 280° and 300° (northwest), on ice-polished outcrop. Tipper (1971) described and interpreted various glacial landforms north and west of Quesnel Lake as evidence for two distinct glaciations during the Pleistocene. Given the proximity of Shiko Lake to the Cariboo Mountains, the glacial sediments occurring there are likely the product of the most recent Late Wisconsinan glacial advance (i.e., Fraser Glaciation) and subsequent deglaciation. A predominantly sandy till was deposited that, on steeper slopes, has been mobilized and reworked into colluvium. Sand and gravel deposited during deglaciation have accumulated to a considerable thickness on the floors of major valleys, such as the Horsefly River valley located south of Shiko Lake. Levson and Giles (1993) described an exposure north of Horsefly where a Late Wisconsinan diamicton and glaciofluvial sand and gravel overlie Au-bearing Miocene gravel.

Humo-ferric Podzolic and Brunisolic soils have developed on the better drained sandy till, whereas organic and Gleysolic soils are common in poorly drained depressions. Western red cedar, white spruce and Douglas-fir, lodgepole pine, common paper birch, black cottonwood and trembling aspen form the canopy. Willow, alder and devils club grow thickly in poorly drained areas. The ridge and surrounding area have been extensively logged.

An early Jurassic intrusive complex, which was emplaced in hornfelsed metasedimentary rocks, volcanoclastic rocks and massive plagioclase-pyroxene basalt, dominates the geology of the Shiko Lake property. The intrusive stock consists of an older biotite-pyroxene monzodiorite phase and younger potassium-feldspar syenite and alkaline-feldspar phases. The dominant phase near the centre of the stock is a medium to coarse-grained monzonite containing traces of magnetite, sphene and pyrite. Fine-grained, pink quartz syenite veins and dikes intrude the monzonite and form an intrusive breccia that has a matrix containing chalcopyrite and pyrite. At this mineral occurrence, chalcopyrite, bornite and gold occur in veins and as coarse disseminations, mainly in the youngest quartz syenite but also in the other intrusive phases. Fracture-controlled pervasive potassium alteration and epidote alteration of the volcanoclastic rocks is associated with the Cu mineralization. Earlier potassium and epidote alteration has been cut by late-stage calcite-filled veinlets (Logan and Mihalynuk, 2005). Soil profile sampling focused on the North, Northeast and East zones, where, in addition to recent diamond-drilling, a detailed overburden geochemical survey has been completed by NovaGold Resources Inc.

Soda Creek

Soil profiles were sampled near Soda Creek in an area west of the Fraser River (Fig 1). With gently undulating to flat topography at an elevation of 1000 m, this area has numerous lakes and poorly defined marshy streams. The land surface slopes steeply towards the Fraser River, reflecting erosion of the plateau basalt cover. Tipper (1972) interpreted a few drumlin-like landforms, visible on air photographs, as indicating a northward ice-flow event during the Late Wisconsinan Fraser Glaciation. Till, exposed in roadcuts, has a silty clay matrix and, in one section sampled, is carbonate rich. Soils are predominantly Brunisolic and organic, and support mainly white spruce, Douglas-fir and lodgepole pine.

The Eocene to Pleistocene Chilcotin Group plateau basalt, covering Permian to Triassic Cache Creek marine sedimentary and volcanic rocks, underlies the area surveyed. The thickness of the Chilcotin Group in the area around Coyote Lake is unknown, but Mihalynuk (2007) predicted that, close to the Fraser River valley, the thickness of these volcanic rocks may exceed 100 m.

PRELIMINARY RESULTS

Threshold Values

Mean, median, quartile and percentiles calculated from aqua regia digestion – ICP-MS analyses of 158 upper B and lower B-horizon samples are listed in Table 2. Soil Cu and Au results have been contoured with Manifold GIS software to create sections across the surveyed areas using median and quartile values for contour intervals. Quartiles, as opposed to percentiles, have been used because they are a more robust statistic when the data are suspected to contain several populations. For example, upper B, lower B and C-horizon geochemistry can be expected to represent separate data populations and, ideally, different anomaly thresholds should be calculated for each horizon. The difference between upper B and lower B-horizon geochemistry is demonstrated using the T statistic, which compares the means of the datasets for each element in the two horizons. The T statistic is calculated from the pooled variance and the means from element values for 79 upper B and 79 lower B-horizon samples (Davis, 1973). Table 3 lists the T

TABLE 2. STATISTICS FOR ELEMENTS DETERMINED BY AQUA REGIA – ICP-MS ANALYSIS IN 158 B-HORIZON SAMPLES. THE UPPER FENCE VALUE HAS BEEN CALCULATED BY MULTIPLYING THE DIFFERENCE BETWEEN THE 3RD AND 1ST QUARTILES BY 1.5.

Element	Units	Median	1 st quartile	3 rd quartile	Upper fence	Maxi- mum	Mean	95 th percentile	98 th percentile	99 th percentile
Ag	ppb	73	46.5	129	252.75	580	99.29	228.2	376.2	470.84
Al	%	1.605	1.28	2.33	3.905	3.83	01.79	3.016	3.3086	3.4358
As	ppm	4.4	2.225	6.1	11.9125	13.2	04.45	9.33	10.93	12.288
Au	ppb	1.2	0.225	3.275	7.85	239.1	07.68	28.69	99.394	142.054
Ba	ppm	77.8	63.425	93.275	138.05	304.2	83.66	131.775	203.498	245.51
Bi	ppm	0.09	0.07	0.12	0.195	0.26	00.10	0.17	0.1986	0.2143
Ca	%	0.315	0.24	0.4	0.64	0.88	00.33	0.613	0.713	0.7686
Cd	ppm	0.125	0.08	0.19	0.355	0.69	00.15	0.38	0.4672	0.6045
Co	ppm	12.8	9.425	18.6	32.3625	34.4	14.27	27.115	30.79	32.188
Cr	ppm	47.2	37.225	63.3	102.4125	128.8	53.10	92.98	104.534	119.167
Cu	ppm	29.255	20.105	43.35	78.2175	482.95	48.82	157.9815	246.3706	276.7893
Fe	%	3.06	2.4325	3.8975	6.095	6.79	03.18	4.8365	5.1216	5.9732
Ga	ppm	5	4	6.7	10.75	13	05.45	9.115	10.23	11.229
Hg	ppb	30	17	40.75	76.375	176	33.39	71.75	125.72	130.29
K	%	0.07	0.05	0.11	0.2	0.4	00.09	0.2215	0.2586	0.333
La	ppm	8.3	6.6	10.9	17.35	21.3	09.10	15	17.93	18.931
LOI	%	6.4	4.5	8.5	14.5	22.5	06.72	10.675	13.994	16.648
Mg	%	0.585	0.44	0.81	1.365	1.94	00.65	1.2215	1.303	1.4216
Mn	ppm	294	223.5	375	602.25	2504	333.07	579.75	811.84	936.73
Mo	ppm	0.59	0.4325	0.74	1.20125	6.09	00.74	1.741	2.8504	3.6046
Na	%	0.008	0.006	0.014	0.026	0.035	00.01	0.028	0.029	0.03229
Ni	ppm	32.5	24.75	53.925	97.6875	205	42.80	97.615	116.268	122.919
P	%	0.0685	0.047	0.10125	0.182625	0.235	00.08	0.1616	0.185	0.22001
Pb	ppm	4.685	4.035	5.875	8.635	15.35	05.22	9.576	10.6248	11.5679
S	%	0.01	-0.01	0.01	0.04	0.05	00.00	0.02	0.03	0.0343
Sb	ppm	0.195	0.1425	0.39	0.76125	0.76	00.26	0.5315	0.6072	0.7001
Sc	ppm	3.2	2.7	4.2	6.45	11.9	04.07	10.015	11.272	11.615
Se	ppm	0.3	0.2	0.4	0.7	1.7	00.29	0.6	0.872	0.9
Sr	ppm	24.2	18.125	29.675	47	87.6	25.89	44.305	65.984	70.367
Te	ppm	0.02	-0.02	0.03	0.105	0.14	00.01	0.06	0.1086	0.13
Th	ppm	2	1.4	2.6	4.4	5.6	02.19	4.2	4.572	4.843
Ti	%	0.083	0.065	0.1155	0.19125	0.637	00.10	0.1777	0.28906	0.44421
Tl	ppm	0.06	0.05	0.0775	0.11875	0.19	00.06	0.1	0.11	0.1329
U	ppm	0.4	0.3	0.4	0.55	1.6	00.39	0.6	0.6	1.5
V	ppm	61	49	71	104	155	61.91	98.45	122.16	130.58
W	ppm	-0.1	-0.1	0.1	0.4	0.7	-00.03	0.2	0.286	0.3
Zn	ppm	72	56.325	85.675	129.7	160.4	73.53	117.655	139.336	151.49

statistic at the 90% confidence level, together with the upper B and lower B means for each element. At the 90% confidence level, for a sample size of 79, a T statistic greater than 2 indicates that there is a significant difference between population means. Most elements (including Cu and Au) do have a T statistic that is greater than 2, although Mo, Ag, Pb and Mn have T statistics less than 2, so there may be no significant difference between their means. An interpretation of these results might be that, although the difference between the population means for upper B and lower B elements is small, there is a significant difference in the soil chemistry for many of the elements. This difference could be the result of different soil-forming processes active in the two horizons and also the presence or absence of metals introduced from mineralized bedrock. Care is needed when collecting samples from soil profiles to avoid the misleading geochemical trends that are introduced by

TABLE 3. T STATISTICS FOR ELEMENTS DETERMINED BY AQUA REGIA – ICP-MS ANALYSIS IN UPPER AND LOWER B-HORIZON SAMPLES. DATA FROM ALL SAMPLE AREAS WERE USED TO CALCULATE THE STATISTICS REPRESENTED HERE.

Element	Units	Upper B horizon mean	Lower B horizon mean	T statistic
Ag	ppb	103.76	99.29	2.03
Al	%	1.68	1.79	6.56
As	ppm	4.01	4.45	6.27
Au	ppb	5.01	7.68	3.96
Ba	ppm	86.52	83.66	3.17
Bi	ppm	0.10	0.10	0.12
Ca	%	0.31	0.33	5.81
Cd	ppm	0.17	0.15	5.53
Co	ppm	12.77	14.27	9.70
Cr	ppm	48.89	53.10	7.89
Cu	ppm	40.61	48.82	5.43
Fe	%	2.97	3.18	8.73
Ga	ppm	5.32	5.45	2.82
Hg	ppb	32.33	33.39	1.65
K	%	0.09	0.09	4.29
La	ppm	8.46	9.10	7.67
LOI	%	7.05	6.72	4.55
Mg	%	0.57	0.65	11.67
Mn	ppm	336.13	333.07	0.54
Mo	ppm	0.71	0.74	1.49
Na	%	0.01	0.01	3.49
Ni	ppm	35.73	42.80	10.59
P	%	0.08	0.08	0.78
Pb	ppm	5.20	5.22	0.36
S	%	0.00	0.00	2.25
Sb	ppm	0.25	0.26	4.43
Sc	ppm	3.54	4.07	8.82
Se	ppm	0.27	0.29	4.89
Sr	ppm	24.17	25.89	5.96
Te	ppm	0.01	0.01	1.57
Th	ppm	1.96	2.19	9.42
Ti	%	0.09	0.10	3.20
Tl	ppm	0.06	0.06	5.60
U	ppm	0.36	0.39	6.70
V	ppm	58.76	61.91	6.05
W	ppm	-0.03	-0.03	0.19
Zn	ppm	78.12	73.53	7.61

mixing sample populations (e.g., different sample media from different sample depths).

Element Associations

Correlation matrices were calculated from element data for upper B, lower B and C-horizon samples from the Mouse Mountain and Shiko Lake areas, to examine variations of element association between soil horizons. The Soda Creek area was excluded because there is no confirmed source of metal for any geochemical variations in the soil. Strong (less than +0.70 coefficient) element correlations are revealed between Cu, Co, Fe, Au, W and Se in the C horizon (53 samples); between Cu, Ag, Fe, Au, W and Se in the lower B horizon (53 samples); and between Cu, V, Al, Sc and Ga in the upper B horizon (58 samples). The element associations show that there has been only slight modification of the parent glacial sediment (till) geochemistry into the lower part of the soil profile, but more redistribution of elements due to soil-forming processes in the upper part of the soil.

Mouse Mountain Results

Soil profiles were sampled at 11 stations along traverses north and south of Highway 26. Figure 3 shows the location of profiles across the Mouse Mountain Rainbow mineralized zone. The variation of Cu and Au in the soil over the Rainbow zone is displayed as contoured sections in Figures 4 and 5. Copper values generally increase with depth from the B to the C horizon, and the highest values are in the C horizon towards the east end of the traverse. Increased Cu in the soil from the B to the C horizon may partly reflect a higher metal content in the <0.063 mm fraction of the glacial sediment compared to that in the <0.180 mm fraction in B-horizon soil. At profile 7, there is a C-horizon Cu anomaly (up to 123 ppm) with elevated Ag, V and Hg, and up to 16 ppb Au. The B-horizon pH tends to increase from the upper B to the lower B, with most values being above pH 6. Towards the east end of the traverse, however, where Cu and Au are higher the soil, pH is lower than at profile 6.

Figure 6 shows the locations of eight vertical profiles along logging roads south of Highway 26, an area underlain by geology similar to that at Mouse Mountain. The aim of sampling this area was to compare soil geochemistry with a region remote from Mouse Mountain and that is thought to be unmineralized. Figure 7 shows that the highest Cu (89.9 ppm) in the C horizon at profile 40 is associated with elevated V and Co and the lowest B-horizon pH values (5.47) measured along the traverse. While there are background levels of Cu in profile 39 to the west, the Hg content of the C horizon reaches 482 ppb. Gold values in the soil west of profile 40 are below 5 ppb. However, to the east in profile 44, the Au content of the lower B horizon increases to 24 ppb (Fig 8). Lower values were detected in the underlying C horizon. The higher Au and Cu in profiles could reflect an undetected Cu-Au-mineralized source to the south of the traverse.

Shiko Lake

Figure 9 shows the locations of 30 vertical profiles on the Shiko Lake property, where soil samples were taken. The Cu and Au geochemistry for only five of these profiles will be described here because they show element varia-

tions parallel to the regional ice-flow direction (i.e., in the down-ice direction). In addition to the analytical results generated by this study, there is a large database of bedrock, overburden and soil geochemical results generated by NovaGold Resources exploration work on and around the property. Although these company data will be used in conjunction with new analyses from this study when they are available, they will only be used at this time to identify apparent element associations in bedrock and till, and to corroborate the trends observed in selected soil profiles. For example, an element correlation matrix from data for 486 company analyses of overburden samples collected greater than 1 m below the surface reveals an association (coefficient greater than +0.45) between Cu, V and Co, and between Ag, Cd and Pb.

Figure 10 shows Cu variation in soil between profiles 56 and 59. The highest Cu recorded is 1096 ppm in the C horizon of profile 60 at the southeastern end of the traverse. In this profile, Cu values increase from 155 ppm in the upper B horizon to 1096 ppm in the C horizon. A com-

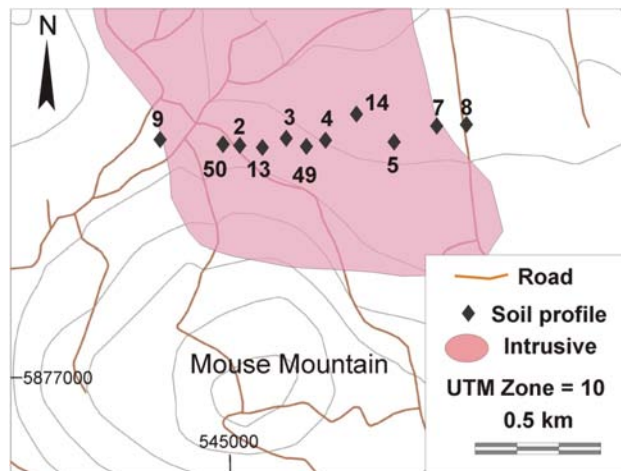


Figure 3. Soil profile locations over the Rainbow zone, Mouse Mountain (geology after Jonnes and Logan, 2007).

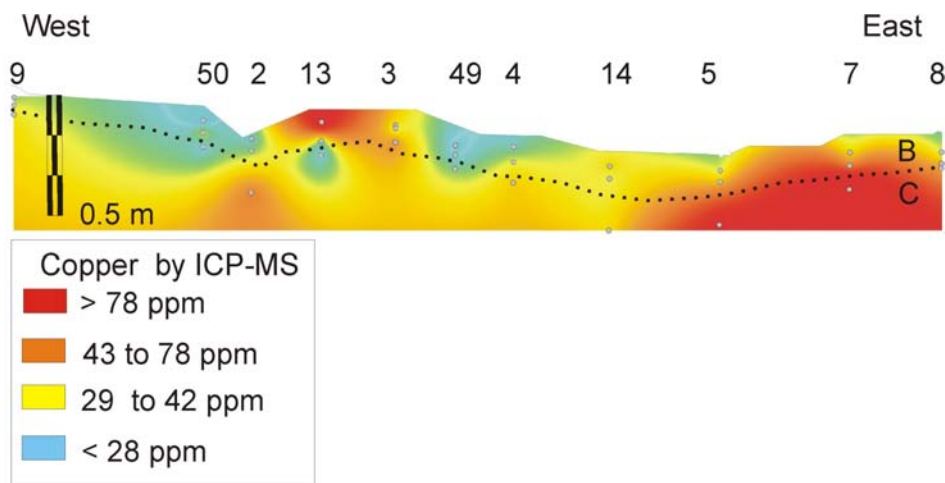


Figure 4. Contoured Cu in soil over the Rainbow zone, Mouse Mountain.

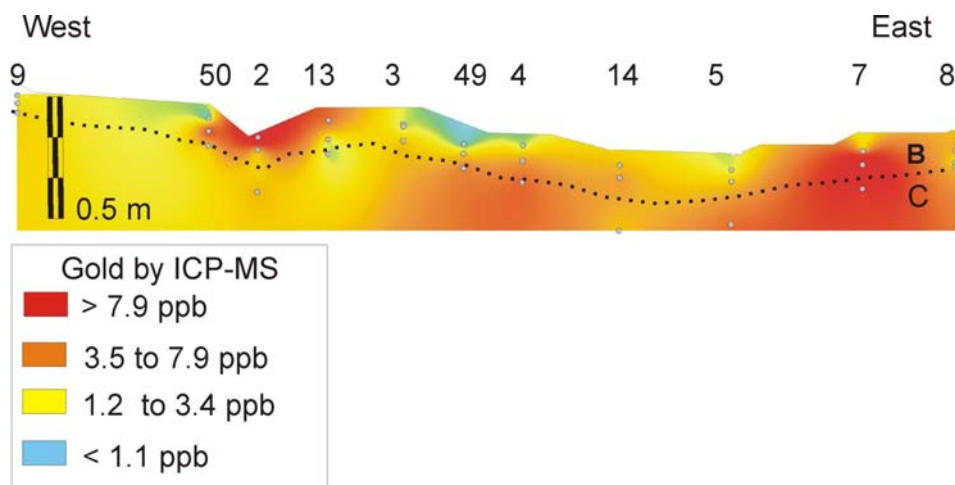


Figure 5. Contoured Au in soil over the Rainbow zone, Mouse Mountain.

pany overburden sample (S-28-18-6), taken near profile 60, contained 487 Cu and 69 ppb Au at 1 m depth. Both lower B and C-horizon samples at profile 60 also have elevated Ag, Co, V and W, with up to 244.8 ppb Au in the C horizon. Element concentrations fall sharply from profile 60 to 62, and Cu values are typically below 120 ppm for soil sampled northwest of profile 62. Gold values, shown in Figure 11, are more variable along the traverse and reach a maximum 156 ppb in the lower B horizon at profile 56. This maximum Au value corresponds to the highest Cu content in the soil.

Soda Creek

Soil samples were taken from vertical profiles located at intervals of about 1 km along two traverses that paralleled forestry access roads east and north of Yorston and Coyote lakes (Fig 12). Soil profiles were sampled to determine if the source of a government regional geochemical survey (RGS) Cu-Ni anomaly in stream sediments collected from Coyote Creek (Jackaman, 2001) could be detected. Copper content in the original stream sediment sam-

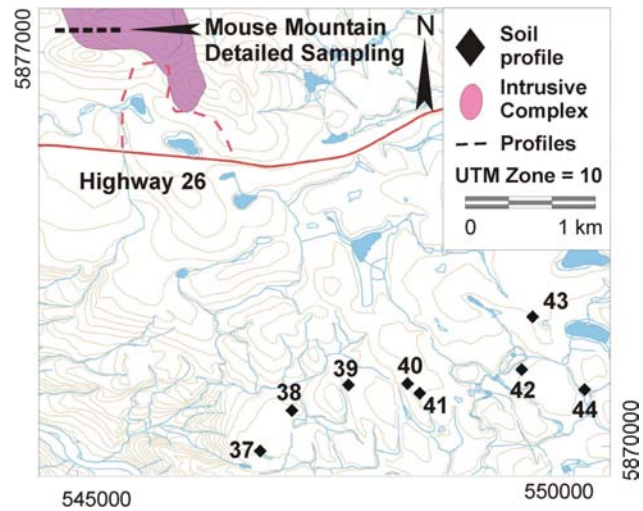


Figure 6. Locations of soil profiles in the area south of Highway 26.

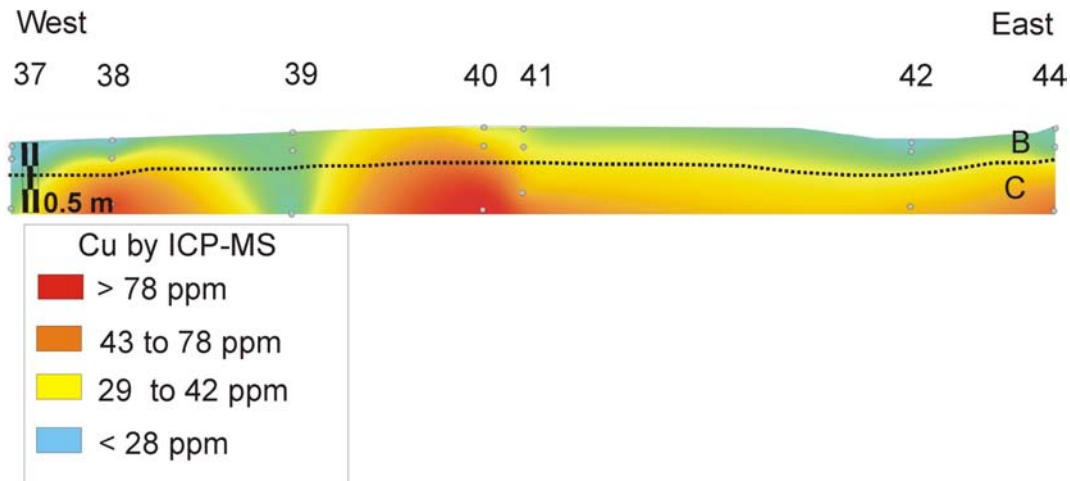


Figure 7. Contoured Cu in soil from profiles south of Mouse Mountain.

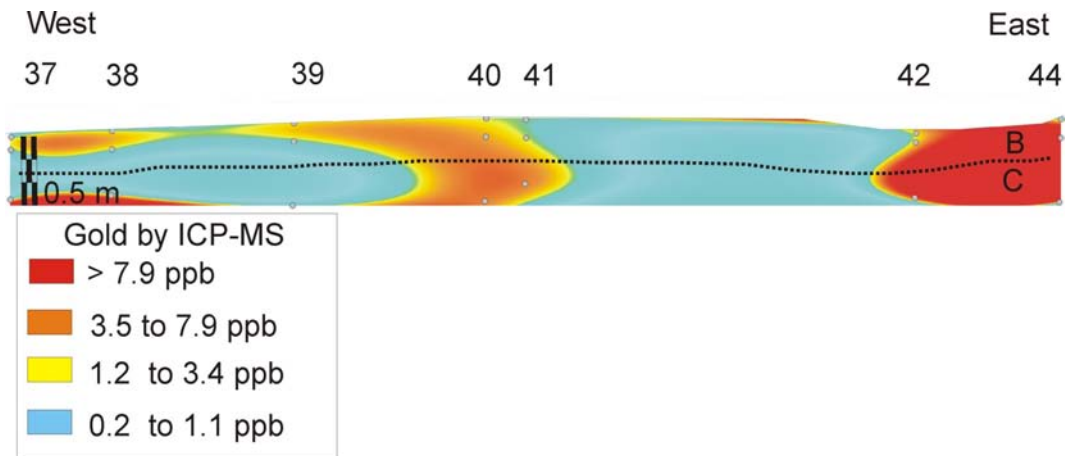


Figure 8. Contoured Au in soil from profiles south of Mouse Mountain.

ple (93B805009) was 164 ppm and the Ni content was 190 ppm. A stream sediment sample collected as part of this study from roughly the same stream site and analyzed by a similar method (<0.180 mm size fraction and aqua regia digestion – ICP-MS) contained 33.4 ppm Cu and 72.6 ppm Ni. Although the sediment has only background Cu values, it still has anomalous Ni as defined by Jackaman (2001) for the NTS 93B regional survey 95th percentile. Part of the geochemical variation between the two samples may be due to the high organic content of the sediment and the stagnant character of the stream. Weathered vesicular basalt boulders lined the stream reach that was sampled, and weathering of these boulders could contribute some of the Cu and Ni to the sediment. Soil profile sampling was also aimed at detecting a possible northwest mineral-rich trend revealed by contoured RGS Cu values. This trend extends beneath the plateau basalts from Quesnel Terrane rocks in the east.

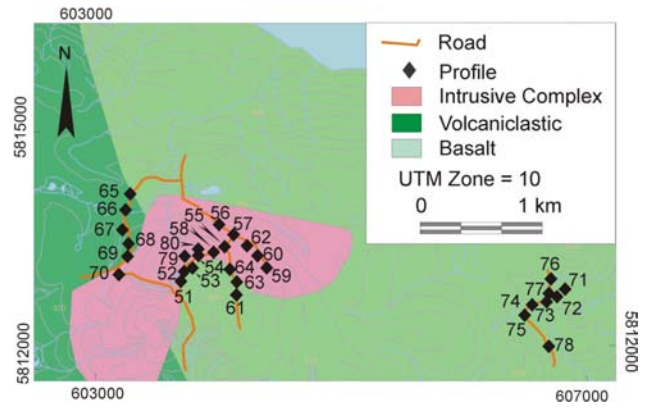


Figure 9. Soil profile locations over the Shiko Lake property (geology after Massey et al., 2005).

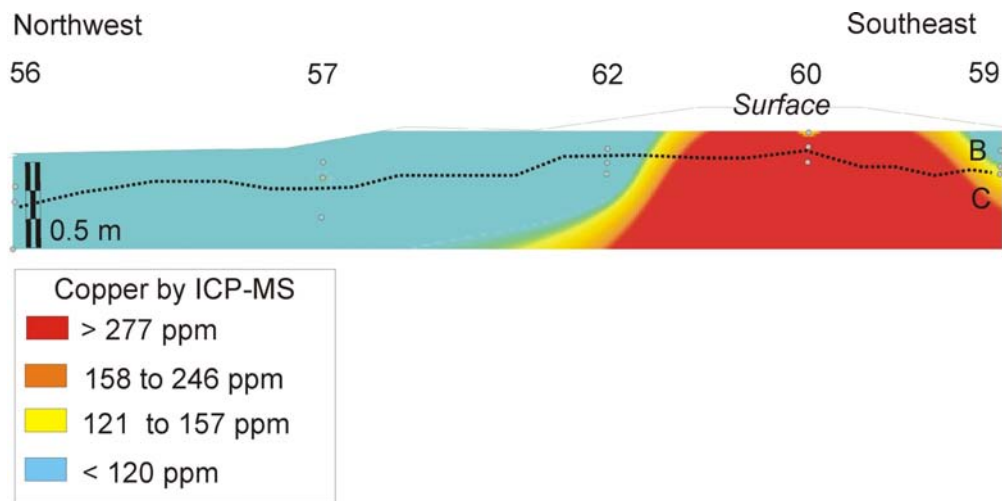


Figure 10. Contoured Cu in soil between profiles 56 and 59, Shiko Lake.

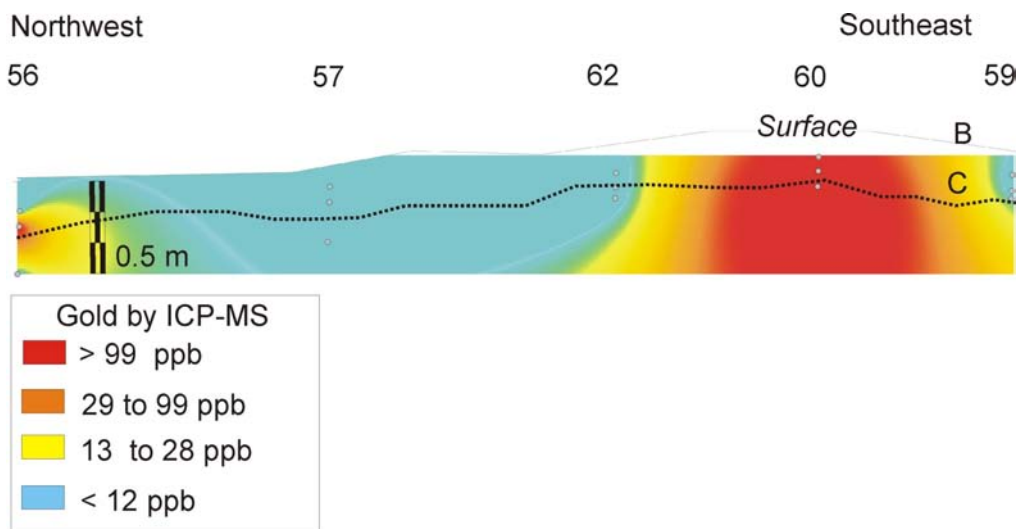


Figure 11. Contoured Au in soil from between profiles 56 and 59, Shiko Lake.

Figures 13 and 14 show contoured soil Cu and Ni along the north-south traverse. Copper is relatively uniform along the traverse and the highest value (50.1 ppm) occurs in the C horizon at profile 20. There is more variation in Ni, however, and values reach 124.9 ppm in the lower B horizon at profile 23. The anomalous Ni is associated with elevated Cr, Fe and Mg, suggesting that the source for these metals may be ultramafic rock incorporated in the till from a source area to the south. Soil pH values range from 5.26 in the upper B horizon to 7.11 in the lower B, and there is no obvious relationship between Ni and Cu chemistry and soil pH. There are no significant changes in Cu and Ni values in soil along the east-west traverse (profiles 10–19 in Fig 11), although the highest Ni value from this study (102.7 ppm) occurs in the C horizon at profile 19. Most Ca values in soil (from either traverse) are below 0.5%, but elevated Ca (2.81%) in the C horizon at profile 11 corresponds to a strong soil reaction with dilute (10%) hydrochloric acid. This Ca-rich C horizon could be till derived from Cache Creek Group rocks to the south.

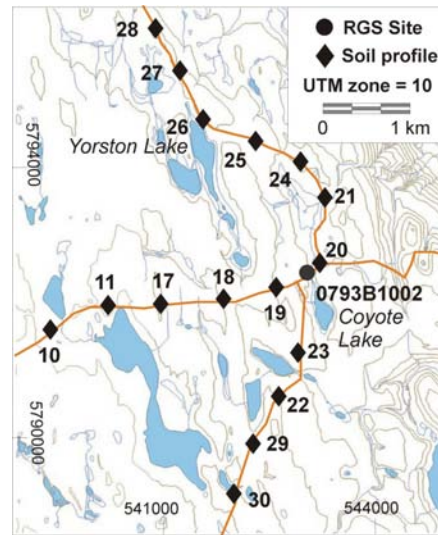


Figure 12. Profile locations in the Yorston and Coyote lakes (Soda Creek) area. Abbreviation: RGS, regional geochemical survey.

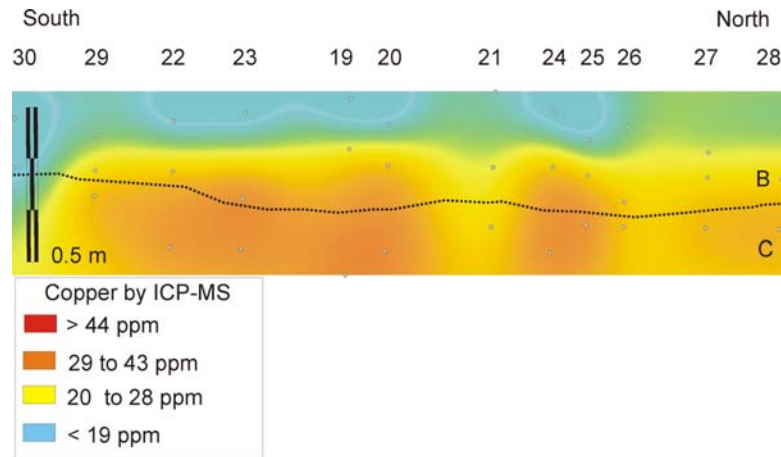


Figure 13. Contoured Cu in soil along a north-south traverse, Yorston and Coyote lakes (Soda Creek) area.

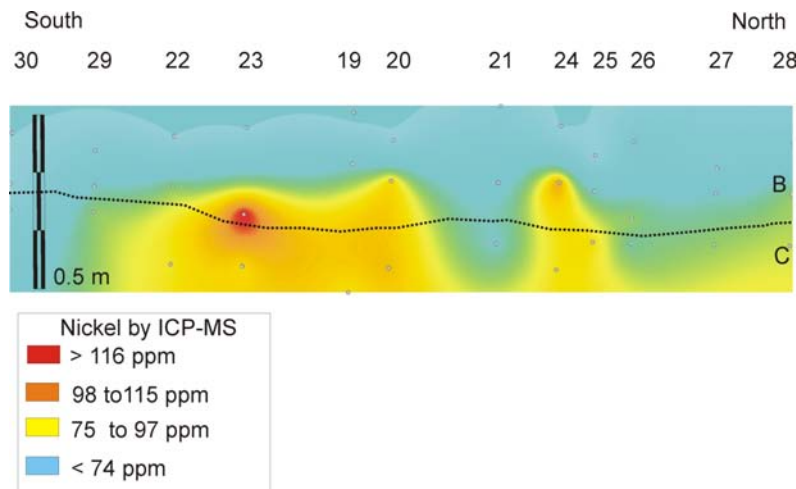


Figure 14. Contoured Ni in soil along a north-south traverse, Yorston and Coyote lakes (Soda Creek) area.

DISCUSSION

There will only be a preliminary discussion of geochemical results in this paper because various analyses (e.g., Enzyme LeachSM, Soil Gas HydrolysisSM and Mobile Metal IonSM) are still pending, and these additional data are necessary for a full interpretation of the soil geochemistry within the areas studied. An association of Cu and Au with Ag, V±W and ±Co in the lower B and C horizons at Mouse Mountain and Shiko Lake most likely reflects detrital transport in till of material from mineralized bedrock. At Mouse Mountain, the regional ice flow is from the south and, at Shiko Lake, it is from the southeast. Although sampling at Mouse Mountain has not been sufficient to define the extent of a till dispersal train, the soil sampling at Shiko Lake, coupled with an examination of results from a company till program, suggest that dispersal trains are relatively short and perhaps less than 0.5 km. Levson (2001) reported a displacement distance of less than 100 m for near-surface geochemical anomalies in areas where the till thickness was less than 1 m, whereas the anomalies in thicker till could be displaced more than 500 m from their bedrock source. Given the regional ice-flow direction, the Cu-Au-V-Co anomaly in the C horizon south of Mouse Mountain is intriguing because it suggests a presently unknown mineral source to the south in Nicola Group rocks. Near Yorston and Coyote lakes, west of Soda Creek, the anomalous Ni values in soil are most likely caused by ultramafic rock entrained in the till and transported from the Cache Creek Group to the south.

A provisional model is proposed here for the transport of elements from bedrock into soil based on the geochemical patterns revealed in the soil profiles. The lower B horizon is a product of the underlying C horizon (till), so the geochemistry of the lower B horizon is most closely related to this lowermost horizon. Redistribution of elements in the upper B horizon by soil-forming processes explains the geochemical difference between the upper and lower B horizons. The upper B horizon is the part of the soil profile where adsorption of elements to secondary minerals (e.g., Fe and Mn oxides) is most active. Hence, reagents that selectively remove metal bound to oxide and other minerals will be most effective for enhancing anomaly contrast and for detecting subtle geochemical changes caused by the presence of mineralized material. Superimposed on the soil chemistry (that is related to dispersal of metals in till) may be a secondary signature of near-vertical migration of volatile elements such as halogens or halogen-metal complexes (Cook and Dunn, 2007). Figure 15 is a provisional model showing the relationship between these various element dispersion pathways. In the model, Cu, Ag, Au, W, V, Co, Se and Hg from porphyry-style mineralization beneath till contribute to a detrital dispersal train down-ice from the source of mineralized material. The vertical projection of mineralized subcrop onto the till layer is shown with the expected trace of volatile components migrating upward from bedrock. Both of the patterns are reflected in the lower B-horizon layer, but the soil anomaly related to till geochemistry in the upper B horizon is more dispersed and larger. The model has not attempted to predict different element mobility in response to changing soil pH.

CONCLUSIONS

- Anomalous Cu and Au with Ag, V±W and ±Co in the C and lower B horizons appears to reflect bedrock Cu-Au mineralization.
- Differences between lower and upper B-horizon soil chemistry have implications for soil sampling during routine geochemical surveys. The lower B horizon (generally more than 20 cm below the surface litter horizon) is more effective for detecting mineralized bedrock dispersed in till, as it is the derivative of this lowermost horizon. The shallow upper B horizon, however, is most commonly sampled, even though metal concentrations in this horizon are less related to those in underlying till (first derivative of bedrock), since they are more the result of various soil-forming and hydromorphic processes. The lower B and C horizons and till are preferred for routine soil surveys, provided that the genesis of the parent glacial material can be interpreted with confidence (including transport direction), and colour and texture variations down soil profiles can be recognized in the field.
- A provisional model for element dispersion from Au-Cu porphyry mineralization into soil presented here distinguishes between geochemical anomalies that could form by ice-transported material (i.e., detrital transport) and elements that may have migrated as volatile compounds. Further sample analyses for elements and organic compounds will focus on confirming this model. Results of this research will be published as a British Columbia Geological Survey GeoFile in 2008.

ACKNOWLEDGMENTS

Sheila Jonnes is sincerely thanked for generously guiding the authors on the Mouse Mountain property. Permission to collect samples on this property from Peter Bernier, President, Richfield Ventures Corp., is very much appreciated. Scott Petsel, NovaGold Resources Inc., and Rudi Dufeld willingly allowed access to the Shiko Lake property for sampling and are thanked for encouraging the fieldwork. The Geological Survey of Canada very gener-

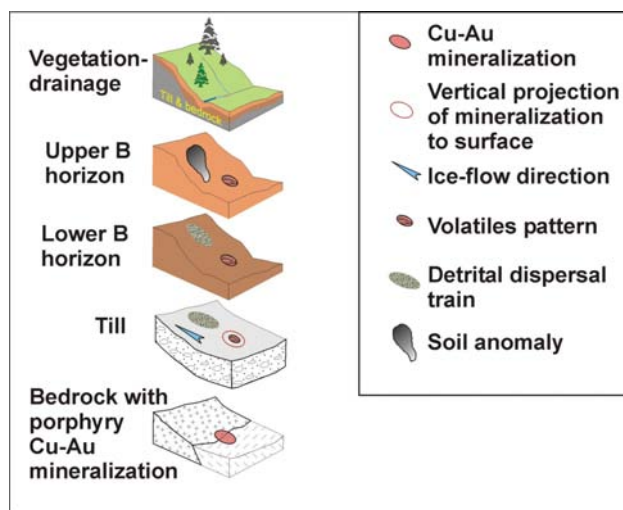


Figure 15. Provisional model for the transport of elements from mineralized bedrock into soil.

ously funded much of the sample preparation and analysis. Critical reviews of a draft of this paper by Travis Ferbey and Tania Demchuk are very much appreciated.

REFERENCES

- Bradshaw, P.M.D. (1975): Conceptual models in exploration geochemistry: the Canadian Cordillera and Canadian Shield; *Journal of Geochemical Exploration*, Volume 4, Number 1, 223 pages.
- Butt, C.R.M., Robertson, I.D.M., Scott, K.M. and Cornelius, M. (2005): Regolith expression of Australian ore systems; *Co-operative Research Centre for Landscape Environmental and Mineral Exploration* Publication, 424 pages.
- Canada Soil Classification Working Group (1998): The Canadian system of soil classification, 3rd Edition; *National Research Council Press*, Ottawa, Ontario, 187 pages.
- Cameron, E.M., Hamilton, S.M., Leybourne, M.I., Hall, G.E.M. and McClenaghan, M.B. (2004): Finding deeply buried deposits using geochemistry; *Geochemistry: Exploration, Environment, Analysis*, Volume 4, pages 7–32.
- Clark, J.R. (1999): Concepts and models for interpretation of Enzyme Leach data for mineral and petroleum exploration; in *Geoanalysis: With Emphasis on Selective Extractions*, 19th International Geochemical Exploration Symposium, Short Course, April 10, 1999, Vancouver, BC.
- Cook, S.J. and Dunn, C.E. (2007): A comparative assessment of soil geochemical methods for detecting buried mineral deposits: 3Ts epithermal Au-Ag prospect, central British Columbia, Canada; *Geoscience BC Report 2007-7*, 130 pages.
- Davis, J.C. (1973): *Statistics and data analysis in geology*; John Wiley and Sons, 550 pages.
- Hall, G.E.M. (1998): Analytical perspective on trace element species of interest in exploration; in *Journal of Geochemical Exploration Special Issue on Selective Extractions*, Hall, G.E.M. and Bonham-Carter, G.F., Editors, Volume 61, pages 1–9.
- Hoffman, S.J. and Perkins, D. (1990): Report on the Cat and Betty mineral claims: geology, geochemistry, geophysics and drill exploration; *BC Ministry of Energy, Mines and Petroleum Resources*, Assessment Report 19956, 383 pages.
- Holland, S.S. (1976): Landforms of British Columbia — a physiographic outline; *BC Ministry of Energy, Mines and Petroleum Resources*, Bulletin 48, 138 pages.
- Jackaman, W. (2001): British Columbia regional geochemical survey, NTS 93B — Quesnel; *BC Ministry of Energy, Mines and Petroleum Resources*, RGS 6/54 and *Geological Survey of Canada*, Open File 777, 138 pages.
- Jonnes, S. and Logan, J.M. (2007): Bedrock geology and mineral potential of Mouse Mountain, central BC; in *Geological Fieldwork 2006*, *BC Ministry of Energy, Mines and Petroleum Resources*, Paper 2007-1 and *Geoscience BC*, Report 2007-1, pages 55–66.
- Lett, R.E.W. and Bradshaw, P. (2002): Atlas of landscape geochemical models for porphyry copper, VMSD and gold deposits in the Cordillera from Alaska to Nevada; *Association of Exploration Geochemists*, *Explore* (newsletter), Number 118, pages 20–23.
- Levson, V.M. and Giles, T.R. (1993): Geology of Tertiary and Quaternary gold-bearing placers in the Cariboo region, British Columbia (93A, B, G and H); *BC Ministry of Energy, Mines and Petroleum Resources*, Bulletin 89, 201 pages.
- Levson, V.M. (2001): Regional till geochemical surveys in the Canadian Cordillera: sample media, methods and anomaly evaluation; in *Drift Exploration in Glaciated Terrain*, McClenaghan, M.B., Bobrowsky, P.T., Hall, G.E.M. and Cook, S.J., Editors, *Geological Society*, Special Publication 185, pages 45–68.
- Logan, J.M. (2008): Geology and mineral occurrences of the Quesnel Terrane, Cottonwood map sheet, central British Columbia (NTS 093G/01); *BC Ministry of Energy, Mines and Petroleum Resources*, Paper 2008-1, pages 69–86.
- Logan, J.M. and Mihalynuk, M.G. (2005): Regional geology and setting of the Cariboo Bell, Springer and Northeast porphyry Cu-Au zones at Mount Polley, south-central British Columbia; in *Geological Fieldwork 2004*, *BC Ministry of Energy, Mines and Petroleum Resources*, Paper 2005-1, pages 249–270.
- Lord, T.M. (1982): Soils of the Quesnel area, British Columbia; *Agriculture Canada*, British Columbia Soil Survey Report 31, 93 pages.
- Lord, T.M. (1984): Soils of the Horsefly area, British Columbia; *Agriculture Canada*, British Columbia Soil Survey Report 32, 108 pages.
- Mann, A.W., Birrell, R.D., Mann, A.T., Humphreys, D.B. and Perdix, T. (1998): Application of mobile metal ion technique to routine geochemical exploration; in *Journal of Geochemical Exploration Special Issue on Selective Extractions*, Hall, G.E.M. and Bonham-Carter, G.F., Editors, Volume 61, pages 87–102.
- Massey, N.W.D., MacIntyre, D.G., Desjardins, P.J. and Cooney, R.T. (2005): Digital map of British Columbia; *BC Ministry of Energy, Mines and Petroleum Resources*, GeoFile 2005-1.
- Mihalynuk, M.G. (2007): Neogene and Quaternary Chilcotin Group cover rocks in the Interior Plateau, south-central British Columbia: a preliminary 3-D thickness model; in *Geological Fieldwork 2006*, *BC Ministry of Energy, Mines and Petroleum Resources*, Paper 2007-1 and *Geoscience BC*, Report 2007-1, pages 143–147.
- Panteleyev, A., Bailey, D.G., Bloodgood, M.A. and Hancock, K.D. (1996): Geology and mineral deposits of the Quesnel River – Horsefly map area, central Quesnel Trough, BC; *BC Ministry of Energy, Mines and Petroleum Resources*, Bulletin 97, 156 pages.
- Tipper, H.W. (1971): Glacial geomorphology and Pleistocene history of central British Columbia; *Geological Survey of Canada*, Bulletin 196, 89 pages.
- Yeager, J.R., Clarke, J.R., Mitchell, W. and Renshaw, R. (1998): Enzyme Leach anomalies associated with deep Mississippi Valley – type zinc ore bodies in the Elmwood Mine, Tennessee; in *Journal of Geochemical Exploration Special Issue on Selective Extractions*, Hall, G.E.M. and Bonham-Carter, G.F., Editors, Volume 61, pages 103–112.

Towards a Drainage Geochemical Atlas of British Columbia

by R.E. Lett, E.C. Man and M.G. Mihalynuk

KEYWORDS: regional geochemical surveys, contouring, geochemical atlas

INTRODUCTION

Drainage geochemical surveys utilize a combination of water and stream or lake sediment media collection and chemical analysis for rapid and effective evaluation of mineral resources within fluvial catchment areas. Low-density surveys (typically at a density of one sample site per $\sim 10 \text{ km}^2$) are a cost-effective method for regional mineral exploration covering thousands of square kilometres. Drainage geochemical surveys are based on the principal that the bedrock and surficial geology underlying the drainage catchment area upstream from a sample site will be reflected in the sediment chemistry. Background element variations in drainage sediment can characterize the source bedrock geochemistry and may outline metallogenic belts. Elevated metal contents may indicate mineralized bedrock or rock types that are the potential hosts of economic mineral deposits. However, low density (e.g., an average of one sample per 13 km^2 in British Columbia) sampling is not sufficient to detect all mineral deposits unless their surface exposure is substantial.

Internationally, regional surveys for geochemical mapping, metallogenic studies and mineral exploration have been carried out by governments and mining companies for over 30 years. Darnley (1990) reported on the beginning of an international geochemical mapping (IGM) project in 1988 that was sponsored by the International Union of Geological Sciences and UNESCO. Since then, there have been more examples of national mapping surveys from many countries, including the United Kingdom (Plant et al., 1989, 1997), Greenland (Steenfeld, 1993) and China (Xie and Ren, 1993). The results of national geochemical surveys are commonly displayed in the form of an atlas that shows the spatial distribution of elements as either symbol or contour maps. One of the first of these to be produced was the Wolfson *Geochemical Atlas of England and Wales* (Webb, 1978); since then, there have been several others, such as the *Geochemical Atlas of Alaska* (Weaver, 1983).

Much of British Columbia is a mountainous terrain with numerous rivers, an ideal physiography for the application of drainage geochemical mapping. Consequently, the BC Geological Survey started a regional stream sediment and stream water geochemical survey (RGS) in 1976 as part of the Geological Survey of Canada's National Geochemical Reconnaissance Program (NGR). Since its incep-

tion, 70% of the province has been surveyed, with the collection and multi-element analysis of more than 50 000 stream sediment, lake sediment and surface water samples at an average density of one sample per 13 km^2 . Since 2006, Geoscience BC has contributed to the RGS database with information from stream and lake sediment geochemical surveys (e.g., Jackaman, 2006).

With the widespread use of personal computers, multi-element RGS data analysis and spatial analysis have been used to identify regions of high mineral potential. The data have also proven useful for establishing environmental baseline geochemistry.

Advantages of the RGS for geochemical mapping are that 1) few changes have been made to analytical and sample preparation methods since the start of the survey, and 2) strict quality control has been maintained during sample preparation and analysis. Thus, the data from all survey areas can be combined into a relatively seamless geochemical database. This paper reports on the first, comprehensive, province-wide, geochemical atlas products arising from the integration of this database through the use of GIS spatial analysis. The *Geochemical Atlas of British Columbia* (Lett et al., in press) is an ongoing project, with updates of the atlas anticipated as new data come available to augment the stream sediment, moss-mat sediment (moss sediment) and lake sediment results that are distributed over approximately 70% of the province, as shown in Figure 1.

SOURCE DATA

Information used to create the *Geochemical Atlas of British Columbia* has been extracted from the British Columbia Regional Geochemical Survey database, a Microsoft Access® database implemented in the late 1980s and most recently revised in 2007 for the BC Geological Survey's MapPlace portal. Among the database tables used for the atlas are the following:

RGS Sample Location Information: This table has a unique sample identification number that combines NTS map sheet, year and sample number. It also contains a code for the sample type (e.g., 1, stream sediment; 7, moss-mat sediment; 9, lake sediment), location co-ordinates (UTM Zone, northing and easting, datum used [i.e., NAD 83]) and a quality-control sample code identifying field replicate samples. There are presently 56 475 sample locations in the database.

RGS Field Stream Lake: This table has all of the field information for stream sediment, lake sediment and surface water samples. It includes such criteria as water colour, stream depth, stream width, bank composition and sediment texture.

RGS Routine Water: This table includes pH, F and U results from the analysis of surface stream and lake water. For

This publication is also available, free of charge, as colour digital files in Adobe Acrobat® PDF format from the BC Ministry of Energy, Mines and Petroleum Resources website at http://www.em.gov.bc.ca/Mining/Geolsurv/Publications/catalog/cat_fldwk.htm

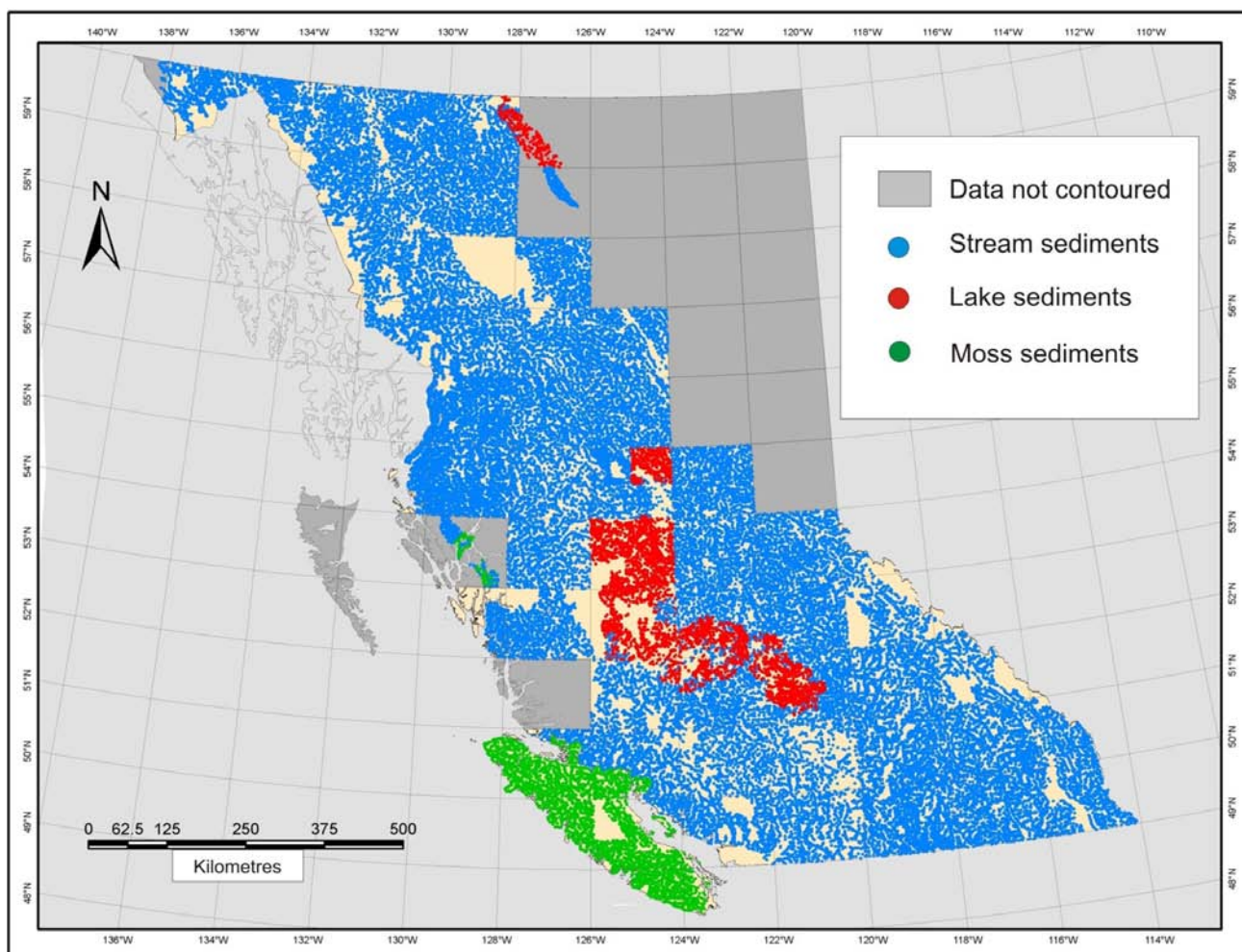


Figure 1. Distribution of stream sediment, moss-mat sediment (moss sediment) and lake sediment geochemical sample sites in British Columbia.

recent surveys (since 2002), water conductivity was also recorded.

RGS Stream Sediment AAS: This table comprises analytical data for stream sediment, moss-mat sediment and lake sediment analyzed by an aqua regia (HCl-NH₃) digestion followed by atomic absorption spectrophotometry (AAS). The table also includes the results for samples analyzed for Au by lead-collection fire assay (FA) and AAS, and for loss-on-ignition at 500°C.

RGS Stream Sediment ICP-MS: This table comprises analytical data for stream sediment, moss-mat sediment and lake sediment analyzed by an aqua regia (HCl-NH₃) digestion followed by inductively coupled plasma – mass spectrometry (ICP-MS).

RGS Stream Sediment INAA: This table comprises analytical data for stream sediment, moss-mat sediment and lake sediment determined by instrumental neutron activation analysis (INAA).

Data Merging — Analytical Methods Comparison

The RGS database comprises analytical results for more than 70 elements determined by a combination of

aqua regia – AAS, aqua regia – ICP-MS and INAA. However, province-wide coverage exists for only 40 of these elements and the data can be used to create maps showing their regional variation. Thirty of the elements are not considered because they are determined by a variety of methods that produce incompatible results. In addition, the data may be limited by high instrumental detection limit, interelement inferences or analysis of only a small number of samples for a particular element (e.g., Sn).

All of the samples have been analyzed for a core group of ore-indicator elements (e.g., Au, Cu, Co, Ni, Pb, Zn), but there exist differences in the detection limits for aqua regia – AAS and aqua regia – ICP-MS, as shown in Table 1. Samples from surveys prior to 1999 were analyzed by aqua regia – AAS, whereas those from more recent surveys were analyzed by aqua regia – ICP-MS, and there are few examples where drainage samples were analyzed by both methods. As a basis for comparison between these two main analytical techniques, 1152 stream sediments from the McLeod Lake regional survey that were initially analyzed by aqua regia – AAS were later reanalyzed by aqua regia – ICP-MS for up to 37 elements, including Cu (Lett and Bluemel, 2006). Near-perfect correlation between the two methods is shown for Cu in Figure 2, where the scatterplot

TABLE 1. INSTRUMENTAL DETECTION LIMITS FOR ELEMENTS DETERMINED BY AQUA REGIA – AAS AND AQUA REGIA – ICP-MS.

Element	Units	ICP-MS	AAS
Ag	ppb	2	100
Al	%	0.01	nd
As	ppm	0.1	1
Au*	ppb	0.2	nd
B	ppm	1	nd
Ba	ppm	0.5	nd
Bi	ppm	0.02	nd
Ca	%	0.01	nd
Cd	ppm	0.01	0.1
Co	ppm	0.1	2
Cr	ppm	0.5	nd
Cu	ppm	0.01	2
Fe	%	0.01	0.01
Ga	ppm	0.2	nd
Hg	ppb	5	5
K	%	0.01	nd
La	ppm	0.5	nd
Mg	%	0.01	nd
Mn	ppm	1	5
Mo	ppm	0.01	1
Na	%	0.001	nd
Ni	ppm	0.1	2
P	%	0.001	nd
Pb	ppm	0.01	2
S	%	0.02	nd
Sb	ppm	0.02	1
Sc	ppm	0.1	nd
Se	ppm	0.1	nd
Sr	ppm	0.5	nd
Te	ppm	0.02	nd
Th	ppm	0.1	nd
Ti	%	0.001	nd
Tl	ppm	0.02	nd
U	ppm	0.1	nd
V	ppm	2	5
W	ppm	0.2	nd
Zn	ppm	0.1	2

shows a strong linear relationship with a correlation coefficient of +0.957. Similar correlation between the original and reanalyzed results for other elements of the McLeod Lake survey, especially those that underwent essentially the same digestion method used since the start of the RGS program, justify the merger of AAS and ICP-MS analytical results into datasets for production of maps for the *Geochemical Atlas of British Columbia*. A modified form of exploration data analysis has been used to compare populations of data produced by different analytical techniques, because few samples from the broader RGS database have been reanalyzed by aqua regia – ICP-MS.

EXPLORATION DATA ANALYSIS

Exploration data analysis (EDA) is designed to detect trends or structures in geochemical data. It involves graphical and numerical techniques that are independent of assumptions about element distributions. In

this way, EDA resolves problems related to the common failure that statistical assumptions have in describing real data, and the overwhelming influence that large populations have on smaller but often significant distributions (Kurzl, 1988). Box plots and Q-Q plots can also be used to compare geochemical data, such as subsets from the RGS database generated by different analytical methods and from different sample media. Pseudo – box plot divisions have been constructed from the following statistical ranges to compare datasets. The divisions are as follows:

Lower fence ($Q1 - 1.5(Q3 - Q1)$) — also known as interquartile range/whisker

First quartile 1

Median

Third quartile 3

Upper fence ($Q3 + 1.5(Q3 - Q1)$) — also known as interquartile range/whisker

Values above or below the fences are considered outliers

Based on the techniques described by Kurzl (1988) and Grunsky (2007), a pseudo – box plot approach has been applied to statistically examine the relationship between the results produced by the different analytical methods. An example of a pseudo – box plot for Cu by AAS and ICP-MS is shown in Figure 3. All of the box plots will accompany maps in the final *Geochemical Atlas of British Columbia* (Lett et al., in press). The graphs can be used to determine if the data need to be levelled with a correction factor so that misleading trends in plotted data are avoided. The first stage of the statistical analysis has been to calculate median, 1st quartile, 3rd quartile, and ‘fence’ values from Pb, Co, V, Fe, Mo, Hg, Sb, Cd, Bi, Zn and Cu results by AAS and ICP-MS. These statistics were plotted as a function of concentration on a simple line graph to produce a pseudo – box plot. In the same fashion, U by delayed neutron counting (NADNC) was compared to U by INAA, and Au by INAA was compared to the data produced by lead-collection fire assay – AAS. Arsenic results by AAS, ICP-MS and INAA were also compared, and the similarity be-

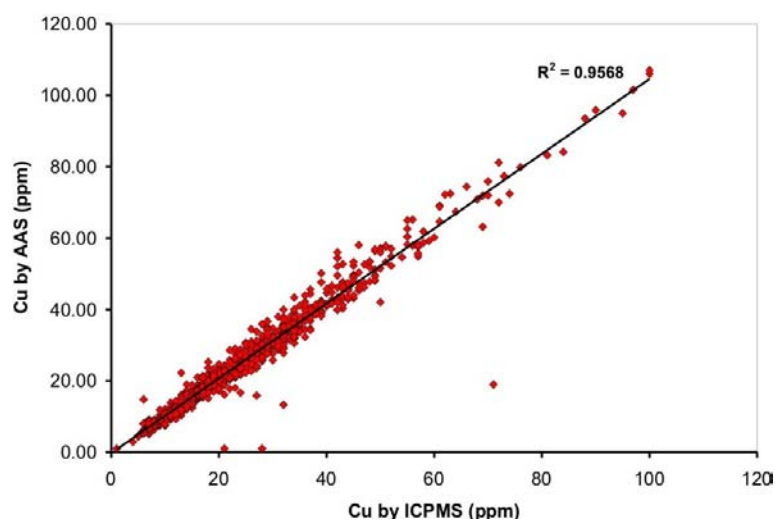


Figure 2. Scatterplot for 1152 stream sediment samples from the McLeod Lake map sheet (NTS 93J) initially analyzed for Cu by aqua regia – AAS and later reanalyzed for Cu by aqua regia – ICP-MS (Lett and Bluemel, 2006). Abbreviations: ppm Cu-AAS, Cu by AAS (ppm); ppm Cu-ICPMS, Cu by ICP-MS (ppm).

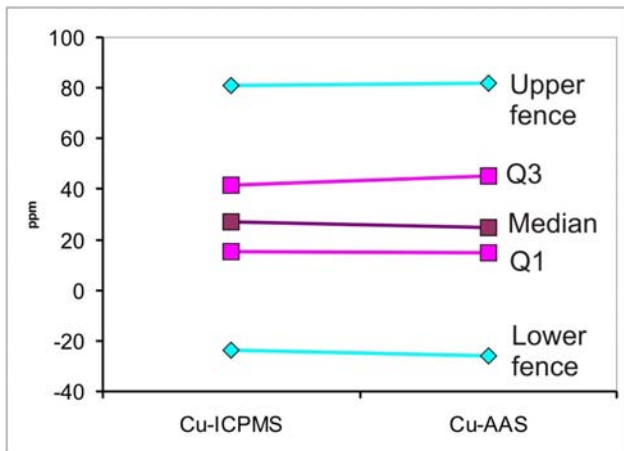


Figure 3. Pseudo – box plot comparing median, quartile and fence values for Cu by AAS and ICP-MS. The graph was prepared from 46 379 AAS determinations and 12 132 ICP-MS determinations. Q1 and Q3 are the 1st and 3rd quartiles, respectively. Abbreviations: Cu_ICPMS, Cu by ICP-MS; Cu_AAS, Cu by AAS.

tween results produced by all three methods justified merging the three datasets. This is the only case where INAA results were merged with aqua regia – ICP-MS/AAS results (Lett et al., in press).

Comparison of pseudo – box plots reveals that most RGS elements have almost identical median and quartile values for AAS, ICP-MS and INAA methods, indicating that no levelling is needed. Consequently, data from the following methods can be merged into a single file for map plotting:

- Pb — AAS with ICP-MS
- Co — AAS with ICP-MS
- U — NADNC with INAA
- V — AAS with ICP-MS
- Au — FA with INAA
- Fe — AAS with ICP-MS
- Mo — AAS with ICP-MS
- Mn — AAS with ICP-MS
- Ni — AAS with ICP-MS
- Hg — AAS with ICP-MS
- As — AAS with ICP-MS or INAA
- Sb — AAS with ICP-MS
- Cd — AAS with ICP-MS
- Bi — AAS with ICP-MS
- Zn — AAS with ICP-MS
- Cu — AAS with ICP-MS

DATA MERGING — SAMPLE MEDIA COMPARISON

Element data for stream sediment, moss-mat sediment and lake sediment were compared using pseudo – box plots in the same way that different analytical methods were treated. Data from the same analytical technique (e.g., aqua regia – AAS) were used to compare two different sample types, such as stream sediment and moss-mat sediment. An example of a pseudo – box plot for Cu in stream sediment

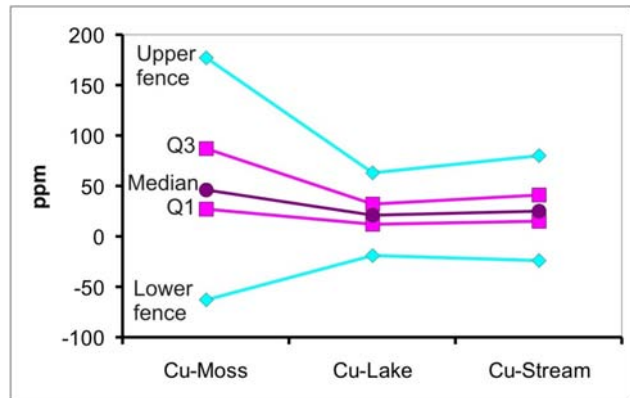


Figure 4. Pseudo – box plot comparing Cu in stream sediment (Cu_Stream) with Cu in moss-mat sediment (Cu_Moss) before levelling. Q1 and Q3 are the 1st and 3rd quartiles, respectively.

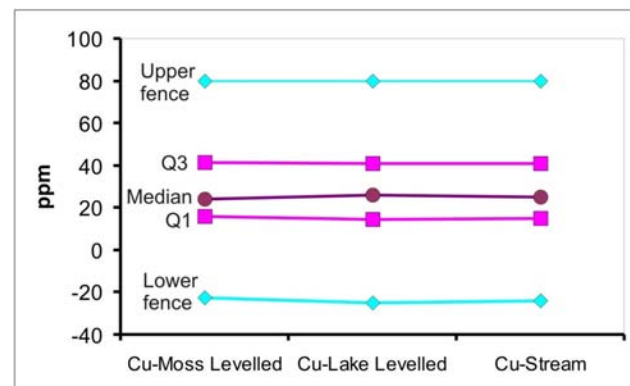


Figure 5. Pseudo – box plot comparing Cu in stream sediment (Cu_Stream Levelled) with Cu in moss-mat sediment (Cu_Moss Levelled) after levelling. Q1 and Q3 are the 1st and 3rd quartiles, respectively.

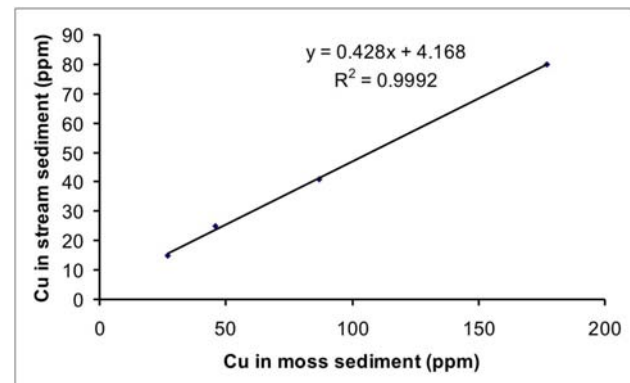


Figure 6. Example of a Q-Q plot for Cu in stream sediment and Cu in moss (moss-mat) sediment.

compared to lake sediment and moss (moss-mat) sediment is shown in Figure 4. Levelling of moss-mat sediment or lake sediment data to stream sediment data was carried out with Q-Q graphs, where the 1st quartile, 3rd quartile, median, lower fence and upper fence for each sample media dataset were plotted on a scatter graph. Least-squares best-

TABLE 2. LEVELLED AND UNLEVELLED CU AND NI VALUES FOR THE PERCENTILES USED FOR CONTOURING IN FIGURES 7, 8, AND 9. ABBREVIATIONS: L, LEVELLED; NL, UNLEVELLED.

Percentile	Cu NL (ppm)	Cu L (ppm)	Ni NL (ppm)	Ni L (ppm)
10	9	9	5	4.68
20	13	13	8	8
30	17	17	12	12
40	21	21	15	16
50	26	25	19	20
60	31	30	24	25
70	38	37	30	31
80	47	46	40	41
85	54	52	48	49
90	65	61	62	64
95	89	80	94	95
98	132	114	148	148
99	170	151	250	251

fit regression lines were generated (in the simple form, $y = mx + b$, where 'm' is the slope and 'b' is the intercept) and a common intercept ('b') was used to level the moss-mat sediment or lake sediment element values with stream sedi-

ment data. A pseudo – box plot is shown in Figure 5 and an example of a Q-Q plot for Cu is shown in Figure 6. Substituting the analyzed moss-mat and lake sediment values ('x') into the equation for stream sediment results in transformed data distributions with a least-squared best-fit regression line having a slope ('m') and intercept ('b') like that of stream sediment data distribution for the element of interest.

MAP PLOTTING

Of the 10th, 20th, 30th, 40th, 50th, 60th, 70th, 80th, 85th, 90th, 95th, 98th and 99th percentile values calculated from the raw and levelled data for each element, only those above the 50th percentile were used for plotting the atlas maps. The unlevelled and levelled Cu and Ni values that correspond to the percentiles shown on the maps are listed in Table 2. Percentiles for the levelled data were used as intervals for contours on the atlas maps. The maps were prepared using both ESRI ArcMap[®] 9.2 and Manifold System 8. Each program produces slightly different representations, but the same trends and patterns are maintained. Attribute tables for each element were queried and imported from Microsoft Access. Contours were created by kriging using the spatial analysis tool in each program. Output cell size

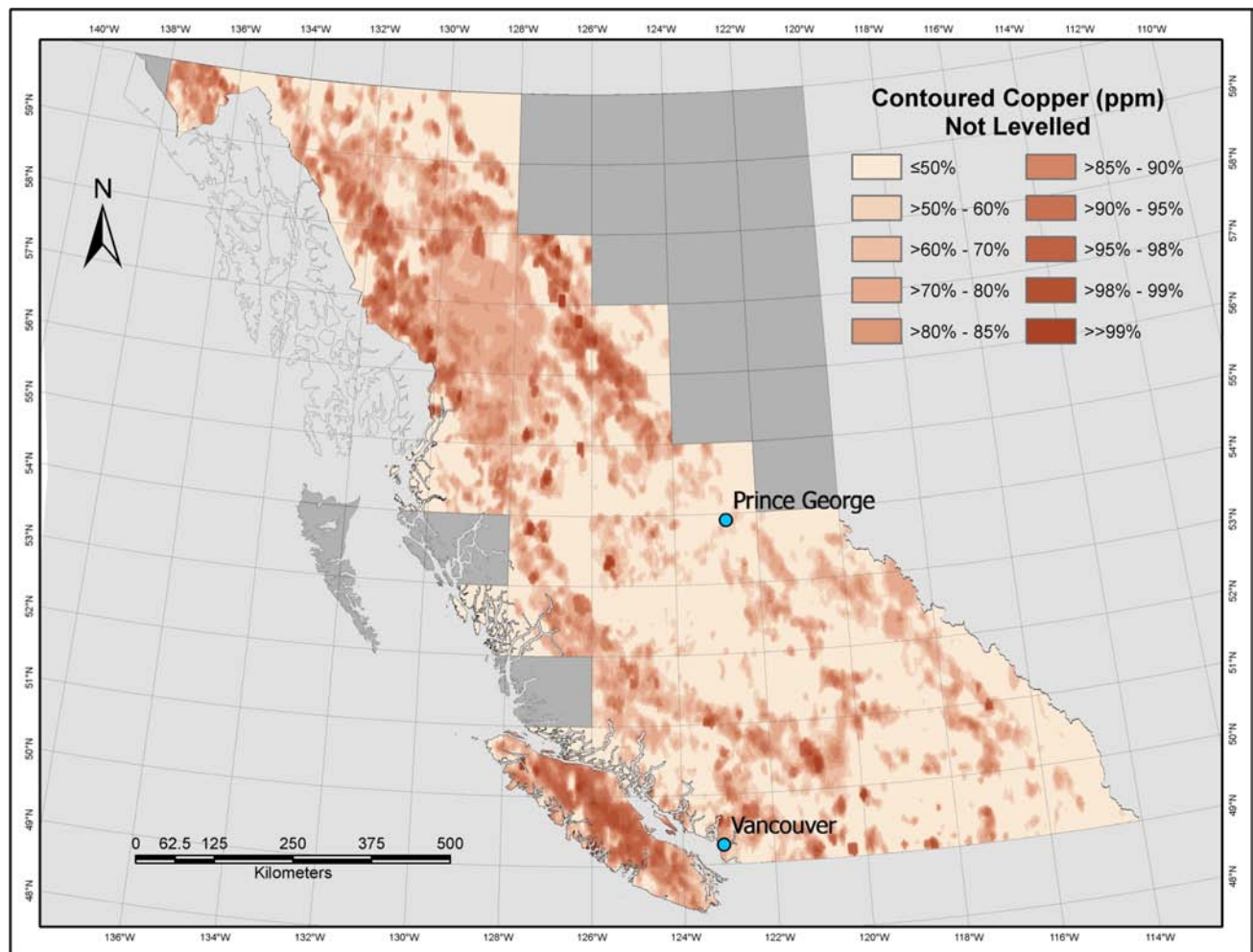


Figure 7. Contoured unlevelled Cu from merged AAS and ICP-MS stream sediment, lake sediment and moss (moss-mat) sediment data.

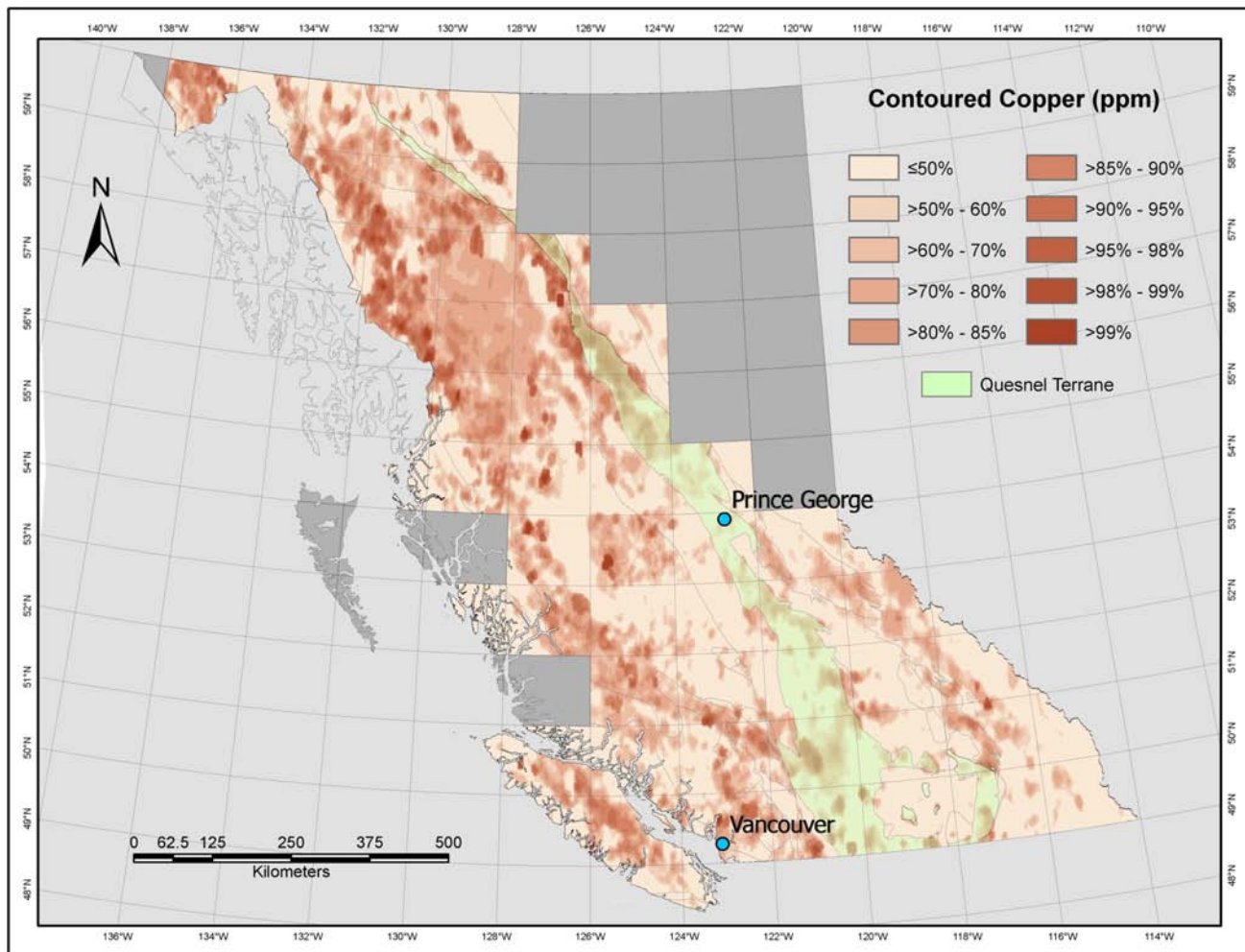


Figure 8. Contoured levelled Cu in stream sediment, lake sediment and moss-mat sediment, determined by combined AAS and ICP-MS.

was set to 0.05 of a degree, the search radius was set to 'program determined' and the number of neighbour points on which to base the prediction was set to 10. The resultant raster surface was combined with data from the digital geographic base map of British Columbia.

Contoured maps plotted from unlevelled and levelled Cu data are shown in Figures 7 and 8. Although the Cu trends are essentially the same in both contoured maps, there is an enhancement of Cu geochemistry in the unlevelled dataset (Fig 7) for some parts of British Columbia, such as Vancouver Island. This apparent enhancement reflects differences in the sample media, with higher Cu background in the moss-mat sediments that were collected mainly on Vancouver Island, compared to stream sediments collected in most other parts of the province. The levelled drainage sediment Cu data (Fig 8) reveal several belts where the elevated Cu shows a spatial relationship to geological terranes. For example, northwest-trending belts of elevated sediment Cu in central BC correspond to the volcanic island-arc sequences that form much of Quesnel Terrane. The outline of the Quesnel Terrane on the contoured Cu map is shown in Figure 8. Contoured Ni values in Figure 9 illustrate how this element can help outline metallogenic belts when the data are presented in an atlas format.

CONCLUSIONS

- Selected Pb, Co, V, Fe, Mo, Hg, Sb, Cd, Bi, Zn and Cu data for up to 56 000 reconnaissance-scale stream, lake and moss-mat drainage survey sediment samples have been compiled to form the basis for the *Geochemical Atlas of British Columbia*.
- Levelling methods have been applied to correct population differences arising from differences in analytical technique and/or sample media.
- To date, ESRI ArcMap® 9.2 and Manifold System 8 layouts for the atlas maps have been produced for selected elements. Data files and documentation that will constitute the first-generation atlas will be available as BC Ministry of Energy, Mines and Petroleum Resources GeoFile 2008-1 (Lett et al., in press).
- Future use of the geochemical atlas and derivative products will help to better define metallogenic belts with new mineral deposits.

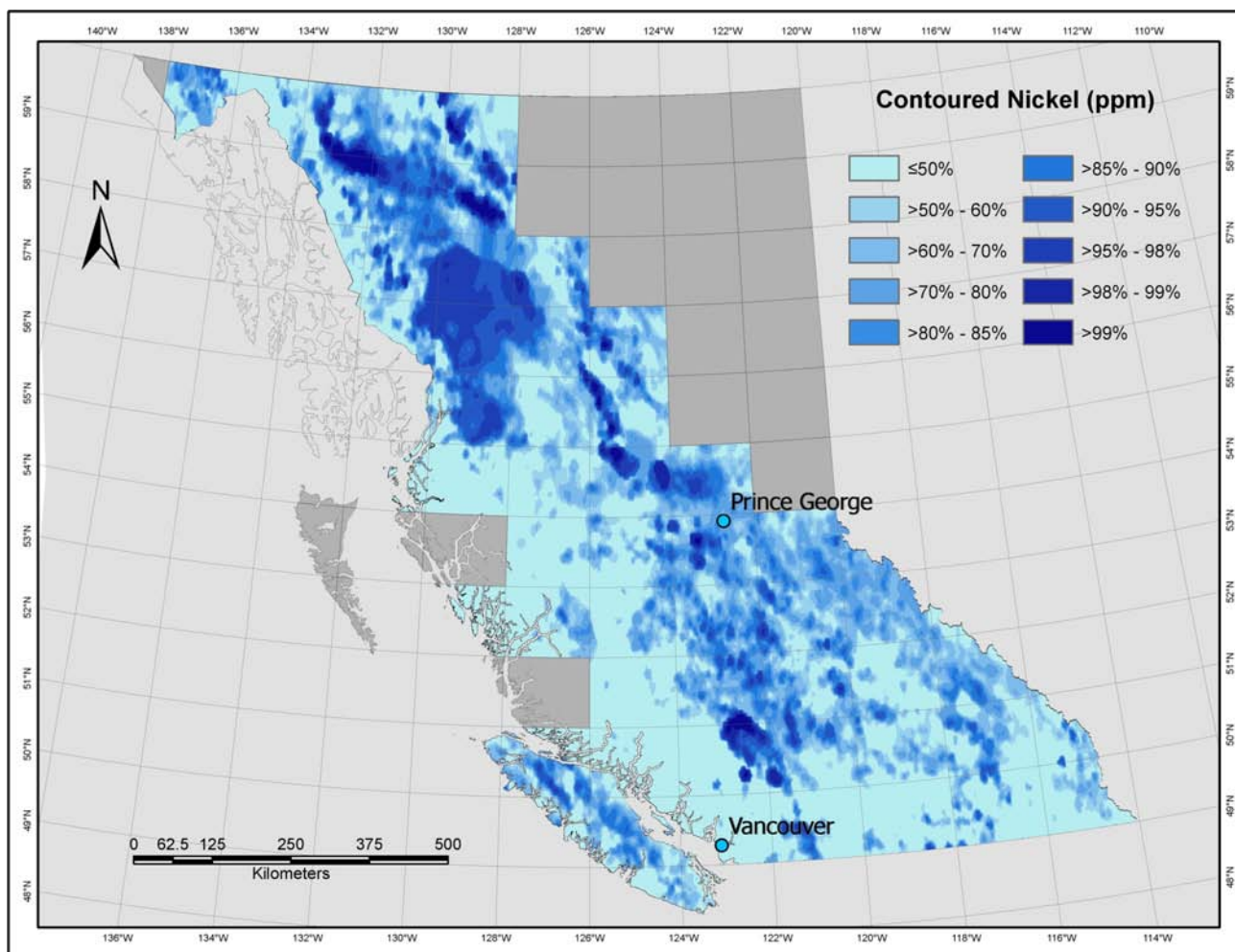


Figure 9. Contoured levelled Ni in stream sediment, lake sediment and moss-mat sediment determined by combined AAS and ICP-MS.

ACKNOWLEDGMENTS

Encouragement from Brian Grant during the early stages of this project and advice from Eric Grunsky on procedures for data levelling were very much appreciated by the authors.

REFERENCES

- Darnley, A.G. (1990): International geochemical mapping: a new global project; *Journal of Geochemical Exploration*, Volume 39, Numbers 1–2, pages 1–13.
- Grunsky, E.C. (2007): The interpretation of regional geochemical survey data; in *Proceedings of Exploration '07*, Fifth Decennial International Conference on Mineral Exploration, Milkereit, B., Editor, X-CD Technologies Inc., CD publication, pages 384–404.
- Jackaman, W. (2006): Regional drainage sediment and water geochemical survey data, Anahim Lake – Nechako River, central British Columbia (NTS maps sheets 093C and 093F); *Geoscience BC*, Report 2006-4 and *BC Ministry of Energy, Mines and Petroleum Resources*, GeoFile 2006-11.
- Kurzl, H. (1988): Exploration data analysis: recent advances for interpretation of geochemical data; *Journal of Geochemical Exploration*, Volume 30, pages 309–322.
- Lax, K. and Selinus, O. (2005): Geochemical mapping at the Geological Survey of Sweden; *Geochemistry, Exploration, Environment and Analysis*, Volume 5, Part 4, pages 337–346.
- Lett, R.E., Man, E.C., Mihalynuk, M.G. and Grant, B.G. (in press): A geochemical atlas for British Columbia; *BC Ministry of Energy, Mines and Petroleum Resources*, GeoFile 2008-1.
- Lett, R.E. and Bluemel, B. (2006): Re-analysis of regional geochemical stream sediment samples from the McLeod Lake area (NTS map sheet 093J); *BC Ministry of Energy, Mines and Petroleum Resources*, GeoFile 2006-9, 13 pages.
- Plant, J.A., Hale, M. and Ridgeway, J. (1989): Regional geochemistry based on stream sediment sampling; in *Proceedings of Exploration '87*, Third Decennial International Conference on Geophysical and Geochemical Exploration for Minerals and Groundwater, Garland, D.G., Editor, *Ontario Geological Survey*, Special Volume 3, pages 384–404.
- Plant, J.A., Klaver, G., Locutura, J., Salminen, R., Vrana, K. and Fordyce, F.M. (1997): The forum of European Geological Surveys Geochemistry Task Group inventory 1994–1996; *Journal of Geochemical Exploration*, Volume 59, Number 2, pages 123–146.
- Steenfelt, A. (1993): Geochemical mapping — progress in Greenland; *Journal of Geochemical Exploration*, Volume 49, Numbers 1–2, pages 5–14.

Webb, J.S., editor (1978): The Wolfson Geochemical Atlas of England and Wales; Oxford University Press, Oxford, United Kingdom, 70 pages.

Weaver, T.A. (1983): The geochemical atlas of Alaska; *Los Alamos National Laboratory*, Report GJBX-32 (83), 9 pages and maps.

Xie, X and Ren, T. (1993): National geochemical mapping and environmental geochemistry — progress in China; *Journal of Geochemical Exploration*, Volume 49, Numbers 1–2, pages 15–34.

Geology and Mineral Occurrences of the Quesnel Terrane, Cottonwood Map Sheet, Central British Columbia (NTS 093G/01)

by J. Logan

KEYWORDS: Quesnel, Cache Creek, Crooked amphibolite, Snowshoe Group, Nicola Group, Naver pluton, Mouse Mountain, alkalic Cu-Au porphyry mineralization, copper, gold

INTRODUCTION

A large prospective area for Cu-Au porphyry that is mostly covered by recent basalt and glacial deposits lies between Prince George and Quesnel Lake. The high mineral potential of the Quesnel Terrane rocks that underlie the area has been mostly untested in the past due to the difficulty of seeing through the thick overburden that blankets the area. Producing porphyry Cu-Au, Au and Cu-Mo mines occur both north and south of this 20 000 km² area and high mineral potential is inherent with geological continuity along the length of the belt.

Regional mapping in the Quesnel area was initiated by the BC Geological Survey in 2006 and continued in 2007 as part of a multi-year program designed to study and promote exploration of BC porphyry deposits. The 2006–2007 fieldwork is a continuation of regional mapping and mineral deposit studies initiated in the area around Mount Polley (Logan and Mihalynuk, 2005; Logan and Bath, 2006; Logan et al., 2007a) and extends coverage north-westward to test the area north and east of Quesnel. The project area covers the 1:50 000 scale Cottonwood map sheet, NTS 093G/01 (Fig 1).

The project objectives are to

- determine arc history and tectonics of the Quesnel Terrane in order to understand the evolution of magmatism and porphyry mineralization over the life of the arc (ca. 230–185 Ma);
- extend geological mapping northwestward towards Prince George into the overburden-covered, poorly understood area of Quesnel Terrane rocks;
- acquire a suite of samples from the various mineralized zones as well as a suite of least-altered volcanic and intrusive rocks for major and trace-element analysis;
- continue dating intrusive rocks to establish the magmatic history of the arc.

The Cottonwood map area is covered by thick deposits of unconsolidated Holocene and Pleistocene sedimentary rocks with rock exposures confined to less than 3% of the

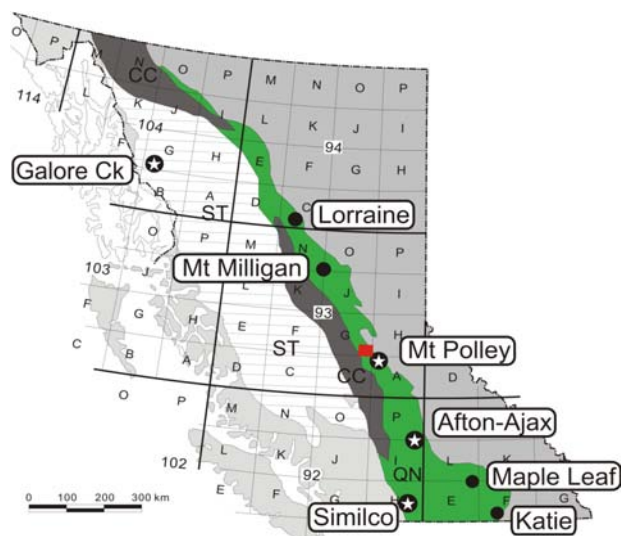


Figure 1. Location of BC Cu-Au-Ag±PGE alkaline porphyry deposits showing the Cottonwood map area in red (093G/01), green band indicates the Quesnel Terrane, grey band indicates the Cache Creek Terrane. Abbreviation: ST, Stikine Terrane.

map, usually in the main river valleys and tops of hills. The ‘Rocks to Riches’ low-level airborne magnetic and radiometric survey covered about two-thirds of the project area (Carson et al., 2006) and provided good baseline data that assisted exploration and mapping rock types, alteration and structure across the map.

REGIONAL GEOLOGY

The regional setting of the central Quesnel belt is summarized by Logan et al. (2007a), and is only briefly reviewed here. The Quesnel Terrane represents an extensive (>2 000 km) west-facing, calcalkaline to alkaline Late Triassic to Early Jurassic arc that developed outboard or marginal to the western margin of North America (Mortimer, 1987; Mihalynuk et al., 1994). It is characterized by Mesozoic arc volcanic and sedimentary rocks of the Nicola, Takla and Stuhini groups and coeval plutonic rocks, which intrude and inflate the sequence. At this latitude, the temporal, chemical and facies architecture of the Nicola Group rocks reflects a shift in magmatism from the fore arc volcanoclastic-dominated successions eastward across the arc into back arc Middle to Late Triassic fine-grained clastic rocks (the black phyllite unit of Rees, 1987). The eastern boundary of the Quesnel Terrane is marked by the Eureka thrust (Struik, 1988a), an easterly verging fault zone. Variably sheared mafic and ultramafic rocks of the Crooked amphibolite that occupy this boundary are as-

This publication is also available, free of charge, as colour digital files in Adobe Acrobat® PDF format from the BC Ministry of Energy, Mines and Petroleum Resources website at http://www.em.gov.bc.ca/Mining/Geosurv/Publications/catalog/cat_fldwk.htm

signed to the Slide Mountain Terrane, a Late Paleozoic marginal basin assemblage (Schiarizza, 1989; Roback et al., 1994) of oceanic basalt and chert that separated Quesnellia from North America until its closure in the Early Jurassic (?). The footwall to the Eureka thrust comprises the Proterozoic to Paleozoic Snowshoe Group rocks of the Barkerville subterrane (Struik, 1986), a northern extension of the Kootenay Terrane (Monger and Berg, 1984), which are pericratonic and likely represent distal sedimentation of ancestral North America (Colpron and Price, 1995). West of the Quesnel Terrane is Late Paleozoic to Jurassic oceanic rocks of the Cache Creek Terrane with Late Triassic blueschist-facies rocks (Patterson and Harakal, 1974; Ghent et al., 1996) representing the remnants of a subduction-accretionary complex (Travers, 1977; Mihalyuk et al., 2004) that generated the Quesnel Arc. Younger rocks include mid-Cretaceous granitic plutons, Eocene sedimentary and volcanic sequences and Miocene flood basalt.

STRATIGRAPHY

The Cottonwood map area is underlain by four major Canadian Cordilleran terranes that include, from east to west: Kootenay, Slide Mountain, Quesnel and Cache Creek. The rock packages that define each are fault-bounded and trend to the northwest, parallel to the dominant regional fabric in the map. Unconsolidated Holocene and Pleistocene glacial deposits are thick and cover the majority of the map area. Surficial deposits completely mask the Cache Creek Terrane, projected to underlie the southwest corner of the map (Fig 2).

Kootenay Terrane — Snowshoe Group

The Snowshoe Group, a Late Proterozoic to Paleozoic package of predominately siliciclastic rocks, dominates the Barkerville subterrane of the Kootenay Terrane. The stratigraphic nomenclature for these pelitic and psammitic rocks has evolved since the earliest work by Bowman (1889), who first designated them as the Cariboo schists. Regional maps by Struik (1988) in the Wells-Barkerville area subdivide the Snowshoe Group into 14 informal units that he correlated with Proterozoic to Paleozoic successions in the Kootenay Lake and Adams Lake areas. Recently, Ferri and Schiarizza (2006) proposed a revised stratigraphy and structural interpretation for these rocks in the Barkerville area that implied the upper Snowshoe Group is a structural repetition of the lower succession. They redefined the stratigraphy into three major units, which, from oldest to youngest, are the Downey, Harveys Ridge and Goose Peak successions. The Downey combines rocks formally assigned to the Downey, Keithley, Ramos, Kee Khan and Tregillus successions (Struik, 1988b). It consists of greenish-grey, micaceous quartzite or feldspathic quartzite, phyllite, schist, locally with a distinctive orthoquartzite at the top of the succession. The Harveys Ridge succession includes rocks formerly of the Harveys Ridge and Hardscrabble Mountain successions and comprises dark grey to black phyllite, siltstone and quartzite that become more arenaceous upsection. The Goose Peak succession includes rocks formally assigned to the Goose Peak and Eaglesnest successions: light grey and green quartz and feldspathic quartzite with interbedded grey phyllite and siltstone.

Reconnaissance mapping only was carried out over the eastern portion of the Cottonwood map area that is underlain by the Snowshoe Group (Fig 2). Building on the regional mapping of Struik (1988b), but following the stratigraphic re-interpretation of Ferri and Schiarizza (2006), traversing focused on the western contact relationships between the Snowshoe Group and the Slide Mountain – Quesnel terranes, and evaluating its Besshi-type volcanogenic massive sulphide (VMS) mineral potential. The Harveys Ridge succession of the Snowshoe Group hosts Besshi-type VMS mineralization 50 km southeast at Cariboo Lake (Høy and Ferri, 1998; Ferri, 2000) and may have the potential to host similar mineralization in the study area. Mapping determined that micaceous quartzite and schist of the Downey succession underlie the majority of the eastern one-third of the map area. Two isolated packages of dark grey to black siltite, quartzose phyllite, calcareous schist and limonitic micaceous quartzite interpreted to be Harveys Ridge succession crop out in the northern and southern parts of the map, adjacent to the Eureka thrust.

Grey and olive micaceous quartzite, schist, phyllite and calcareous schist comprise the majority of the Downey succession. The dominant rock type is a light brown-weathering micaceous quartzite consisting of recrystallized quartz, sparse feldspar and foliation-parallel metamorphic biotite and muscovite. Layers of micaceous quartzite that range from several to tens of centimetres thick are interlayered with schist. Resistant micaceous quartzite and light grey orthoquartzite occupy most of the higher peaks along the eastern boundary of the map. A distinctive white quartzite granule to cobble conglomerate overlies a sequence of orthoquartzite and interbedded grey phyllite and micaceous quartzite near the summit of a northwest-trending ridge on the eastern boundary of the map area. The quartzite weathers grey and light brown to orange. It is medium to coarse-grained and rhythmically bedded with dark grey phyllite. Micaceous units are poorly sorted with up to 20% matrix mica (muscovite > biotite), vitreous to white-coloured quartz, potassium feldspar and plagioclase grains 2 to 4 mm in size. Struik (1988b) mapped these rocks in the Wells area as the Tregillus clastic rocks. These units have been deformed and metamorphosed to upper greenschist grades. Metamorphic assemblages in the micaceous quartzite include biotite-muscovite-albite and retrograde synkinematic garnet rimmed with chlorite. Detrital mineral assemblages of quartz, muscovite and zircon populations are indicative of North American continental sources.

The Harveys Ridge succession to the east consists of black and grey siltite, micaceous quartzite, phyllite and limestone and is characterized by black and dark grey rocks (Struik, 1988b). In the map area, Harveys Ridge rocks occur at the south and north boundaries of the map. In addition, Struik (1988b) shows a 1 km wide belt projecting into the map area from the eastern boundary. The Harveys Ridge rocks in the southeast corner of the map occupy the upper limb of a northwest-plunging anticline overturned to the southwest and cored by Downey succession rocks. The rocks include interbedded black siltite, phyllite and brown-green weathering micaceous quartzite. The black siltite contains narrow (1–2 mm) sheeted white quartz veins that parallel bedding. Thinly laminated, fine-grained black quartzite and a distinctive micaceous quartzite with coarse, randomly oriented metablasts of chloritoid and/or actinolite occur within the southern sequence. At the northern occurrence, black quartzite and well-foliated argillite and phyllite of the Harveys Ridge succession comprise the

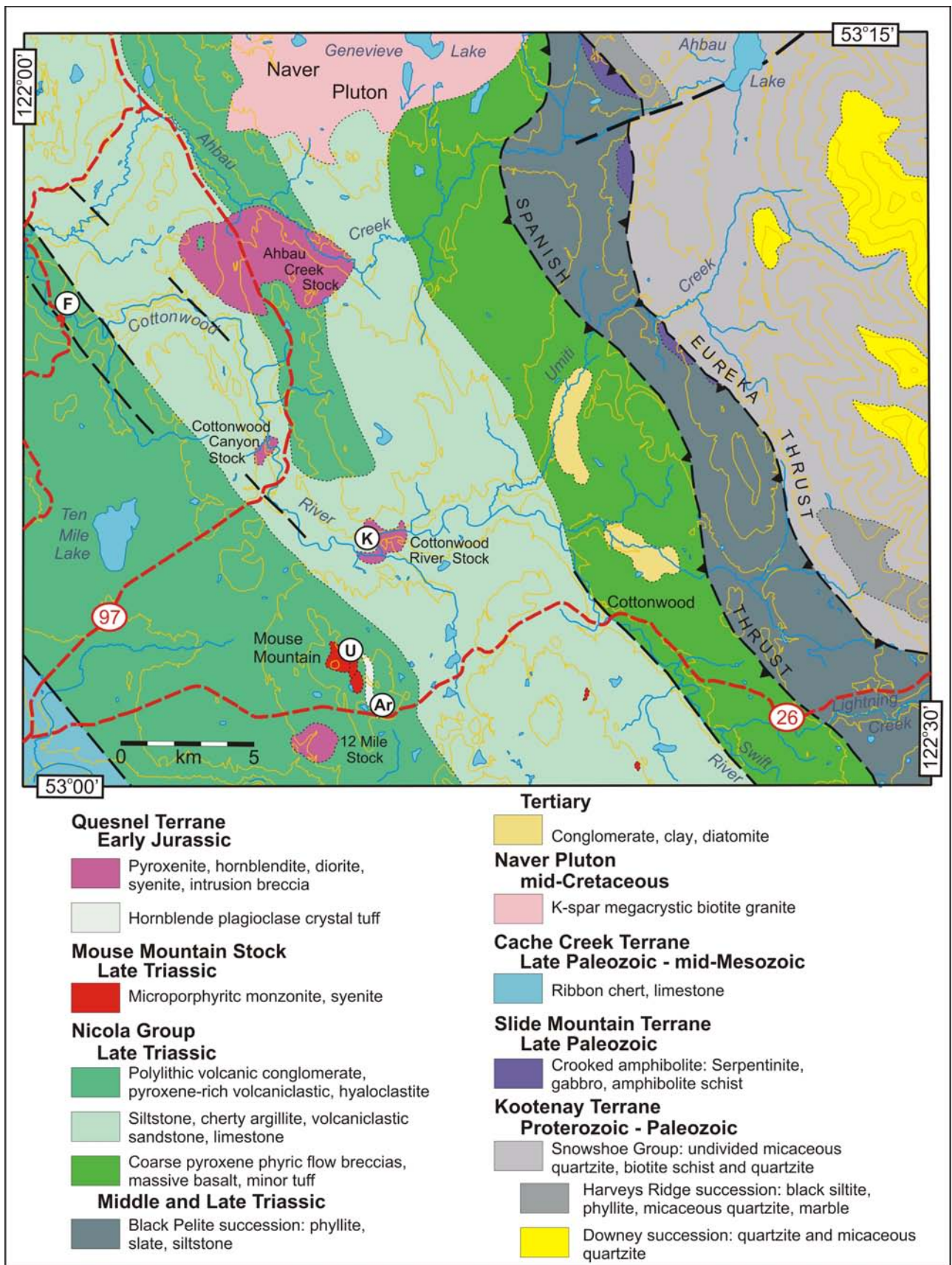


Figure 2. Generalized geology of the Cottonwood map area (093G/01), based on 2007 fieldwork and interpretation of low-level airborne geophysical survey (Carson et al., 2006). The map shows the location of macrofossil and geochronological samples.

hilltop located 5 km west of Ahbau Lake. An isolated outcrop of thinly foliated micaceous marble and quartzite is seen on the western slope of the hill forming the footwall to the Eureka thrust and the serpentinitized pyroxenite exposed at the base of the hill. Bedrock exposure is limited, but anomalous base-metal soil geochemistry is known from the area underlain by the Harveys Ridge succession (Ahbau Lake Property in the Mineralization section).

Slide Mountain Terrane — Crooked Amphibolite

The Slide Mountain Terrane consists of the Antler Formation, the Crooked amphibolite (Campbell, 1978; Struik, 1982) and the Fennell Formation farther south (Schiarizza and Preto, 1987). All consist of imbricated oceanic assemblages of basalt, gabbro and chert in thrust contact with the pericratonic Kootenay Terrane. Variably sheared and tectonically thickened/thinned (?) mafic and ultramafic rocks of the Crooked amphibolite separate rocks of the Quesnel Terrane and the Barkerville subterrane over a distance of 200 km from Prince George (Struik et al., 1990) south to Hendrix Lake (Schiarizza and Macauley, 2007).

The Crooked amphibolite is well exposed in the northern part of the Cottonwood map area, southwest of Ahbau Lake and as small isolated subcrop occurrences south of Umiti Creek (Fig 2). It consists of a variety of dark green, typically FeCO₃-altered schistose ultramafic and mafic metavolcanic rocks and coarser-grained plutonic rocks. These rocks have high magnetic susceptibilities due to the magnetite produced during the alteration and breakdown of olivine to serpentine. As a result, follow-up of magnetic high anomalies generated from the 2005 airborne geophysical survey was successful in delineating a number of previously unknown occurrences of this unit. South of Ahbau Creek, variably foliated metavolcanic schist and coarse-grained amphibolite characterized by acicular, centimetre-long crystal aggregates of actinolite (~75%) and interstitial white plagioclase define the unit. In the southeastern corner of the map area, the Crooked amphibolite (not shown on the map) consists of a thinly foliated metavolcanic rock less than 50 m thick that strikes parallel to the dominant foliation in the micaceous quartzite and schist of the Snowshoe Group and can be traced for several hundreds of metres.

Quesnel Terrane — Nicola Group

BLACK PELITE SUCCESSION

Between the Eureka and Spanish thrusts is a low area with variable relief and few outcrops. Here, defining the eastern part of Quesnel Terrane, are scattered outcrops of silty to fine sandy black slate, calcareous slate and rare volcanic tuff interbedded with black recessive-weathering phyllite and lesser quartz sandstone.

The black fine-grained siliceous and calcareous clastic rocks structurally overlie sheared serpentinite of the Crooked amphibolite in the eastern portion of the map (Fig 2). The nature of the contact is not exposed, but it follows a north-trending magnetic high that corresponds to sheared serpentine and talc-altered mafic volcanic rocks mapped as part of the Crooked amphibolite. These fine-grained black clastic rocks are correlated with the black phyllite unit of Rees (1987), which has been dated as Middle and Late Triassic from conodont-bearing calcareous horizons at Quesnel Lake (Struik and Orchard, 1985). Thin

interbedded grey and black phyllite, graphitic±pyritic argillite, buff and grey siltstone and fine quartz sandstone crop out along Highway 26 in the southeastern corner of the map area. The rocks are weakly metamorphosed to lower greenschist facies and mostly unaltered. A slaty cleavage is common, but recrystallization along it is lacking. Bedding and cleavage trend northwest. Open to subisoclinal folds that trend northwest are seen locally. On the limbs of these folds, cleavage has transposed bedding, producing lensoidal quartz sandstone breccia in a black graphitic or calcareous phyllite matrix that can be traced into interbedded quartz sandstone and black siltstone. Detrital quartz and muscovite present in sandstone imply a continental margin rather than a fore arc volcanic setting.

A coarse polyolithic clastic unit, the Wingdam conglomerate of Struik (1988b), is exposed adjacent to the southeast corner of the map area. It strikes northwesterly and projects into the map area but was not encountered during current mapping. The conglomerate is included in the Middle and Late Triassic black clastic sequence of the Nicola Group (Struik, 1988b). The conglomerate contains rounded clasts of deformed and foliated serpentinite, mafic volcanic rocks and pyroxenite, micaceous quartzite, black quartzite, white vein quartz, graphitic phyllite and shale within a dolomitic and siliceous matrix. All of the clast types in the conglomerate can be derived locally from the Crooked amphibolite and the Snowshoe Group. Recognition of deformed and metamorphosed (?) Slide Mountain Terrane and Kootenay Terrane fragments deposited on the Quesnel Terrane led McMullin et al. (1990) to suggest that the Slide Mountain and Kootenay terranes must have been imbricated prior to the Middle to Late Triassic deposition of the Quesnel Terrane. This implies that the contact between the Slide Mountain and Quesnel terranes is an erosional unconformity that was later tectonized and metamorphosed in the Middle Jurassic.

Contact relations between the black pelite succession and the overlying volcanic rocks are both depositional (Bloodgood, 1987; Rees, 1987; Panteleyev et al., 1996) and structural (Struik, 1986, 1988a, 1990) in the Quesnel Lake area farther south, but not exposed in the current study area. The black pelite succession is considered to be broadly coeval with the eastern volcanoclastic Nicola Group and may be an eastern back arc facies onto which arc volcanic and volcanoclastic rocks were deposited.

EASTERN VOLCANICLASTIC SUCCESSION

An eastern belt of mafic olivine-pyroxene, pyroxene and pyroxene-plagioclase-phyric volcanic flows, breccia, fine-grained tuff and volcanoclastic rocks structurally overlie black clastic rocks of the black pelite succession (Fig 3). Outcrop is sparse but defines a 5 km wide north-trending belt of rocks, which at its northern extent appears to wrap around the southeastern margin of the Naver pluton south of Genevieve Lake. Outcrop distribution, airborne geophysical total field magnetic and first vertical derivative plots coincide to define the eastern volcanoclastic succession.

In the north part of the map area, black, vesicular, coarse-grained clinopyroxene-phyric block flow breccia, ash and lapilli-supported autoclastic breccia and coherent basalt flows occupy an east-trending belt that follows the southeastern margin of the Naver pluton. The flows are characterized by euhedral to stubby 2 to 3 mm pyroxene crystals and sparse <1 mm plagioclase laths in a weak



Figure 3. Coarse monolithic block to lapilli volcanic breccia containing pyroxene-phyric and pyroxene-plagioclase-phyric basalt fragments. Clast to matrix supported, eastern volcanoclastic succession, Ahbau Creek.

chloritic aphanitic groundmass. Outcrops show vague pillowed forms with chilled altered margins and concentrically distributed white calcite and/or albite-filled amygdulites. The basalt is cut by narrow (1–2 cm wide), east-trending sheeted albite veins. The rocks have relatively high magnetic susceptibility and can be traced southward.

Outcrops in Ahbau Creek consist of coarse, angular, block to boulder clast-supported volcanic breccia dominated by pyroxene-phyric and pyroxene-plagioclase-phyric basalt. White calcite, pyroxene crystals and/or sand-sized lithic fragments comprise the matrix (<3%) to the mainly clast-supported breccia (Fig 3).

At the southern end of the belt, in the Cottonwood River and Lightning Creek drainages, pyroxene-phyric and pyroxene-plagioclase-phyric coherent flow and breccia flow units are common. Rubbly flow breccia consists of monolithic angular to rounded, block to lapilli-sized clasts of pyroxene-phyric basalt. Often clast supported, or within a matrix of ash, rarely carbonate fills the interstices. Flows are, for the most part, submarine and subordinate to clastic volcanic rocks in overall abundance.

COTTONWOOD RIVER SUCCESSION

Fine clastic sedimentary rocks dominated by thin parallel-laminated grey, green, buff and black cherty argillite, volcanic siltstone, slate and grey or buff limestone form a continuous belt of rocks approximately 9 km wide that occupies the western third of the map (Fig 2). These rock types are best exposed along the length of the Cottonwood River and have been assigned to the Cottonwood River succession (Fig 4).

The Cottonwood River succession consists mainly of grey to green or rusty weathering black cherty argillite and fine-grained, parallel-laminated, volcanic siltstone. Centimetre-thick grey limestone beds occur interlayered with the cherty argillite sequence or as tens of metres thick black and buff-coloured silty limestone interbedded with graphitic phyllite. The sequence is dominated by massive sandstone, planar-laminated siltstone units and rare wavy to small-scale crossbeds that are interpreted to represent turbidite deposition distal from the main arc. The succession is characteristically cleaved parallel to bedding into 50 mm thick cherty domains by 2 mm phyllite partings.

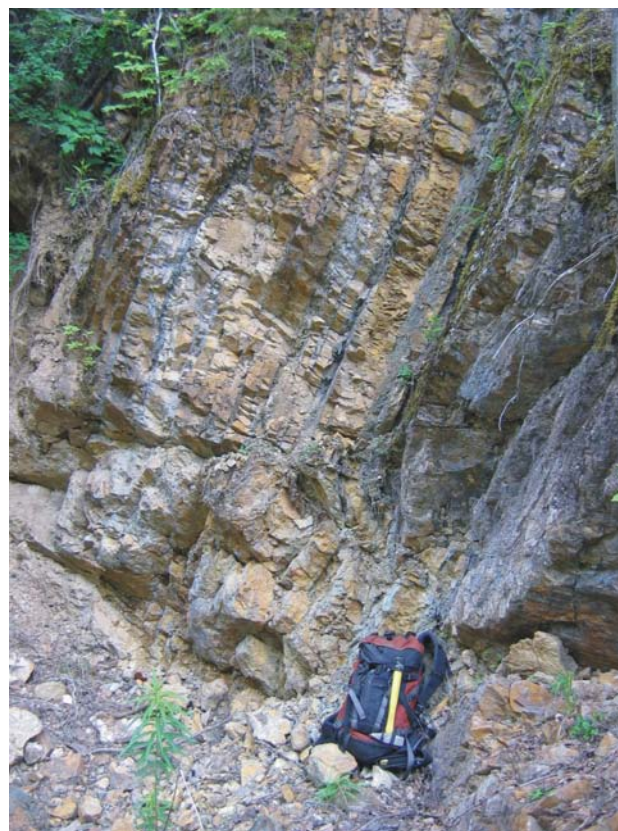


Figure 4. Rusty-weathering siltstone and cherty argillite interbedded with massive grey-green volcanic sandstone of the Cottonwood River succession. Photo is looking northwest along the sinistral fault zone, downstream of Cottonwood River.

South of Highway 26, the sedimentary rocks are coarser grained, consisting of thinly bedded volcanic sandstone, poorly sorted volcanic debris flows or greywacke and black cherty argillite. Relatively minor amounts of dark green coarse pyroxene-phyric basalt breccia occur interbedded with the sedimentary rocks in the central sedimentary sequence.

The upper contact with the western volcanoclastic succession is not well established, although east of the Cottonwood River it appears that volcanoclastic material increases in grain size and proportion upsection, passing gradually into volcanic breccia of the western volcanoclastic succession. The Cottonwood River succession is not dated within the map area, but samples of limestone and calcareous black siltstone have been submitted to the Geological Survey of Canada Micropaleontology Laboratory in Vancouver.

WESTERN VOLCANICLASTIC SUCCESSION

The western volcanoclastic succession of the Nicola Group is the most heterogeneous unit in the map area. It forms a north and northwest-trending belt, 2.5 and 9 km wide, respectively, of pyroxene-phyric basalt breccia, heterolithic volcanic conglomerate, crystal-lithic sandstone and fine-grained heterolithic volcanoclastic rocks (Fig 2). The north-trending belt follows Highway 97 for 20 km from the Cottonwood River to the northern edge of the map. Contact relationships are apparently gradational with fine clastic rocks of the Cottonwood River succession exposed along the Umiti Creek Road. Contact relationships

for the western belt are less understood. On the east it is bound by northwest-trending faults and to the southeast its relation to the Cache Creek Terrane is obscured by thick overburden.

Volcaniclastic rocks of the western succession are well-exposed in the CN Rail quarry north of Ahbau Creek. They consist of northwest-trending units of massive coherent basalt flows, hyaloclastite, coarse pyroxene-phyric breccia and clastic deposits. Rare 1 m wide fine-grained tuffaceous cherty siltstone defines the regional trend. Basalt flows are approximately 5 m thick and characterized by brecciated margins. Flows vary from coarse crowded pyroxene porphyry to sparse and aphyric, commonly highly vesicular, varieties. The volcaniclastic package is hornfelsed and flooded by pyrite and/or pyrrhotite, abundant calcite and chlorite probably related to the emplacement of the Naver pluton.

Interbedded with the volcaniclastic rocks are well-sorted planar laminated argillite and siltstone units and 10 m thick channel deposits of unsorted chaotic slump deposits of sedimentary and volcanic-derived material. These coarse-grained intervals consist of angular boulder to granule-sized volcanic clasts and centimetre-sized rip-up clasts of cherty argillite supported within a matrix of pyroxene and plagioclase-rich sand and/or mud. The grain flow deposits are dominated by clasts of pyroxene-phyric basalt. The pyroxene crystal-rich sandstone, volcaniclastic breccia and conglomerate horizons contain abundant detrital magnetite and a relatively high magnetic susceptibility, which is evident on the airborne magnetic maps. Stratigraphically low in the volcaniclastic succession are sedimentary units characterized by bedding couplets generally less than 1.0 mm thick of olive grey sandstone and orange-black thinly laminated cherty siltstone and 10 to 12 m thick massive outcrops of pale green, fine to medium-grained, well-sorted pyroxene and plagioclase crystal (1–4 mm) sandstone.

The western belt of volcaniclastic rocks is best exposed in the area between Highways 97 and 26, where it extends from Mouse Mountain northwestward as a 5 km wide belt of pyroxene-phyric breccia, heterolithic maroon pyroxene and plagioclase-phyric volcaniclastic and massive green tuffaceous rocks (Fig 2). The majority of outcrops in the western belt consist of massive, heterolithic pyroxene-dominated volcaniclastic to conglomeratic units. Bedding is rarely observed and often preserves slumping and soft sedimentary deformation. Rocks are variably green and/or maroon and hematitic, suggesting marine and subaerial deposition. In the vicinity of Mouse Mountain, the breccia contains detrital biotite, orthoclase and altered intrusive rocks related to the Cu-Au mineralizing system.

The minimum age of the western volcaniclastic succession is constrained by the Late Triassic age of the Mouse Mountain pluton.

Early Jurassic

SEDIMENTARY ROCKS

Rocks exposed at the old Prince George highway bridge crossing the Cottonwood River comprise a structurally disrupted and sheared sequence of heterolithic maroon volcanic breccia, calcareous green volcaniclastic rock and grey limestone. Overlying this Triassic (?) volcanic sequence is a grey and brown sedimentary sequence of fine

sandstone, siltstone and shale. Ten to twenty millimetre thick beds of olive sandstone with black siltstone partings are interbedded with thinly laminated sooty black shale and siltstone. Poorly preserved ammonoids and bivalves were collected from the sandstone and shale. The fossils have been assigned an Early Jurassic Sinemurian age (T. Poulton, pers comm, 2007).

The contact relationship between the two packages is believed to be depositional because similar stratigraphic relationships occur at Morehead Lake in the Mount Polley area (Bailey, 1978; Logan et al., 2007b).

VOLCANIC ROCKS

Grey to white plagioclase-hornblende porphyritic volcanic and subvolcanic intrusive rocks crop out in a north-northwest-trending belt in the vicinity of Mouse Mountain (Fig 2). The rocks are coarsely porphyritic with tabular white plagioclase phenocrysts up to 2.5 cm in diameter and noticeably finer acicular hornblende crystals in a green, grey or maroon aphanitic matrix. Brecciated lithic fragments, crystal shards and eutaxitic textures indicate that the unit represents a welded crystal-ash flow (ignimbrite). The rock was mapped and interpreted variably as a subvolcanic intrusive to flow unit (Jonnes and Logan, 2007) that cross-cut or overlay the pyroxene porphyry and volcaniclastic units. Observations from the summer mapping recognized heterolithic breccia at Mouse Mountain and along strike to the south that contain plagioclase-hornblende porphyritic volcanic clast-rich horizons interbedded with coarse pyroxene-phyric breccia flows, suggesting temporal relationships for these units (Fig 5).

Major and trace-element rock geochemistry of the plagioclase porphyry unit plots in the andesite field on Winchester and Floyd (1977) rock discrimination diagram. On the SiO₂ vs. K₂O andesite series plot of Gill (1981), the hornblende-plagioclase crystal tuff unit occupies the high-potassium andesite field.

Hornblende was separated from the plagioclase crystal tuff and analyzed to constrain the cooling age of the ignimbrite. Argon-argon plateau ages for hornblende separates determined at the Geochronology Laboratory, the

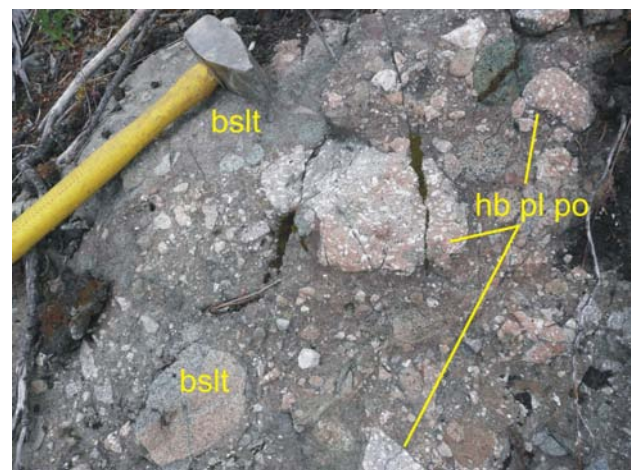


Figure 5. Heterolithic volcanic breccia composed primarily of subangular to rounded pyroxene-phyric basalt (bslt) and hornblende-plagioclase-phyric andesite (hb-pl po), in a sand-sized, crystal-rich volcaniclastic matrix, 1 km southeast of Mouse Mountain.

University of British Columbia returned an Early Jurassic cooling age of 192 ± 1.3 Ma (T. Ullrich, pers comm, 2007). This Early Jurassic age coincides with the ca. 193 Ma plutons of the Takomkane–Thuya suite (Parrish et al., 1987; Breitsprecher and Mortensen, 2004), suggesting that these high-potassium andesite units may represent extrusive equivalents to a well-established Early Jurassic plutonic event in the Quesnel Terrane.

Intrusive Rocks

Intrusive rocks within the Cottonwood map area include a Late Triassic and Late Triassic to Early Jurassic suite that comprise the constructive period of the Quesnel magmatic arc and a younger post-accretionary suite of Cretaceous age. A Middle Jurassic suite of plutons intrudes the Quesnel Arc north and south of the current study area (Struik et al., 1992; T. Ullrich, pers comm, 2006; Logan et al., 2007a), but has not been recognized in the Cottonwood map area.

LATE TRIASSIC

Mouse Mountain Monzonite

Small, isolated, quartz undersaturated stocks interpreted to be Late Triassic in age intrude the Cottonwood River succession of fine-grained clastic rocks in the south-central part of the map area (Fig 2). Most are less than 0.5 km^2 in area and occur south of Highway 26. They are similar in composition, regional distribution and temporal relationships to the suite of latest Triassic alkaline intrusive rocks that define the medial arc axis and magmatic centres at Mount Polley, QR and Cantin Creek, where they are associated with alteration and Cu-Au mineralization (Logan and Mihalyuk, 2005; Jonnes and Logan, 2007). The Mouse Mountain pluton is also characteristic of this suite, is larger and intrudes the western volcanoclastic succession.

Leucocratic fine-grained intrusive rocks underlie the main area of Mouse Mountain, encompassing an area of approximately 1.3 km^2 (Jonnes and Logan, 2007). Microporphyratic monzonite to monzodiorite rocks characterize the main intrusive sequence, but coarse orthoclase megacrystic syenite dikes are also known to intrude the area. Contact relationships with the Late Triassic Nicola Group country rock are presumably intrusive, but unseen. Separating the monzonite into two bodies is a monolithic breccia made up primarily of intrusive clasts of monzonite in a rock flour matrix. Jonnes and Logan (2007) interpreted this breccia to be a hydrothermal breccia or eruptive diatreme located near the top of the intrusive pile.

A 20 kg sample of least-altered, pink pyroxene monzonite was collected from the Valentine zone and dated using laser ablation inductively coupled plasma – mass spectrometry (ICP-MS) U-Pb techniques at the University of British Columbia. Zircon grains extracted from the sample yielded a Late Triassic crystallization age for the monzonite of 207.42 ± 0.58 Ma (R. Friedman, pers comm, 2007), thus providing a maximum age for Cu-Au mineralization at the Valentine zone.

Additional intrusive bodies in the map include a distinctive white-weathering plug of crowded megacrystic orthoclase porphyritic syenite that crops out approximately 3 km south of the community of Cottonwood (Fig 2). The main body of the syenite consists of aligned orthoclase crystals up to 5 cm in length, which comprises 80% of the

rock. Equigranular pyroxene-hornblende monzodiorite containing sparse (2–3%) megacrysts of orthoclase define 25 m wide marginal phases to the plug. Trace amounts of chalcopyrite and pyrite replace mafic xenoliths and mafic minerals along weak alteration fronts cutting the monzodiorite.

Three kilometres west-northwest of the megacrystic syenite is a poorly exposed fine to medium-grained, equigranular to microporphyratic pyroxene monzodiorite plug. Both the intrusion and the country rock contains 1 to 1.5% pyrrhotite and elevated Cu and Zn (07GLE22-111, Table 1).

LATE TRIASSIC TO EARLY JURASSIC (?)

Mafic-Ultramafic Plutonic Complexes

The map area contains a number of small, generally less than 1 km^2 composite mafic-ultramafic intrusive bodies (Fig 2). These and other Alaskan-type complexes in BC are confined to the Quesnel and Stikine terranes and are spatially and genetically associated with Late Triassic to Early Jurassic volcanic arc rocks of the Nicola-Takla-Stuhini groups (Irvine, 1974; Mortimer, 1986; Nixon et al., 1997). The mafic biotite-bearing phases of these plutons have elevated concentrations of magnetite and hand samples typically display high magnetic susceptibility readings that correspond to magnetic highs on residual total magnetic field plots. Two apparently similar composite plutons exposed in the Cottonwood River consist of pyroxenite, pyroxene-hornblende diorite and monzodiorite. In detail, the pyroxene-biotite diorite phase is absent and both stocks have much lower magnetic susceptibilities and no magnetic high signature.

The Ahbau Creek stock is the largest of these mafic complexes. It is centred on Highway 97 at the Greening rail siding and is interpreted primarily on the basis of its magnetic signature to cover an elliptical area of just over 20 km^2 between Ahbau Creek and the Cottonwood River. The northwestern margin of the stock is exposed for approximately 3 km in Ahbau Creek from the railroad trestle upstream to the upper falls. Outcrop exposures include clinopyroxenite, pyroxene-biotite diorite and intrusion breccia comprising fragments of pyroxenite, gabbro and diorite within an intermediate to felsic, medium-grained hornblende monzodiorite matrix (Fig 6). The pyroxene-biotite diorite to monzodiorite is medium grained; plagioclase and pyroxene crystals are subequal in size and display intergranular texture, while interstitial coarse poikilitic biotite envelops the plagioclase and pyroxene (Fig 7). Coarse (1.5 mm) euhedral apatite crystals and magnetite are evenly disseminated throughout the matrix is greater than 5 vol%. Magnetic susceptibility values for this unit average between 75 and 100 SI units. The matrix to the igneous breccia is leucocratic, medium to coarse grained and enriched in alkali minerals compared to the earlier crystallized phases. Orthoclase occurs as megacrysts and late optically continuous interstitial crystals that together with coarse poikilitic hornblende envelop subhedral crystals of apatite and pyroxene. Hornblende also locally replaces clinopyroxene. Magnetite is noticeably less abundant, present in only trace amounts. Coarse euhedral sphene crystals and andradite garnet occupy cusped late-stage voids that trapped hydromagmatic fluids.

The 12 Mile stock is a similar mafic plutonic complex to the Ahbau Creek stock. It is located south of High-

way 23, approximately 19.3 km (12 mi) east of Quesnel. Like the Ahbau Creek stock, it has a distinctive circular magnetic high anomaly on the residual total magnetic field plot and is poorly exposed. Exposures are limited to a creek gully located approximately 3 km south of Mouse Mountain. Outcrops consist of pyroxenite and pyroxene-biotite diorite and intrusion breccia with angular blocks of gabbro, pyroxenite and diorite within an equigranular pyroxene-hornblende monzodiorite. Joints and fractures are coated with chlorite, serpentine and calcite. The plagioclase is extensively sericitized, particularly along outer zones of the phenocrysts and/or sausseritized (epidote+sericite±carbonate±chlorite), chiefly in the interior of the phenocrysts. Apatite and magnetite are abundant and associated with poikilitic biotite. At the northern end of the outcrop the intrusion breccia is cut by an 8 m wide northwest-trending dike of microporphyrific pink biotite-pyroxene monzonite similar to the Mouse Mountain monzonite.

The Cottonwood River (Bailey, 1988) and the Cottonwood Canyon stocks are two additional mafic plutonic complexes that occur within the study area. Both crop out

along the Cottonwood River, are <1 km² and intrude fine-grained cherty tuff, siltstone and volcanoclastic rocks of the central Nicola facies. The plutons are complexly zoned, composite bodies of igneous breccia comprising coarse-grained clinopyroxenite, hornblende clinopyroxenite, gabbro and/or monzodiorite, veined by more felsic medium to coarse-grained hornblende-pyroxene monzodiorite to monzonite phases. The youngest intrusions consist of crowded orthoclase megacrystic monzonite to pegmatitic syenite dikes. These latter orthoclase megacrystic phases commonly exhibit a well developed trachytic flow fabric defined by aligned orthoclase phenocrysts (Fig 8).

A sample of pyroxene-hornblende gabbro collected by D. Bailey from the Cottonwood River stock was dated using K-Ar isotopic techniques at the University of British Columbia by J. Harakal. Hornblende from the gabbro yielded an Early Jurassic cooling age of 187 ±7 Ma (Panteleyev et al., 1995). Schiarizza and Macauley (2007) describe similar ultramafic-mafic plutonic complexes that intrude the eastern side of the Quesnel Terrane in the Canim Lake area (150 km southeast of the study area). They report

TABLE 1. ASSAYS OF ROCK SAMPLES COLLECTED DURING SUMMER 2007 FIELDWORK, COTTONWOOD MAP SHEET (093G/01); ANOMALOUS SAMPLES HIGHLIGHTED IN YELLOW.

Station Number	Easting	Northing	Element																			
			Ag	Al	As	Au	Ba	Bi	Ca	Cd	Ce	Co	Cr	Cu	Fe	Hf	K	La	Li	Mg	Mn	Mo
Units			(ppm)	(%)	(ppm)	(ppb)	(ppm)	(ppm)	(%)	(ppm)	(ppm)	(ppm)	(ppm)	(%)	(ppm)	(%)	(ppm)	(ppm)	(%)	(ppm)	(ppm)	
Method			TICP	TICP	TICP	FA	TICP	TICP	TICP	TICP	TICP	TICP	TICP	TICP	TICP	TICP	TICP	TICP	TICP	TICP	TICP	
07GLE10-53	541694	5893709	1	6.74	14	4	78	2.9	0.13	2.6	60	0.5	57.4	3.8	0.63	3.5	3.93	33.7	10.9	0.1	69	14.2
07JLO10-54	540602	5897830	1	7.1	7	34	1667	0.2	2.57	0.1	36	15.8	102.5	127.3	3.38	0.9	3.14	18	78.5	2.27	414	0.8
07JLO14-87	567045	5877649	<1	10.87	<1	19	17	0.5	14.54	0.3	107	11.3	84.2	0.5	10.04	0.8	0.02	55.7	15.8	2.82	3215	0.2
07JLO18-118	554373	5879944	<1	3.99	324	5	35	0.1	0.63	0.7	82	62.4	685.1	59.9	5.94	2	1.63	40.5	10	0.52	2273	0.2
07JLO18-126	554332	5875955	0.1	11.09	1	18	737	<1	4.91	0.1	10	9.9	36.2	47.3	3.33	1.1	4.42	4.7	9.9	0.95	894	0.1
07GLE20-106	542139	5894516	0.5	9.5	3	17	307	<1	7	0.3	18	34.6	85.8	283.1	8.85	2.4	1.5	7.9	39.5	4.06	1673	0.7
07JLO20-131	551661	5881262	0.2	8.23	2	<2	1024	0.1	6.95	0.2	12	20	52.9	173.9	4.88	1.5	2.41	5.9	12.1	1.72	1133	0.2
07JLO21-141	546726	5881716	0.1	5.46	14	<2	440	<1	8.66	0.1	33	13.6	55.7	85.1	3.96	1.2	2.77	17.8	33.2	3.56	2392	0.5
07JLO22-147-2	547698	5881795	0.2	11.55	106	6	1247	<1	3.31	0.7	16	13.5	28.8	96.4	4.02	1.1	3.51	7.8	11.7	0.64	445	1.5
07GLE26-119	546480	5876166	0.1	7.03	6	19	1158	0.1	8.43	<1	22	29.2	70.2	53.1	6.37	1.2	3.45	11.6	55.8	2.36	1328	0.5
07GLE29-137	535507	5889129	0.1	7.47	5	8	81	<1	10.62	0.1	18	15.7	24.9	37.8	4.76	2.5	0.33	7.2	15.2	1.13	1354	0.4
07GLE23-114	555518	5895807	<1	9.09	1	70	158	0.1	6.45	0.2	35	43.7	354.1	32.1	6.97	1.6	0.63	17.6	34.3	3.26	996	0.3
07JLO13-83	544811	5902426	<1	7.54	2	1216	0.2	1.2	0.1	67	2.8	96.7	6	1.36	1.3	3.88	37.4	65	0.38	365	0.3	
07GLE3-10	546610	5896809	0.1	8.08	3	1264	0.1	1.77	0.1	55	4.9	83.2	8.4	1.84	1.3	3.22	29.2	42.6	0.76	420	0.4	
07GLE31-147	544702	5895672	0.1	8.74	12	1816	0.1	4.04	0.4	108	16.1	61.3	21.5	4.55	3.4	2.34	57.9	26.6	2.02	839	1.8	
07JLO13-80	555424	5898275	0.1	0.86	11	29	0.1	0.29	0.2	10	121.3	1201.1	14.8	6.92	<1	0.02	5.3	10.3	21.32	538	0.1	
07JLO20-134	546542	5881292	<1	8.97	2	1453	<1	6.38	0.1	15	21.5	45.1	30.3	6.19	1.4	5.05	6.5	22.6	1.81	1303	0.6	
07GLE26-126	546469	5881403	0.2	9.13	1	874	<1	8.44	0.2	15	34.8	52.1	421.5	7.44	1.4	3.23	7	24.4	3.21	1507	0.2	
07GLE22-111	551521	5876622	0.1	8.6	<1	568	<1	6.18	0.3	18	35	73.5	116	8.03	2.2	1.5	7.4	20.6	3.48	1450	0.1	
07JLO25-177	542458	5885376	<1	7.57	1	1209	<1	6.24	0.1	19	26.4	47.9	55.1	6.91	1.7	3.23	9	35.1	2.56	1438	<1	
07JLO27-190	544116	5892126	0.1	9.14	3	1152	<1	7.46	0.1	14	38.4	17	165.3	9.09	0.5	2.45	6.7	30.5	3.59	1424	0.1	
Std CANMET WPR1			0.6	1.67	-1	43	21	0.1	1.6	0.2	5	202.2	2595.2	1722.9	10.56	0.5	0.09	2	5.7	18.09	1397	0.3
Recommended			0.7	1.64	1.4	42.2	22	0.19	1.43	0.43	6	180	3300	1640	9.93	0.61	0.165	2.2	4.2	18.69	1549	0.9
% Difference			15.4	1.8	1200	1.9	4.7	62.1	11.2	73.0	18.2	11.6	23.9	4.9	6.1	19.8	58.8	9.5	30.3	3.3	10.3	100
Station Number	Easting	Northing	Element																			
			Na	Nb	Ni	P	Pb	Rb	S	Sb	Sc	Sn	Sr	Ta	Th	Ti	U	V	W	Y	Zn	Zr
Units			(%)	(ppm)	(ppm)	(%)	(ppm)	(ppm)	(%)	(ppm)	(ppm)	(ppm)	(ppm)	(ppm)	(ppm)	(%)	(ppm)	(ppm)	(ppm)	(ppm)	(ppm)	(ppm)
Method			TICP	TICP	TICP	TICP	TICP	TICP	TICP	TICP	TICP	TICP	TICP	TICP	TICP	TICP	TICP	TICP	TICP	TICP	TICP	TICP
07GLE10-53	541694	5893709	2.903	36.5	2.1	0.005	627.6	185.6	<1	1.3	2	10	52	2.7	28.7	0.064	8.6	5	6.2	10.9	289	81.6
07JLO10-54	540602	5897830	1.155	7.9	38.9	0.076	12.6	102.6	0.5	4	14	1.3	472	0.6	5.3	0.335	1.4	141	1.3	15	58	31.3
07JLO14-87	567045	5877649	0.111	19	26.7	0.073	27.2	2	<1	0.9	12	4.8	2075	1.4	15.7	0.405	4.6	86	0.8	27.6	85	17.4
07JLO18-118	554373	5879944	0.016	19.7	540	0.196	8.4	55.9	<1	122.2	16	1	228	1	6.2	0.421	1.6	142	0.8	13.5	99	75.7
07JLO18-126	554332	5875955	3.272	2.9	8.9	0.13	13.2	106.6	0.2	0.4	8	0.5	1684	0.2	0.8	0.18	1.5	135	0.2	7.8	52	38.8
07GLE20-106	542139	5894516	1.933	3.8	45.1	0.132	2.7	53.2	0.1	4	31	1.2	1165	0.3	1	0.868	0.6	399	0.8	23.8	84	63.3
07JLO20-131	551661	5881262	2.974	1.7	25.9	0.063	5.5	58.8	<1	0.7	25	0.9	345	0.1	0.8	0.415	1.3	256	1.3	12.9	84	43.8
07JLO21-141	546726	5881716	0.643	5.7	38.4	0.043	6	49.4	0.2	32.5	14	1.1	284	0.5	3.8	0.259	1.2	199	3.6	12.3	79	30.7
07JLO22-147-2	547698	5881795	3.09	2.8	16.5	0.21	12.1	91.7	1.5	1.7	9	1.8	1455	0.2	1.5	0.255	0.8	176	0.5	11.6	89	39.9
07GLE26-119	546480	5876166	1.188	1.9	30.9	0.293	6.6	44.1	0.2	0.4	21	0.6	382	0.2	1.3	0.328	1.5	273	0.9	10.8	85	30.3
07GLE29-137	535507	5889129	2.854	2.4	6.1	0.098	5.3	5.6	0.1	0.6	21	1	195	0.2	0.8	0.537	0.8	175	0.2	24.6	64	61.8
07GLE23-114	555518	5895807	2.575	9.7	149.2	0.188	5.1	13.4	0.4	0.2	30	1.3	513	0.7	2.3	0.931	0.5	269	0.3	25.9	80	43.9
07JLO13-83	544811	5902426	3.171	15.9	5	0.055	25.1	157.3	0.1	<1	4	2.2	311	1.2	19.4	0.171	7.6	28	0.3	14	45	32.3
07GLE3-10	546610	5896809	3.06	15.7	15.5	0.075	17.4	128.2	<1	0.2	5	2.2	373	1.2	13.9	0.281	3.2	48	0.2	11.6	42	31.7
07GLE31-147	544702	5895672	3.557	23.3	20.8	0.277	15.5	55.1	0.1	0.6	11	1.4	1228	0.9	11.6	0.634	4.1	155	0.8	16.6	88	125.4
07JLO13-80	555424	5898275	0.013	1.5	2304.3	0.001	2.7	2.1	<1	2.5	10	0.6	23	0.1	0.2	0.012	0.9	31	0.6	1.5	55	1.6
07JLO20-134	546542	5881292	1.967	1	12.7	0.23	5.8	87.3	0.2	0.1	15	0.7	1923	0.1	0.5	0.39	0.2	309	2.6	13.5	80	42.4
07GLE26-126	546469	5881403	1.733	2.1	29.4	0.322	4.6	63.2	0.1	<1	24	0.6	1326	0.1	0.6	0.46	0.2	299	0.5	14.6	101	45.2
07GLE22-111	551521	5876622	2.945	4.2	28.6	0.139	3	36.5	0.6	0.2	34	1.2	1081	0.2	1.2	0.923	0.5	370	0.2	26.4	113	79.7
07JLO25-177	542458	5885376	1.796	2.5	16.6	0.335	8.5	56.9	0.1	0.3	23	0.7	1358	0.1	1	0.448	0.6	319	0.2	15.4	101	61
07JLO27-190	544116	5892126	1.475	1.8	13.9	0.235	1.9	59.2	0.3	0.2	32	0.7	909	0.1	0.6	0.626	0.3	437	0.1	12.4	85	12.8
Std CANMET WPR1			0.021	1.7	3293	0.02	5.7	4.7	0.7	0.8	11	0.8	8	0.1	0.2	0.192	0.1	81	-0.1	3.8	96	14.6
Recommended			2.4	2900	0.013	6	5	0.9	0.9	12	1.1	7	8	0.4	0.179	0.2	65				95	18
% Difference			200.0	34.1	12.7	42.4	5.1	6.2	25.0	11.8	8.7	31.6	13.3	200.0	66.7	7.0	66.7	21.9	200.0	200.0	1.0	20.9

06JLO: TICP= Four acid digestion - inductively coupled plasma emission/mass spectrometry analysis. FA - Lead collection fire assay - ICPE Finish. Acme analytical, Vancouver



Figure 6. Intrusion breccia, Ahbau Creek mafic-ultramafic complex, upper falls on Ahbau Creek.

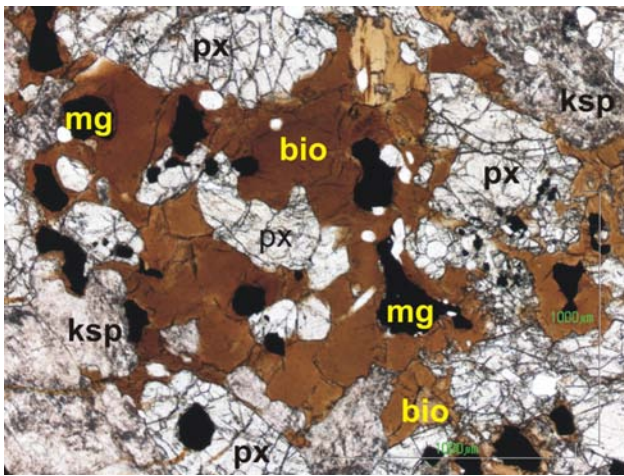


Figure 7. Photomicrograph of pyroxene-biotite diorite from the Ahbau Creek mafic-ultramafic complex, shows subhedral pyroxene, plagioclase and magnetite grains enveloped by large poikilitic biotite (07JLO10-59). Plane-polarized light. Abbreviations: bio, biotite; ksp, K-feldspar; mg, magnetite; px, pyroxene.

a number of overlapping Early Jurassic ages that include a concordant U-Pb titanite age of 188.3 ± 0.5 Ma, and Ar-Ar plateau ages from hornblende (187.7 ± 1.1 Ma) and biotite (186.34 ± 0.96 Ma). Another Early Jurassic U-Pb zircon age of 186 ± 2 Ma is reported for late-stage pegmatite from the Polaris complex (Nixon et al., 1997). Samples of the Ahbau Creek and Cottonwood River stocks have been collected for Ar-Ar dating. Results are pending.

CRETACEOUS PLUTONS

Naver Pluton

The Naver pluton is a north-trending 500 km^2 body of mainly granite composition that underlies the area from Mount George southward into the current map area at Genevieve Lake (Fig 2; Struik et al., 1992). North of the map area, it intrudes the Eureka thrust, providing a minimum age for the suture between the Quesnel, Slide Mountain and Kootenay terranes. The southern end of the pluton extends into the study area and is represented by three isolated, well-rounded and subdued outcrops of white weathering granite. The texture of the granite varies from feld-



Figure 8. Medium-grained melanocratic pyroxene-hornblende monzodiorite and trachytic orthoclase megacrystic syenite phases of the Cottonwood mafic-ultramafic complex, Cottonwood Creek.

spar megacrystic to coarsely equigranular. Mafic minerals commonly form less than 7% of the rock. Biotite predominates with hornblende present in some of the more mafic border phases. The southern border of the pluton is characterized by a narrow zone (20–200 m) containing xenoliths of metavolcanic and metavolcaniclastic rocks.

Modal mineral contents based on point counts and nomenclature following the classification of Streckeisen (1973) indicates primarily granite composition and rare granodiorite (Struik et al., 1992). Thin sections show 30 to 40% plagioclase, 30 to 35% orthoclase, 25 to 30% rounded quartz and 5 to 7% biotite±muscovite. Accessory minerals include sphene, zircon and magnetite. Alteration of plagioclase includes minor sericite, clay and saussurite±calcite. The texture and mineralogy of the granite is well exhibited in staining off-cut thin-section blocks with sodium cobaltinitrate (Fig 9).

Northerly trending porphyritic granite dikes intrude hornfelsed Nicola Group volcanic and volcaniclastic country rocks peripheral to the southern margin of the Naver pluton. The dikes trend southerly, dipping steeply to the east and rarely exceeding 5 m in width. Mineral composition is similar to the main pluton and comprises 2 to 3 mm phenocrysts of euhedral to resorbed quartz, 2 to 5 mm plagioclase and finer grained 1 mm crystals of chloritic and/or sericitic biotite in a fine orthoclase-rich matrix. The fine-grained groundmass with resorbed porphyritic phenocrysts suggest the rapid cooling and quenching characteris-

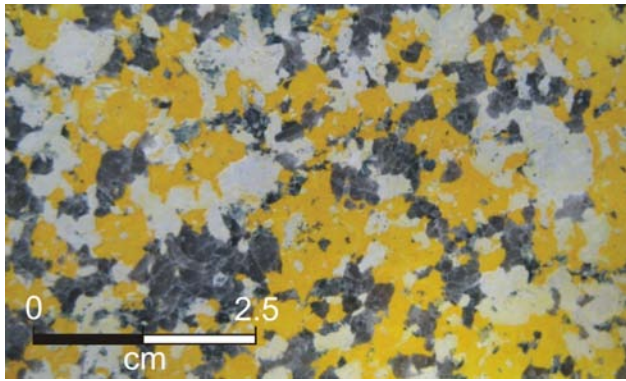


Figure 9. Equigranular granite phase of the Naver pluton stained with sodium cobaltinitrate to determine the percentages of plagioclase, potassium feldspar and quartz.

tic of narrow dikes; the composition and proximity to the Naver pluton suggest consanguinity.

The Naver pluton was assigned a mid-Cretaceous age by Wanless et al. (1967) on the basis of K-Ar biotite ages of 107.3 ± 5 Ma and 109 ± 6 Ma. Hunt and Roddick (1988) confirmed the age with new K-Ar isotopic ages of biotite that yielded 98 ± 3 and 101 ± 2 Ma dates. Uranium-lead age determinations on zircon and monazite fractions from an additional two samples suggest a 113 ± 1 Ma crystallization age for the pluton (Struik et al., 1992). The ca. 100 Ma K-Ar biotite dates are cooling ages indicating relatively slow cooling after crystallization.

Tertiary Sedimentary Rocks

Struik et al. (1990) mapped a narrow belt of poorly consolidated and generally undeformed Tertiary sedimentary rocks exposed on Umiti and Mary creeks in the eastern portion of the map (Fig 2). These areas were not visited during the current study and the following description summarizes earlier work.

Struik et al. (1990) correlated these sedimentary rocks with three mid-Tertiary formations, the Australian Creek, Fraser Bend and Crownite, which are confined to a belt no more than 15 km wide along the Fraser River, west and south of Quesnel. Rouse and Matthews (1979) interpreted the preservation of these Oligocene to Late to Middle Miocene fluvial and paludal sedimentary rocks exposed along the Fraser River to their position in postdepositional down-faulted blocks rather than a valley-fill deposition model. The Australian Creek and Fraser Bend formations consist of well-sorted gravel, alternating finer and less well-sorted gravel and silt, clay and seams of lignite; the overlying Crownite Formation is almost pure diatomite with some clay.

Quaternary Cover

Unconsolidated Holocene and Pleistocene sediments cover much of the area. Bedrock is limited to deeply incised creeks and rivers and hilltops. Deglaciation outwash, lake and drift deposits comprise much of the sediments.

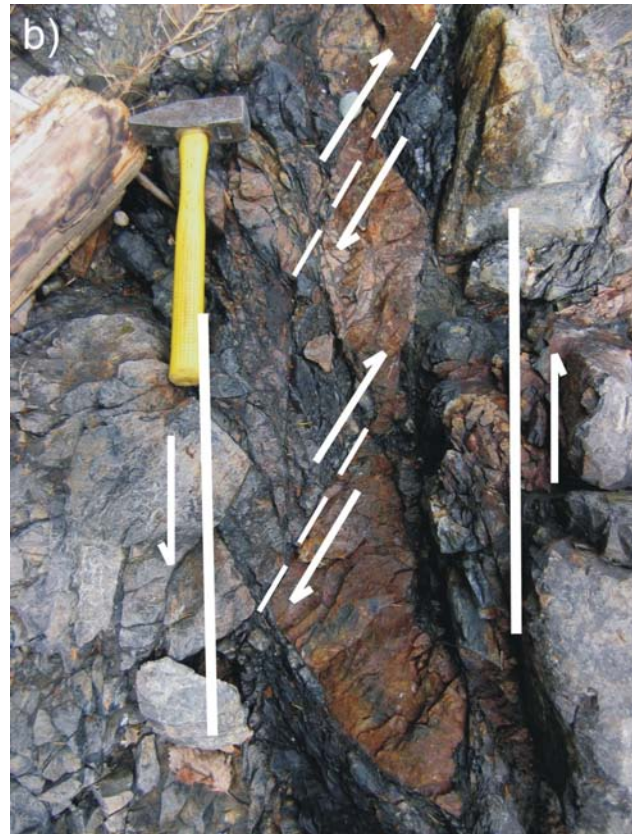


Figure 10. a) Northwest-trending brittle shear zone showing shear bands and asymmetry suggestive of dextral shear in a fault, cutting Cottonwood succession fine-grained volcanoclastic and sedimentary rocks, Ahbau Creek; coloured pencil for scale. b) Brittle shear zone, cutting Cottonwood succession fine-grained sedimentary rocks in Cottonwood River, same location as Figure 4. The anti-thetic slip along fracture planes indicates a sinistral sense of shear along the fault.

STRUCTURE

The general accepted structural evolution of the Cordillera at this latitude invokes from three to as many as five phases of regional folding (Rees, 1987; Struik, 1988a; McMullin, 1990). Evidence for the earliest deformation

that affects rocks of the Barkerville subterrane is not recorded in Quesnellia. The second phase of deformation produced tight to isoclinal northwest-trending folds, which Rees (1987) suggested had northeast to easterly vergence. This second phase of folding was synmetamorphic (i.e., phyllosilicate mineral growth parallels foliation). The third phase of regional deformation (McMullin, 1990), D_2 in Quesnellia, produced upright to inclined southwest to westward-verging backfolds. These northwest-trending fold structures are responsible for much of the regional map-scale patterns. The D_2 phase is responsible for the z-shaped folded terrane boundary (Barkerville subterrane and Quesnel Terrane) demarked by the Crooked amphibolite. Younger deformation (D_3) is evidenced by open upright folds and warps that lack a penetrative axial planar cleavage. Younger structures include prominent systems of Eocene dextral strike-slip and extensional faults (Panteleyev et al., 1996).

Structure in the Cottonwood map area is not well known due primarily to the poor exposure and lack of any distinctive marker units within the fine-grained clastic and volcanoclastic units that dominate the map. The study area lies on the west flank of a broad northwesterly plunging arch, cored by Snowshoe Group rocks and the Naver pluton. The regional trend of the units is northwesterly; faults trend north-northwest and northeast.

The Eureka and Spanish thrust faults separate the imbricated terranes and are the earliest structures recognized (Struik, 1986, 1988a). The Eureka thrust (Struik, 1983) separates the Quesnel Terrane in the hangingwall from the Barkerville subterrane in the footwall. It trends northerly and is marked by discontinuous serpentinite and amphibolite of the Crooked amphibolite and/or isolated magnetic highs on the residual total magnetic field plots reflecting covered serpentinitized ultramafic rocks. The hangingwall Nicola Group sedimentary rocks and footwall Snowshoe Group rocks are penetratively foliated adjacent to the structure. The Spanish thrust trends northerly and imbricates the eastern volcanoclastic succession with Nicola Group sedimentary rocks of the black pelite succession (Struik et al., 1990). The contact between the eastern sedimentary rocks and the eastern volcanoclastic succession was not located and therefore evidence for, or the degree of, imbrication along this structure could not be evaluated.

A number of northwest-trending parallel lineaments are defined by the drainage patterns of the Cottonwood River and Ahbau Creek in the northwestern portion of the map area. Northwest-trending discrete brittle fault structures from several metres up to tens of metres wide have been mapped in creek exposures along both of these drainage systems. Shear band orientation and asymmetric rotation of augen indicate a consistent dextral sense of shear for some of the northwest-trending faults (Fig 10a). Alternatively, similar northwest-trending brittle shears exposed along strike have shear sense indicators, which show sinistral motion along these fault structures (Fig 10b).

Struik et al. (1990) mapped a northeast-striking fault at the south end of Ahbau Lake that shows apparent dextral offset. The distribution of serpentinite and amphibolite units across the fault is consistent with dextral offset of the Crooked amphibolite and Eureka thrust across this lineament (Fig 2).

The volcanoclastic and sedimentary rocks of the Quesnel Terrane are tightly folded, locally refolded and sheared with intensity of deformation increasing eastward

(i.e., down section). The sedimentary rocks of the black pelite and Cottonwood River successions and some of the finer-grained volcanoclastic rocks show minor fold structures that consistently show northwest-trending, northeast-verging folds. Sparse structural data for the western volcanoclastic succession along Umiti Road suggest these rocks occupy the upper limb of a northeast-verging antiform.

METAMORPHISM

Metamorphism increases from west to east across the map area from prehnite-pumpellyite and zeolite grades to greenschist for the Mesozoic arc rocks and as high as garnet to amphibolite (?) facies for some of the Barkerville subterrane rocks (Greenwood et al., 1991; Read et al., 1991). A sharp transition from low to higher metamorphic grade is apparent at the terrane boundary between the Quesnel Terrane, the Crooked amphibolite and the Barkerville subterrane. Metamorphic mineral assemblages of the black pelite unit are characterized by chlorite-muscovite without biotite. Penetrative deformed rocks of the Crooked amphibolite are characterized by chlorite-epidote-amphibolite±biotite and/or antigorite-chlorite±tremolite and talc assemblages, whereas micaceous quartzite and schist of the Snowshoe Group contain a synkinematic metamorphic assemblage of biotite, muscovite±garnet and actinolite, locally retrograded to biotite and chlorite.

Rocks of the Quesnel Terrane and Barkerville subterrane, the black pelite and Snowshoe Group are penetratively deformed in the vicinity of the terrane boundary. West from this tectonic boundary, rocks of the Quesnel Terrane are not penetratively deformed or metamorphosed beyond lower greenschist facies.

Contact metamorphism affects a 1.5 to 2.0 km wide zone adjacent to the southern margin of the mid-Cretaceous Naver pluton. The volcanoclastic rocks are variably altered to a fine-grained, brown to dark purple biotite, chlorite, actinolite±pyrrhotite hornfels, with limited skarn and calcisilicate development in thin calcareous horizons. Overprinting the dark hornfels are fracture-controlled pale anastomosing bleached zones of Na and/or K-enriched hydrothermal alteration. No sulphide introduction was recognized.

MINERALIZATION

MINFILE indicates ten mineral occurrences and three different mineral deposit models applicable to the Cottonwood map area that include seven past-producing surficial placer gold deposits located along the Cottonwood River and tributaries, four zones of alkaline porphyry Cu-Au mineralization known to occur at Mouse Mountain and auriferous polymetallic veins that have been the focus of past and current exploration on the G-South developed prospect (Table 2). North of the area, limited production is recorded for gold-quartz veins near Hixon and showings of molybdenum and tungsten mineralization occur near the western margin of the Naver pluton. South of the map area, Cu±Mo porphyry mineralization associated with calcalkaline intrusive complexes at the Gibraltar mine and Cu±Au porphyry and propylitic Au replacement associated with alkaline intrusive centres at the Mount Polley mine and the QR mine,

TABLE 2. MINFILE OCCURRENCES WITHIN THE COTTONWOOD MAP SHEET (093G/01).

MINFILE #	Name (Status)	Easting	Northing	Commodity	Description
Surficial Placers					
093G 009	Hannador Lightning Creek (past producer)	552929	5882203	Au	region underlain to the west by Mesozoic sedimentary and volcanic rocks of the Quesnel Terrane and to the east by Proterozoic to Paleozoic dominantly metasedimentary rocks of the Omineca Belt quartz veins in greenschist facies rocks of the Omineca Belt are commonly auriferous the Hannador deposit occurs on Lightning Creek at the junction of Angus Creek in the southeastern corner of the map area. This deposit is one of several past placer gold producers on Lightning and other creeks draining the Omineca Belt. These placer deposits occur in late Tertiary (Miocene) gravels
093G 022	MacMillian, Cottonwood River (past producer)	550695	5882365	Au	the pre-Tertiary geology of this area consists of mafic volcanic and sedimentary rocks of the Upper Triassic Nicola Group and Lower Jurassic volcanoclastic rocks of the Quesnel Terrane the Cottonwood workings produced alluvial platinum and gold
093G 025	Cottonwood Placer (past producer)	560751	5880164	Au, Pt	mafic volcanic and sedimentary rock of the Upper Triassic Nicola Group of the Quesnel Terrane Cottonwood workings produced alluvial platinum and gold
093G 026	Mary Creek, Norton Creek, Old San Juan (past producer)	562718	5873544	Au	ultimate source of gold may have been the auriferous veins of the Barkerville subterrane from which the Cottonwood River drains pre-Tertiary geology of this area consists of mafic volcanic and sedimentary rocks of the Upper Triassic Nicola Group and Lower Jurassic volcanoclastic rocks of the Quesnel Terrane gold from the Mary Creek placer deposit produced from pay gravels a few centimetres to a few metres thick. The roundness of the
093G 059	Gagen Creek (past producer)	562718	5873544	Au	well-worn, fairly coarse placer gold in bench-type deposits primarily basalt
093G 060	Mostique Creek (past producer)	565811	5875007	Au	primarily underlain by argillite cut by intrusions at the mouth of Mostique Creek, coarse placer gold occurs in a buried channel deposit, and fine gold originated mainly from post-glacial gravels overlying the deposit
Polymetallic veins					
093G 007	G-South (developed prospect)	542976	5894496	Au, Cu, Zn, Pb, Ag	sulphide mineralization occurs disseminated in the country rocks and in stockworks and breccia infillings with quartz, calcite, epidote and chlorite; two main types of mineralization: 1) disseminated and fracture-controlled pyrite, pyrrhotite and rare chalcocopyrite in volcanic or along contacts with rhyolite dikes and 2) massive sulphide mineralization within gouge zones up to 1.9 m wide consisting of pyrite, arsenopyrite and sphalerite and occasionally chalcocopyrite and galena high gold and silver values are not coincident and do not appear to be associated with the percentage of sulphides present. The best mineralization is suggested to occur at or near the intersection of regional fault structures that trend northerly and southeasterly
Porphyry Cu-Au; alkalic					
093G 003	Mouse Mountain (past producer)	545508	5878048	Cu, Ag, Au	Mineralization is mainly chalcocopyrite, with bornite and minor tetrahedrite. Mineralization occurs within felsic to intermediate breccias as fracture fillings. Disseminated copper mineralization also occurs within the feldspar porphyry stock. Associated alteration in the volcanic rocks is mainly argillic and propylitic with some potassic alteration of the stock small felsic to intermediate alkaline plutons of Late Triassic and Early Jurassic intrude basalt and volcanoclastic rocks of the upper part of the Nicola Group
093G 005	Mouse Mountain (showing)	543824	5876796	Cu	Upper Triassic to Lower Jurassic sedimentary and volcanic rocks; Intruding these rocks are small felsic to intermediate alkalic plutons of Late Triassic and Early Jurassic age. These are in part comagmatic with the volcanic rocks of the upper part of the Nicola stratigraphy. Mouse Mountain is underlain by one of these alkalic plutons (Mouse Mountain Stock). The stock is composed of syenite, syeno-monzonite, with minor gabbro. The stock has intruded Late Triassic basaltic rocks and is mantled unconformably (?) by Early Jurassic intermediate tuffs and polyolithic breccias <i>Chalcocopyrite mineralization is reported to occur within gabbro bodies</i>

respectively, comprise important exploration models for this part of the Nicola Arc (Fox, 1975; Bailey, 1990).

Proven and probable reserves at Gibraltar (0.2% Cu cutoff) total 232 Mt of 0.318% Cu and 0.010% Mo with an addition 554 Mt of measured and indicated at 0.28% Cu and 0.008% Mo and 15 Mt of oxide (0.10% acid-soluble Cu) at 0.148% Cu (Taseko Mines Limited, 2007). Proven and probable reserves at the Mount Polley mine incorporate the open pit mining of the Southeast zone, the C2 zone and the Springer zone in addition to the Wight and Bell pits and totals 59.9 Mt of 0.36% Cu, 0.27 g/t Au and 0.73 g/t Ag (Imperial Metals Corporation, 2007), with an addition of measured and indicated resources of 73.5 Mt of 0.356% Cu, 0.302 g/t Au and 1.42 g/t Ag. Reserves for the QR estimated by Kinross Gold Corporation at January 1, 1997 were 1.57 Mt grading 3.99 g/t Au, with the main zone hosting an estimated 0.6 Mt of 4.4 g/t Au (MINFILE 093A 121). The mill and related surface facilities have been rehabilitated by Cross Lake Minerals Ltd. and the restart of operations and development of the QR mine is projected to commence in the third quarter of 2007 (Cross Lake Minerals Ltd., 2007).

Twenty-one rock geochemical samples were collected during the course of the summer mapping program of alteration and mineralization to assess the mineral potential of the area (Table 1). Sampling of the mineralization at Mouse Mountain was carried out last year (Jonnes and Logan, 2007).

EXPLORATION ACTIVITY

With the exception of placer leases, Richfield Ventures Corporation holds the majority of mineral claims that cover the 093G/01 map area and have been actively exploring the Quesnel belt since 2004. They have completed soil geochemical sampling programs, following up multi and single-element regional geochemical survey anomalies and geophysical anomalies generated by the low-level helicopter-borne geophysical survey completed in 2005 over the G-South, Ahbau Lake and Mary Creek targets (Tempelman-Kluit, 2006).

The multisensor (gamma-ray spectrometric and magnetic) airborne geophysical data for the Cottonwood-Wells area was collected by Fugro Airborne Surveys under contract to the Geological Survey of Canada (Carson et al., 2006). It was one of ten areas flown in the summer months of 2004 and 2005 in central British Columbia. Funding was derived from a joint 'Rocks to Riches' program involving a number of provincial, industry and First Nations partners and supported by Natural Resources Canada. The K, K-Th, magnetic total field and magnetic vertical gradient maps can be used to identify potassic alteration, and magnetite enrichment/depletion zones associated with Cu-Au mineralization (Fig 11) and have been used successfully to define porphyry targets elsewhere in the Quesnel Terrane (Shives, 2004).

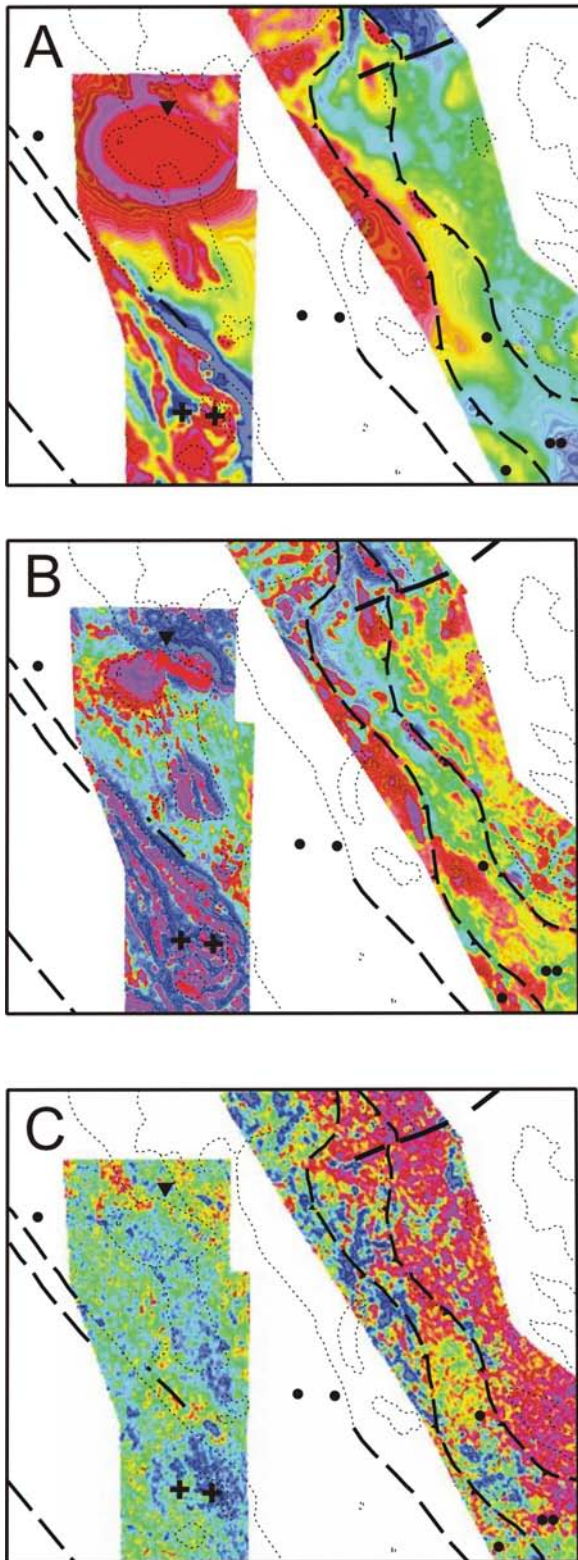


Figure 11. Contacts and faults from Figure 2 are shown together with airborne magnetic total field (a) for NTS 093G/01 (each map is 33.5 by 27.7 km); magnetic vertical gradient (b) and potassium-thorium ratio maps (c). Also shown are MINFILE occurrences for 093G/01: filled circles denote surficial placer gold, the inverted filled triangle denotes auriferous base-metal vein mineralization and crosses represent alkalic Cu-Au.

In the map area, the magnetic total field map can be used to recognize the distribution of magnetite-bearing intrusions, serpentinized ultramafic rocks of the Crooked amphibolite and demark the location of most of the pyroxene-phyric breccia and volcanoclastic rocks (Fig 11a). Utilizing the first vertical gradient magnetic plot (Fig 11b) provides a more precise location for variations in the magnetic field that can reflect lithological contacts and provide a means to trace contacts beneath overburden. From Figure 11b, the large first-order magnetic anomaly centred in the map can be seen to be composed of a number of discrete magnetic identities which, upon mapping, reveal small isolated plugs of the pyroxene-biotite-magnetite diorite coincident with the northern margin of a probable composite intrusion. Figure 11c is a plot of the ratio of eTh/K, which provides a negative anomaly (dark blue colour) that corresponds to anomalous K screened against equivalent Th values.

The Cu-Au mineralized showings on Mouse Mountain have become the main focus of Richfield Ventures Corporation's exploration efforts since 2006.

Mouse Mountain

Mouse Mountain is a Cu, Au and Ag past producer situated 9 km east-northeast of Quesnel in central BC. Some time around 1950, 20 t of hand-sorted ore grading 1.55 g/t Au, 15.5 g/t Ag and 5.6% Cu was produced from open pits and shipped to the Tacoma smelter (Sutherland Brown, 1957). A thorough account of the background history and development of the property is provided by Greig and Tempelman-Kluit (2007). Recent exploration work carried out on the Mouse Mountain property includes ground geophysical surveys, excavator trenching, mapping and rock sampling (Jonnes, 2006; Greig and Tempelman-Kluit 2007; Jonnes and Logan, 2007).

Mouse Mountain is underlain by a roughly equant stock of very fine grained, leucocratic syeno-monzonite, which coincides with a 1 km by 0.5 km airborne magnetic high and a much broader coincident airborne radiometric (K-Th) anomaly (Carson et al., 2006). The monzonite appears to be intimately related to the mineralization identified along the northeast flank of Mouse Mountain (Jonnes, 2006). Three discrete zones of Cu-Au mineralization are known and include, from north to south, the Rainbow, Valentine and High-grade zones. The character of mineralization, alteration and metal tenor for each of the three zones is reported in Jonnes and Logan (2007).

A deep-focus three-dimensional induced polarization (IP) survey has defined an 800 m long, northeast-trending chargeability target and eastward-offset resistivity target on the west flank of the mountain. A 10 000 m diamond drill program initiated October 2007 is currently underway to test the chargeability, resistivity and magnetic highs that flank Mouse Mountain on the west. Results from the current drilling program have not been released.

Alteration assemblages at the Valentine zone include a pervasive K-feldspar replacement of the monzonite (?) matrix, alteration and replacement of plagioclase crystals with orthoclase rims and at the same time introduction of magnetite, pyrite and chalcopyrite (Fig 12a). A secondary green pyroxene diopside occurs as vein and breccia fillings associated with minor chalcopyrite (Fig 12b). Following the main Cu-Au mineralization is a structure-controlled FeCO₃-silica-pyrite alteration event, which is texture and grade destructive.

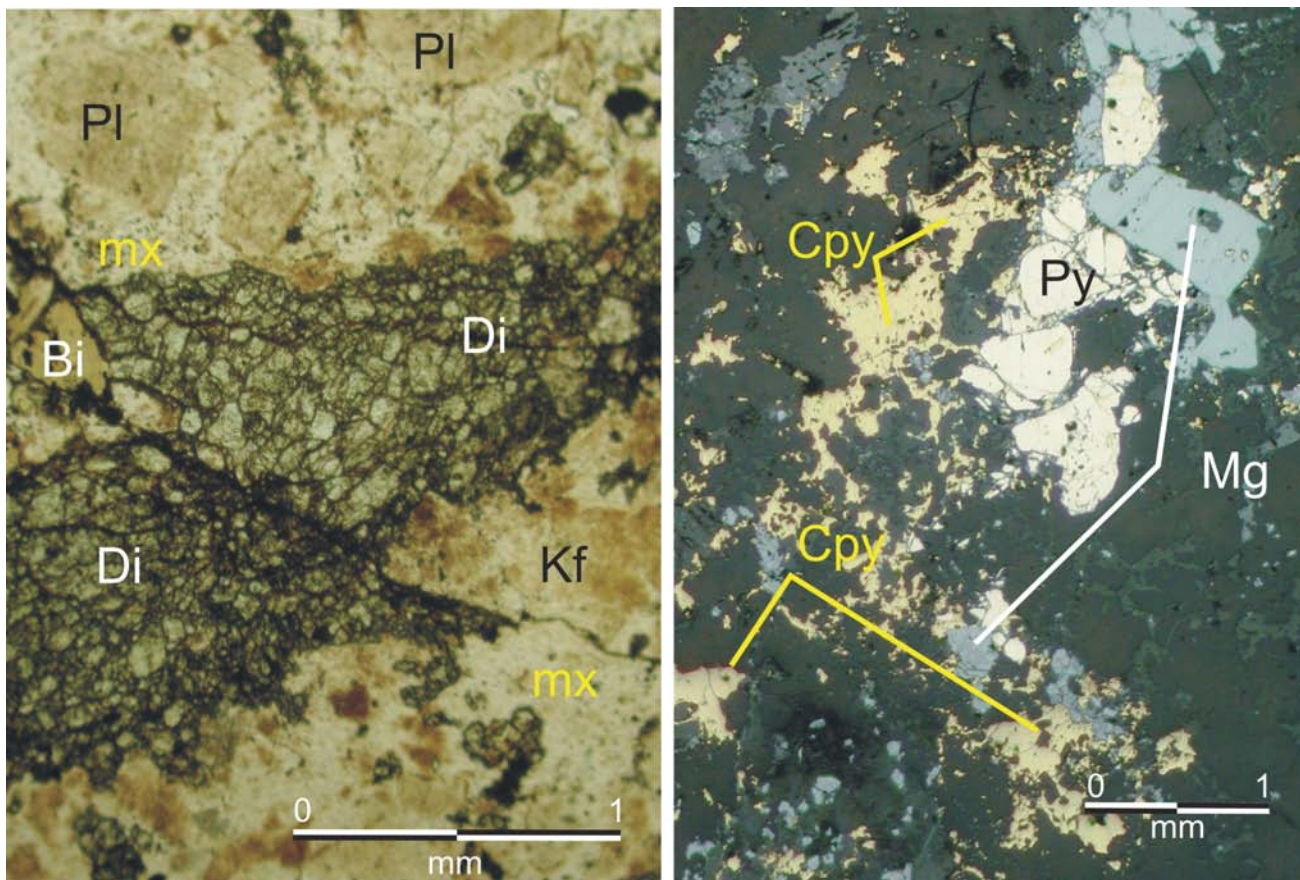


Figure 12. Polished thin section photomicrographs of Mouse Mountain monzonite from the Valentine zone: a) K-flooded microporphyritic monzonite breccia, altered by secondary diopside; plane polarized light; b) opaque mineralogy consists of subhedral, coarse-grained, early pyrite and magnetite and relatively younger chalcopyrite and magnetite intergrowths occupying interstices in the breccia; reflected light. Abbreviations: Cpy, chalcopyrite; Di, diopside; Kf, K-feldspar; Pl, plagioclase; Py, pyroxene; Mg, magnetite; mx, matrix.

The distribution of multiple intrusive rocks of composite composition, the magnetic signature, alteration assemblages, chalcopyrite-magnetite mineralization are similar to the characteristics of alkalic Cu-Au porphyry mineralization known to be hosted by Nicola volcanic and plutonic rocks of the Quesnel Arc. Uranium-lead (zircon) dating of the monzodiorite that hosts mineralization at the Valentine zone returned a crystallization age of 207.4 ± 0.58 Ma. Alteration and mineralization overprint, however, appear to be closely linked to the monzodiorite and were probably generated from late-stage fluids associated with the Mouse Mountain monzonite.

G-South

The G-South developed prospect (MINFILE 093G 007) is located approximately 28 km north-northeast of Quesnel in a 2 by 1 km² area north of Ahbau Creek. Here, auriferous base-metal veins occupy north and northeasterly trending brittle shears that cut hornfelsed Nicola Group volcanic and volcanoclastic sedimentary rocks. The volcanic rocks are intruded to the south by a Late Triassic to Early Jurassic ultramafic-mafic plutonic complex and to the north by the mid-Cretaceous Naver pluton. Narrow northeast-trending dikes of granite related (?) to the Naver pluton occupy mineralized structures and are weakly mineralized.

Gold-bearing sulphide veins of the Ahbau Au zone were staked and explored beginning in the 1960s. In 1968, Equatorial Resources Ltd. and then in 1971, Texas Gulf Sulphur explored the property for volcanogenic massive sulphide mineralization. Several narrow zones of subeconomic auriferous sulphide vein mineralization were delimited, but the economic potential of the property (i.e., continuity) was considered low due to disruption by faulting (Newell and Podolsky, 1971). Between 1982 and 1988, Gabriel Resources Inc. conducted fieldwork over the property that included heavy-mineral concentrate sampling, soil and rock geochemistry, very low frequency electromagnetic (VLF-EM) and magnetometer surveys, geological mapping, an airborne geophysical survey, backhoe trenching and percussion and diamond drilling (Troup and Ridley, 1982; Ridley et al., 1983; Butterworth et al., 1985; Walcott, 1986; Kowalchuk, 1987; Kowalchuk and Mathison, 1987; Lechow, 1987a, b; Newton, 1988). Diamond drilling completed in 1986 (1896 m in 25 holes) and 1987 (2809 m in 21 holes), while relatively shallow (all less than 200 m), did intersect considerable Au grades in narrow discontinuous brittle fault structures. Newton (1988) reported anomalous Au values in more than 120 drill intersections of greater than or equal to 0.34 g/t Au.

Gold mineralization occurs in north-trending brittle shear zones, a northwest-trending apparently younger fault, the Discovery zone and as disseminated and

stockwork replacements localized in cherty tuff and fine-grained volcanoclastic rocks.

Mineralization associated with the north-trending structures consists primarily of pyrite and pyrrhotite with lesser amounts of sphalerite, galena, chalcopyrite and arsenopyrite and is confined to <1.0 m and often <0.5 m wide breccia zones. The mineralized zones are sulphide-rich and either gangue-poor massive sulphide or intergrown with variable amounts of quartz-carbonate±chlorite gangue in veins, stockworks and breccia. Leucocratic, variably but characteristically FeCO₃ and clay altered, northerly trending quartz and orthoclase porphyritic dikes intrude along and across the north-trending structures at the G-South. The dikes are characterized by crystal aggregates of euhedral quartz, fine-grained relict biotite and disseminated pyrite and associated with sparse chalcopyrite and gold±galena mineralization.

Mineralization at the Discovery zone is hosted within a massive sulphide vein that strikes 227° and dips 35° to the northwest. It has been traced for about 50 m by trenching, but along-strike extension of the mineralized structure could not be demonstrated with follow-up drilling (Kowalchuk and Mathison, 1987). Selected assay results from Trench 1 on the Discovery zone show consistent mineralization over widths of 1.0 and 2.0 m. Mean values from three 1.0 m wide samples from the Discovery zone trench are 8.48 g/t Au, 38.74 g/t Ag, 0.75% Cu, 0.76% Zn, 0.04% Pb, 0.95% As; from three 2.0 m wide samples also from the Discovery zone trench are 6.74 g/t Au, 38.79 g/t Ag, 0.43% Cu, 0.40% Zn, 0.08% Pb, 0.49% As (Kowalchuk and Mathison, 1987). The Discovery zone trench was not located during regional mapping and could not be sampled.

Irregular sulphide stockworks, in fractured cherty tuffaceous argillite and fine volcanoclastic units (east zone of Newell and Podolsky, 1971), have returned grab samples with impressive 1 to 3% Cu values. Mapping and sampling in this area could not duplicate the high-grade mineralization reported.

Auriferous base-metal mineralization on the G-south property occupy north and southwest-trending structures that locally host weakly mineralized porphyritic granite apophyses of the Naver pluton and infer a temporal and possible genetic relationship with mid-Cretaceous plutonism.

Ahbau Lake Property

The Ahbau Lake property comprises two exploration targets situated approximately 2.5 km west and 3 km south of the outflow of Ahbau Lake. The claims straddle the boundary between micaceous quartzite, phyllite and schist of the Snowshoe Group and black pelite of the eastern Nicola Group (Tipper, 1960; Struik et al., 1990) and cover 25 anomalous values of Au (>20 ppb) in silt and pan concentrate samples obtained in a regional geochemical survey ca. 1980. Follow-up work by Leishman (1986, 1987) resulted in the recognition of a small (1 by 0.5 km) ultramafic body of Crooked amphibolite in the northern grid area that R. Wells studied petrographically and described as serpentinized pyroxenite. Dark, fine-grained Harveys Ridge rocks crop out east of the serpentinite and include calcareous, quartz, muscovite schist and micaceous (biotite+muscovite) marble.

A 2006 soil sampling program was undertaken to assess the continuity of previously determined Au anomalies

and to test for anomalous soil geochemical signatures in other metals. A total of 2834 samples were collected and analyzed by ICP-MS for 24 elements. The results for the southern grid were geochemically flat, but the north grid area shows a strong geochemical responsiveness with two distinctive multi-element anomalous areas (Tempelman-Kluit, 2007). In addition, each geochemical anomalous zone corresponds to a distinctive target generated from the 2005 airborne multiparameter survey, a U target and a total field magnetic high. Anomalous Au values in the north grid cluster locally, defining areas of prospecting interest but with no consistent trend or spatial relationship to other elements.

The airborne magnetic high trends northwest (Fig 11a) and shows a direct spatial relationship to outcrops of serpentinized pyroxenite and a strong multi-element soil geochemical response for Ni, Co, Cr and Mg. The U airborne target is a tabular 1 km² zone within fine-grained, dark-coloured Harveys Ridge phyllite and micaceous quartzite in the footwall to the Eureka thrust. Coincident with the U target is a large, northwest-trending (1 km by 0.5 km) multi-element soil geochemistry anomaly defined by Zn but also includes Cu, Cd, Pb, Ag, Ba and P. Copper-zinc and low Pb content is typical of Besshi deposits together with anomalous concentrations of a number of metals, including Co, Mo, Bi, As and Ni (Slack, 1993).

CONCLUSIONS

The Cottonwood map area is underlain by Proterozoic to Paleozoic siliciclastic rocks of the Kootenay Terrane, Late Paleozoic mafic schist of the Slide Mountain Terrane and Middle Triassic to Early Jurassic sedimentary, volcanic and plutonic rocks of the Quesnel Terrane. Middle Jurassic and mid-Cretaceous post-accretionary granitic stocks intrude this part of the Quesnel Terrane. Isolated Miocene sedimentary rocks are preserved beneath a thick Quaternary cover of glaciofluvial, lacustrine and lodgment till deposits.

The Nicola Group in the Cottonwood map area includes four main subdivisions: a Middle to Late Triassic eastern black pelite succession comprising dark phyllite, siltite and slate; a Late Triassic eastern volcanic package of pyroxene-phyric flow breccia and tuff that structurally overlies the black pelite; a central belt of siltstone, cherty argillite, limestone and volcanoclastic sandstone of the Cottonwood River succession; and a pyroxene-rich volcanoclastic succession characterized by polyolithic volcanic conglomerate containing sedimentary, plutonic and volcanic clasts that overlies the Cottonwood River succession in apparent depositional contact. The Cottonwood River succession and conformably overlying western volcanoclastic succession are Late Triassic or older because the upper part of the succession is cut by monzonite of the Late Triassic Mouse Mountain stock.

Small isolated exposures of Early Jurassic sedimentary and volcanic rocks have been recognized through fossil and radiometric dating techniques, respectively.

Intrusive rocks in the map area include the Late Triassic (ca. 205 Ma) Mount Polley, Early Jurassic (ca. 187 Ma) Polaris and mid-Cretaceous (ca. 110 Ma) Naver intrusive suites.

Copper-gold mineralization at Mouse Mountain probably formed from late-stage fluids associated with the Late

Triassic (ca. 207 Ma) Mouse Mountain monzonite. The auriferous base-metal-mineralized brittle shear zones, cutting mid-Cretaceous hornfelsed volcanic and volcanoclastic rocks of the Nicola Group at the G-South property, probably formed from fluids related to the quartz porphyritic granite apophyses of the Naver pluton. Base-metal soil geochemical anomalies reported from the Ahbau Lake property are consistent with a Besshi-type of volcanogenic massive sulphide mineralization, but further work is required to test this hypothesis. The Early Jurassic (?) mafic-ultramafic intrusive complexes that intrude the Cottonwood River succession do not appear to have anomalous associated Au or Cu sulphide mineralization.

ACKNOWLEDGMENTS

The manuscript benefited from a critical review by Brian Grant of the BC Ministry of Energy, Mines and Petroleum Resources. Leslie Able, Graham Leroux and Brian Hawes from the University of Victoria provided capable and enthusiastic field assistance. Sheila Jonnes is thanked for sharing her knowledge of the geology and Cu-Au mineralization at Mouse Mountain. Many thanks are extended to Richard Friedman and Thomas Ullrich of the Pacific Centre for Isotopic and Geochemical Research at the University of British Columbia for providing the geochronological analyses that are so critical to these mapping projects.

REFERENCES

- Bailey, D.G. (1978): The Geology of the Morehead Lake Area; unpublished Ph.D. thesis, *Queen's University*, 198 pages.
- Bailey, D.G. (1988): Geology of the central Quesnel belt, Swift River, south-central British Columbia (93B/16, 93A/12, 93G/1); in *Geological Fieldwork 1988, BC Ministry of Energy, Mines and Petroleum Resources*, Paper 1989-1, pages 167–172.
- Bailey, D.G. (1990): Geology of the central Quesnel belt, British Columbia; *BC Ministry of Energy, Mines and Petroleum Resources*, Open File 1990-31, 1:100 000 map with accompanying notes.
- Bloodgood, M.A. (1987): Deformational history, stratigraphic correlations and geochemistry of eastern Quesnel Terrane rocks in the Crooked Lake area, central British Columbia, Canada; unpublished M.Sc. thesis, *The University of British Columbia*, 165 pages.
- Bowman, A. (1889): Report on the geology of the mining district of Cariboo, British Columbia; *Geological Survey of Canada*, Annual Report for 1887–1888, Volume 3, Part 1, pages 1–49.
- Breitsprecher, K. and Mortensen, J.K. (2004): BC Age 2004A-1: A database of isotopic age determinations for rock units from British Columbia; *BC Ministry of Energy, Mines and Petroleum Resources*, Open File 2004-03.
- Butterworth, B.P., Freeze, J.C. and Troup, A.G. (1985): Geology, geophysics and geochemistry report for the Ahbau Creek property; submitted by Gabriel Resources Inc., *BC Ministry of Energy, Mines and Petroleum Resources*, Assessment Report 13 712.
- Campbell, R.B. (1978): Quesnel Lake (93A) map-area; *Geological Survey of Canada*, Open File Map 574.
- Carson, J.M., Dumont, R., Potvin, J., Shives, R.B.K., Harvey, B.J.A. and Buckle, J.L. (2006): Geophysical series – NTS 93G/1, 93G/8 and 93B/16 – Cottonwood, British Columbia; *Geological Survey of Canada*, Open File 5289, 10 maps.
- Colpron, M. and Price, R.A. (1995): Tectonic significance of the Kootenay Terrane, southeastern Canadian Cordillera: an alternative model; *Geology*, Volume 23, pages 25–28.
- Cross Lake Minerals Ltd. (2007): Website, URL <<http://www.crosslakeminerals.com/s/Home.asp>> [November 2007].
- Ferri, F. (2000): Geological setting of the Frank Creek massive sulphide occurrence near Cariboo Lake, east-central BC; in *Geological Fieldwork 1999, BC Ministry of Energy, Mines and Petroleum Resources*, Paper 2000-1, pages 31–50.
- Ferri, F. and Schiarizza, P. (2006): Re-interpretation of Snowshoe Group stratigraphy across a southwest-verging nappe structure and its implications for regional correlation within the Kootenay Terrane; in *Paleozoic Evolution and Metallogeny of Pericratonic Terranes at the Ancient Pacific Margin of North America, Canadian and Alaskan Cordillera*, Colpron, M. and Nelson J.L., Editors; *Geological Association of Canada*, Special Paper 45, pages 415–432.
- Fox, P.E. (1975): Alkaline rocks and related mineral deposits of the Quesnel trough, British Columbia (abstract); *Geological Association of Canada*, Program with Abstracts, page 12.
- Ghent, E.D., Erdmer, P., Archibald, D.A. and Stout, M.Z. (1996): Pressure-temperature and tectonic evolution of Triassic lawsonite – aragonite blueschists from Pinchi Lake, British Columbia; *Canadian Journal of Earth Sciences*, Volume 33, pages 800–810.
- Gill, J.B. (1981): *Orogenic Andesites and Plate Tectonics*; *Springer-Verlag*, 390 pages.
- Greenwood, H.J., Woodsworth, G.J., Read, P.B., Ghent, E.D. and Evenchick, C.A. (1991): Metamorphism, Chapter 16; in *Geology of the Cordilleran Orogen in Canada*, Gabrielse, H. and Yorath, C.J., Editors, *Geological Survey of Canada*, *Geology of Canada*, Number 4, pages 533–570 (also *Geological Society of America*, *The Geology of North America*, Volume G-2).
- Greig, C.J. and Tempelman-Kluit, D.J. (2007): Geological report on the Quesnel trough project; specifically the Mouse Mountain prospect, Quesnel River area, Cariboo Mining Division, British Columbia; unpublished report, *Richfield Ventures Corporation*, 68 pages.
- Höy, T. and Ferri, F. (1998): Stratatound base-metal deposits of the Barkerville subterranean, central British Columbia (093A/NW); in *Geological Fieldwork 1997, BC Ministry of Energy, Mines and Petroleum Resources*, Paper 1998-1, pages 13-1–13-12.
- Hunt, P.A. and Roddick, J.C. (1988): A compilation of K-Ar ages, Report 18; in *Radiogenic Age and Isotopic Studies*, Report 2; *Geological Survey of Canada*, Paper 88-2, pages 127–153.
- Imperial Metals Corporation (2007): Imperial reports production statistics and up dated Mount Polley resource: Imperial Metals Corporation, press release, March 2, 2007, URL <http://www.imperialmetals.com/s/News-2007.asp?ReportID=175026&_Type=News-Release-2007&_Title=Imperial-Reports-2006-Production-and-Updated-Mount-Polley-Reserve> [November 2007].
- Irvine, T.N. (1974): Alaskan-type ultramafic-gabbroic rocks in the Aiken Lake, McConnell Creek and Toodoggone map-areas; *Geological Survey of Canada*, Paper 76-1A, pages 76–91.
- Jonnes, S. (2006): Progress report concerning bedrock geology data from Mouse Mountain; unpublished report, *Richfield Ventures Corp.*, 20 pages.
- Jonnes, S. and Logan, J.M. (2007): Bedrock geology and mineral potential of Mouse Mountain (NTS 093G/01), central British Columbia; in *Geological Fieldwork 2006, BC Ministry of Energy, Mines and Petroleum Resources*, Paper 2007-1 and *Geoscience BC*, Report 2007-1, pages 55–66.
- Kowalchuk, J.M. (1987): An interim report on the diamond drilling program on the Yardley Lake property, Cariboo Mining

- Division; submitted by Gabriel Resources Inc., *BC Ministry of Energy, Mines and Petroleum Resources*, Assessment Report 15 744.
- Kowalchuk, J.M. and Mathison, D.A. (1987): Geology, trenching and diamond drilling report on the Ahbau Creek property, Cariboo Mining Division; submitted by Gabriel Resources Inc., *BC Ministry of Energy, Mines and Petroleum Resources*, Assessment Report 15 927.
- Lechow, W.R. (1987a): Report on combined helicopter borne electromagnetic, magnetic, and VLF-EM survey, Yardley Lake area; submitted by Gabriel Resources Inc., *BC Ministry of Energy, Mines and Petroleum Resources*, Assessment Report 16 503.
- Lechow, W.R. (1987b): Report on combined helicopter borne electromagnetic, magnetic, and VLF-EM survey, Yardley Lake area; submitted by Gabriel Resources Inc., *BC Ministry of Energy, Mines and Petroleum Resources*, Assessment Report 16 645.
- Leishman, D.A. (1986): Geochemical Report on the Ahbau Lake property of Eureka Resources Inc. NTS 93G/1E; submitted by Eureka Resources Inc., *BC Ministry of Energy, Mines and Petroleum Resources*, Assessment Report 15 113
- Leishman, D.A. (1987): Geological and Geochemical Report on the Ahbau Lake property of Eureka Resources Inc. NTS 93G/1E; submitted by Eureka Resources Inc., *BC Ministry of Energy, Mines and Petroleum Resources*, Assessment Report 16 374.
- Logan, J.M. and Bath, A.B. (2006): Geochemistry of Nicola Group basalt from the central Quesnel Trough at the latitude of Mount Polley (NTS 093A/5, 6, 11, 12), central BC; in *Geological Fieldwork 2005*, *BC Ministry of Energy, Mines and Petroleum Resources*, Paper 2006-1, pages 83–98.
- Logan, J.M. and Mihalynuk, M.G. (2005): Regional geology and Setting of the Cariboo, Bell, Springer and northeast Porphyry Cu-Au Zones at Mount Polley, south-central British Columbia; in *Geological Fieldwork 2004*, *BC Ministry of Energy, Mines and Petroleum Resources*, Paper 2005-1, pages 249–270.
- Logan, J.M., Mihalynuk, M.G., Ullrich, T. and Friedman, R.M. (2007a): U-Pb ages of intrusive rocks and $^{40}\text{Ar}/^{39}\text{Ar}$ plateau ages of copper-gold-silver mineralization associated with alkaline intrusive centres at Mount Polley and the Iron Mask batholith, south and central British Columbia; in *Geological Fieldwork 2006*, *BC Ministry of Energy, Mines and Petroleum Resources*, Paper 2007-1 and *Geoscience BC*, Report 2007-1, pages 93–116.
- Logan, J.M., Bath, A.B., Mihalynuk, M.G., Ullrich, T.D., Friedman, R. and Rees, C.J. (2007b): Regional geology of the Mount Polley area, central British Columbia; *BC Ministry of Energy, Mines and Petroleum Resources*, Geoscience Map 2007-1.
- McMullin, D.W.A., Greenwood, H.J. and Ross, J.V. (1990): Pebbles from Barkerville and Slide Mountain terranes in a Quesnel Terrane conglomerate: evidence for pre-Jurassic deformation of the Barkerville and Slide Mountain terranes; *Geology*, Volume 18, pages 962–965.
- Mihalynuk, M.G., Erdmer, P., Ghent, E.D., Cordey, F., Archibald, D.A., Friedman, R.M. and Johannson, G.G. (2004): Coherent French Range blueschist: subduction to exhumation in <2.5 m.y.?; *Geological Society of America Bulletin*, Volume 116, Number 7/8, pages 910–922.
- Mihalynuk, M.G., Nelson, J. and Diakow, L. (1994): Cache Creek Terrane entrapment: oroclinal paradox within the Canadian Cordillera; *Tectonics*, Volume 13, pages 575–595.
- MINFILE (2007): MINFILE BC mineral deposits database; *BC Ministry of Energy, Mines and Petroleum Resources*, URL <<http://www.em.gov.bc.ca/Mining/Geosurv/Minfile/>> [December 2007].
- Monger, J.W.H. and Berg, H.C. (1984): Lithotectonic terrane map of western Canada and southeastern Alaska: in *Lithotectonic Terrane Maps of the North American Cordillera*, Siberling, N.J. and Jones, D.L., Editors, *United States Geological Survey*, Open File Report 84-523.
- Mortimer, N. (1987): The Nicola Group: Late Triassic and Early Jurassic subduction-related volcanism in British Columbia; *Canadian Journal of Earth Sciences*, Volume 24, pages 2521–2536
- Newell, J.M. and Podolsky, G. (1971): Geological, geochemical and geophysical report on the Thunder and Kim claim group and Rain 1-20 mineral claims; submitted by Texasgulf, *BC Ministry of Energy, Mines and Petroleum Resources*, Assessment Report 3385.
- Newton, D. (1988): Geological, geophysical, geochemical and percussion drilling report on the Ahbau Creek property; submitted by Gabriel Resources Inc., *BC Ministry of Energy, Mines and Petroleum Resources*, Assessment Report 17 309.
- Nixon, G. T., Hammack, J.L., Ash, C.H., Cabri, L.J., Case, G., Connelly, J.N., Heaman, L.M., Laflamme, J.H.G., Nuttall, C., Paterson, W.P.E. and Wong, R.H. (1997): Geology and platinum-group-element mineralization of Alaskan-type ultramafic-mafic complexes in British Columbia; *BC Ministry of Energy, Mines and Petroleum Resources*, Bulletin 93, 141 pages.
- Panteleyev, A., Bailey, D.G., Bloodgood, M.A. and Hancock, K.D. (1996): Geology and mineral deposits of the Quesnel River – Horsefly map area, central Quesnel trough, British Columbia; *BC Ministry of Energy, Mines and Petroleum Resources*, Bulletin 97, 156 pages.
- Parrish, R., Roddick, J.C., Loveridge, W.D. and Sullivan, R.W. (1987): Uranium lead analytical techniques at the Geochronology Laboratory, Geological Survey of Canada; in *Radiogenic Age and Isotopic Studies*, Report 1, *Geological Survey of Canada*, Paper 87-2, pages 3–7.
- Patterson, I. and Harakal, J. (1974): Potassium-argon dating of blueschists from Pinchi Lake, central British Columbia; *Canadian Journal of Earth Sciences*, Volume 11, pages 1007–1011.
- Read, P.B., Woodsworth, G.J., Greenwood, H.J., Ghent, E.D. and Evenchick, C.A. (1991): Metamorphic map of the Canadian Cordillera: Geological Survey of Canada, Map 1714A, scale 1:2 000 000.
- Rees, C.J. (1987): The Intermontane – Omineca Belt boundary in the Quesnel Lake area, east central British Columbia: tectonic implications based on geology, structure and paleomagnetism; unpublished PhD thesis, *Carleton University*, 421 pages.
- Ridley, J.C., Butterworth, B.P. and Troup, A.G. (1983): Geology, geophysics and geochemistry report for the G-South property; submitted by Gabriel Resources Inc., *BC Ministry of Energy, Mines and Petroleum Resources*, Assessment Report 12 211.
- Roback, R.C., Sevigny, J.H. and Walker, N.W. (1994): Tectonic setting of the Slide Mountain Terrane, southern British Columbia; *Tectonics*, Volume 13, pages 1242–1258.
- Rouse, G.E. and Mathews, W.H. (1979): Tertiary geology and palynology of the Quesnel area, British Columbia; *Bulletin of Canadian Petroleum Geology*, Volume 27, pages 418–445.
- Schiarizza, P. (1989): Structural and stratigraphic relationships between the Fennell Formation and Eagle Bay Assemblage, western Omineca Belt, south-central British Columbia: implications for Paleozoic tectonics along the paleocontinental margin of western North America; unpublished MSc thesis, *University of Calgary*, 343 pages.

- Schiarizza, P. and Preto, V. (1987): Geology of the Adams Plateau – Clearwater – Vavenby area; *BC Ministry of Energy, Mines and Petroleum Resources*, Paper 1987-2, 88 pages.
- Schiarizza, P. and Macauley, J. (2007): Geology and mineral occurrences of the Hendrix Lake area, south-central British Columbia (93A/02); in *Geological Fieldwork 2006*, *BC Ministry of Energy, Mines and Petroleum Resources*, Paper 2007-1 and *Geoscience BC*, Report 2007-1, pages 179–202.
- Shives, R.B.K., Thomas, M.D., Cathro, M.S. and Diakow, L.J. (2004): Interpretation of Airborne Geophysics; Kamloops Exploration Conference and Trade Show 2004, April 1, Kamloops, Short Course notes.
- Slack, J.F. (1993): Description and grade-tonnage models for Besshi-type massive sulphide deposits in Mineral Deposits Modeling, Kirkham, R.V., Sinclair, W.D., Thorpe, R.I. and Duke, J.M., Editors; *Geological Association of Canada*, Special Paper 40, pages 343–371.
- Streckeisen, A. (1973): Plutonic rocks, classification and nomenclature recommended by the IUGS subcommission on the systematics of igneous rocks; *Geotimes*, Volume 18, Number 10, pages 26–30.
- Struik, L.C. (1982): Bedrock geology of Cariboo Lake (93A/14), Spectacle Lake (93H/3), Swift River (93A/13) and Wells (93H/4) map areas; *Geological Survey of Canada*, Open File 858.
- Struik, L.C. (1983): Bedrock geology of Spanish Lake (93A/11) and parts of adjoining map areas, central British Columbia; *Geological Survey of Canada*, Open File Map 920, scale 1:50 000.
- Struik, L.C. (1986): Imbricated terranes of the Cariboo gold belt with correlations and implications for tectonics in southeastern British Columbia; *Canadian Journal of Earth Sciences*, Volume 23, pages 1047–1061.
- Struik, L.C. (1988a): Regional imbrication within Quesnel Terrane, central British Columbia, as suggested by conodont ages; *Canadian Journal of Earth Sciences*, Volume 25, pages 1608–1617.
- Struik, L.C. (1988b): Structural geology of the Cariboo gold mining district, east-central British Columbia; *Geological Survey of Canada*, Memoir 421, 100 pages.
- Struik, L.C., Fuller, E.A. and Lynch, T.E. (1990): Geology of Prince George (east half) map area (93G/E); *Geological Survey of Canada*, Open File 2172.
- Struik, L.C. and Orchard, M.J. (1985): Late Paleozoic conodonts from ribbon chert delineate imbricate thrusts within the Antler Formation of the Slide Mountain Terrane, central British Columbia; *Geology*, Volume 13, pages 794–798.
- Struik, L.C., Parrish, R.R. and Gerasimoff, M. D. (1992): Geology and age of the Naver and Ste Marie plutons, central British Columbia; in *Radiogenic age and isotopic studies: Report 5*; *Geological Survey of Canada*, Paper 91-2, pages 155–162.
- Sutherland Brown, A. (1957): Mouse Mountain (53° 122° S.E.); in *Minister of Mines Annual Report 1956*, *BC Ministry of Energy, Mines and Petroleum Resources*, page 33.
- Taseko Mines Limited (2006): Taseko adds 74 Million Tons to Gibraltar's Mineral Reserves, press release, December 12, 2006, URL < http://www.tasekomines.com/tko/NewsReleases.asp?ReportID=162562&_Type=News-Releases&_Title=Taseko-Adds-74-Million-Tons-To-Gibraltars-Mineral-Reserves > [November 2007].
- Tipper, H.W. (1960): Prince George map area, Cariboo District, British Columbia; *Geological Survey of Canada*, Map 49-1960.
- Tempelman-Kluit, D.J. (2006): Geological Report on the Quesnel trough project including the G-South, Mouse Mountain, Blackstone, Chubby Bear, Quesnel River area, Cariboo Mining Division, British Columbia; unpublished report, *Richfield Ventures Corporation*, May 8, 2006, 95 pages.
- Tempelman-Kluit, D.J. (2007): Soil geochemistry of the Ahbau Lake property, Quesnel River Area, Cariboo Mining Division, British Columbia; unpublished report, *Richfield Ventures Corporation*, 31 pages.
- Travers, W.B. (1977): Overturned Nicola and Ashcroft strata and their relations to the Cache Creek Group, southwestern Intermontane Belt, British Columbia; *Canadian Journal of Earth Sciences*, Volume 15, pages 99–116.
- Troup, A.G. and Ridley, J.C. (1982): Geology, geophysics and geochemistry report for the G-South property; submitted by Gabriel Resources Inc., *BC Ministry of Energy, Mines and Petroleum Resources*, Assessment Report 11 061.
- Walcott, P.E. (1986): A geophysical report on an induced polarization survey, Hixon area; submitted by Gabriel Resources Inc., *BC Ministry of Energy, Mines and Petroleum Resources*, Assessment Report 15 084.
- Wanless, R.K., Stevens, R.D., Lachance, G.R. and Edmonds, C.M. (1967): Age determinations and geological studies, K-Ar isotopic ages, Report 8; *Geological Survey of Canada*, Paper 67-2, Part A.
- Winchester, J.A and Floyd, P.A. (1977): Geological discrimination of different magma series and their differentiation products using immobile elements; *Chemical Geology*, Volume 20, pages 325–342.
- Woodsworth, G.J., Anderson, R.G. and Armstrong, R.L. (1991): Plutonic Regimes; Chapter 15, in *Geology of the Cordilleran Orogen in Canada*, Gabrielse, H. and Yorath, C.J., Editors, *Geological Association of Canada*, *Geology of Canada*, Volume 4, pages 491–531.

Boundary Project: McKinney Creek (NTS 82E/03) and Beaverdell (NTS 82E/06E, 07W, 10W, 11W) Areas, South-Central British Columbia

by N.W.D. Massey and A. Duffy

KEYWORDS: Quesnellia, Paleozoic, Knob Hill Complex, Anarchist schist, Wallace Formation, McKinney Creek, Beaverdell

INTRODUCTION

The Boundary Project was initiated in 2005 with the purpose of better characterizing the lithological and geochemical variations within and between the various Paleozoic sequences in the southern Okanagan region along the United States border. These occur within the Quesnel Terrane, which is dominated by such Paleozoic mafic volcanic and pelitic sedimentary rocks, unconformably overlain by Triassic and Jurassic volcanic and sedimentary rocks. In the Boundary district, these are exposed between down-faulted blocks of Tertiary volcanic and sedimentary cover rocks preserved in structural keels between gneissic domes (Fig 1).

The individual Paleozoic sequences of the Boundary district have had a variety of names depending upon their location and appear to form three north-south belts. They are called the Knob Hill Complex and Attwood Formation in the Greenwood area; the Anarchist schist (or Group) in the Osoyoos – Rock Creek and Beaverdell areas; and the Kobau Group in the area between Oliver and Keremeos. The terms Kobau and Anarchist have also been used in Washington, though not always for directly correlatable rock packages.

The Paleozoic rocks of the Greenwood – Rock Creek area are preserved in a series of north-dipping thrust sheets (Little, 1983; Fyles, 1990). Many of the bounding thrusts are marked by serpentinite layers or pods. Tertiary extensional faulting has disrupted and modified the thrust sheets and makes correlation difficult between the Greenwood and Rock Creek areas. However, mafic volcanic flows and chert in the Johnstone Creek area are contiguous with similar outcrops of the Knob Hill Complex on the east side of the Kettle River valley (Fyles, 1990; Massey, 2007a). Massey (2007b) thus proposed to extend the Knob Hill Complex designation to these rocks. The term Anarchist schist was retained for the sequence of metasedimentary and metabasaltic rocks south of Highway 3, between Osoyoos and Rock Creek. It was also proposed to apply the Anarchist schist designation to similar rocks in

the Greenwood area, which Fyles (1990) had included in the Knob Hill Complex.

Following these revisions in nomenclature of the Paleozoic rocks of the Greenwood – Rock Creek area, the regional map now appears to show an east-west pattern, in keeping with pre-Tertiary structural grain, rather than the previous north-south pattern. Continuing this pattern further to the west led Massey (2007b, Fig 15) to suggest that the McKinney Creek area may be underlain by rocks of the Knob Hill Complex. Scattered serpentinite occurrences just south of the McKinney Creek pluton could possibly mark the bounding thrust, now intruded and hidden by the pluton. Mapping in the McKinney Creek area was designed to test this hypothesis.

The relationship of the Paleozoic rocks east of Beaverdell to the sequences in the south is uncertain due to extensive Mesozoic and Tertiary intrusive bodies. Mapping in this area was focused on better documenting these rocks and their possible relationships and correlations.

MCKINNEY CREEK AREA

Previous Work

The McKinney Creek area has a mining history dating from the discovery of vein gold deposits at Camp McKinney in 1887. The first geological report, by Bauerman (1885), was done as part of the Boundary Commission Expedition of 1859–1861. Regional mapping has been undertaken by Cairnes (1940), Little (1957, 1961), and Tempelman-Kluit (1989a, b). Detailed investigations of the lode gold mineralization at Camp McKinney were undertaken by Cockfield (1935), Cairnes (1937) and Hedley (1940). Much of the southern, lower lying parts of the area are covered by extensive glaciofluvial and moraine deposits (Kowall, 1986c).

Pre-Jurassic Rocks

The suggested extension of the Knob Hill Complex into the McKinney Creek area proved to be unfounded. Although outcrop is limited in many areas due to extensive Quaternary cover, all observed outcrops of Paleozoic rocks belong to the Anarchist schist (Fig 2). The age of the Anarchist schist is still poorly determined, as no paleontological or geochronological data are available. Rubidium-strontium geochronology in the Osoyoos area only records Tertiary metamorphic ages (Ryan, 1973). In the McKinney map area, the rocks of the Anarchist schist are intruded by plutons and smaller bodies of Jurassic and Eocene age.

This publication is also available, free of charge, as colour digital files in Adobe Acrobat® PDF format from the BC Ministry of Energy, Mines and Petroleum Resources website at http://www.em.gov.bc.ca/Mining/Geolsurv/Publications/catalog/cat_fldwk.htm

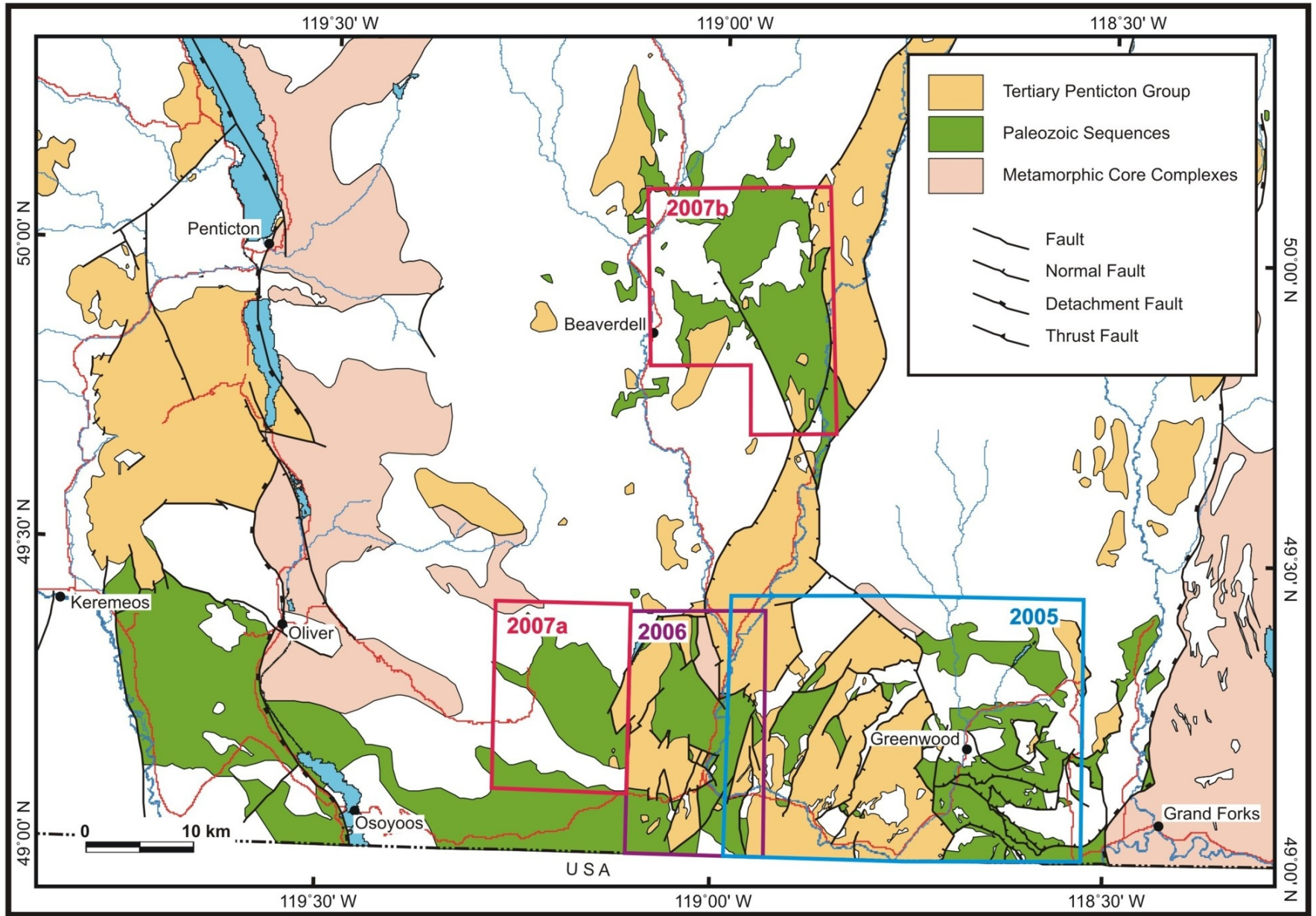


Figure 1. Distribution of Paleozoic Quesnellian rock suites in the boundary district (south-central part of NTS 82E), amended from Massey et al. (2005). Boxes outline the areas studied in 2005 (Greenwood), 2006 (Rock Creek) and 2007 (a, McKinney Creek; b, Beaverdell).

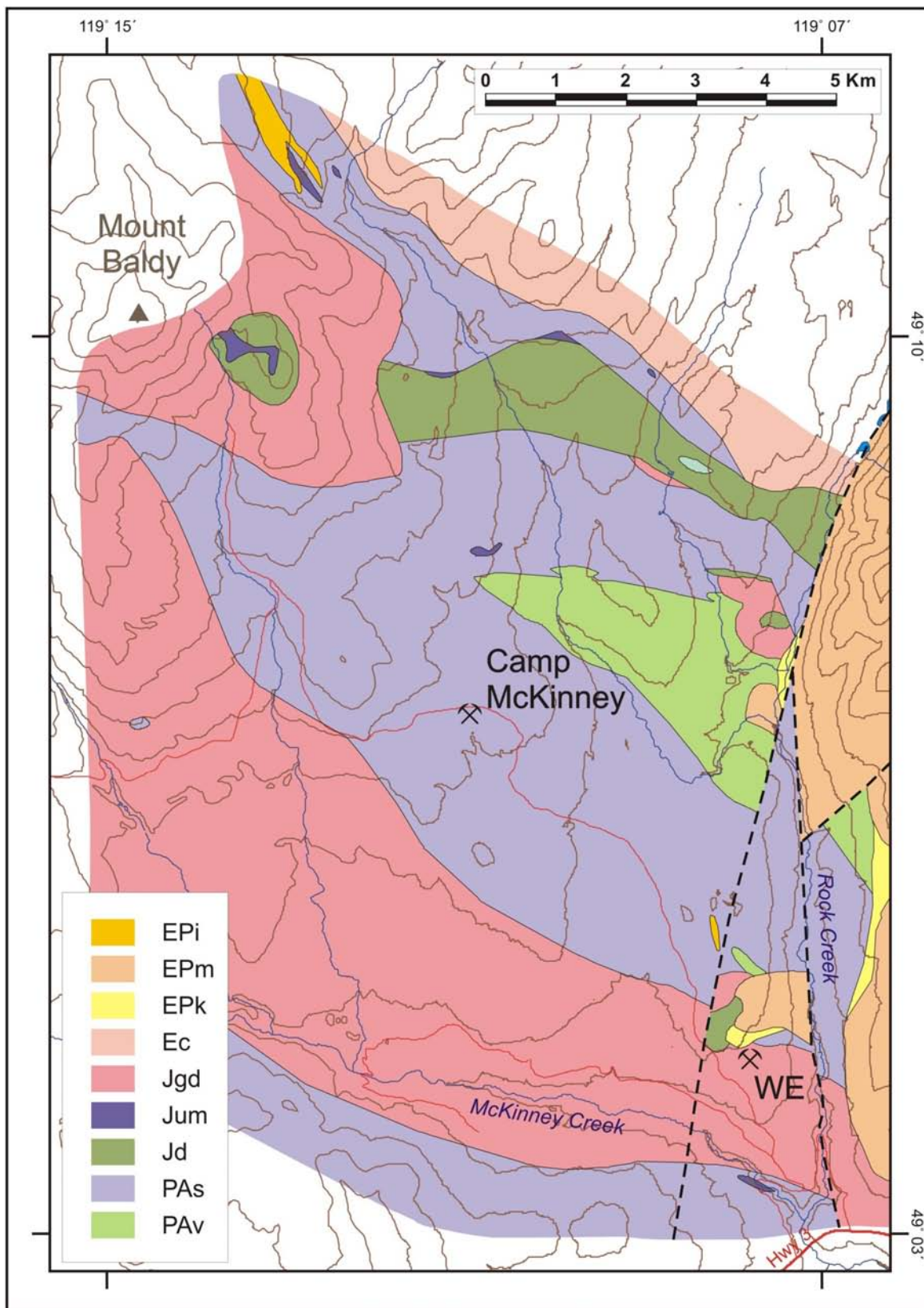


Figure 2. Geological sketch map of the McKinney Creek area. Extent of coloured polygons shows the limit of area mapped in 2007. Abbreviation: WE, War Eagle (Dayton Property). Legend: PAv, metavolcanic unit of Anarchist schist; PAs, metasedimentary unit of Anarchist schist; Jd, diorite-gabbro intrusions; Jum, pyroxenite and serpentinite intrusions; Jgd, granodiorite intrusions (Nelson suite); Ec, K-feldspar megacrystic granite (Coryell suite); EPk, Kettle Valley Formation; EPm, Marron Formation; Epi, minor porphyry intrusions consanguineous with Marron Formation.

ANARCHIST SCHIST

The Anarchist schist can be subdivided into a metasedimentary unit and a metavolcanic unit, delineated on the dominant rock types within them. The stratigraphic relationship between the units is uncertain. Deformation of the schist involves at least two phases of deformation. Schistosity generally trends southeast with medium to steep southwesterly dips in the northern part of the map area, and steep northeasterly dips in the south. The Camp McKinney area is also marked by northeasterly trending schistositities with moderate southeasterly dips. Secondary spaced cleavages in quartzite and crenulation cleavage in quartzite (Fig 3a) and meta-argillite also trend north to northeast. Small-scale folds of foliations generally tend to plunge southwest with shallow dips. The general map pattern of the metasedimentary and metavolcanic units seems to define a major northwesterly trending fold (Fig 2). However, the lack of conclusive way-up structures and stratigraphic relationship precludes determining if the fold is antiformal or synformal.

Metasedimentary unit

The metasedimentary unit is dominated by quartzite, argillaceous quartzite, and meta-argillite with minor metabasalt and limestone. Quartzite is metachert that is variably recrystallized with a fine to medium-grained sugary texture (Fig 3b), and typically has a white to pale grey or darker bluish grey colour. Beds are usually 1 to 2 m thick (Fig 3c) but can vary up to 10 m, and may show a knobby or irregular weathered surface. They may be massive or show dark and light laminations and banding (Fig 3d). Ribbon bedding is rarely preserved.

Phyllitic to schistose argillaceous metasedimentary rocks are darker, with fine-grained black chlorite or biotite schist layers interlayered with lighter quartz-rich layers. Epidote laminae and bands suggest fine-grained tuffaceous interbeds. The schistosity is commonly crenulated and contorted (Fig 4a). Quartz veining may also be contorted, disrupted and augened. Some thicker, less siliceous meta-argillite beds are carbonaceous. Minor limestone beds vary from one to two centimetres (Fig 4b) up to 10 m thick (Fig 4c). They are white to grey in colour, fine to medium grained and recrystallized.



Figure 3. Quartzite of the Anarchist schist: a) crenulation cleavage (s_2) developed in a foliated quartzite (s_1 parallel to s_0) (07NMA07-17; UTM Zone 11, 5443051N, 338954E, NAD83); b) recrystallized quartzite (07NMA11-12; UTM Zone 11, 5442153N, 339187E, NAD83); c) quartzite beds with meta-argillite (chlorite-quartz schist) interbeds (07NMA02-14; UTM Zone 11, 5444292N, 344895E, NAD83); d) laminated quartzite (07NMA01-10; UTM Zone 11, 5450727N, 337896E, NAD83).

Metavolcanic unit

The metavolcanic unit comprises greenstone flows with minor breccia, tuff and metasedimentary rocks. Greenstone flows are massive and medium to dark grey or black in colour. They are fine grained and generally aphyric, though rare feldspar and pyroxene crystals are seen. Chlorite±epidote alteration is common, along with veining of quartz±chlorite±calcite. Chlorite and brown to black oxides are present on fractures. Tuffaceous interbeds are altered to green quartz–chlorite±sericite schist with epidote pods and laminae (Fig 4d).

Jurassic Intrusions

Intrusive rocks rim the McKinney Creek area on its north, west and south sides (Fig 2). These comprise two major bodies — the McKinney Creek and Mount Baldy granodiorites — as well as an unnamed suite of ultramafic and mafic intrusions. The granodiorites have been correlated with the mid-Jurassic Nelson Intrusions and the Jura-Cretaceous Okanagan batholith, respectively (Little, 1961; Tempelman-Kluit, 1989a, b), though geochronological

data are lacking. The mafic rocks may be an older phase of the Nelson Intrusions and are intruded by granodiorite and included as xenoliths in granodiorite.

Diorite-gabbro

A belt of diorite occurs along the northeastern edge of the map area, intruding the Anarchist schist (Fig 2). Medium to coarse-grained diorite to gabbro is black to grey, weathering dark greenish grey. It comprises varying quantities of equigranular greenish black hornblende and white feldspar and occasional minor quartz (Fig 5a). Shear zones are common, accompanied by flattening and stretching of minerals (Fig 5b), white veinlets of feldspar and quartz, and chloritization. Pegmatitic diorite veins are also found (Fig 5c). The belt is a composite body with fine-grained chilled contacts between different diorite phases (Fig 5d). These fine grained chilled contacts can be difficult to distinguish from basaltic dikes in small outcrops.

Ultramafic intrusions

Significantly, there are several ultramafic intrusions spatially associated with the belt of diorite, and presumably



Figure 4. Less siliceous rocks of the Anarchist schist: a) chlorite-quartz schist (meta-argillite), pencil along axis of minor s-folding of foliation (07NMA05-12; UTM Zone 11, 5446337N, 341735E, NAD83); b) calcareous band within chlorite-quartz schist (07NMA05-12; UTM Zone 11, 5446337N, 341735E, NAD83); c) laminated marble (07NMA06-06; UTM Zone 11, 5448311N, 341637E, NAD83); d) quartz-chlorite schist with epidote pods (metatuff) (07NMA04-06; UTM Zone 11, 5447546N, 342904E, NAD83).

genetically related. These are pyroxenite, feldspathic pyroxenite and melanogabbro with grain sizes up to two to three centimetres. They are black to greenish black or grey and commonly weather orange-brown with a knobby, uneven surface (Fig 6a). They are partially to completely altered to serpentinite and, in one case, to talc and soapstone. Serpentinite is variably foliated. Black seams of magnetite (Fig 6b) and chromite up to several centimetres occur in some bodies and have received some attention in the past for their Cr and Ni potential.

This belt of diorite and ultramafic rocks is probably correlative with diorite seen on the Dayton property and may form the western extension of the belt that hosts the Old Nick deposit just east of Bridesville. It may also be contemporaneous with Jurassic ultramafic intrusions in the Greenwood area, e.g., on the Sappho property (Nixon, 2002).

Granodiorites

The McKinney Creek granodiorite is composed of two distinct phases — an early biotite granodiorite and a later porphyritic granodiorite. The biotite granodiorite is coarse

grained, up to 4 mm, and white to grey (Fig 7a). It is equigranular with typical salt and pepper texture made up of white feldspar, translucent quartz and black biotite plates. Biotite also forms clots up to 1 cm in size. Colour index averages 25. Small rounded amphibolite xenoliths are common (Fig 7b). Chlorite is often developed on fractures and joints.

The porphyritic granodiorite contains large white feldspar phenocrysts up to 2 cm in size (Fig 7c). The phenocrysts are euhedral laths or square in shape and show good twinning. The phenocrysts, which vary in amount from a few to 25%, are set in a coarse grained groundmass of white tabular feldspar, irregular translucent quartz and platy biotite. Biotite is less abundant than in the biotite granodiorite. Mafic xenoliths were observed but are not common. The porphyritic granodiorite intrudes the biotite granodiorite with good chilled contacts (Fig 7d). Pegmatite and aplite veins crosscut both granodiorite phases.

A smaller stock of granodiorite also crops out northwest of Fish Lake. It is medium to coarse grained, massive, pale grey to white, and generally equigranular, with euhedral white feldspar, rounded to irregular grey translu-

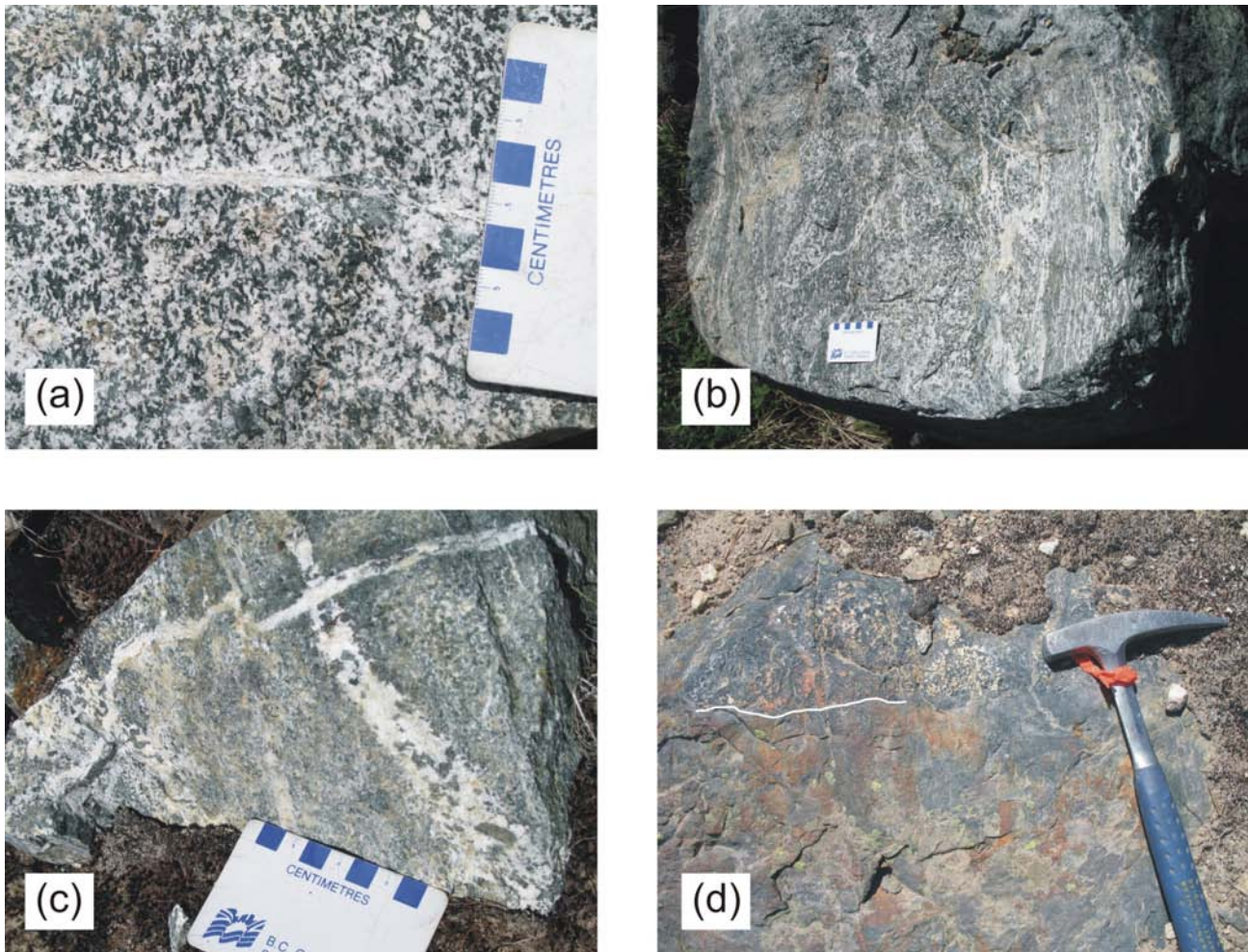


Figure 5. Jurassic diorite: a) typical coarse grained diorite (07NMA05-15; UTM Zone 11, 5447025N, 342198E, NAD83); b) shearing in diorite (07NMA01-03; UTM Zone 11, 545042N, 337675E, NAD83); c) hornblende-feldspar pegmatitic veins crosscutting diorite (07NMA05-15; UTM Zone 11, 5447025N, 342198E, NAD83); d) fine-grained chilled contact between two diorite phases, white line is emphasizing part of the contact (07NMA04-13; UTM Zone 11, 5446751N, 342696E, NAD83).

cent quartz, acicular greenish black hornblende and flakes of biotite. The colour index varies from 5 to 15. This granodiorite contains xenoliths of diorite and amphibolite. A similar body is found on the southern part of the Dayton property, though it tends to be finer grained and has a higher mafic content (colour indices ranging up to 25). Hornblende may occur as phenocrysts up to 1 cm in size.

The Mount Baldy granodiorite is medium to coarse grained, ranging from 2 to 5 mm, showing an equigranular, phaneritic texture. It is light grey to dark grey. It comprises euhedral white feldspar, irregular grey quartz and black tabular biotite. There is some chlorite alteration within the rock. The granodiorite is crosscut by feldspar porphyry dikes, assumed to be Tertiary in age. Isotropic, lath-shaped hornblende may be developed in the granodiorite around some porphyry dikes.

Tertiary Intrusions

The northeastern margin of the map area is marked by a white to pinkish potassium feldspar megacrystic granite intrusion typical of the Coryell Suite. Euhedral, lath to

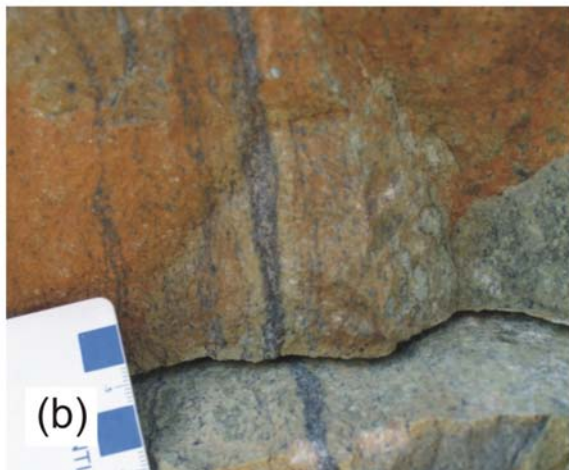


Figure 6. Jurassic ultramafic rocks: a) typical orange-brown outcrop of serpentinized pyroxenite (07NMA01-11; UTM Zone 11, 5450754N, 337817E, NAD83); b) magnetite seam in pyroxenite (07NMA01-14; UTM Zone 11, 5450311N, 338058E, NAD83).

square-shaped phenocrysts of pink K-feldspar are commonly 3 to 4 cm in size, though they range up to 8 cm. They are set in a coarse-grained groundmass of white and pink subhedral feldspar and polycrystalline quartz eyes up to 1 cm in size. Biotite is commonly less than 5%.

Pyroxene-feldspar porphyry, feldspar porphyry, and hornblende-feldspar porphyry dikes intrude all older rocks throughout the map area. These probably were feeders to the volcanic rocks of the Eocene Marron Formation.

BEAVERDELL AREA

Previous Work

The first and still only detailed regional map of the Beaverdell area is that of Reinecke (1915). He assigned the oldest stratified rocks to the Wallace group and correlated them, in part, with other Paleozoic sequences to the south, including the Anarchist schist and the Attwood 'Series'. Little (1957, 1961) and Tempelman-Kluit (1989a, b) extended this work to the east and west, including the older rocks in the "Anarchist Group". Detailed work on the mineral deposits of the area, including the silver-lead-zinc veins of the Beaverdell camp and the gold veins of the Carmi camp, has been reported by White (1949), Kidd and Perry (1957), Christopher (1975a, b; 1976), Peatfield (1978), Watson et al. (1982), Godwin et al. (1986) and Church (1995). Mathews (1988) reported on the Neogene volcanic rocks of the area while Kowall (1986a, b) mapped the Quaternary deposits.

Pre-Jurassic Rocks

The pre-Jurassic rocks of the Beaverdell area (Fig 8) differ significantly from the type Anarchist schist to the south. They are dominated by fine to medium-grained clastic sedimentary rocks which are essentially unmetamorphosed, though they do show extensive hornfelsing from Jurassic plutons. Limestone and greenstone members occur in the Crouse Creek area, and are the lowest exposed units. Significantly, no chert is developed in the sequence. Except for one small area, to the west of Crouse Creek, no penetrative deformation was observed.

Continuing correlation of these rocks with the Anarchist schist seems to be ill advised. It is proposed here to revert to Reinecke's original term — "Wallace" — for these rocks, though at the formation rather than group level. It should, however, be noted that not all of the area originally mapped as Wallace by Reinecke (1915) is actually underlain by pre-Jurassic rocks. There is a significant amount of younger intrusive material. In particular, a lot of the so-called pyroxene-phyric 'volcanics' in Reinecke's Wallace prove to be porphyry dikes of Tertiary age and, in one area east of Collier Lake, flows of the Eocene Marron Formation.

No geochronological or paleontological data are presently available for the Wallace formation rocks, though limestone samples have been collected for potential conodont determinations. Correlation of the Wallace is thus difficult. It is lithologically dissimilar to any of the Paleozoic sequences to the south. It does, however, show some similarities to parts of the Middle Triassic Brooklyn Formation of the Greenwood area or the Franklin Camp, though lack-

ing the distinctive basal sharpstone conglomerate, perhaps due to non-exposure.

WALLACE FORMATION

Larse Creek limestone member

A significant limestone unit occurs in the Larse Creek area, forming the lowest exposed unit in the Wallace formation. Contact with the overlying greenstone member is not exposed, but the limestone is estimated to be at least 100 m thick. It is grey on weathered surfaces, varying from black to grey to white on fresh surfaces. It is massive to well bedded and laminated (Fig 9a, b). Thin siliceous and minor calcsilicate veins weather positively. Macrofossils appear to be absent.

Fine to medium grained, grey to light blue marble occurs in the Trapping Creek area as xenoliths and pendants in the Jurassic granodiorite. These may be derived from the Larse Creek limestone member. However, their isolated position and metamorphism preclude certainty in correlation.

Crouse Creek greenstone member

A greenstone unit overlies the limestone member in the Crouse Creek area. This comprises mostly massive mafic flows, though amygdules are occasionally seen. The flows are medium to dark green-grey, bluish green or black. They may show bright green epidosite patches up to 30 cm across (Fig 10a) and veins of quartz-chlorite±epidote±calcite. Many flows are fine grained and aphyric, but feldspar-phyric and pyroxene-feldspar-phyric flows are also common. Phenocrysts are approximately 1 to 2 mm in size. Volcanic breccia, lapilli tuff, pyroxene lapilli tuff and chloritic metatuff (Fig 10b, c, d) are also found interbedded in the flows, as is laminated limestone. Some volcanic breccias also contain limestone and clastic sedimentary rock clasts.

Clastic sedimentary rocks

Most of the exposed Wallace formation is typically interbedded and laminated siltstone-argillite (Fig 11a). Siltstone beds are light coloured, buff to pale grey, while argillite beds are dark grey. Weathered surfaces may be broken with a coating of rusty oxides. Individual beds can range up to 3 cm thick with laminations about 1 to 2 mm



Figure 7. McKinney Creek granodiorite: a) typical biotite granodiorite (07NMA14-17; UTM Zone 11, 5437528N, 338967E, NAD83); b) rounded feldspar-amphibolite xenolith in biotite granodiorite 907NMA14-04; UTM Zone 11, 5437967N, 337557E, NAD83); c) porphyritic granodiorite phase, note sun glinting on feldspar twin plane in upper right (07NMA14-17; UTM Zone 11, 5437528N, 338967E, NAD83); d) chilled contact of porphyritic granodiorite against biotite granodiorite (07NMA14-17; UTM Zone 11, 5437528N, 338967E, NAD83).

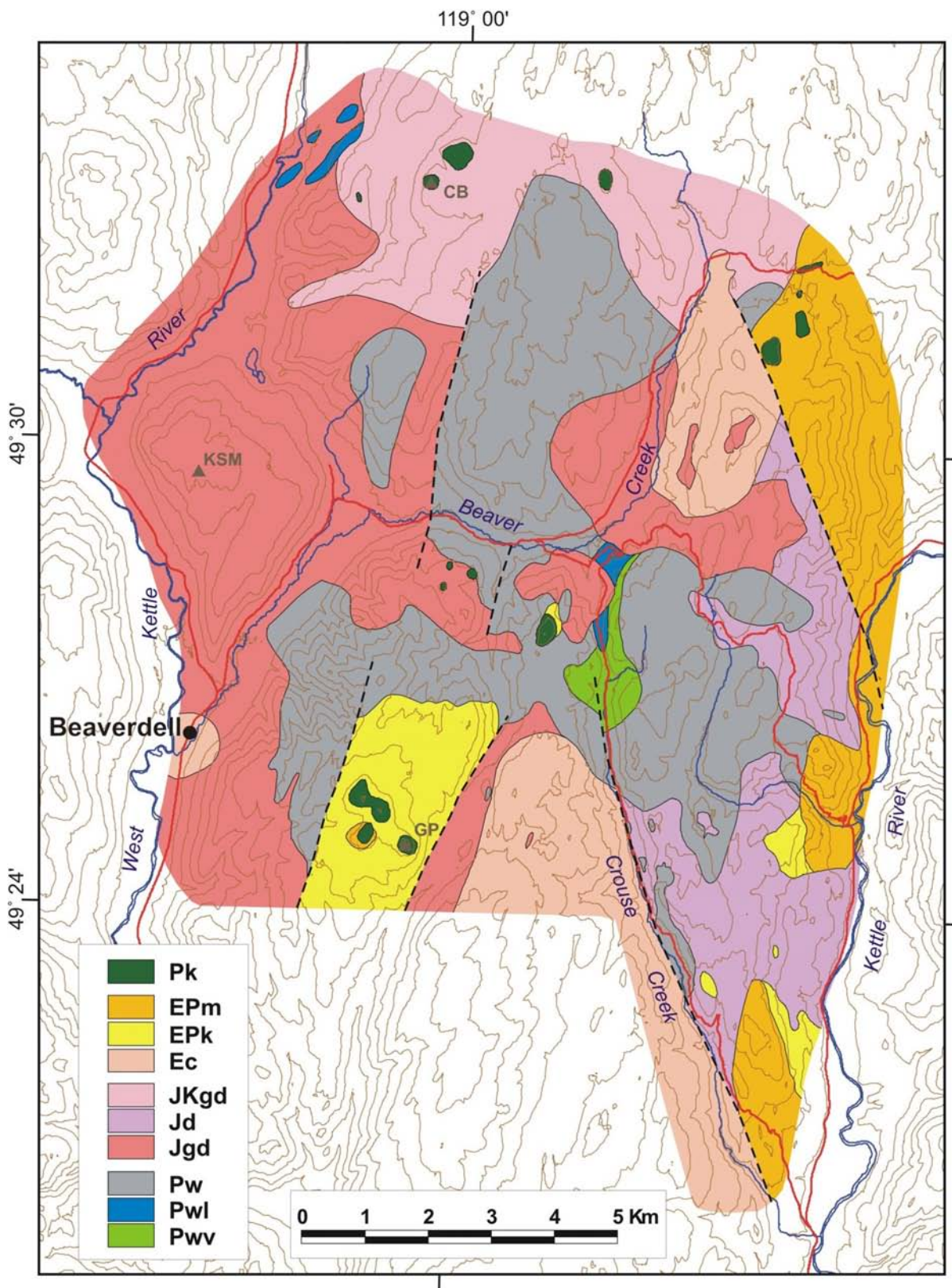


Figure 8. Geological sketch map of the area east of Beaverdell. Extent of coloured polygons shows the limit of area mapped in 2007. Abbreviations: CB, China Butte; GP, Goat Peak; KSM, King Solomon Mountain. Legend: Pw, Wallace formation; Pwl, Larse Creek limestone member of the Wallace formation; Pwv, Crouse Creek greenstone member of the Wallace formation; Jgd, granodiorite intrusions (Westkettle batholith, Nelson suite); Jd, diorite-quartz diorite intrusions (?Westkettle batholith, Nelson suite); Ec, K-feldspar megacrystic granite (Coryell suite); EPK, Kettle Valley Formation; EPm, Marron Formation; Pk, Kallis Formation.

thick. The sedimentary units are often siliceous or porcelaneous and may be recrystallized due to hornfelsing by Jurassic intrusions.

Coarser clastic beds are also found, though less common than the siltstone-argillite interbeds. Sandstone beds are grey, medium to coarse grained and generally massive. Hornfelsing sandstone is recrystallized to feldspar-quartz-amphibole assemblages that can be difficult to discriminate from microdiorite or microgranodiorite in the field. Conglomerate and pebbly sandstone have matrix-supported, rounded to subangular clasts (Fig 11b). The clasts are dominantly of siliceous siltstone and argillite, but also can include limestone, usually larger. All clasts appear to be intraformational and no exotic rock types have been observed.

Occasional white, tan or grey limestone interbeds vary from several centimetres up to five metres thick (Fig 11c). The limestone interbeds are massive and may be sparry or recrystallized due to hornfelsing, or may be variably silicified and skarned (Fig 11d).

Post-Triassic intrusions

Intrusive rocks envelope the Wallace formation in the Beaverdell area (Fig 8). These comprise several major granodiorite plutons and stocks in the western and central parts of the map area, designated the Westkettle batholith (Reinecke 1915) and probably correlative with the mid-Jurassic Nelson Intrusions (Little, 1961; Tempelman-Kluit, 1989a, b). Tempelman-Kluit (1989a, b) has also ascribed some of the granodiorite bodies to the north of the area as being part of the Jura-Cretaceous Okanagan batholith. No

geochronological data are available for these rocks in the area.

Megacrystic granite of the Coryell suite forms two intrusions in the east and south of the map area, as well as the small Beaverdell stock. Tertiary-age porphyry dikes abound through the area, intruding all older rocks. The Beaverdell stock has yielded a biotite K-Ar date of 58.8 ± 2.0 Ma (Godwin et al., 1986). Crosscutting dikes have been dated at 50.6 ± 1.5 Ma and 61.9 ± 2.2 Ma by whole-rock K-Ar methods by Watson et al. (1982). The latter also report biotite K-Ar dates for the Eugene Creek and Tuzo Creek stocks, west of Beaverdell, of 54.5 ± 1.9 Ma and 49.5 ± 2 Ma, respectively. A biotite K-Ar age of 49.4 ± 0.7 Ma has also been obtained from the megacrystic granite of the Margranite quarry, south of Beaverdell (Church, 1995).

JURASSIC

The Westkettle batholith is composed of granodiorite, quartz diorite and microgranodiorite with minor aplite and pegmatite. The granodiorite is white to light grey, medium to coarse grained equigranular with a typical salt-and-pepper texture (Fig 12a). Weathered surfaces are white to grey but can be greenish or slightly pink. The rock comprises white subhedral feldspar, translucent irregular quartz, greenish black tabular hornblende and black biotite flakes. Pink feldspar is minor. Quartz contents vary from about 5 to 20%, or may be absent in dioritic phases. Colour index is about 10 to 15, but may range up to 25 in diorite and quartz diorite. Chlorite and epidote occur in veins; chlorite and iron oxides, on fracture surfaces. Xenoliths of amphibolite and microdiorite are occasionally seen.

Bodies of diorite, quartz diorite, microdiorite and microgranodiorite intrude the sedimentary rocks of the



Figure 9. Larse Creek limestone member of the Wallace Formation: a) bedded limestone (07NMA21-13; UTM Zone 11, 5482534N, 358653E, NAD83); b) close up of laminations in limestone (07NMA22-04; UTM Zone 11, 5481427N, 357652E, NAD83).

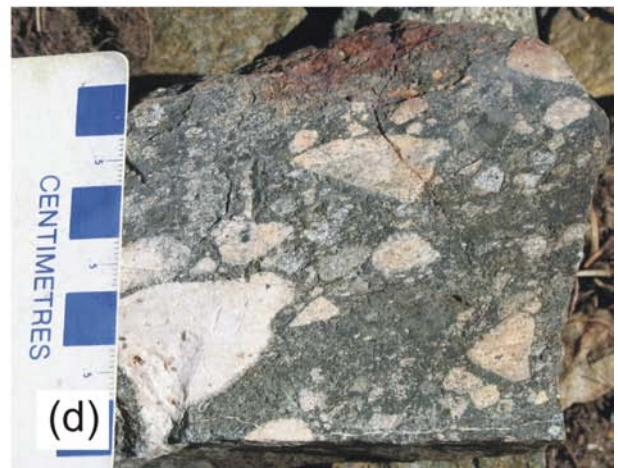
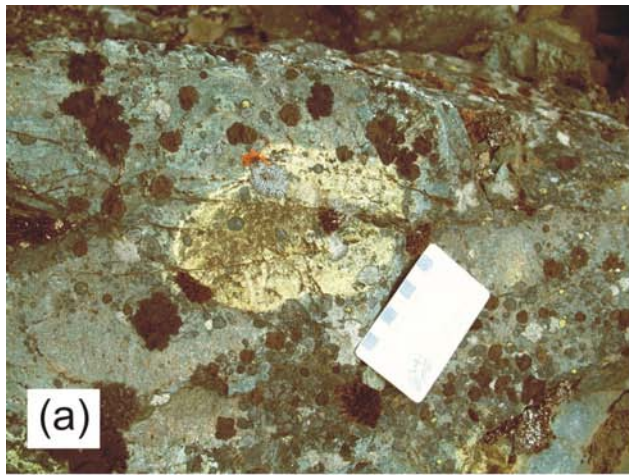


Figure 10. The Crouse Creek greenstone member of the Wallace Formation. a) epidosite patch in massive greenstone (07NMA31-01; UTM Zone 11, 5479991N, 358567E, NAD83); b) pyroxene crystal lapilli tuff (07NMA32-04; UTM Zone 11, 5479062N, 358777E, NAD83); c) pyroxene-feldspar crystal tuff (07NMA33-02; UTM Zone 11, 5479283N, 357806E, NAD83); d) pyroxene crystal lapilli tuff with rhyolite clasts (07NMA32-04; UTM Zone 11, 5479062N, 358777E, NAD83).

Wallace formation to the east of Crouse creek. These tend to be medium to coarse-grained, equigranular rocks composed of white feldspar, green-black hornblende and variable amounts of quartz. One distinctive unit, termed the “hornblende crowded feldspar diorite” by Grieg and Flasha (2005), underlies much of the GK Property. This is characterized by abundant, subrounded to subhedral, lath-shaped, white feldspar crystals in a finer grained black groundmass of acicular hornblende and feldspar (Fig 12b). Tabular hornblende phenocrysts may also be developed. Quartz is rare or absent. The diorite is variably mineralized with up to 5% disseminated pyrrhotite, lesser pyrite and rare arsenopyrite (Grieg and Flasha, 2005). The relationship of the dioritic rocks to the Westkettle granodiorite is presently unknown, though they are suspected to be correlative.

Foliated granodiorite occurs in the China Creek area in the northern part of the map area. This granodiorite comprises varying amounts of rounded sugary quartz, euhedral white feldspar, biotite and isotropic, lath-shaped hornblende. Minor pyrite can also be seen in hand sample. The grain size varies from fine to medium grained. Foliation is marked by dark and light colour banding due to vary-

ing mineral proportions and alignment of biotite plates. Foliations show an average trend of $134^{\circ}/73^{\circ}$ but are not continuous throughout the area. Tempelman-Kluit (1989a, b) assigned the foliated granodiorite to the Jura-Cretaceous Okanagan batholith. However, the foliated granodiorite is never seen in contact with the massive Westkettle granodiorite and relative age relations are unknown.

EOCENE

Megacrystic K-feldspar granite and quartz monzonite form three intrusions in the area — the Crystal Mountain, Collier Lake and Beaverdell stocks. Typical of Coryell intrusions, they have euhedral, lath to square-shaped phenocrysts of pink K-feldspar that are commonly 3 to 4 cm in size, though they range up to 8 cm (Fig 12c). They are set in a coarse-grained groundmass of white and pink subhedral feldspar and quartz. Quartz occurs as polycrystalline quartz eyes up to 1 cm in size or as irregular patches interstitial to the groundmass feldspars. Biotite is usually minor, varying from 5 to 10%. The Collier Lake stock differs to the other stocks in having lower quartz contents, less than 5%, and a

medium-grained porphyritic microquartz monzonite chill phase (Fig 12d).

Pyroxene-feldspar porphyry, feldspar porphyry, hornblende-feldspar porphyry and K-feldspar megacrystic porphyry dikes occur throughout the map area. These are offshoots from the Coryell intrusions or feeders to the volcanic rocks of the Eocene Marron Formation. Orange to brown weathering dikes of black olivine basalt and aphyric basalt occur in the western part of the map area and are related to the Neogene Kallis Formation plateau basalts (Mathews, 1988).

REGIONAL CORRELATION OF PALEOZOIC SEQUENCES

The Paleozoic rocks of the Greenwood area are preserved in a series of northward-dipping thrust sheets (Little, 1983; Fyles, 1990) with many of the bounding thrusts being marked by serpentinite layers or pods. Despite disruption and modification of the thrust sheets by Tertiary extensional faulting, Massey (2007a) traced the Knob Hill Complex and Anarchist schist westward from the Green-

wood area into the Johnstone Creek and Bridesville areas. Mapping in 2007 has identified all the Paleozoic rocks of the McKinney Creek area as being Anarchist schist and not Knob Hill Complex. Correlation of the belt of Jurassic diorite and ultramafic rocks with similar rocks underlying the Old Nick property and east to Rock Creek suggests dextral motion of about 10 km on the Conkle Lake fault (in addition to eastward downdrop). Rocks of the Knob Hill Complex west of the Conkle Lake fault would thus have to be displaced northwards (Fig 13). However, this area is underlain by Jura-Cretaceous intrusions, apart from minor outcrop areas of greenstone and chert in the Ripperno Creek area (Church, 1980), probably the furthest west remnants of the Knob Hill Complex. The Anarchist schist extends further westwards before passing into the granitic gneiss of the Okanagan batholith (Ryan, 1973; Tempelman-Kluit, 1989a, b).

West of the Okanagan fault, the Kobau Group is lithologically similar to the Anarchist schist and also has a complex deformational history (Okulitch, 1973; Mäder et al., 1989). Its direct correlation with the Anarchist schist is however unclear due to the intervening Okanagan Fault. To the south, in Washington State, the Kobau Group structur-



Figure 11. Clastic sedimentary rocks of the Wallace formation. a) laminated argillite-siltstone overlain by fine-grained sandstone bed (07NMA20-15; UTM Zone 11, 5479573N, 356006E, NAD83); b) pebbly sandstone (07NMA42-17; UTM Zone 11, 5476122N, 361189E, NAD83); c) limestone interbedded in siltstone-argillite (07NMA21-06; UTM Zone 11, 5481228N, 356427E, NAD83); d) garnet skarn (07NMA33-08; UTM Zone 11, 5478697N, 358233E, NAD83).

ally overlies the Palmers Mountain Greenstone. The bounding thrust is probably marked by serpentinite in the Chopaka Mountain area (Rinehart and Fox, 1972) but has been poorly defined elsewhere in the Loomis map area.

The Palmer Mountain Greenstone comprises mafic flows and pyroclastic rocks with variably textured gabbro ('amphibolite' of Rinehart and Fox, 1972) that can be correlated with the Knob Hill Complex. These, in turn, structurally overlie the Anarchist Group along the Chesaw thrust (Cheney et al., 1994), though the 'Anarchist Group' of Rinehart and Fox (1972) includes much undeformed sharpstone conglomerate, limestone and finer clastic sedimentary rocks that are probably Brooklyn Formation equivalent.

If the suggested correlations and structural interpretations are correct, the thrust model developed in the Greenwood area by Fyles (1990) is thus apparently traceable west to the Loomis and Oliver areas. Throughout the Boundary district, the ophiolitic Knob Hill Complex is sandwiched between more complexly deformed quartzite-schist-greenstone sequences — the Anarchist to the south and Kobau to the north. In the Greenwood area, the latter is represented by the quartzite and schist of the Eholt Creek val-

ley and Mount Roderick Dhu (Massey, 2006; see also Fig 13). However, it is still unclear how the Kobau Group and Anarchist schist correlate with each other, or with the Knob Hill Complex. They may be the same package structurally repeated or, perhaps, represent opposite sides of an oceanic basin (the Knob Hill Complex) that is now closed and telescoped. It is hoped that continuing petrochemical studies will help shed some light on this problem.

ACKNOWLEDGMENTS

The senior author is much indebted to Jim Fyles and Neil Church for all their invaluable help and advice during the planning stages of this project and since. Both authors acknowledge the indispensable assistance of Kevin Paterson and Bev Quist during fieldwork and in the office. The collaboration, support and ready welcome of the Boundary district exploration community continue to be exceptional.

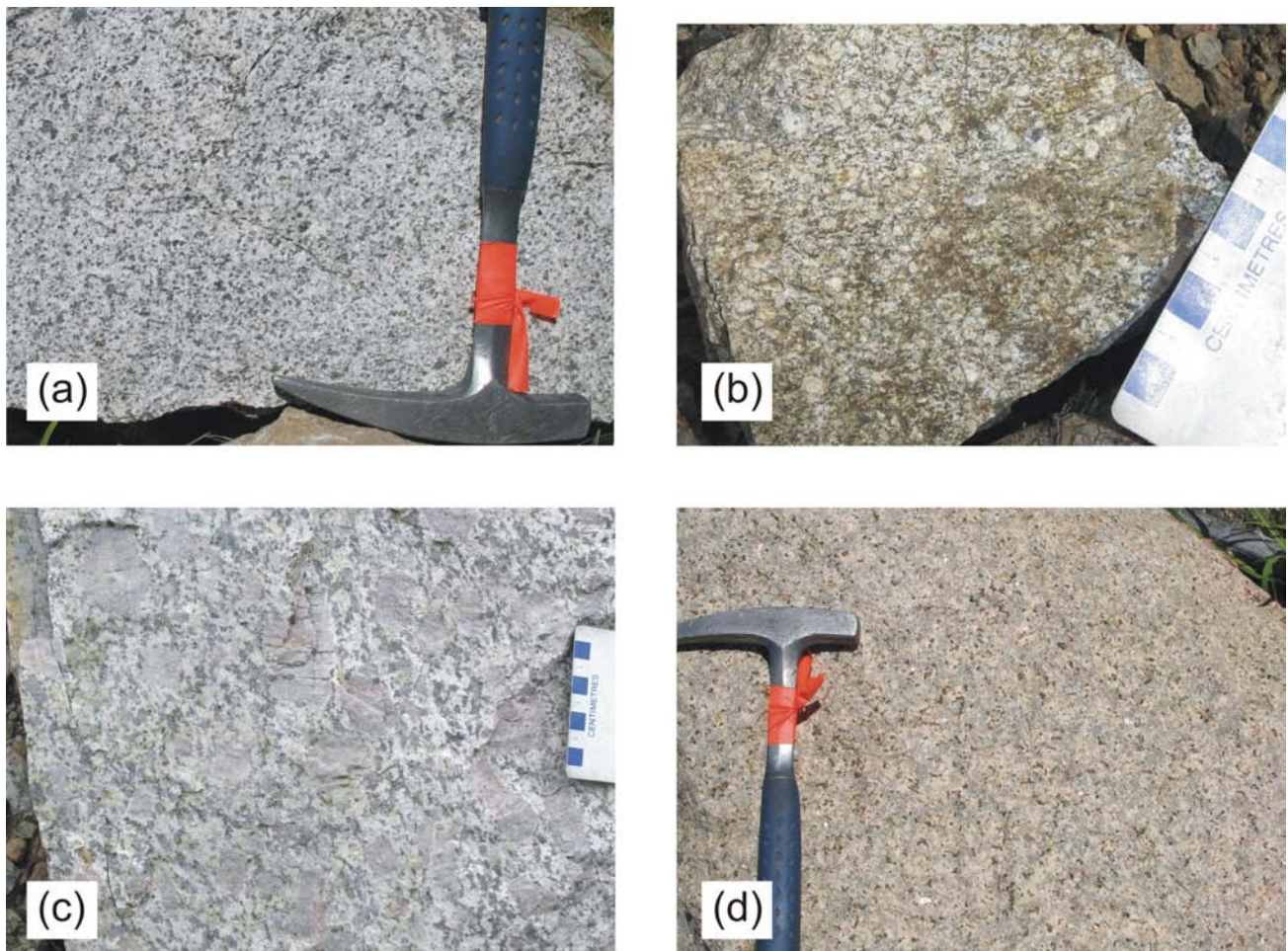


Figure 12. Intrusions of the Beaverdell area. a) hornblende-biotite granodiorite of the Jurassic Westkettle batholith (07NMA28-20; UTM Zone 11, 5484322N, 360440E, NAD83); b) hornblende crowded feldspar diorite (07NMA34-13; UTM Zone 11, 5474088N, 359662E, NAD83); c) typical K-feldspar megacrystic granite of the Eocene Coryell suite (07NMA45-09; UTM Zone 11, 5475024N, 355570E, NAD83); d) pink quartz monzonite of the Eocene Coryell suite (07NMA28-17; UTM Zone 11, 5486026N, 360995E, NAD83).

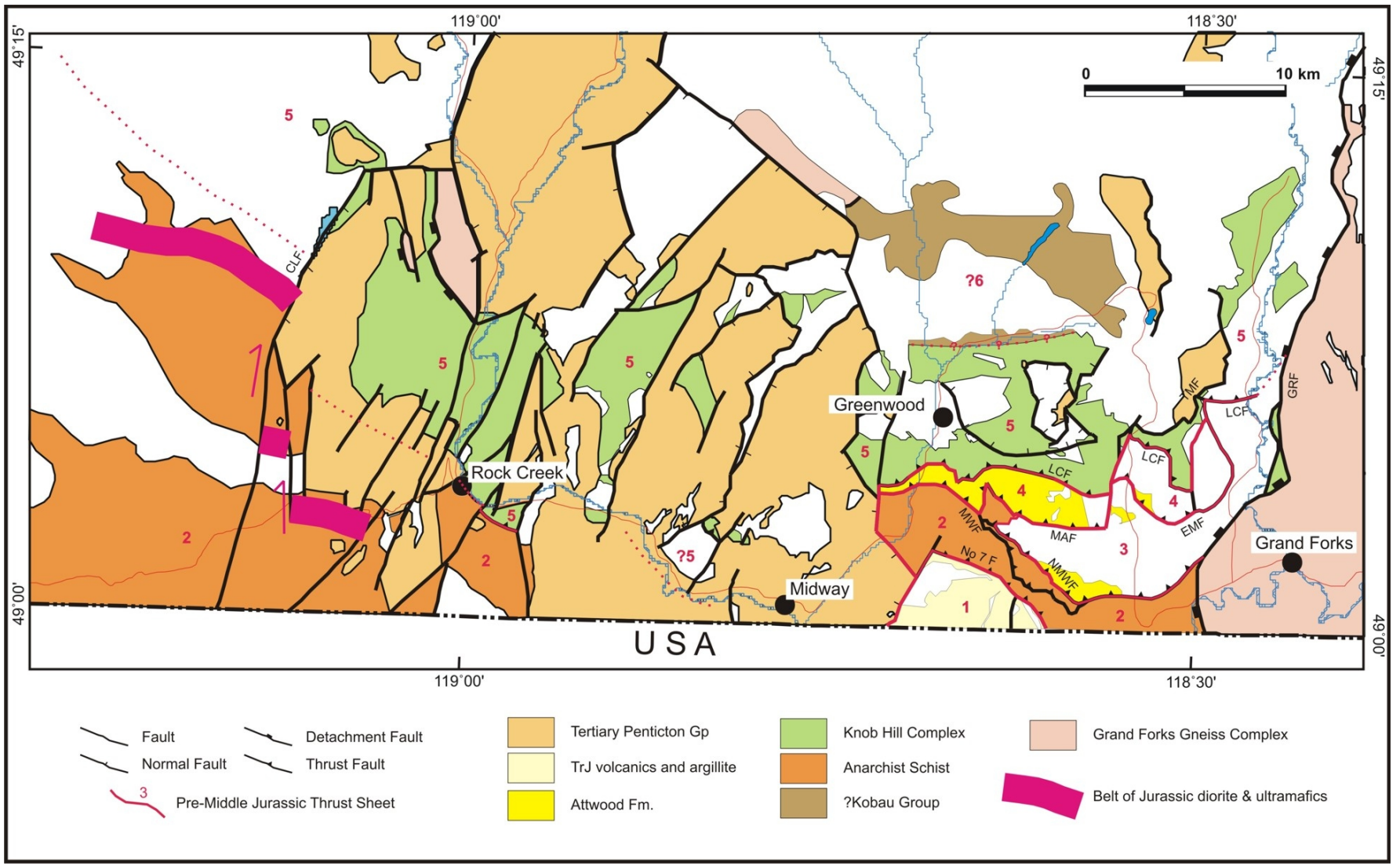


Figure 13. Main structural elements of the Boundary district, outlining the major thrust sheets (numbered 1–6) containing the Paleozoic and Mesozoic sequences (modified from Fyles, 1990; geology modified from Massey et al., 2005). Abbreviations: No 7 F, Number 7 fault; MWF, Mount Wright fault; NMWF, North Mount Wright fault; MAF, Mount Attwood fault; LCF, Lind Creek fault; EMF, Eagle Mountain fault; TMF, Thimble Mountain fault; GRF, Granby River fault; CLF, Conkle Lake fault. Jurassic diorite and ultramafic belt in the McKinney Creek area is shown diagrammatically as a thick magenta line. Arrows indicate relative lateral offsets along the Conkle Lake fault system.

REFERENCES

- Bauerman, H. (1885): Geology of the country near the forty-ninth parallel of north latitude, west of the Rocky Mountains; *Geological Survey of Canada*, Report of Progress, 1882–1884, pages 5B–42B.
- Cairnes, C.E. (1937): Mineral Deposits of the West Half of Kettle River Area, British Columbia; *Geological Survey of Canada*, Paper 37-21, 58 pages.
- Cairnes, C.E. (1940): Kettle River (West Half), British Columbia; *Geological Survey of Canada*, Map 538A, scale 1:253 440.
- Cheney, E.S., Rasmussen, M.G. and Miller, M.G. (1994): Major faults, stratigraphy, and identity of Quesnellia in Washington and adjacent British Columbia; *Washington Division of Geology and Earth Resources*, Bulletin 80, pages 49–71.
- Christopher, P.A. (1976a): Carmi-Beaverdell area (82 E/6 11); in *Geological Fieldwork 1975*, *BC Ministry of Energy, Mines and Petroleum Resources*, Paper 1976-1, pages 27–31.
- Christopher, P.A. (1975b): Highland Bell (Beaverdell) Mine (82 E/6E); in *Geology 1975*, *BC Ministry of Energy, Mines and Petroleum Resources*, pages G30–G33.
- Christopher, P.A. (1977): Beaverdell area (82 E/6E); in *Geological Fieldwork 1976*, *BC Ministry of Energy, Mines and Petroleum Resources*, Paper 1977-1, page 15.
- Church, B.N. (1980): Geology of the Rock Creek Tertiary outlier (082E/03E, 02W); *BC Ministry of Energy, Mines and Petroleum Resources*, Preliminary Map 41, 1:50 000 scale.
- Church, B.N. (1996): Several new industrial mineral and ornamental stone occurrences in the Okanagan-Boundary district (82E, 82L); in *Exploration in British Columbia 1995*, *BC Ministry of Energy, Mines and Petroleum Resources*, pages 123–130.
- Cockfield, W.E. (1935): Lode gold deposits, Fairview camp, Camp McKinney and Vidette Lake area and the Dividend-Lakeview property near Osoyoos, BC; *Geological Survey of Canada*, Memoir 179, 38 pages.
- Fyles, J.T. (1990): Geology of the Greenwood – Grand Forks area, British Columbia (NTS 82E/1, 2); *BC Ministry of Energy, Mines and Petroleum Resources*, Open File 1990-25, 19 pages.
- Greig, C.J. and Flasha, S.T. (2005): Geological, geochemical, geophysical and diamond drill report on the GK Property, submitted by Bitterroot Resources Ltd.; *BC Ministry of Energy, Mines and Petroleum Resources*, Assessment Report 28179, 325 pages.
- Godwin, C.I., Watson, P.H. and Shen, K. (1986): Genesis of the Lass vein system, Beaverdell silver camp, south-central British Columbia; *Canadian Journal of Earth Sciences*, Volume 23, pages 1615–1626.
- Hedley, M. S. (1940): Geology of Camp McKinney and of the Cariboo-Amelia mine, Similkameen District; *BC Ministry of Energy, Mines and Petroleum Resources*, Bulletin 6, 39 pages.
- Kidd, D.F. and Perry, O.S. (1957): Beaverdell Camp, B.C.; in *Structural Geology of Canadian Ore Deposits*, *Canadian Institute of Mining and Metallurgy*, Congress Volume, pages 136–141.
- Kowall, R. (1986a): Soils of the Pentiction map area 82E: Almond Mountain sheet (82E/7); *BC Ministry of Environment*, 1:50 000 scale.
- Kowall, R. (1986b): Soils of the Pentiction map area 82E: Beaverdell sheet (82E/6); *BC Ministry of Environment*, 1:50 000 scale.
- Kowall, R. (1986c): Soils of the Pentiction map area 82E: Osoyoos sheet (82E/3); *BC Ministry of Environment*, 1:50 000 scale.
- Little, H.W. (1957): Kettle River (east half), Similkameen, Kootenay and Osoyoos districts, British Columbia; *Geological Survey of Canada*, Preliminary Map 6-1957, 1:253 440 scale.
- Little, H.W. (1961): Kettle River (west half), British Columbia; *Geological Survey of Canada*, Preliminary Map 15-1961, 1:253 440 scale.
- Little, H.W. (1983): Geology of the Greenwood map area, British Columbia; *Geological Survey of Canada*, Paper 79-29, 37 pages.
- Mäder, U., Lewis, P. and Russell, J.K. (1989): Geology and structure of the Kobau Group between Oliver and Cawston, British Columbia: with notes on some auriferous quartz veins (82E/4E); in *Geological Fieldwork 1988*, *BC Ministry of Energy, Mines and Petroleum Resources*, Paper 1989-1, pages 19–25.
- Massey, N.W.D. (2006): Boundary Project: reassessment of Paleozoic rock units of the Greenwood area (NTS 82E/02), southern British Columbia; in *Geological Fieldwork 2005*, *BC Ministry of Energy, Mines and Petroleum Resources*, Paper 2006-1 and *Geoscience BC*, Report 2006-1, pages 99–107.
- Massey, N.W.D. (2007a): Geology and Mineral Deposits of the Rock Creek Area, British Columbia (82E/02W; 82E/03E); *BC Ministry of Energy, Mines and Petroleum Resources*, Open File 2007-7, 1:25 000 scale.
- Massey, N.W.D. (2007b): Boundary Project: Rock Creek area (82E/02W, 03E), southern British Columbia; in *Geological Fieldwork 2006*, *BC Ministry of Energy, Mines and Petroleum Resources*, Paper 2007-1 and *Geoscience BC*, Report 2007-1, pages 117–128.
- Massey, N.W.D., MacIntyre, D.G., Desjardins, P.J. and Cooney, R.T. (2005): Digital geology map of British Columbia; *BC Ministry of Energy, Mines and Petroleum Resources*, Open File 2005-02, DVD.
- Mathews, W.M. (1988): Neogene geology of the Okanagan highland, British Columbia; *Canadian Journal of Earth Sciences*, Volume 25, pages 725–731.
- Nixon, G.T. (2002): Alkaline hosted Cu-PGE mineralization: the Sappho alkaline plutonic complex, south-central British Columbia; *BC Ministry of Energy, Mines and Petroleum Resources*, Open File 2002-7, 2 map sheets at 1:5 000 scale.
- Okulitch, A.V. (1973): Age and correlation of the Kobau Group, Mount Kobau, British Columbia; *Canadian Journal of Earth Sciences*, Volume 10, pages 1508–1518.
- Peatfield, G. R. (1978): Geologic history and metallogeny of the “Boundary District”, southern British Columbia and northern Washington; PhD thesis, *Queen’s University*, 249 pages.
- Reinecke, L. (1915): Ore deposits of the Beaverdell map area; *Geological Survey of Canada*, Memoir 79, 178 pages.
- Rinehart, C.D. and Fox, K.F., Jr. (1972): Geology and mineral deposits of the Loomis Quadrangle, Okanogan County, Washington; *Washington Department of Conservation and Development*, Division of Geology, Bulletin 64, 124 pages.
- Ryan, B.D. (1973): Structural geology and Rb-Sr geochronology of the Anarchist Mountain area, south-central British Columbia; PhD thesis, *University of British Columbia*, 256 pages.
- Tempelman-Kluit, D.J. (1989a): Geological map with mineral occurrences, fossil localities, radiometric ages and gravity field for Pentiction map area (NTS 82/E), southern British Columbia; *Geological Survey of Canada*, Open File 1969, 17 pages.
- Tempelman-Kluit, D.J. (1989b): Geology, Pentiction, West of Sixth Meridian, British Columbia; *Geological Survey of Canada*, Map 1736A, scale 1:250 000.
- Watson, P.H., Godwin, C.I. and Christopher, P.A. (1982): General geology and genesis of silver and gold veins in the Beaverdell area, south-central British Columbia; *Canadian Journal of Earth Sciences*, Volume 19, pages 1264–1274.

White, W.H. (1949): Beaverdell (49° 119° S.E.); *BC Department of Mines*, Annual Report of the Minister of Mines, 1949, pages A138–A148.

Newly Discovered Volcanic-Hosted Massive Sulphide Potential within Paleozoic Volcanic Rocks of the Stikine Assemblage, Terrace Area, Northwestern British Columbia (NTS 1031/08)

by M. McKeown, J. Nelson and R. Friedman¹

KEYWORDS: volcanic-hosted massive sulphide, Kuroko, Stikine assemblage, Mount Attree volcanics, Terrace, porphyritic, phyllic

INTRODUCTION

Mineralization and alteration consistent with a distal, Kuroko-type volcanic-hosted massive sulphide (VHMS) system were discovered within a package of highly altered, Paleozoic volcanic rocks 23 km southeast of Terrace, British Columbia (Fig 1).

The VHMS potential of the area was investigated during the 2007 field season in conjunction with a regional-scale mapping project (Fig 3; Nelson et al., 2008). The 2007 mapping project covers NTS map 1031/08, expanding on mapping carried out in the Terrace area over the last two years (Nelson et al., 2006 Nelson and Kennedy, 2007).

Key to this discovery was the recognition of a group of Palaeozoic, submarine volcanic rocks, named the Mount Attree volcanics, which had previously been mapped as part of the Lower Jurassic Telkwa Formation (Woodsworth et al., 1985). The Lower Telkwa volcanic rocks are not considered prospective for VHMS deposits because they formed in a subaerial, compressional environment, whereas the Paleozoic volcanic rocks formed in a submarine setting and an extensional tectonic environment favourable to VHMS formation. Furthermore, the Paleozoic volcanic rocks are correlative with the Stikine assemblage which is host to multiple, significant VHMS deposits within BC (Fig 2).

In order to fully assess the VHMS potential of the prospective area, known as the Gazelle property, 1:10 000 scale mapping delimiting alteration zones and mineralization was conducted, along with thin section examination, geochemical analysis and U-Pb dating. Results of samples sent for whole-rock analysis are pending. The results of this investigation indicate there is strong potential for Kuroko-type VHMS deposits in the area.

Mineral exploration in the Terrace area has historically focused on copper and gold vein, skarn and porphyry deposits. The discovery of Kuroko-type mineralization

within the Paleozoic volcanic rocks is significant as it opens up a newly defined exposure of the Stikine assemblage to exploration, in an area that was previously not considered prospective for VHMS deposits.

Volcanic-Hosted Massive Sulphide Deposits

Volcanic-hosted massive sulphide (VHMS) deposits are an important source of copper, zinc, lead and precious metals in Canada. A specific BC example is the currently-producing Myra Falls mine on Vancouver Island. These deposits are attractive exploration targets since they are high-grade, commonly contain significant amounts of precious metals, and are polymetallic, which offers protection against fluctuating metal prices.

Volcanic-hosted massive sulphide deposits form by focused discharge of metal-rich hydrothermal fluids on the seafloor. This results in the formation of sulphide lenses at, or near, the seafloor, hosted in submarine volcanic rocks and deep basal sedimentary strata (Galley et al., 2007). The deposits vary considerably in their metal contents, alteration and mineralization styles. There are, however, several features that characterize these deposits: they generally have concordant lenses of massive (>40%), polymetallic sulphide minerals that stratigraphically overlie a crosscutting discordant zone of intense alteration and mineralization, often as stockwork veining.

Hoy (1991) provides a useful summary of Kuroko-type occurrences, which are the most common type of VHMS occurrences in British Columbia. The polymetallic lenses are rich in copper, lead, zinc, silver and gold, and are commonly comprised of massive pyrite, sphalerite, galena and chalcopyrite. They are associated with bimodal, calc-alkaline suites that typically form during a rifting event during constructive development of an island arc complex. The host rocks are often felsic volcanic rocks with well-developed alteration zones beneath the sulphide lenses. The stockwork zone and immediate deposit are characterized by magnesium chlorite-sericite alteration and local silicification. VHMS deposits in BC are principally of Early Paleozoic, Devonian–Mississippian, Permian or Triassic ages (Massey, 1999).

VHMS Deposits within Stikinia

Stikinia, the largest terrane of the Intermontane Belt, (Fig 2) is comprised of island arc volcanic, sedimentary and plutonic rocks. Island arc building began in Stikinia during the middle to late Paleozoic (Price and Monger, 2003). This followed a shift from a passive ancestral North American margin to an extensional tectonic environment due to both

¹Pacific Centre for Isotopic and Geochemical Research, Department of Earth and Ocean Sciences, University of British Columbia, Vancouver, BC

This publication is also available, free of charge, as colour digital files in Adobe Acrobat® PDF format from the BC Ministry of Energy, Mines and Petroleum Resources website at http://www.em.gov.bc.ca/Mining/Geolsurv/Publications/catalog/cat_fldwk.htm

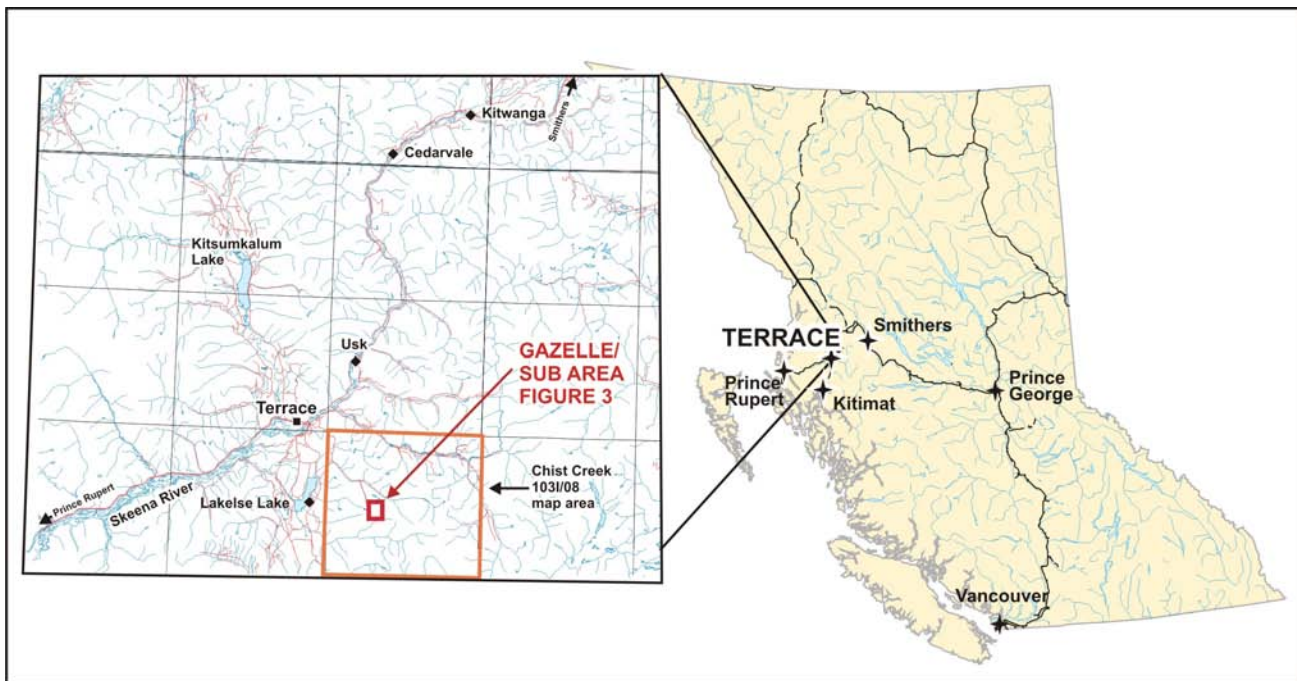


Figure 1. Location map of the project area southeast of Terrace, British Columbia.

the start of active subduction during the Late Devonian (between 390 Ma and 360 Ma) and retreat of the arc away from the western margin of the continent (Price and Monger, 2003). Paleozoic arc and associated rocks, mainly exposed in northern Stikinia, are referred to collectively as the Stikine assemblage. Younger overlapping arc assemblages include the Triassic Takla Group and Jurassic Hazelton Group. Stikinia is host to VHMS deposits of mid-Paleozoic, Triassic and mid-Jurassic age (Hoy, 1991). The most significant VHMS deposits include the Paleozoic Tulsequah Chief deposit and Foremore prospect as well as the Mesozoic Granduc, Eskay, and Anyox mines (Fig 2; Massey, 1999).

The Tulsequah Chief deposit, located in far northwestern BC (Fig 2), is currently moving towards production with indicated resources of 6 Mt grading 1.40% Cu, 1.24% Pb, 6.41% Zn, 2.67 g/t Au and 99 g/t Ag (Arsenault et al., 2007). The Tulsequah Chief and nearby Big Bull deposit are hosted by a sequence of Devonian to Mississippian felsic and mafic volcanoclastic rocks and flows of the Stikine assemblage. The deposits comprise several lenses in which the sulphides are massive and also banded to disseminated (Sebert et al., 1994). Quartz-sericite alteration is well-developed in footwall felsic rock types, and cordierite is locally abundant, probably as a result of metamorphic recrystallization of hydrothermal clays (Sebert et al., 1994). Rhyolite in the immediate footwall of the Tulsequah Chief deposit has been dated at ca. 327 Ma, Late Mississippian, by U-Pb methods on zircons (Childe, 1997). The mainly volcanic sequence that hosts it is overlain regionally by Pennsylvanian bioclastic limestone (Mihalynuk et al., 1994).

The Foremore deposit (MINFILE 104G 148, 181, 182; MINFILE, 2007) is also hosted by the Stikine assemblage (Logan, 2003). It consists of multiple lenses of massive sulphide minerals that occur in at least two separate stratigraphic levels, hosted in pyritic-quartz-sericite phyllite and

schist within a larger alteration zone of chloritic, hematitic and carbonaceous phyllite. The mineral horizons occur near the contact between felsic and overlying mafic volcanic rocks along a strike length of several kilometres. Grades and thicknesses vary considerably, due in part to strong deformation. In 2004, the best drill intersection was 3.1 m with 14.6 g/t Au, 1114 g/t Ag, 0.2% Cu, 1.2% Pb and 6.6% Zn (MINFILE 104G 148). One of the footwall rhyolite units has yielded a preliminary Devonian–Mississippian U-Pb zircon date of ca. 359 Ma (J. Logan, pers comm, 2004).

The now-closed Granduc mine was developed on a series of massive sulphide lenses associated with a banded iron formation. Granduc is hosted by an unusual Late Triassic sequence, compared to the main Takla-Stuhini arc of Stikinia. It is associated with very primitive tholeiitic basalt that represents either a primitive arc or a back-arc setting (Childe, 1997). Ore reserves, before production began in 1971, were nearly 40 Mt grading 1.73 % Cu (MINFILE 104B 021).

The Eskay Creek mine is now nearing closure after production of nearly a hundred tonnes of gold between 1995 and 2008. It is hosted by a Lower to Middle Jurassic sequence of bimodal basalt and rhyolite flows and interbedded sedimentary strata that were deposited within a north-trending rift graben after main Hazelton arc volcanism had ceased (Alldrick et al., 2005). The deposits consist of stratabound massive sulphide layers with unusually high Ag-Au contents (Hoy, 1991). The Anyox mine was developed on a copper-rich massive sulphide deposit hosted by primitive basalt. It is thought to be the same age as Eskay Creek, and to lie along the trend of the Eskay rift to the south (Fig 2; Evenchick and McNicoll, 2002).

The above examples show that the most prospective hosts for VHMS mineralization within Stikinia are the Paleozoic Stikine assemblage, an unusual Triassic facies, and

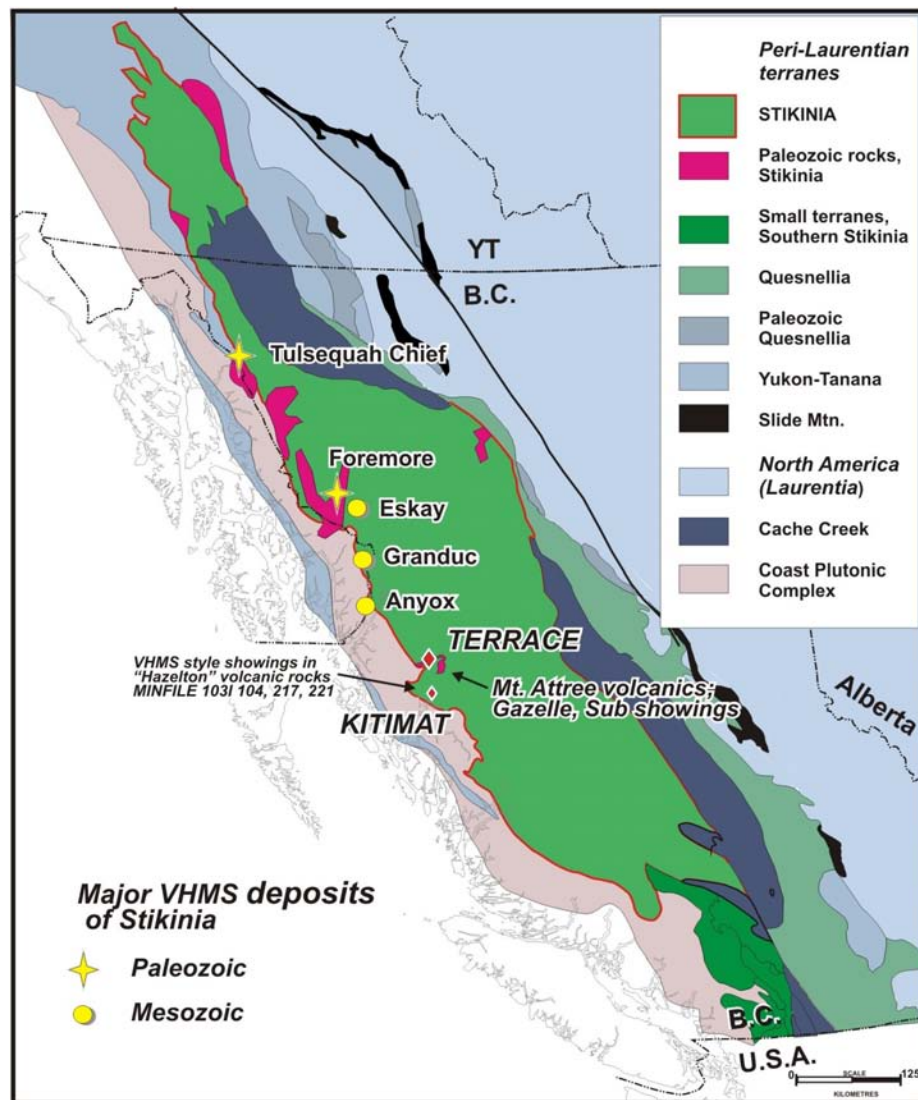


Figure 2. British Columbia terrane map, showing Stikinia and selected volcanic-hosted massive sulphide deposits within it.

post-Hazelton rift facies. None of them are hosted by the Lower Jurassic Telkwa Formation or its correlatives. This is to be expected, because Telkwa volcanic sequences are generally developed in shallow marine or subaerial settings. In particular, the Howson facies between Terrace and Smithers (*see* Tipper and Richards, 1976) formed in a subaerial, compressional environment that is not prospective for VHMS deposits. Thus, the recognition of Paleozoic volcanogenic strata in an area previously included within the Telkwa Formation is significant as it opens up the potential for the presence of deposits similar to, for instance, Tulsequah Chief.

PREVIOUS WORK

Previous regional geological mapping of the Terrace area carried out by Duffell and Souther (1964) and later by Woodsworth et al. (1985) provides excellent groundwork for later mapping. However, because so little regional mapping has been conducted in the Terrace area, as for most of

northern BC, many fascinating mysteries remain regarding the complex geological history of the area as well as its mineral potential.

Mineral exploration south of Williams Creek dates back to at least 1922, with the discovery of copper, iron and zinc showings. Several claims were staked in 1968; however, there are no assessment reports on government record until 1984, when the Gazelle showing was discovered (Hooper, 1984, 1985). The showing consists of multiple lenses of semi-massive to massive sulphides that were identified by D. Hooper. He noted that the style of mineralization and extensive quartz-sericite alteration of the hostrocks are consistent with a VHMS system. Despite the potential of the property, there has been no follow-up to this work in over 20 years.

Stratigraphy

The regional map area (NTS 1031/08) is underlain by a conformable sequence of pre-Permian to Permian subma-

rine volcanic rocks and overlying limestone of the Zymoetz Group. This in turn is unconformably overlain by Lower Jurassic, subaerial volcanic and clastic strata of the Telkwa Formation. These units are intruded by the Early Jurassic Kleanza pluton, unnamed Paleocene (?) plutons, and the Eocene Williams Creek pluton. Structurally, the Paleozoic rocks occupy the core of a northeasterly-trending, north-plunging, regional anticline (Fig 3; Nelson et al., 2008).

The Zymoetz Group consists of Mt Attree volcanics overlain by limestone of the Ambition Formation (Nelson et al., 2008). The Mt Attree volcanics are a compositionally variable volcanogenic sequence that consists largely of dark green andesite flows, tuff and breccia with lesser rhyolite flows, tuff and breccia. The unit contains minor limestone and bedded calc-silicate. The Ambition Formation is a thick unit of grey limestone that is generally well-bedded, with some highly fossiliferous beds. In some areas it contains minor layers of green interbedded tuff and red silicified chert. The fossil assemblage includes horn and colonial corals, bryozoans, brachiopods, gastropods, fusulinids and sporifera. Brachiopods are of Pennsylvanian–Permian age, and fusulinids from one locality are specifically Early to mid-Permian (Duffell and Souther, 1964).

The lowest part of the Lower Jurassic Telkwa Formation is composed primarily of polymictic conglomerate and breccia. The basal Telkwa conglomerate, where present, is dominated by limestone and volcanic clasts. The conglomerate passes upsection into andesite and dacite breccia that are overlain by coherent and fragmental dacite and rhyolite of the lower felsic marker (Nelson et al., 2008). Vent-proximal units are often brick-red and feature spectacular pyroclastic textures.

Where the limestone is not present, having been removed by erosion, Telkwa Formation conglomerate, andesite tuff and breccia directly overlie the andesite tuff of the Mt Attree volcanics. Due to the compositional and textural similarities of the two units, past regional maps have included the Mt Attree volcanics within the Telkwa Formation (Woodsworth et al., 1985). An important goal of this project was to distinguish between the two groups in order to delimit their boundaries within the map area. Paleozoic age was established by referring to the following evidence:

- **Stratigraphic position:** The Paleozoic volcanic rocks lie depositionally below the Permian limestone. This is evident from:
 - the sharp, unshaped contacts between the highest Mt Attree flow or tuff and the overlying limestone and
 - the presence of fine, green tuff layers interbedded with the limestone unit in some areas, likely representing the last throes of explosive volcanism.
- **Distinctive volcanic sequences:** The Paleozoic volcanic sequence is distinguished from the Telkwa Formation based on volcanic textures, compositions, metamorphic grade and presence of foliation. Paleozoic andesite features large, blocky augite, and smaller anhedral plagioclase. Rhyolite typically contains large, embayed quartz phenocrysts. Lapilli tuff characteristically contains abundant unflattened scoria clasts. Rare marble-calc-silicate interbeds are important in that they indicate submarine deposition. Greenschist-facies assemblages and well-developed foliation also distinguish these rocks. Defining characteristics of the Telkwa andesite include abundant, large, generally ir-

regularly-shaped amygdules which indicate subaerial eruption, and well-formed plagioclase phenocrysts that range from 1 millimetre to over a centimetre in length. Rhyolite is best distinguished by the presence of devitrification textures, including spherulites and a lavender-coloured matrix. They are plagioclase-phyric and lack quartz phenocrysts, except in rare cases. Foliation is never observed in Lower Telkwa rocks, and metamorphic grades are mostly sub-greenschist. Incipient actinolite development under static conditions is probably related to contact metamorphism. Table 1 expands on the differences between these two sequences.

GEOLOGY OF GAZELLE AREA

The Gazelle property is located on a 1200 to 1500 m high ridge between Williams Creek and Chist Creek, approximately 4.3 km east of Gunsight Peak (Fig 3). It is an area of very strong alteration, with prominent gossans, as shown in Figure 4 and on the detailed map (Fig 5).

All of the ground is covered by claims that are in good standing, those in the south held by Paget Resources and those in the north, by J. Wang (claims 549673, 555399, 564134, 550358, 564181).

Stratigraphy

The centre of the map area is dominated by an apparently homoclinal sequence of layered Paleozoic felsic to intermediate volcanoclastic rocks with large zones of intense alteration. Permian limestone of the Ambition Formation unconformably overlies the Mt Attree volcanics to the east. It is in turn unconformably overlain by Telkwa dacite breccia at the eastern-most edge of the map sheet. There are multiple stages of intrusions, including Triassic quartz-feldspar-rhyolite porphyry (Fig 5, 6, 7, Table 2) and extensive Eocene granodiorite of the Williams Creek pluton (Fig 5).

Lithological Units

MOUNT ATTREE VOLCANICS

The volcanic rocks are well foliated, thoroughly altered and recrystallized in greenschist facies; the reconstructions of primary rock types, therefore, are based on textural and mineralogical relicts. Rhyolite protoliths are distinguished by the presence of relict quartz phenocrysts and lesser plagioclase and alkali feldspar, whereas andesite protoliths contain plagioclase phenocrysts and lack quartz eyes. The volcanic sequence is dominated by dark green, plagioclase-augite-phyric andesite tuff. Also abundant are white, quartz-phyric rhyolite tuffs, breccias and flows. The rhyolite crystal-lapilli tuffs contain heavily embayed quartz porphyroblasts and rare relict plagioclase.

An anomalous 12 m wide zone of limestone breccia occurs along East Creek, at the contact between the quartz-sericite schist and andesite tuff units (Fig 5). The limestone clasts are enclosed within a green, fine-grained, plagioclase-phyric matrix. The breccia may have formed as a slump deposit. This limestone unit was not seen at this contact anywhere else.

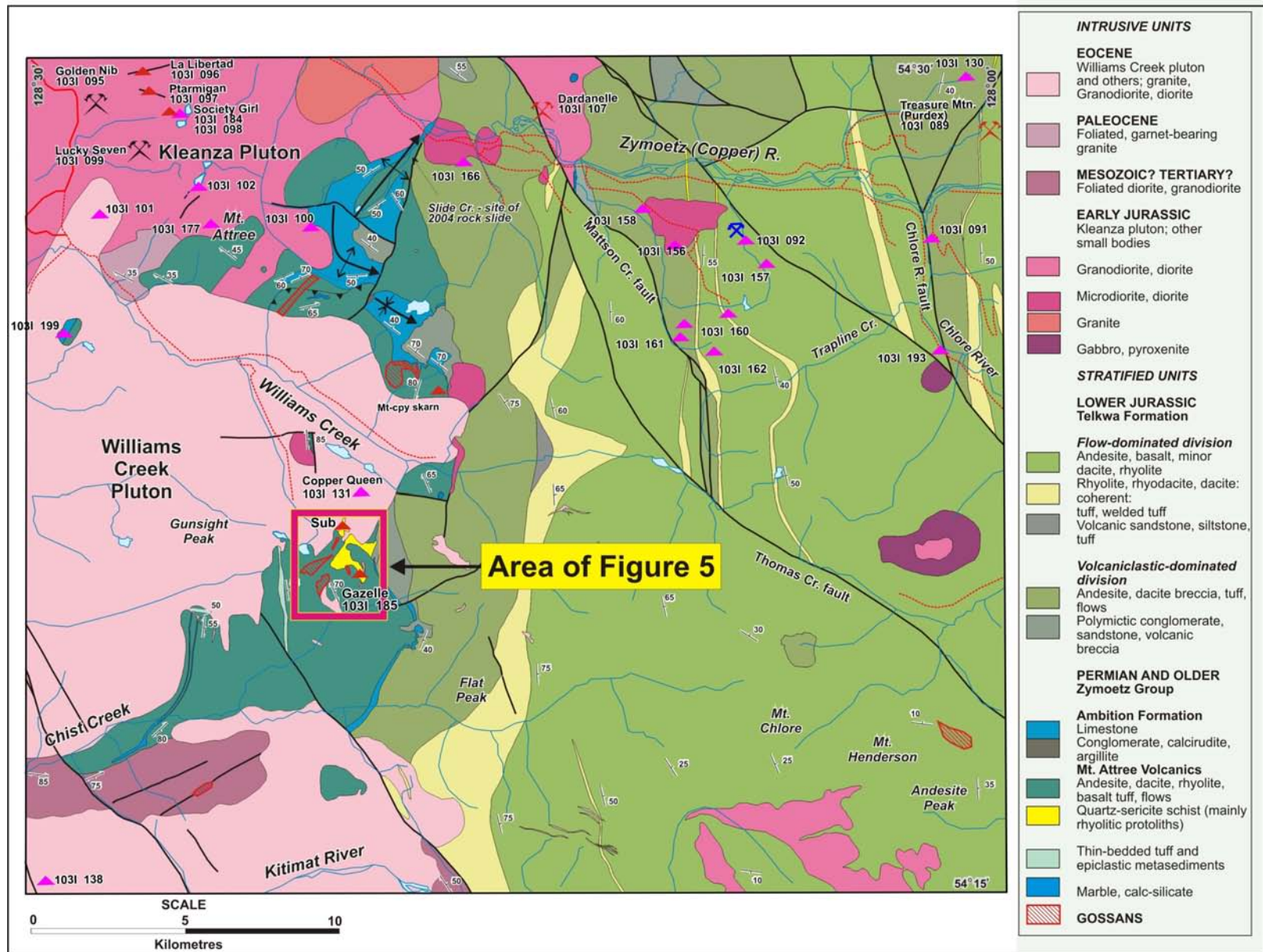


Figure 3. Regional geological map of the Chist Creek area (NTS 1031/08), based on 2007 mapping (Nelson et al., 2008). Inset shows the location of the detailed Gazelle geological map (Fig 5), focused on extensive alteration zones within the Paleozoic Mt Attree volcanics.

TABLE 1. COMPARISON OF DISTINGUISHING CHARACTERISTICS OF THE PALEOZOIC MT ATTREE VOLCANICS AND LOWER JURASSIC TELKWA FORMATION VOLCANIC ROCKS.

Distinguishing characteristics	Paleozoic volcanic rocks	Telkwa volcanic rocks (Lower Jurassic)
Phenocryst assemblage and textures:	Plagioclase: anhedral, broken, altered Augite: large, blocky, abundant	Plagioclase: well-formed, may be large (up to several cm) Augite: rare, only in some basal volcaniclastics
Features of intermediate volcaniclastics:	Vesicular clasts	Lithic clasts
Texture of felsic volcaniclastics:	Quartz phenocrysts, sericitized ash lapilli	Devitrification, spherulites
Metamorphic grade:	Greenschist	Subgreenschist to albite-actinolite hornfels
Deformation:	Distinct foliation	Not foliated

AMBITION FORMATION

A white to grey limestone unit consisting of well-bedded, recrystallized marble with fossiliferous zones correlates with Ambition Formation limestone in the headwaters of Eight Mile Creek (Fig 3). In particular, it contains red chert layers and nodules, siliceous, networked veins and silicified crinoid and brachiopod fossils. Interbedded, fine, green tuffaceous laminae indicate continuity with the Mt Attree volcanics.

TRIASSIC INTRUSIONS

A small Late Triassic quartz-feldspar rhyolite porphyry stock is exposed in the central map area, cutting actinolite schist of the Mt Attree volcanics. It is weakly foliated and relatively unaltered (Fig 5, 6c, d). U-Pb isotopic dating conducted by R. Friedman of the Pacific Centre for Isotopic and Geochemical Research at the University of British Columbia, with assistance from H. Lin and Y. Feng, has provided an age of 211.16 ± 0.41 Ma (Fig 7, Table 2). Thin section analysis revealed embayed, euhedral quartz phenocrysts and lesser plagioclase phenocrysts within a matrix dominated by fine-grained alkali feldspar, recrystallized quartz and minor biotite in fine, discontinuous trains (Fig 6c, d).

LOWER JURASSIC TELKWA FORMATION VOLCANIC ROCKS AND RELATED INTRUSIONS

The Lower Telkwa Formation can be distinguished from the Mt Attree volcanics by its lack of greenschist



Figure 4. Mountain-scale gossan, quartz-sericite schist, Gazelle area. View from the ridge looking southeast towards Nifty creek (Fig 5).

metamorphism and foliation, as well as the presence of red dacite clasts and crowded feldspar porphyry clasts. The Telkwa Formation is locally dominated by a polymict dacite breccia interbedded with minor flows. The breccia contains abundant millimetre-scale anhedral plagioclase clasts, local concentrations of limestone clasts and rare, subangular, red dacite clasts with fluidal boundaries, all within an aphanitic light grey to slightly maroon matrix. Towards the southern part of the map area there are localized zones containing crowded feldspar porphyry clasts up to 6 mm in diameter that contain blocky mafic phenocrysts and have a slight purple tinge, perhaps due to hornfelsing. These may have been derived from the Mt Attree volcanics. There are also localized, patchy zones of glassy, flow-foliated dacite that contain carbonate veinlets.

EOCENE INTRUSION: WILLIAMS CREEK PLUTON

The large intrusive body dominates the northern part of the map area. It engulfs the northern end of the Paleozoic exposure and forms abundant dykes and plugs throughout the property. The intrusion is a postkinematic, unfoliated, white-weathering biotite-hornblende granodiorite.

Structure and Metamorphism

The presence of chlorite, actinolite and minor biotite in the metavolcanic rocks indicates metamorphism in greenschist facies. Metamorphic grade increases downsection, towards the south, where an abundance of biotite and well-formed darker green amphibole, as well as calcic plagioclase show the rocks are in upper greenschist to amphibolite facies.

The Mt Attree volcanics on the Gazelle property are generally well-foliated. There are two dominant foliations, striking northerly and to the northeast. The felsic, altered rocks have a strong F1 schistosity parallel to compositional layering. The foliation is fairly consistent throughout the property and the rocks show signs of multiple isoclinal folding, perhaps due to progressive deformation. There is small-scale faulting with, however, very few documentable offsets. The shears are oriented northeast and north-north-westerly. There is a major shear oriented north-northeast along East Creek and another small-scale fault, oriented north-northwest, exposed along Nifty creek. A steeply-plunging fold occurs along the ridge parallel to Ice Bridge Lake with a north-northeast fold axis plunging 45° .

The geological units of different ages display varying degrees of deformation. The Paleozoic volcanic rocks have undergone intense and likely multiple stages of deformation early in their history, while the Triassic stock is only

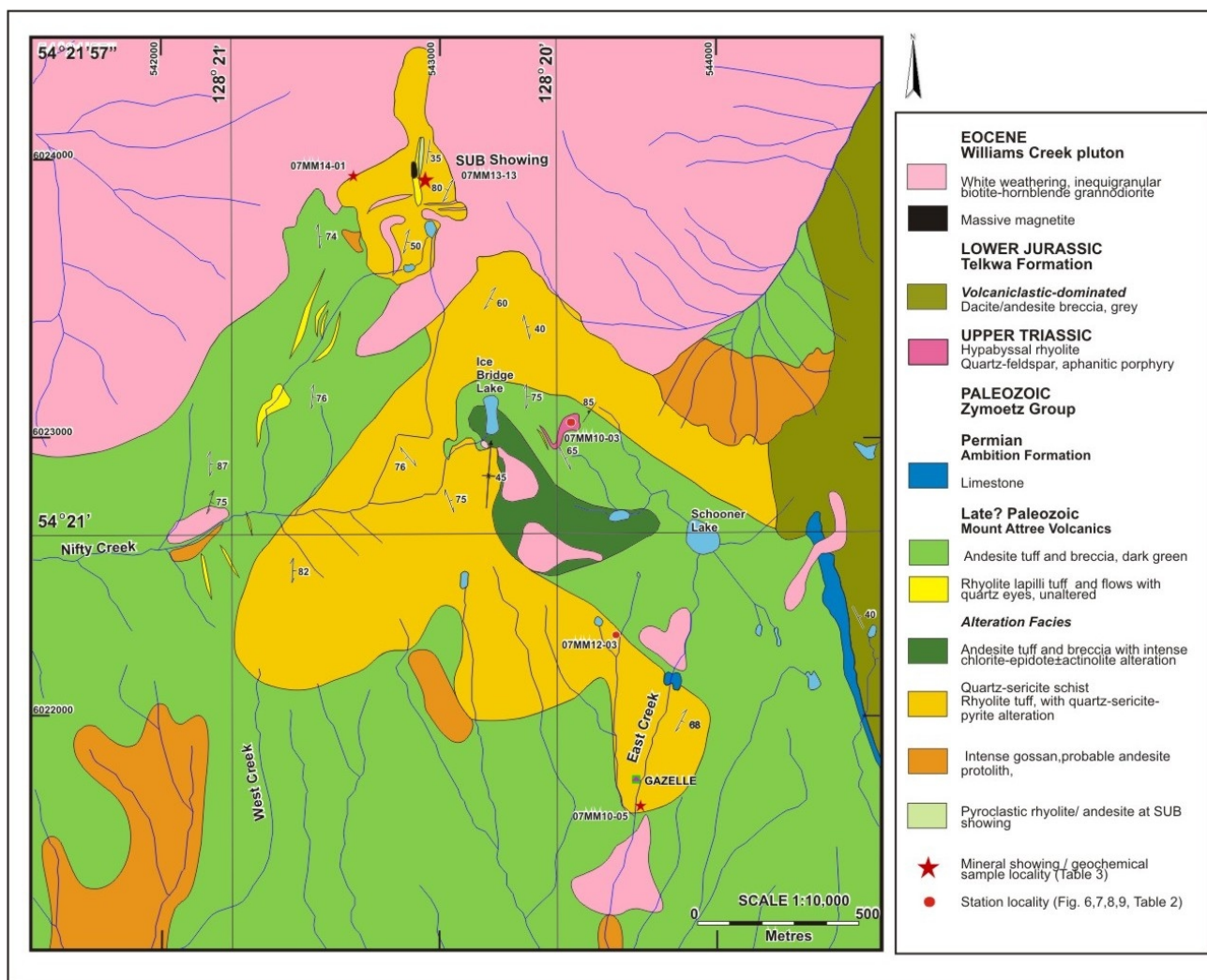


Figure 5. Detailed map of Gazelle area. Field work done in 2007 by M. McKeown and J. Nelson. Data also from Hooper (1984, 1985).

slightly deformed (Fig 6c, d) and the Telkwa dacite does not appear deformed. Although this likely indicates multiple stages of deformation, the variable intensity of deformation of the rock units may be in part a function of their position within the regional-scale fold, with the highly deformed Paleozoic volcanic rocks in the nose of the fold and the undeformed Telkwa breccia nearer the limb, and certainly a function of clastic versus coherent texture and intensity of alteration.

Crosscutting relationships and the unfoliated, fresh textures of the Eocene (?) Williams Creek pluton show that it was intruded after all ductile deformation had ceased. There is also evidence that the Paleozoic volcanic rocks have undergone earlier deformation, some likely shortly after deposition. On Mt Attree (Fig 3), clasts of foliated Paleozoic volcanic rocks occur as clasts within diorite assigned to the Jurassic Kleanza pluton (Nelson et al., 2008). On the Gazelle property, the Paleozoic rocks have undergone intense prekinematic alteration whereas the Triassic intrusion is largely unaltered, which suggests two different deformation events.

Alteration

The property features extensive, intense gossans (Fig 4, 5) that occur in the quartz-sericite schist as well as in the silicified, chlorite-pyrite andesite tuff. In plan view, they are prominent, linear alteration zones oriented perpendicular to each other in northeast and northwest directions (Fig 5).

The two alteration types in the area are phyllic, consisting of quartz-sericite-pyrite (quartz-sericite schist), and propylitic, consisting of chlorite-epidote-actinolite±pyrite. Feldspar phenocrysts in porphyritic rocks have been completely altered to sericite, leaving only quartz phenocrysts. Propylitic alteration occurs in the form of chlorite-altered matrixes and quartz-epidote veins.

The andesite and rhyolite volcanic rocks were likely deposited at the same time (or the rhyolite only slightly after) and have undergone the same alteration and deformation. The difference in alteration type is greatly influenced by the composition of the protolith. The feldspars in rhyolite are preferentially altered to sericite, which in turn enables deformation. In andesite, primary phases such as the clinopyroxene and hornblende are metamorphosed to as-

TABLE 2. U-PB THERMAL IONIZATION MASS SPECTROMETRY ANALYTICAL DATA FOR ZIRCON.

Fraction ¹	Wt (µg)	U ² (ppm)	Pb ³ (ppm)	²⁰⁶ Pb ⁴ ²⁰⁴ Pb	Pb ⁵ (pg)	Th/U ⁶	Isotopic ratios ±1σ% ⁷			ρ ⁸	% ⁹ discordant	Apparent ages ±2σMa ⁷		
							²⁰⁶ Pb/ ²³⁸ U	²⁰⁷ Pb/ ²³⁵ U	²⁰⁷ Pb/ ²⁰⁶ Pb			²⁰⁶ Pb/ ²³⁸ U	²⁰⁷ Pb/ ²³⁵ U	²⁰⁷ Pb/ ²⁰⁶ Pb
07MM-10-03, deformed quartz-feldspar porphyry, UTM 543533E, 6023013N; 211.2 ± 0.4 Ma														
A	2.0	787.4	27.1	2351	1.4	0.47	0.03332 ± 0.15	0.2307 ± 0.35	0.05020 ± 0.30	0.49727	-3.4	211.3 ± 0.6	210.8 ± 1.3	204.5 ± 13.9/14.0
B	3.1	1129.7	37.4	3030	1.5	0.38	0.03285 ± 0.21	0.2285 ± 0.37	0.05046 ± 0.28	0.64689	3.7	208.3 ± 0.9	209.0 ± 1.4	216.2 ± 13.0/13.1
C	3.8	472.5	15.7	2460	1.5	0.39	0.03293 ± 0.31	0.2282 ± 0.42	0.05026 ± 0.26	0.78363	-0.8	208.8 ± 1.3	208.7 ± 1.6	207.2 ± 12.0/12.1
D	2.8	322.1	10.8	1376	1.4	0.39	0.03329 ± 0.10	0.2314 ± 0.53	0.05042 ± 0.50	0.38923	1.5	211.1 ± 0.4	211.4 ± 2.0	214.2 ± 23.0/23.3
E	4.8	472.9	16.1	1151	4.1	0.45	0.03309 ± 0.17	0.2297 ± 0.34	0.05035 ± 0.28	0.56056	0.6	209.8 ± 0.7	209.9 ± 1.3	211.0 ± 13.1/13.2

¹ All analyzed zircon grains air abraded; all single grain analyses

² U blank correction of 0.2 pg ± 20%; U fractionation corrections were measured for each run with a double ²³³⁻²³⁵U spike

³ Radiogenic Pb

⁴ Measured ratio corrected for spike and Pb fractionation of 0.23/amu ± 20% (Daly collector) a value determined by repeated analysis of NBS Pb 982 reference material throughout the course of this study

⁵ Total common Pb in analysis based on blank isotopic composition. ²⁰⁶Pb/²⁰⁴Pb = 18.5 ± 3%, ²⁰⁷Pb/²⁰⁴Pb = 15.5 ± 3%, ²⁰⁸Pb/²⁰⁴Pb = 36.4 ± 3%

⁶ Model Th/U derived from radiogenic ²⁰⁸Pb and the ²⁰⁷Pb/²⁰⁶Pb age of fraction

⁷ Blank correction of 1.0 pg Pb with blank isotopic composition listed above; 0.2 pg U; remaining common Pb is based on Stacey-Kramers model Pb isotopic composition at 211 Ma (Stacey and Kramers, 1975)

⁸ Correlation coefficient

⁹ Discordance in % to origin



Figure 6. Photomicrographs from Gazelle property: a) hypabyssal quartz-feldspar porphyry in cross-polarized and b) plane-polarized light (Sample 07MM12-03) with large recrystallized and embayed quartz porphyroblast (right), a heavily embayed ash fragment (left), and a matrix dominated by recrystallized quartz and sericite; c) Palaeozoic andesite lapilli-tuff in contact with Triassic quartz-feldspar rhyolite porphyry in cross-polarized and d) plane-polarized light (Sample 07MM10-03) with visible chlorite and sericite in the foliation.

semblages of actinolite±epidote±chlorite. These rocks are less prone to deformation, since micas are not abundant. Clastic rocks of either composition are more readily altered than their coherent counterparts, due to increased permeability.

Textural evidence shows that primary alteration occurred prior to deformation, since micas are not abundant. Sericite and pyrite are found mostly along foliation that, in turn, has been cut by quartz-epidote veins showing signs of folding and shearing. Sericite forms rootless, isoclinal folds and pyrite is smeared into the lineation in the most deformed rocks.

Mineralization

There are two unrelated types of mineralization within the Gazelle property: syngenetic, VHMS-related, and that related to later intrusions.

Volcanic-hosted massive sulphide – style mineralization includes small lenses of semi-massive to massive (>50%) chalcopyrite and sphalerite that were identified by previous assessment work in the East Creek Fault Zone (Fig 5; Hooper, 1984, 1985). During the 2007 field season, minor disseminated chalcopyrite±galena was found within the sheared quartz-sericite schist, near the Gazelle showing along East Creek (Fig 5). More importantly, the Sub showing, a new zone of silicification with base-metal sulphide deposits as well as barite, was discovered during 2007 mapping (*see below*).

Later mineralization related to the Williams Creek pluton includes small skarn and porphyry occurrences. There is a small skarn zone where Telkwa dacite and Permian limestone have been intruded by granodiorite (Fig 5). It is marked by 0.5 metre-wide zones of epidote alteration, minor disseminated to blebby magnetite and malachite staining. Quartz veins containing abundant disseminated pyrite, chalcopyrite and minor molybdenite occur in the northern map area (Fig 5). Three sets of the veins, up to 50 cm in width, occur within bright orange quartz-sericite schist in contact with granodiorite.

U-Pb Geochronology

All sample preparation and analytical work for the U-Pb radiometric age presented here were conducted using the thermal ionization mass spectroscopy (TIMS) technique at the Pacific Centre for Isotopic and Geochemical Research, located in the Department of Earth and Ocean Sciences of the University of British Columbia. Details of analytical techniques are presented in Logan et al. (2007). U-Pb results are plotted on a standard concordia diagram (Fig 7) and listed in Table 2.

Uranium-lead single-grain analyses were performed on air-abraded zircons (Table 2). All of the analyzed grains gave statistically concordant results but three yielded slightly younger ages, likely due to minor Pb loss (Fig 7). An age estimate of 211.2 ± 0.4 Ma is based on a two-point

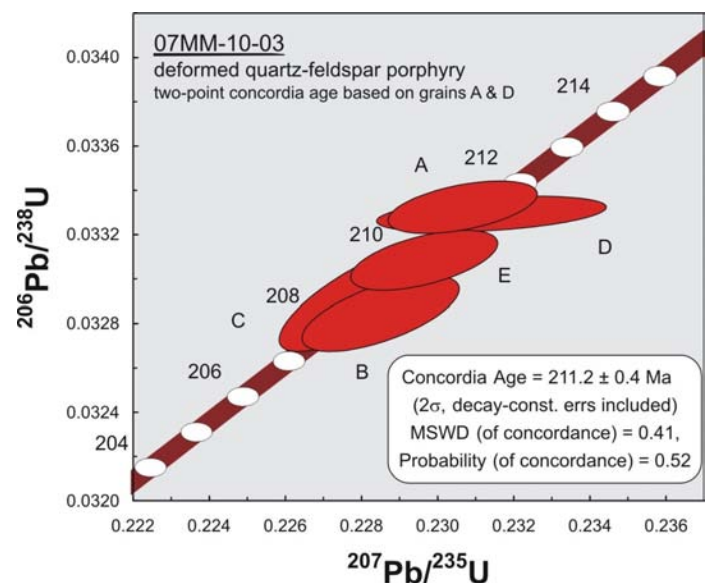


Figure 7. U-Pb concordia diagram for sample 07MM-10-03 with data plotted at the 2σ confidence level. Concordia curve is shown as a band that includes decay-constant errors. Details of the concordia age interpretation are listed on the diagram and discussed in the text.

concordia interpretation (Ludwig, 2003) for older, concordant, and overlapping grains A and D. Although these grains were air abraded, we cannot rule out that they did not also undergo very minor Pb loss; however, this is considered unlikely to significantly affect the crystallization age estimate.

SUB SHOWING

Mineralization indicative of a VHMS deposit has been discovered in an intensely-altered body within the Mt Attree volcanics. The body is approximately 250 by 50 m, trending north-south (Fig 5, 8) and is partially enclosed by the Williams Creek pluton.

Stratigraphy

The mineralized unit is part of a stratigraphic sequence dominated by rhyolite tuffs, breccias and flows. Intensely altered quartz-sericite schist (Fig 8a) is overlain by rhyolite flows (Fig 8b, c), which in turn are overlain by a heterolithic, plagioclase-phyric, (andesite?) breccia that contains clasts of the underlying rhyolite (Fig 8c). The breccia grades into thinly-layered, fine-grained tuff and welded tuff (Fig 8b). The sequence youngs to the east, consistent with facing directions from the surrounding area (Nelson et al., 2008).

Mineralization and Alteration

There are two types of mineralization in the Sub showing, both hosted in sericitized rhyolite tuff with intense silica flooding and pyritic alteration:

- A small, localized zone, 1 metre thick and 4 metres long, of massive barite occurs in an intensely-altered quartz-sericite schist. Thin sections reveal a protomylonitic texture, with barite porphyroblasts within a foliated matrix of finer-grained barite neoblasts (Fig 8, 9a, b). The predeformational, coarse grain sizes indicate barite veins, rather than exhalite (Samples from stations 07MM13-13 01A and 07MM13-13 01B; *see* Table 3).
- Massive to semi-massive galena is hosted within intensely-silicified, pyritic rhyolite in a zone 2 metres thick and 10 metres long (Fig 5; Sample 07MM13-13 01C; *see* Table 3). The mineralization occurs in a zone situated stratigraphically below the barite. Disseminated galena also occurs over a larger zone within the quartz-sericite schist in the northern area of the showing.

Interpretation

The styles of mineralization and alteration at the Sub showing, as throughout the Gazelle area, most likely represent a VHMS feeder zone below the seafloor. The intense sericitization and silicification, in zones both parallel to bedding and crosscutting bedding at a high angle, suggest that low pH fluids were channelled both along structures and along permeable, fragmental layers in the volcanic pile. The originally coarse-grained barite is more likely to have crystallized in a vein, rather than as part of a bedded sequence. In addition to pyrite, local showings of galena, sphalerite and chalcopyrite indicate that the fluids transported base metals. High silver values accompany high

lead values in the barite sample at the Sub showing (Table 3). The low copper values, as well as the moderate zinc and high lead values, indicate the showing is part of a distal VHMS system. Higher copper values would likely occur more proximal to the system. The slightly high gold values represent the enrichment of precious metals which is common for a VHMS deposit.

EXPLORATION POTENTIAL

Alteration and mineralization discovered in the Gazelle map area likely represent that of a distal VHMS system. The Mt Attree volcanics correlate with the pre-Permian volcanic hostrocks of the Stikine Assemblage, which host the Tulsequah Chief deposit and Foremore prospect.

The extent of the alteration identified thus far is approximately 18 kilometres along strike and up to 10 kilometres in width. However, it is likely that more could be identified with further mapping and exploration (*see* Nelson et al., 2008, Fig 3). An immediate target for exploration are the intense gossans and malachite staining in the southwest corner of the map sheet, spotted from a helicopter in the cliffs south of Chist Creek (Fig 3). Their northeasterly strikes are parallel to the transposed layering of the Mt Attree volcanics in that area.

At some distance from there, it is possible that the northeasterly striking Mt Attree volcanics in lower Chist Creek could project southwest across the Kitimat valley, into an area of foliated metavolcanic rocks that are currently included in the Telkwa Formation (Woodsworth et al., 1985). Within the foliated basaltic to rhyolitic flows and tuff are three showings of probable or possible volcanogenic character. Two of the showings occur within a coarse pyroclastic belt approximately 8 kilometres long and at least 1.5 kilometres wide (Belik, 1987). The Bowbyes showing (MINFILE 103I 104) comprises two massive sulphide/magnetite lenses, each about 1 metre thick and 3 to 4 metres long, in chloritic schist. Mineralization consists of massive, crudely-banded chalcopyrite, pyrite and magnetite. Quartz-eye rhyolite overlies and underlies the mineralized horizon. A selected sample assayed 11.4 % Cu and 124.8 g/t Ag (Belik, 1987). At the Barite showing (MINFILE 103I 217), white to grey, dense to thinly-laminated semi-massive barite occurs in foliated, silicified and pyritized breccia and tuff, which are concordantly underlain by a coarse quartz-eye rhyolite. (Belik, 1987). Close to the showing, several lenses of massive barite up to 1.1 metres thick and 15 metres long occur in altered and recrystallized, intermediate to felsic pyroclastic volcanic rocks, that may be favourable for VHMS deposits (Gunning, 1988). Chip samples from this showing were anomalous in silver, gold, copper and zinc. Quartz-sericite schists occur 1.5 km to the northeast of this showing. The sericite has a distinct northeast foliation, similar to the Gazelle property schist. The J showing (MINFILE 103I 221) is considered to be of either Kuroko or Besshi type. Mineralization is exposed along a CNR railway cut on the south side of the Wedeene River. Stratiform pyrite and pyrite-chalcopyrite mineralization occurs within bedded tuff, with a maximum exposed width of about 0.5 m. A grab sample assayed 0.265 g/t Au, 13.3 g/t Ag, 1.978 % Cu and 11.069 % Fe (Raynor, 1987).

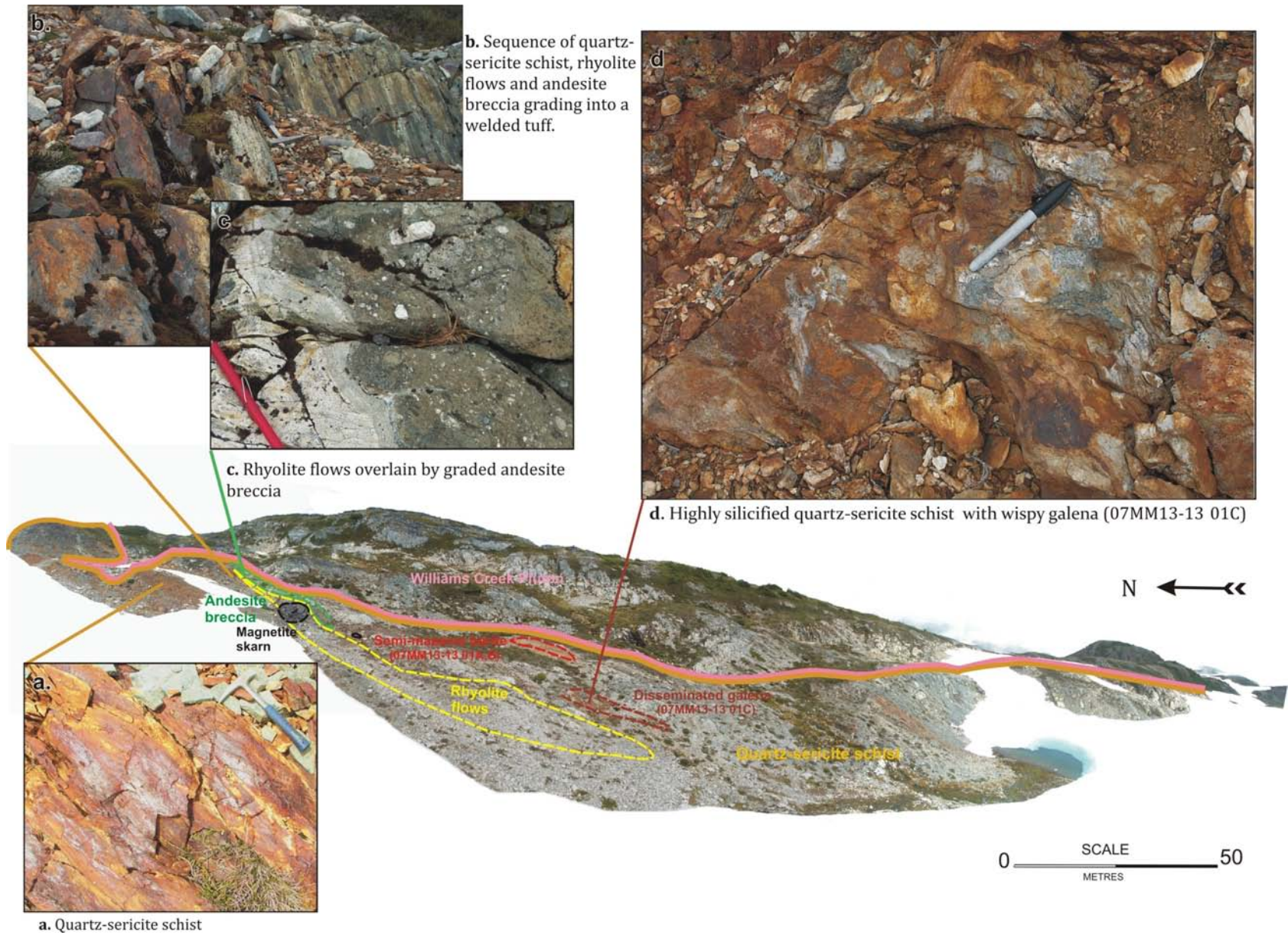


Figure 8. Photomosaic of the Sub showing units: a) quartz-sericite schist; b) sequence of quartz-sericite schist, rhyolite flows and andesite breccia grading into a welded tuff; c) rhyolite flows overlain by graded andesite breccia; d) highly silicified quartz-sericite schist with wispy galena and also a magnetite-clinopyroxene-amphibole skarn.

TABLE 3. GEOCHEMICAL DATA FROM SAMPLES COLLECTED DURING THE 2007 FIELD SEASON IN THE GAZELLE AREA.

Station number	UTM Easting Northing		Description	Element:	Cu	Zn	Pb	Ag	Au	Ba	Mo
				Units:	(ppm)	(ppm)	(ppm)	(ppb)	(ppb)	(ppm)	(ppm)
				Method:	ARMS	ARMS	ARMS	ARMS	ARMS	LMB	ARMS
				Lab:	ACM	ACM	ACM	ACM	ACM	ACM	ACM
				Detection limit:	0.01	0.1	0.01	2	0.1	5	0.01
07MM13-13 01A	543083	6023645	Grab sample: barite in highly silicified quartz-sericite schist	11.26	267.9	643	72787	362.4	>50000	22.77	
07MM13-13 01B	543083	6023645	Representative sample: barite in highly silicified quartz-sericite schist	37.78	7956	>10000.00	>100000	208.4	>50000	35.71	
07MM13-13 01C	543083	6023645	Highly silicified quartz-sericite schist with a lens of disseminated to massive galena (2 x 25 m zone)	212.8	4439	3107	18324	275.1	>50000	33.7	
07MM12-01	542901	6022437	Float sample: quartz-sericite schist with abundant pyrite	70.19	103.3	18.35	237	7.2	1063	0.35	
07MM13-13 07	543083	6023645	Magnetite skarn	25.02	70.6	46.78	1364	3.9	116	1.85	
07MM14-01	542162	6022812	Quartz vein within quartz-sericite schist near granodiorite; mineralization is related to the intrusion	46.45	312.2	406.7	3428	2988	852	95.44	

Analysis of steel-milled crushed rock prepared by ACME Analytical Laboratories Ltd.; duplicate on crushed rock

Abbreviations: ACM, ACME Analytical Laboratories Ltd., Vancouver, BC; ARMS, aqua regia digestion followed by inductively coupled plasma – mass spectrometry (15 gram sample); LMB, lithium metaborate fusion followed by inductively coupled plasma – emission spectroscopy / inductively coupled plasma – mass spectrometry

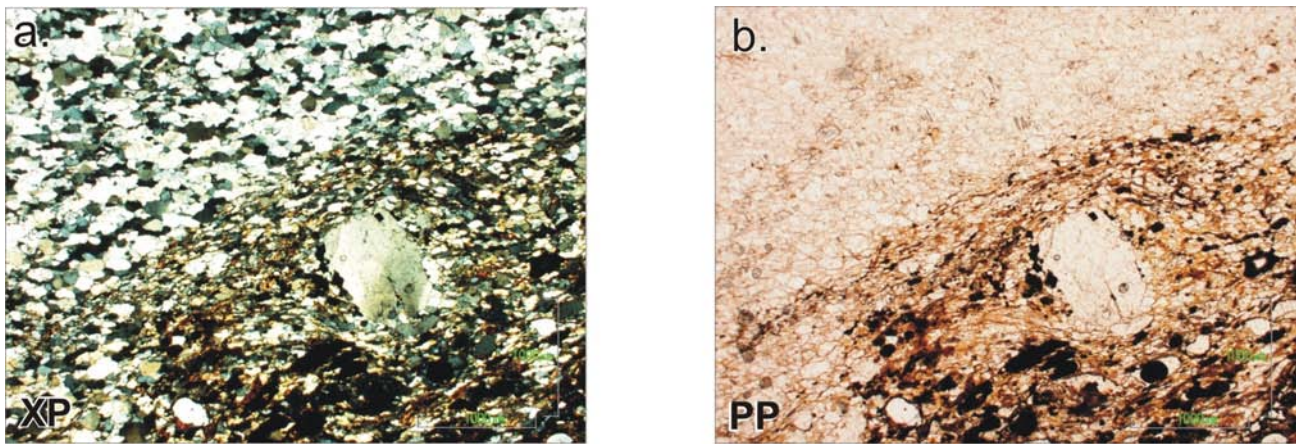


Figure 9. Photomicrograph of barite vein in a) cross-polarized and b) plane-polarized light. Large (pre-tectonic) barite porphyroblast within finer-grain barite (Sample 07MM13-13 01A).

CONCLUSIONS

Through regional and local mapping, the stratigraphy of Paleozoic and Jurassic volcanic rocks in the area southeast of Terrace has been clarified and a new unit that is prospective for VHMS deposits has been identified. The host-rock age, lithology, alteration and mineralization styles identified on the Gazelle property are characteristic of other pre-Permian VHMS deposits within Stikinia. The results of U-Pb, assay and whole-rock samples that are pending will further test this correlation. Possible extensions of

the favourable belt to the southwest require further study to evaluate their stratigraphic age and potential for hosting significant VHMS deposits.

ACKNOWLEDGMENTS

We thank Dave Lefebure for his insights while in the field, as well as for his thoughtful review of the manuscript. We also thank Ray Lett for his tireless and efficient work, providing us with the results of geochemical analysis in time for this publication.

REFERENCES

- Alldrick, D.J., Nelson, J.L. and Barresi, T. (2005): Geology and mineral deposits of the upper Iskut River area: tracking the Eskay rift through northern British Columbia (104G/1,2; 104B/9,10,15,16); in Geological Fieldwork 2004, *BC Ministry of Energy, Mines and Petroleum Resources*, Paper 2005-1, pages 1–30.
- Arseneault, G., Deter, K., Nichols, A., McVey, S., Bruce, I., Broughton, S., Dudson, E. and Eng, G. (2007): Tulsequah: Feasibility study; *Wardrop Engineering Inc.*, URL <<http://www.redcorp-ventures.com/main/?tFeasibilityStudy>> [December 2007]
- Belik, G.D. (1987): Geological and geochemical report on the Billy property, Skeena Mining District, British Columbia; *BC Ministry of Energy, Mines and Petroleum Resources*, Assessment Report 15528, 51 pages.
- Childe, F.C. (1997): Timing and tectonic setting of volcanogenic massive sulphide deposits in British Columbia: constraints from U-Pb geochronology, radiogenic isotopes and geochemistry; PhD thesis, *University of British Columbia*, Vancouver, BC, 298 pages.
- Duffell, S. and Souther, J.G. (1964): Geology of Terrace map-area, British Columbia; *Geological Survey of Canada*, Memoir 329, 117 pages.
- Evenchick, C.A. and McNicoll, V.J. (2002): Stratigraphy, structure and geochronology of the Anyox pendant, northwest British Columbia, and implications for mineral exploration; *Canadian Journal of Earth Sciences*, Volume 39, pages 1313–1332.
- Galley, A., Hannington, M. and Jonasson, I. (2007): Volcanogenic massive sulphide deposits; in Mineral Deposits of Canada, A Synthesis of Major Deposit Types, District Metallogeny, the Evolution of Geological Provinces, and Exploration Methods, Goodfellow, W.D., Editor, *Geological Association of Canada*, Special Publication 5, pages 141–162.
- Gunning, M.H. (1988): Kitimat project; in Exploration in British Columbia 1987, *BC Ministry of Energy, Mines and Petroleum Resources*, pages B67–B70.
- Hooper, D.G. (1984): Geological report on the Gazelle claim, record number 4229; *BC Ministry of Energy, Mines and Petroleum Resources*, Assessment Report 12717, 41 pages.
- Hooper, D.G. (1985): Gazelle claim geological report; *BC Ministry of Energy, Mines and Petroleum Resources*, Assessment Report 14076.
- Hoy, T. (1991): Volcanic massive sulphide deposits in British Columbia, in Ore Deposits, Tectonics and Metallogeny in the Canadian Cordillera; *BC Ministry of Energy, Mines and Petroleum Resources*, Paper 1991-4, pages 89–124.
- Logan, J. (2003): Preliminary litho-geochemistry and polymetallic VHMS mineralization in Early Devonian and(?) Early Carboniferous volcanic rocks, Foremore property; in Geological Fieldwork 2002, *BC Ministry of Energy, Mines and Petroleum Resources*, Paper 2003-1, pages 105–124.
- Logan, J.M., Mihalynuk, M.G., Ullrich, T. and Friedman, R.M. (2007): U-Pb ages of intrusive rocks and $^{40}\text{Ar}/^{39}\text{Ar}$ plateau ages of copper-gold-silver mineralization associated with alkaline intrusive centres at Mount Polley and the Iron Mask Batholith, southern and central British Columbia; in Geological Fieldwork 2006, *BC Ministry of Energy, Mines and Petroleum Resources*, Paper 2007-1, pages 93–116.
- Ludwig, K.R. (2003): User's manual for Isoplot 3.00: a geochronological toolkit for Microsoft Excel; *Berkeley Geochronology Center*, Special Publication 4, 74 pages.
- Massey, N.W.D. (1999) Volcanogenic massive sulphide deposits of British Columbia; *BC Ministry of Energy, Mines and Petroleum Resources*, Open File 1999-2.
- Mihalynuk, M.G., Smith, M.T., Hancock, K.D. and Dudka, S. (1994): Regional and economic geology of the Tulsequah River and Glacier areas; in Geological Fieldwork 1993, *BC Ministry of Energy, Mines and Petroleum Resources*, Paper 1994-1, pages 171–197.
- MINFILE (2007): MINFILE BC mineral deposits database; *BC Ministry of Energy, Mines and Petroleum Resources*, URL <<http://www.em.gov.bc.ca/Mining/Geolsurv/Minfile/>> [November 2007].
- Nelson, J.L., Barresi, T., Knight, E. and Boudreau, N. (2006): Geology of the Usk map area (1931/09); *BC Ministry of Energy, Mines and Petroleum Resources*, Open File 2006-3, scale 1:50 000.
- Nelson, J. and Kennedy, R. (2007): Terrace Regional Mapping Project Year 2: new geological insights and exploration targets (NTS 1031/16S, 10W), west-central British Columbia; in Geological Fieldwork 2006, *BC Ministry of Energy, Mines and Petroleum Resources*, Paper 2007-1, pages 149–162.
- Nelson, J., Kyba, J., McKeown, M. and Angen, J. (2008): Terrace Regional Mapping Project, year 3: contributions to stratigraphic, structural and exploration concepts, Zymoetz River to Kitimat River, east-central British Columbia (NTS 1031/08); in Geological Fieldwork 2007, *BC Ministry of Energy, Mines and Petroleum Resources*, Paper 2008-1, pages 159–174.
- Price, R.A. and Monger, J.W.H. (2003): A transect of the southern Canadian Cordillera from Calgary to Vancouver, field trip guidebook; *Geological Association of Canada*, Vancouver 2003, pages 1–24.
- Raynor, G.H. (1987): A geological report on the J claim group; *BC Ministry of Energy, Mines and Petroleum Resources*, Assessment Report 16860, 21 pages.
- Sebert, C.F., Curtis, K.M., Barrett, T.J. and Sherlock, R.L. (1994): Geology of the Tulsequah Chief volcanogenic massive sulphide deposit, northwestern British Columbia (104K/12); in Geological Fieldwork 1994, *BC Ministry of Energy, Mines and Petroleum Resources*, Paper 1995-1, pages 529–539.
- Stacey, J.S. and Kramer, J.D., 1975. Approximation of terrestrial lead isotope evolution by a two-stage model; *Earth and Planetary Science Letters*, Volume. 26, pages 207–221.
- Tipper, H.W. and Richards, T.A. (1976): Jurassic stratigraphy and history of north-central British Columbia; *Geological Survey of Canada*, Bulletin 270, 73 pages.
- Woodsworth, G., van der Heyden, P. and Hill, M.L. (1985): Terrace East map area; *Geological Survey of Canada*, Open File 1136, scale 1:125 000.

Regional Geology and Resource Potential of the Chezacut Map Area, Central British Columbia (NTS 093C/08)

by M.G. Mihalynuk, C.R. Peat, K. Terhune and E.A. Orovan¹

KEYWORDS: regional geology, structure, litho-geochemistry, mineral potential, Chezacut, Chilcotin River, mountain pine beetle

INTRODUCTION

Mountain pine beetles are a natural part of western North American forest ecosystems. They range from British Columbia to northern Mexico. Human intervention in the natural cycle of forest fires, which rejuvenate forests and create barriers to the transmission of disease and pests, has resulted in mature to overmature pine forests throughout interior British Columbia. These stands of trees are particularly susceptible to widespread mountain pine beetle infestation. A combination of enhanced beetle survival during recent mild winters and regionally overmature forests has resulted in a beetle-infested area of historically unprecedented size. In 2005, the area of contiguous infestation recorded by the 2004 Forest Health Survey (BC Ministry of Forests and Range, 2005a) was coextensive with the Interior Plateau (Fig 1). We refer to this area as the Beetle Infested Zone (BIZ; Mihalynuk, 2007).

Substantial increases to the annual allowable timber harvest in most of the BIZ will help to capture economic value from the dead trees, speed up regeneration and enhance economies of forestry-dependent communities in the BIZ (BC Ministry of Forests and Range, 2005b). However, inevitable degradation of the available trees will lead to an industry downturn. The provincial government is supporting economic diversification to help reduce the long-term economic impact of the mountain pine beetle, including geological mapping programs aimed at locating areas of potential interest to the mining and petroleum industries.

The Chezacut area was targeted for revision mapping because of relatively good logging road access and a historical lack of mineral exploration that we believe is underserved. Herein we report on results of geological mapping and resource evaluation of the area in the 2007 field season and confirm that further mineral exploration is warranted. Significant mineralization was discovered within the first two weeks of mapping (see 'Mineralization' section). Geological mapping also demonstrated that rock exposures are more extensive, and Chilcotin basalt is less extensive, than previously recognized — additional incentives for future mineral exploration in the area.

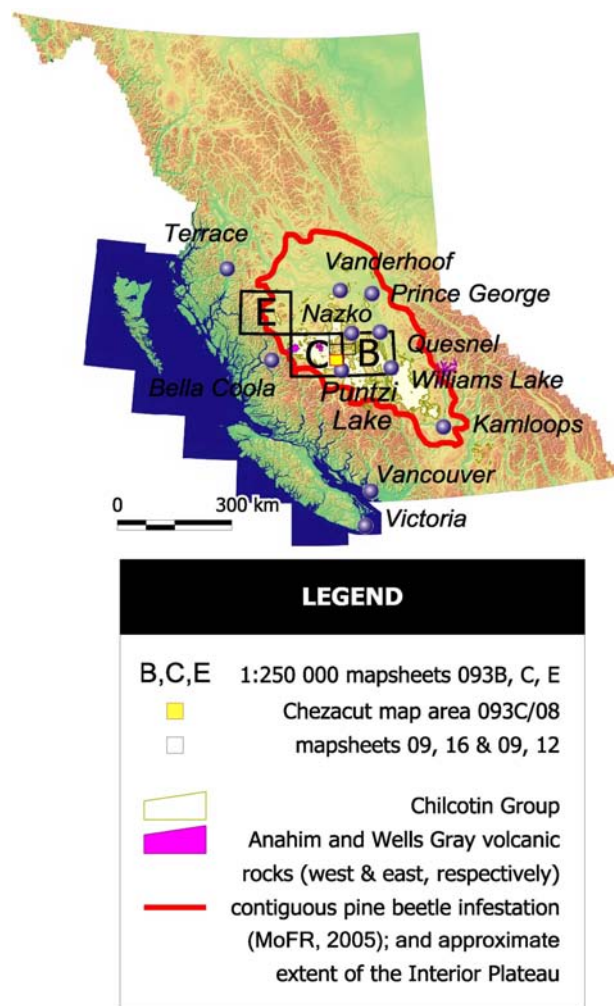


Figure 1. Location of the Chezacut map area, showing areas mentioned in the text as well as the distribution of rocks of the Chilcotin Group (after Massey et al., 2005).

LOCATION AND ACCESS

The map area covers approximately 950 km², and is located about 200 km west of Williams Lake on the Fraser Plateau (the Interior Plateau, Fig 1). It is immediately north of the resort community of Puntzi Lake, a former military air base on the north side of Highway 20 approximately halfway between Williams Lake and Bella Coola. Midway along the eastern edge of the map area is the tiny ranching community of Chezacut, serviced from the main Chezacut forest service road. A second major forest service road, the

¹ Carleton University, Ottawa, ON

This publication is also available, free of charge, as colour digital files in Adobe Acrobat® PDF format from the BC Ministry of Energy, Mines and Petroleum Resources website at http://www.em.gov.bc.ca/Mining/Geosurv/Publications/catalog/cat_fldwk.htm

Puntzi Lake road, transects the south-central and western parts of the map area. Hundreds of kilometres of secondary logging roads branch off the major forestry trunk roads. Many of these are decommissioned and best accessed by mountain bike or, where extensively degraded or overgrown, on foot. Many roadbeds are partly constructed on glaciolacustrine deposits, which are common at low elevations (*see* ‘Surficial Deposits’ section). During dry spells this material forms smooth, albeit dusty, roadways. When soaked by rains, however, the clay-rich glaciolacustrine materials turn greasy and travel can be treacherous.

Major drainages include the Clusko and Chilcotin rivers. Both have eroded through Neogene volcanic rocks, exposing older Eocene and Mesozoic rocks. The paleo-Chilcotin River valley probably channelled lava flows in the Chezacut area: this is particularly evident along the river’s lower stretches, as can be seen from the Bella Coola Highway (Highway 20) at the spectacular cliffs in Bull Canyon Provincial Park (Gordee et al., 2007). Travellers of this route are left with the impression that the Chilcotin basalts are a thick, widespread blanket, and this impression has negatively impacted mineral exploration within the Interior Plateau.

REGIONAL GEOLOGICAL SETTING AND PREVIOUS WORK

The Chezacut map area is located in the west-central part of the Interior Plateau (Fig 1), in which Mesozoic volcanic-arc strata and their plutonic roots are exposed in a basement high that is draped by Eocene, Miocene and Quaternary volcanic rocks. Results of geological fieldwork presented here build upon the regional geological framework established by Tipper (1969), compiled by Massey et al. (2005) and recomputed with regional revisions by Riddell (2006). To the immediate northeast, in the Clisbako area (NTS 093C/9), Metcalfe et al. (1997) focused on volcanological studies, mapping and determination of potential for epithermal mineralization in the Eocene volcanic rocks. Surficial deposits and glacial physiography have been mapped regionally by Tipper (1971) and in more detail by Kerr and Giles (1993), who also conducted till geochemical surveys (*cf.* Levson and Giles, 1997). Our 1:50 000 scale mapping is available in hard copy or digital format (Mihalyuk et al., 2008).

FIELD TECHNIQUES

We relied heavily upon 1:20 000 scale digital orthophotographs (0.5 m resolution) for the identification of areas of outcrop and definition of geological lineaments. Remotely sensed, multispectral ASTER imagery that was captured from orbit mid-season was also utilized.

Rocks exposed as a consequence of road construction form only a small percentage of those mapped within the area (only 2.4% of outcrops are within 15 m of roads; Fig 2). Mapping restricted to roadways leaves a negative impression of the percentage of outcrop within the area, probably because rocky areas are avoided in order to minimize road construction costs. Most outcrops are exposed along glacially scoured ridges and along the margins of glacial meltwater channels: both appear as open areas on orthophotographs and ASTER images.

Clast counts in basal till were used locally to help establish geological contacts beneath the till blanket. However, large portions of the western half of the map area are covered by reworked or potentially far-travelled hummocky glacial deposits (Fig 2). In these areas, we have relied upon gravity (Riddell, 2006) and aeromagnetic survey data (Geological Survey of Canada, 1994) to guide our interpretation of unit contacts.

LAYERED ROCKS

Rocks within the Chezacut map area can be assigned to one of four successions: Mesozoic, Eocene, Oligocene–Pleistocene or Pleistocene–Holocene (Fig 3). The presumed oldest rocks are undated, poorly fossiliferous strata that correlate with Late Triassic and Early Jurassic volcanic arc – related strata of the Stikine Terrane (Tipper, 1969; Massey et al., 2005). These arc rocks and their high-level plutonic roots were folded prior to the deposition of widespread Eocene volcanic rocks. Eocene and/or subsequent deformation produced broad folds in the Eocene volcanic strata. Erosion of the deformed terrain during the Miocene created paleotopographic lows into which effusive outpourings of Miocene and younger basalt ponded. The youngest bedrock units probably range from Quaternary to Recent in age, and belong to the alkaline Anahim volcanic belt of possible hot-spot origin (Bevier et al., 1979).

Mesozoic Strata

Volcanic strata of presumed Jurassic age were mapped by Tipper (1969) in three areas: Puntzi Ridge, on the slopes north of Chilcotin Lake and in the Punkutlaenkut Creek area (northwesternmost NTS 093C/08). Rocks north of Chilcotin Lake more closely resemble Eocene strata (an opinion also expressed by Nebocat, 1983); however, we have extended areas of Mesozoic strata in the other two areas on the basis of outcrop found during the 2007 mapping, as well as aeromagnetic and gravity data. We interpret part of Tipper’s ‘Eocene (?)’, ‘Oligocene (?)’ unit as belonging to the Mesozoic succession, which is exposed in two belts that merge towards Puntzi Ridge, in the southeastern part of the map area (Fig 2).

VARIEGATED LAPILLI ASH TUFF

The most voluminous Mesozoic unit is green or variegated lapilli tuff, which may be more than 1000 m thick. It typically weathers to green or orange angular blocks, with tabular feldspar phenocrysts ≤ 3 mm in size comprising 15% of the rock. Lapilli are angular to subrounded and tend to be supported by an ash matrix that can contain up to 25% feldspar crystals. Less commonly, clasts are trachytic, with up to 3% subhedral pyroxenes that are < 3 mm in diameter, and are quartz-calcite-chlorite amygdaloidal. The unit is of dominantly basaltic andesite composition.

POLYMYCTIC BOULDER CONGLOMERATE

Spectacular polymictic boulder conglomerate is exposed on the west flank of Luck Mountain. The most conspicuous clasts are well-rounded boulders of pink monzonite in excess of 1.5 m in diameter. Other major source rock types include feldspar porphyry and lapilli tuff. No calcareous or fine-grained sedimentary rock clasts were identified, suggesting that only the upper parts of the Mesozoic section were exposed to erosion at the time of forma-

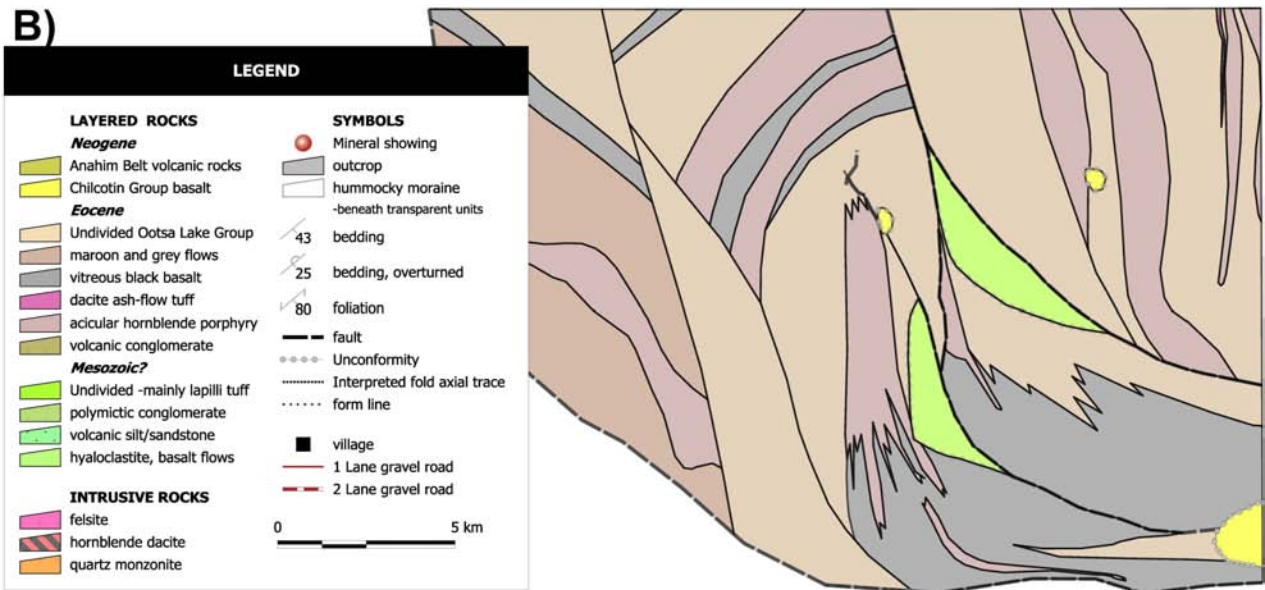
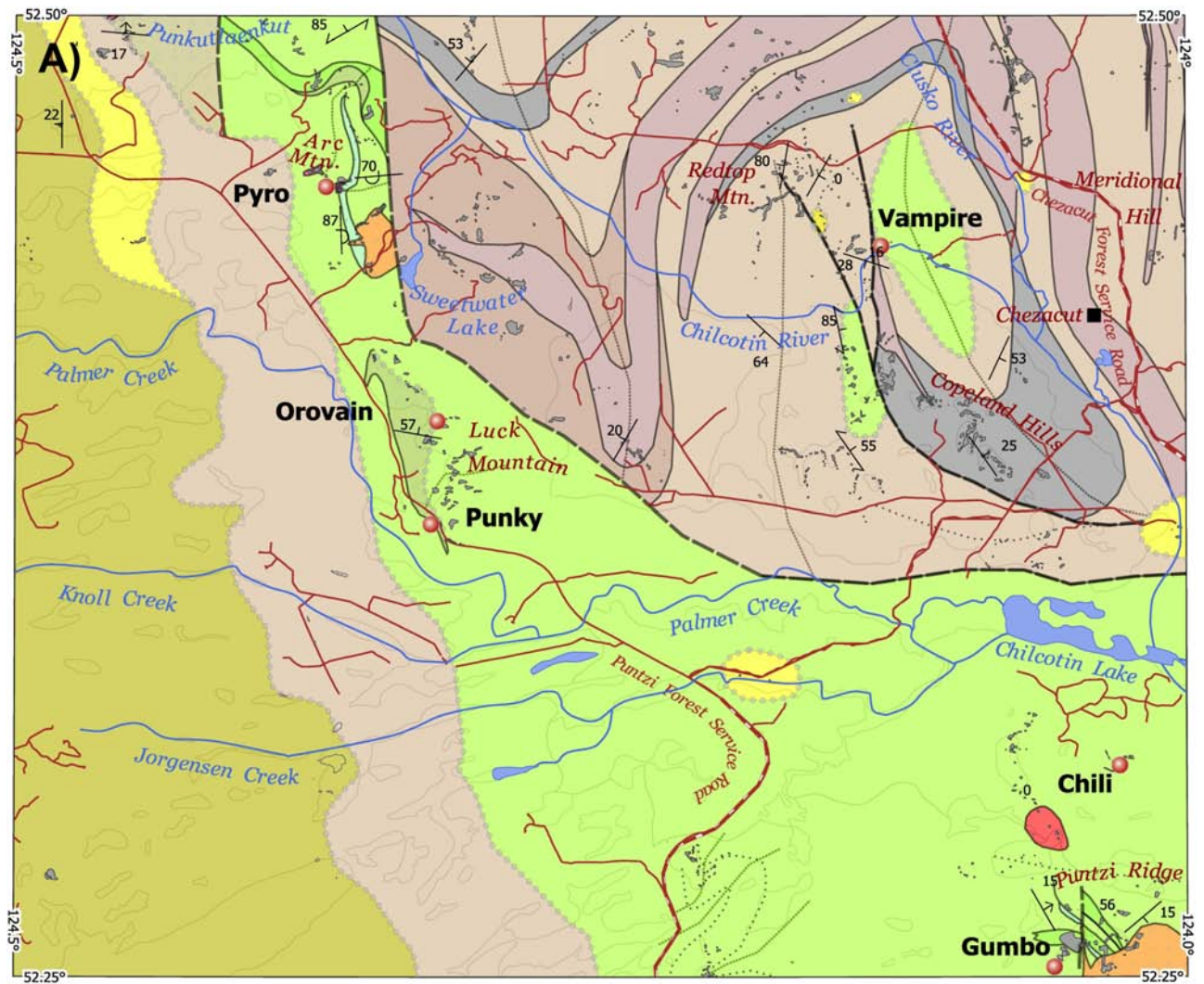


Figure 2. A) Generalized geology of the Chezacut map area, including work by Tipper (1969) and Nebocat (1983). B) Alternative interpretation for the Eocene geology of the map area.

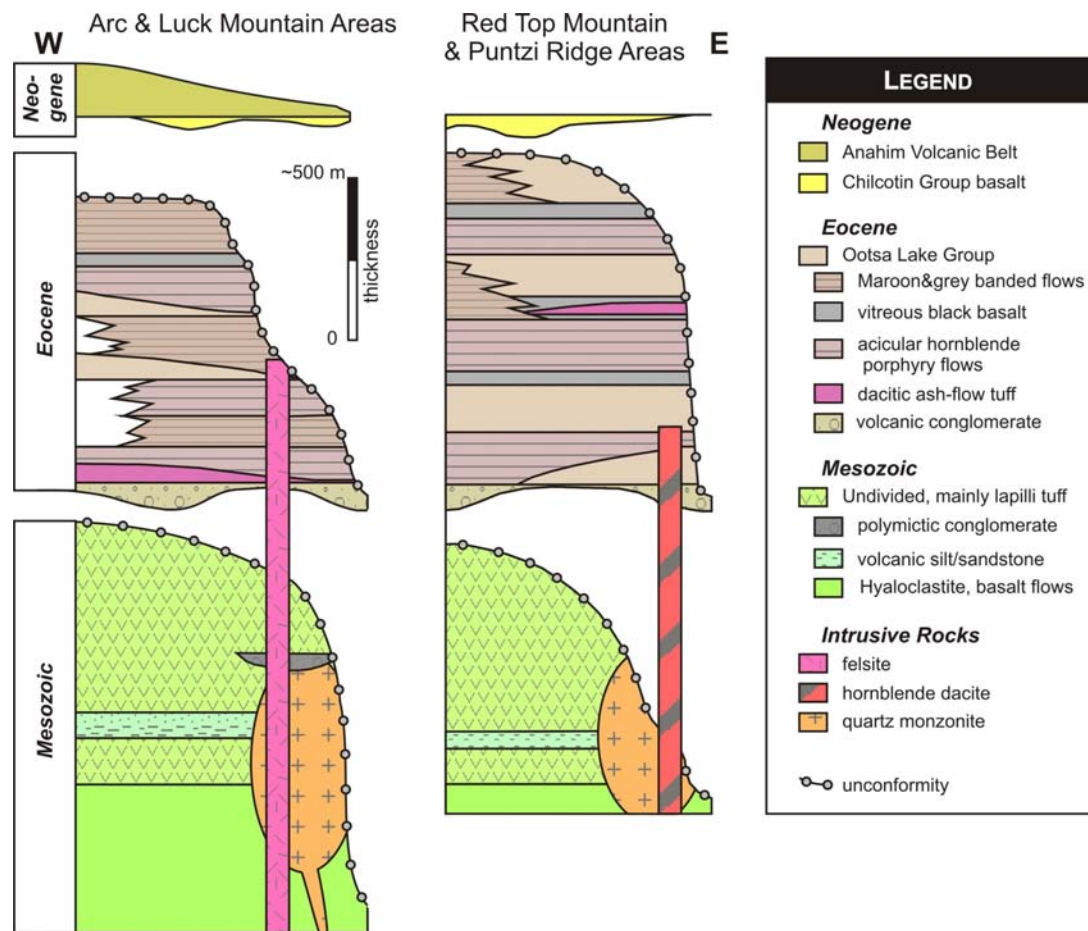


Figure 3. Schematic stratigraphic columns for the northwestern and southeastern parts of the Chezacut map area. Each column shows facies changes from west to east.

tion of this conglomerate. This unit apparently sits above, and grades upwards into, lapilli tuff and tuffite. On this basis, we interpret it as an intraformational conglomerate.

CALCAREOUS FOSSILIFEROUS SANDSTONE

Tan to yellow and rusty-weathering, calcareous volcanic sandstone crops out at one locality on the northern flank of Arc Mountain. Only about 5 m is exposed, and maximum thickness cannot be more than about 50 m. Internal and external moulds of fossil belemnoids (?) and corals are poorly preserved within the coarse-grained feldspathic sandstone. They are best exposed on weathered surfaces, presumably through dissolution of the calcareous fossil. Pyrrhotite, lesser pyrite (up to 4% combined) and traces of chalcopyrite/cubanite and possibly bornite can be observed in hand samples (all sulphides except bornite have been confirmed by petrographic analysis; Fig 4).

Some grains in the sandstone may have a chert protolith, supporting correlation of this unit with the calcareous chert pebble conglomerate unit described below.

CALCAREOUS CHERT PEBBLE CONGLOMERATE

Well-rounded pebbles and granules of white rhyolite typically form white and black conglomerate beds,

1 to 30 cm thick. Together with sandstone interbeds, they form a unit approximately 25 m thick. Other interbeds include siltstone, siliceous volcanic mudstone and hyaloclastite. Conglomerate beds are clast-supported with a recessive, sandy, carbonate-rich matrix. Clasts are up to 4 cm in diameter and well sorted. On the south flank of Arc Mountain, the matrix material of the conglomerate is replaced by mats of tourmaline (Fig 5), perhaps due to a subjacent mass of aplite that forms much of the southwestern flank of Arc Mountain.

HYALOCLASTITE

Bright green hyaloclastite forms a layer approximately 200 m thick near Arc Mountain and in the Puntzi Ridge area. Hyaloclastite typically consists of monomict aphanitic basalt fragments, but may contain fine-grained pyroxene phenocrysts. Clasts are most commonly lapilli sized, ranging up to small blocks. The matrix is sparry calcite, which may locally contain up to 1% pyrite cubes. Near Arc Mountain and in the western Copeland Hills, hyaloclastite passes laterally into massive basalt, possibly pillowed.

BASALT

Dark green, massive, blocky weathering pyroxene basalt is approximately 100 m thick and grades into the hyaloclastite unit. Carbonate-chlorite amygdules up to

1 cm form $\leq 10\%$ of the rock. Concentric zones with more abundant amygdules are interpreted to parallel pillow margins. Tabular to xenomorphic plagioclase and euhedral pyroxene form $\sim 15\%$ and $\sim 5\%$ of the rock, respectively. Epidote and chlorite-coated joint surfaces are ubiquitous.

VOLCANIC SILTSTONE/SANDSTONE

Green to brown or rust-coloured, commonly recessive, volcanic siltstone and mudstone form a unit approximately 80 m thick. The unit weathers into small (1–5 cm) angular fragments. Rusty zones may contain up to 3% pyrite and/or pyrrhotite. The sedimentary rocks are typically laminated to thinly bedded (1–2 cm). Ripple cross-stratification, scours and flutes, and graded bedding are locally preserved.

Ootsa Lake Group

Volcanic strata of the Eocene Ootsa Lake Group were defined in the Whitesail Lake area (NTS 093E) by Duffell (1959), approximately 200 km northwest of the Quesnel and Anahim Lake areas (NTS 093B, C; Fig 1) where they were mapped between 1954 and 1957 by Tipper (1959,

1969). Metcalfe et al. (1997) conducted revision mapping in NTS area 093C/09 and 16, and 093B/12 and 13, which are widely underlain by correlative strata. The southwestern corner of this four-sheet block is the Clisbako sheet (NTS 093C/09), located immediately north of the Chezacut sheet (NTS 093C/08). Metcalfe et al. (1997) renamed the Ootsa Lake Group in this area to ‘Clisbako volcanics’ and published isotopic age determinations ranging from ca. 53.4 ± 0.6 Ma to ca. 44.2 ± 0.4 Ma, in agreement with palynological age data. Map units identified as part of the Chezacut project do not easily fit with the assemblages defined across the map boundary by Metcalfe et al. (1997), probably because of the paucity of data observation points that Metcalfe et al. (1997) had upon which to base their interpretations. We have therefore retained the broader ‘Group’ designation of Tipper (1969). We have found it advantageous to map units based upon phenocryst content and texture, rather than on broader unit assemblages. For example, we separate a regionally significant hornblende-phyric unit, which is included by Metcalfe et al. (1997) within their ‘pyroxene-bearing assemblage’. This has allowed us to map out units that could be outlining broad folds in the Eocene volcanic rocks.

A minimum composite thickness for the Ootsa Lake Group in the Chezacut map area is shown in Figure 3 as approximately 1.5 km. However, at a location just 20 km north of the map area, the petroleum exploration well CanHunter b22/093-C-09 penetrated Eocene strata from surface to nearly 3800 m (Riddell et al., 2007). Four detrital zircon age determinations on well cuttings confirm Eocene

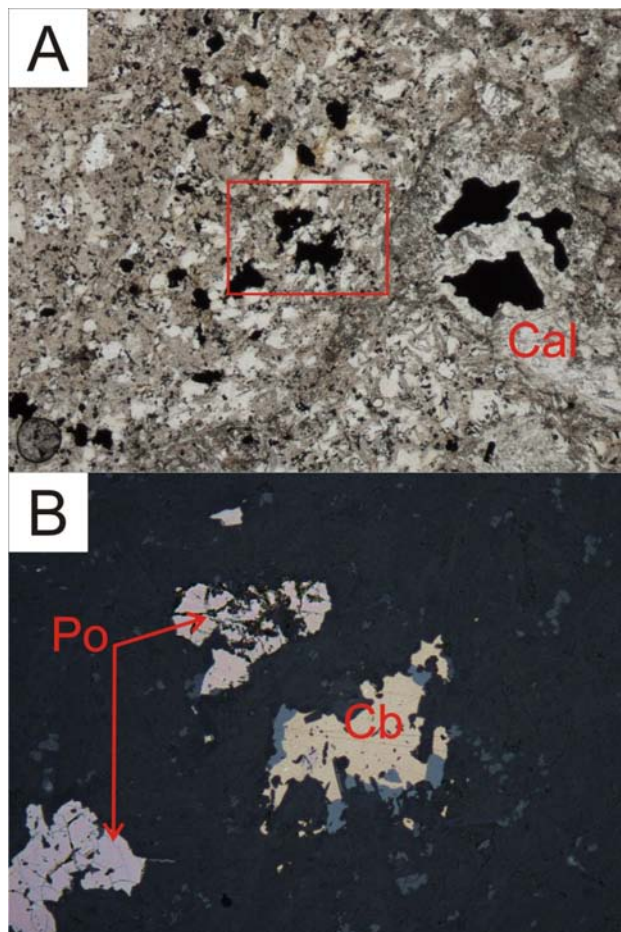


Figure 4. Photomicrographs of thermally metamorphosed calcareous volcanic sandstone on the northeast flank of Arc Mountain: A) calcite (Cal) and intergrown secondary tremolite are conspicuous in transmitted cross-polarized light; B) reflected light shows skeletal pyrrhotite (Po) and cubanite (Cb). Width of rectangle in A represents approximately 1 mm and shows the extent of photograph B.



Figure 5. Tourmaline and silica replacing the matrix within rhyolite pebble conglomerate.

TABLE 1. CHARACTERISTICS FOR DISTINGUISHING BETWEEN VOLCANIC-DOMINATED SUCCESSIONS WITHIN THE CHEZACUT MAP AREA.

	Chilcotin Group	Ootsa Lake Group	Mesozoic Strata
<i>Composition</i>	Mainly basalts	Glassy basalt to dacite	Mainly andesitic
<i>Vesiculation</i>	Highly vesicular – spongy	Amygdaloidal, some vesicles	No vesicles – amygdules only
<i>Magnetic Susceptibility</i>	4.5 ±1.7 (1σ)	3.5 ±4 (1σ); sediment/tuff ~1; flows 1–17	3.9 ±6.4 (1σ); tuffite/tuff 0.1–18; flows 1–20
<i>Alteration</i>	Unaltered – olivine and feldspars vitreous	Feldspars turbid, olivine altered, pyroxene-hornblende are fresh	Feldspars sericitized, ±chlorite-epidote altered; no unaltered olivine; pyroxene epidote-chlorite altered
<i>Deformation</i>	Warping, local high-angle faults	Broad folds, local spaced cleavage, weak foliation	Tight folds, overturned, foliation common

ages down to 3745 m; all dates are equivalent within the limits of error (ca. 52 ±2 Ma; Riddell et al., 2007).

DISTINGUISHING FEATURES

The Ootsa Lake Group volcanic rocks can be difficult to distinguish from Mesozoic volcanic rocks; however, they are typically less altered, lacking the pervasive epidote-chlorite alteration typical of the Mesozoic strata. Some mafic units, especially an olivine-phyric unit near the base of the Ootsa Lake Group, can be mistaken for Chilcotin Group basalt; however, the latter is generally unaltered, with vitreous feldspars, and tends to be highly vesicular. Ootsa Lake Group volcanic rocks, on the other hand, have cloudy feldspars, are clay-chlorite altered, and are amygdaloidal (Table 1).

Basal portions of the Ootsa Lake Group lie with angular unconformity atop Mesozoic rocks. Details of the stratigraphy vary from place to place, but the following generalized succession can be described for the five most important units:

- poorly exposed basal conglomerate
- recessive, maroon-brown flows and breccias, herein termed the Peaty unit
- acicular hornblende porphyry flows (through to all but the very highest levels)
- ‘maroon and grey flow-banded’ and ‘vitreous black’ units (both interlayered with the acicular hornblende porphyry unit)

BASAL CONGLOMERATE

Biotite-rich basal conglomerate is a recessive unit at the base of the Ootsa Lake Group. It is typically yellow to white weathering, poorly indurated, feldspathic and clast supported (Fig 6). It locally grades into coarse-grained sandstone. Euhedral biotite booklets up to 0.5 cm in diameter are characteristic of this unit, commonly forming up to 10% of the rock, either as single crystals within the sandy matrix or as phenocrysts in dacitic clasts. Sandy beds may display reverse grading (interpreted as a water-laid tuffaceous component), scouring and crossbedding. Green clasts, probably derived from the underlying Mesozoic units, are conspicuous and may form up to 30% of the rock.

PEATY BASALT

The Peaty basalt unit is composed of flows and related breccias. Weathered surfaces are a peat-brown colour. Fresh surfaces are dark grey and may display coarse, black, subidiomorphic olivine and idiomorphic, ochre-weathering sanidine (?), each forming up to 2% of the rock. Very fine-grained carbonate is pervasive within the matrix but is not visible as discrete veins or patches, except as amygdules that are otherwise composed of green and amber, chalcedonic quartz. Amygdules are present in vesicu-

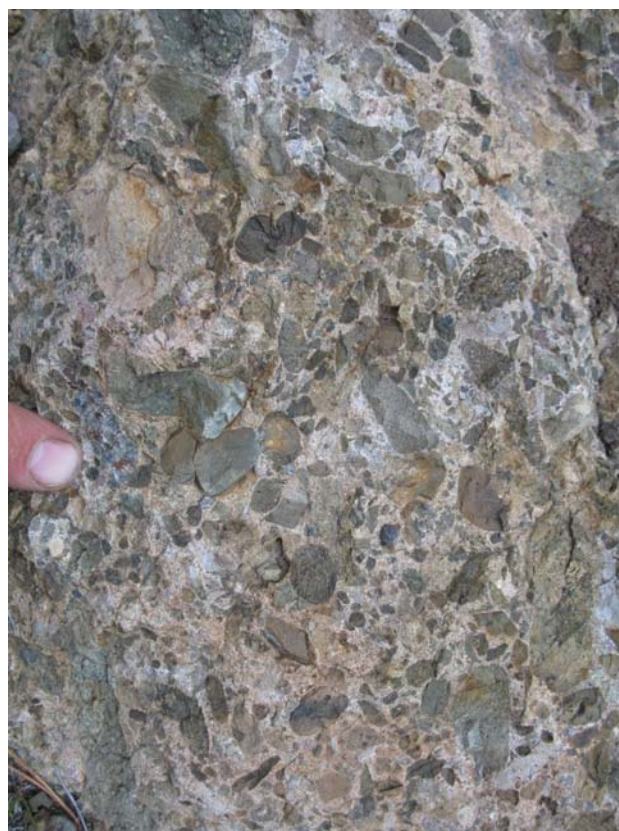


Figure 6. Basal conglomerate of the Ootsa Lake Group. Some of the dark green clasts may be derived from the underlying Mesozoic volcanic strata. Biotite crystals are abundant within the matrix and in Eocene (?) clasts.

lar flow tops, which are developed in the top 1.5 m of the approximately 10 to 70 m thick sequence of flows and breccia that forms this unit.

ACICULAR HORNBLENDE DACITE

Northeast of Arc Mountain, acicular hornblende dacite flows are probably deposited directly atop the Triassic–Jurassic succession. Acicular hornblende porphyry is the dominant exposed rock type in the eastern parts of the map area. It is resistant, commonly underlying ridges. Hornblende displays trachytic alignment within well-developed layers, which are interpreted as flow banding. Parting along flow band surfaces causes the outcrops to break into thin plates that are typical of this unit. Slopes adjacent to outcrops are covered by tan to pink or rusty, angular, poker-chip scree. Fresh surfaces are pinkish tan to grey and display black hornblende needles that are generally less than 4 mm long and form less than 3% of the rock. Typically, hornblende is less than 1%, altered to a punky brown and best displayed on weathered parting surfaces. Salmon-coloured idiomorphic crystals of sanidine (?) locally form up to 2% of the unit.

Two variants of this unit occur locally. One contains coarse hornblende comprising about 5% of the rock. It may display variegated flow bands and flattened pumice lapilli. The other is strongly rusty weathering and limonite and jarosite (?) stained, and is best exposed on the eastern slopes of Redtop Mountain.



Figure 7. Platy-weathering dacitic acicular hornblende-phyric flow unit with characteristic pinkish colour. Photo shows an example of a vesicular flow top, which are not commonly exposed.

Where well exposed, dense flow and vesicular flow-top facies can be identified (Fig 7). Flows range from a couple of metres to perhaps ten metres in thickness, with the top 0.5 to 2 m highly vesicular and recessive weathering. Interflow and autobreccia are well developed in some localities.

AMYGDALOIDAL PYROXENE-PHYRIC BASALT

Brown-green, rubbly weathering, highly vesicular, sparse pyroxene (~2 mm, <3%) and fine plagioclase porphyry is commonly brecciated and forms irregular layers and lenses. Green and amber amygdules of chalcedonic quartz are characteristic. Amygdules are commonly elongate and can be more than 10 cm long. Irregular cavities more than 30 cm in diameter are lined with terminated quartz crystals or filled with geopetal layers of varicoloured (mainly white or amber) chalcedony. This unit is interpreted as a succession of gas-rich basalt flows infilling an irregular topography.

OCHRE BRECCIA AND FLOW LOBES

Ochre-weathering breccia can form layers more than 10 m thick. Dominant clast types are black or maroon, scoriaceous to nonvesicular, aphanitic to rare crowded tabular feldspar porphyries. Pyroxene crystals are a common but minor constituent. Ochre staining and clay alteration may be developed within en échelon tabular zones inter-



Figure 8. Flattened pumice blocks and possible weak welding producing flame-like textures (F) in chlorite-altered (Chl) hornblende-biotite dacite (quartz, hornblende and biotite phenocrysts fall outside the field of view). Diameter of circle around the crosshairs is ~200 µm.

preted as fumarole fissures. These may be filled with secondary breccias. At one locality in the northeastern part of the map area, agglutinated, flattened blocks of black obsidian are interpreted as part of a spatter breccia. Dense, brown to black lobes are interpreted as fingers of basalt flows within the breccia-dominated unit.

DACITE ASH-FLOW TUFF

White, blocky-weathering hornblende-biotite dacite forms a layer up to approximately 100 m thick. Idiomorphic hornblende and biotite form up to 15% of the unit in subequal amounts. Flattened blocks interpreted as collapsed pumice may display local weak welding (Fig 8) and are suggestive of an ash flow origin. This unit crops out at four localities between the northeastern corner of the map area and west of Redtop Mountain (two are large enough to be shown on Fig 2). These isolated ash-flow tuff layers are interpreted as penecontemporaneous, or deposited during one ignimbritic eruptive episode. Two other occurrences of this unit are located within different stratigraphic intervals and are unlikely to have been deposited during the same eruptive episode.

MAROON AND GREY BANDED RHYOLITE

A ridge-forming rhyolitic unit composed of alternating, millimetre-thick, maroon and grey flow bands (Fig 9) is an attractive and easily distinguished rock type within the north-central part of the map area. It is interlayered with flow top/bottom breccias of the same composition. Most commonly it is aphanitic, but feldspar phenocrysts locally



Figure 9. Typical outcrop of maroon and grey flow-banded unit.

form up to 1% of the rock. The unit is interpreted as a series of low-relief dacitic flow domes.

VITREOUS BLACK DACITE

Vitreous, black, sparse pyroxene porphyritic dacite flows and breccia display a distinctive yellow-tan pelagonite rind where weathered surfaces are well developed (Fig 10),

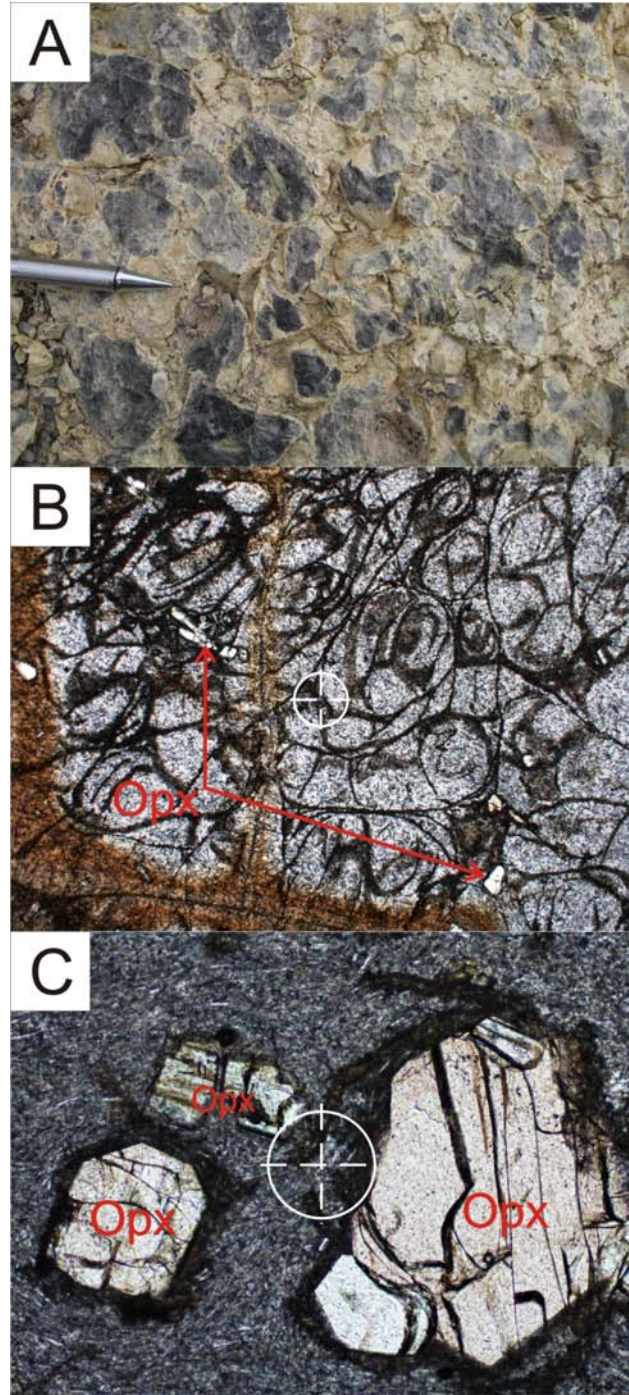


Figure 10. A) Typical pelagonite alteration within vitreous black basalt. (B) Perlitic fracturing and pelagonite alteration along joint surfaces. (C) Plagioclase microlites in glassy matrix surrounding orthopyroxene (? orthoferrosilite) phenocrysts. Circle at crosshairs in photomicrographs is ~200 µm in diameter.

such as among the roots of ubiquitous dead and blown-down pine trees. Phenocrysts include <1% fine, bright green orthopyroxene as anhedral and granular aggregates less than 2 mm in size, and <1% transparent, lath-shaped plagioclase up to 4 mm in size (Fig 9). Euhedral black pyroxenes (up to 1 cm and 1%) were identified within a single flow of this unit. Flow tops are commonly vesicular (less than 5 mm thick, 30% irregularly shaped vesicles), with vesicles lined by yellow-orange to tan mineral aggregates. Interflow breccia facies are less commonly developed.

Neogene Volcanic Rocks

Neogene volcanic rocks encompass two broad rock packages: the Late Oligocene to early Pleistocene Chilcotin Group, which extends over 50 000 km² of the Interior Plateau of British Columbia between the Coast Mountains and the Quesnel Highlands (Bevier, 1983b), and the Pleistocene to Holocene Anahim volcanic belt (Mathews, 1989). The Chilcotin Group is composed of submarine and subaerial basalts and associated pyroclastic and sedimentary rocks deposited in a back-arc basin (Bevier, 1983a; Anderson et al., 2001), whereas the Anahim belt rocks are attributed by Bevier (1989) to a hot spot that tracked eastward, with the easternmost volcanic manifestations in the Wells Grey area (Fig 1). However, a swarm of earthquakes in a formerly aseismic region near Nazko cone (Fig 1) may be caused by the movement of magma at depths of approximately 20 km (Pynn, 2007), calling into question simple passage of the hotspot.

CHILCOTIN GROUP

The Chilcotin Group was first described in south-central British Columbia by Tipper (1971) and later redefined by Bevier (1983b) and Mathews (1989). The lava plateau formed from a series of topographically low shield volcanoes that amalgamated into a single, flat terrain. Vents for Chilcotin basalt flows appear to be represented by six basaltic and gabbroic plugs intruded into the flows (Bevier, 1983a), none of which occur within the map area. The Chilcotin Group postdates most tectonism within the area, although regional tilting is reported along the southwest flank of the Interior Plateau (Parrish, 1983).

Chilcotin Group basalt flows rest unconformably on all older rock units. They consist mainly of thin (2–15 m thick), flat-lying, dark brown to grey, columnar-jointed pahoehoe flows. Outcrops in the Chezacut map area are mainly massive or columnar-jointed flows, locally displaying flow-parallel layers of vesicles, or vesicle pipes (Fig 11). These vesicle pipes are a common feature reported by Bevier (1983a), suggesting that the extruded lavas were rich in volatiles.

The average composite thickness of the Chilcotin Group, according to Bevier (1983a), is 67 m, with a maximum known thickness of 141 m. However, 500 m of 'mafic volcanics' were penetrated by petroleum exploration well CanHunter b-16-J/93-B-11 in the Nazko River area, about 60 km east-northeast of the Chezacut map area (Riddell et al., 2007). A preliminary thickness model for the Chilcotin Group indicated that it is less than 25 m thick across approximately 80% of its extent, and more than a third may be less than 5 m in thickness (Mihalynuk, 2006; readers interested in more refined thickness models are referred to Andrews and Russell (2007) and subsequent publications by those and affiliated authors). Despite its limitations, the

preliminary thickness model is consistent with the basalt observed in the Chezacut map area, where only six areas with Chilcotin outcrop were found (Fig 2), even though the Chezacut map area is located near the centre of the approximately 50 000 km² extent of the Chilcotin Group (Massey et al., 2005).

Anahim Volcanic Belt

Northwest of the Chezacut map area, relict stratovolcanos of the Rainbow, Itcha and Ilgatchuz ranges are products of the compositionally diverse Anahim volcanic belt. Volcanic units include alkaline basalts like hawaiite and basanite, and peralkaline rhyolite and phonolite (Souther and Souther, 1994) of mainly Pliocene and Pleistocene age (Bevier, 1989). Previous petrogenetic studies have focused primarily on the hawaiites (Stout and Nicholls, 1983; Charland et al., 1995), which appear to be derived from the mantle at the base of the crust.

Rocks of the Anahim volcanic belt are sporadically exposed along the western margin of the Chezacut map area. A hill in the southwestern part of the area is underlain by shallowly east-dipping black or pinkish grey, fine to medium-grained, crystal-rich trachybasalt flows. Petrographic analyses of the latter show them to contain conspicuous skeletal olivine with inclusions of devitrified melt (Fig 12A).

Broken outcrops on an isolated knob along the western border of the map area at the headwater of Palmer Creek are composed of light green and grey-weathering basalt. The

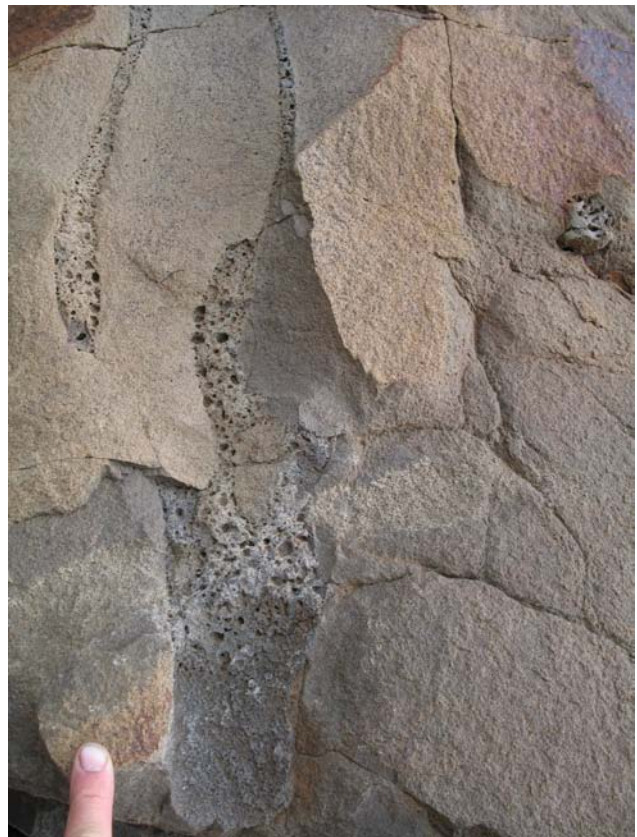


Figure 11. Vesicle pipes, like those shown here, form within and between metre-thick columns of the Chilcotin Group basalt flows.

light green colour is imparted by an approximately 10% aegirine content and a predominance of alkali feldspars (Fig 12B).

A knob 7 km west-northwest of Arc Mountain is underlain by well-developed alternating layers of scoria and flows (Fig 13). Exposures at the lowest elevations are pink

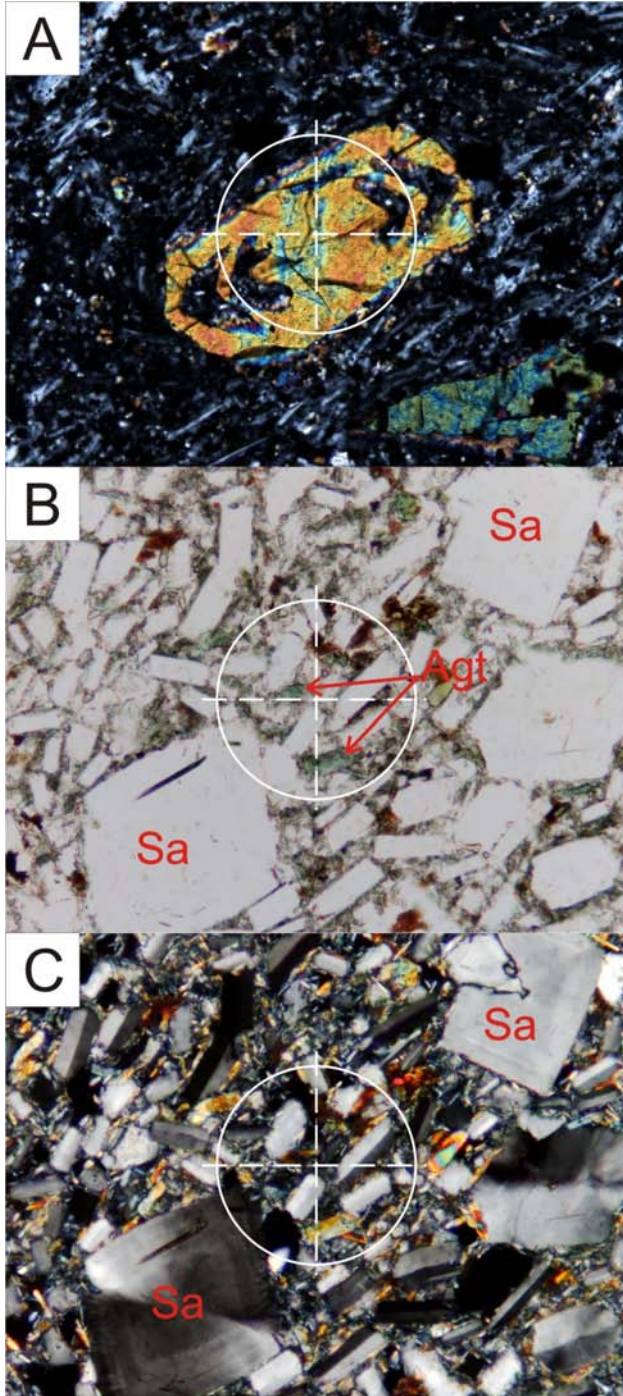


Figure 12. Photomicrographs of A) skeletal olivine that has trapped melt (now devitrified) during rapid growth (cross-polarized light); and B) and C) aegirine (Agt) and Baveno-twinned sanidine (Sa) within a phonolite flow (?) of the alkalic Anahim volcanic belt in plane polarized light (B) and cross-polarized light (C). Circle at crosshairs in photomicrographs is 200 µm in diameter.

tuff with sparse euhedral quartz eyes. Above a covered contact is an approximately 10 m thickness of crowded, coarsely bladed feldspar porphyry flows. On the incised western flank of the knob are beautifully exposed scoria layers (Fig 13) containing lapilli to breccia-sized feldspar crystals (Fig 13, inset) and interlayered, dark grey, sparsely feldspar-phyric flows. These strata dip west, indicating that an elevated magma source was located to the east prior to glaciation.

All exposures of Anahim volcanic belt rocks are mantled by a thin veneer of fluvially modified glacial deposits. Therefore, they predate the latest glaciation. Glacial erratics of Anahim volcanic belt rocks are commonly more than a metre in diameter. One of the most conspicuous rock types that forms these erratics is coarse-grained K-feldspar porphyry with quartz ‘eyes’ up to 3 cm in size.

SURFICIAL DEPOSITS

Till, glaciofluvial and glaciolacustrine deposits are widespread within the Chezacut map area. These deposits have been discussed as part of a study by Levson and Giles (1997), and were mapped by Kerr and Giles (1993). Readers interested in surficial geology should refer to these publications, as we discuss relatively few salient points here.

Undisturbed basal till is not abundant within the Chezacut map area. The most widespread unit is hummocky moraine, interpreted to have been deposited mainly during ice retreat. Where present, however, basal till is a reasonable proxy for the local bedrock geology through geochemical analysis of the silt fraction and composition of the entrained clasts. Geochemical analyses are reported in Peat et al. (2008). One notable sample is MMI07-20-4 (52.4609°N, 124.0849°W), which contains significant Ag (6 ppm).

Glaciolacustrine deposits are widespread within the Chezacut map area. They extend up to a consistent elevation of approximately 1150 m across the area (Fig 14), and are interpreted to have been deposited from a late glacial lake that inundated approximately 65% of the map area at its peak level.



Figure 13. Eroded flank of an Anahim volcanic belt stratovolcano. Inset photo demonstrates the very coarse size attained by the feldspars within these units.

INTRUSIVE ROCKS

Three intrusive bodies, each approximately 1 km in diameter, crop out in a northwest-trending belt in the map area. From south to north, these are the Puntzi Ridge quartz monzonite, the Chili dacite, and the ‘Sweetwater Lake’ monzonite. The latter informal name is taken from a kilometre-long, deep lake 3 km southeast of Arc Mountain (Fig 2).

Puntzi Ridge Quartz Monzonite

Pink to grey quartz monzonite crops out on the southeastern flank of Puntzi Ridge and ‘Sweetwater Lake’. Composition varies from quartz diorite to monzodiorite and grain size varies from medium to coarse. Mafic minerals include biotite and subordinate hornblende. Late fractures in the monzonite at Puntzi Ridge are commonly annealed with K-feldspar and display pink halos that are 2 cm or more wide (Fig 15A). Chlorite±epidote alteration and coatings on late joint surfaces affect most parts of the intrusions to some degree.

Dikes of monzodiorite extend from the main body at ‘Sweetwater Lake’, and a varitextured diorite apophysis is locally foliated. Thermal metamorphic halos affect Mesozoic country rocks for at least 30 m from the intrusive contacts, but some of the Mesozoic units may postdate intrusion of the bodies. For example, a biotite-bearing dacite/latite tuff at Puntzi Ridge is, in places, almost indis-

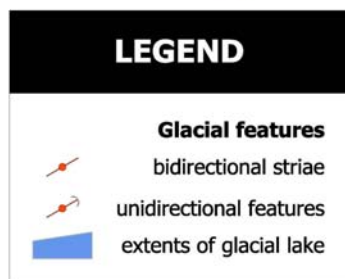
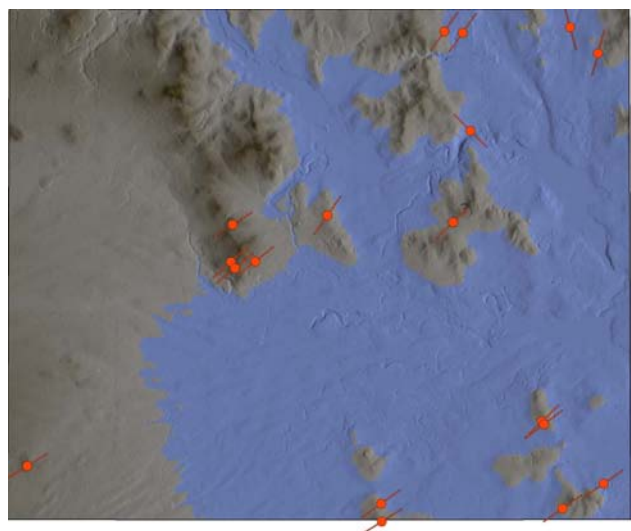


Figure 14. Distribution of glaciolacustrine deposits within the Chezacut map area is consistent with an enormous glacial lake having a surface elevation of 1153 m, which would have inundated approximately 65% of the map area.

tinguishable from the intrusion (Fig 15B) and, on this basis, is interpreted as a coeval extrusive equivalent. However, latest phases of the intrusion may cut volcanic units at



Figure 15. A) K-feldspar alteration halos on parallel fractures within Puntzi Ridge quartz monzonite. B) Quartz monzonite tuff interpreted as comagmatic with the Puntzi Ridge quartz monzonite.

stratigraphic levels higher than the dacite/latite tuff. Samples of the plutons were collected for isotopic age determination. The extensively altered 'Sweetwater Lake' pluton was sampled for U-Pb zircon/titanite determination(s), and one of the rare zones of fresh biotite and K-feldspar in the Puntzi pluton was sampled for $^{40}\text{Ar}/^{39}\text{Ar}$ age determination.

Chili Dacite

Porphyritic dacite crops out sporadically across an approximately 200 m by 1000 m area, about 3 km northwest of Puntzi Ridge. It is white to grey-weathering and medium-grained, composed of ~2% euhedral hornblende and ~15% biotite booklets, as well as equant white feldspar, possibly sanidine. In one of the highest exposures, an ~100 m long zone contains quartz-lined mirolitic cavities up to 2 cm across, knots of coarse biotite and abundant xenoliths (probably autoliths).

The Chili dacite is lithologically similar to dikes and ash-flow tuff units within the Ootsa Lake Group, and is therefore considered as a potential subvolcanic feeder. To test this correlation, a sample containing fresh biotite was collected for $^{40}\text{Ar}/^{39}\text{Ar}$ age determination.

STRUCTURE AND DEFORMATION

Evidence of deformation can be found in rocks of all ages within the Chezacut map area. Deformation is most intense in the oldest rocks — folded strata of presumed Mesozoic age. However, even rocks that may be as young as Quaternary display evidence of contractional deformation. Mesozoic rocks are dominated by massive volcanic strata that do not readily reveal deformational fabrics, but tight folds and overturned beds can be observed where these rocks are interbedded with sedimentary strata. In some areas, a spaced cleavage or weak phyllitic fabric is developed.

Deformation of strata of the Ootsa Lake Group is mainly displayed by variably dipping strata, locally vertical, which are interpreted to outline kilometre-scale folds. An open, north-plunging antiformal culmination is interpreted in the northeastern part of the Chezacut map area. It has a wavelength of at least 15 km and exposes Mesozoic strata in its core. Oppressed limbs have resulted in escape structures, such as sinistral shear zones on the eastern limb and thrust faulting within the fold core. Penetrative, closely spaced cleavage and weak phyllitic fabrics are best developed north of Meridional Hill (Fig 16A) and in the Cope-land Hills where they extend across 50 to 200 m.

Our interpretation of large-scale folds is a departure from the more classic view of widespread block-faulting and extension during Eocene magmatism. In fact, nowhere can we conclusively demonstrate a fold closure by walking volcanic stratigraphy through a fold hinge. The outcrop distribution of the Ootsa Lake Group is sufficiently sparse to easily accommodate a more classic interpretation. For example, Figure 2B presents one of many possible alternative interpretations of the Eocene geology, but it does not explain the spaced cleavage and weak phyllitic fabrics that are exposed in most areas with abundant outcrop.

Within the northwestern part of the map area, Neogene Anahim volcanic rocks display evidence of high-angle reverse faulting (Fig 16B). Inexplicably, the discrete fault

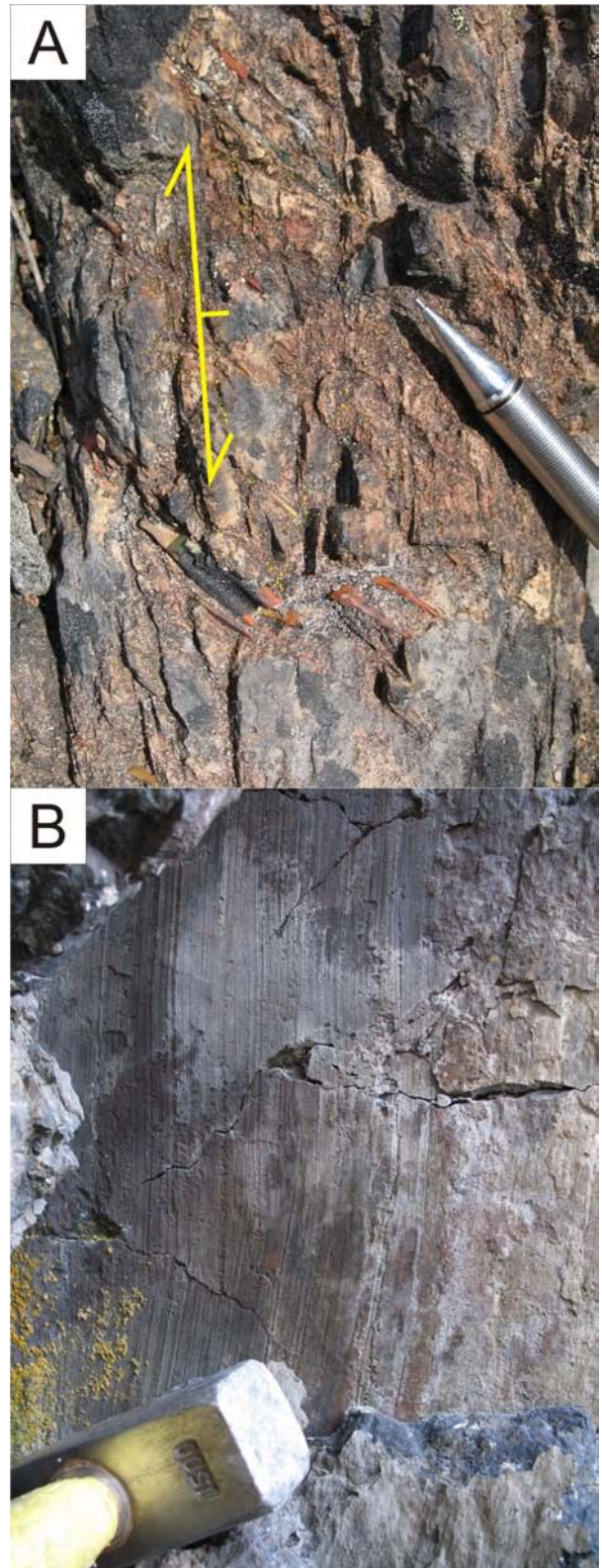


Figure 16. A) Spaced cleavage (oriented parallel to length of photo) pervasively overprints a basalt flow containing elongated amygdules (with pencil aligned). B) Steeply plunging striae on fault surfaces commonly occur within flow units of the Anahim volcanic belt at this locality. Possible causes of the faulting include loading by ice or volcanic deposits, or previously undocumented tectonism.

planes are focused in dense flows, not in the adjacent, less competent scoriaceous layers.

Because of the very low relief and extensive hummocky moraine within the southwestern part of the map area, contacts between the Mesozoic, Eocene and Neogene units are based largely on gravity and aeromagnetic lineaments.

Deformation Age and Significance

The age of pre-Miocene deformation cannot be well constrained within the map area. Possible correlations with deformational events defined outside of the map area are as follows:

- Paleocene–Middle Eocene: Kinematic linkage with 110 km of dextral offset on the crustal-scale Yalakom Fault system (Umhoefer and Schiarizza, 1996), and/or Eocene unroofing of the Tatla Lake metamorphic complex (Friedman and Armstrong, 1988; Friedman, 1992), located 30 km south of the Chezacut map area. Eocene extension is consistent with rapid Early Eocene cooling (55–50 Ma), as determined from apatite fission track studies in the region (Riddell et al., 2007).
- Middle Jurassic (Bajocian): Emplacement of the Cache Creek Terrane (Ricketts et al., 1992; Mihalynuk et al., 2004). Cache Creek rocks are juxtaposed with Mesozoic strata about 80 km to the east.

A sub-Eocene structural discontinuity is interpreted because the younger strata are not observed to be isoclinally folded (although flow fabrics displaying all manner of folding are common within Tertiary units of dacitic and rhyolitic composition, they are not tectonic in origin). In addition, a sandstone and conglomerate unit containing clasts of the Mesozoic unit is interpreted as a sub-Eocene basal conglomerate. It also contains vitreous, euhedral, biotite booklets and ‘dacitic’ clasts containing biotite, probably attributable to syndepositional volcanism. Samples of this biotite were collected for isotopic age determination. The occurrence of biotite may mark the onset of volcanism of the Ootsa Lake Group in this area, constraining the age of the angular unconformity to early Eocene.

MINERALIZATION

Prior to 2007, only a single MINFILE occurrence was reported for the Chezacut area. Identified as MINFILE 093C 011 (MINFILE, 2007), the Chili (formerly Punt) occurrence is a shear-related quartz stockwork with argentiferous and auriferous chalcopyrite (Nebocat, 1983; see also new analysis 1.5 ppm Au and 69 ppm Ag in Table 2b) within probable Mesozoic volcanic strata (Fig 2). The quartz stockwork cuts epidote-chlorite-altered feldspar-pyroxene porphyry and lapilli tuff. The quartz is greasy grey in places, probably related to its elevated Ag content.

During the course of our work, five new mineral occurrences were discovered. From north to south these are the Pyro, Orovain, Punky, Vampire and Gumbo showings. Coarse-grained pyrolusite-rich breccias dominate isolated outcrops at the Pyro showing. Both the Punky and Orovain occurrences are copper sulphide and native copper – bearing veins. Mineralization at the Vampire and Gumbo show-

ings is disseminated copper sulphides in altered igneous rocks.

Pyro Showing

The Pyro showing is located at the southwestern base of Arc Mountain (Fig 2). This area is part of a thermally metamorphosed zone characterized by silicification and secondary tourmaline in outcrops exposed for more than 350 m along a glacial outflow channel. Tourmaline grains provide a nucleation site for nonpleochroic hexagonal crystals that grow in optical continuity with the tourmaline and replace up to 50% of the rock matrix (Fig 17). Mineralization at the Pyro showing is not well exposed but, over a 10 m by 25 m area, it consists of sooty, rust-coloured, coarse-grained breccia with hematite-goethite-pyrolusite-rich cement (>1% Mn, the analytical upper concentration limit for determination of this element by the ICP-MS method; see Table 2a) and vein-like bodies up to 35 cm thick. A low-angle fault zone that cuts the mineralization is tentatively interpreted as a top-to-the-southeast thrust fault.

Analysis (Table 2a, b; results to two significant figures for INAA and ICP-MS values, respectively) of two samples of sooty mineralization, including a chip sample at 20 cm intervals across 4 m (sample MMI07-48-4B), reveal elevated values for Au (90, 160 ppb), As (530, 1200 ppm), Sb (34, 6 ppm) and Zn (840, 3000 ppm); and, for ICP-MS analyses only, 11 ppm Ag, 30 ppm Bi, 2.3 ppm Tl and 13 ppm Te. Most surprising is Te enrichment, which is more than 4000 times the average crustal abundance in analogous volcanic-arc rocks (Yi et al., 2000). Conclusive classification of this deposit is not possible given the cursory nature of our observations; however, in consideration of the tourmaline and silica alteration and induration, a skarn origin is possible. If so, the aplite body that forms much of the southwestern flanks of Arc Mountain is the likely cause of the thermal-metamorphism. Silver-zinc-lead skarns are commonly enriched in Mn and have elevated Bi and Au (Ray, 1995); however, the Te enrichment is unusual for a skarn. On the basis of elevated Au and Ag values alone, this occurrence warrants further investigation.

Punky and Orovain Showings

Both the Orovain and Punky showings are copper-bearing vein occurrences located near the peak and on the southwestern flank of Luck Mountain, respectively (Fig 2). Mineralization at the Orovain occurrence is within a set of 0.5 to 8 cm thick quartz-epidote-prehnite veins. Veins cut feldspar-phyric lapilli tuff and are generally subparallel and west trending, with a spacing of approximately 1 m, and exposed over a 50 by 75 m area. Mineralization occurs as disseminations of native copper mantled by chalcocite (Fig 18). Copper mineralization is most abundant within the vein material, but sporadically occurs within the alteration envelope adjacent to the vein. Alteration mineralogy of the envelopes is similar to that of the veins, and total envelope thickness is about equal to that of the veins. Analysis of the veins reveals between 1026 ppm and >1% Cu (Table 2a, samples MMI07-37-7, 8 and 9).

Veining at the Punky occurrence is more sporadic with a less well developed vein set than at the Orovain occurrence. Quartz-carbonate veins up to 12 cm thick are copper stained. Preliminary petrographic analysis of the veins reveals no primary copper mineralization; however, calcite-

TABLE 2. SELECTED ANALYTICAL RESULTS FROM MINERALIZED SAMPLES WITHIN THE CHEZACUT MAP AREA: A) SELECTED ICP-MS RESULTS, B) SELECTED INAA RESULTS. A DIGITAL REPORT AND DATABASE OF ALL SAMPLES ANALYZED AS PART OF THE CHEZACUT MAPPING PROJECT ARE AVAILABLE IN PEAT ET AL. (2008).

(a)	Sample number	Sample type	Latitude	Longitude	Cu (ppm)	Pb (ppm)	Zn (ppm)	Ag (ppb)	Fe (%)	As (ppm)	Au (ppb)	Sb (ppm)	Bi (ppm)	Tl (ppm)	Hg (ppb)	Te (ppm)	Mn (ppm)
	KTE07-13-12 Punky	Hand - assay	52.3697	-124.3204	1925	2.82	23.5	222	1.80	4.8	0.2	0.08	<0.02	<0.02	21	0.04	535
	KTE07-13-8 Punky	Hand - assay	52.3678	-124.3224	1100	13.36	9.7	401	0.79	3.7	0.2	0.07	<0.02	<0.02	<5	0.04	393
	MMI07-1-4	Hand - assay	53.4212	-125.7519	98	37.93	83.5	448	14.39	6.8	23.9	2.15	3.78	0.08	13	0.06	1653
	MMI07-17-11B Vampire	Hand - assay	52.4403	-124.1284	2839	2.22	55.5	556	2.01	6.4	0.5	0.66	0.04	<0.02	<5	0.07	660
	MMI07-17-7 Vampire East	Hand - assay	52.4402	-124.1287	95	1.55	48.4	685	2.88	95.3	8	0.63	0.16	<0.02	6	1.11	514
	MMI07-17-8 Vampire	Hand - assay	52.4402	-124.1294	1188	1.41	44.9	266	2.16	39.7	9	0.29	0.02	<0.02	<5	0.63	838
	MMI07-17-9 Vampire	1.1 m chip sample	52.4400	-124.1301	2145	1.07	95.9	232	2.63	7.4	1.5	0.19	<0.02	<0.02	<5	0.10	798
	MMI07-17-9rep Vampire	1.1 m chip sample	52.4400	-124.1301	2347	1.44	95.4	270	2.62	7.9	0.9	0.23	<0.02	0.02	<5	0.11	811
	MMI07-18-6 Chilcotin cutbank	Hand - assay	52.4350	-124.1036	224	504.18	408.0	395	1.29	2.3	44.6	0.10	0.19	<0.02	697	0.04	719
	MMI07-37-7	Hand - assay	52.3945	-124.3197	2613	7.84	7.3	296	1.48	9.2	0.4	0.05	<0.02	<0.02	20	0.05	384
	MMI07-37-8	Hand - assay	52.3945	-124.3200	>10000	6.10	17.0	3182	1.90	26.7	1.1	0.09	<0.02	<0.02	184	0.03	405
	MMI07-37-9	Hand - assay	52.3940	-124.3199	1026	4.15	6.8	58	1.46	2.0	0.5	<0.02	<0.02	<0.02	5	<0.02	194
	MMI07-38-7	Hand - assay	52.3824	-124.3140	1928	6.27	42.0	284	3.53	6.7	2.4	0.03	0.04	<0.02	15	0.03	544
	MMI07-44-1	Hand - assay	52.2527	-124.0568	196	0.61	32.2	77	2.81	<0.1	1.1	0.02	0.04	0.04	<5	<0.02	356
	MMI07-48-4 Pyro	Hand - assay	52.4555	-124.3672	44	475.30	2984.0	11276	7.39	1227.0	163.5	6.46	29.78	0.45	670	12.59	>10000
	MMI07-48-4B Pyro	Hand - assay	52.4555	-124.3672	9	30.45	569.0	800	11.21	547.2	9.7	2.36	1.53	2.27	308	0.53	>10000
			<i>Detection limit:</i>		0.01	0.01	0.1	2	0.01	0.1	1	0.02	0.02	0.02	5	0.02	1

(b)	Sample number	Sample type	Latitude	Longitude	Au (ppb)	Ag (ppm)	As (ppm)	Ni (ppm)	Zn (ppm)	Sb (ppm)
	KTE07-6-6 Chili occurrence	Hand - assay	52.3069	-124.0269	1530	69	15.2	20	470	3.5
	MMI07-18-6 Chilcotin cutbank	Hand - assay	52.4350	-124.1036	50	< 5	9.1	<20	480	6.6
	MMI07-44-1	Hand - assay	52.2527	-124.0568	<2	< 6	<0.5	150	180	<0.1
	MMI07-48-4 Pyro	Hand - assay	52.4555	-124.3672	90	< 7	526.0	130	840	33.8
	MMI07-48-4B Pyro	4 m chip sample	52.4555	-124.3672	<2	< 8	249.0	<20	200	10.5
			<i>Detection limit:</i>		2	5	0.5	20	50	0.1

Notes: A full list of samples and elements analyzed can be obtained for both INAA and ICP-MS suites from http://www.em.gov.bc.ca/Mining/Geosurv/Publications/catalog/cat_geof.htm

epidote alteration patches within the tuffaceous host rocks do contain native copper mantled by chalcocite and hematite. These observations suggest that sampling that was bi-

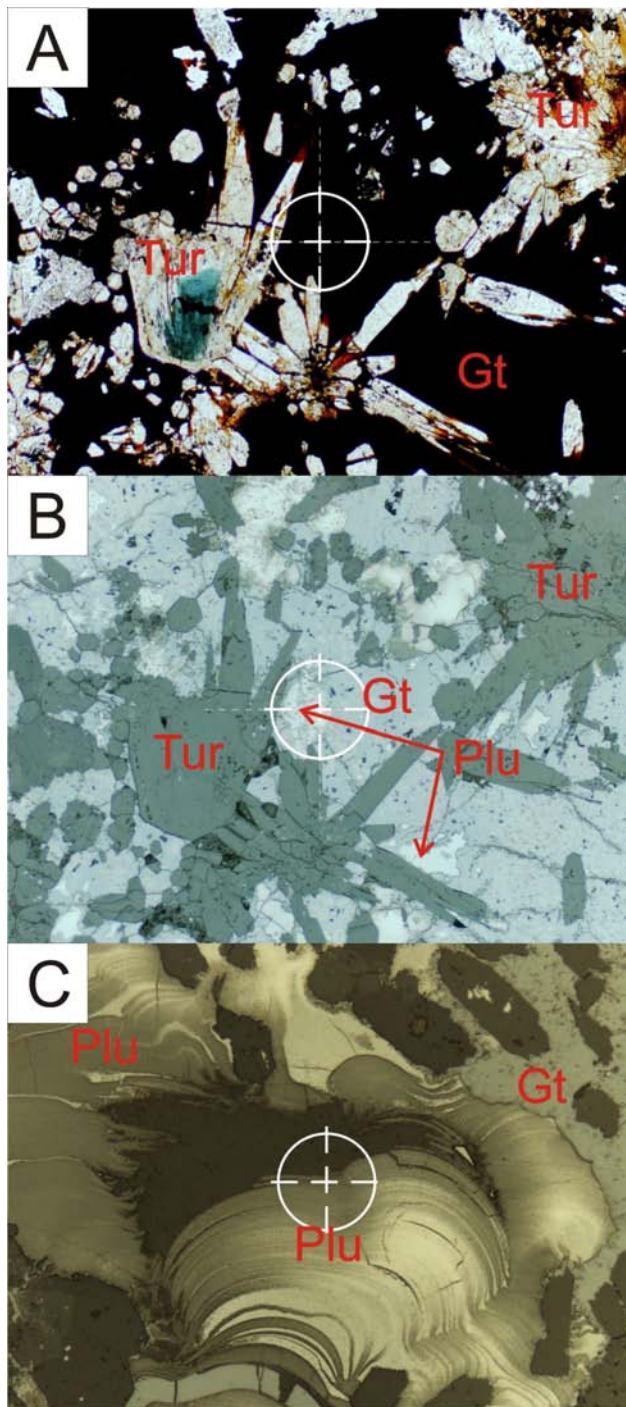


Figure 17. Photomicrographs of mineralization at the Pyro occurrence: A) plane-polarized light shows nucleus of olive-blue pleochroic tourmaline (Tur) overgrown by radiating mat of nonpleochroic tourmaline; B) and C) opaque and semi-opaque minerals are tentatively identified in reflected light (B) as goethite (Gt, red internal reflections), hematite and pyrolusite (Pru) and/or other Fe-Mn oxides that, in partly uncrossed polarized light (C), display botryoidal and/or geopetal textures. Circle at crosshairs in photomicrographs is 200 μ m in diameter.

ased towards copper-stained vein material may have underrepresented the copper content of the outcrop, and future investigators should look carefully at the tuffaceous host rocks for signs of mineralization. Analysis of the vein material yielded Cu values of between 1925 and 1100 ppm (Table 2a).

Gold and silver values at both occurrences are negligible.

Vampire Showing

Disseminated chalcopyrite occurs within a belt of outcrops of mainly intermediate volcanic breccia, located between the old homestead access road and the Chilcotin River, about 5 km above its confluence with the Clusko River (Fig 2). At this locality, epidote-quartz-chlorite-pyrite alteration (propylitization) is widespread in feldsparphyric volcanic breccia and sparse white, dacitic (?) tuff layers (Fig 19), producing green and rust outcrops that extend sporadically for approximately 110 m along the river valley. Analysis of samples with visible chalcopyrite returned values of between 0.12% and 0.28% Cu, including a 1.1 m chip sample across one well-mineralized outcrop that returned 0.21% Cu. No significant Au or Ag enrichment

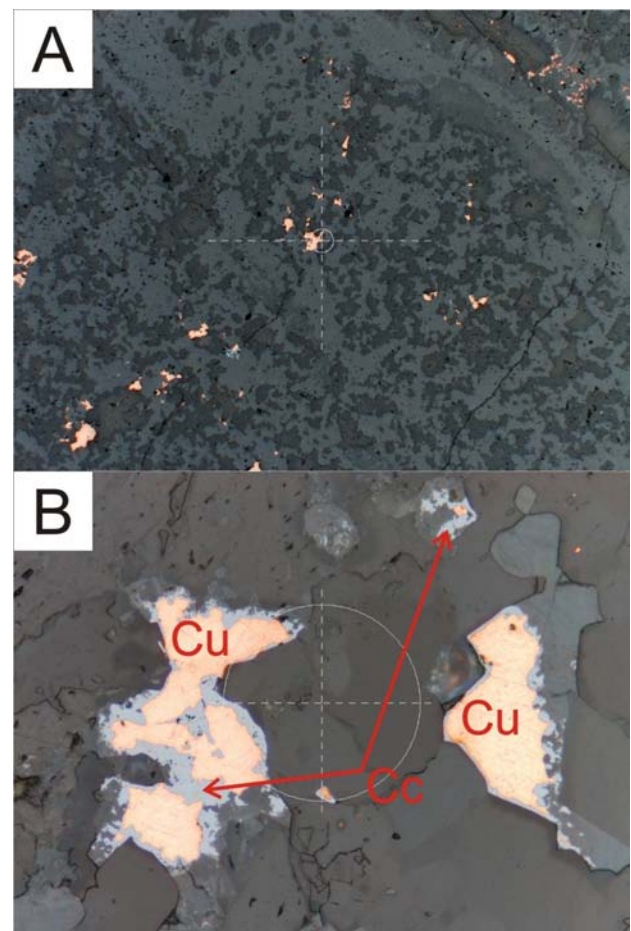


Figure 18. Reflected light photomicrographs of samples of mineralization at the Orovain occurrence showing: A) disseminated native copper within a well-mineralized vein, and B) close-up of a typical native copper (Cu) grain showing a mantle of chalcocite (Cc). Circle at crosshairs in photomicrographs is 200 μ m in diameter.

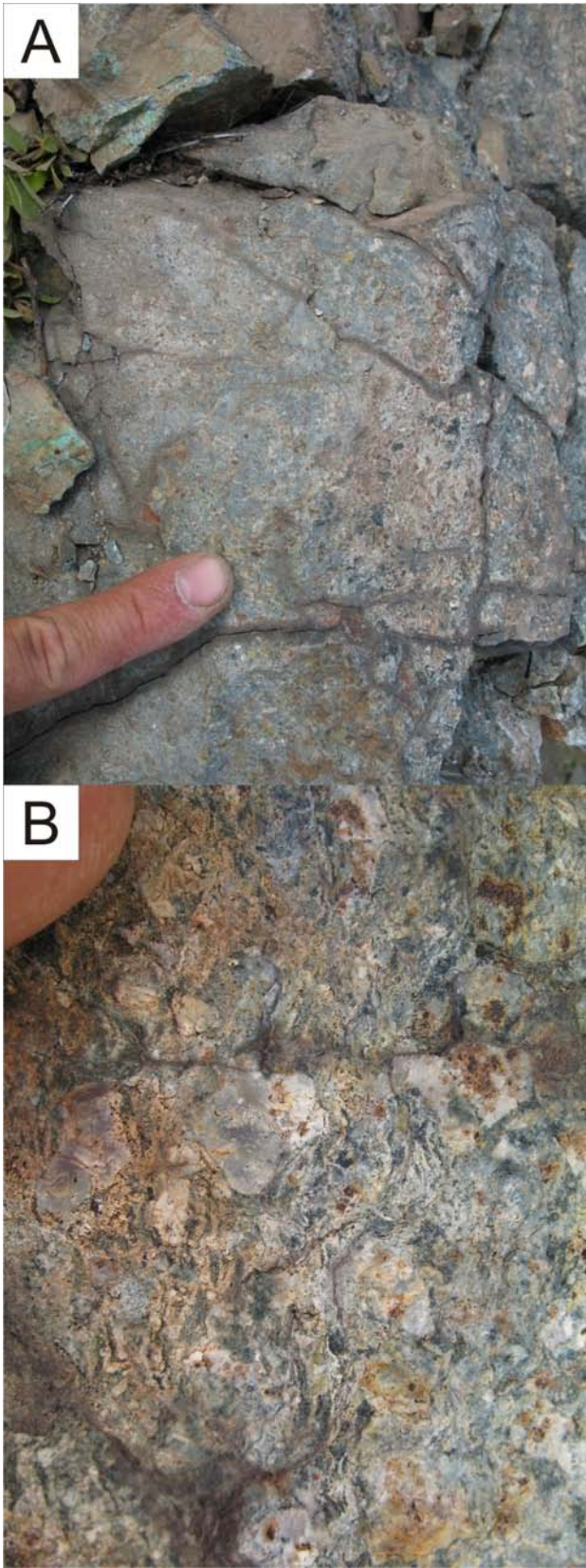


Figure 19. Photographs of the Vampire occurrence, showing: A) an outcrop of intermediate tuff mineralized with chalcopyrite (recessive rusty) and sparsely copper-stained, fresh fracture surfaces; and (B) a thin interbed of felsic tuff.

was detected. Of the chalcopyrite-bearing samples analyzed, the highest Au value returned is 9 ppb and the highest Ag value is 0.5 ppm (Table 2a).

Gumbo Showing

Mineralization at the Gumbo showing occurs as local accumulations of disseminated chalcopyrite and pyrrhotite (Fig 20A) in an altered, porphyritic, mafic igneous unit (Fig 20B). Relict phenocrysts are probably plagioclase and pyroxene. Sporadic low outcrops of this unit are dark green-grey with rust patches (oxidized pyrrhotite), and well indurated with angular, blocky jointing. Samples from the showing returned elevated levels of Cr (518 ppm, possible contamination from mill), Ni (150 ppm) and Zn (180 ppm) relative to other samples analyzed.

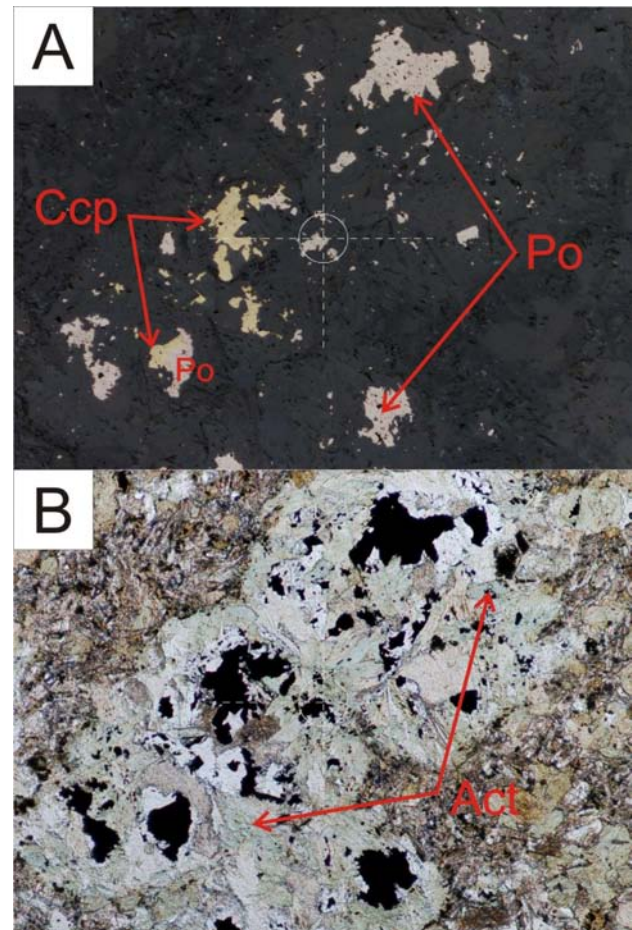


Figure 20. Photomicrographs of altered pyroxene-phyric volcanic or intrusive rock at the Gumbo occurrence, showing A) pinkish pyrrhotite (Po) and yellow chalcopyrite (Cpy) as irregular clots (in places intergrown) and as dustings in the rock matrix (reflected light); and; B) sulphides replacing the cores of altered phenocrysts, possibly pyroxene (plane-polarized transmitted light); pale green actinolite (Act), and chlorite also replace pyroxene (?). Circle at crosshairs in photomicrographs is 200 µm in diameter. Remainder of the rock is hornblende diorite.

SUMMARY

Geological field investigations within the Chezacut map area demonstrated the following:

- Rumours of a relatively unbroken blanket of glacial cover are ill-founded. Bedrock exposure is more extensive than is generally perceived.
- With the aid of detailed digital orthophotos and multispectral imagery, strategies were successfully devised to maximize the chances of encountering outcrops.
- The extent of the Chilcotin Group is much less than anticipated: a 96% decrease in the area originally included in Massey et al. (2005). If the Anahim volcanic belt is included with the Chilcotin Group, there is still a 62% decrease in young volcanic cover.
- Mesozoic strata are more abundant and more extensively intruded than previously thought. If our interpretation is correct, Mesozoic units now account for nearly 240% of the distribution shown in Massey et al. (2005).
- Eocene strata are probably deformed by broad folding, not solely by block faulting. If this interpretation is correct, it appears that Mesozoic strata are exposed in the core of a broad anticline.
- Neogene volcanic rocks are commonly highly vesicular (25%), resulting in lower than expected density (possible gravity lows, not the highs normally anticipated from basalt).
- Significant new mineral occurrences can still be discovered at surface within the Chezacut map area (in our case, within 1.5 weeks of commencing the mapping project).
- Discovery of four new mineral occurrences during the course of the Chezacut regional mapping project is a demonstration of the underexplored status of this area. The region clearly deserves much more exploration attention than it has received in the past.

ACKNOWLEDGMENTS

Larry Diakow helped with geological reconnaissance and introduced our field crew to the nebulous geology of the Nechako Plateau. He also kindly reviewed and improved an earlier draft of this manuscript. Travis Ferbey taught us why, where and how to dig till and mix daiquiris. Our crew was joined near season's end by the highly energetic and helpful Margot McKeown. The parched plateau was made more pleasurable through the kindness of Kevin Newberry of Chezacut Ranch Ltd. We offer our apologies to George Maybee, whose freshly graded dirt road turned to mud and then ruts with the barely controlled passage of our truck.

REFERENCES

- Anderson, R.G., Resnick, J., Russell, J.K., Woodsworth, G.J., Villeneuve, M.E. and Grainger, N.C. (2001): The Cheslatta Lake suite: Miocene mafic, alkaline magmatism in central British Columbia; *Canadian Journal of Earth Sciences*, Volume 38, pages 697–717.
- Andrews, G.D.M. and Russell, J.K. (2007): Mineral exploration potential beneath the Chilcotin Group (NTS 092O, P; 093A, B, C, F, G, I, J, K), south-central British Columbia: preliminary insights from volcanic facies analysis; in *Geological Fieldwork 2006, BC Ministry of Energy, Mines and Petroleum Resources*, Paper 2007-1, and *Geoscience BC*, Report 2007-1, pages 229–238.
- BC Ministry of Forests and Range (2005a): The state of British Columbia's forests 2004; *BC Ministry of Forests and Range*, URL <<http://www.for.gov.bc.ca/hfp/sof/2004/>> [November 2007].
- BC Ministry of Forests and Range (2005b): British Columbia's Mountain Pine Beetle Action Plan 2005–2010; Government of British Columbia, 20 pages, <www.for.gov.bc.ca/hfp/mountain_pine_beetle/actionplan/2005/actionplan.pdf> [October 2, 2006].
- Bevier, M.L., Armstrong, R.L. and Souther, J.G. (1979): Miocene peralkaline volcanism in west-central British Columbia — its temporal and plate-tectonic setting; *Geology*, Volume 7, Number 8, pages 389–392.
- Bevier, M.L. (1983a): Implications of chemical and isotopic composition for petrogenesis of Chilcotin Group basalts, British Columbia; *Journal of Petrology*, Volume 24, pages 207–226.
- Bevier, M.L. (1983b): Regional stratigraphy and age of Chilcotin Group basalts, south-central British Columbia; *Canadian Journal of Earth Sciences*, Volume 20, pages 515–524.
- Bevier, M.L. (1989): A lead and strontium isotopic study of the Anahim volcanic belt, British Columbia: additional evidence for widespread suboceanic mantle beneath western North America; *Geological Society of America Bulletin*, Volume 101, pages 973–981.
- Charland, A., Francis, D. and Ludden, J. (1995): The relationship between the hawaiites and basalts of the Itcha Volcanic Complex, central British Columbia; *Contributions to Mineralogy and Petrology*, Volume 121, pages 289–302.
- Duffell, S. (1959): Whitesail Lake map area, British Columbia; *Geological Survey of Canada*, Memoir 299, 119 pages.
- Friedman, R.M. and Armstrong, R.L. (1988): Tatla Lake metamorphic complex: an Eocene metamorphic core complex on the southwestern edge of the Intermontane Belt of British Columbia; *Tectonics*, Volume 7, pages 1141–1166.
- Friedman, R.M. (1992): P-T-t path for the lower plate of the Eocene Tatla Lake metamorphic core complex, southwestern Intermontane Belt, British Columbia; *Canadian Journal of Earth Sciences*, Volume 29, pages 972–983.
- Geological Survey of Canada (1994): Magnetic residual total field, Interior Plateau of British Columbia; *Geological Survey of Canada*, Open File 2785, 19 Maps, 1:100 000 and 1:250 000 scale.
- Gordee, S., Andrews, G.D.M., Simpson, K.A. and Russell, J.K. (2007): Subaqueous channel-confined volcanism within the Chilcotin Group, Bull Canyon Provincial Park (NTS 093B/03), south-central British Columbia; in *Geological Fieldwork 2006, BC Ministry of Energy, Mines and Petroleum Resources*, Paper 2007-1 and *Geoscience BC*, Report 2007-1, pages 285–290.
- Kerr, D.E. and Giles, T.R. (1993): Surficial geology of the Chezacut map area (NTS 93C/8); *BC Ministry of Energy, Mines and Petroleum Resources*, Open File 1993-17, 1:50 000 scale.
- Levson, V.M. and Giles, T.R. (1997): Quaternary geology and till geochemistry studies in the Nechako and Fraser plateaus, central British Columbia (NTS 93C/1, 8, 9, 10; F/2, 3, 7; 93L/16; 93M/1); in *Interior Plateau Geoscience Project: Summary of Geological, Geochemical and Geophysical Studies*, Diakow, L.J., Metcalfe, P. and Newell, J., Editors, *BC Ministry of Energy, Mines and Petroleum Resources*, Paper 1997-2, pages 121–145.
- Massey, N.W.D., MacIntyre, D.G., Desjardins, P.J. and Cooney, R.T. (2005): Digital geology map of British Columbia:

- whole province; *BC Ministry of Energy and Mines*, GeoFile 2005-1, 1:250 000 scale, URL <<http://www.em.gov.bc.ca/Mining/Geolsurv/Publications/GeoFiles/Gf2005-1/toc.htm>>.
- Mathews, W.H. (1989): Neogene Chilcotin basalts in south-central British Columbia: geology, ages, and geomorphic history; *Canadian Journal of Earth Sciences*, Volume 26, pages 969–982.
- Metcalfe, P., Richards, T.A., Villeneuve, M.E., White, J.M. and Hickson, C.J. (1997): Physical and chemical volcanology of the Eocene Mount Clisbako volcano, central British Columbia (93B/12, 13; 93C/9, 16); in Interior Plateau Geoscience Project: Summary of Geological, Geochemical and Geophysical Studies, Diakow, L.J., Metcalfe, P. and Newell, J., Editors, *BC Ministry of Energy, Mines and Petroleum Resources*, Paper 1997-2, pages 31–61.
- Mihalynuk, M.G., Erdmer, P., Ghent, E.D., Cordey, F., Archibald, D.A., Friedman, R.M. and Johannson, G.G. (2004): Coherent French Range blueschist: subduction to exhumation in <2.5 m.y.?; *Geological Society of America*, Bulletin, Volume 116, pages 910–922.
- Mihalynuk, M.G., Peat, C.R., Orovan, E.A., Terhune, K., Ferby, T. and McKeown, M.A. (2008): Chezacut area geology (NTS 93C/8); *BC Ministry of Energy, Mines and Petroleum Resources*, Open File 2008-2, 1:50 000 scale.
- MINFILE (2007): MINFILE BC mineral deposits database; *BC Ministry of Energy, Mines and Petroleum Resources*, URL <<http://www.em.gov.bc.ca/Mining/Geolsurv/Minfile/>> [November 2007].
- Nebocat, J. (1983): Geological and geochemical report on the Chili claim; *BC Ministry of Energy, Mines and Petroleum Resources*, Assessment Report 11 685, 48 pages.
- Parrish, R.R. (1983): Cenozoic thermal evolution and tectonics of the Coast Mountains of British Columbia: 1, Fission track dating, apparent uplift rates, and patterns of uplift; *Tectonics*, Volume 2, pages 601–631.
- Peat, C., Mihalynuk, M.G., Ferby, T. and Diakow, L.J. (2008): Analytical results from investigations in the Chezacut map area (NTS 93C/08) and other select areas within the Beetle Infested Zone 2007; *BC Ministry of Energy, Mines and Petroleum Resources*, GeoFile 2008-2.
- Pynn, L. (2007): Quakes near Quesnel may signal lava flow; *The Vancouver Sun*, October 16, 2007.
- Ray, G.E. (1995): Pb-Zn Skarns; in Selected British Columbia Mineral Deposit Profiles, Volume 1 — Metallics and Coal, Lefebvre, D.V. and Ray, G.E., Editors, *BC Ministry of Energy of Employment and Investment*, Open File 1995-20, pages 61–62.
- Ricketts, B.D., Evenchick, C.A., Anderson, R.G. and Murphy, D.C. (1992): Bowser Basin, northern British Columbia; constraints on the timing of initial subsidence and Stikinia – North America terrane interactions; *Geological Society of America*, Geology, Volume 20, pages 1119–1122.
- Riddell, J.M. (2006): Geology of the southern Nechako Basin (NTS 92N, 92O, 93C, 93F, 93G), sheet 3 of 3 — geology with contoured gravity underlay; *BC Ministry of Energy, Mines and Petroleum Resources*, Petroleum Geology Map 2006-1, 1:400 000 scale.
- Riddell, J.M., Ferri, F., Sweet, A.R. and O’Sullivan, P.B. (2007): New geoscience data from the Nechako Basin project; in The Nechako Initiative — Geoscience Update 2007, *BC Ministry of Energy, Mines and Petroleum Resources*, Petroleum Geology Open File 2007-1, pages 59–98.
- Souther, J.G. and Souther, M.E.K. (1994): Geology, Ilgachuz Range and adjacent parts of the Interior Plateau, British Columbia; *Geological Survey of Canada*, Map 1845A, 1:50 000 scale.
- Stout, M.Z. and Nicholls, J. (1983): Origin of the hawaiites from the Itcha Mountain Range, British Columbia; *Canadian Mineralogist*, Volume 21, pages 575–581.
- Tipper, H.W. (1959): Geology, Quesnel; *Geological Survey of Canada*, Map 12-1959, 1:253 440 scale.
- Tipper, H.W. (1969): Geology, Anahim Lake; *Geological Survey of Canada*, Map 1202A, 1:253 440 scale.
- Tipper, H.W. (1971): Surficial geology, Anahim Lake; *Geological Survey of Canada*, Map 1289A, 1:250 000 scale.
- Umhoefer, P.J. and Schiarizza, P. (1996): Latest Cretaceous to early Tertiary dextral strike-slip faulting on the southeastern Yalakom fault system, southeastern Coast Belt, British Columbia; *Geological Society of America Bulletin*, Volume 108, pages 768–785.
- Yi, W., Halliday, A.N., Alt, J.C., Lee, D.-C., Rehkämper, M., Garcia, M.O. and Su, Y. (2000): Cadmium, indium, tin, tellurium and sulfur in oceanic basalts: implications for chalcophile element fractionation in the Earth; *Journal of Geophysical Research – Solid Earth*, Volume 105, pages 18 927–18 948.

Geochronological Results from Reconnaissance Investigations in the Beetle Infested Zone, South-Central British Columbia

by M.G. Mihalynuk, R.M. Friedman¹ and T.D. Ullrich¹

KEYWORDS: geochronology, isotopic age, uranium-lead zircon, $^{40}\text{Ar}/^{39}\text{Ar}$, mineral potential, mountain pine beetle, economic diversification, Stikine Terrane, Cache Creek Terrane

INTRODUCTION

Forestry is the principal economic engine for many communities within the interior of British Columbia. Infestations of mountain pine beetle have affected most forests in this part of the province (Fig 1) and, as a result of widespread pine tree mortality, a downturn within the forestry sector is anticipated. The BC government is working to stimulate economic diversification within the Beetle Infested Zone (BIZ) to soften these negative economic impacts.

Mineral exploration and mineral resource development within the BIZ have lagged behind other prospective parts of the province (Mihalynuk, 2007a). Low levels of historical exploration mean more opportunity for future mineral discoveries and, as such, these industries could bring economic diversification to the BIZ. To help the mineral exploration industry justify investments in the BIZ, the BC Geological Survey has refocused most of its field programs into the area (see 'Foreword', page iii). We report here on geochronological data arising from a 2006 reconnaissance field program that investigated methods to enhance the efficacy of geological fieldwork within the BIZ (e.g., Mihalynuk, 2007b; Mihalynuk et al., 2008).

LOCATION

Data reported here are from samples collected in three widespread areas within the BIZ — east of southern Babine Lake, near Riske Creek and west of the Iron Mask batholith (Fig 1).

Samples were collected from three sites east of southern Babine Lake — two sites are along the main logging haul road (named 'Phantom Road') between 4 and 6 km northwest of Boling Point on Babine Lake (samples MMI06-7-12 and MMI06-24-4, Table 1), and the third site is a recently active borrow pit approximately 1 km southwest of Cunningham Lake (sample MMI06-5-1, Table 1).

All three sites are within an area most recently mapped at 1:100 000 scale by MacIntyre and Schiarizza (1999).

Samples from the Riske Creek area were collected from a site 27 km southwest of Williams Lake, located between Cotton Road and the village of Toosey (sample MMI06-34-8, Table 1). This area has been most recently mapped at 1:50 000 scale by Mihalynuk and Harker (2007; see also Mihalynuk et al., 2007), who included the sample location and age (without data) on their map.

Sample collection in the Iron Mask batholith area was from west of the batholith, approximately 2 km south of Jacko Lake and 15 km southwest of Kamloops (sample MMI04-11-7b, Table 1). A recent regional mapping and data compilation that covered this area (Logan and Mihalynuk, 2006) included the sample site within the 'Cherry Creek tectonic zone'.

METHODS

All sample preparation and analytical work for the U-Pb and $^{40}\text{Ar}/^{39}\text{Ar}$ isotopic ages presented here was conducted at the Pacific Centre for Isotopic and Geochemical Research (PCIGR) at the Department of Earth and Ocean Sciences, The University of British Columbia.

The U-Pb isotopic age determinations reported here were by Thermal Ionization Mass Spectroscopy (U-Pb TIMS). The $^{40}\text{Ar}/^{39}\text{Ar}$ isotopic age determinations were by the laser-induced step-heating technique. Details of the both analytical techniques are presented in Logan et al. (2007).

ISOTOPIC AGE DETERMINATIONS

A synoptic description of the sample set and geochronological results are presented in Table 1. Results of U-Pb isotopic analyses are reported in Table 2, and summary data for $^{40}\text{Ar}/^{39}\text{Ar}$ plots are reported in Table 3. Complete digital data sets are available in Ullrich et al. (2008).

Uranium-lead analyses were performed on zircons recovered from samples MMI06-5-1 and MMI06-24-11. Zircons from the populations analyzed are pictured in Figure 2, both before and after air abrasion treatment. Four single zircon grains analyzed from sample MMI06-5-1 produced good quality data with four concordant and overlapping 2σ error ellipses contributing to a best estimate concordia age of 171.44 ± 0.39 Ma (Fig 3A) at 95% confidence (2σ decay constant errors included). The mean square of weighted deviates (MSWD) of concordance is 1.3 and the probability of concordance is 0.25.

Three single zircon grains analyzed from sample MMI06-24-11 also produced good-quality data with con-

¹ Pacific Centre for Isotopic and Geochemical Research, The University of British Columbia, Vancouver, BC

This publication is also available, free of charge, as colour digital files in Adobe Acrobat® PDF format from the BC Ministry of Energy, Mines and Petroleum Resources website at http://www.em.gov.bc.ca/Mining/Geosurv/Publications/catalog/cat_fldwk.htm

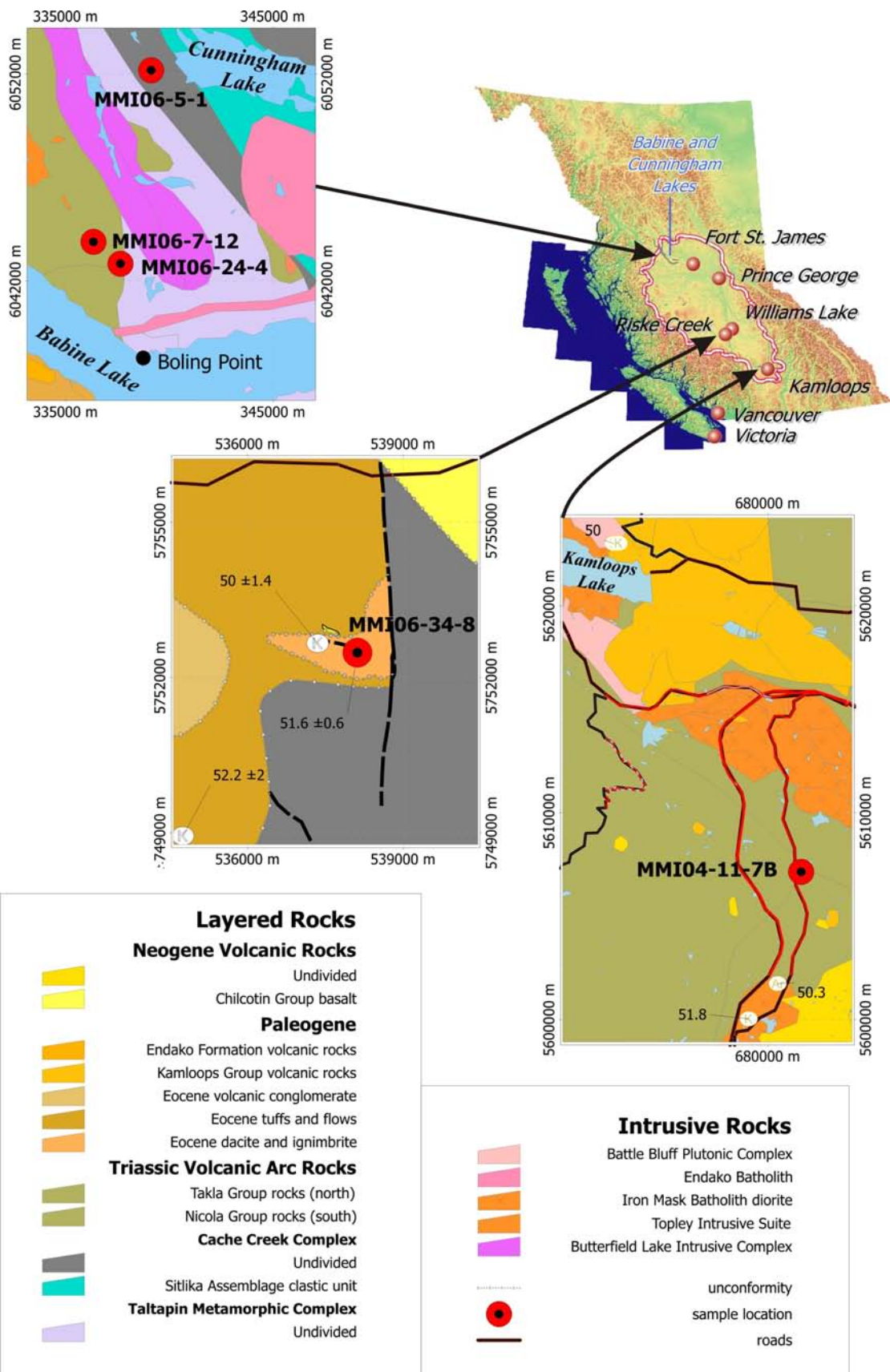


Figure 1. Location of the samples analyzed. Geological maps are modified after Massey et al. (2005) and Mihalyuk and Harker (2007).

TABLE 1. SUMMARY INFORMATION FOR GEOCHRONOLOGICAL SAMPLES.

Sample number	Method and interpreted best age ¹	Location (UTM zone 10)	Lithology sampled	Reason for geochronological age determination
MMI06-5-1	U-Pb zircon 171.4 ±0.4 Ma	339119E, 6052178N; Cunningham Lake	Foliated dacitic ignimbrite	To confirm affiliation of quartz-phyric volcanic unit with the Sitkika assemblage and Kutcho-type volcanogenic massive sulphide potential
MMI06-24-11	U-Pb zircon 218.7 ±0.4 Ma	335309E, 6045571N; Babine Lake	Quartz eye porphyry dike, synkinematic, variable ductile (quartz elongation) fabric	Fabric relationships show that this intrusion was emplaced during deformation; age determination will date the deformation, probably ca. 200 Ma
MMI04-11-7b	⁴⁰ Ar/ ³⁹ Ar muscovite/ whole rock 53.39 ±0.45 Ma	681606E, 5607143N; Iron Mask batholith	Fine-grained muscovite-quartz-carbonate schist	Sample is within the Cherry Creek tectonic zone; age determination will provide a minimum age for this deformation
MMI06-24-4	⁴⁰ Ar/ ³⁹ Ar biotite 134.65 ±0.74 Ma	337638E, 6042831N; Babine Lake	Sparse biotite booklets in porphyritic, intermediate to mafic volcanic breccia, deformed to chlorite-actinolite-epidote schist	Cooling age of metamorphism, which has not previously been dated
MMI06-34-8	⁴⁰ Ar/ ³⁹ Ar hornblende 51.65 ±0.58 Ma	538117E, 5752479N; Riske Creek	Ignimbritic lapilli tuff-breccia composed of acicular hornblende (10%), biotite (1%), quartz eyes (15%) and feldspar (40%, mainly K-feldspar) in a fine-grained, light grey matrix	Cooling age of eruptive unit; K-Ar whole rock age on same package of rocks was reported as 50 ±1.4 Ma (Hunt and Roddick, 1994; MacIntyre et al., 2001)

¹ Precision for all interpreted ages at 95% confidence limit, decay constant errors included.

cordant and overlapping 2σ error ellipses contributing to a best estimate concordia age of 218.74 ± 0.44 Ma (Fig 3B) at 95% confidence (2σ decay constant errors included). The MSWD of concordance is 2.0 and the probability of concordance is 0.19.

Argon-40/argon-39 analyses were performed on three samples: MMI04-11-7b (whole rock containing white mica), MMI06-24-4 (biotite) and MMI06-34-8 (hornblende).

Whole rock sample MMI04-11-7b produced a good 53.39 ± 0.45 Ma plateau age (2σ , including J-error of 0.5%) representing 82.7% of the ³⁹Ar gas released (Fig 4A). The MSWD of concordance is 0.76 and the probability of concordance is 0.55. The inverse isochron has an initial ⁴⁰Ar/³⁶Ar intercept of 311 ± 19 Ma, within error of the accepted atmospheric value, and yielded an age of 52.82 ± 0.83 Ma (MSWD = 0.115).

The biotite separate (sample MMI06-24-4) produced a convincing plateau for intermediate heating steps only (Fig 4B). Accounting for 51.7% of the ³⁹Ar gas released, the plateau age is 134.65 ± 0.74 Ma (2σ , including J-error of 0.5%). The MSWD of concordance is 1.00 and the probability of concordance is 0.41. The inverse isochron is poorly constrained due to radiogenic argon dominating the heating steps, yielding an initial ⁴⁰Ar/³⁹Ar intercept of 290 ± 98 Ma, an age of 134.9 ± 4.3 Ma, and a MSWD = 1.3, but nonetheless supports the plateau age.

The hornblende separate (sample MMI06-34-8) produced a 51.65 ± 0.58 Ma plateau age (2σ , including J-error of 0.5%) representing 90% of the ³⁹Ar gas released

(Fig 4C). The MSWD is 0.49 and the probability of concordance is 0.61. Again, the inverse isochron is dominated by radiogenic argon, yielding a poorly constrained but supportive initial ⁴⁰Ar/³⁶Ar intercept of 275 ± 64 Ma and age of 51.8 ± 2.1 Ma (MSWD = 0.71).

GEOLOGICAL IMPLICATIONS OF GEOCHRONOLOGICAL RESULTS

Babine Lake

Geological fieldwork was conducted in the southern Babine Lake area as a consequence of province-wide Regional Geochemical Stream sediment compilations that showed correlations between phosphorous and copper (Mihalynuk et al., 2007; cf., Lett et al., 2008). These elements show strong correlation in alkalic copper-gold porphyry camps such as the Iron Mask batholith and Mount Polley. Mineralization at most alkalic copper-gold porphyry deposits within the province is between 205 and 200 Ma (Logan et al., 2007). One objective of the work in the Babine Lake area was to determine if any intrusive rocks of this critical age are present.

BOLING POINT AREA: SYNKINEMATIC DIKE, SAMPLE MMI06-24-11

Between approximately 1 km and 7 km northwest of Boling Point on Babine Lake (Fig 1), exposures are dominated by foliated mafic volcanic rocks. These are mainly coarse-grained pyroxene-porphyritic breccias in which

TABLE 2. U-PB TIMS ANALYTICAL DATA FOR ZIRCON.

Fraction ¹	Weight (µg)	U ² (ppm)	Pb ³ (ppm)	²⁰⁶ Pb/ ²⁰⁴ Pb ⁴	Pb ⁵ (pg)	Th/U ⁶	Isotopic ratios ±1σ(%) ⁷			ρ ⁸	% ⁹ discordant	Apparent ages ±2σ (Ma) ⁷		
							²⁰⁶ Pb/ ²³⁸ U	²⁰⁷ Pb/ ²³⁵ U	²⁰⁶ Pb/ ²⁰⁶ Pb			²⁰⁶ Pb/ ²³⁸ U	²⁰⁷ Pb/ ²³⁵ U	²⁰⁶ Pb/ ²⁰⁶ Pb
Sample MMI06-5-1														
A	10	294.65	8.20	2639	1.9	0.468	0.02698 ±0.10	0.1843 ±0.25	0.04955 ±0.22	0.47733	1.5	171.6 ±0.4	171.8 ±0.8	174.1 ±10.4/10.4
B	7	293.07	8.10	1604	2.2	0.426	0.02699 ±0.11	0.1840 ±0.36	0.04945 ±0.33	0.39715	-1.5	171.7 ±0.4	171.5 ±1.1	169.1 ±15.2/15.4
C	11	237.42	6.70	2712	1.6	0.547	0.02692 ±0.08	0.1854 ±0.45	0.04995 ±0.42	0.47712	11.3	171.3 ±0.3	172.7 ±1.4	192.8 ±19.5/19.7
D	10	199.10	5.70	1454	2.3	0.566	0.02697 ±0.33	0.1844 ±0.47	0.04959 ±0.49	0.30548	2.5	171.5 ±1.1	171.8 ±1.5	175.9 ±22.5/22.8
Sample MMI06-24-11														
C	11	184.71	6.20	218.2	21.6	0.275	0.03443 ±0.27	0.23994 ±1.17	0.05054 ±1.02	0.637034	0.8	218.2 ±1.2	218.4 ±4.6	220.0 ±46.4/47.7
D	13	174.11	6.00	1216	4.0	0.317	0.03453 ±0.10	0.23949 ±0.27	0.05031 ±0.23	0.515749	-4.6	218.8 ±0.4	218.0 ±1.0	209.3 ±10.6/10.7
E	8	153.68	5.30	1282	2.1	0.319	0.03456 ±0.23	0.24065 ±0.61	0.05050 ±0.55	0.457242	-0.4	219.0 ±1.0	219.0 ±2.4	218.2 ±25.1/25.5

¹ All grains air abraded; all single grains processed and analyzed, except where noted by number of grains after fraction ID.

² U blank correction of 0.2pg ± 20%; U fractionation corrections were measured for each run with a double ²³³⁻²³⁵U spike.

³ Radiogenic Pb: all raw Pb data corrected for fractionation of 0.23%/amu ± 20% determined by repeat analysis of NBS-982 reference material.

⁴ Measured ratio corrected for spike and Pb fractionation.

⁵ Total common Pb in analysis based on blank isotopic composition: ²⁰⁶Pb/²⁰⁴Pb = 18.5 ± 3%, ²⁰⁷Pb/²⁰⁴Pb = 15.5 ± 3%, ²⁰⁸Pb/²⁰⁴Pb = 36.4 ± 0.5%.

⁶ Model Th/U derived from radiogenic ²⁰⁸Pb and the ²⁰⁷Pb/²⁰⁶Pb age of fraction.

⁷ Fractionation, blank and common Pb corrected: Pb procedural blanks were ~2.0 pg and U <0.2 pg. Common Pb compositions are based on Stacey-Kramers (Stacey and Kramers, 1975) model Pb at the interpreted age of the rock — 219 Ma for sample MMI06-24-11 and 172 Ma for sample MMI06-5-1.

⁸ Correlation coefficient.

⁹ Discordance in % to origin.

TABLE 3. $^{40}\text{Ar}/^{39}\text{Ar}$ AR STEP HEATING GAS RELEASE DATA.

Laser power (%)	$^{40}\text{Ar}/^{39}\text{Ar}$	$^{38}\text{Ar}/^{39}\text{Ar}$	$^{37}\text{Ar}/^{39}\text{Ar}$	$^{36}\text{Ar}/^{39}\text{Ar}$	Ca/K	Cl/K	% ^{40}Ar atm	f ^{39}Ar	$^{40}\text{Ar}/^{39}\text{ArK}$	Age
Sample MMI04-11-7b: whole rock white mica, J = 0.010308±0.000012, integrated age = 53.26±0.43 Ma (2σ)										
2	16.155 ±0.012	0.064 ±0.083	0.097 ±0.057	0.049 ±0.037	1.75	0.008	85.21	1.18	2.270 ±0.545	41.74 ±9.91
2.3	4.884 ±0.026	0.027 ±0.045	0.435 ±0.027	0.010 ±0.058	9.218	0.002	46.86	4.94	2.470 ±0.187	45.36 ±3.38
2.4	3.767 ±0.014	0.018 ±0.054	0.627 ±0.019	0.005 ±0.073	13.35	0	19.99	8.37	2.903 ±0.121	53.19 ±2.18
2.7	3.115 ±0.007	0.014 ±0.029	0.099 ±0.020	0.001 ±0.095	2.089	0	4.71	21.18	2.892 ±0.036	53.00 ±0.65
3	3.880 ±0.004	0.013 ±0.039	0.007 ±0.033	0.003 ±0.029	0.126	0	22.92	29.73	2.931 ±0.031	53.70 ±0.56
3.2	3.672 ±0.004	0.014 ±0.029	0.008 ±0.057	0.003 ±0.050	0.139	0	18.45	15.22	2.909 ±0.041	53.30 ±0.75
3.4	3.856 ±0.005	0.014 ±0.056	0.010 ±0.057	0.003 ±0.104	0.165	0	20.46	8.19	2.940 ±0.102	53.87 ±1.84
3.7	3.860 ±0.005	0.015 ±0.044	0.013 ±0.039	0.003 ±0.100	0.236	0	17.17	7.86	3.062 ±0.087	56.06 ±1.56
4	4.729 ±0.006	0.014 ±0.076	0.030 ±0.058	0.006 ±0.075	0.518	-0.001	27.3	3.33	3.199 ±0.131	58.54 ±2.36
Total/average	3.807 ±0.001	0.015 ±0.008	1.167 ±0.001	0.003 ±0.011	2.138	0.001		100	2.907 ±0.012	
Sample MMI06-24-4: biotite ± hornblende, J = 0.010300±0.000012, integrated age = 136.01±0.31 Ma (2c)										
2	20.276 ±0.012	0.053 ±0.043	0.036 ±0.075	0.041 ±0.031	0.661	0.007	55.68	0.42	8.556 ± 0.393	152.38 ±6.72
2.2	13.069 ±0.006	0.036 ±0.074	0.031 ±0.055	0.025 ±0.037	0.581	0.004	51.64	0.62	5.981 ± 0.271	107.85 ±4.74
2.4	9.411 ±0.004	0.023 ±0.029	0.022 ±0.023	0.012 ±0.024	0.457	0.002	35.57	3.03	5.942 ± 0.088	107.16 ±1.54
2.7	8.631 ±0.004	0.020 ±0.022	0.019 ±0.026	0.005 ±0.027	0.408	0.001	17.21	5.37	7.045 ± 0.053	126.38 ±0.93
2.9	8.398 ±0.005	0.019 ±0.022	0.025 ±0.017	0.003 ±0.037	0.537	0.001	9.79	7.09	7.486 ± 0.049	134.00 ±0.85
3.1	8.388 ±0.005	0.019 ±0.026	0.038 ±0.014	0.003 ±0.037	0.817	0.001	9.38	8.19	7.517 ± 0.048	134.54 ±0.83
3.3	8.307 ±0.005	0.019 ±0.020	0.072 ±0.014	0.003 ±0.027	1.554	0.001	8.68	11.32	7.517 ± 0.042	134.53 ±0.72
3.4	8.255 ±0.004	0.020 ±0.020	0.102 ±0.017	0.003 ±0.033	2.202	0.001	7.94	7.94	7.518 ± 0.044	134.56 ±0.75
3.5	8.378 ±0.004	0.019 ±0.017	0.089 ±0.015	0.003 ±0.032	1.92	0.001	8.83	7.37	7.553 ± 0.043	135.17 ±0.73
3.6	8.404 ±0.004	0.020 ±0.023	0.097 ±0.014	0.003 ±0.022	2.085	0.001	9.46	9.77	7.537 ± 0.040	134.87 ±0.69
3.7	8.570 ±0.005	0.018 ±0.029	0.082 ±0.018	0.003 ±0.030	1.777	0.001	8.47	8.29	7.763 ± 0.045	138.78 ±0.78
3.8	8.685 ±0.005	0.019 ±0.027	0.092 ±0.017	0.003 ±0.045	1.994	0.001	7.69	6.23	7.923 ± 0.055	141.52 ±0.94
3.9	8.711 ±0.004	0.019 ±0.019	0.112 ±0.015	0.003 ±0.040	2.424	0.001	7.53	5.27	7.951 ± 0.048	142.01 ±0.83
4.1	8.586 ±0.005	0.018 ±0.024	0.072 ±0.016	0.002 ±0.033	1.548	0.001	6.92	7.5	7.905 ± 0.045	141.22 ±0.77
4.3	8.683 ±0.004	0.017 ±0.018	0.051 ±0.018	0.002 ±0.035	1.099	0.001	5.91	5.97	8.069 ± 0.040	144.03 ±0.69
4.6	8.680 ±0.005	0.017 ±0.016	0.077 ±0.015	0.002 ±0.042	1.657	0.001	6.04	5.64	8.053 ± 0.048	143.76 ±0.82
Total/average	8.516 ±0.001	0.019 ±0.003	0.829 ±0.001	0.003 ±0.004	1.517	0.002		100	7.522 ± 0.008	
Sample MMI06-34-8: hornblende, J = 0.010322 ±0.000010, integrated age = 48.86 ±0.69 Ma (c)										
2	241.226 ±0.033	0.374 ±0.114	0.688 ±0.071	0.883 ±0.050	8.829	0.05	108.61	0.1	-17.807 ±9.833	-366.40 ±224.33
2.2	78.656 ±0.026	0.187 ±0.177	0.361 ±0.077	0.311 ±0.071	4.971	0.029	119.43	0.22	-12.214 ±6.083	-243.12 ±129.62
2.5	15.918 ±0.012	0.061 ±0.174	0.246 ±0.050	0.056 ±0.082	4.737	0.009	100.72	0.94	-0.118 ±1.339	-2.20 ±24.97
2.8	13.347 ±0.006	0.069 ±0.060	0.074 ±0.040	0.039 ±0.049	1.357	0.011	83.05	2.34	1.984 ±0.563	36.58 ±10.28
3.1	6.864 ±0.008	0.164 ±0.033	0.115 ±0.042	0.018 ±0.055	2.269	0.034	68.77	2.31	1.653 ±0.293	30.52 ±5.37
3.4	5.019 ±0.007	0.378 ±0.017	0.276 ±0.024	0.011 ±0.062	5.949	0.084	50.02	4.09	2.066 ±0.203	38.06 ±3.70
3.7	3.744 ±0.005	0.343 ±0.010	0.356 ±0.014	0.004 ±0.037	7.854	0.076	21.83	22.89	2.785 ±0.051	51.13 ±0.92
4	3.143 ±0.005	0.259 ±0.010	0.366 ±0.013	0.002 ±0.056	8.318	0.057	7.33	40.62	2.809 ±0.042	51.57 ±0.76
4.3	3.313 ±0.005	0.252 ±0.011	0.379 ±0.013	0.003 ±0.069	8.611	0.055	9.35	26.49	2.862 ±0.060	52.52 ±1.08
Total/average	3.941 ±0.001	0.273 ±0.003	4.276 ±0.001	0.005 ±0.011	7.849	0.045		100	2.819 ±0.019	

Notes:Gas volume measurements to 10^{-13} cm³

Neutron flux monitors: 28.02 Ma FCs (Renne et al., 1998)

Isotope production ratios: ($^{40}\text{Ar}/^{39}\text{Ar}$)K = 0.0302 ±0.00006, ($^{37}\text{Ar}/^{39}\text{Ar}$)Ca = 1416 ±0.5, ($^{36}\text{Ar}/^{39}\text{Ar}$)Ca = 0.3952 ±0.0004, Ca/K = 1.83 ±0.01 ($^{37}\text{ArCa}/^{39}\text{ArK}$)

pyroxene crystals have acted as strain markers and display flattening and orogen-parallel elongation within the foliation planes. Elongation strain averages about 3 but can exceed 10 (Fig 5). Foliation and lineation fabrics are cut by a granodioritic pluton 6 km in length and by smaller stocks less than a kilometre in length (MacIntyre and Schiarizza, 1999). All are elongated in a northwest direction, parallel with the mineral elongation direction which averages approximately 335°.

Hornblende dacite dikes generally cut the foliation of the deformed volcanic country rocks (Fig 6). The dikes are

1 to 5 m thick and have an average strike/dip of approximately 145°/60°. They all display protomylonitic textures. Locally, the dikes are transposed by the 335° ductile fabric. These relationships are taken to indicate late synkinematic emplacement of the dikes.

The U-Pb zircon age determination of 218.7 ± 0.4 Ma for sample MMI06-24-11, collected from one of the synkinematic dacite dikes, is slightly younger than the crystallization age of 226 ± 3 Ma estimated from a stock 2 km to the southeast by MacIntyre et al. (2001). This stock displays a decimetre thick ultramylonite zone (approx. 205°/40°) that is overprinted by later dilational brecciation textures (Fig 7).

The new age is identical, within the limits of error, to the oldest parts of the Endako Batholith (the Stern Creek phase) where dated, approximately 65 km to the southeast.

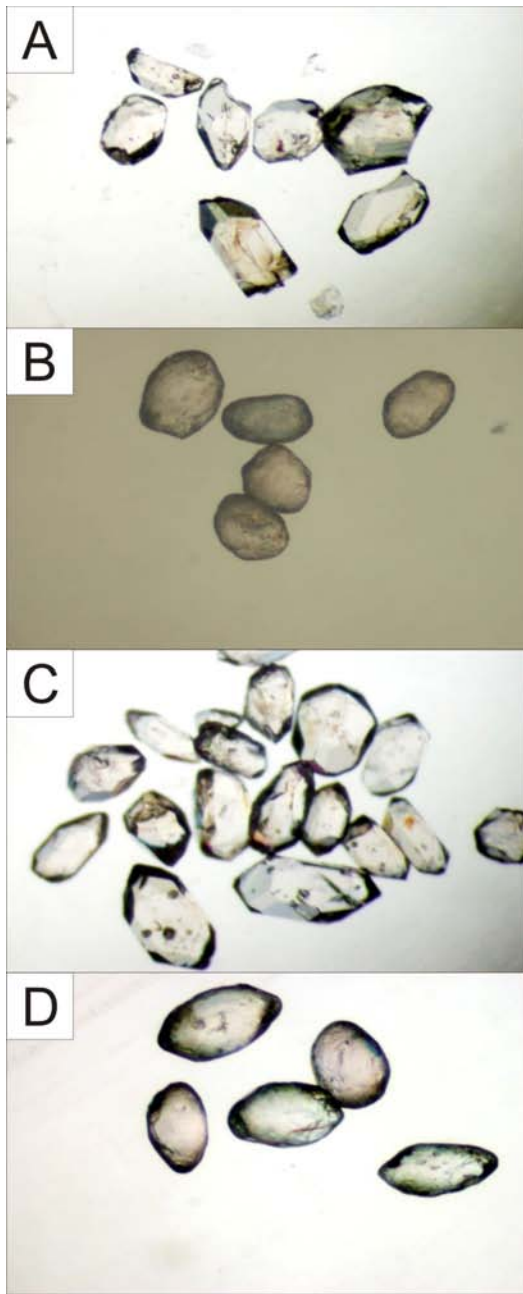


Figure 2. Photomicrographs of zircons analyzed from sample MMI06-5-1 before (A) and after (B) air abrasion, and from sample MMI06-24-11 before (C) and after (D) air abrasion. Horizontal dimension of photos represents approximately 1 mm.

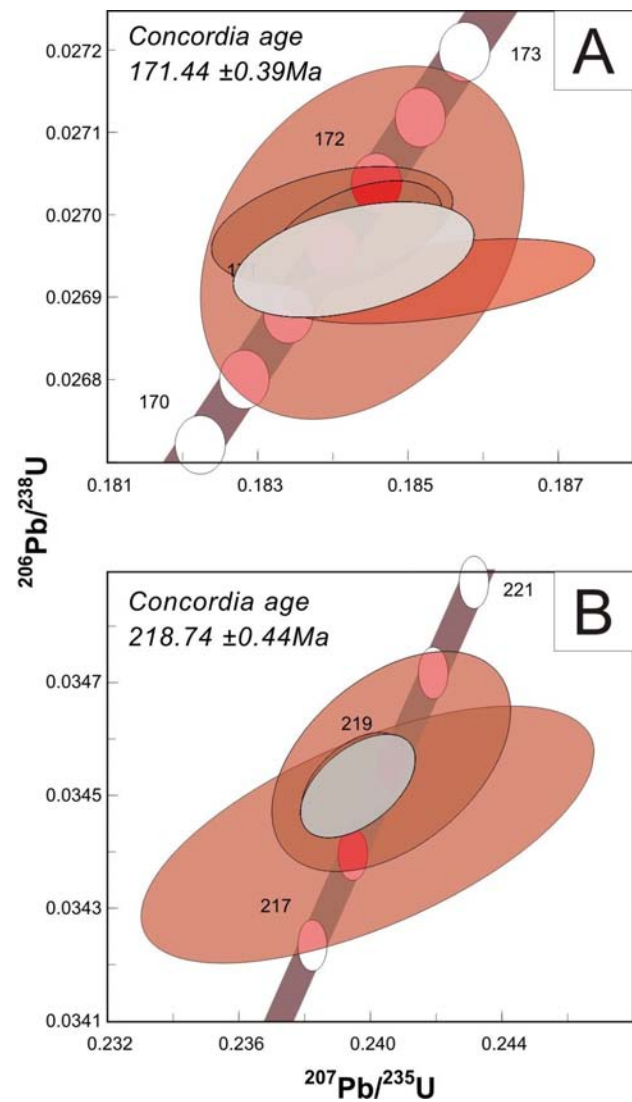


Figure 3. Concordia plots for U-Pb TIMS data for: A) sample MMI06-5-1, and (B) sample MMI06-24-11. 2σ error ellipses for individual analytical fractions are shown in red. These data are combined to produce the best estimate age shown by the grey ellipse. Concordia bands include 2σ errors on U decay constants.

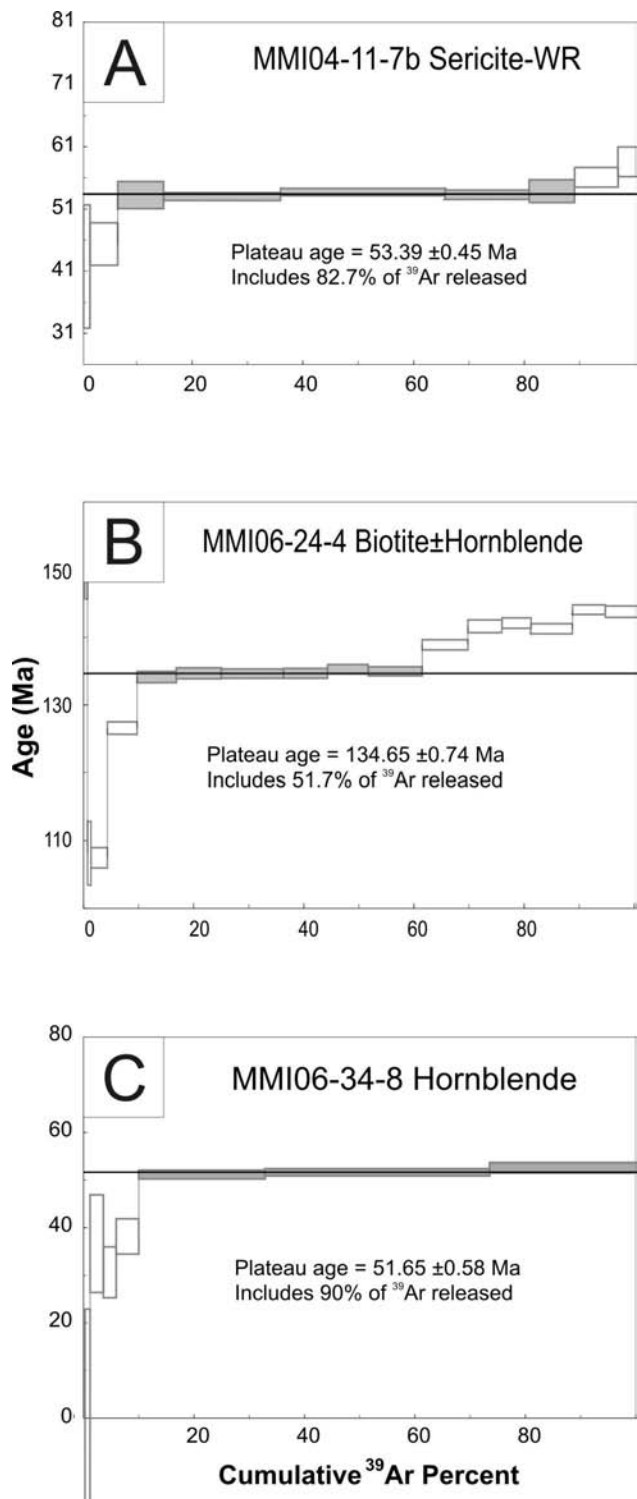


Figure 4. Step heating Ar gas release spectra for: A) sample MMI04-11-7b, B) sample MMI06-24-4, and C) sample MMI06-34-8. Plateau steps are filled, rejected steps are open. Box heights at each step are 2σ .

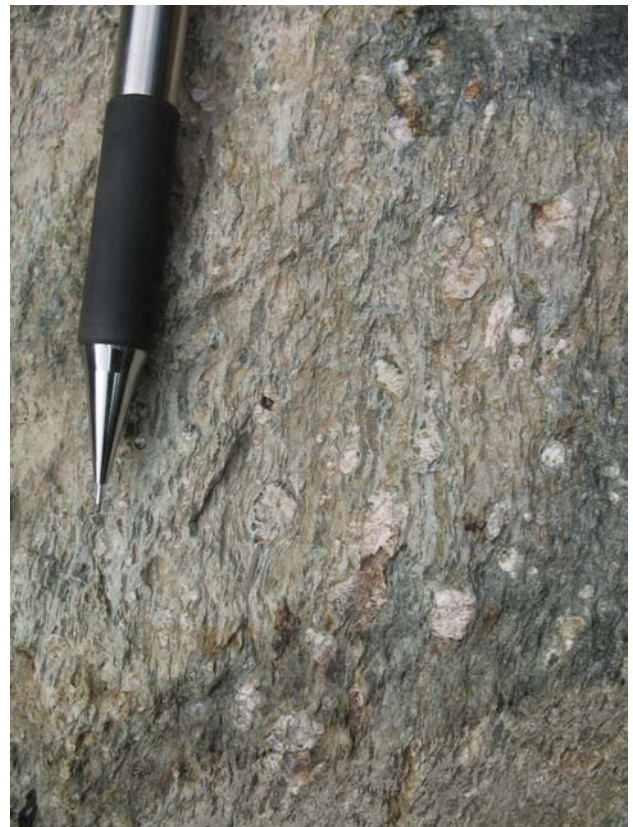


Figure 5. Coarse augite crystals characterize the porphyritic volcanic rocks near Boling Point. They are good strain markers and commonly display a strong lineation. Strain averages about 3, but is locally 10 or more.



Figure 6. Dacite dike contact shows weakly to non-foliated dike margin in contact with foliated tuffaceous country rocks.



Figure 7. a) Dacite dikes are locally infolded with augite porphyry breccia. Fold axes are oriented $345^{\circ}/20^{\circ}$. b) Close-up view of dacite outcrop showing foliation at this locality plus cataclastically reduced quartz eyes. c) Strong fabric development in augite porphyry country rocks.

Villeneuve et al. (2001) report an age for this phase of 219.3 ± 0.4 Ma.

CUNNINGHAM LAKE: FOLIATED TUFF WITH DACITIC CLASTS, SAMPLE MMI06-5-1

Sample MMI06-5-1 was collected from a unit mapped as Sitlika assemblage, which is described by MacIntyre and Schiarizza (1999) as mainly metabasalt with lesser amounts of felsic volcanic and sedimentary units. At the sample locality, white, flow-banded and quartz-phyric, coarse lapilli-sized clasts constitute about 5% of a dark brown tuffaceous unit. The clasts display elongation with gentle northwest plunges within a steep, north-northwest-striking foliation (Fig 8).

Age determination was sought to help test the correlation with the Sitlika assemblage because such a correlation points to an environment with potential for volcanogenic massive sulphide mineralization, similar to that seen at the Kutcho Creek deposit (MINFILE 104I 060). Unfortunately, the correlation is not borne out by the new U-Pb age determination of ca. 171 Ma (versus the expected age of ca. 250 Ma for Sitlika strata). However, these volcanic rocks may be extrusive equivalents to a belt of intrusive

rocks that includes the Spike Peak intrusive suite, dated at 171.8 ± 0.6 Ma (U-Pb zircon; MacIntyre et al., 2001) about



75 km along strike to the northwest and the Sugarloaf phase of the Endako Batholith, dated at 171 ± 1.7 Ma ($^{40}\text{Ar}/^{39}\text{Ar}$; Villeneuve et al., 2001) about 90 km to the southeast. The deformation event that produced the strong lineation displayed by these pyroclastic strata must be younger than ca. 171 Ma.

BOLING POINT: BIOTITE GRADE METATUFF, SAMPLE MMI06-24-4

Late Triassic augite porphyritic volcanic and related sedimentary rocks are in presumed contact with serpentinized ultramafic rocks along their eastern margin (MacIntyre and Schiarizza, 1999) in the Boling Point area, but the contact is obscured by surficial deposits. At the sample locality, augite porphyry breccia contains sparse, possibly andesitic, clasts containing euhedral biotite booklets. Biotite was extracted from one of these clasts for geochronological age determination and yielded a cooling age of 134.65 ± 0.74 Ma (Table 3).

Elongation fabrics at the sample locality are similar to other parts of the Late Triassic package near Boling Point and the Middle Jurassic section at Cunningham Lake. To the immediate east, however, polydeformed, fine-grained tuffaceous sedimentary rocks may have been deformed into sheath folds (Fig 9). In consideration of the protolith age of the sample from Cunningham Lake (ca. 171 Ma), the strong metamorphic fabric was probably imparted on this belt of rocks between ca. 171 and ca. 135 Ma.



Figure 8. Lineation of felsic clasts within exposures near Cunningham Lake.

Riske Creek area

Two K-Ar whole rock ages are reported from unnamed Eocene volcanic rocks in the Riske Creek area. They are 52.2 ± 2 Ma and 50 ± 1.4 Ma (Hunt and Roddick, 1994). A clean fresh sample of hornblende-porphyritic tuff was collected to obtain a more robust $^{40}\text{Ar}/^{39}\text{Ar}$ age. The aim was to test the chronostratigraphic correlation of these rocks with lithologically similar rocks more than 100 km to the west-northwest, now the subject of geological investigation (Mihalynuk et al., 2008), and a growing body of radiometric age data that points to a voluminous ca. 52 Ma eruptive epoch (Riddell et al., 2007).

RISKE CREEK: IGIMBRITIC TUFF, SAMPLE MMI06-34-8

Slabby-weathering, cream-coloured dacitic ignimbrite cooling units are stacked more than 100 m thick near the sample site. Lahar layers up to 5 m thick locally separate the dacite flows. Lapilli compaction and flow fabrics dip shallowly east-northeast, defined partly by the alignment of oxyhornblende (10%) and biotite (1%, not present in dated sample), together with trails of feldspar (40%) and quartz (15%), in a fine-grained, cream-coloured matrix. These rocks are juxtaposed across a steeply dipping, north-trending fault with Paleozoic chert and argillite of the Cache Creek complex (Mihalynuk and Harker, 2007).

Hornblende separated from a sample of the freshest and densest dacite yielded a $^{40}\text{Ar}/^{39}\text{Ar}$ age of 51.65 ± 0.58 Ma. Previously reported K-Ar age determina-

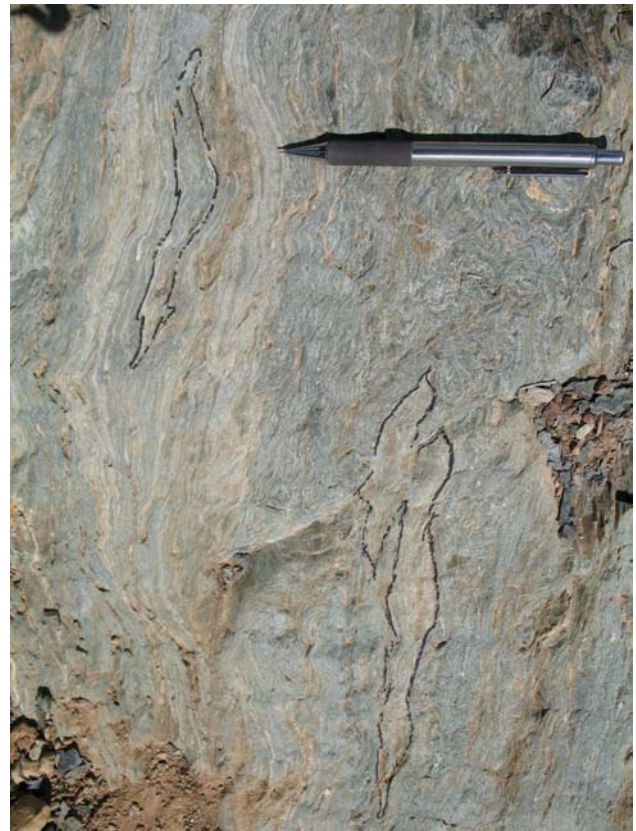


Figure 9. Possible sheath folds within epidote-chlorite-altered tuffaceous siltstone and fine-grained sandstone are outlined in black marker.

tions (Hunt and Roddick, 1994) were from samples of basaltic andesite and dacite tuff collected approximately 0.75 km west and approximately 5 km southwest of sample site MMI06-34-8. The dacite tuff sampled and reported on by Hunt and Roddick (1994) is likely the same unit that is reported on here. The two ages are identical within limits of error. The rocks are equivalent in age to the Ootsa Lake Group to the northwest and the Kamloops Group to the southeast.

Iron Mask batholith

The Iron Mask batholith is an important copper-gold resource as it contains at least eight separate alkalic, porphyry-style copper-gold-silver deposits; five of which are significant past producers. Phyllitic fabrics and minor folds are locally developed in parts of the batholith (Logan et al., 2007). Fabrics with similar orientation are well developed within the Late Triassic arc strata outside the western margin of the batholith. This deformation could affect the distribution of mineralization within the batholith; therefore, it is important to understand its timing as a first step to determining the cause of the deformation.

CHERRY CREEK TECTONIC ZONE PHYLLITE, SAMPLE MMI04-11-7B

In the most coarsely crystalline samples of the phyllite unit, individual mica crystals can be discerned in hand sample. A sample of this calcareous quartz-mica schist was collected from a low, white-weathering outcrop approximately 2 km south of Jacko Lake. Unfortunately, the sample was not sufficiently coarse-grained to permit separation of white mica, so a whole rock determination was performed. It yielded an Eocene $^{40}\text{Ar}/^{39}\text{Ar}$ age of 53.39 ± 0.45 Ma.

Numerous samples collected from within 20 km north and south of Jacko Lake display early Tertiary cooling ages (Matthews, 1964; Preto et al., 1979; Breitsprecher and Mortensen, 2004), but none are from the Mesozoic volcanic section. Two cooling ages for samples of porphyritic granodiorite of the Nicola batholith (Preto et al., 1979) collected from sites approximately 6 and 8 km to the south-southeast of sample site MMI04-11-7b were interpreted on later compilations as having a crystallization age of Late Triassic–Early Jurassic (Kwong, 1987; Massey et al., 2005). The ages are 50.3 ± 0.4 Ma ($^{40}\text{Ar}/^{39}\text{Ar}$, Ghosh, 2003) and 51.8 ± 2 Ma (K-Ar, Preto et al., 1979). Volcanic strata of the Kamloops Group, sampled approximately 18 km to the north (approx. 1 km north of Kamloops Lake, Fig 1), have produced a cooling age of 50 ± 4 Ma (Matthews, 1964). This sample site is within 100 m of an Eocene pluton that is part of the Battle Bluff plutonic complex (Massey et al., 2005), and the age may partly reflect cooling of that body.

Ductile Eocene deformation may be related to emplacement of an Eocene component of the Nicola batholith, recognized by Preto et al. (1979) but not represented in subsequent compilations. Deformation of this age has not been widely acknowledged in this region. Such deformation may have significant implications for mineral exploration, particularly as deeper structural levels of the Iron Mask batholith are targeted.

ACKNOWLEDGMENTS

Assistance with U-Pb geochronology was provided by H. Lin (mineral separations and support with mass spectrometry) and R. Lishansky (grain selection, abrasion and cleanlab work). Sample MMI04-11-7B was collected as part of the Alkalic Copper-Gold Porphyry project, under the sage leadership of James Logan. C. Peat painstakingly created Figure 1.

REFERENCES

- Breitsprecher, K. and Mortensen, J.K. (2004): BCAGE 2004A - a database of isotopic age determinations for rock units from British Columbia. *BC Ministry of Energy and Mines*, Open File 2004-3 (Release 2.0), 7766 records, 9.3 Mb, URL <<http://www.em.gov.bc.ca/Mining/Geosurv/Publications/OpenFiles/OF2004-03/toc.htm>> [December, 2007].
- Ghosh, S. (2003): Petrology, geochemistry, geochronology and tectonic history of the Nicola Horst, B.C.; M.Sc. thesis, *Simon Fraser University*, Vancouver, 155 pages.
- Hunt, P.A. and Roddick, J.C. (1994): A compilation of K-Ar and $^{40}\text{Ar}/^{39}\text{Ar}$ ages: Report 24; in Radiogenic Age and Isotopic Studies, Report 8, *Geological Survey of Canada*, Paper 1994-F, pages 125–155.
- Kwong, Y.T.J. (1987): Evolution of the Iron Mask batholith and its associated copper mineralization, *BC Ministry of Energy, Mines and Petroleum Resources*, Bulletin 77, includes 1:50 000 scale map, 56 pages.
- Lett, R.E., Man, E.C. and Mihalynuk, M.G. (2008): Towards a drainage geochemical atlas for British Columbia; in Geological Fieldwork 2007, *BC Ministry of Energy, Mines and Petroleum Resources*, Paper 2008-1, pages 61–68.
- Logan, J.M. and Mihalynuk, M.G. (2006): Geology of the Iron Mask batholith, southern British Columbia (NTS 0921/9, 10), *BC Ministry of Energy, Mines and Petroleum Resources*, Open File 2006-11, 1:25 000 scale, URL <<http://www.em.gov.bc.ca/Mining/Geosurv/Publications/OpenFiles/OF2006-11/toc.htm>> [November, 2007].
- Logan, J.M., Mihalynuk, M.G., Ullrich, T. and Friedman, R.M. (2007): U-Pb ages of intrusive rocks and $^{40}\text{Ar}/^{39}\text{Ar}$ plateau ages of copper-gold-silver mineralization associated with alkaline intrusive centres at Mount Polley and the Iron Mask batholith, southern and central British Columbia; in Geological Fieldwork 2006, *BC Ministry of Energy, Mines and Petroleum Resources*, Paper 2007-1, pages 93–116, URL <<http://www.em.gov.bc.ca/DL/GSBPubs/GeoFldWk/2006/11-Logan.pdf>> [November, 2007].
- MacIntyre, D.G. and Schiarizza, P. (1999): Bedrock geology, Cunningham Lake area (NTS 93K/11, 12, 13, 14), *BC Ministry of Energy, Mines and Petroleum Resources*, Open File 1999-11, 1:100 000 scale.
- MacIntyre, D.G., Villeneuve, M.E. and Schiarizza, P. (2001): Timing and tectonic setting of Stikine Terrane magmatism, Babine-Takla lakes area, central British Columbia; *Canadian Journal of Earth Sciences*, Volume 38, pages 579–601.
- Massey, N.W.D., MacIntyre, D.G., Desjardins, P.J. and Cooney, R.T. (2005): Digital Geology Map of British Columbia: Whole Province, *BC Ministry of Energy and Mines*, GeoFile 2005-1, 1:250 000 scale, URL <<http://www.em.gov.bc.ca/Mining/Geosurv/Publications/GeoFiles/Gf2005-1/toc.htm>> [November 2007].
- Matthews, W.H. (1964): Potassium-argon age determinations of Cenozoic volcanic rocks from British Columbia; *Geological Society of America*, Bulletin, Volume 75, pages 465–468.
- Mihalynuk, M.G. (2007a): Evaluation of mineral inventories and mineral exploration deficit of the Interior Plateau Beetle In-

- fested Zone (BIZ); in *Geological Fieldwork 2006, BC Ministry of Energy, Mines and Petroleum Resources*, Paper 2007-1, pages 137–142, URL <<http://www.em.gov.bc.ca/DL/GSBPubs/GeoFldWk/2006/14-Mihalynuk.pdf>> [November 2007].
- Mihalynuk, M.G. (2007b): Neogene and Quaternary Chilcotin Group cover rocks in the Interior Plateau, south-central British Columbia: A preliminary 3-D thickness model; in *Geological Fieldwork, BC Ministry of Energy, Mines and Petroleum Resources*, Paper 2007-1, pages 143–147, URL <<http://www.em.gov.bc.ca/DL/GSBPubs/GeoFldWk/2006/15-Mihalynuk.pdf>> [November 2007].
- Mihalynuk, M.G. and Harker, L.L. (2007): Riske Creek geology (NTS 92O/16W), *BC Ministry of Energy, Mines and Petroleum Resources*, Open File 2007-6, 1:50,000 scale, URL <<http://www.em.gov.bc.ca/DL/GSBPubs/OF/2007-6/OF2007-6-RiskeCk-Mihalynuk-Harker.pdf>> [November 2007].
- Mihalynuk, M.G., Harker, L.L., Lett, R. and Grant, B. (2007): Results of reconnaissance surveys in the Interior Plateau Beetle Infested Zone (BIZ); *BC Ministry of Energy, Mines and Petroleum Resources*, GeoFile 2007-5, URL <<http://www.em.gov.bc.ca/Mining/Geosurv/Publications/GeoFiles/Gf2007-5/toc.htm>> [November 2007].
- Mihalynuk, M.G., Peat, C.R., Terhune, K. and Orovan, E.A. (2008): Regional geology and resource potential of the Chezacut map area, central British Columbia (NTS 093C/08); in *Geological Fieldwork 2007, BC Ministry of Energy, Mines and Petroleum Resources*, Paper 2008-1, pages 117–134.
- MINFILE (2007): MINFILE BC mineral deposits database; *BC Ministry of Energy, Mines and Petroleum Resources*, URL <<http://www.em.gov.bc.ca/Mining/Geosurv/Minfile/>> [November 2007].
- Preto, V.A., Osatenko, M.J., McMillan, W.J. and Armstrong, R.L. (1979): Isotopic dates and strontium isotopic ratios for plutonic and volcanic rocks in the Quesnel Trough and Nicola Belt, south-central British Columbia; *Canadian Journal of Earth Sciences*, Volume 16, pages 1658–1672.
- Riddell, J.M., Ferri, F., Sweet, A.R. and O’Sullivan, P.B. (2007): New geoscience data from the Nechako Basin project; in *The Nechako Initiative – Geoscience Update 2007, BC Ministry of Energy, Mines and Petroleum Resources*, pages 59–98, URL <http://www.em.gov.bc.ca/dl/OilGas/COG/Nechako_Sheet3.pdf> [November 2007].
- Ullrich, T., Friedman, R.M., Mihalynuk, M.G. and Logan, J.M. (2008): Results of field investigations in the Beetle Infested Zone 2006: radiometric age determination data; *BC Ministry of Energy, Mines and Petroleum Resources*, GeoFile 2008-3.
- Villeneuve, M.E., Whalen, J.B., Anderson, R.G. and Struik, L.C. (2001): The Endako batholith: episodic plutonism culminating in formation of the Endako porphyry molybdenite deposit, north-central British Columbia; *Economic Geology*, Volume 96, pages 171–196.

Origin of the Kootenay Lake Metamorphic High, Southeastern British Columbia

by D.P. Moynihan¹ and D.R.M. Pattison¹

KEYWORDS: Canadian Cordillera, Kootenay Arc, metamorphism, structural geology, Tertiary extension, normal faulting, differential exhumation

INTRODUCTION

A narrow, elongate region of anomalously high metamorphic grade runs parallel to Kootenay Lake, in the central part of the Kootenay Arc, southeastern British Columbia. Metamorphic grade ranges from the chlorite/biotite zones on the flanks to the sillimanite+K-feldspar zone in the centre of the high. In this paper, we present a summary of structural, metamorphic and geochronological data and discuss the origin of this pattern. It is suggested that the metamorphic high results from differential exhumation during early Tertiary extensional deformation.

Background Geology

The Kootenay Arc is a narrow, curvilinear, metamorphosed and polydeformed region straddling the boundary between rocks formed on the North American continental margin and those developed in an oceanic setting to the west (Klepacki, 1985; Colpron and Price, 1995; Thompson et al., 2007). It extends in an eastward-convex arch from northern Washington State to Revelstoke, BC, and lies on the western flank of the Purcell Anticlinorium, an area characterized by open folds of Mesoproterozoic to Neoproterozoic strata. The transition from the Purcell Anticlinorium into the Kootenay Arc is characterized by an increase in metamorphic grade and complexity of deformation, and a decrease in stratigraphic age (Warren, 1997).

Neoproterozoic to Triassic metasedimentary and metavolcanic rocks host numerous Middle Jurassic (ca. 165 Ma) and mid-Cretaceous (ca. 115–100 Ma) granitic plutons and minor intrusive bodies (Fig 1). The oldest units are the quartzite-dominated Hamill Group and the carbonate Badshot-Mohican Formation. These are similar to coeval strata in the Purcell and Rocky mountains, whereas the overlying Lardeau Group differs from rocks of similar age farther east (Colpron and Price, 1995). The Lardeau Group comprises black, grey and green schist, argillite, calcisilicate and quartzofeldspathic gneiss, marble, quartzite, metaconglomerate and metabasite (Fyles, 1967; Hoy,

1980). It is unconformably overlain by the Milford Group, which includes marble, siliceous argillite, schist and chert. This is followed by the Kaslo Group, a package of mafic volcanic and volcanoclastic rocks. The youngest unit, the Slocan Group, is dominated by argillite and limestone. A summary of rock types and their ages is included in Figure 1.

There is a general westward-younging trend in the rock units across the Kootenay Arc. This is partly due to a series of subparallel normal faults mapped by Fyles (1967) on the west side of Kootenay Lake. Three major west-dipping faults were recognized. From east to west, these are the Lakeshore, Josephine and Gallagher faults (Fig 1, 2). The Schroeder fault is probably a continuation of the Lakeshore fault north of Kaslo (Klepacki, 1985).

The Middle Jurassic plutonic suite is represented by the calcalkaline Nelson batholith and associated minor bodies. The Nelson batholith is an 1800 km² body intruded during the interval 173 to 159 Ma (Ghosh, 1995). It ranges in composition from diorite to granite, but is dominated by porphyritic hornblende granodiorite. The Nelson batholith is unaffected by ductile deformation, except for narrow zones along its eastern margin and southern tail. It is truncated on its western margin by the Eocene Slocan Lake (normal) fault (Carr et al., 1987), but an intrusive margin is preserved along much of its eastern boundary. A contact metamorphic aureole is locally well developed around its intrusive margins (Pattison and Vogl, 2005).

The second major plutonic suite was intruded during the interval 117 to 100 Ma. Rock types include hornblende and biotite granodiorite, biotite granite and two-mica granite, which are interpreted to have been derived from crustal anatexis (Brandon and Lambert, 1993). The largest bodies of this age in the area are the Fry Creek and Bayonne batholiths, which are for the most part undeformed. Deformed equivalents include the Baldy pluton and numerous minor sheet-like bodies in higher grade areas. Locally, igneous sheets make up a high percentage of the country rock, resulting in gradational margins to parts of the Baldy pluton, the Proctor pluton and the Shoreline stock.

STRUCTURAL RELATIONS

Deformations D_1 and D_2

The outcrop pattern in the central Kootenay Arc is dominated by two generations of regionally developed folds (Fig 1, 2; Fyles, 1964, 1967; Hoy, 1980; Leclair, 1988). The earliest folds are a series of high-amplitude isoclinal folds with an axial-planar schistosity containing a gently plunging stretching lineation. The most clearly defined F_1 folds are westward-closing recumbent anticlines

¹ Department of Geoscience, University of Calgary, Calgary, AB

This publication is also available, free of charge, as colour digital files in Adobe Acrobat® PDF format from the BC Ministry of Energy, Mines and Petroleum Resources website at http://www.em.gov.bc.ca/Mining/Geolsurv/Publications/catalog/cat_fldwk.htm

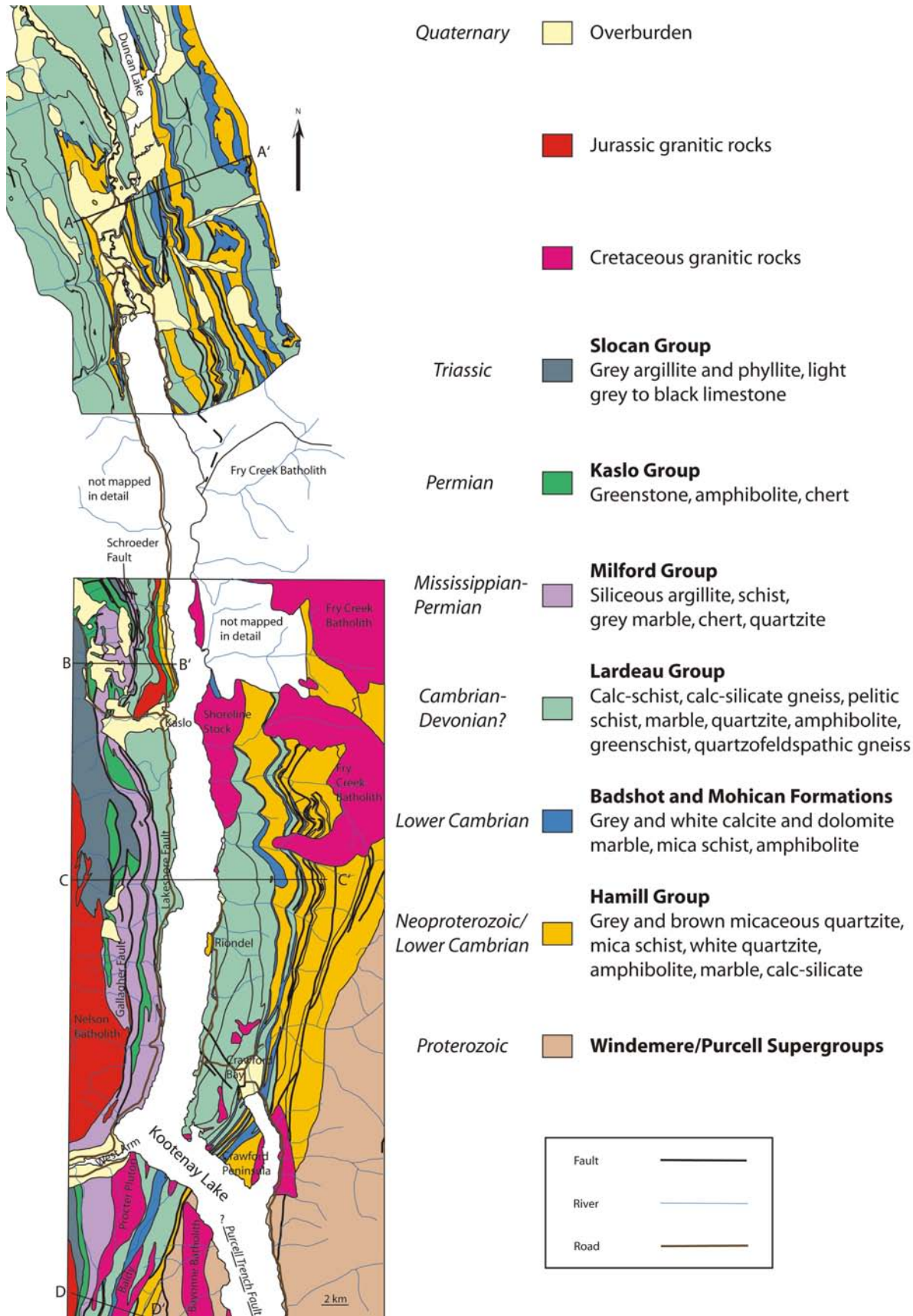


Figure 1. Geology of the central Kootenay Arc, compiled from Fyles (1964) and Reesor (1996). The lines of cross-sections shown in Figure 2 are displayed.

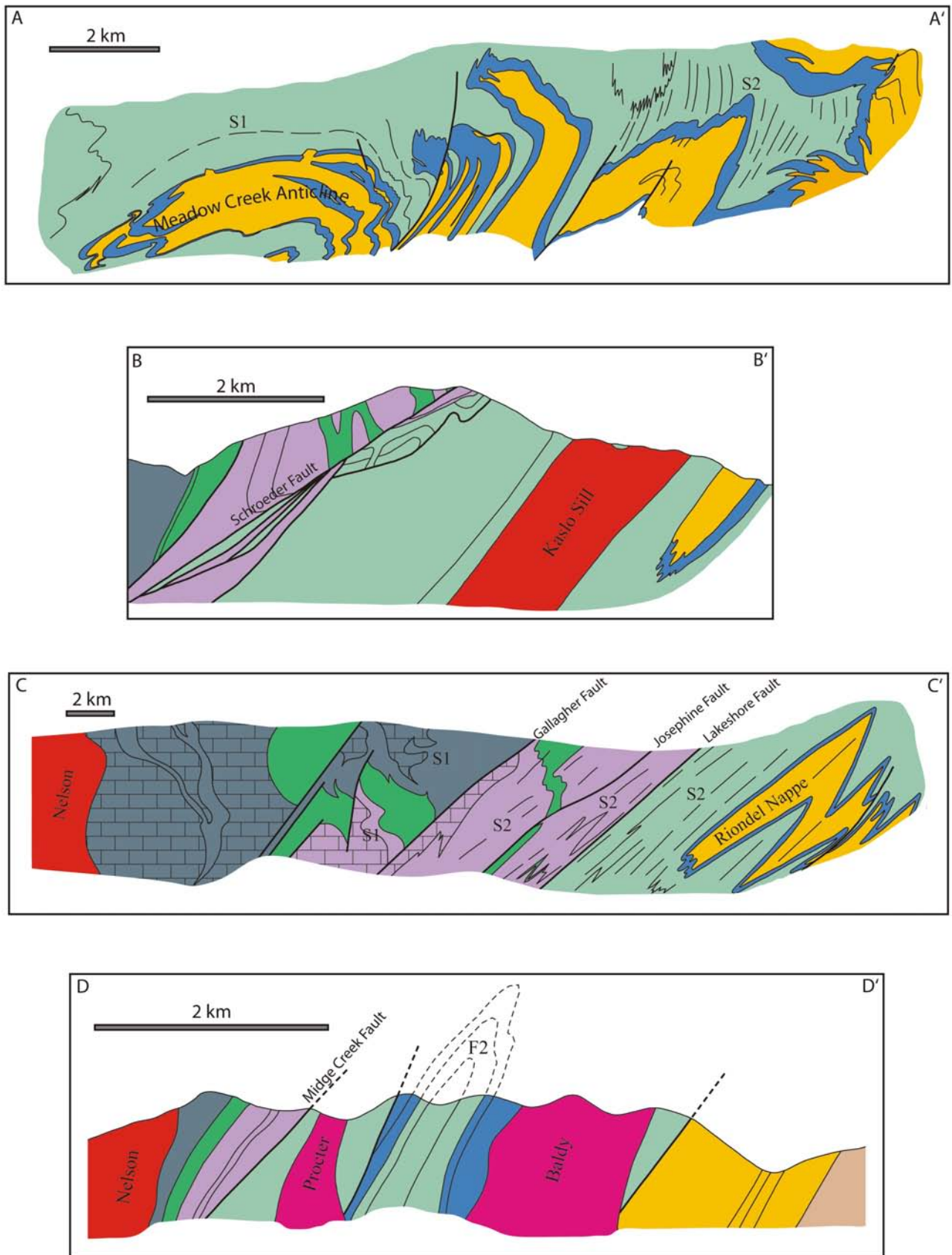


Figure 2. Vertical cross-sections across the central Kootenay Arc from Fyles (1964; A–A'), Klepacki (1985; B–B'), Brown et al. (1981; C–C') and Leclair (1988; D–D'). No vertical exaggeration. The lines of section are shown in Figure 1.

cored by the Hamill Group. The largest of these, the Riondel nappe (equivalent to the Meadow Creek anticline in the Duncan Lake area), has a 20 km long overturned lower limb (Fig 2a, c). Folds with similar geometry and characteristics are also developed in the Mesozoic strata exposed west of Kootenay Lake, but their full definition is hindered by a lack of continuous marker horizons. The main body of the Nelson batholith is undeformed, but foliated minor bodies of approximately the same age indicate the age of D_1 is Middle Jurassic (Warren, 1997).

The F_1 isoclines were coaxially refolded around gently plunging F_2 axes, giving rise to a type 3 interference pattern (Ramsay, 1967). Second-generation (F_2) axial planes generally dip gently to moderately steeply to the west, but steepen towards higher structural levels in the Purcell Anticlinorium (Hoy, 1980). The F_2 axes plunge gently north over most of the area, as do L_2 stretching (mineral and elongation) lineations, resulting in exposure of progressively lower structural levels towards the south.

There is spatial variation in the intensity of D_2 deformation. In the northern part of the area, and west of the Gallagher fault (i.e., at higher structural levels), F_2 folds are open to close, and are outlined by S_1 and transposed S_0 . Second-phase schistosity (S_2) commonly forms a crosscutting spaced or crenulation cleavage, but rarely forms the dominant schistosity in the rock. Minor F_2 folds have curvilinear hinges, which locally diverge slightly from the trend of the L_2 stretching lineation. East of the Gallagher fault in the southern part of the area (lower structural levels), D_2 folds are tight to isoclinal and S_2 forms a continuous schistosity; S_1 is unrecognizable outside of the hinge zones of competent layers. Second-generation (F_2) fold hinges are rectilinear and are invariably parallel to the well-developed L_2 stretching lineation. Low-angle cutoffs and discontinuous lithological sequences indicate local transposition of primary compositional layering parallel to S_2 . The tighter folds, straightening of fold hinges, and parallelism between fold axes and the stretching lineation are manifestations of higher D_2 strain. There is, therefore, a broad correspondence between structural level and intensity of D_2 . This variation is evident across the normal faults (particularly the Gallagher and Schroeder faults) on the west side of Kootenay Lake (Fig 2). In the hangingwall of the Gallagher fault, S_1 is the dominant planar fabric and it is folded by open F_2 folds; S_1 is truncated against the fault. In the footwall, F_2 folds are tighter and S_2 is well developed.

The 115 Ma Fry Creek batholith (Brandon and Lambert, 1993) truncates D_2 folds and fabrics in the eastern part of the Riondel area. However, the northern part of the 117 Ma Baldy pluton is deformed by D_2 structures (Leclair, 1988). Although D_2 is ostensibly mid-Cretaceous, the possibility that D_2 is diachronous and/or composite cannot be ruled out.

Deformation D_3

First (D_1) and second-generation (D_2) structures share common characteristics for great lengths along strike, and have been tentatively correlated along much of the arc, from Salmo to the central Lardeau area (Fyles, 1967). This along-strike continuity contrasts with the distribution of later (D_3) structures. There is a change in the nature of D_3 deformation around the latitude of the West Arm (Fig 1), where the trend of Kootenay Lake changes from south to south-southeast. Two distinct styles of later (D_3) deforma-

tion are evident; these are referred to as D_{3N} and D_{3S} (subscripts 'N' and 'S' stand for north and south, respectively). Although described in sequence here, no age relationship between the two is implied.

DEFORMATION D_{3N}

In the central and northern parts of the area, east of the Gallagher and Schroeder faults, shear bands are variably but ubiquitously developed in micaceous horizons (Fig 3a, b). Shear bands cut down to the west more steeply than S_2 foliation, and bound lenses of rock that display sigmoidal deflections of S_2 foliation into the shear bands. The L_2 stretching lineation is folded around the open (F_{3N}) hinges. The shear bands range from sharp (commonly chlorite-rich) cleavage-forming surfaces with discrete offsets, to broader, more diffuse, inclined shear zones. These fabrics are referred to as S-C' fabric, extensional crenulation cleavage or shear band foliation (Platt and Vissers, 1980; Ponce de Leon and Chouckroune, 1980; White et al., 1980), and record extension of S_2 during west-side-down ductile shearing (Williams and Price, 1990). Shear bands merge with S_2 and are laterally discontinuous. The shear bands and their associated folds/extensional crenulations impart an irregular, undulatory character to the S_2 surface; F_{3N} hinges have a preferred orientation, but they are discontinuous and non-cylindrical. Shear bands and associated folds are developed on a centimetre scale in pelitic layers, but metre-scale folds with the same geometry are also evident on the east shoreline of Kootenay Lake in the Riondel area (the F_3 warps of Livingstone, 1968 and Hoy, 1980). Hinges of F_{3N} folds and indistinct shear band — S_2 intersections plunge gently to moderately steeply southwest throughout the affected area. Third-generation deformation (D_{3N}) fabrics are restricted to the footwall of the Gallagher and Schroeder faults. They extend eastward from the fault a horizontal distance of >10 km (>5 km structural thickness), but much of the most intensely developed shear band foliation is found in the immediate footwall of the Gallagher fault.

The northwest margin of the mid-Cretaceous Fry Creek batholith is also affected by west-side-down ductile shearing (Fig 3d). Although the remainder of the batholith is undeformed, this zone displays S-C fabrics (Berthé et al., 1979). The affected area is along strike from a normal fault that truncates the Meadow Creek anticline, which itself lies within the region of diffuse west-side-down ductile shearing (Fig 2).

The Gallagher fault (and Schroeder fault further north) marks the upper (western) boundary of D_{3N} deformation; west-side-down S-C' fabrics are not developed in the hangingwall to any significant degree. A broad region in the footwall is characterized by widespread, variably intense, ductile normal-sense fabrics accompanied by discrete normal faults. Although there is no direct evidence, the ductile fabrics and discrete faults are interpreted as having formed approximately synchronously, based on spatial distribution and kinematic compatibility.

DEFORMATION D_{3S}

Whereas D_{3N} resulted in extension of S_2 , S_2 was shortened in the area affected by D_{3S} . Shortening is manifested in buckle folds and crenulations of S_2 , with L_2 folded around hinges (Fig 3e, f). Third-generation (F_{3S}) buckles range from open to tight, and locally an axial-planar S_3 schistosity is developed. Third-generation (F_{3S}) folds plunge either

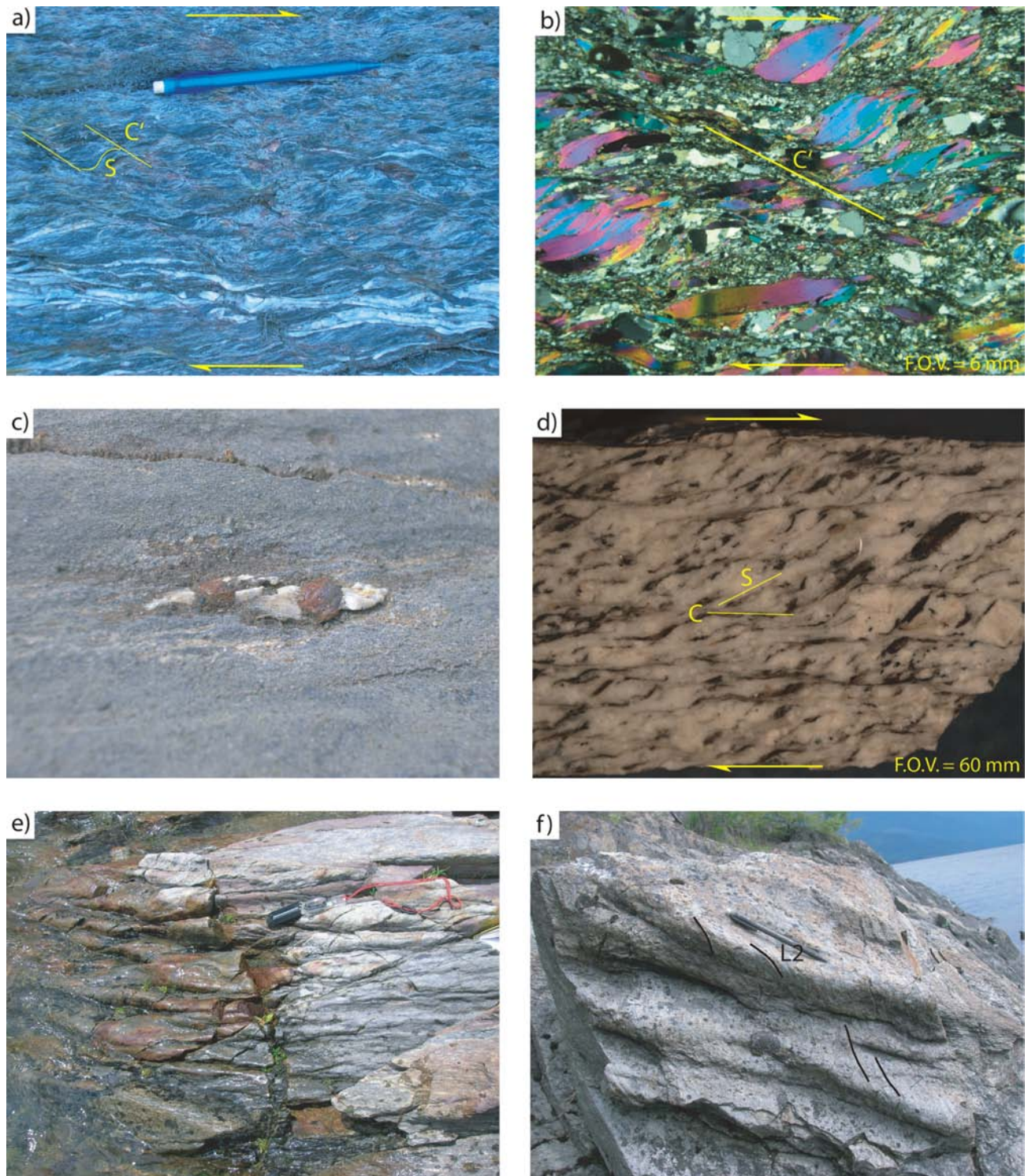


Figure 3. a) An example of S-C' fabric in Milford Group schist in the footwall of the Gallagher fault. b) Photomicrograph of S-C' fabric in Hamill Group schist, east side of Kootenay Lake. c) Subhorizontal stretching on S_1 is indicated by quartz-filled strain shadows on pyrite from the Slocan Group west of the Schroeder fault (width of photo is 5 cm). d) An example of S-C fabric indicating west-side-down shearing on the northwest margin of the Fry Creek batholith. e) Discontinuous F_{3S} hinges in the Hamill Group, Crawford Peninsula. f) Southwest-plunging F_{3S} folds showing steeply plunging L_2 passing around hinges.

southwest or northwest; over most of the Crawford Peninsula, F_3 folds plunge gently to the southwest (Fig 4). Axial planes dip moderately steeply northwest or southeast, depending on the orientation of the S_2 – S_0 enveloping surface. Hinge lines of F_{3S} folds are curvilinear and discontinuous, unlike F_2 folds, which have cylindrical axes parallel to L_2 . Third-generation (F_{3S}) folds range from centimetre-scale crenulations of micaceous layers and buckles of thin layers, up to folds with wavelengths >100 m. Deformation D_{3S} correlates with the D_3 of Leclair (1988) in the northern part of the Midge Creek area (south of the West Arm), and may continue further south.

RELATIONSHIP BETWEEN D_{3N} AND D_{3S} , AND TIMING OF D_3

The areas affected by D_{3N} and D_{3S} are approximately outlined in Figure 5. A question arises as to the timing relationship between D_{3N} and D_{3S} , and the reason for the change in the nature of D_3 around the bend in Kootenay Lake. Deformations D_{3N} and D_{3S} affect the same rock units. There is no difference in the nature of the layering that could lead to preferential development of buckles/shear bands in one area over the other. There is also no systematic difference in the orientation of the layering between the two areas. It is therefore concluded that there was spatial variation in the kinematics of D_3 deformation.

The location of the change between D_{3N} and D_{3S} — the bend in Kootenay Lake — coincides with the tip zone of the Purcell Trench fault, an Eocene extensional structure (Archibald et al., 1984; Doughty and Price, 1999). There is no reason why D_{3S} should be restricted to the tip zone of the fault, or that the change from D_{3N} to D_{3S} should occur at this location, unless the ductile D_{3S} deformation is genetically linked to the development of the Purcell Trench fault. As the age of the fault is known (Eocene), so is the age of D_{3S} . Given the relationship of D_{3N} to the early Tertiary Gallagher fault and the lack of overprinting relationships between D_{3N} and D_{3S} , this is most likely also the age of D_{3N} .

METAMORPHIC CONSIDERATIONS

The configuration of isograds based on the distribution of index minerals in pelitic rocks is shown in Figure 5. Pelitic layers are widely distributed, but they are commonly thin and discontinuous, and make up a small percentage of the rock volume. Their sparse occurrence in some areas introduces uncertainty into the exact position of isograds, but their wide distribution facilitates the recognition of trends in metamorphic grade. While future identification of important assemblages may locally shift the position of some isograds, the regional pattern is well established. Isograds south of the study area (in the southernmost part of Fig 5) are more poorly constrained.

Isograds run approximately parallel to strike along the central part of Kootenay Lake, but diverge from strike and converge in the northern Kootenay Lake – Duncan Lake area. South of the bend in Kootenay Lake, isograds also

transect strike; they run approximately parallel to the Purcell Trench fault (PTF), which marks the eastern boundary of the Priest River complex (Doughty and Price, 1999). The amphibolite facies belt of central and northern Kootenay Lake is continuous with the Priest River complex. At the latitude of Creston, to the south, there is a gradual decrease in grade westward from the PTF, a pattern that likely continues northward towards the bend in the lake. North of here, the western boundary of the amphibolite-facies belt is for the most part fault-bounded, whereas there is a monotonic decrease in metamorphic grade on its east side, from the sillimanite+K-feldspar zone in the centre of the high to the biotite zone in the Purcell Anticlinorium. The highest grade rocks are >5 km east of the fault, around the shoreline of Kootenay Lake.

The Gallagher fault marks the western boundary of the Barrovian metamorphic high along the central part of Kootenay Lake, and it juxtaposes two contrasting metamorphic field gradients. Pelite in the footwall directly east of the fault contains garnet and staurolite, with kyanite in contemporaneous quartz-rich veins (Fig 6a). The fault marks the garnet and staurolite ‘isograds’. Eastward from here, the grade increases, with pelitic rocks containing the assemblages garnet-staurolite-kyanite, garnet-kyanite, garnet-kyanite-sillimanite, garnet-sillimanite and garnet-sillimanite-K-feldspar (all with muscovite, biotite, quartz, plagioclase and accessory minerals). Porphyroblasts are wrapped by S_2 , and elongate porphyroblasts (staurolite, kyanite, sillimanite) are aligned (L_2) parallel to D_2 fold axes. Deformation D_2 is mid-Cretaceous, and Leclair et al. (1993) also interpreted this as the age of peak metamorphism.

Rocks in the hangingwall of the fault record a different metamorphic history. At the latitude of Figure 2c, rocks in the hangingwall display a Buchan (low pressure) contact aureole sequence (Pattison and Vogl, 2005). Rocks immediately west of the fault are low-grade chlorite-muscovite-bearing phyllite; metamorphic grade increases towards the Nelson batholith, with hornfelsic biotite-staurolite-andalusite (\pm garnet) and biotite-sillimanite-garnet assemblages

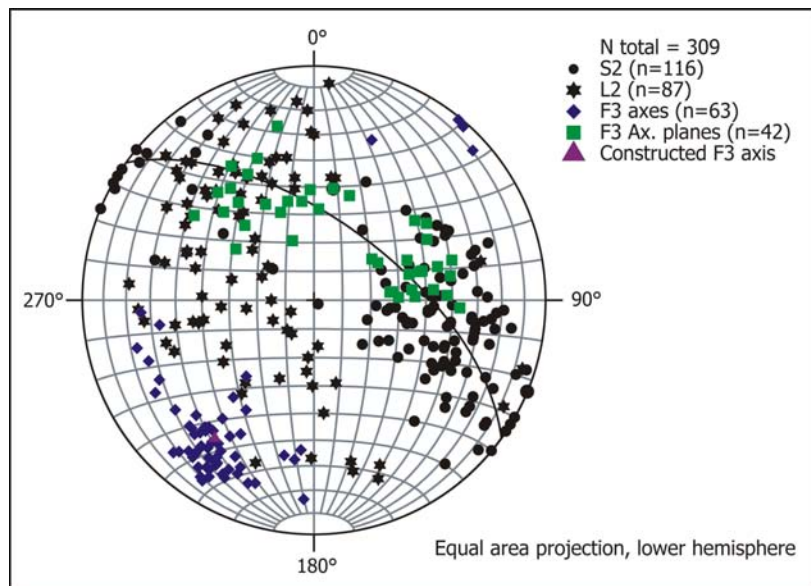


Figure 4. Structural data from the southwest-facing shoreline of the Crawford Peninsula, showing the folding of D_2 structures around F_{3S} axes.

developed close to its margin (Fig 6b). Southward from the latitude of Figure 2c, this low-pressure carapace (comprising the contact aureole and low-grade phyllite outside it) is progressively cut out by the Gallagher fault. It is absent from the easternmost part of the Nelson batholith, where the Gallagher fault separates deformed porphyritic granodiorite from Barrovian garnet-staurolite (+ vein kyanite)-bearing pelite.

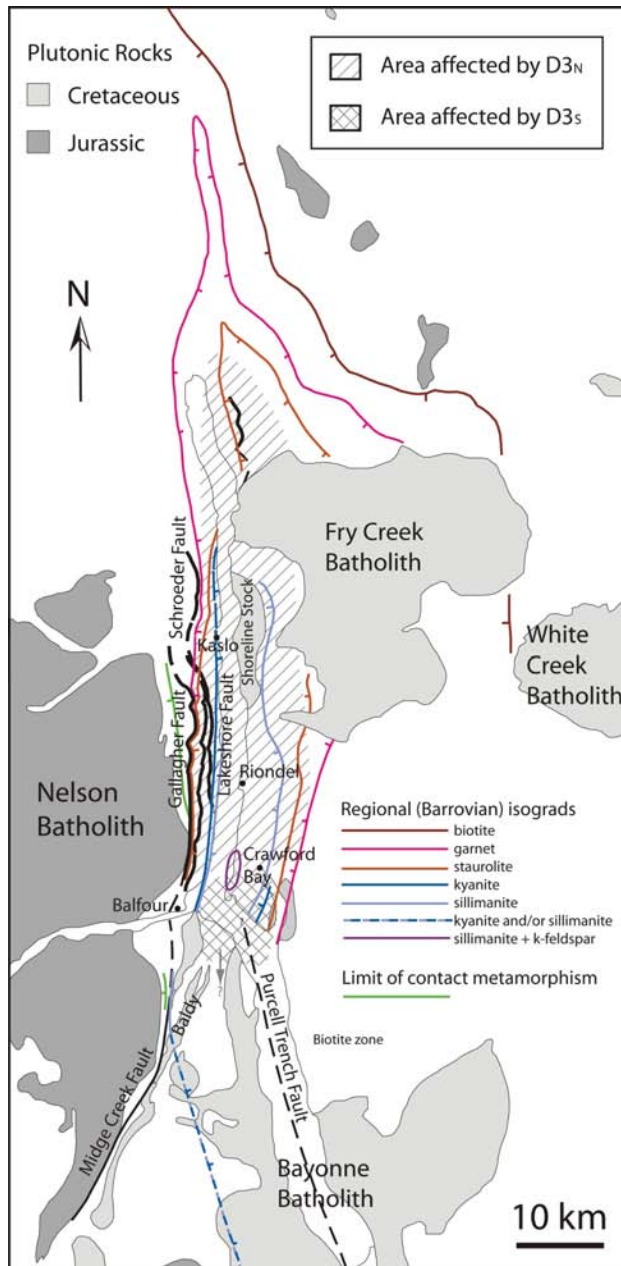


Figure 5. Isograd map of the central Kootenay Arc, compiled from Fyles (1964, 1967), Reesor (1973), Hoy (1980), Klepacki (1985), Leclair (1988) and new data. Ticks are on the high-grade side of the lines. Major normal faults are shown. The areas affected by D_{3N} and D_{3S} are approximately outlined, as are normal faults discussed in the text. Deformation D_{3S} correlates with the D_3 of Leclair (1988) in the northern part of the Midge Creek area (south of the West Arm), and may continue further south.

An appreciation for the significance of the metamorphic contrast across the Gallagher fault is gained by considering the pressure-temperature conditions under which assemblages on either side of the fault formed. Figure 7 displays the stable mineral assemblage as a function of pressure and temperature for a rock with the composition of an average pelite. The temperature ranges of the two sets of assemblages overlap, but there is a difference in pressure. Rocks in the contact aureole (hangingwall) were metamorphosed during the intrusion of the Nelson batholith at 3.5 to 4 kb, which is equivalent to approximately 12 to 14 km (for a crustal density of 2900 kg/m^3). Kyanite-bearing Barrovian rocks in the footwall were metamorphosed at approximately 7 kb, or a depth of around 25 km.

ARGON-ARGON GEOCHRONOLOGY

Archibald et al. (1984) carried out an extensive $^{40}\text{Ar}/^{39}\text{Ar}$ study concentrated on the southern-central part of the Kootenay Arc. They documented a trend whereby amphibolite-facies rocks in the centre of the metamorphic high yield early Tertiary mica cooling ages, whereas rocks in lower grade areas cooled earlier. North of the bend in Kootenay Lake, there is a monotonic rise in biotite cooling ages, from $<55 \text{ Ma}$ in the centre of the metamorphic high to $>90 \text{ Ma}$ in the central Purcell Anticlinorium (Fig 8). The western margin of the amphibolite-facies belt was not studied, but biotite from the main (mid-Jurassic) body of the Nelson batholith yielded Jurassic to early Cretaceous cooling ages, consistent with earlier studies.

Mathews (1983) dated samples along an east-west transect around the latitude of Figure 2c (Fig 9). Samples from the footwall of the Gallagher fault yielded $^{40}\text{Ar}/^{39}\text{Ar}$ ages of 59 Ma (muscovite) and 53 Ma (whole rock), whereas the lone hangingwall sample yielded a whole-rock cooling age of 131 Ma (early Cretaceous). The Purcell Trench fault also marks the locus of a discrete change in $^{40}\text{Ar}/^{39}\text{Ar}$ cooling ages. The difference in cooling ages across the Purcell Trench decreases from south to north, leading Archibald et al. (1984) to conclude that the fault dies out in the central Kootenay Lake region, around the inflection point in the lake.

DISCUSSION

The structural, metamorphic and geochronological evidence presented above reveals contrasts in the thermal and tectonic histories of rocks now exposed around central and northern Kootenay Lake. There is a systematic variation in structural, metamorphic and isotopic characteristics with structural level. Rocks from low structural levels, in the centre of the metamorphic high, apparently reached peak metamorphic conditions in the mid-Cretaceous and did not cool below 350°C (the closure temperature of muscovite) until the early Tertiary, when they were exhumed by D_3 extensional deformation. They record considerable D_2 strain, and experienced further ductile deformation during exhumation. Lower grade rocks at high structural levels were metamorphosed and cooled earlier, underwent mild D_2 deformation and did not experience D_3 . The area west of the Gallagher fault was deformed and metamorphosed in the mid-Jurassic and cooled through the biotite closure temperature ($\sim 250^\circ\text{C}$) by the early Cretaceous. It has remained at high crustal levels since then, behaving as a

relatively unmodified 'lid', while rocks at lower levels were metamorphosed and intensely deformed.

These different structural levels are juxtaposed across the Gallagher fault on the west flank of the amphibolite-facies belt. There is a discrete change in structural geology, in metamorphic grade and in $^{40}\text{Ar}/^{39}\text{Ar}$ cooling ages. This contrasts with the eastern margin, where there is a monotonic decrease in metamorphic grade and rise in cooling ages. This east-west asymmetry is a first-order characteristic of the metamorphic high and is interpreted to reflect the control of the Gallagher fault and related extensional structures on its structural, metamorphic and thermochronological architecture. In the Creston area,

where the PTF marks the eastern margin of the Priest River complex, there is a similar, but reversed, east-west asymmetry in grade and cooling ages. The area south of the West Arm is a horst situated in the transfer zone between the two major faults. Early Tertiary extension did not just involve normal faulting; there was also widespread extensional shearing and folding around the tip zone of the PTF.

Given the significance of the Gallagher fault just north of the West Arm, and the close proximity of Barrovian and Buchan rocks along strike to the south (west of the Baldy pluton), the fault probably continues across the West Arm. One possibility is that it is represented by the Midge Creek fault, which separates the Lardeau and Milford groups and

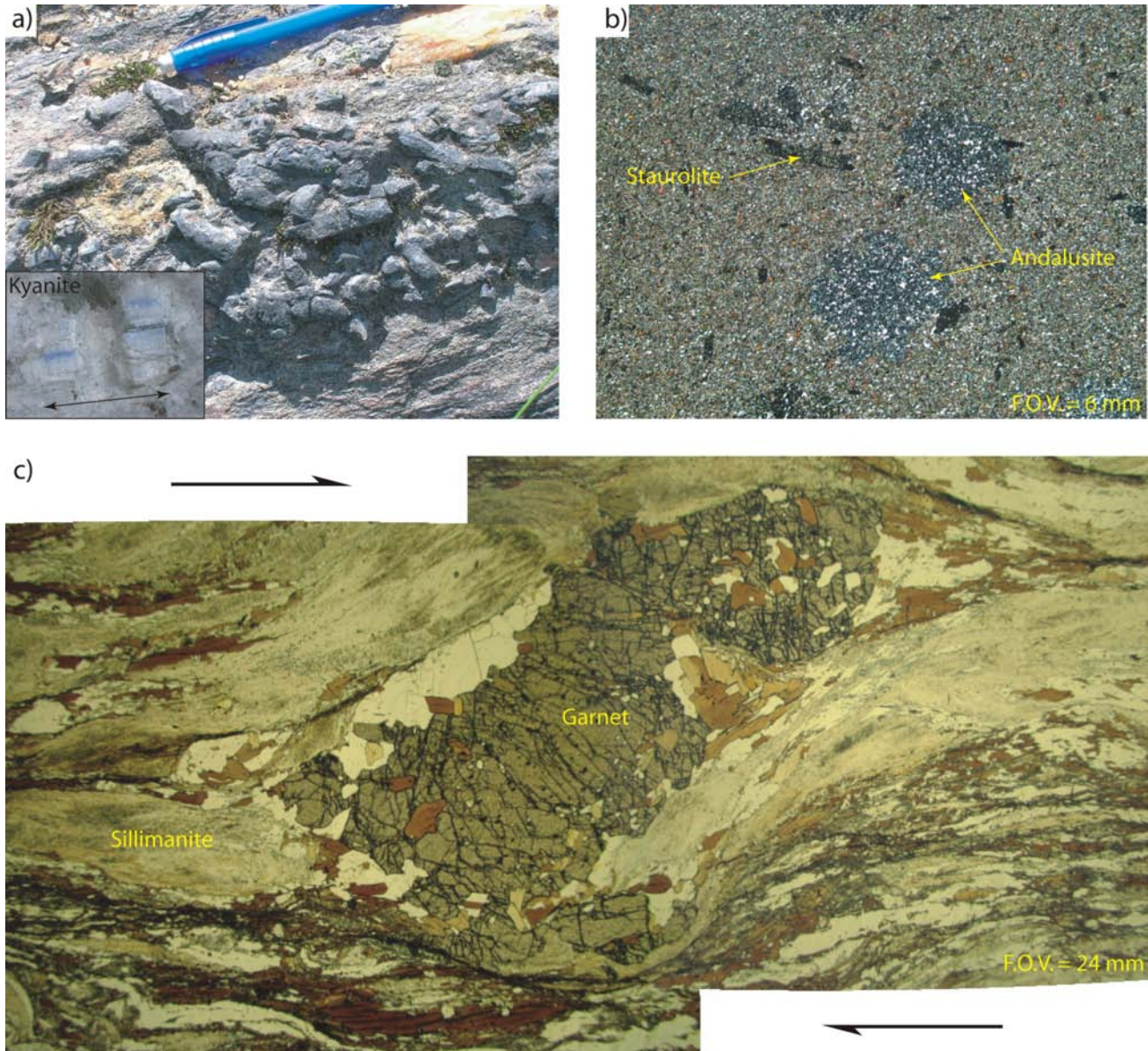


Figure 6. a) Staurolite porphyroblasts in garnet-staurolite schist directly east of the Gallagher fault (footwall). Kyanite is present in veins at this locality. Veins are synmetamorphic, as there is an increase in the abundance and size of porphyroblasts adjacent to vein boundaries. The kyanite is boudinaged, with a subhorizontal extension direction. b) Staurolite and andalusite porphyroblasts in contact metamorphosed pelite from the hangingwall of the Gallagher fault. This assemblage indicates metamorphism under significantly lower pressure conditions than the rock shown in a). c) Asymmetric strain shadows on garnet porphyroblast in garnet-sillimanite schist from the Rionde l area. Evidence for west-side-down shearing such as this is restricted to the Barrovian rocks in the footwall of the Gallagher fault.

lies between the contact aureole of the Nelson batholith and regional sillimanite zone rocks (Fig 2d). To the north, the staurolite isograd diverges from the trace of the Gallagher fault as the contrast in metamorphic grade across the fault decreases. Around Kaslo, staurolite and kyanite are restricted to the footwall of the Lakeshore-Schroeder fault, as are D_{3N} structures (Fig 5). As is the case with the Gallagher fault further south, the hangingwall contains low-grade phyllite, unaffected by D_{3N} . It appears, therefore, that as the Gallagher fault dies out, the Schroeder fault becomes the major structure marking the western boundary of the metamorphic high. The relationship between isograds and faults cannot be documented in the Duncan Lake area due to the northward decrease in grade and the relative scarcity of indicative mineral assemblages.

Although there is a ~ 3 kb pressure difference between the contact aureole and kyanite-bearing rocks (equivalent to approximately 10 km), this cannot be translated into an estimate of vertical offset across the Gallagher fault. Assessment of displacement is complicated by uncertainty in

the pressure difference across the fault itself, in the age(s) of Barrovian metamorphism and in the spacing of isobars in the footwall rocks.

There is a west to east increase in metamorphic grade in the immediate footwall of the Gallagher fault, and possibly also in the pressure of peak metamorphism. Rocks directly east of the fault (garnet-staurolite (+ vein kyanite)-bearing pelite) were metamorphosed in the kyanite field, but the pressure may not have been as high as in slightly higher grade rocks further east. This issue will be clarified with future detailed petrological study. Low-grade phyllite outside the contact aureole of the Nelson batholith was regionally metamorphosed prior to the intrusion of the batholith. If the amphibolite-facies Barrovian metamorphism is a similar age, exhumation prior to the intrusion of the Nelson batholith could account for much of the observed pressure difference. However, Leclair et al. (1993) presented evidence for a mid-Cretaceous age for Barrovian metamorphism in the sillimanite zone. If Barrovian metamorphism is mid-Cretaceous directly east of the fault, this

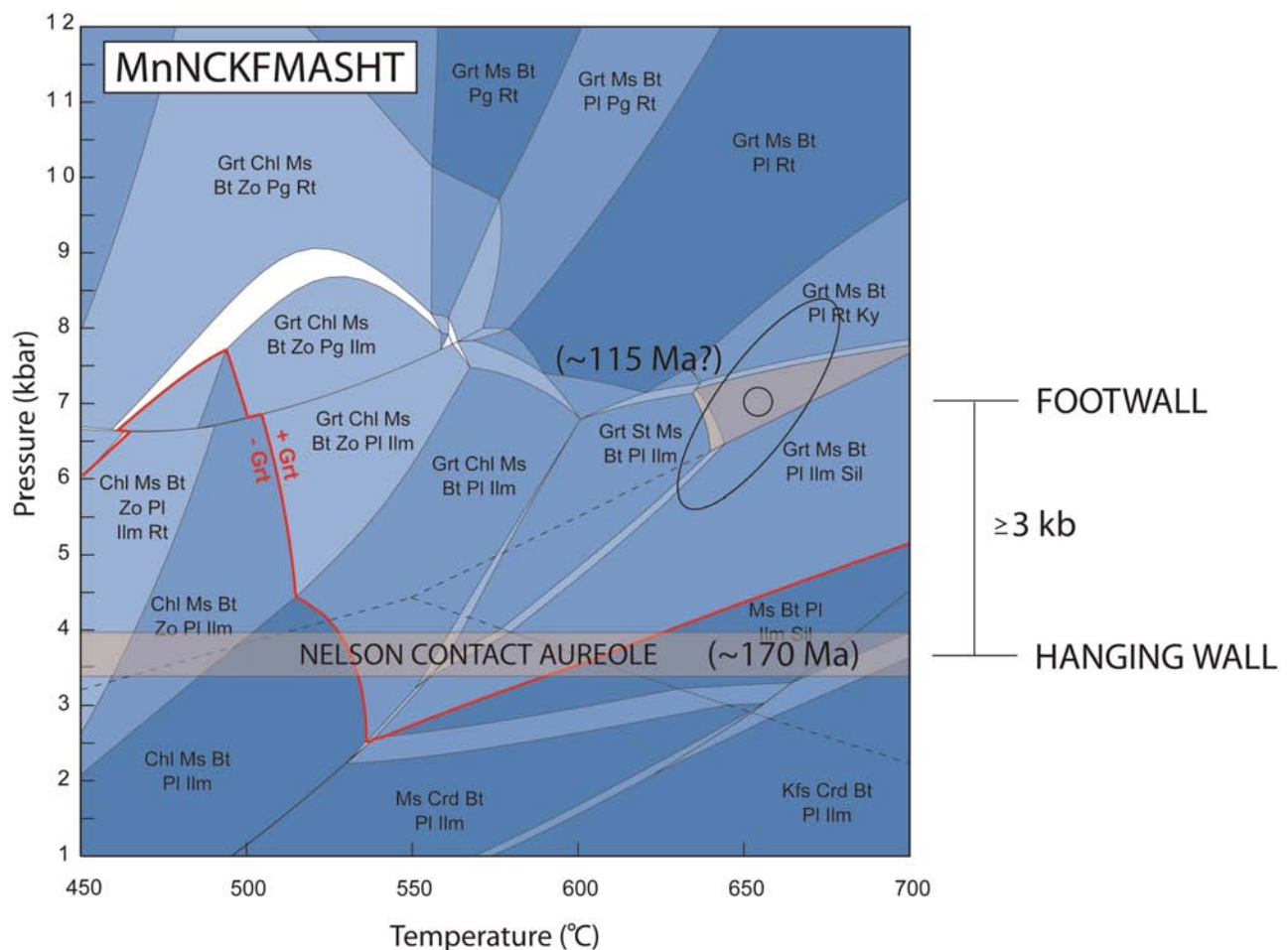


Figure 7. Mineral assemblage stability diagram for an average pelite composition from Tinkham and Pattison (pers comm, 2007). The lower shaded band indicates the pressure during contact metamorphism in the hangingwall of the Gallagher fault. The upper shaded areas are the garnet-staurolite-kyanite and garnet-kyanite fields (each with quartz, muscovite, biotite, plagioclase and ilmenite). These assemblages are developed in the footwall of the Gallagher fault and indicate pressures approximately 3 kb higher than those in the hangingwall. This is equivalent to a difference in burial depth of ~ 10 km. Also shown is a Thermocalc (Powell and Holland, 1988) average P-T estimate (with 2σ error ellipse) from a garnet-staurolite-kyanite schist collected close to the Lakeshore fault northwest of the Riondel nappe. Contact metamorphism accompanied the intrusion of the Nelson batholith around 170 Ma, whereas Barrovian metamorphism probably took place in the mid-Cretaceous.

rules out pre-Nelson batholith exhumation, and appears to require a much larger offset on the fault. Planned U-Pb dating will clarify the age(s) of peak metamorphism throughout the Barrovian sequence.

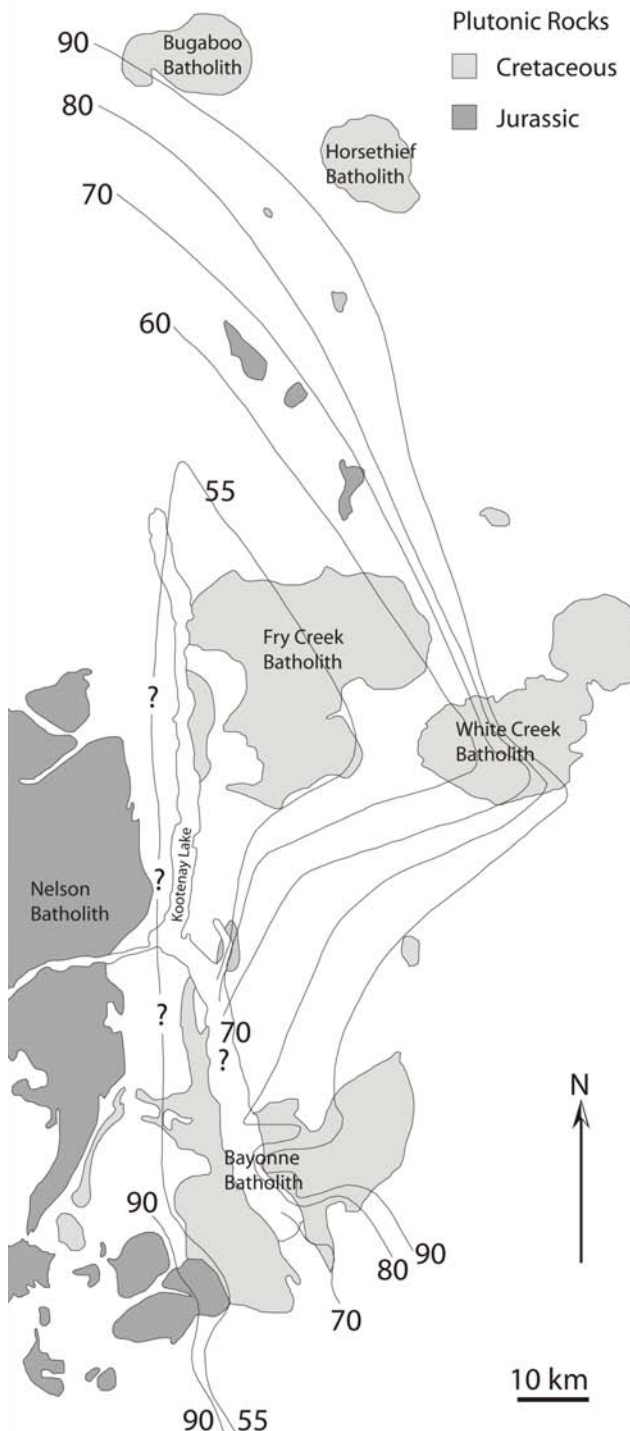


Figure 8. Biotite $^{40}\text{Ar}/^{39}\text{Ar}$ cooling ages from Archibald et al. (1984). The geometry is similar to that of the isograds (Fig 5). Cooling ages rise steadily from <55 Ma in the centre of the metamorphic high to >90 Ma in the Purcell Anticlinorium. The difference in cooling ages across the Purcell Trench decreases northward towards the bend in Kootenay Lake, where the Purcell Trench fault dies out and the Gallagher fault becomes the main extensional structure.

Aside from uncertainties in the peak metamorphic pressure profile and age(s) of Barrovian metamorphism, the use of metamorphic pressure contrasts to infer displacement is potentially problematic. Another complicating factor that must be considered is the possibility of late- D_2 deformation of isobars and isograds. As isobars and isograds behave as passive markers in the rock after peak metamorphic quenching, post-peak metamorphic (late D_2) thinning could have resulted in telescoping of isobars, thereby reducing the amount of offset required on the Gallagher fault to account for the observed pressure difference. Although the Gallagher fault represents a major geological discontinuity, the fact that isograds diverge from the fault trace south of Kaslo provides support for a relatively conservative estimate.

CONCLUSIONS

The metamorphic high in the central Kootenay Arc results from differential exhumation during early Tertiary extensional deformation. Deformation involved discrete faulting and ductile footwall strain. North of the bend in Kootenay Lake, the amphibolite-facies belt is fault-bounded on its west side; south of the bend it is fault-bounded on the east side. The bend in the lake marks the area where extensional strain was transferred from the Purcell Trench fault to the Gallagher-Schroeder fault system. Normal faulting was accompanied by west-side-down shearing and extension of S_2 in the footwall north of the bend, whereas S_2 was simultaneously buckled around the tip zone of the Purcell Trench fault. Normal faulting and related shearing has juxtaposed rocks with different structural and P-T-t histories.

ACKNOWLEDGMENTS

This work was funded by the Targeted Geoscience Initiative III, and Natural Sciences and Engineering Research Council (NSERC) Discovery Grants to Pattison (037233) and Philip Simony. Thanks to Travis Murphy and Hannah Mills for excellent field assistance, and to Thomas Choquette, Gennyne McCune and Chris Coüeslan for additional help.

REFERENCES

- Archibald, D.A., Krogh, T.E., Armstrong, R.L. and Farrar, E. (1984): Geochronology and tectonic implications of magmatism and metamorphism, southern Kootenay Arc and neighbouring regions, southeastern British Columbia. Part II: mid-Cretaceous to Eocene; *Canadian Journal of Earth Sciences*, Volume 21, pages 567–583.
- Berthé, D., Choukroune, P. and Jegouzo, P. (1979): Orthogneiss, mylonite and non coaxial deformation of granites: the example of the South Armorican Shear Zone; *Journal of Structural Geology*, Volume 1, pages 31–42.
- Brandon, A.D. and Lambert, R.S.J. (1993): Geochemical characterisation of mid-Cretaceous granitoids of the Kootenay Arc in the southern Canadian Cordillera; *Canadian Journal of Earth Sciences*, Volume 30, pages 1076–1090.
- Brown, R.L., Fyles, J.T., Glover, J.K., Hoy, T., Okulitch, A.V., Preto, V.A. and Read, P.B. (1981): Southern Cordillera cross-section – Cranbrook to Kamloops; in Field guides to geology and mineral deposits, Calgary 1981 Annual Meeting, Thompson, R.I. and Cook, D.G., Editors, *Geological Association of Canada*, pages 335–372.

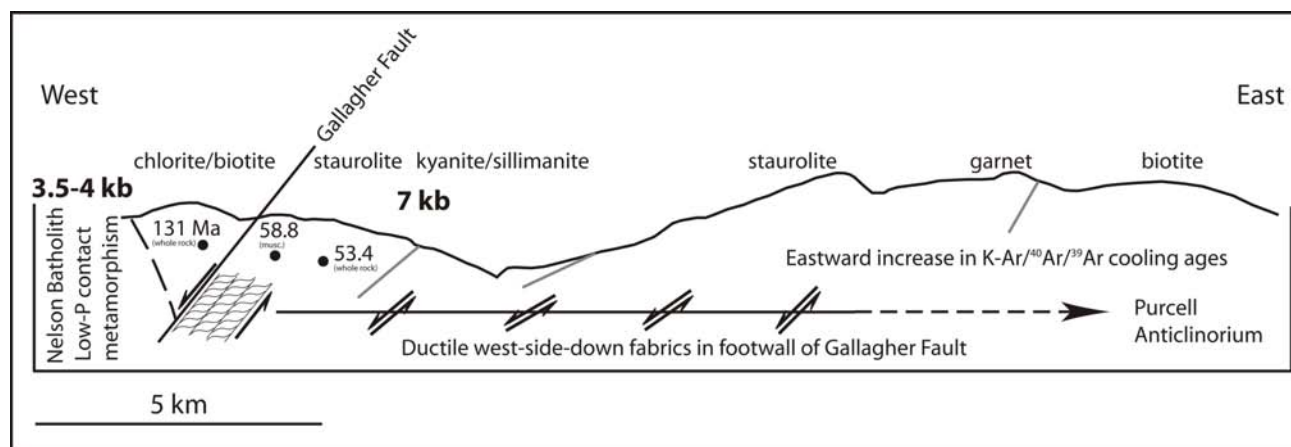


Figure 9. Cross-section across the central part of the Kootenay Arc, showing the data of Mathews (1983) in relation to the Gallagher fault, and emphasizing the asymmetry in the distribution of metamorphic grade and cooling ages. There is a sharp break in grade, structures and cooling ages across the fault, whereas the east side of the high is characterized by gradational changes in grade and cooling ages.

- Carr, S.D., Parrish, R. and Brown, R.L. (1987): Eocene structural development of the Valhalla complex, southeastern British Columbia; *Tectonics*, Volume 6, pages 175–196.
- Colpron, M. and Price, R.A. (1995): Tectonic significance of the Kootenay Terrane, southeastern British Columbia: an alternative model; *Geology*, Volume 23, pages 25–28.
- Doughty, P.T. and Price, R.A. (1999): Tectonic evolution of the Priest River complex, northern Idaho and Washington: a reappraisal of the Newport fault with new insights on metamorphic core complex formation; *Tectonics*, Volume 18, pages 375–393.
- Fyles, J.T. (1964): Geology of the Duncan Lake area, British Columbia; *BC Ministry of Mines, Energy and Resources*, Bulletin 49, 87 pages.
- Fyles, J.T. (1967): Geology of the Ainsworth-Kaslo area, British Columbia; *BC Ministry of Energy, Mines and Petroleum Resources*, Bulletin 53, 125 pages.
- Ghosh, D.K. (1995): U-Pb geochronology of Jurassic to early Tertiary granitic intrusives from the Nelson-Castlegar area, southeastern British Columbia, Canada; *Canadian Journal of Earth Sciences*, Volume 32, pages 1668–1680.
- Hoy, T. (1980): Geology of the Riondel area, Central Kootenay Arc, southeastern British Columbia; *BC Ministry of Energy, Mines and Petroleum Resources*, Bulletin 73, 89 pages.
- Klepachki, D.W. (1985): Stratigraphy and structural geology of the Goat Range area, southeastern British Columbia; unpublished PhD thesis, *Massachusetts Institute of Technology*, Cambridge, Massachusetts, U.S.A., 268 pages.
- Leclair, A.D. (1988): Polyphase structural and metamorphic histories of the Midge Creek area, southeast British Columbia: implications for tectonic processes in the central Kootenay Arc; unpublished PhD thesis, *Queens University*, Ontario, Canada, 264 pages.
- Leclair, A.D., Parrish, R.R. and Archibald, D.A. (1993): Evidence for Cretaceous deformation in the Kootenay Arc on U-Pb and $^{40}\text{Ar}/^{39}\text{Ar}$ dating, southeastern British Columbia; Current Research, Part A, *Geological Survey of Canada*, Paper 93-1A, pages 207–220.
- Livingstone, K.W. (1968): Geology of the Crawford Bay Map-Area; unpublished MSc thesis, *The University of British Columbia*, Vancouver, Canada, 87 pages.
- Mathews, W.H. (1983): Early Tertiary resetting of potassium-argon dates in the Kootenay Arc, southeastern British Columbia; *Canadian Journal of Earth Sciences*, Volume 20, pages 867–872.
- Pattison, D.R.M. and Vogl, J.J. (2005): Contrasting sequences of metapelitic mineral-assemblages in the aureole of the tilted Nelson batholith, British Columbia: implications for phase equilibria and pressure determinations in andalusite-sillimanite-type settings; *The Canadian Mineralogist*, Volume 43, pages 51–88.
- Platt, J.P. and Vissers, R.L.M. (1980): Extensional structures in anisotropic rocks; *Journal of Structural Geology*, Volume 2, pages 397–410.
- Ponce de Leon, M.I. and Choukroune, P. (1980): Shear zones in the Iberian Arc; *Journal of Structural Geology*, Volume 2, pages 63–68.
- Powell, R. and Holland, T.J.B. (1988): An internally consistent thermodynamic dataset with uncertainties and correlations. 3. Application to geobarometry methods, worked examples and a computer program; *Journal of Metamorphic Geology*, Volume 6, pages 173–204.
- Ramsay, J.G. (1967): *Folding and Fracturing of Rocks*; McGraw Hill, Inc., 568 pages.
- Reesor, J.E. (1996): Geology, Kootenay Lake, British Columbia; *Geological Survey of Canada*, Map 1864A, scale 1:100 000.
- Reesor, J.E. (1973): Geology of the Lardeau map-area, east half, British Columbia; *Geological Survey of Canada*, Memoir 369, 129 pages.
- Thompson, R.I., Glombick, P., Erdmer, P., Heaman, L.M., Lemieux, Y. and Daughtry, K.L. (2007): Evolution of the ancestral Pacific margin, southern Canadian Cordillera: insights from new geologic maps; in *Palaeozoic Evolution and Metallogeny of Pericratonic Terranes at the Ancient Pacific Margin of North America*, Canadian and Alaskan Cordillera, Colpron, M. and Nelson, J.L., Editors, *Geological Association of Canada*, Special Paper 45, pages 433–482.
- Warren, M.J. (1997): Crustal extension and subsequent crustal thickening along the Cordilleran rifted margin of ancestral North America, western Purcell Mountains, southeastern British Columbia; unpublished PhD thesis, *Queens University*, Ontario, Canada, 361 pages.
- White, S.E., Burrows, S.E., Carreras, J., Shaw, N.D. and Humphreys, F.J. (1980): On mylonites in ductile shear zones; *Journal of Structural Geology*, Volume 2, pages 175–187.
- Williams, P.F. and Price, G.P. (1990): Origin of kinkband and shear-band cleavage in shear zones: an experimental study; *Journal of Structural Geology*, Volume 12, pages 145–164.

Terrace Regional Mapping Project, Year 3: Contributions to Stratigraphic, Structural and Exploration Concepts, Zymoetz River to Kitimat River, East-Central British Columbia (NTS 103I/08)

by J. Nelson, J. Kyba¹, M. McKeown and J. Angen²

KEYWORDS: Terrace, Stikinia, regional geology, VMS, Paleozoic, Telkwa

INTRODUCTION

Now in its third year, the Terrace regional mapping and mineral potential evaluation project focuses on bringing modern geological concepts to bear on the region around Terrace, BC — an area that has seen comparatively little recent exploration-oriented regional geological work (Fig 1; see Nelson et al., 2006a; Nelson and Kennedy, 2007a).

Geological mapping in the summer of 2007 has now extended coverage into the Christ Creek map area, 103I/08, continuing south from the Usk (103I/09) area to the north completed in 2005 (Nelson et al., 2006b). Two and a half months were spent in the area, with traverses by four-wheel drive along main roads; on foot, bicycle and horse on decommissioned and overgrown forest roads; and out of helicopter-accessed remote camps on foot and ski, the last made necessary due to exceptional snow levels from the winter of 2006–2007.

The most important new geological and exploration-related observations include

- recognition of an extensive Paleozoic metavolcanic unit that stratigraphically underlies Lower Permian limestone over a strike length of 25 km, from Zymoetz River to Chist Creek and probably beyond;
- recognition of the exploration potential of the Paleozoic volcanic unit, in that it contains broad zones of syngenetic alteration (quartz-sericite schist) accompanied by local occurrences of volcanogenic sulphide occurrences;
- definition of regional northeast-trending folds within the combined Paleozoic to Early Mesozoic stratigraphy;
- delineation of two felsic marker units that serve as a basis for stratigraphy within the Telkwa Formation;
- probably continuation of the Eocene Skeena River detachment fault system into the lowest elevations along Williams Creek, Chist Creek and the Kitimat River.

¹ Hard Creek Nickel Corporation, Vancouver, BC

² University of Victoria, School of Earth and Ocean Sciences, Victoria, BC

This publication is also available, free of charge, as colour digital files in Adobe Acrobat® PDF format from the BC Ministry of Energy, Mines and Petroleum Resources website at http://www.em.gov.bc.ca/Mining/GeolSurv/Publications/catalog/cat_fldwk.htm

PREVIOUS WORK

The first modern geological mapping in the Terrace area is by G. Woodsworth and colleagues (Woodsworth et al., 1985; Gareau et al., 1997a, b; G. Woodsworth, unpublished 1:100 000 scale maps), which has provided an invaluable framework for subsequent study. As part of that project, M. Mihalynuk completed a MSc thesis, which involved mapping of ridges south of the Zymoetz (Copper) River (Mihalynuk, 1987); this, along with his unpublished field maps, gave us a much-appreciated introduction to stratigraphy and structure in the Chist Creek map area.

GEOLOGY

Overview

Stratified units in the Chist Creek map area range in age from pre-Early Permian to Early Jurassic (Fig 2, 3). They include volcanic, volcanoclastic and overlying carbonate strata of the Permian and older Zymoetz Group (Nelson et al., 2006a), overlain by extensive exposures of the mainly subaerial volcanic Howson facies of the Early Jurassic Telkwa Formation (see Tipper and Richards, 1976). The sequence is deformed into a broad, regional northeasterly plunging anticline cored by the pre-Permian volcanic unit. On the limbs, faulted panels of Telkwa Formation strata dip to the east and north-northeast (Fig 2, 3). This folded Paleozoic to Early Mesozoic stratigraphic sequence, along with Early Jurassic granitoid rocks of the Kleanza pluton, lies in the hangingwall of the Skeena River fault system. The Skeena River fault system is a zone of regional detachment located within the Skeena River valley, with interpreted early thrust and later, Eocene normal, top-to-the-northeast sense of motion (Gareau et al., 1997a, b; Nelson and Kennedy, 2007a, b). A few outcrops of ductilely deformed metavolcanic and plutonic rocks in the Williams Creek, Chist Creek and Kitimat River valleys probably constitute a continuation of the detachment surface. Undeformed granite and granodiorite of the Williams Creek pluton cuts both the hangingwall panel and the ductilely deformed zones. This pluton is assumed to be of Eocene age, in that it closely resembles the Carpenter Creek pluton in the Usk map area to the northwest.

Stratified Units

ZYMOETZ GROUP

The name Zymoetz Group was proposed by Nelson et al. (2006a) for a section of Permian volcanogenic and marine sedimentary strata overlain by limestone that outcrops

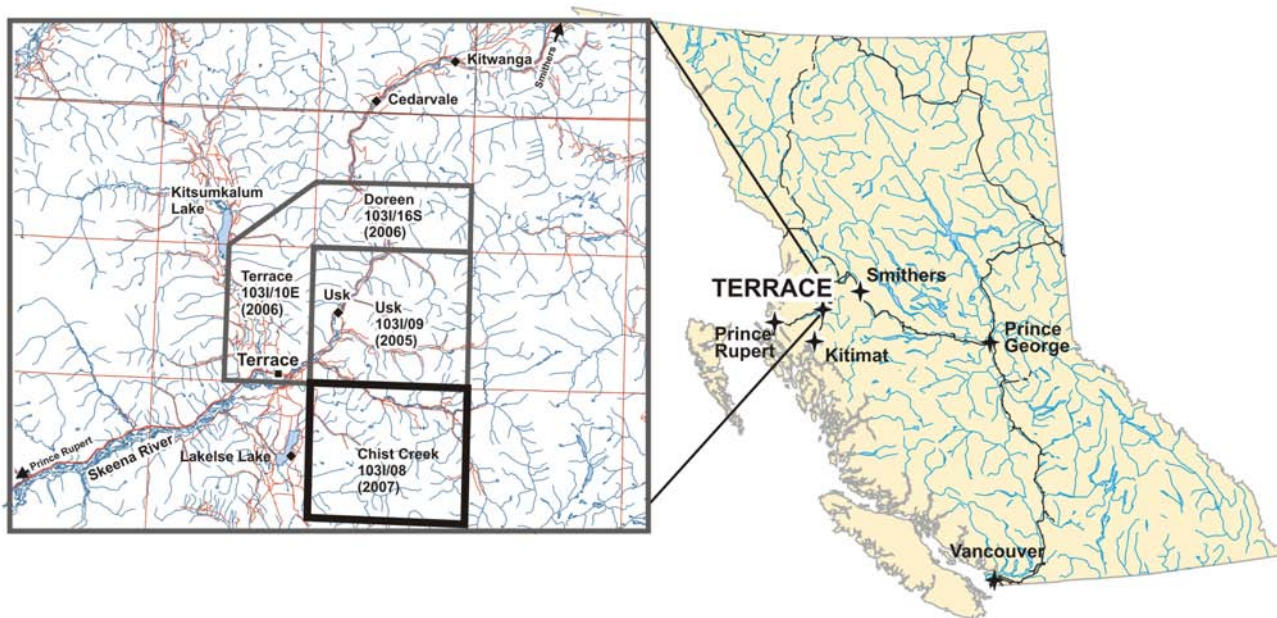


Figure 1. Location of the Chist Creek map area near Terrace, BC.

within and south of the lower Zymoetz River valley in the Usk map area. These strata have now been traced over 25 km to the south in the lower reaches of Chist Creek, and may well extend farther south and west. The Zymoetz Group is divided into two units: a lower, volcanogenic unit named the Mount Attree volcanics, overlain by Lower Permian limestone that is age-equivalent to, and correlative with, the Ambition Formation of Gunning et al. (1994).

Mount Attree Volcanics

This unit is named for Mt Attree, a prominent summit on the ridge between the Zymoetz River and Williams Creek. Its dominant composition is andesitic and it is seen as flows, pyroclastic and epiclastic beds (Fig 4).

On Mt Attree and along the ridge to the east, dark green plagioclase and augite-phyric andesite and basalt flows are interbedded with volcanic breccia and lapilli tuff, with minor marble and calcsilicate layers. At two localities 7 km east of Mt Attree, the upper part of the unit is an unusual succession of rhyolite, quartz-sericite schist, grey cordierite-bearing graphitic phyllite and conglomerate (Fig 2; Nelson et al., 2008). The lower conglomerate beds interfinger with black argillite, phyllite and greywacke; they grade up into fossiliferous calcirudite with siliceous, tuffaceous laminae. Clasts tend to be very well rounded, in contrast to the more subrounded to angular clasts in the basal Telkwa conglomerate rocks. They are dominantly of siliceous composition, a further suggestion of maturity and significant reworking. Clasts include recrystallized chert and argillite, plagioclase-rich dacite, and large, embayed single quartz phenocrysts, enclosed in a variably foliated matrix of sericite, quartz, biotite, actinolite and in some cases, postkinematic andalusite. The high degree of foliation within this sequence contrasts with the limestone above it, and suggests that an episode of deformation affected the unit prior to the deposition of the overlying limestone. North of the present area, tuff within the upper part of the volcanogenic unit have yielded a ca. 285 Ma, Early Permian, U-Pb age (Gareau et al., 1997a).

South of Williams Creek, well-bedded volcanoclastic units — fine-grained andesite, dacite and rhyolite tuff and lesser coarse plagioclase and augite-phyric volcanic breccia — are more abundant than flows. The degree of foliation and metamorphic grade increases towards the south and west. The dark green phyllite that outcrops along Chist Creek was probably the source of its name, as locals pronounce it ‘Schist Creek’. The succession south of Williams Creek contains an upper marker unit composed of thinly bedded epiclastic sandstone, mudstone and tuff; and a lower unit of thin calcsilicate and marble interlayered with tuffaceous phyllite. These units define a gently warped trend (Fig 2). Facing directions along it are to the northeast and southeast, and no structural repetition is indicated. On the ridge between Williams and Chist Creek, a broad area of quartz-sericite schist alteration and strong gossan development occurs within the Mt Attree volcanics (Fig 5).

Although heavily masked by alteration, felsic intrusive and extrusive phases form an integral part of this system, which is described in a separate paper (McKeown et al., 2008). Within the quartz-sericite schist, there are small, widespread areas of base-metal sulphides; and a new showing, the Sub, contains barite as well silica-facies alteration zones that together define a small syngenetic exhalative system (McKeown et al., 2008).

The Mt Attree volcanics are a newly defined unit that occupies an area assigned to the Jurassic Telkwa Formation on earlier regional maps (cf. Woodsworth et al., 1985). Although some rock types within it, such as plagioclase and augite-phyric andesite breccia, resemble the lower Telkwa, it differs critically from the Telkwa in a number of important respects:

- It is depositionally, probably unconformably, overlain by Permian limestone, which forms a continuous band from the ridge east of Mt Attree, to the ridge west of Flat Top Mountain.
- It contains marble, calcsilicate and black phyllitic units that are incompatible with the terrestrial origin of the Telkwa Formation in this area.

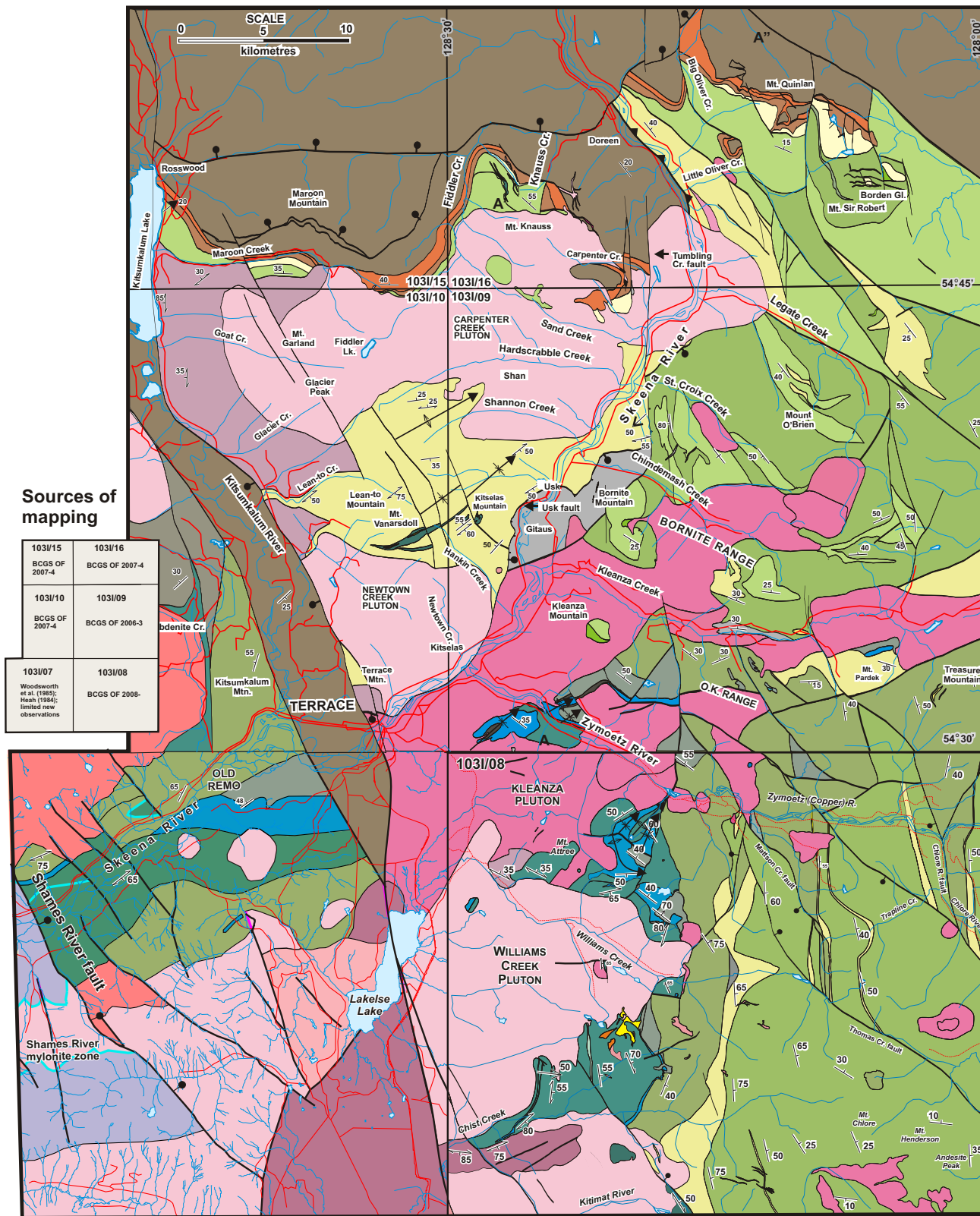
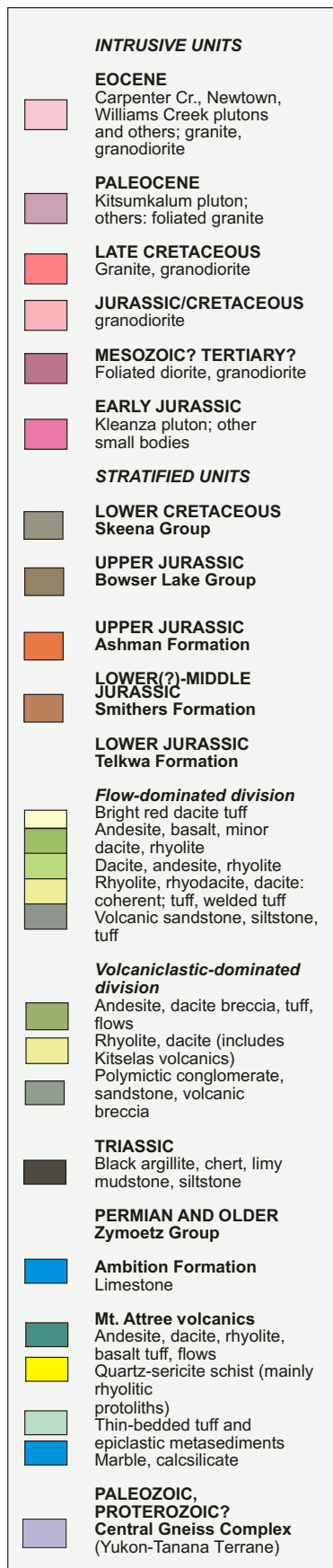


Figure 3. Geology of the Terrace area, compiled from field mapping at 1:20 000 scale in 2005 to 2007 (Nelson et al., 2006b; Nelson and Kennedy, 2007b), with additional data from Woodsworth et al. (1985) and Heah (1991) via the BC Geological Survey compilation on the MapPlace.



Legend for Figure 3.

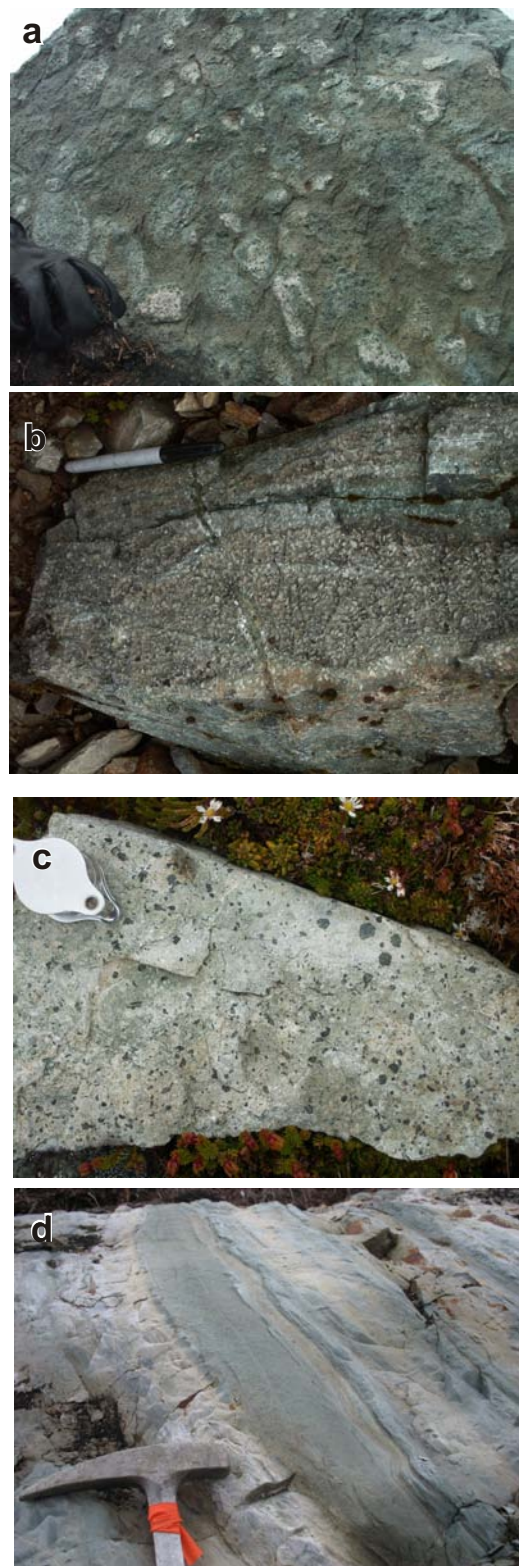


Figure 4. Andesite volcanic variations in the Mt Attree volcanics: a) pyroclastic breccia of augite-plagioclase-phyric andesite clasts, Chist Creek; station 07JK16-1; b) typical plagioclase-phyric coherent andesite, flow on ridge east of Mt Attree; station 07MM18-02; c) augite-plagioclase-phyric coherent andesite, flow on ridge east of Mt Attree; station 07JN17-04; d) bedded andesitic tuff and epiclastic greywacke and mudstone, Chist Creek; station 07JK16-12.

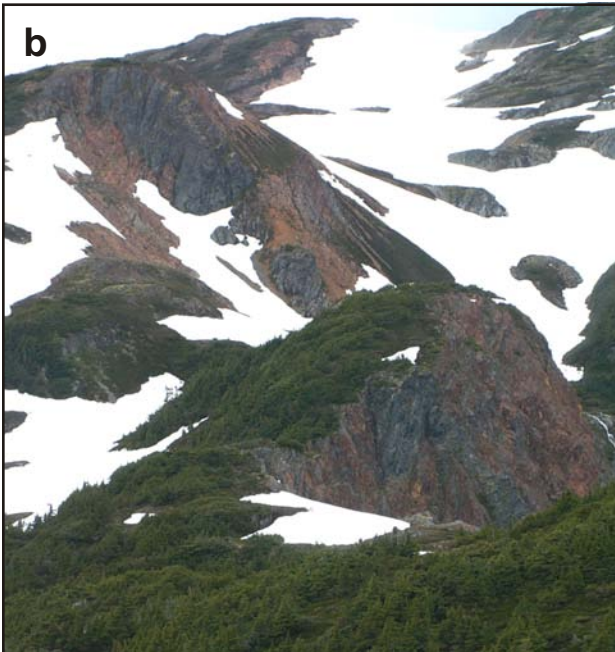


Figure 5. a) Rusty, pyritic quartz-sericite schist in Mt Attree volcanics south of Williams Creek. The protolith is a quartz-phyric rhyolite lapilli tuff. b) Gossanous, pyritic quartz-sericite schist; dark areas are highly silicified. c) Aphanitic rhyolite breccia with chlorite infillings.

- It contains significant areas of quartz-sericite schist, which are absent in the Telkwa.
- It contains rhyolite that is typically quartz-phyric, unlike the dominantly plagioclase-phyric rhyolite of the Telkwa. More siliceous compositions are suggested. The characteristic coarse, polymictic welded tuff of the Telkwa Formation is not present.
- Andesite flows in it contain only small amygdules, if any, in contrast to the large, irregular amygdules that are common in the Telkwa Formation.
- Characteristic stubby, ragged shapes of plagioclase grains in the andesite are unlike the lath-shaped phenocrysts in Telkwa andesite (compare Fig 4b with Fig 7e).
- The degree of foliation within it stands in strong contrast to overlying Telkwa volcanic units, which are completely unfoliated.
- Greenschist to lower-amphibolite grade, synkinematic metamorphic assemblages contrast with the nearby basal Telkwa, which locally contains epidote-actinolite contact-related assemblages but is regionally metamorphosed in zeolite facies (Mihalynuk, 1987).

It should be noted that some conglomeratic units that were included within the Paleozoic section north of the Zymoetz River by Nelson et al. (2006a, b) have been re-assigned to the basal Telkwa in current mapping (compare Fig 3, this paper, with Fig 4, Nelson et al., 2006a). Work in 2007 has enhanced our appreciation of the variability within the basal Jurassic conglomerate rocks and reinforced their stratigraphic position above the Permian limestone.

Ambition Formation

A unit of thick, in part richly fossiliferous, limestone outcrops from the Zymoetz River through the ridge east of Mt Attree, across Williams Creek and south to the ridge west of Flat Top Mountain (Fig 6a, b).

Macrofossil identifications by previous workers have identified the limestone as of Permian age (Duffell and Souther, 1964; Woodsworth et al., 1985; Gareau et al., 1997b). It is correlative with the Ambition Formation in the Iskut area of northern Stikinia (Gunning et al., 1994). White and red secondary chert replace beds in some areas and thin tuff beds are present locally, particularly near the base of the unit. North of the Zymoetz River, a mixed carbonate-volcaniclastic facies consists of calcarenite interbedded with limy volcanic sandstone.

The base of the Ambition Formation on top of the Mt Attree volcanics is sharp, with small-scale irregular relief. Pods of limestone within the top few decimetres of the volcanic pile may attest to slumping and the formation of olistostrome deposits, and/or to the deposition of limy material within open spaces in its substrate.

TELKWA FORMATION (HAZELTON GROUP)

Basal Unconformity

The Telkwa Formation lies above an unconformable surface. Bedding-parallel relationships between strata above and below it, for instance between Permian limestone and greywacke in the basal Telkwa, are consistent with a paraconformable contact. Regionally, however, the unconformity bevels through the thin Upper Triassic unit

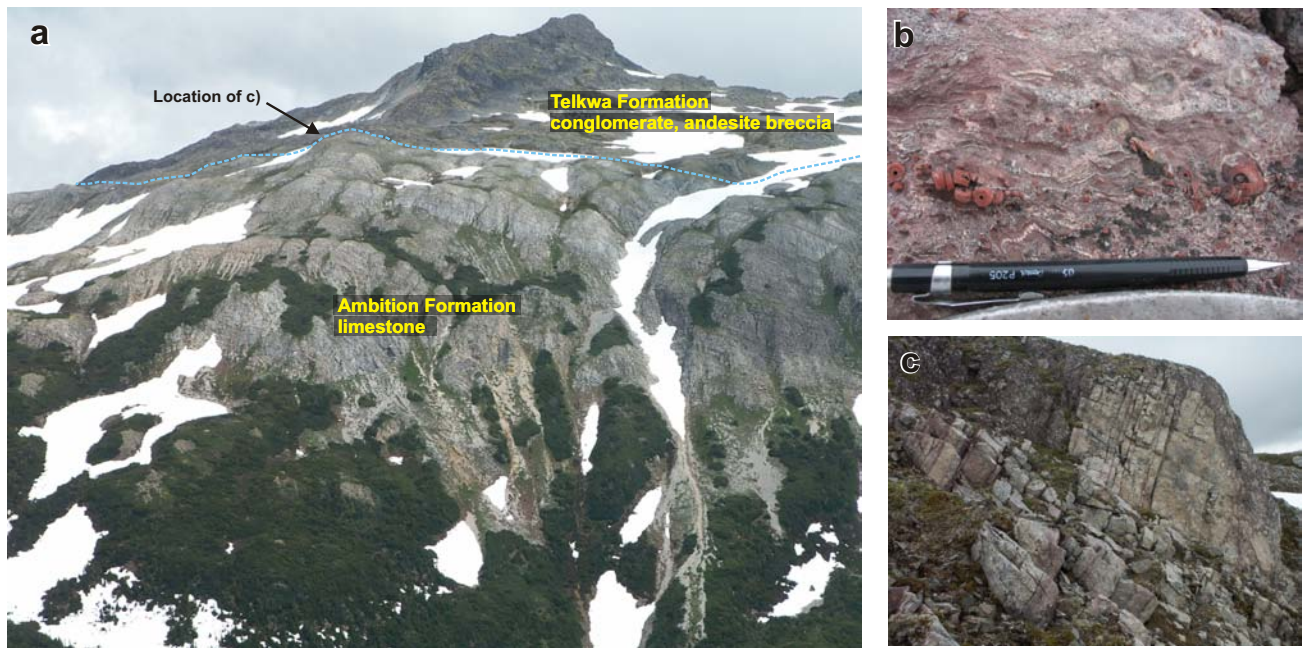


Figure 6. a) Ambition Formation at the headwaters of 8 Mile Creek. Here the well-bedded, fossiliferous limestone is overlain by conglomerate and breccia at the base of the Telkwa Formation. b) Silica-hematite-replaced crinoid segments in limestone. Note the crinoid calyx at the far left; station 07JK24-11. c) Detail of basal Telkwa unconformity. Note the strong relief on contact and the penetration of conglomerate along bedding planes. Overall both limestone and conglomerate dip steeply northeast: this part of the basal contact was originally steep and possibly karst controlled.

north of the Zymoetz River and in part through the Permian limestone. At a number of localities on the ridge east of Mt Attree, Telkwa conglomerate directly overlies the Mt Attree volcanics (Fig 2). In the headwaters of 8 Mile Creek and near Flat Peak, local relief on the unconformity is shown by channels cut into the limestone (Fig 6c).

Lower Telkwa Formation

The lowest unit of the Telkwa Formation, directly above the unconformity, includes both polymictic conglomerate and breccia with sparse thin interbeds of greywacke and, in a few areas, pyroclastic breccia. It grades up into, and interfingers with, polymictic and monolithic volcanic breccia sourced wholly from within the lower Telkwa. The conglomerate is overall polymictic, but in many exposures tends to be dominated by one or a few clast types that reflect local sources. For instance, limestone clasts concentrate directly above the Ambition Formation (Fig 7a), whereas augite and plagioclase-phyric andesite clasts concentrate above the Mt Attree volcanics.

In some clasts, volcanic textures are identical to those in the immediately underlying Paleozoic unit, which identifies them as externally rather than internally derived. Volcanic centres within the lower Telkwa also strongly influence the clastic composition of the conglomerate and breccia, with concentrations of felsic clasts in some areas (Fig 7b), and plagioclase-phyric or plagioclase-hornblende-augite-phyric clasts in others. The breccia in Figure 7c is related to a small dioritic centre at the base of the Telkwa Formation near Williams Creek. Early Telkwa volcanism seems to have been sourced from a series of small, explosive centres, the products of which mixed with clastic deposits.

North of the Zymoetz River and west of Dardanelle Creek, limestone olistostromes occur, containing blocks up to several metres across. Also present in these conglomerate rocks are black argillite clasts, probably derived from the Triassic beds, and densely plagioclase-phyric andesite clasts with textures similar to those seen in volcanic breccia throughout the lower Telkwa. These exposures are continuous with rocks that were interpreted as Paleozoic (Nelson et al., 2006a, b); however, the conglomerate passes transitionally upwards into typical lower Telkwa pyroclastic units, so they are redefined here as basal Telkwa.

Felsic Marker Units and the Upper Telkwa Formation

As in the Usk map area to the north, the mainly clastic and volcanoclastic lower Telkwa Formation is overlain by an upper, flow-dominated unit. In the Usk map area, the contact is marked by a discontinuous, thinly bedded sedimentary unit of volcanic greywacke and mudstone (Nelson et al., 2006a, b). Here, it is marked instead by a dacite-rhyolite unit of regional extent, the 'lower felsic marker'. There is a higher rhyolite unit within the upper flow sequence, the 'intraflow felsic marker'.

The lower felsic marker is exposed as part of continuous sections along the Mattson Creek logging road and on the road to the repeater tower east of Mattson Creek, on Treasure Mountain, and on remote ridges in the eastern part of the map area. It varies from a few hundred metres to nearly 1 km in thickness. Highly variable volcanic textures (Fig 8a–c) document a widespread felsic volcanic event. There are coherent rhyolite and dacite units with local strong flow banding and even folded flow bands; welded rhyolite tuff; bedded rhyolite and dacite lapilli tuff; and interbedded polymictic andesitic breccia, possibly derived

from uplifted parts of the underlying section or from more distant penecontemporaneous volcanic centres.

In the far southern part of the map area, between Chist Creek and the Kitimat River, the lower volcanoclastic



Figure 7. Compositional variations in the lowermost Telkwa conglomerate and breccia: a) limestone breccia, 10 m above Permian limestone, headwaters of 8 Mile Creek; b) breccia dominated by Telkwa felsic fragments, 20 m above Permian limestone, from a ridge northeast of Mt Attree; station 07JN20-3; c) plagioclase-augite-phyric pyroclastic breccia in the lowermost Telkwa Formation south of Williams Creek; note the flattened bombs.

Telkwa thins, and andesite flows occupy the section below the lower felsic marker.

Although a few andesite flows occur within the lower Telkwa, above the lower felsic marker, andesite and lesser dacite flows are dominant. These subaerial flows typify the terrestrial Howson facies of the Telkwa Formation, which extends from this area eastwards into the Howson Range to Smithers (*see* Tipper and Richards, 1976). They are generally plagioclase-phyric, with phenocrysts ranging from millimetre to centimetre scale (Fig 8e). They are also characteristically amygdaloidal (Fig 8d). Amygdules tend to be large and irregular, filled with quartz, calcite, epidote, chlorite, zeolite and rarely piedmontite. In places, zones of them define flow centres and flow tops. Flow breccia is also present, and minor maroon polymictic volcanic breccia is identical to those in the lower Telkwa.

The remote massif of Mt Clore, Mt Henderson and Andesite Peak was unmapped prior to this project (*see* Woodsworth et al., 1985). Through work in 2007, we now assign it to the upper Telkwa Formation. It is underlain by a thick section of moderately to gently dipping andesite, dacite, basalt and rhyolite flows and rhyolitic ash flow deposits, with minor maroon polymictic andesitic breccia and tuff (Fig 8f), intruded by probably comagmatic intermediate plutons (*see* Intrusive Rocks, below). It is a likely candidate for the remains of a major volcanic centre.

Intraflow Felsic Marker

A second felsic unit of regional extent occurs within the upper, flow-dominated part of the Telkwa Formation, between a few hundred metres to 2 km stratigraphically above its base. It outcrops along strike from the repeater tower road in the north, to near the Kitimat River in the south. Its maximum stratigraphic separation from the lower felsic marker is near the Kitimat River, leading to the inference that a volcanic centre was located near there, perhaps in the Clore-Henderson-Andesite massif. This intraflow felsic marker is distinguished from the lower felsic marker only by its position above and below identical, mainly andesite flows. It comprises coherent rhyolite and dacite flows, welded tuff with strong eutaxitic fabrics, and rhyolite and dacite tuff and breccia.

The upper flow-dominated unit of the Telkwa Formation is the highest stratigraphic unit exposed in the Chist Creek map area. Younger units, such as the brick-red tuff of the uppermost Telkwa or Nilkitkwa formations, or the overlying 'pyjama beds' and Bowser Lake Group, are only seen far to the north (Nelson and Kennedy, 2007a, b) near Mt Quinlan, and to the east in the Smithers map area.

Intrusive Rocks

Within the Chist Creek map area, there are at least four inferred generations of plutonic rocks. As there are no modern U-Pb dates from the area, correlations are based on relationships to supracrustal units, and continuity with or similarity to well-dated bodies farther to the north (*see* Gareau et al., 1997a). Representative samples have been collected for U-Pb dating. In order of inferred geological age, the plutonic suites are

- small hypabyssal intrusions related to the Paleozoic Mt Attree volcanics;
- Early Jurassic intrusions, including the large Kleanza pluton and scattered smaller bodies that are probably comagmatic with the Telkwa Formation;

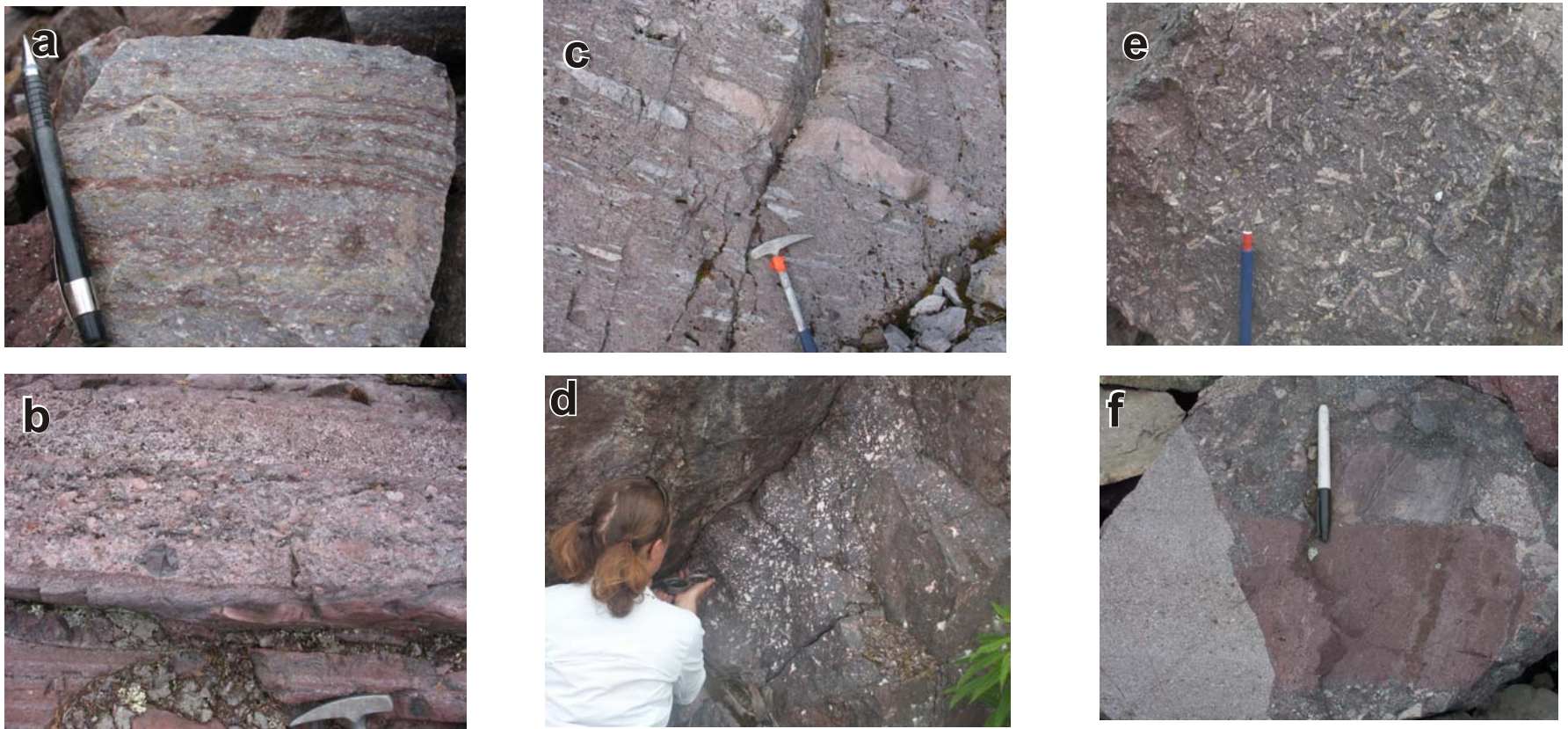


Figure 8. a) Flow-banded plagioclase-phyric dacite, near the base of upper Telkwa Formation, west of Mattson Creek; station 07JK03-04. b) Rhyolite-dacite polymictic lapilli tuff with fine-grained tuff interbeds, lower felsic marker at the base of the upper Telkwa Formation, Mattson Creek repeater road; station 07JK08-07. c) Eutaxitic texture in a welded rhyolite lapilli tuff, in the intraflow felsic marker unit, upper Telkwa Formation; station 07JK44-3. d) Zone of large, irregular amygdules in andesite flow, upper Telkwa Formation; station 07MM05-07. e) Plagioclase megacrystic andesite flow, upper Telkwa Formation; station 07MM05-07. f) Polymictic breccia with second-cycle clasts, upper Telkwa Formation near Mt Clore; station 07JN24-04.

- Cretaceous to Paleocene (?), ductilely deformed, mainly granitic bodies that outcrop at low elevations in the valleys of Williams Creek, Chist Creek and the Kitimat River;
- a large bulbous granitic to granodioritic body of probable Eocene age, the Williams Creek pluton.

PALEOZOIC INTRUSIONS

These are of limited extent, but of an importance that is disproportionate to their size. The rhyolitic volcanic centre that is associated with syngenetic quartz-sericite alteration and base-metal sulphide mineralization in the Mt Attree volcanics south of Williams Creek is partly defined by the presence of white, aphanitic rhyolite dikes and sills, and small, apparently cross-cutting bodies of foliated quartz-feldspar porphyry. One of the latter has been collected for U-Pb dating, and results are anticipated within the next few months.

EARLY JURASSIC INTRUSIVE SUITE

The largest intrusion of this suite is the southern extension of the Kleanza pluton, dated by Gareau et al. (1997a) as ca. 200 Ma, which sprawls along the Zymoetz River and Kleanza Creek to the north (Fig 3). It extends onto Mt Thornhill and the area around 8 Mile Creek. Its southern boundary lies on the slopes north of Williams Creek, where it is cut off by the Williams Creek pluton. As elsewhere, this pluton consists of a variety of phases that range from microdiorite, gabbro and minor clinopyroxene-bearing ultramafite, through coarse-grained tonalite and granodiorite, to quartz-rich granite. Hypabyssal phases that form part of the Kleanza pluton and exhibit transitional relationships to upper Telkwa andesite flows have been documented farther north (Nelson et al., 2006). In the present map area, deeper levels of the Kleanza pluton are exposed.

A number of smaller plutons show more direct ties to Early Jurassic arc-related volcanism in the Telkwa Formation. A small mafic pluton intrudes the base of the formation on the ridge east of Mt Attree. It is texturally highly variable, ranging from gabbro to microdiorite. Intrusive breccia is well developed near its margins (Fig 7c). It is surrounded by andesitic breccia, which grades outwards from monolithic bomb and pyroclastic breccia to more heterolithic breccia with andesite and diorite clasts, and lastly, an uppermost unit of thinly bedded andesitic turbidite overlain by welded tuff of the lower felsic marker. Clearly depicted here is a high-level intrusion and its apron of pyroclastic to reworked epiclastic products. Similar relationships are shown between a small body of microdiorite and porphyritic andesite east of 'Slide Creek', and nearby andesite breccia that contains clasts with identical igneous textures.

There are two small ultramafic to mafic intrusions that intrude the upper Telkwa flow-dominated unit in the eastern part of the map area. The best exposed of the two, located southeast of Moraine Creek, is roughly 1.5 km in diameter. It consists of a thick outer rim of gabbro, diorite and clinopyroxene-rich ultramafite, and a core of plagioclase-rich leucogabbro. The other intrusion is a body of clinopyroxenite and gabbro exposed over a few hundred metres west of the Clore River.

Irregular intrusive bodies outcrop extensively within the Clore-Henderson-Andesite massif (Fig 2). They are generally intermediate to felsic, of dioritic, tonalitic and dacitic compositions. Textures vary from fairly coarse

grained equigranular to porphyritic with a very fine grained matrix. They are accompanied by swarms of andesite and dacite dikes, such that the boundary between intrusive and extrusive regimes is difficult to pinpoint. Their outcrop pattern suggests the gently undulating roof of a magma chamber, with gently dipping andesite and dacite flows in its cupola. This massif is interpreted as a volcanic centre, based on its thick accumulation of flows; the presence of an inferred subjacent intrusion strengthens that supposition.

LATE CRETACEOUS-PALEOCENE (?) INTRUSIONS

These are limited in extent, occurring along one logging road on the north side of Williams Creek, near the mouth of Chist Creek and at one locality north of the Kitimat River. They are defined primarily by the presence of strong ductile fabrics. They intrude highly foliated Paleozoic metavolcanic rocks, and both are cut by unfoliated granite of probable Eocene age.

The body in Williams Creek is composed of granite and lesser granodiorite. In a small quarry along the main logging road, it shows strong foliation and metamorphic recrystallization under amphibolite conditions, and transposed igneous layering (Fig 9a). Higher above the valley, the intensity of foliation decreases, but the body is still characterized by clumps of dynamically recrystallized biotite. One phase also contains tiny pink garnets, both single grains and clusters that outline pelitic xenoliths that are now completely resorbed except for these delicate pseudomorphs.

Highly foliated tonalite near the mouth of Chist Creek is more mafic than the Williams Creek granite, but shows a similar texture of wispy, recrystallized biotite aggregates. A metamorphic complex exposed on a logging branch north of the Kitimat River comprises green phyllite allied with the Mt Attree volcanics and also fine-grained metadiorite with pegmatite and aplite dikes and sills.

The occurrence of these strongly foliated intrusive bodies associated with other deformed rocks in topographically low areas is reminiscent of the character and external relations of the ca. 58 Ma Kitsumkalum granite suite within the Kitselas complex (Gareau et al., 1997a, b; Nelson and Kennedy, 2007a). This Paleocene body is interpreted as being emplaced during tectonic unroofing of the complex during early Tertiary detachment faulting. A similar interpretation of these granitoid bodies is explored later in this paper (*see* Structure, below).

EOCENE INTRUSIONS

A large, bulbous undeformed body, mainly of granite and granodiorite, underlies the valley of Williams Creek and the western ridges to the south of it, including the drainage of the eponymous Granite Creek. South of a re-entrant near the mouth of Chist Creek, another salient extends along the valley of the Kitimat River. This body is named the Williams Creek pluton for its extensive exposures there. Its roof is exposed at middle elevations on the ridges north and south of the creek; overall, its geometry is the classic 'balloon' shape typical of granite emplaced into the upper crust.

Compared to the Jurassic Kleanza pluton, the Williams Creek body is compositionally more homogeneous and tends towards more felsic compositions. Most abundant are granite and granodiorite. Textures range from equigranular to inequigranular with euhedral, blocky white plagioclase

and/or K-feldspar phenocrysts up to 1 cm in length. Planar pink pegmatite and aplite dikes are common (Fig 9b). Unlike Kleanza granite, biotite in the Williams Creek pluton is more abundant than hornblende, and both are unaltered and fresh. A key identifying characteristic is the presence of small, clear, euhedral, amber-coloured titanite grains.

The Williams Creek body strongly resembles the ca. 53 Ma Carpenter Creek pluton west of the Skeena River (Gareau et al., 1997a; Nelson and Kennedy, 2007a, b). Both are predominantly felsic, both are large, bulbous bodies and both are postkinematic to ductile deformation events. Titanite also occurs in the slightly older Kitsumkalum intrusive suite (Gareau et al., 1997a; Nelson and Kennedy, 2007a). Pending ongoing U-Pb dating, the Williams Creek pluton is assigned a probable Eocene age.

Granitic and granodioritic dikes related to the Williams Creek pluton are widespread, but concentrate near

the pluton margins. They crosscut all older units and all fabrics.

In addition to felsic plutonic rocks, medium-grained equigranular diorite is abundant south of Chist Creek and near the Kitimat River. Because they are fresh and postkinematic, and are associated with the more typical granite, they are also assigned to the Eocene suite.

Structure and Metamorphism

MAJOR STRUCTURES

The Paleozoic to Jurassic stratigraphic sequence in the Chist Creek map area is deformed into a northeast-trending, regional-scale anticline. Its shape is outlined by the curvilinear outcrop pattern of the Ambition Formation limestone, which strikes north-northeast near Chist Creek, changing to north-northwest on the ridge south of Williams Creek, west-northwest on the ridge east of Mt Attree, and is then deformed into a series of northeasterly plunging folds in the hinge area from 'Slide Creek' into the Zymoetz River valley and on Copper Mountain (Fig 2, 3). The Mt Attree volcanics occupy its core.

An east to east-northeast-striking band of Permian limestone, overlain by Triassic radiolarian chert and limy shale, and then fragmental volcanic rocks of the Telkwa Formation, extends west towards Old Remo (Fig 3). A similar northeasterly striking succession is recognized near the Shames River, although there it may be complicated by thrust faulting (Heah, 1991). However, it is plausible that the northeasterly trending anticline outlined in the Chist Creek area extends west as far as the Shames River fault. Heah (1991) reports a U-Pb age of 331 to 317 Ma from a quartz diorite body east of the Shames River, and G. Woodsworth has obtained a Mississippian age from an intrusion in the eastern Coast Mountains near Kitimat (pers comm, 2006).

Regional attitudes in the Telkwa Formation reflect the east limb and hinge of the anticline. Predominant strikes in most of the Chist Creek map area are northerly, with moderate dips and facings to the east (Fig 3). To the north, across a series of east-west faults, the prevailing strike changes to west-northwesterly, with shallow dips to the northeast; these attitudes are seen over a broad region from near Kleanza Creek in the south to Mt Quinlan and Maroon Creek to the north, with the exception of rotated fault blocks near Mt O'Brien (Fig 2, 3).

A set of northwest-striking faults in the Chist Creek map area repeat the Telkwa stratigraphy. Displacement across them was southwest-side-down and/or dextral, based on offsets of the two felsic markers within the section. Although these faults have strong topographic expressions and significant offsets within the Chist Creek area, they are more or less truncated by westerly faults and elongate apophyses of the Kleanza pluton between the Zymoetz River and Chindemash Creek (Fig 3).

Doubt has been cast on the imbricated thrust faults shown near the Zymoetz River (Nelson et al., 2006a, b). Detailed remapping of this area has redefined coarse volcanic-derived clastic strata as Telkwa rather than Paleozoic volcanogenic units. It has also shown that structural repeats of Ambition Formation and basal Telkwa conglomerate are separated by the Triassic sedimentary unit, in normal stratigraphic order: they are northeasterly trending folds, not older-over-younger thrust faults. Contrary to Nelson et al.



Figure 9. Contrasting Paleocene (?) and Eocene intrusions: a) strongly deformed granite in Williams Creek; station 07JA05-01; b) undeformed, inequigranular granite with a pegmatite dike, Williams Creek pluton; station 07JN11-06.

(2006a), there is no longer a case for post-Triassic, pre-Jurassic thrusting in this area. Deposition of the basal Telkwa was preceded by strong uplift, but not necessarily crustal compression.

North of Terrace, a major low-angle fault system is recognized along the valley of the Skeena River, separating a footwall of metamorphosed Telkwa-equivalent rocks and ductilely deformed Paleocene granitoid rocks to the west from a hangingwall composed of northeast-younging Paleozoic to Upper Jurassic stratified rocks, intruded at lower stratigraphic levels by the Jurassic Kleanza pluton, to the east (Gareau et al., 1997a, b; Nelson and Kennedy, 2007a, b). This, the Skeena River fault system, is expressed as zones of strong ductile deformation and shearing, with superimposed high-angle normal faults. It probably was the locus first of late Mesozoic thrust motion, followed by Eocene down-to-the-east detachment (Nelson and Kennedy, 2007a). Prior to 2007 mapping, its southernmost known extent was near the base of Terrace Mountain, where it separates granitoid rocks with strong ductile fabrics from unfoliated K-feldspar-megacrystic granite that is the western extension of the Kleanza pluton on Copper Mountain.

In the Chist Creek map area, zones of strong ductile deformation occur at low topographic elevations near the mouths of Williams and Chist creeks, and on the north side of the Kitimat River. Strong foliations, and in some cases shears, are developed both in metavolcanic rocks and in granitoid rocks. The postkinematic Williams Creek pluton crosscuts all of them. The zone in west Williams Creek involves garnet-bearing biotite granite of probable Paleocene age that intrudes, and is deformed with mafic metavolcanic rocks of the Mt Attree volcanics. At the elevation of Williams Creek, the granite is a streaky protomylonite cut by top-to-the-northeast shear bands. Farther up the north slope, it is foliated but not mylonitic. Foliated andesite breccia that it intrudes is identical, except in its higher metamorphic grade and degree of deformation, to the sporadically foliated Mt Attree volcanics on the ridge above. At 400 m elevation above the creek, foliation is weak in the meta-andesite, and undeformed gabbro of the Kleanza pluton occurs. This upward decrease in intensity of deformation and metamorphism is consistent with a position in the immediate hangingwall of a low-angle detachment fault. The fault itself would lie below the lowest outcrop in the valley. Similarly, the biotite schist and metaplutonic rocks at low elevations in western Chist Creek, although at higher metamorphic grade and degree of ductile deformation compared to higher and more easterly outcrops, show continuity with them and are interpreted as the base of the hangingwall of a subjacent shear zone. The metavolcanic-metaplutonic exposure in the Kitimat River valley is isolated from undeformed ridge-top exposures, so its position above or below the major detachment is unknown.

Based on these three exposures, we hypothesize that the Skeena River fault zone extends at depth below the Chist Creek area, with the folded section of Mt Attree volcanics, Ambition Formation limestone and overlying Telkwa Formation in its hangingwall.

West of Terrace, the low-angle Shames River mylonite zone and the northwest-striking Shames River fault (Fig 3) both show top-to-the-northeast, normal sense of displacement. Both mylonitic deformation and north faulting are constrained as Eocene, ca. 54 to 47 Ma (Heah, 1991; Andronicos et al., 2003), approximately coeval with

unroofing of the Kitselas complex along the Skeena River fault zone. These structures make up a set of crustal-scale detachments along which the eastern Coast Belt was exhumed in transtensional conditions.

FABRICS, STRUCTURES AND REGIONAL METAMORPHISM WITHIN THE ZYMOETZ GROUP

Penetrative cleavage in the Mt Attree volcanics increases from sporadic development in favourable rock types north of Williams Creek, to weakly pervasive south of it, to strong and prevalent in the Chist Creek drainage. One of the northernmost indicators of penetrative deformation is a small marble body that forms an isoclinal fold in a headwall south of 8 Mile Creek, within metavolcanic strata that are otherwise only locally foliated. By contrast, south of Williams Creek, layering in the metavolcanic units has been completely transposed into the foliation, although measured facings are consistently to the east, in the overall direction of stratigraphic younging. Foliation attitudes in general are generally parallel to bedding; they are folded in the same manner around the major anticline (Fig 2).

The conglomerate-phyllite unit at the top of the Mt Attree volcanics north of Williams Creek is affected by two generations of cleavage. One is parallel to layering and a second is axial planar to a minor syncline that affects both metavolcanic rocks and overlying limestone, but apparently not the basal Telkwa conglomerate. On Mt Attree, zones of cleavage in the metavolcanic rocks are crosscut by a dioritic phase of the Kleanza pluton, a demonstration of pre-Early Jurassic penetrative deformation.

A top-to-the-north thrust fault is mapped in the headwaters of 8 Mile Creek, where sheared Mt Attree andesite rests structurally above the Ambition Formation. No other thrust faults were documented in the Paleozoic section. The Mt Attree volcanics show an increase in metamorphic grade from greenschist on the Mt Attree ridge and the Gazelle area south of Williams Creek, to amphibolite on the ridge between Chist Creek and Schulbuckhand Creek. Amphibolite-grade metamorphism is also seen at low topographic elevations in western Williams Creek, near the mouth of Schist Creek and in the valley of the Kitimat River. Greenschist facies assemblages in mafic rocks consist of pale-green to medium-green feathery and acicular actinolite, chlorite, epidote and albite after primary plagioclase. Felsic rocks contain albite, K-feldspar, sericite, biotite and chlorite. In mafic assemblages transitional to amphibolite, chlorite disappears followed by epidote, plagioclase becomes calcic, amphibole becomes more equant and darker in colour, and biotite becomes more abundant. The highest observed metamorphic grades are near the mouth of Chist Creek, where knotted green biotite schist contains cordierite grains with relict garnet in their cores.

Hornfelsic overprinting affects rocks near the Williams Creek pluton. Spongy metamorphic clinopyroxene occurs in amphibolite; and postkinematic cordierite and andalusite occur in the aluminum-rich altered metasedimentary rocks — biotite phyllite and conglomerate — north of Williams Creek. In this area, garnet and diopside are widespread in Ambition Formation limestone, filling fractures and in some cases delicately replacing silica-hematite-replaced fossils.

MINERAL OCCURRENCES AND MINERAL POTENTIAL

Traditionally, the mineral potential of the Chist Creek area was linked mainly to gold in polymetallic veins and redbed-style copper in the upper Telkwa, with lesser emphasis on small skarns. We have visited and sampled a number of known occurrences in the course of this project. Further, the identification of the Paleozoic Mt Attree volcanics and recognition of indicators of significant volcanogenic massive sulphide potential within them adds a new and promising development to the area (McKeown et al., 2008).

Precious metal-bearing polymetallic veins are associated with the Kleanza pluton. Of the many veins on Mt Thornhill, two, the Golden Nib and Lucky Seven, produced on a small scale in the early years of the 20th century. Grab samples collected in 2007 from vein occurrences, the Society Girl and Ptarmigan on Mt Thornhill, show variably high contents of copper and lead, and anomalous silver and gold (Table 1). Veins on Mt Thornhill were observed to contain pyrite, chalcopyrite, sphalerite, galena and arsenopyrite. They occur within northeasterly and west-northwesterly shears.

Regional prospecting along an abandoned logging road north of Williams Creek in 2007 located a sulphide+sulphosalt – bearing quartz vein with high geochemically determined contents of Ag and Au. Sample 07JK17-5, shown on Table 1, contains >10 000 ppb Ag and 14 098 ppb Au. It is exposed in a ditch, cutting metamorphosed Mt Attree andesite. Further extensions are possible.

The most significant vein-type occurrence in the area, also mined in the period of 1910 to 1935, is the Dardanelle (MINFILE 1031 107). In 1983, S. Reamsbottom reported that the property may contain reserves of approximately 181 440 t grading about 7.5 g/t Au and 17.1 g/t Ag (this estimate does not conform to NI43-101 requirements; MINFILE, 2007). The most recent drill program was by Trade Winds Ventures Inc. in 2005 (Burton, 2005). The main vein at Dardanelle lies within a steep, east-northeasterly (250°/80°) shear zone within granodiorite, immediately east of its strongly sheared and faulted western contact with the lower Telkwa Formation (Fig 2). The vein has been traced on the surface and in part underground for 2 km (Burton, 2005). A pink aplite dike occupies the same structure. The width of the vein is highly variable, and its gold grades range from trace amounts to over 33 g/t (Burton, 2005). The vein shows regular dark grey carbonaceous bands typical of orogenic gold-quartz deposits (Fig 10a).

Throughout the region, maroon to red andesite and dacite of the upper Telkwa Formation are host to numerous occurrences of fracture and shear-controlled copper mineralization, typically of high-oxidation assemblages of bornite and chalcocite with hematite, calcite and epidote. Showings on Treasure Mountain, in the northeast corner of the map area, are of particular note. Although most are shear-controlled (Nelson et al., 2006a), the Purdex showing (Snow, MINFILE 1031 090) also exhibits matrix replacement textures over significant widths (Fig 10b). A 26 m surface chip sample from this showing assayed 2.44% Cu and 0.4 g/t Ag (BC Ministry of Energy, Mines and Petroleum Resources, 1965); this is confirmed by our grab sample, which contained 6.21% Cu (Table 1, 07JK47-01). Recently, exploration of this property has been reactivated,

with re-opening of surface roads and a limited diamond drill program (Burton, 2006).

In the course of field mapping in 2007, we sampled a number of copper showings within Telkwa volcanic rocks. The most interesting analysis is of sample 07MM07-10 from a shear zone east of the Clore River, which contains 1.35% Cu, 16 ppm Ag and 295 ppb Au.

A series of magnetite-garnet-chalcopyrite+sulphosalt+galena skarn showings are located at and near the base of the Ambition Formation north of the Williams Creek pluton. Some of these show evidence of historic workings, including a well-preserved set of hand tools; but they are not listed in the MINFILE database. Two of our samples from these returned high Cu-Ag values (Table 1). Sample 07MM17-01 contains 13.09% Cu, >100 000 ppb Ag; and 07MM17-04, from a hand-dug pit, contains 7.62% Cu and 70 247 ppb Ag.

The Paleozoic Mt Attree volcanics host several broad zones of quartz-sericite schist, most notably around the Gazelle and Sub showings but also north of Williams Creek (Fig 2). Particularly in the Gazelle-Sub area, the quartz-sericite schist is associated with zones of strong silicifica-

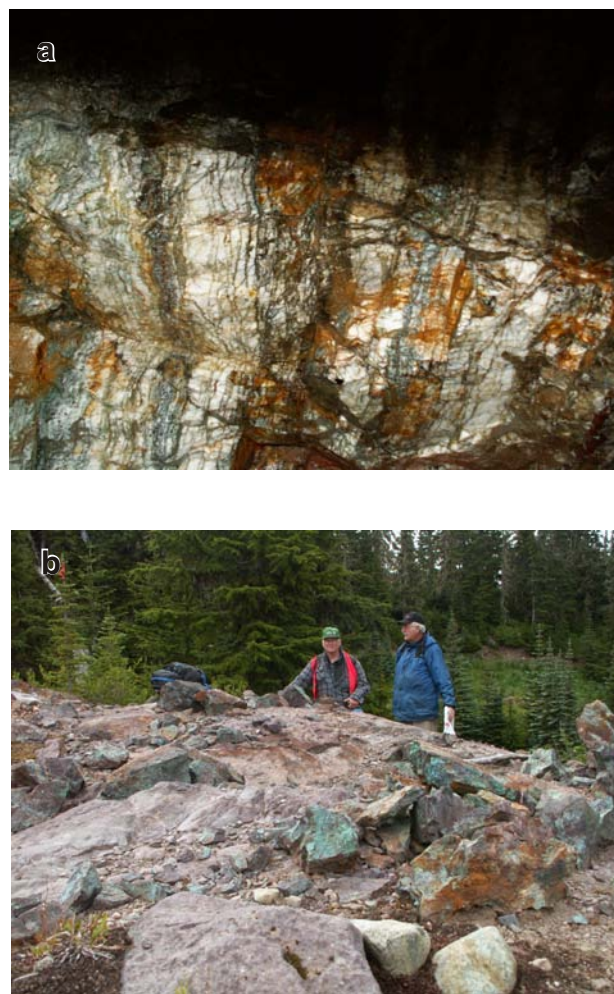


Figure 10. a) Underground exposure of the Dardanelle vein, approximately 200 m from the portal. Width is over 1 m at this point. b) A. Burton and G. Chinn at the Purdex showing on Treasure Mountain, where matrix replacement by copper minerals is shown by malachite staining over a broad area.

TABLE 1. GEOCHEMICAL AND ASSAY RESULTS FOR THE NTS 1031/08 MAP AREA, 2007. ABBREVIATIONS: ALT, ALTERATION; AZ, AZURITE; BO, BORNITE; BX, BRECCIA; CPY, CHALCOPYRITE; DISSEM, DISSEMINATED; GL, GLAUCOPHANE; GN, GARNET; L.JUR., LOWER JURASSIC; MAL, MALACHITE; MB, MOLYBDENITE; MIN, MINERALIZATION; MT, MAGNETITE; PLAG, PLAGIOCLASE; PO, PYRRHOTITE; PY, PYRITE; PZ, PALEOZOIC; QTZ, QUARTZ. ANOMALOUS VALUES ARE HIGHLIGHTED IN YELLOW.

Station number	Easting	Northing	Location	MINFILE	Sample Type	Minerals noted	Description	Element													
								Units		Mo	Cu	Pb	Zn	Ag	As	Au	Cd	Sb	Bi	W	
								(ppm)	(ppm)	(ppm)	(ppm)	(ppb)	(ppm)	(ppb)	(ppm)	(ppm)	(ppm)	(ppm)	(ppm)	(ppm)	
Method		ARMS	ARMS	ARMS	ARMS	ARMS	ARMS	ARMS	ARMS	ARMS	ARMS	ARMS	ARMS	ARMS							
Detection Limit		0.01	0.01	0.01	0.1	2	0.1	0.1	0.01	0.02	0.02	0.2	0.2								
		% if listed	% if listed																		
07JA01-03	536737	6016764	Chist Creek	none	2 m cont chip	py	Phyllite with dissem py	4.62	39.96	4.87	240.3	129	0.6	7.5	0.09	<0.02	0.34	0.1			
07JA10-10	569870	6047786	Many Bear Creek (093L/12)	93L 323	grab	py	pyritic-silicified rhyolite bx (adv. argillic alt.)	1.77	24.78	4.62	3.4	40	16.7	0.3	0.04	0.52	0.24	<0.1			
07JK03-05	562345	6032779	Clore R.	103L 091	2 m disc chip	bo, cpy, po	Amygdaloidal andesite/dacite with min. in amygdales	0.43	3801	9.24	295.3	14200	3.1	0.5	0.15	0.09	0.03	0.3			
07JK05-02	548992	6036878	Clore R.	none	5 m disc chip	py, cpy	Vein hosted within andesite lapilli tuff	3.71	105.5	3.1	40.9	873	8.4	79.9	0.11	0.34	0.24	<0.1			
07JK15-04	550803	6034687	Mattson Creek W.	none	grab	py	Highly silicified plag phyruc andesite with up to 15% dissem py.	1.27	29.65	8.36	64.7	69	5.7	0.6	0.08	0.35	0.02	0.1			
07JK16-02	543404	6021282	Chist Creek spur	none	grab	py	L.Jur. sericite schist, up to 15% pyrite within quartz veins	63.46	3620	195.9	7496	4847	8.6	82.3	95.24	0.21	1.14	0.1			
07JK17-5	535839	6031689	West Williams Creek	none	grab	py, mb?, sulphosalts?	quartz vein exposed over 1 X 4 metres minimum	18.21	3843	165.4	114.8	>100000	1	14098	3.12	0.3	48.53	0.9			
07JK17-13	536358	6033218	West Williams Creek	none	grab	py	pyritic qtz-(sericite?) also diorite with blue opal beads - epithermal? Abundant sulphide alteration	2.03	79.98	14.99	3.1	394	2.1	8.2	<0.01	0.11	0.19	<0.1			
07JK27-01	536824	6037770	Mt. Thornhill	near Society Girl 1031 184	grab	py, gn	Smoky qtz vein hosting dissem. pyrite and minor galena	3.32	751.2	1.12%	55.8	45655	80.3	275.3	2.74	13.13	1.56	<0.1			
07JK27-02	536633	6038304	Mt. Thornhill	Ptarmigan 1031 097	grab	py, cpy, mal	Qtz vein w dissem and blebby sulphides	1	2.15%	8.47	77.3	11126	2.4	53.2	1.74	0.21	0.16	<0.1			
07JK28-03	537977	6034609	Mt. Thornhill south	none	grab	py	Shear with silica/pyritic alteration up to 30% dissem pyrite some massive	2.2	60.61	2.68	42.3	156	11.2	5.9	0.04	0.04	0.7	<0.1			
07JK33-02	551598	6030194	Ridge SW of Mattson Cr.	none	grab	mal, minor mt	Amygdaloidal plag phyruc andesite with mt, jasper	0.19	9122	9.53	364.5	3056	0.4	474.5	1.3	0.31	<0.02	<0.1			
07JK44-03	551409	6014982	Ridge NW of Hunter Creek	none	grab	py >cpy	Highly silicified volcanics with up to 15% fine dissem py	0.75	32.04	7.03	48.5	155	2.9	3.4	0.03	0.11	0.41	0.1			
07JK44-04	563863	6016810	Ridge NW of Hunter Creek	none	grab	py	Intense gossan within andesite, pyritic + jarosite	4.37	103.3	6.15	23.9	57	34.2	0.6	0.09	0.3	3.31	<0.1			
07JK47-01	563945	6037713	Treasure Mountain	Purdex 1031 090	grab	cpy,po,mal,az	Dacite with fine dissem sulphides	0.44	6.21%	537.7	161.6	35650	1.9	3	0.4	0.39	0.14	0.3			
07JN01-03	544844	6039018	N. Zymoetz	none	grab	mt, cpy, gn	Skarn - lenses of calcsilicate metaseds. Mt rich zone with garnet, epidote, diopside	0.32	20.37	2.57	55.2	33	1.5	0.4	0.09	0.18	0.18	0.3			
07JN01-06	546451	6039356	N. Zymoetz	none	grab	mal, cpy	Sulphide rich zone within Lower Telkwa, limestone dominated bx.	6.37	7.21%	15.68	97.9	5279	17.1	5.5	0.77	0.42	0.23	0.3			
07JN08-05	560476	6034700	W. of Clore	none	grab	zeolite?	Rotten dacite bx silicified (possibly some pink zeolite?)	9.61	60.56	338.3	36	4624	182.8	60.5	0.49	3.48	11.14	>100			
07JN17-01	541737	6031336	Camp 2	none	grab	py	Gossan within Pz lapilli tuff, patchy, intense silicified-pyritic zone	0.34	41.74	10.71	72.9	517	8.5	2.3	0.67	0.77	0.64	0.2			
07JN24-05	563735	6016931	Clore-Henderson-Andesite Peak	none	grab	py>>cpy	Gossanous diorite with up to 15% py intruding Telkwa rhyolite	1.86	100.3	9.74	15.4	102	10.1	0.8	0.03	0.41	12.92	<0.1			
07MM07-10	563650	6033284	E. Clore	none	2m cont chip	mal, cpy, bo	Hosted in porphyritic andesite (Telkwa), likely shear controlled, min over 15 ft	0.38	1.35%	4.43	298.3	15847	2.5	295.5	0.27	0.07	0.34	0.4			
07MM17-01	546260	6028880	Summit E. of Mt. Attree	none	grab over 20 m	mt, cpy, gl	Skarn - base of Permian limestone over andesite flow, massive galena and trace grey sulphosalts	1.07	13.09%	248.7	1457	>100000	8.2	72.8	44.48	0.25	124.4	34.3			
07MM17-04	546379	6028416	Summit E. of Mt. Attree	none	grab	cpy, mt, gn?	Magnetite skarn within Pz andesite, plag phyruc flow	208.3	7.62%	36.6	367.6	70247	2.7	27.1	30.6	0.08	67.99	>100			
07MM18-06	545017	6029157	Summit E. of Mt. Attree	none	2 m chip	py	silic-pyritic zone overlying highly foliated quartz-sericite schist	1.28	198.8	5.94	166.5	308	5.4	0.5	0.38	0.04	0.28	2.7			

tion and local base-metal sulphide concentrations; massive barite is present at the Sub showing (McKeown et al., 2008). The alteration and mineralization are prekinematic, and are interpreted as syngenetic. This suggests that the Mt. Attree volcanics have the potential for hosting volcanogenic massive sulphide deposits similar to Tulsequah Chief, which is associated with Late Mississippian rhyolite in northern Stikinia.

SUMMARY AND CONCLUSIONS

Field mapping in 2007 of the Chist Creek map area southeast of Terrace has clarified regional geological understanding as well as pointing to volcanogenic massive sulphide potential in newly defined Paleozoic hosts. The western half of the Chist Creek area is underlain in part by Paleozoic volcanic and related strata of the Mt Attree volcanics, which are separated from overlying lower Mesozoic strata by the Permian Ambition Formation limestone. Together the Paleozoic volcanic strata and the limestone form the core of a regional, northeasterly trending anticline. Correlatives of the Zymoetz Group may extend westwards into the eastern Coast Mountains.

ACKNOWLEDGMENTS

We appreciate the expert piloting of Canadian Helicopters, and expediting by Jean and Lorna Black. Dan Parker gave us yet another summer of safe and skillful driving. Tony Wass, Soleil and Jed are thanked for logistical support in the field. Lael and Dave McKeown provided a field base of unparalleled excellence. Bill McRae is always handy with oral history of mining and exploration in the Terrace area. Glenn Woodsworth and Mitch Mihalynuk provided useful discussions and clarifications.

REFERENCES

- Andronicos, C.L., Chardon, D., Hollister, L.S., Gehrels, G. and Woodsworth, G.J. (2003): Strain partitioning in an obliquely convergent orogen, plutonism, and synorogenic collapse: Coast Mountains batholith, British Columbia, Canada; *Tectonics*, Volume 22, Number 2, doi: 10.1029/2001TC001312, pages 7-1-7-24.
- BC Ministry of Energy, Mines and Petroleum Resources (1965): Minister of Mines, Annual Report 1965; *BC Ministry of Energy, Mines and Petroleum Resources*, 271 pages.
- Burton, A., 2005: Assessment report on the Dardanelles property, Skeena Mining Division, for Trade Wind Ventures, Inc.; *BC Ministry of Energy, Mines and Petroleum Resources*; Assessment Report 28303, 60 pages.
- Burton, A. 2006: Technical assessment report on the Treasure Mountain property, Skeena Mining Division; *BC Ministry of Energy, Mines and Petroleum Resources*, Assessment Report 28304, 27 pages.
- Duffell, S. and Souther, J.G. (1964): Geology of Terrace map area, British Columbia; *Geological Survey of Canada*, Memoir 329, 117 pages.
- Gareau, S.A., Friedman, R.M., Woodsworth, G.J. and Childe, F. (1997a): U-Pb ages from the northeastern quadrant of Terrace map area, west-central British Columbia; *in Current Research, Geological Survey of Canada*, Paper 1997-A/B, pages 31-40.
- Gareau, S.A., Woodsworth, G.J. and Rickli, M. (1997b): Regional geology of the northeastern quadrant of Terrace map area, west-central British Columbia; *in Current Research, Geological Survey of Canada*, Paper 1997-A/B, pages 47-55.
- Gunning, M.H., Bamber, E.W., Brown, D.A., Rui, L., Mamet, B.L. and Orchard, M.J. (1994): The Permian Ambition Formation of northwestern Stikinia, British Columbia; *in*, Pangea: Global Environments and Resources, Embry, A.F., Beauchamp, B., and Glass, D.J., Editors, *Canadian Society of Petroleum Geologists*, Memoir 17, pages 589-619.
- Heah, T.S.T. (1991): Mesozoic ductile shear and Paleogene extension along the eastern margin of the Central Gneiss Complex, Coast Belt, Shames River area, near Terrace, British Columbia; unpublished MSc thesis, *The University of British Columbia*, 155 pages.
- McKeown, M., Nelson, J.L. and Friedman, R. (2008): Newly discovered volcanic-hosted massive sulphide potential within Paleozoic volcanic rocks of the Stikine assemblage, Terrace area, northwestern British Columbia (NTS 103I/08); *in Geological Fieldwork 2007, BC Ministry of Energy, Mines and Petroleum Resources*, Paper 2008-1, pages 103-116.
- Mihalynuk, M.G. (1987): Metamorphic, structural and stratigraphic evolution of the Telkwa Formation, Zymoetz River area (NTS 103I/08 and 93L/05), near Terrace, British Columbia; MSc thesis, *University of Calgary*, 128 pages.
- MINFILE (2007): MINFILE BC mineral deposits database; *BC Ministry of Energy, Mines and Petroleum Resources*, URL <<http://www.em.gov.bc.ca/Mining/Geolsurv/Minfile/>> [December 2007].
- Nelson, J.L., Barresi, T., Knight, E. and Boudreau, N. (2006a): Geology and mineral potential of the Usk map area (103I/09) near Terrace, British Columbia; *in Geological Fieldwork 2005, BC Ministry of Energy, Mines and Petroleum Resources*, Paper 2006-1 and *Geoscience BC*, Report 2006-1, pages 117-134.
- Nelson, J.L., Barresi, T., Knight, E. and Boudreau, N. (2006b): Geology of the Usk map area (193I/09); *BC Ministry of Energy, Mines and Petroleum Resources* Open File 2006-3, 1:50 000 scale.
- Nelson, J.L. and Kennedy, R. (2007a): Terrace regional mapping project Year 2: New geological insights and exploration targets (NTS 103I/16S, 10W), west-central British Columbia; *in Geological Fieldwork 2006, BC Ministry of Energy, Mines and Petroleum Resources*, Paper 2007-1 and *Geoscience BC*, Report 2007-1, pages 149-162.
- Nelson, J.L. and Kennedy, R. (2007b): Geology of the Doreen south half (103I/16S) and Terrace east half (103I/10E) map areas, near Terrace, British Columbia; *BC Ministry of Energy, Mines and Petroleum Resources*, Open File 2007-4, 1:50 000 scale.
- Nelson, J.L., Kyba, J., McKeown, M. and Angen, J. (2008): Geology of the Chist Creek map area (103I/08); *BC Ministry of Energy, Mines and Petroleum Resources*, Open File 2008-3.
- Tipper, H.W. and Richards, T.A. (1976): Jurassic stratigraphy and history of north-central British Columbia; *Geological Survey of Canada*, Bulletin 270, 73 pages.
- Woodsworth, G., van der Heyden, P. and Hill, M.L. (1985): Terrace East map area; *Geological Survey of Canada*, Open File 1136, 1:125 000 scale.

High-Mg Lavas in the Karmutsen Flood Basalts, Northern Vancouver Island (NTS 092L): Stratigraphic Setting and Metallogenic Significance

G.T. Nixon, J. Larocque¹, A. Pals¹, J. Styan¹, A.R. Greene² and J.S. Scoates²

KEYWORDS: Vancouver Island, NTS 092L, Wrangellia, Vancouver Group, Karmutsen Formation, stratigraphy, volcanology, metallogeny, flood basalt, high-Mg basalt, picrite, Ni-Cu-PGE

INTRODUCTION

The occurrence of high-Mg lavas in the Triassic Karmutsen flood basalts of the Wrangellia Terrane on northern Vancouver Island has recently been documented by Greene et al. (2006). They identified a number of separate occurrences of high-Mg or picritic pillow lavas and subvolcanic dikes, and designated the excellent exposures of pillowed flows at Keogh Lake as the type locality. Although all currently known picritic basalt flows clearly formed in the submarine environment, their precise stratigraphic position within the Karmutsen Formation has remained uncertain.

The expansion of new logging road systems on northern Vancouver Island over the last decade or so has provided access to more remote areas underlain by Karmutsen volcanic rocks. It is now possible to map distinct stratigraphic subunits within the Karmutsen Formation, similar to those established by earlier workers elsewhere on Vancouver Island. This report, therefore, describes the internal stratigraphy of the Karmutsen Formation, as revealed by recent mapping, and attempts to place known occurrences of high-Mg basalt in the context of this new stratigraphic framework.

The existence of high-Mg basalts in the Karmutsen succession has important ramifications for the mineral potential of this Triassic flood basalt province. Northern Vancouver Island is well known for a number of significant metal prospects and deposits, including intrusion-related Cu-Au-Ag(-Mo) porphyry (e.g., Hushamu, MINFILE 92L 240; the former Island Copper mine, MINFILE 92L 158; MINFILE, 2007); base and precious-metal skarns (e.g., Merry Widow, MINFILE 92L 044); and epithermal precious-metal environments (e.g., Mount McIntosh – Hushamu, MINFILE 92L 240). All such styles of mineralization have strong genetic links to supra-subduction zone metallogenic events associated with the

Late Triassic to Early Jurassic Bonanza magmatic arc (Nixon and Orr, 2007). However, additional exploration opportunities exist in the flood basalt environment, which is known to host world-class magmatic Ni-Cu-PGE deposits associated with high-Mg basalts or their intrusive counterparts.

REGIONAL SETTING

The geology of northern Vancouver Island has been published in a series of 1:50 000 scale maps (Nixon et al., 2006a–d), and revisions to the Early Mesozoic stratigraphy were made recently by Nixon and Orr (2007). A generalized geology map and stratigraphic column for northern Vancouver Island are presented in Figures 1 and 2.

Vancouver Island belongs to the Wrangellia tectonostratigraphic terrane (Jones et al., 1977) of Late Paleozoic to Early Mesozoic rocks, which extends northwards through the Queen Charlotte Islands into southern Alaska (Wheeler and McFeely, 1991). Wrangellia was amalgamated with the Alexander Terrane in the Alaska panhandle to form the Insular Superterrane as early as the Late Carboniferous (Gardner et al., 1988), and was accreted to inboard terranes of the Coast and Intermontane belts as late as the mid-Cretaceous (Monger et al., 1982) or as early as the Middle Jurassic (van der Heyden, 1991; Monger and Journeay, 1994). At the latitude of northern Vancouver Island, Wrangellia is intruded to the east by granitoid rocks of the Coast Plutonic Complex and fault bounded to the west by the Pacific Rim Terrane and metamorphosed and intrusive rocks of the Westcoast Crystalline Complex (Wheeler and McFeely, 1991). Devonian to Early Permian island-arc volcanic, volcanoclastic and sedimentary rocks of the Sicker and Buttle Lake groups (Massey, 1995a–c), which form the basement to Wrangellia, are exposed on southern and central Vancouver Island, and the overlying Middle Triassic shale ('*Daonella* beds') at the base of the Karmutsen is well exposed in the Schoen Lake area, some 30 km southeast of the area shown in Figure 1.

The stratigraphy of northern Vancouver Island is founded upon the Triassic tripartite sequence of Karmutsen flood basalt, Quatsino limestone and Parson Bay mixed carbonate-clastic-volcanic succession, which is diagnostic of Wrangellia (Jones et al., 1977). The occurrence of island-arc volcanic and volcanoclastic strata in the Parson Bay Formation led Nixon and Orr (2007) to take the Parson Bay Formation out of the Vancouver Group and place it in the Late Triassic–Middle Jurassic Bonanza Group. The latter group of volcanic and sedimentary rocks, together with coeval granitoid intrusions of the Island Plutonic Suite,

¹ University of Victoria, Victoria, BC

² University of British Columbia, Vancouver, BC

This publication is also available, free of charge, as colour digital files in Adobe Acrobat® PDF format from the BC Ministry of Energy, Mines and Petroleum Resources website at http://www.em.gov.bc.ca/Mining/GeolSurv/Publications/catalog/cat_fldwk.htm

constitute the main phase of magmatism of the Bonanza island arc (Northcote and Muller, 1972; DeBari et al., 1999).

A major contractional event is marked by an angular unconformity underlying Jurassic–Cretaceous clastic sequences deposited on the eroded surface of the Bonanza

Group. This episode of deformation is constrained by strata of Late Jurassic age (Oxfordian–Tithonian) that locally underlie more widespread Cretaceous sedimentary rocks on northern Vancouver Island and in the Queen Charlotte Islands (Gamba, 1993; Haggart, 1993; Haggart and Carter, 1993).

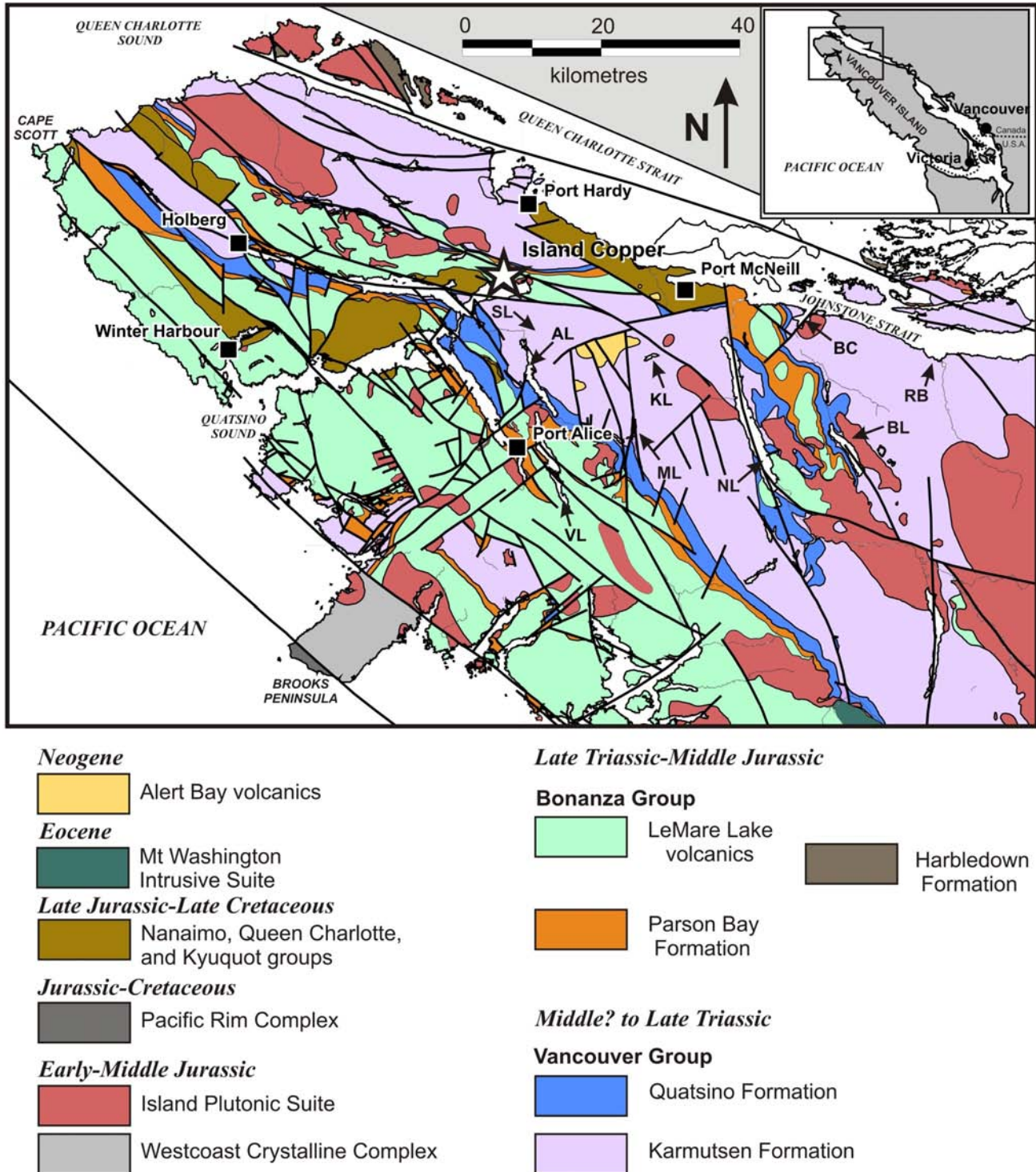


Figure 1. Regional geology of northern Vancouver Island (compiled by Massey et al., 2005). Abbreviations for selected geographic localities: AL, Alice Lake; BC, Beaver Cove; BL, Bonanza Lake; KL, Keogh Lake; ML, Maynard Lake; NL, Nimpkish Lake; RB, Robson Bight; SL, Sara Lake; VL, Victoria Lake.

The history of faulting on northern Vancouver Island is complex and embodies Cretaceous transpression and Tertiary extension. The present crustal architecture exhibits a dominant northwesterly-trending structural grain manifested by the distribution of major lithostratigraphic units and granitoid plutons (Fig 1). Numerous fault-bounded

blocks of homoclinal, Early Mesozoic strata generally dip to the southwest and west (Muller et al., 1974). Jura-Cretaceous clastic strata are preserved as disparate fault-bounded remnants of formerly more extensive Cretaceous basins (Muller et al., 1974; Jeletzky, 1976; Haggart, 1993). The relatively low relief and high heat flow of northern

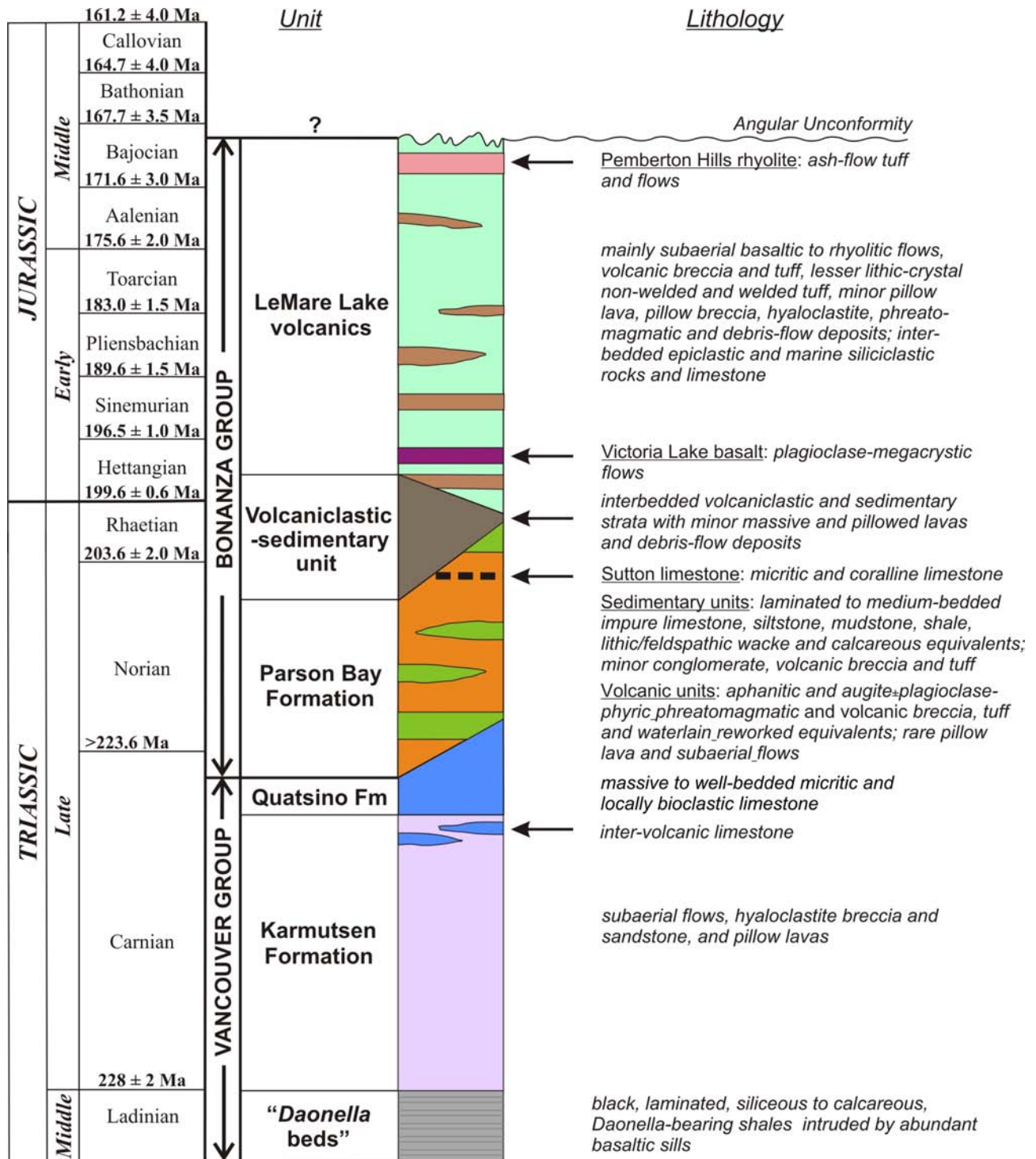


Figure 2. Early Mesozoic stratigraphy of northern Vancouver Island, using the nomenclature for Triassic–Jurassic lithostratigraphic units proposed by Nixon and Orr (2007). The geological time scale is that of Gradstein et al. (2004) except for the Carnian–Norian stage boundary, which is taken from Furin et al. (2006).

Vancouver Island reflect tectonism associated with the development of the Queen Charlotte Basin, a Tertiary transtensional province related to oblique convergence of the Pacific and Juan de Fuca plates with the North American Plate (Riddihough and Hyndman, 1991; Lewis et al., 1997). The distribution of Tertiary volcanic centres appears to be strongly influenced by high-angle faults. The north-easterly-trending Brooks Peninsula fault zone appears to coincide with the southern limit of Neogene volcanism in the region and delineate the southern boundary of the Tertiary extensional regime in the Queen Charlotte Basin (Armstrong et al., 1985; Lewis et al., 1997).

WRANGELLIAN FLOOD BASALTS

The geological setting and evolution of the Triassic flood basalts in the Wrangellia Terrane of northern Vancouver Island was recently reviewed by Greene et al. (2006). The weight of currently available geological evidence indicates that the voluminous ($>10^6$ km³) Wrangellian flood basalts represent an accreted oceanic plateau formed by the rise and demise of a mantle plume (Richards et al., 1991). From fauna and lithostratigraphic correlations, Carlisle and Suzuki (1974) concluded that the Karmutsen basalts range from Middle to Late Triassic (Ladinian–Norian) in age and were emplaced within approximately 2.5 to 3.5 Ma. More recent U-Pb and geochronological studies have so far failed to accurately resolve the age and longevity of Karmutsen volcanism, which is placed at ca. 217 to 233 Ma (see Greene et al., 2006). Despite their age and low (prehnite-pumpellyite) grade of ‘burial’ metamorphism (see Greenwood et al., 1991 and references therein), volcanological and petrographic features of the basalts are typically well preserved, as shown below.

KARMUTSEN FORMATION

The early work of Gunning (1932) established the ‘Karmutsen volcanics’, named for the type area in the Karmutsen Range just west of Nimpkish Lake, as the dominant member of the Vancouver Group. Subsequently, this unit was elevated to formal lithostratigraphic status by Sutherland Brown (1968) and Muller and Carson (1969). The Karmutsen succession in central and northern Vancouver Island was later subdivided by D. Carlisle and coworkers (Carlisle, 1963, 1972; Carlisle and Suzuki, 1974; Muller et al., 1974) into three distinct and mappable volcanic units: 1) closely packed pillow lavas in the lower part of the succession (2900 ± 150 m); 2) pillow breccia and ‘aquagene tuff’ in the middle (610–1070 m); and 3) massive flows at the top (2600 ± 150 m). Intervolcanic sedimentary lenses, principally micritic to bioclastic limestone and black siliceous shale, occur near the top and, less commonly, near the base of the massive flow unit, and are locally associated with pillow lavas, pillow breccias and finer grained, bedded volcanoclastic deposits. The base of the Karmutsen succession overlies a thick (760–920 m) sequence of black siliceous to calcareous shale (‘*Daonella* beds’) of Middle Triassic age, intruded by abundant mafic sills that are considered comagmatic with Karmutsen volcanic rocks (Carlisle, 1972; Carlisle and Suzuki, 1974; Muller et al., 1974). The shale unit is exposed south of the current area of interest near Schoen Lake (see Greene et al., 2006). According to previous work, estimates for the cumulative thickness of the Karmutsen Formation exceed 6000 m.

Yorath et al. (1999) proposed that the excellent exposures along Buttle Lake on central Vancouver Island represent the most complete section.

Recent mapping of the Karmutsen Formation on northern Vancouver Island has resulted in a tripartite division of the volcanic succession (Fig 3–5), analogous to the sub-units originally established by Carlisle (1963, 1972): 1) a pillow lava unit at the base, dominated by closely packed pillowed flows with minor intercalated sheet flows; 2) an overlying hyaloclastite unit characterized by pillow-fragment breccias and fine-grained hyaloclastite deposits, and intercalated locally with pillowed flows throughout the succession; and 3) an upper massive flow unit dominated by subaerial lavas but including minor limestone, fine-grained siliciclastic sedimentary rocks, pillow lavas and volcanoclastic deposits near the top and base. The genetic term ‘hyaloclastite’ has been adopted to denote volcanic rocks formed by quench-fragmentation and autobrecciation during interaction with water, rather than the classic term ‘aquagene tuff’, as originally employed by Carlisle (1963), which may connote an origin via explosive fragmentation and deposition directly by pyroclastic processes (Cas and Wright, 1987). Although certain basaltic shard morphologies described by Carlisle (1963) may have a pyroclastic origin, generated, for example, by steam explosions where lava flows entered the ocean, there is abundant evidence to conclude that the overwhelming majority of volcanoclastic products in the Karmutsen succession are related to the emplacement and granulation of pillowed flows, as well as resedimentation of hyaloclastites in the submarine environment.

Pillow Lava Unit

Pillow lavas in the basal part of the Karmutsen Formation are exposed on the coast north of Robson Bight, and in roadcuts and quarries along logging roads stretching west from the Karmutsen Range to Sara Lake, just west of Twin Peaks (Fig 3). The base of the pillow lava unit is typically cut off by faulting and is not exposed in the map area. The top of the unit appears broadly conformable with overlying beds of hyaloclastite, and map patterns northwest of Maynard Lake indicate interdigitation of pillows and the basal part of the hyaloclastite unit. The minimum thickness of the pillow lava sequence, as estimated in a coastal section between Beaver Cove and Robson Bight, is approximately 3000 m, assuming no significant repetition by faults.

Dark grey to grey-green pillows generally exhibit nearly equidimensional to lobate forms up to about 1.5 m in length and 1 m across, and typically are closely packed with very dark grey to black, well-chilled, chlorite-rich selvages (Fig 6A). The majority of the pillow sequence is aphanitic, nonamygdaloidal and strongly to nonmagnetic. However, towards the top of the succession, pillow lavas may carry plagioclase phenocrysts and exhibit amygdaloidal textures. Individual pillows may display pronounced radial jointing, but this is not a common feature. Interstices are commonly devoid of clastic material, or may host subequant to rectangular or distinctly elongate, curvilinear shards that represent the spalled rims of pillows (Fig 6B). This material is commonly partly altered to chlorite, epidote, quartz and carbonate, for which the local term ‘dallasite’ has been coined. Complete replacement or infilling of interstices and irregular fractures by quartz, chlorite, epidote, calcite, potassium feldspar and zeolite usually aids in identifying pil-

low morphologies in blasted outcrops. Rarely, large pillows in cross-section exhibit quartz-filled ledges with flat floors and convex roofs, interpreted to represent cavities evacuated by lava during emplacement (i.e., small lava tubes). These drainage channels provide valuable structural indicators for way-up, flow orientation and flow contacts (bedding). Such features may occur as stacked lava tubes within a single pillow, and have been described previously (e.g., Yorath et al., 1999, Fig 46).

Pockets of pillow breccia and rare, laminated to thinly bedded hyaloclastite sandstone and massive sheet flows are encountered locally throughout the succession. The sheet flows may be more common than appreciated due to the scarcity of well-exposed contacts and similarity of their textures to subvolcanic dikes and sills. The best exposures of sheet flows occur in quarries and high roadcuts (Fig 6C). The convolute nature of their lower contact, which is typically draped over underlying pillows, serves to distinguish the sheet flows from subvolcanic intrusions (Fig 6D). Although most sheet flows lack internal structures, some exhibit a crude curvilinear jointing oriented at a high angle to their contacts. The occurrence of sheet flows deep within the pillow basalt succession, and their generally nonamygdaloidal nature, indicates that they are truly submarine in origin rather than the result of sea-level oscillation between submarine and subaerial conditions. Most appear to have lensoid geometry and likely reflect a local increase in the flow rate relative to the rate of emplacement of pillows.

In thin section, basaltic pillow lavas are weakly to nonamygdaloidal, and aphyric or porphyritic with small amounts of plagioclase and/or olivine phenocrysts. Plagioclase-bearing and/or amygdaloidal lavas begin to appear near the top of the pillow lava succession. Euhedral to subhedral plagioclase and olivine phenocrysts (<2 mm) may form glomerophytic clots, and groundmass plagioclase generally forms acicular crystals. Olivine is completely replaced by fine-grained intergrowths of serpentine, chlorite, carbonate, opaque oxides and/or quartz. In aphyric pillow lavas, clinopyroxene usually forms radiating dendritic to sheaf-like crystals with a variolitic texture, or intergranular microphenocrysts. In porphyritic lavas, clinopyroxene is typically somewhat coarser grained and exhibits a prismatic or ophitic habit.

Hyaloclastite Unit

The hyaloclastite unit crops out on the coast between Beaver Cove and Robson Bight, and can be traced westward through well-forested ground extending from the west flank of the Karmutsen Range to Sara Lake (Fig 3). Where adequate structural control is present, the upper and lower contacts of this unit appear conformable with overlying flow and underlying pillow sequences. The thickness of this unit varies considerably across the map area. It attains an estimated maximum thickness of approximately 1550 ±200 m in a coastal section north of Robson Bight, and may be less than 40 m thick in the Maynard Lake area.

Excellent exposures of the hyaloclastite unit are found along the coast south of Beaver Cove (Fig 3). Massive to thickly bedded volcanic breccia is the dominant lithology, interbedded with subordinate, well-bedded basaltic sandstone and lesser amounts of pillow lava. The relationships between all three rock types and their inherent textural characteristics are well illustrated in the coastal section. At

one locality, for example, dark greenish grey, closely packed pillow lavas are succeeded upward by sandstones and volcanic breccias, and textures and a wealth of sedimentary structures elucidate the origin and mode of deposition of the volcanoclastic rocks (Fig 7). The lowermost pillows (<1 m in length) are aphanitic and nonamygdaloidal, and have locally trapped laminated and deformed sediment in their interstices during emplacement (Fig 7A). The pillows are overlain by pale buff to dark grey-green weathering, thinly laminated to medium-bedded, medium to coarse-grained sandstone composed predominantly of angular to subangular basaltic shards of hyaloclastite origin. The thicker beds of hyaloclastite sandstone may enclose angular to subrounded clasts of basalt (<8 cm across), some of which preserve chilled pillow rinds, whereas laminated horizons may display crossbedding and spectacular slump folds and fluidization structures (Fig 7B, C). At the locality illustrated, slumped beds lie directly beneath a very thick bed of dark grey-green hyaloclastite breccia containing sparse pillow fragments and rare whole pillows, up to 1.5 m in length, set in a finely comminuted sand-size matrix of granulated hyaloclastite material. The clasts are generally matrix supported and poorly sorted. Many clasts are not obviously derived from pillow rims and probably represent fragmented pillow cores. Elsewhere, pillow-fragment breccias are more easily recognized due to the abundance of clasts of broken and whole pillows (Fig 7D). The lower contact of the underlying disturbed-bedding horizon (Fig 7B) is marked by a fairly sharp discontinuity, whereas the upper contact is transitional into the matrix of the breccia bed. Graded bedding is evident in some of the thin sandstone beds, and crude normal grading may be rarely recognized in some of the breccia layers. From these well-preserved sedimentary features, it is clear that the coarse volcanic breccias were emplaced via debris flows carrying unconsolidated hyaloclastite material downslope, thereby causing rapid loading and dewatering, and localized detachment, of semiconsolidated hyaloclastite sandstone deposited previously by turbidity currents.

In thin section, the hyaloclastite sandstone and the breccia matrices are rich in dark brown, angular to subangular, subequant to highly elongate shards of palagonitized and devitrified, pseudo-isotropic basaltic glass, representing the resedimented quench-fragmentation products of pillow lava (Fig 8). Finely comminuted matrices are generally pervasively altered to a fine-grained mixture of chlorite, quartz and prehnite, along with minor epidote, carbonate and iron oxide. The rims of shards and clasts are commonly bleached and/or marked by concentrations of finely crystalline opaque material, and some fragments preserve whole or partial vesicles usually infilled by secondary minerals. Broken plagioclase crystals occur in some matrices, and larger clasts may enclose euhedral to subhedral plagioclase phenocrysts (Fig 8B).

Massive Flow Unit

A thick sequence of subaerial flows caps the lava pile and forms the most aerially extensive map unit in the Karmutsen Formation of northern Vancouver Island. The lower contact with the hyaloclastite unit is essentially conformable (local, irresolvable disconformities probably exist), and flows generally rest on pillow-fragment breccia or pillow lava locally present at the top of the hyaloclastite succession. At some localities, pillow-like morphologies scattered within more massive flows may mark a transition

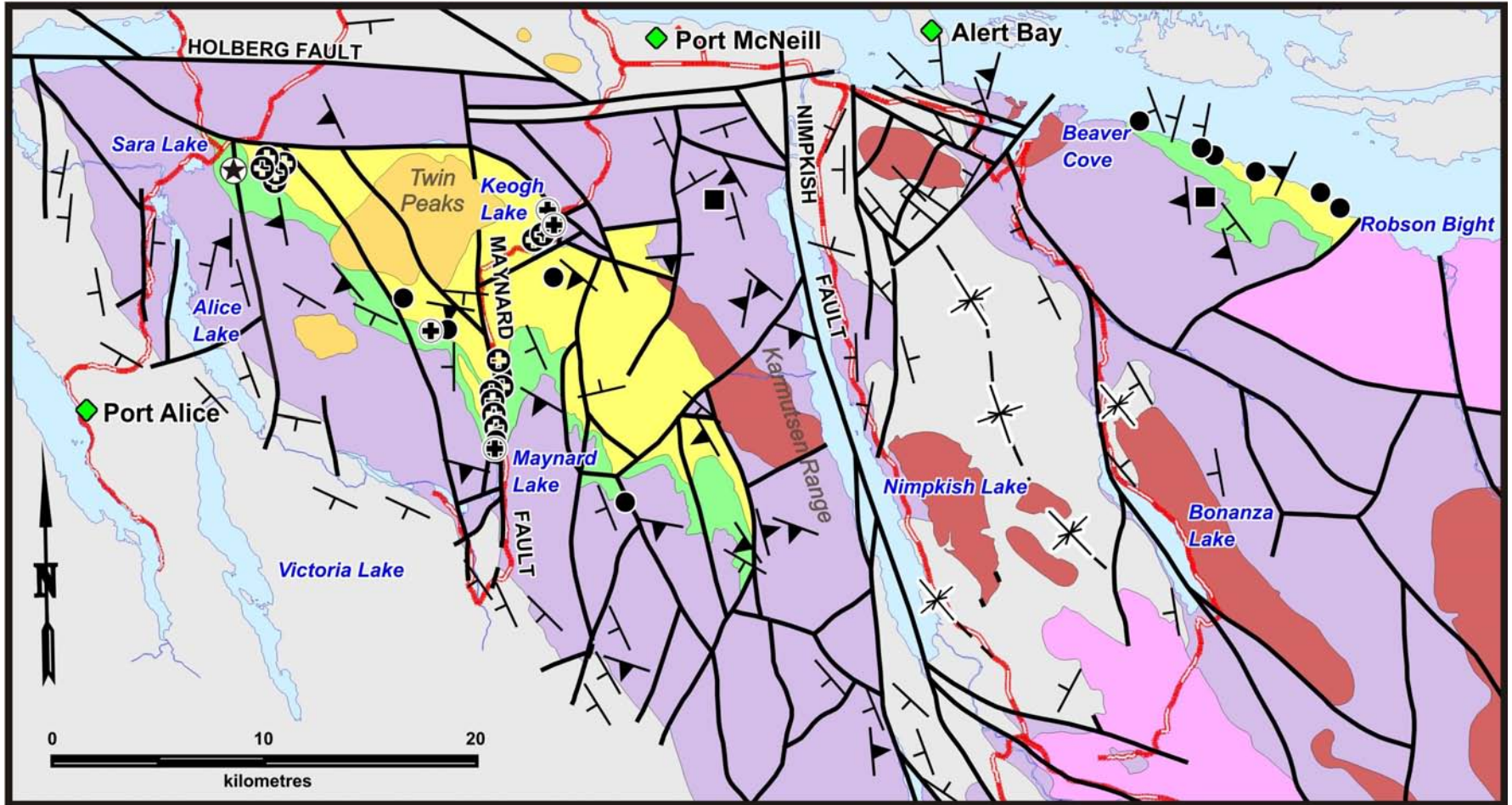


Figure 3. Generalized geology of the Late Triassic Karmutsen Formation in the Port Alice – Port McNeill – Robson Bight area, showing the location of olivine-bearing and high-Mg basalts in relation to the distribution of massive flow, hyaloclastite and pillow lava sequences. Other map units are undifferentiated (grey), except for the Tertiary Alert Bay volcanic rocks and intrusions of the Island Plutonic Suite (see Fig 1).

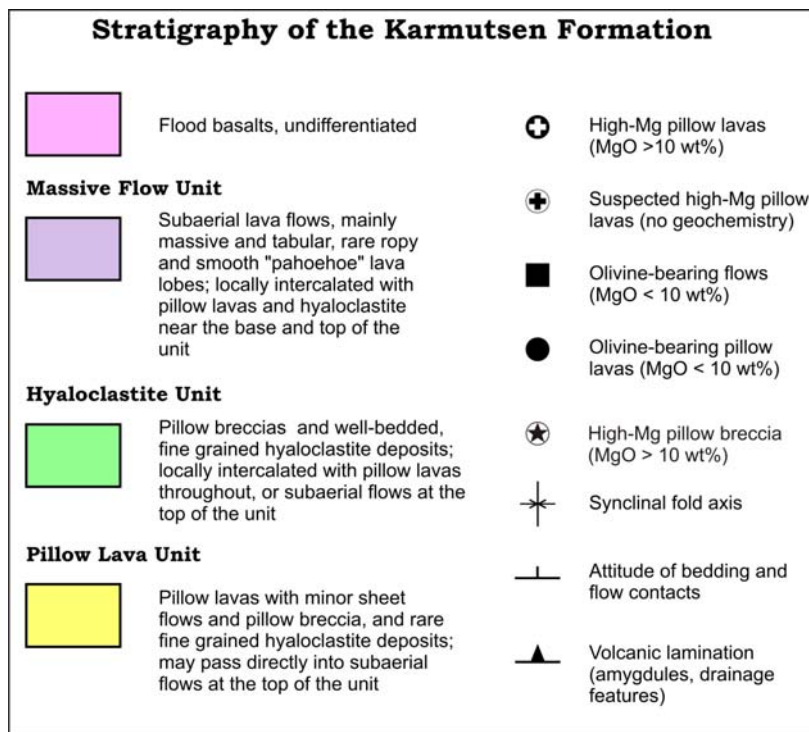


Figure 4. Legend for the geology map of the Karmutsen Formation (Fig 3, opposite).

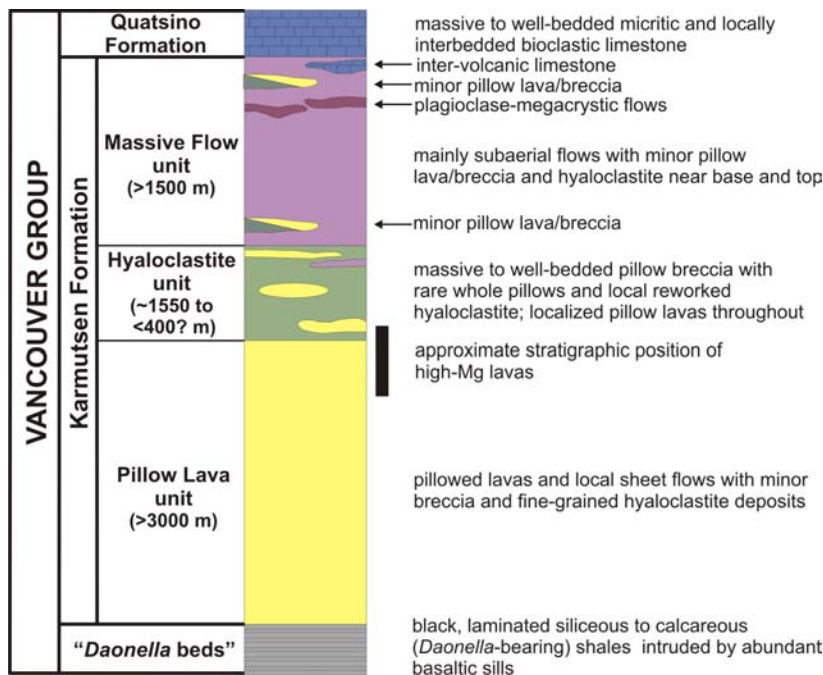


Figure 5. Stratigraphy of the Karmutsen Formation, showing the tripartite subdivision into basal pillow lavas, overlying hyaloclastite deposits and younger massive flow units. Note that known occurrences of high-Mg basalt appear to lie near the top of the pillow lava sequence.

from submarine to subaerial effusive volcanism. At the upper contact, Quatsino limestone rests directly on the flows, or is separated from them by a thin (<1 m) layer of calcareous basaltic sandstone and siltstone representing the water-laid weathering products of the lava shield. The uppermost

part of the flow sequence has a distinctive stratigraphy that includes thin (typically <6 m thick and rarely exceeding 15 m) pockets and lenses of pale grey weathering, micritic to bioclastic, and rarely oolitic, intervolcanic limestone, similar to the Quatsino Formation, and rare shale and siltstone. Locally, intra-Karmutsen limestone is associated with thin sequences of pillow lava and hyaloclastite deposits, which may also occur intercalated between the flows. Distinctive megacrystic lavas, charged with blocky to prismatic, euhedral to subhedral plagioclase crystals reaching 1 to 2 cm in length, are restricted to this part of the section (Fig 5). The minimum thickness of the massive flow unit, as estimated from its upper contact with Quatsino limestone to the granitoid intrusion west of Beaver Cove, is approximately 1500 m.

The dark grey to grey-green or dusky red flows are generally aphanitic to fine grained, especially in flow interiors, or plagioclase phyric, and have strongly amygdaloidal to nonamygdaloidal textures and moderate to strong magnetic response. Plagioclase phenocrysts (typically <4 mm) are more common in the upper part of the flow sequence. Plagioclase megacrysts (usually 1–2 cm) occur in basalts near the top of the unit, generally below intra-Karmutsen limestone, and are evenly distributed throughout the flow (10–20 vol% crystals) or locally concentrated in zones with up to 40 to 50 vol% crystals. The megacrysts are generally arranged haphazardly, presumably due to the high viscosity of these crystal-choked layers.

The morphology of the massive flow unit is commonly rendered as ledges protruding from steep hillsides. The unit is composed predominantly of simple flows, generally ranging from about 2 to 6 m thick, although some flows are thinner (<0.5 m) and others appear to exceed 15 m in thickness. Rarely, ropy and smooth 'pahoehoe' lava crusts and lobes in compound flows are well preserved (Fig 9A–C). The contacts between individual flows are typically sharp and planar to curvilinear, and are indistinct in many outcrops. Definitive features marking flow contacts include amygdaloidal flow tops overlain by dense, compact zones at the base of the overriding flow that locally exhibit hackly joint patterns and/or zones of pipe vesicles commonly filled with quartz and zeolites (Fig 9D).

Contacts may exhibit noticeably different degrees of oxidation, as reflected by hematitic alteration, but flow breccia and paleosol development are entirely absent. As noted by Greene et al. (2006), columnar jointing, common in many continental flood basalt provinces, is completely lacking in

Karmutsen flows. Crude columnar jointing, however, has been observed in certain sills. By far the most common internal fabric is a flow lamination marked by amygdule concentrations ranging from several centimetres to (rarely) 0.5 m thick and commonly arranged in parallel layers within the outcrop. This amygdaloidal layering invariably shares the same orientation as flow contacts, where present, and may be used as a valuable structural indicator in the absence of bedding information (Fig 3). Nested drainage channels filled with drusy quartz crystals, identical to those described previously in the basal pillow lava unit, are sparsely distributed yet provide good substitutes for bedding and clear evidence of local flow orientation (Fig 9E, F).

In thin section, the porphyritic flows contain phenocrysts of plagioclase, or both olivine and plagioclase, set in a fine-grained groundmass containing clinopyroxene, plagioclase and opaque oxides. Subhedral to anhedral olivine crystals (<1.5 mm) are found in lavas with as little as 6 wt% MgO (*see below*). Megacrystic flows contain euhedral laths and blocky crystals of calcic plagioclase up to 2 cm in length and exhibit either a serial size gradation towards the groundmass or hialtal textures. Subhedral olivine commonly forms glomerophyric intergrowths with, or inclusions within, plagioclase phenocrysts. Clinopyroxene may be present as intergranular grains, particularly in aphyric flows, or display subophitic to ophitic textures, most prevalent in plagioclase-phyric lavas, especially the

centres of thick flows. Secondary alteration assemblages and amygdule infillings include quartz, epidote, chlorite, zeolite, potassium feldspar and carbonate, and rarely iron oxides, chalcopryrite and native copper.

High-Mg Lavas

The high-Mg lavas are arbitrarily defined as having MgO >10 wt% and, in the geochemical classification described below, are predominantly magnesian basalt and picrite. The principal outcrops are at Keogh Lake, the type locality, and close to Sara Lake in the west and Maynard Lake in the east (Greene et al., 2006). New exposures of high-Mg lavas identified in this study are situated on the eastern side of the Maynard fault (Fig 3). To date, practically all high-Mg lavas are restricted to the basal pillow basalt unit, where they form both pillowed and sheet flows. A subvolcanic dike and pillow-fragment breccia described by Greene et al. (2006, Fig 7, 8) likewise have high-Mg compositions. The stratigraphic position of these high-Mg rocks, as determined in this study, lies close to the top of the basal pillow basalt sequence and within the base of the overlying hyaloclastite unit (Fig 3, 5).

All high-Mg rocks contain variable amounts of olivine phenocrysts, rarely visible in outcrop due to complete replacement by secondary mineral assemblages (*see* Greene et al., 2006, Fig 6, 7). Olivine phenocrysts, typically accompanied by plagioclase, also occur in rocks with

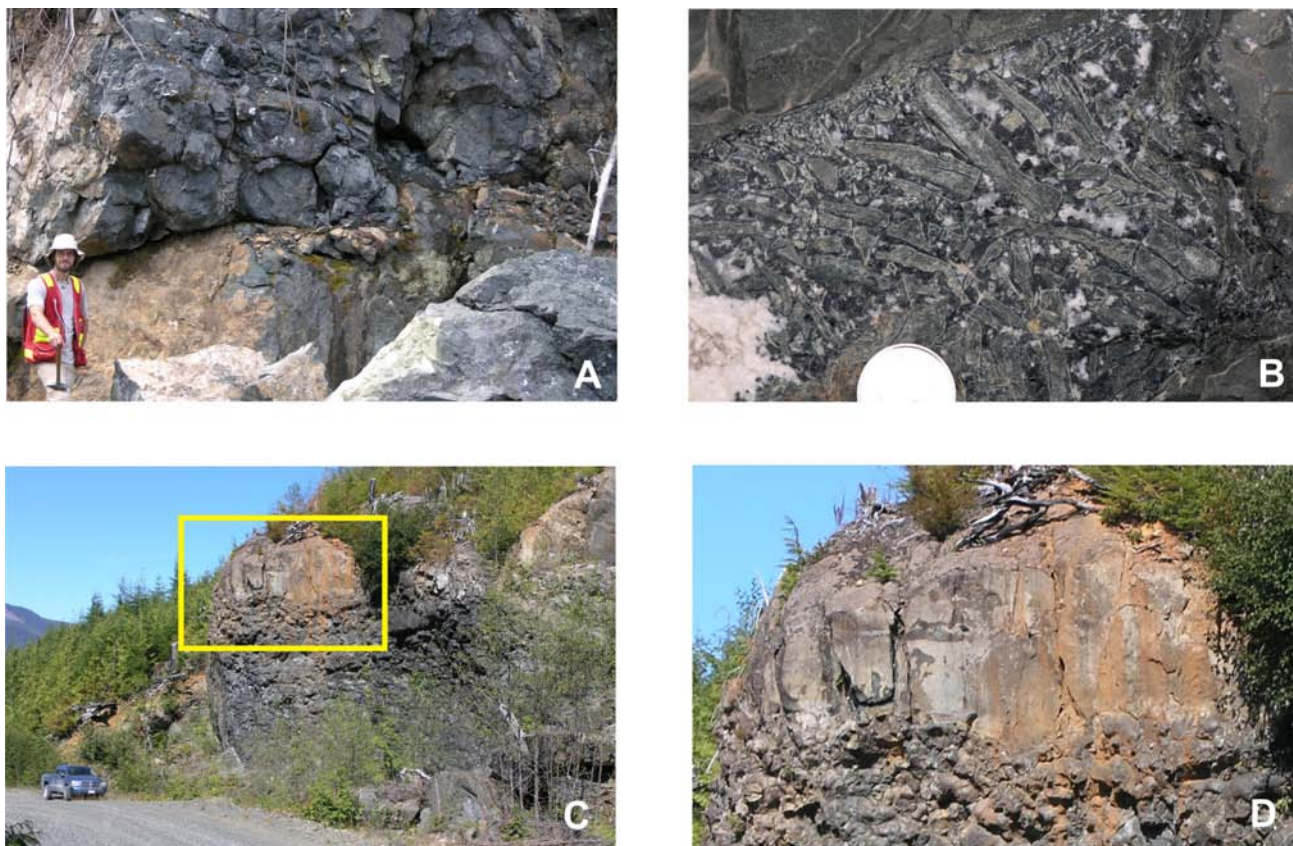


Figure 6. Karmutsen pillow basalt: A) closely packed pillows intercalated with pillow breccias inferred to lie near the top of the massive subaerial flow unit (locality 06GNX3-3-1); B) elongate to curvilinear glassy shards formed from quench-fragmented rinds of tholeiitic pillows in the basal pillow basalt unit, devitrified and altered to chlorite, quartz, epidote and zeolite ('dallasite'); C) localized massive sheet flow intercalated with high-Mg pillow lavas near the top of the pillowed unit (locality 06GNX34-4-1); D) detail of base of sheet flow (inset in C) draped over pillows.

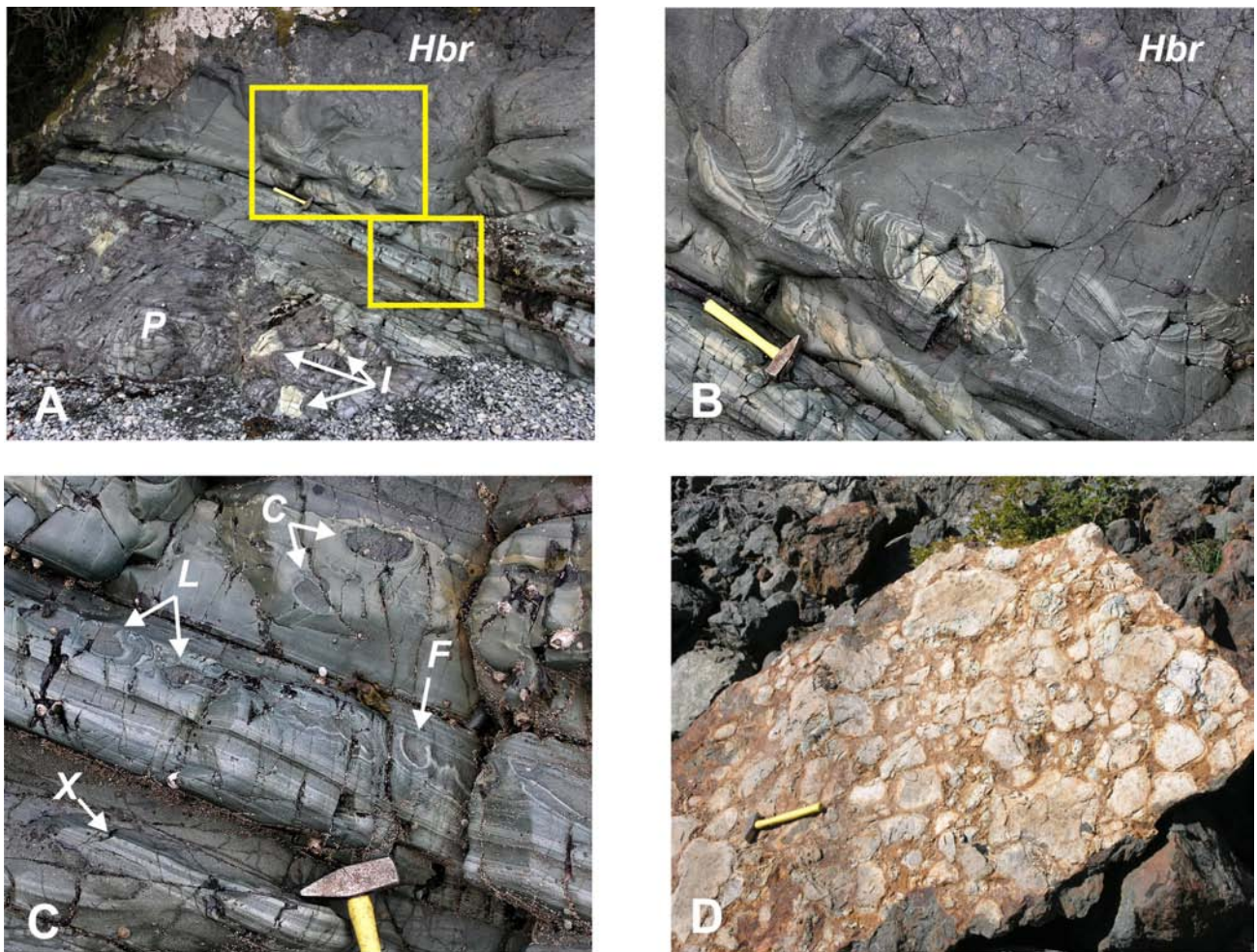


Figure 7. Volcanological and sedimentary features of the hyaloclastite unit: A) intraformational pillow lava (P) with trapped interpillow hyaloclastite sediment (I), overlain by thinly bedded hyaloclastite sandstone exhibiting remobilized bedding near the contact with overlying hyaloclastite breccia (Hbr) rich in broken pillow fragments (locality 07GNX10-5-1); B) slumped and rotated hyaloclastite beds beneath pillow-breccia debris flow (area shown in A); C) well-developed flame structures (F) and load casts (L) in beds below a debris flow that also exhibit crossbeds (X) and contain dispersed basaltic clasts (C; inset shown in A); D) pillow-fragment breccia exhibiting dispersed whole pillows and a rusty, pyritic hyaloclastic matrix (locality 06GNX34-6-1).

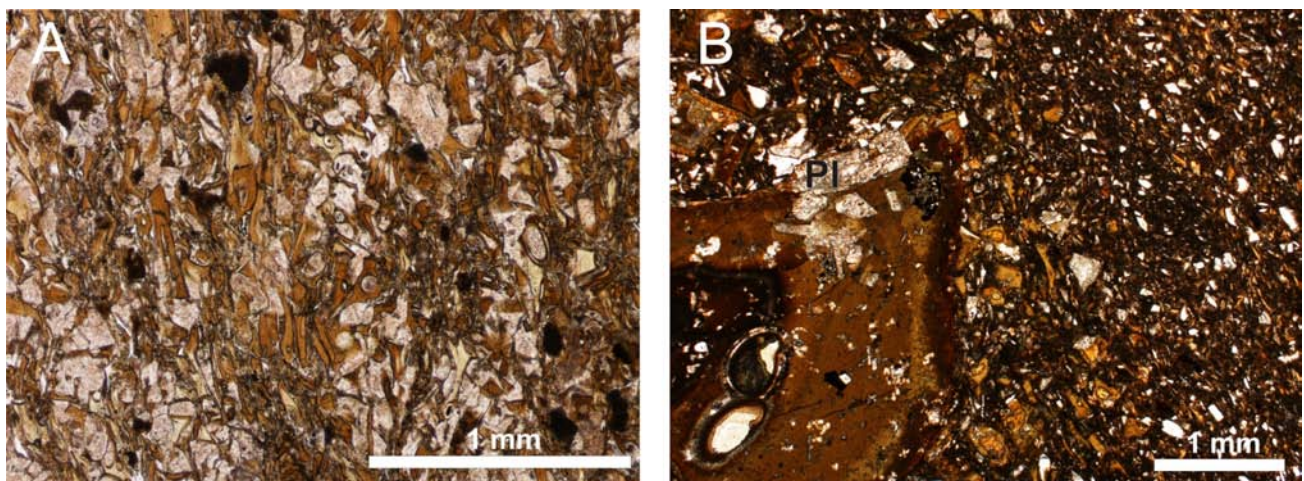


Figure 8. Photomicrographs of hyaloclastite textures: A) dark brown, palagonitized shards of devitrified, pseudo-isotropic basaltic glass and more finely comminuted material in laminated hyaloclastite sandstone, partially replaced and cemented by prehnite (white); B) small angular clast of palagonitized vesicular basalt (lower left) with a partially embedded plagioclase phenocryst (PI) enclosed in hyaloclastite sandstone. Both photomicrographs are of sample 07GNX11-4-1 in plane-polarized transmitted light.

<10 wt% MgO, which appear more widespread (Fig 3). High-Mg lavas are difficult to distinguish from tholeiitic basalt in the field, and positive identification requires geochemical analysis and petrographic observation. The most diagnostic physical property is their generally nonmagnetic

character and extremely low magnetic susceptibility readings.

The dark grey to greenish grey high-Mg pillow lavas are typically closely packed with virtually no interstitial hyaloclastite, and are spatially associated with less

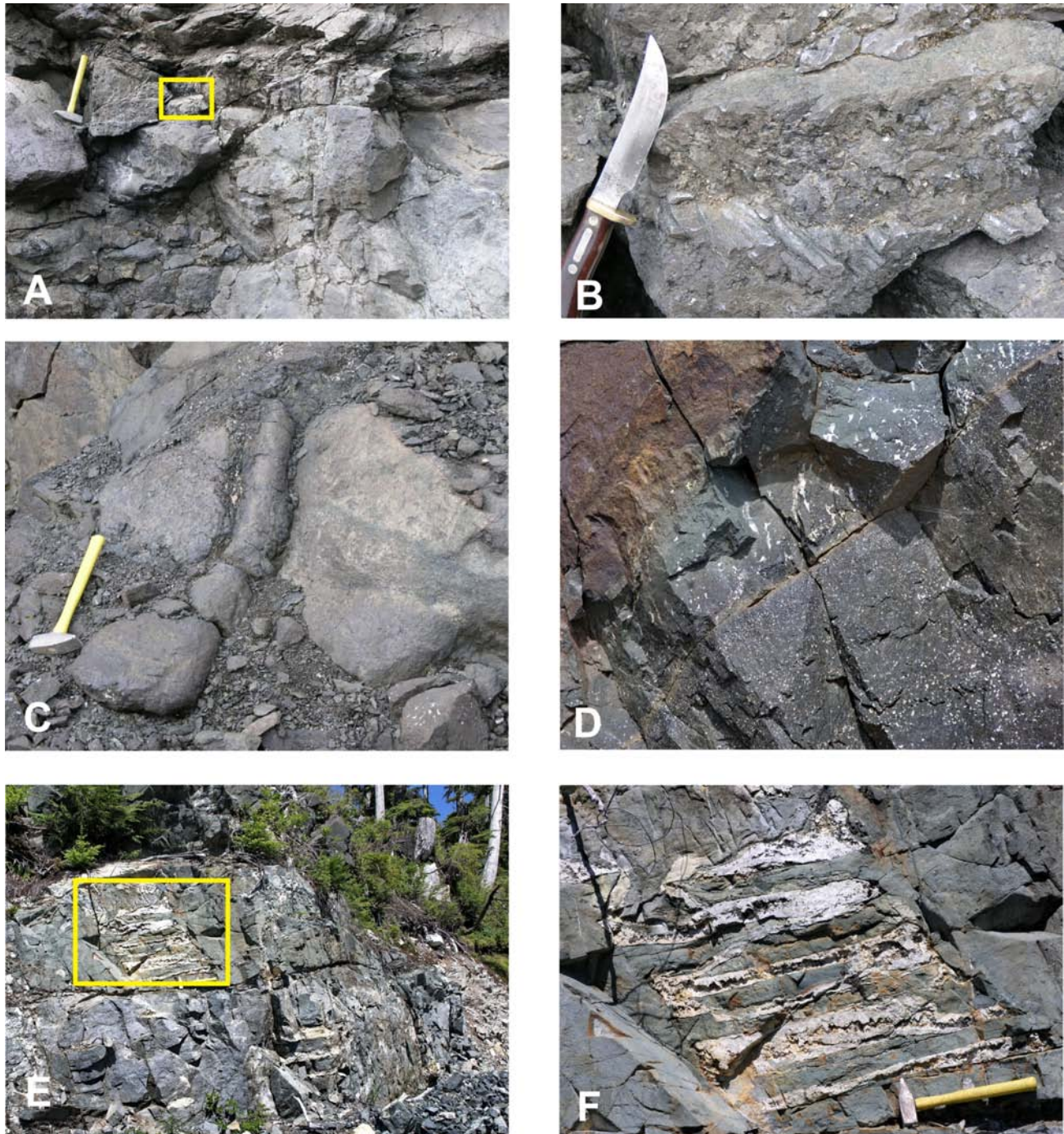


Figure 9. Volcanological features of subaerial Karmutsen basalts: A) cross-section through thin 'pahoehoe' flow lobes with smooth undulatory contacts dipping gently towards camera (locality 06GNX11-5-1); B) close-up of curvilinear, ropy (pahoehoe) lava crust protruding below thin overlying flow (area shown in A); C) smooth pahoehoe flow lobe in the same quarry; D) sharp contact between massive flows, showing amygdule-rich flow top in sharp contact with the dense base of the overlying flow, which exhibits a well-developed zone of pipe vesicles deformed in the direction of flow (left to right; locality 07GNX25-5-1); E) massive flow unit, exhibiting multiple lava drainage ledges (lava tubes) infilled with quartz (locality 07GNX13-5-1); F) close-up of vuggy quartz ledges (area shown in E).



Figure 10. Photomicrograph of high-Mg basalt in a massive sheet flow at the type locality at Keogh Lake. Euhedral to subhedral olivine phenocrysts are set in a groundmass of calcic plagioclase, clinopyroxene and granular opaque oxides. The olivine is completely replaced by talc±chlorite and fine-grained magnetite. Sample 07GNX37-1-1 in plane-polarized transmitted light.

magnesian tholeiitic basalt. The Keogh Lake picritic basalt forms both pillowed flows and minor sheet flows (Fig 10; cf. Greene et al., 2006, Fig 6). The sample of high-Mg pillow breccia taken close to the base of the hyaloclastite unit comes from a dark grey-green, massive layer of chaotically distributed, angular to subrounded, matrix-supported clasts (<35 cm), some of which exhibit chilled pillow margins, set in a chloritized and carbonate-altered clastic matrix.

Petrographically, the high-Mg pillow lavas contain abundant olivine, typically 10 to 25 vol% but reaching 40 vol% in some samples. Euhedral to subhedral olivine crystals (1–4 mm) are the sole phenocryst phase in high-Mg lavas with >12 wt% MgO (i.e., picrite, according to the revised IUGS classification discussed below). The morphology and abundance of olivine phenocrysts is similar in both high-Mg sheet flows associated with the pillow lavas (Fig 10) and the rare dikes that fed these lavas. The olivine in these rocks is predominantly replaced by talc, in contrast to the less magnesian olivine-bearing basalt, where replacement products generally include serpentine, chlorite, carbonate and quartz. Subequant to lath-shaped phenocrysts (<4 mm) of calcic plagioclase generally coexist with olivine in the latter group of lavas. Where olivine and plagioclase form glomerophytic intergrowths, olivine is the subordinate phase. Clinopyroxene in the high-Mg lavas is typically intergrown with calcic plagioclase to form subophitic to well-developed variolitic textures (illustrated by Greene et al., 2006, Fig 5).

GEOCHEMICAL CLASSIFICATION

Whole-rock analyses of Karmutsen basalt from northern Vancouver Island are plotted in Figure 11. All analyzed samples were examined petrographically to determine the degree of alteration, based on the abundance of amygdules infilled by secondary minerals, notably quartz, chlorite, carbonate, epidote, sericite, potassium feldspar, prehnite, zeolites and, rarely, pumpellyite; and the degree of replacement of calcic plagioclase, mainly by sericite and clay minerals but also involving partial replacement by chlorite, car-

bonate and epidote. Accordingly, the geochemical diagrams show only the least altered rocks, except for Figure 11D, where altered and amygdaloidal samples (>10 vol% amygdules) are represented.

A total alkalis versus silica (TAS) plot shows the subalkaline nature of the suite (Fig 11A). The lavas fall within the basalt field in the TAS classification (LeMaitre et al., 1989) and exhibit a large range of total alkali content (approx. 0.5–5.0 wt%) relative to their rather limited variation in silica (approx. 50 ± 2.5 wt%). The AFM diagram (Fig 11B) shows that the subalkaline basalts belong to a tholeiitic lineage with moderate iron enrichment.

Both least-altered and altered basalts are plotted in the IUGS classification scheme for high-Mg lavas (Fig 11C, D, respectively; Le Bas, 2000). Olivine-bearing basalt displays a considerable range of MgO abundances (approx. 5.5–19 wt%), extending from ‘normal’ basalt MgO concentrations through picrite to komatiitic compositions. The sampling is sufficient to illustrate a continuum of MgO abundances in these olivine-bearing lavas. The picrite in this classification scheme is defined by MgO >12 wt%, SiO₂ <52 wt% and Na₂O + K₂O <3 wt%. Komatiite has MgO >18 wt%, SiO₂ <52 wt%, total alkalis <2 wt% and TiO₂ <1 wt% (and see Greene et al., 2006, Fig 2C). Lavas that fall within the picrobasalt field in the high-Mg classification are, in fact, simply basalt in the TAS classification (Fig 11A) because, in order to qualify as ‘picrobasalt’, silica in these rocks must lie within the range 41 to 45 wt% SiO₂ (Le Bas, 2000), which is not the case. Olivine-free basalt falls near the lower limit of MgO concentrations (<7.5 wt%), but there is considerable compositional overlap between the olivine-free and olivine-bearing groups. Magnesium-poor lavas in the latter group are characterized by minor to trace amounts of olivine (Fig 11E).

The amygdaloidal and altered rocks plotted in Figure 11D show a distinct bias towards higher average alkali contents in the Mg-poor part of the compositional spectrum. The compositions of the least altered lavas likewise extend to similar high alkali abundances (Fig 11C). We conclude that this behaviour reflects varying degrees of alkali metasomatism unsuccessfully filtered by petrographic criteria alone.

Greene et al. (2006) observed that the Keogh Lake picritic basalt has the highest MgO abundances presently known within the Wrangellian flood basalt province, and that its primitive nature reflects partial melting generated by the ascent of a mantle plume beneath the oceanic plateau. It must be noted, however, that Karmutsen lavas with the highest MgO contents do not necessarily represent the compositions of such partial melts. For example, it is clear from the strong positive correlation between MgO and modal olivine (Fig 11E) that crystal sorting has played a role in determining the MgO content of these lavas. The high modal abundance of olivine in the most magnesian lavas may be reconciled by crystal accumulation, whereas compositions depleted in MgO likely reflect crystal fractionation of a more magnesian parental magma. It is important to note that rocks falling within the ‘komatiite’ field in the geochemical classification diagram contain approximately 40 vol% polyhedral olivine phenocrysts that are morphologically identical to those observed in the picrite and more magnesian basalt. These textural attributes, together with the complete lack of spinifex textures and close association with picritic basalt, are consistent with a cumulate origin for these MgO-rich compositions (cf. Kerr and

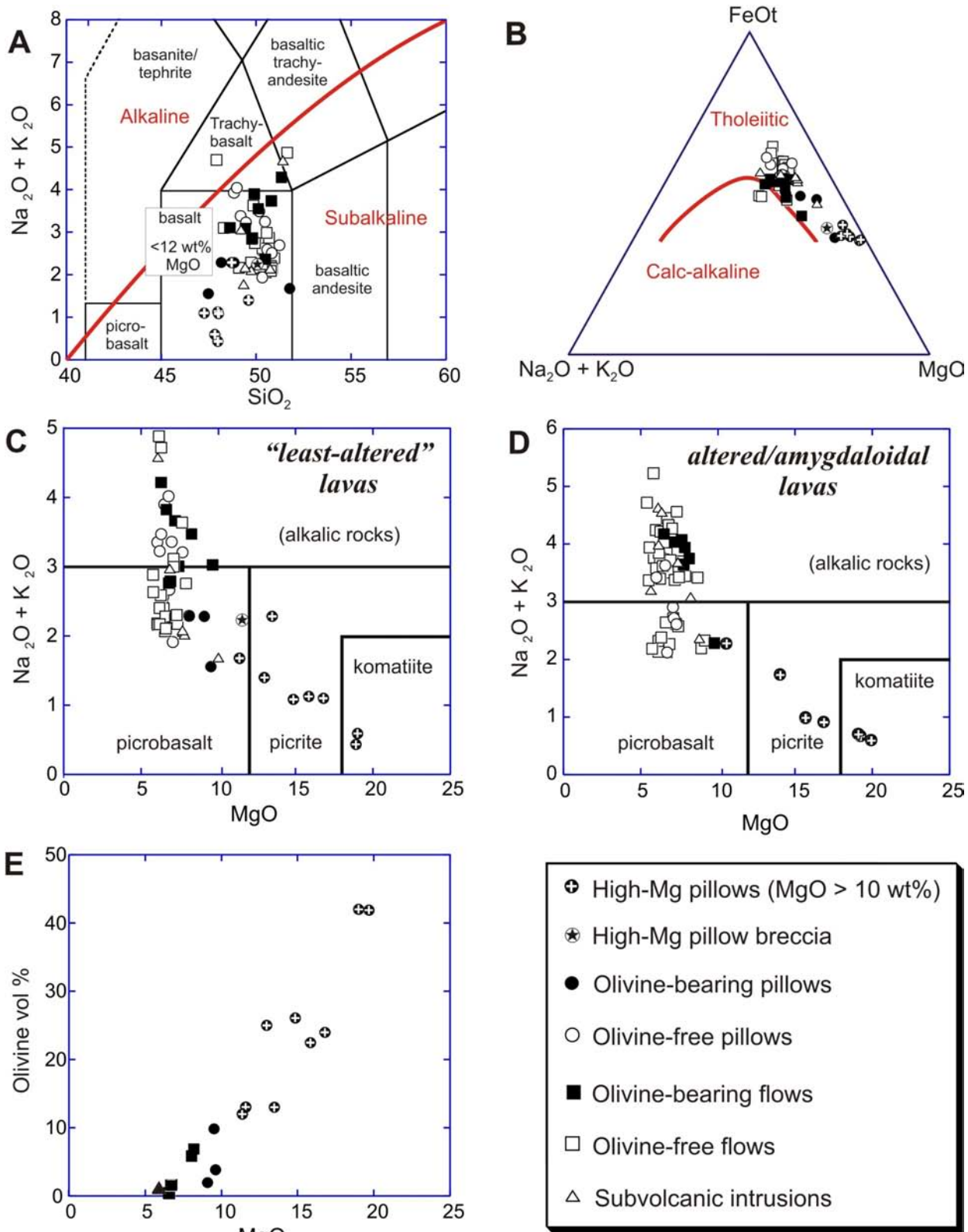


Figure 11. Whole-rock geochemical plots of Karmutsen basalts: A) total alkalis vs SiO₂ plot, showing the discriminant for alkaline and subalkaline rock series (Irvine and Baragar, 1971) and the IUGS classification of LeMaitre et al. (1989); B) total alkalis – total Fe as FeO (FeO_T) – MgO (AFM) plot, showing the discriminant between tholeiitic and calcalkaline rock series (Irvine and Baragar, 1971); C) and D) total alkalis vs MgO plots, showing the IUGS reclassification for high-Mg and picritic volcanic rocks (Le Bas, 2000); 'least altered' samples are shown in C, whereas altered and amygdaloidal samples are plotted in D; E) MgO vs modal olivine (vol%) plot for selected basalt samples. All analyses are recalculated to 100 wt% anhydrous with total iron as FeO.

Arndt, 2001). Thus, the most primitive melts in the Karmutsen Formation may have picritic rather than komatiitic compositions, which has relevance to potential models for Ni-Cu-PGE mineralization in the Wrangellian flood basalt province, as discussed below.

EVOLUTION OF THE OCEANIC PLATEAU

The stratigraphy of the Karmutsen Formation reflects the evolution of the Wrangellia oceanic plateau, a record of events not unlike modern hot-spot volcanoes such as Hawaii. The enormous outpourings of mainly aphyric pillow lava and localized sheet flows, represented by the basal pillow lava unit, mark the initial phase of submarine effusive activity, which constructed a seamount(s) rising from the deep ocean floor. The amygdaloidal nature of the uppermost pillow lavas and breccias in the overlying hyaloclastite unit indicate that, as the volcanic edifice grew and reached relatively shallow depths (<500 m), magmas were able to exsolve small amounts of volatiles. The eruption and emplacement of high-Mg lavas occurred at the transition from pillow lava emplacement to hyaloclastite deposition.

The thick sequence of volcanoclastic rocks deposited at the transition from submarine to subaerial volcanism likely reflects a variety of fragmentation processes, including thermal contraction of cooling pillows and internal expansion of growing pillow tubes, wave action, minor explosive activity triggered by volatile release and seawater-magma interaction, and earthquake-induced and gravitational collapse of oversteepened pillow ramparts. Many pillow-fragment breccias and sandstone horizons are rich in hyaloclastite material, presumably generated in shallow water and redeposited downslope by debris flows and turbidity currents, respectively.

As eruptions breached sea level, outpourings of highly amygdaloidal, fluid basaltic lava began to construct a gently sloping shield volcano. The plagioclase-phyric and megacrystic flows were emplaced late in the evolution of the shield. As volcanism waned due to decay of the mantle plume, thermal contraction of the lithosphere led to submergence of the shield. Localized deposition of intervolcanic limestone, pillow lava and hyaloclastite de-

posits intercalated with subaerial flows at the top of the Karmutsen succession records the final stages of effusive activity as submergence commenced. The presence of thin, discontinuous beds of basaltic sandstone and absence of a well-developed regolith or coarse conglomeratic deposits reflect the lack of deeply incised topography and rapid submergence. Cessation of volcanic activity led to the deposition of platform carbonate, represented by Quatsino limestone.

POTENTIAL FOR NI-CU-PGE MINERALIZATION

Flood basalt volcanism is associated with some important magmatic ore deposits, one premier example being the Ni-Cu-PGE sulphide mineralization of the Noril'sk-Talnakh region of Siberia (Fig 12). Economic concentrations of ore metals (production + reserves) at Noril'sk total some 555 million tonnes of 2.7% Ni, 3.9% Cu, 3 g/t Pt and 12 g/t Pd (Lightfoot and Hawkesworth, 1997). Naldrett (2004) noted that the Noril'sk ores exceed all other deposits, both Ni-Cu and PGE deposits, in the value of *in situ* metals per tonne. The sulphides are hosted by comagmatic intrusions that have been interpreted as conduits for part of a thick (~3.5 km) sequence of continental flood basalts erupted at the Permian-Triassic boundary. Like the Wrangellian flood basalts, the enormous volume of Siberian trap basalts (>2 x 10⁶ km³; Fedorenko, 1994) erupted over such a short time interval (250 ± 1 Ma; Sharma, 1997) that their consequently rapid eruption rate and lack of definitive evidence for emplacement during a major rifting event have been used to support a plume initiation model for their origin (cf. Greene et al., 2006). Aspects of the geology and genesis of the Noril'sk deposits and their related flood basalts, therefore, have metallogenic significance here.

Geochemical studies of the host intrusions and flood basalts at Noril'sk have indicated that, in a general sense (and albeit controversial), the processes that formed the ore deposits are to some degree reflected in the lavas (cf. Arndt et al., 2003; and *see* Naldrett, 2004 for a summary of pertinent controversies). The magmatic sulphides are hosted by gabbro-dolerite (9–16 wt% MgO) and olivine-rich picrite (18–29 wt% MgO) intrusions emplaced in Paleozoic sedi-

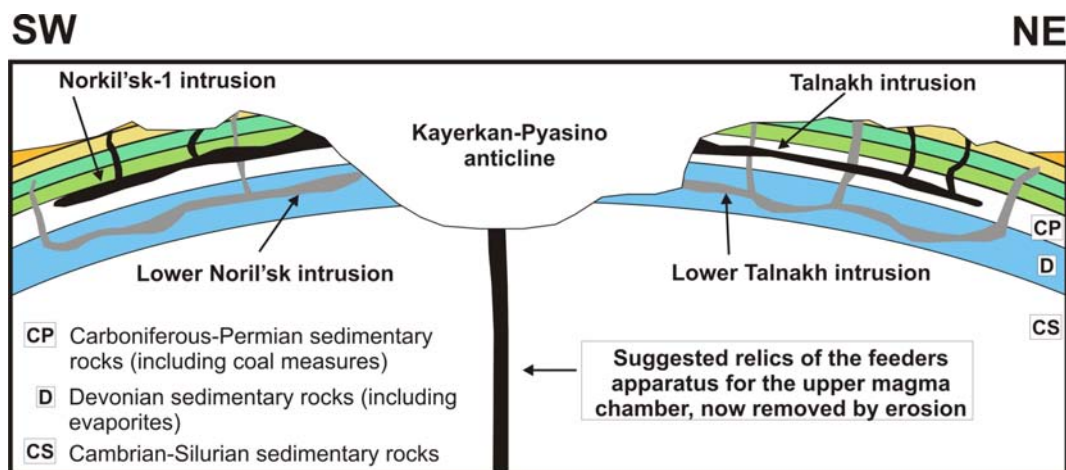


Figure 12. Schematic geological cross-section of the Noril'sk region (after Naldrett, 2004). Vertical scale is greatly exaggerated relative to horizontal scale.

mentary rocks that include sulphate-rich evaporites and coal measures. In order to satisfy the geochemical data, most workers agree that the complex architecture of conduits presently plugged by these intrusions were the sites of dynamic, open magmatic systems feeding the volcanic pile. Hot, primitive high-Mg (picritic) lavas form a small proportion of the overlying flood-basalt stratigraphy in the Noril'sk region (<1% of the stratigraphic thickness, according to Fedorenko, 1994), and are considered to represent parental magmas for the fractionated tholeiite. The presence of high-Mg lavas is nonetheless important, since these magmas inherently contain elevated abundances of Ni, and potentially Cu and PGE, and are the most likely candidates to be sulphur undersaturated and therefore capable of precipitating economic concentrations of metals in magmatic sulphides (Keays, 1995).

Some of the important evolutionary aspects of the Noril'sk-Talnakh system are shown schematically in Figure 13. Lightfoot and Hawkesworth (1997) observed that the chemical stratigraphy of the flood basalt pile records a strong depletion of chalcophile elements, as monitored by Cu, over approximately 200 m of stratigraphy, followed by

a gradual upward recovery in the tenor of Cu, Ni and PGE in the succeeding lavas over a 700 m stratigraphic interval. They emphasized that the lavas that show the strongest depletions of chalcophile elements, reflecting equilibration with sulphide ores at depth, are also those that have experienced the most crustal contamination by lower to midcrustal rocks. They argued that the increase in silica in contaminated magmas was primarily responsible for driving magmas towards sulphide ore formation in shallower crustal magma chambers, and not the addition of crust-derived S from evaporite-rich sediments. Since the sulphide ores contain an unusually high tenor of metals, the immiscible sulphide droplets must have scavenged metals from very large volumes of basaltic magma migrating through the conduit system, leaving the erupted lavas sympathetically depleted in these metals (the 'R factor' of Campbell and Naldrett, 1979). The gradual recovery in metal abundances exhibited by lavas higher in the stratigraphic section is considered to reflect progressive isolation of sulphides from dynamic interaction with fresh inputs of magma, possibly by gravitational settling of heavy sulphide droplets in hydrodynamic traps so as to form the more massive orebodies where Cu-rich ores subsequently fractionated

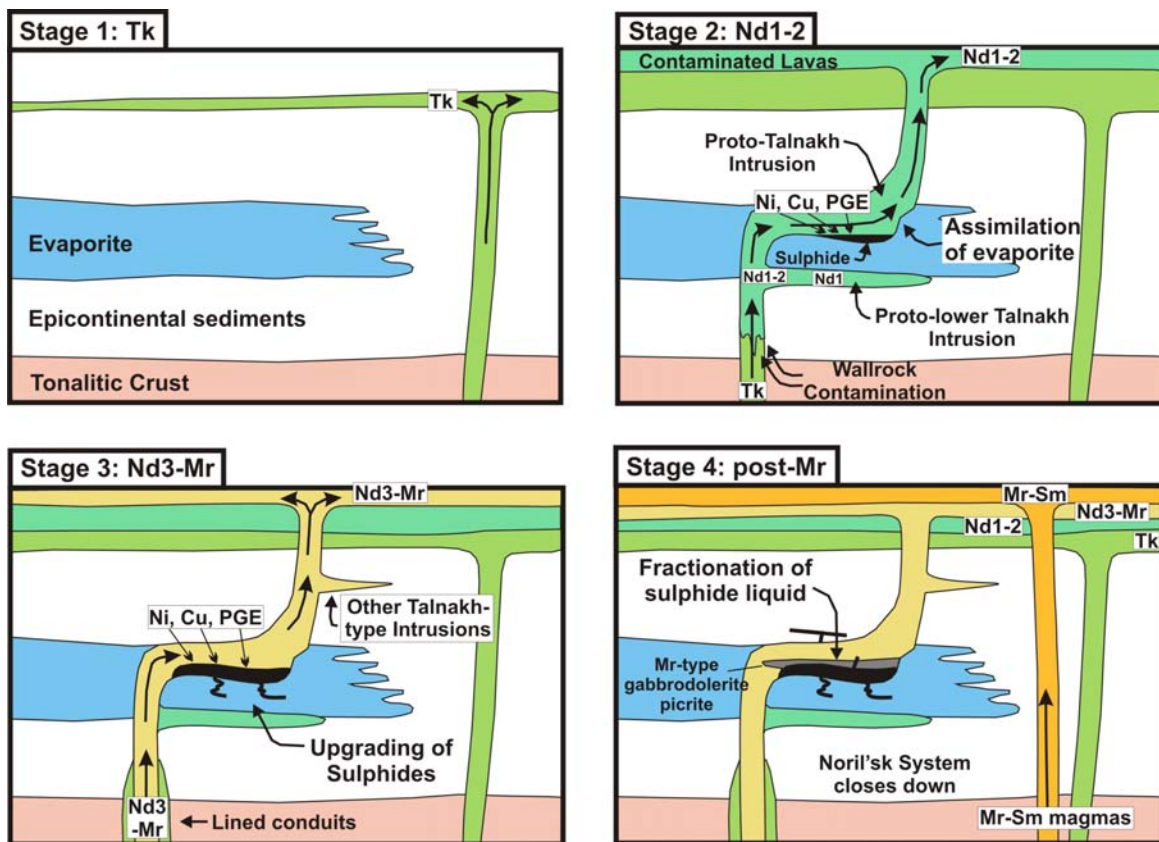


Figure 13. Schematic model for the evolution of the Noril'sk system (after Lightfoot and Hawkesworth, 1997). Stage 1: picritic and tholeiitic lavas of the Tuklonsky Formation (Tk) were erupted through conduits situated east of Noril'sk. Stage 2: Eruption of Nd1 lavas at Noril'sk generated by contamination and crystal fractionation of primitive Tk magmas with granodiorite at depth followed by assimilation of evaporitic sediments at shallow levels in the conduit system; the elevated silica and sulphur contents of contaminated magmas lead to precipitation of immiscible sulphides that ponded and reacted with fresh magma batches of Nd1 (Nadezhdinsky lavas) passing through the conduits. Stage 3: Continued throughput of Nd1 magma upgraded the Ni, Cu and PGE tenor of ponded sulphide liquids, causing the metal depletion observed in the lavas; as subsequent Nd2, Nd3 and Mr (Morongovsky) magmas ascended through the conduits, the sulphides became progressively isolated from the magmas and the degree of metal depletion declined, producing the observed upward increase of chalcophile element abundances with stratigraphic height. Stage 4: The Noril'sk system shut down as magmatism migrated northeast; sulphide liquids fractionated to form the Cu-rich ores.

(Czamanske et al., 1992; Lightfoot and Hawkesworth, 1997).

Exploration strategies for Ni-Cu-PGE deposits associated with the Wrangellian flood basalts should find certain aspects of the Noril'sk model intriguing. The occurrence of high-Mg basaltic lavas in the Karmutsen Formation of northern Vancouver Island demonstrates that this part of the flood basalt province received a supply of hot primitive magma, presumably S-undersaturated and therefore capable of forming magmatic sulphide ores. The lateral extent of these high-Mg lavas is presently unknown, and no systematic geochemical studies of the flood basalt stratigraphy have been undertaken with a view to prospecting for lavas with anomalously low chalcophile-element abundances.

Subvolcanic plumbing systems are exposed at the base of the Karmutsen Formation as dikes and sills in the Middle Triassic 'sediment-sill' unit (Muller et al., 1974, 'Daonella beds' of Fig 2). These pyritic shale and siltstone beds, and the older Paleozoic basement rocks they overlie, are potential sources of the siliceous and sulphur-bearing contaminants apparently required to induce magmatic sulphide segregation in primitive melts. As documented by Greene et al. (2006), small concentrations of disseminated sulphides have been observed at the contact of some subvolcanic Karmutsen sills; and some chemical subtypes of tholeiitic basalt with significant quantities of PGE appear to have erupted close to sulphur saturation (J.S. Scoates, unpublished data). These observations, together with the limited amount of geochemical data currently available for the Triassic flood basalts and their intrusive counterparts, should be particularly encouraging for mineral exploration.

ACKNOWLEDGMENTS

We wish to express our sincere thanks to Margaret Hanuse in Port McNeill and Dave Ross in the community of Holberg for graciously providing shelter from the storm; Kim Pilote for cheerfully dealing with truck and boat logistics; and Brian Grant for a field visit. We also thank Kathryn Gillis, Director of the School of Earth and Ocean Sciences at the University of Victoria, for providing access to point-counting equipment; and Tania Demchuk and Brian Grant for editorial logistics.

REFERENCES

- Armstrong, R.L., Muller, J.E., Harakal, J.E. and Muehlenbachs, K. (1985): The Neogene Alert Bay volcanic belt of northern Vancouver Island, Canada: descending-plate-edge volcanism in the arc-trench gap; *Journal of Volcanology and Geothermal Research*, Volume 26, pages 75–97.
- Arndt, N.T., Czamanske, G.K., Walker, R.J., Chauvel, C. and Fedorenko, V.A. (2003): Geochemistry and origin of the intrusive hosts of the Noril'sk-Talnakh Cu-Ni-PGE sulphide deposits; *Economic Geology*, Volume 98, pages 495–516.
- Campbell, I.H. and Naldrett, A.J. (1979): The influence of silicate:sulphide ratios on the geochemistry of magmatic sulphides; *Economic Geology*, Volume 74, pages 1503–1505.
- Carlisle, D. (1963): Pillow breccias and their aquagene tuffs, Quadra Island, British Columbia; *Journal of Geology*, Volume 71, pages 48–71.
- Carlisle, D. (1972): Late Paleozoic to mid-Triassic sedimentary-volcanic sequence on northeastern Vancouver Island; in Report of Activities, Part B, *Geological Survey of Canada*, Paper 72-1B, pages 24–30.
- Carlisle, D. and Suzuki, T. (1974): Emergent basalt and submergent carbonate-clastic sequences including the Upper Triassic Dilleri and Welleri zones on Vancouver Island; *Canadian Journal of Earth Sciences*, Volume 11, pages 254–279.
- Cas, R.A.F. and Wright, J.V. (1987): Volcanic Successions: Modern and Ancient; *Allen and Unwin*, London, United Kingdom, 528 pages.
- Czamanske, G.K., Kunilov, V.E., Zientek, M.L., Cabri, L.J., Likhachev, A.P., Calk, L.C. and Oscarson, R.L. (1992): A proton-microprobe study of magmatic sulphide ores from the Noril'sk-Talnakh district, Siberia; *The Canadian Mineralogist*, Volume 30, pages 249–287.
- DeBari, S.M., Anderson, R.G. and Mortensen, J.K. (1999) Correlation amongst lower to upper crustal components in an island arc: the Jurassic Bonanza arc, Vancouver Island, Canada; *Canadian Journal of Earth Sciences*, Volume 36, pages 1371–1413.
- Fedorenko, V.A. (1994): Evolution of magmatism as reflected in the volcanic sequence of the Noril'sk region; in Proceedings of the Sudbury-Noril'sk Symposium, Lightfoot, P.C. and Naldrett, A.J., Editors, *Ontario Geological Survey*, Special Volume 5, pages 171–184.
- Furin, S., Preto, N., Rigo, M., Roghi, G., Gianolla, P., Crowley, J.L. and Bowring, S.A. (2006): High-precision U-Pb zircon age from the Triassic of Italy: implications for the Triassic time scale and the Carnian origin of calcareous nannoplankton and dinosaurs; *Geology*, Volume 34, pages 1009–1012.
- Gamba, C.A. (1993): Stratigraphy and sedimentology of the Upper Jurassic to Lower Cretaceous Longarm Formation, Queen Charlotte Islands, British Columbia; in Current Research, Part A, *Geological Survey of Canada*, Paper 93-1A, pages 139–148.
- Gardner, M.C., Bergman, S.C., Cushing, G.W., MacKevett, E.M., Jr., Plafker, G., Campbell, R.B., Dodds, C.J., McClelland, W.C. and Mueller, P.A. (1988): Pennsylvanian pluton stitching of Wrangellia and the Alexander Terrane, Wrangell Mountains, Alaska; *Geology*, Volume 16, pages 967–971.
- Gradstein, F.M., Ogg, J.G. and Smith, A.G. (2004): A geologic time scale 2004; *Cambridge University Press*, Cambridge, United Kingdom, 610 pages.
- Greene, A.R., Scoates, J.S., Nixon, G.T. and Weis, D. (2006): Picritic lavas and basal sills in the Karmutsen flood basalt province, northern Vancouver Island; in Geological Fieldwork 2005, *BC Ministry of Energy, Mines and Petroleum Resources*, Paper 2006-1, pages 39–51.
- Greenwood H.J., Woodsworth, G.J., Read, P.B., Ghent, E.D. and Evenchick, C.A. (1991): Metamorphism; Chapter 16 in *Geology of the Cordilleran Orogen in Canada*, Gabrielse, H. and Yorath, C.J., editors, *Geological Survey of Canada*, Geology of Canada, Number 4, pages 533–570.
- Gunning, H.C. (1932): Preliminary report on the Nimpkish Lake quadrangle, Vancouver Island, British Columbia; *Geological Survey of Canada*, Summary Report, 1931, Part A, pages 22–35.
- Haggart, J.W. (1993): Latest Jurassic and Cretaceous paleogeography of the northern Insular Belt, British Columbia; in *Mesozoic Paleogeography of the Western United States*, Volume II, Book 71, Dunn, G. and McDougall, K., Editors, *Society of Economic Paleontologists and Mineralogists*, Pacific Section, pages 463–475.
- Haggart, J.W. and Carter, E.S. (1993): Cretaceous (Barremian–Aptian) radiolaria from Queen Charlotte Islands, British Columbia: newly recognized faunas and stratigraphic implications; in Current Research, Part E, *Geological Survey of Canada*, Paper 93-1E, pages 55–65.

- Irvine, T.N. and Baragar, W.R.A. (1971): A guide to the chemical classification of the common volcanic rocks; *Canadian Journal of Earth Sciences*, Volume 8, pages 523–548.
- Jeletzky, J.A. (1976): Mesozoic and ?Tertiary rocks of Quatsino Sound, Vancouver Island, British Columbia; *Geological Survey of Canada*, Bulletin 242, 243 pages.
- Jones, D.L., Silberling, N.J. and Hillhouse, J. (1977): Wrangellia — a displaced terrane in northwestern North America; *Canadian Journal of Earth Sciences*, Volume 14, pages 2565–2577.
- Keays, R.R. (1995): The role of komatiitic and picritic magmatism and S-saturation in the formation of ore deposits; *Lithos*, Volume 34, pages 1–18.
- Kerr, A.C. and Arndt, N.T. (2001): A note on the IUGS reclassification of the high-Mg and picritic volcanic rocks; *Journal of Petrology*, Volume 42, pages 2169–2171.
- Le Bas, M.J. (2000): IUGS reclassification of the high-Mg and picritic volcanic rocks; *Journal of Petrology*, Volume 41, pages 1467–1470.
- LeMaitre, R.W., Bateman, P., Dudek, A., Keller, J., Le Bas, M.J., Sabine, P.A., Schmid, R., Sorensen, H., Streckeisen, A., Wooley, A.R. and Zanettin, B. (1989): A classification of igneous rocks and glossary of terms; *Blackwell Scientific Publications*, Oxford, United Kingdom, 193 pages.
- Lewis, T.J., Lowe, C. and Hamilton, T.S. (1997): Continental signature of a ridge-trench-triple junction: northern Vancouver Island; *Journal of Geophysical Research*, Volume 102, pages 7767–7781.
- Lightfoot, P.C. and Hawkesworth, C.J. (1997): Flood basalts and magmatic Ni, Cu and PGE sulphide mineralization: comparative geochemistry of the Noril'sk (Siberian traps) and West Greenland sequences; in Large Igneous Provinces: Continental, Oceanic and Planetary Flood Volcanism, Mahoney, J.J. and Coffin, M.F., Editors, *American Geophysical Union*, Geophysical Monograph 100, pages 357–380.
- Massey, N.W.D. (1995a): Geology and mineral resources of the Alberni-Nanaimo lakes sheet, Vancouver Island, 92F/1W, 92F/2E and part of 92F/7E; *BC Ministry of Energy, Mines and Petroleum Resources*, Paper 1992-2, 132 pages.
- Massey, N.W.D. (1995b): Geology and mineral resources of the Cowichan Lake sheet, Vancouver Island, 92C/16; *BC Ministry of Energy, Mines and Petroleum Resources*, Paper 1992-3, 112 pages.
- Massey, N.W.D. (1995c): Geology and mineral resources of the Duncan sheet, Vancouver Island, 92B/13; *BC Ministry of Energy, Mines and Petroleum Resources*, Paper 1992-4, 112 pages.
- Massey, N.W.D., McIntyre, D.G., Desjardins, P.J. and Cooney, R.T. (2005): Digital geology map of British Columbia: whole province; *BC Ministry of Energy, Mines and Petroleum Resources*, GeoFile 2005-1.
- MINFILE (2007): MINFILE BC mineral deposits database; *BC Ministry of Energy, Mines and Petroleum Resources*, URL <<http://www.em.gov.bc.ca/Mining/GeolSurv/Minfile/>> [November 2007].
- Monger, J.W.H. and Journeay, J.M. (1994): Basement geology and tectonic evolution of the Vancouver region; in *Geology and Geological Hazards of the Vancouver Region*, Southwestern British Columbia, Monger, J.W.H., Editor, *Geological Survey of Canada*, Bulletin 481, pages 3–25.
- Monger, J.W.H., Price, R.A. and Tempelman-Kluit, D.J. (1982): Tectonic accretion and the origin of the two major metamorphic and plutonic belts in the Canadian Cordillera; *Geology*, Volume 10, pages 70–75.
- Muller, J.E. and Carson, D.J.T. (1969): Geology and mineral deposits of Alberni map-area, British Columbia (92F); *Geological Survey of Canada*, Paper 68-50, 52 pages.
- Muller, J.E., Northcote, K.E. and Carlisle, D. (1974): Geology and mineral deposits of Alert Bay – Cape Scott map-area, Vancouver Island, British Columbia; *Geological Survey of Canada*, Paper 74-8, 77 pages.
- Naldrett, A.J. (2004): Magmatic Sulphide Deposits: Geology, Geochemistry and Exploration; *Springer-Verlag*, Berlin, Germany, 727 pages.
- Nixon, G.T. and Orr, A.J. (2007): Recent revisions to the Early Mesozoic stratigraphy of northern Vancouver Island (NTS 102I; 092L) and metallogenic implications, British Columbia; in *Geological Fieldwork 2006*, *BC Ministry of Energy, Mines and Petroleum Resources*, Paper 2007-1, pages 163–177.
- Nixon, G.T., Kelman, M.C., Stevenson, D., Stokes, L.A. and Johnston, K.A. (2006a): Preliminary geology of the Nimpkish map area, northern Vancouver Island (92L/07); *BC Ministry of Energy, Mines and Petroleum Resources*, Open File 2006-5, scale 1:50 000.
- Nixon, G.T., Hammack, J.L., Koyanagi, V.M., Payie, G.J., Haggart, J.W., Orchard, M.J., Tozer, E.T., Friedman, R.M., Archibald D.A., Palfy, J. and Cordey, F. (2006b): Geology of the Quatsino – Port McNeill area, northern Vancouver Island; *BC Ministry of Energy, Mines and Petroleum Resources*, Geoscience Map 2006-2, scale 1:50 000.
- Nixon, G.T., Hammack, J.L., Koyanagi, V.M., Payie, G.J., Snyder, L.D., Panteleyev, A., Massey, N.W.D., Archibald D.A., Haggart, J.W., Orchard, M.J., Friedman, R.M., Tozer, E.T., Tipper, H.W., Poulton, T.P., Palfy, J., Cordey, F. and Barron, D.J. (2006c): Geology of the Holberg – Winter Harbour area, northern Vancouver Island; *BC Ministry of Energy, Mines and Petroleum Resources*, Geoscience Map 2006-3, scale 1:50 000.
- Nixon, G.T., Snyder, L.D., Payie, G.J., Long, S., Finnie, A., Friedman, R.M., Archibald D.A., Orchard, M.J., Tozer, E.T., Poulton, T.P. and Haggart, J.W. (2006d): Geology of the Alice Lake area, northern Vancouver Island; *BC Ministry of Energy, Mines and Petroleum Resources*, Geoscience Map 2006-1, scale 1:50 000.
- Northcote, K.E. and Muller, J.E. (1972): Volcanism, plutonism, and mineralization: Vancouver Island; *Canadian Institute of Mining, Metallurgy and Petroleum*, Bulletin 65, pages 49–57.
- Richards, M.A., Jones, D.L., Duncan, R.A. and DePaolo, D.J. (1991): A mantle plume initiation model for the Wrangellia flood basalt and other oceanic plateaus; *Science*, Volume 254, pages 263–267.
- Riddihough, R.P. and Hyndman, R.D. (1991): Modern plate tectonic regime of the continental margin of western Canada; in *Geology of the Cordilleran Orogen in Canada*, Gabrielse, H. and Yorath, C.J., Editors, *Geological Survey of Canada*, Geology of Canada, Number 4, pages 435–455.
- Sharma, M. (1997): Siberian traps; in Large Igneous Provinces: Continental, Oceanic and Planetary Flood Volcanism, Mahoney, J.J. and Coffin, M.F., Editors, *American Geophysical Union*, Geophysical Monograph 100, pages 273–295.
- Sutherland Brown, A. (1968): Queen Charlotte Islands; *BC Ministry of Energy, Mines and Petroleum Resources*, Bulletin 54, 226 pages.
- van der Heyden, P. (1991): A Middle Jurassic to Early Tertiary Andean-Sierran arc model for the Coast Belt of British Columbia; *Tectonics*, Volume 11, pages 82–97.
- Wheeler, J.O. and McFeely, P. (1991): Tectonic assemblage map of the Canadian Cordillera and adjacent parts of the United States of America; *Geological Survey of Canada*, Map 1712A, scale 1:2 000 000.
- Yorath, C.J., Sutherland Brown, A. and Massey, N.W.D. (1999): LITHOPROBE, southern Vancouver Island: geology; *Geological Survey of Canada*, Bulletin 498, 145 pages.

Geology and Mineral Occurrences of the Timothy Lake Area, South-Central British Columbia (NTS 092P/14)

by P. Schiarizza and J.S. Bligh

KEYWORDS: Quesnel Terrane, Nicola Group, Takomkane batholith, Spout Lake pluton, Peach Lake stock, monzodiorite, monzonite, copper, gold, porphyry, skarn

various industry partners (Carson et al., 2006a, b, c; Coyle et al., 2007; Dumont et al., 2007).

INTRODUCTION

The Takomkane Project is a multiyear bedrock mapping program initiated by the British Columbia Geological Survey in 2005. This program is focused on Mesozoic arc volcanic and plutonic rocks of the Quesnel Terrane in the vicinity of the Takomkane batholith, which crops out in the northern Bonaparte Lake (NTS 092P) and southern Quesnel Lake (NTS 093A) map sheets. Mapping during the 2005 and 2006 field seasons covered the Canim Lake and Hendrix Lake map areas, and is summarized by Schiarizza and Boulton (2006a, b) and Schiarizza and Macauley (2007a, b). Here, we present preliminary results from the third year of mapping for the Takomkane Project, which was carried out by a four-person crew from mid-June to the end of August, 2007. This work covers the 092P/14 NTS map sheet, comprising about 950 km² centred near Timothy Lake (Fig 1).

The Timothy Lake map area is located near the eastern edge of the Interior Plateau physiographic province, within the traditional territories of the Northern Secwepemc te Qelmuw and Esketemc First Nations. Topography is generally subdued, with elevations ranging from about 800 m along Bridge Creek to 1 655 m on Mount Timothy. The town of Lac La Hache, along Highway 97, is located in the southwestern part of the map area, and the village of Forest Grove and the west subdivision of the main Canim Lake Indian reserve are near the southeastern corner of the area. Access to most parts of the map area is easily achieved through extensive networks of public, logging and forest service roads.

The Takomkane Project builds on the geological framework established by the reconnaissance-scale mapping of Campbell and Tipper (1971) and Campbell (1978), as well as subsequent, more detailed studies by Panteleyev et al. (1996), Schiarizza and Israel (2001) and Schiarizza et al. (2002a, b, c). Our geological interpretation of the Timothy Lake map area also incorporates data found in assessment reports available through the BC Geological Survey's Assessment Report Indexing System (ARIS), and airborne geophysical data from a number of recent surveys funded by the Geological Survey of Canada, Geoscience BC and

REGIONAL GEOLOGICAL SETTING

The Timothy Lake map area is underlain mainly by rocks of the Quesnel Terrane, which is characterized by a Late Triassic to Early Jurassic magmatic arc complex that formed along or near the western North American continental margin (Mortimer, 1987; Struik, 1988a, b; Unterschutz et al., 2002; Thompson et al., 2006). An assemblage of mid to Late Paleozoic oceanic basalts and cherts assigned to the Slide Mountain Terrane occurs directly east of the Quesnel belt, and is in turn juxtaposed against a wide belt of Proterozoic and Paleozoic siliciclastic, carbonate and volcanic rocks of the Kootenay Terrane. The Kootenay Terrane is commonly interpreted as an outward facies of the ancestral North American miogeocline (Struik, 1988a; Colpron and Price, 1995), whereas the Slide Mountain Terrane is interpreted as the thrust-imbricated remnants of a Late Paleozoic marginal basin (Schiarizza, 1989; Ferri, 1997). To the west of the Quesnel Terrane are Late Paleozoic through mid-Mesozoic oceanic rocks of the Cache Creek Terrane, which are interpreted as part of the subduction complex that was responsible for generating the Quesnel magmatic arc (Travers, 1978; Struik, 1988a). Younger rocks commonly found in the region include Cretaceous granitic stocks and batholiths, Eocene volcanic and sedimentary rocks, and flat-lying basalt of Neogene and Quaternary age (Fig 1).

Prominent geological structures in the region include Permo-Triassic thrust faults that imbricate the Slide Mountain Terrane and separate it from the underlying Kootenay Terrane (Schiarizza, 1989; Schiarizza and Macauley, 2007a); Late Triassic or Early Jurassic, east-directed thrust faults that imbricate the Quesnel Terrane (Struik, 1988b; Bloodgood, 1990); and predominantly southwest-directed, synmetamorphic folds and thrust faults of Early to Middle Jurassic age that deform the rocks and mutual boundaries of the Kootenay, Slide Mountain and Quesnel terranes (Ross et al., 1985; Mortensen et al., 1987; Rees, 1987; Schiarizza and Preto, 1987). The structural geology of the Quesnel Terrane also includes faults that exerted controls on Triassic-Jurassic volcanic-sedimentary facies distributions and the localization of plutons and associated alteration and mineralization systems (Preto, 1977, 1979; Nelson and Bellefontaine, 1996; Logan and Mihalynuk, 2005b). Younger structures include prominent systems of Eocene dextral strike-slip and extensional faults (Ewing, 1980; Panteleyev et al., 1996; Schiarizza and Israel, 2001).

The Quesnel Terrane is an important metallogenic province, particularly for porphyry deposits containing copper, gold and molybdenum. The world-class Highland

This publication is also available, free of charge, as colour digital files in Adobe Acrobat® PDF format from the BC Ministry of Energy, Mines and Petroleum Resources website at http://www.em.gov.bc.ca/Mining/GeolSurv/Publications/catalog/cat_fldwk.htm

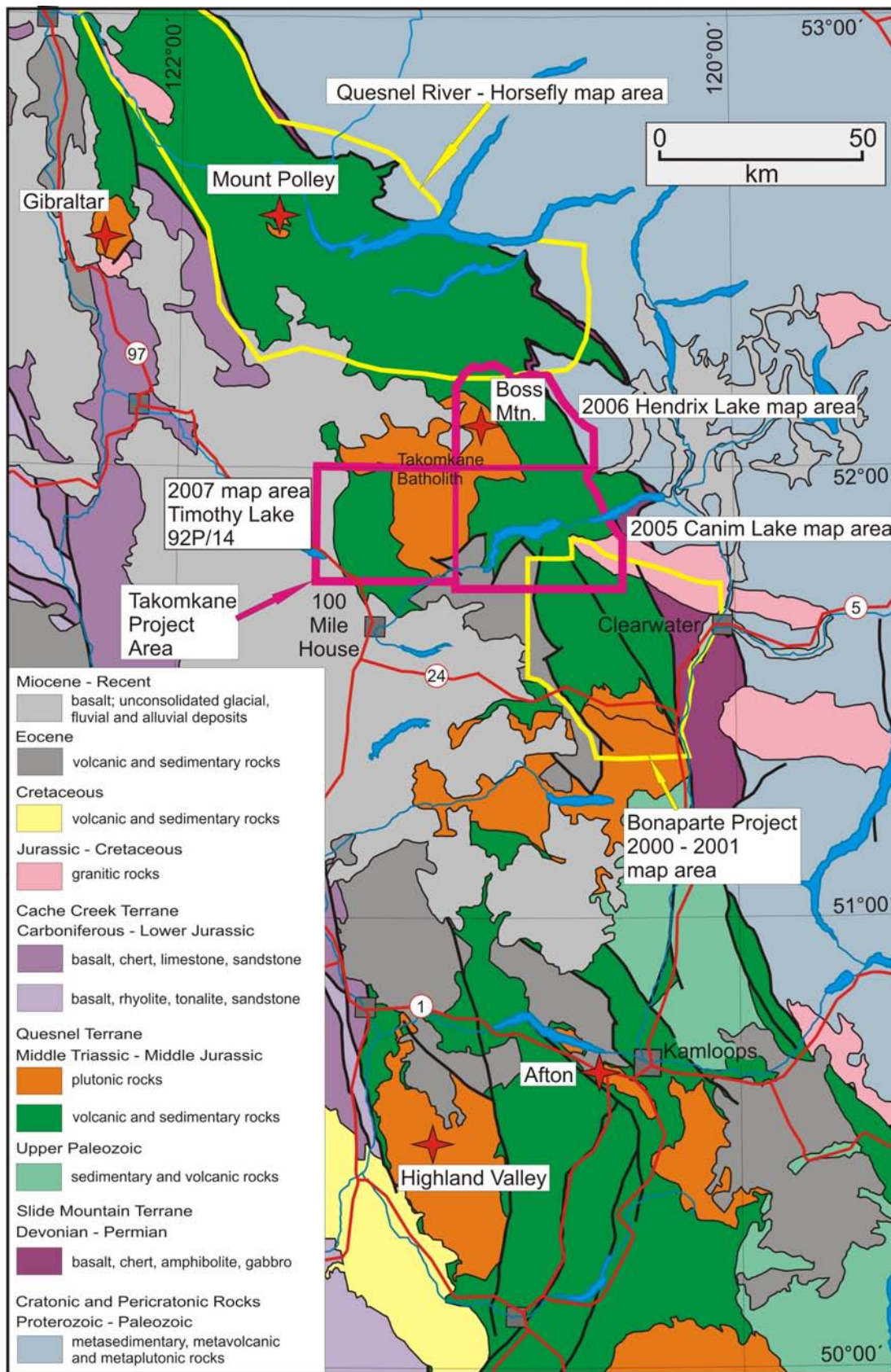


Figure 1. Regional geological setting of the Takomkane Project area, showing the areas mapped in 2005, 2006 and 2007, as well as the area mapped during the 2000–2001 Bonaparte Project, and the Quesnel River – Horsefly map area of Panteleyev et al. (1996). Stars denote locations of selected major mineral deposits.

Valley copper-molybdenum porphyry deposits are in calcalkaline plutonic rocks of the Late Triassic Guichon Creek batholith (Casselmann et al., 1995), which is located in the western part of the Quesnel Terrane, about 150 km south of the Timothy Lake map area. Alkaline plutons, many of latest Triassic age, are scattered across much of the Quesnel Terrane, and host important copper-gold porphyry deposits. These include the Afton Mine and associated occurrences within the Iron Mask batholith, near Kamloops, and the Mount Polley Mine west of Quesnel Lake (Mortensen et al., 1995; Logan and Mihalynuk, 2005a, b). Porphyry and skarn occurrences containing molybdenum and tungsten are associated with Early Cretaceous calcalkaline plutons in the region, and Eocene volcanic rocks and structures locally host epithermal veins that contain gold and silver (Schiarrizza et al., 2002a; Schiarrizza and Boulton, 2006a; Schiarrizza and Macauley, 2007a).

LITHOLOGICAL UNITS

The distribution of the main lithological units within the Timothy Lake map area is shown on Fig 2. The Quesnel Terrane is represented mainly by sedimentary and volcanic rocks of the Upper Triassic Nicola Group and Early Jurassic granodiorite of the Takomkane batholith, but also includes suites of quartz-poor intrusions that crop out mainly in the area of Spout and Peach lakes. Volcanic rocks of the Eocene Skull Hill Formation also underlie significant portions of the map area, and are cut by small dioritic plugs east of Mount Timothy. Olivine-phyric basalt flows of the Miocene-Pliocene Chilcotin Group crop out locally in the southern, western and northern parts of the map area, and Quaternary (?) basalt flows containing lherzolite xenoliths occur on and adjacent to Mount Timothy.

Nicola Group

The Nicola Group, originally named for exposures on the south side of Nicola Lake (Dawson, 1879), comprises a diverse assemblage of Middle and Upper Triassic volcanic, volcanoclastic and sedimentary rocks that crop out over a broad area in south-central British Columbia. The name is applied to Triassic rocks in the Takomkane project area following Campbell and Tipper (1971), and Panteleyev et al. (1996), although the Triassic rocks in the Quesnel Lake map sheet have also been referred to as Quesnel River Group (Campbell, 1978) or Takla Group (Rees, 1987). The Nicola Group in the eastern part of the Takomkane Project area includes two major subdivisions — the Lemieux Creek succession, comprising Middle and Upper Triassic sedimentary rocks that make up the eastern part of the group; and the volcanoclastic succession, an assemblage of volcanoclastic and volcanic rocks that crop out over a broad area to the west (Schiarrizza and Boulton, 2006a, b; Schiarrizza and Macauley, 2007a, b). Most rocks of the Nicola Group in the Timothy Lake map area are here assigned to the volcanoclastic succession. However, two additional units, not recognized to the east, have been mapped in the north-central part of the map area. These are referred to as the polyolithic breccia unit and the red sandstone-conglomerate unit.

VOLCANICLASTIC SUCCESSION

The volcanoclastic succession of the Nicola Group is widespread within the Timothy Lake map area (Fig 2), but

for the most part is represented by small, sparsely scattered exposures that afford no opportunity to establish an internal stratigraphy. Relatively good sets of exposures occur on a series of ridges and hills that extends from Chub Lake northwestward to Greeny Lake, and within the central part of the belt that occurs between the polyolithic breccia unit and the red sandstone-conglomerate unit north of Mount Timothy.

Most exposures within the volcanoclastic succession consist of massive, unstratified volcanic breccia containing fragments of mainly pyroxene-phyric and pyroxene-feldspar-phyric basalt. The breccia is typically dark green or grey-green and rusty brown to greenish-brown-weathered (Fig 3). Locally, such as in exposures south and southeast of Greeny Lake, the colour is mottled because the fragments occur in a variety of colours, including light to dark green, grey and maroon. The fragments commonly range from a few millimetres to more than 10 cm in size, but in some exposures the breccia is finer grained, with fragments up to only a few centimetres. Fragments are typically angular to subangular, poorly sorted and matrix-supported, although clast-supported varieties occur locally and some exposures include a substantial proportion of subrounded clasts. The matrix is composed mainly of feldspar, pyroxene and small mafic lithic grains, and locally is calcareous. In many exposures the compositional similarity between clasts and matrix obscures the fragmental texture of the rock.

A substantial proportion of the volcanoclastic succession consists of medium to coarse-grained, locally gritty, medium to dark green or grey-green sandstone that weathers to lighter shades of green or brownish-green. The sandstone occurs as poorly defined intervals within exposures dominated by volcanic breccia, and as individual outcrops or series of outcrops representing many tens of metres in stratigraphic thickness. Most sandstone units consist of feldspar, mafic mineral grains (mainly pyroxene), mafic lithic grains, and variable proportions of dark, fine-grained matrix material. Many sandstone units are massive, but bedding is locally defined by dark laminations or thin interbeds of fine-grained sandstone or laminated siltstone.

Dark green, brownish-weathered basalt forms rare exposures scattered throughout the volcanoclastic succession, and forms a substantial part of the succession south of Spout Lake, near the contact with the overlying polyolithic breccia unit. Most basalt units consist of a fine-grained, chlorite-epidote-altered groundmass with sparse to abundant, 1 to 5 mm pyroxene and feldspar phenocrysts, and amygdules of mainly epidote and calcite. Similar pyroxene-feldspar porphyry also occurs as dikes cutting breccia, sandstone and basalt units of the volcanoclastic succession.

Light grey-weathered limestone forms a prominent, isolated ridge of outcrop near the southern boundary of the Timothy Lake map area, 10 km southeast of Lac La Hache. Contacts with adjacent rock units are not exposed, but outcrops of volcanic breccia to the west, northwest and north suggest that the limestone is within the volcanoclastic succession. The limestone displays a prominent platy to flaggy layering that dips gently to the north-northeast (Fig 4). The exposure has a strike length of about 600 m and a stratigraphic thickness of 30 to 40 m. In detail, most of the rock comprises irregular domains of very fine grained, pale brown dolomitic (?) limestone cut by abundant veins and patches of white crystalline calcite. Fossil fragments occur locally, and Campbell and Tipper (1971) report that a fossil

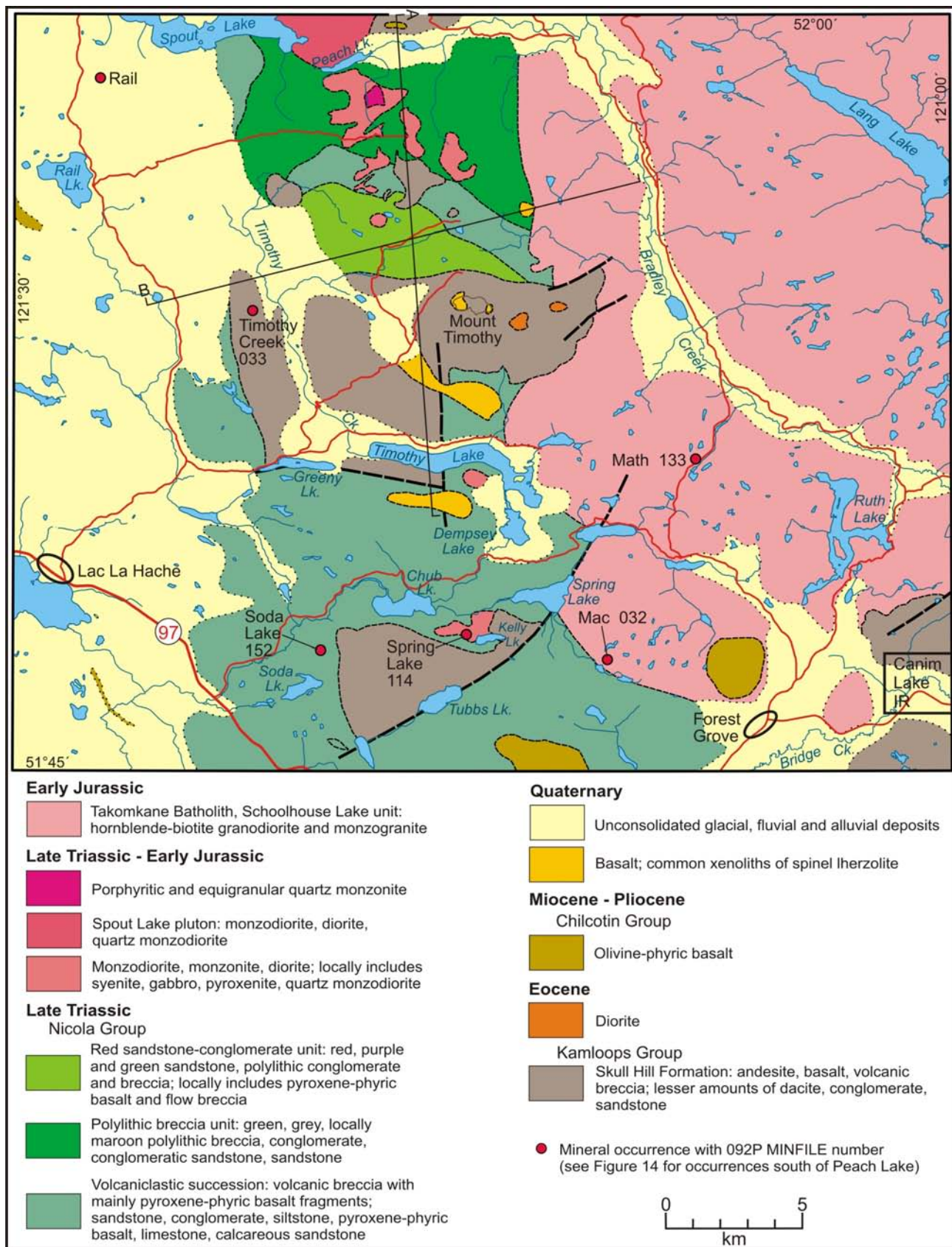


Figure 2. Generalized geology of the Timothy Lake map area, based mainly on 2007 fieldwork.

collection from this exposure indicates a Late Triassic, probably Norian age. This is the only fossil constraint on the age of the Nicola Group within the Timothy Lake map area.

POLYLITHIC BRECCIA UNIT

The polyolithic breccia unit of the Nicola Group crops out in the north-central part of the map area, in an area of relatively good exposure south of Peach Lake. This unit consists mainly of breccia and related conglomerate that contain a variety of clasts, including a significant proportion derived from intrusive rocks. This heterolithic clast population distinguishes the unit from the volcanoclastic succession, where breccia contains fragments of mainly or entirely pyroxene-feldspar-phyric basalt.

The breccia of the polyolithic breccia unit has an overall medium to dark green or greenish-grey colour, and commonly weathers to light shades of brown, greenish-brown or beige. It is characteristically matrix-supported and poorly sorted, with angular to subrounded clasts ranging from a few millimetres to 15 cm in size (Fig 5). The clast population is commonly dominated by fine-grained, equigranular to weakly porphyritic feldspathic rocks rang-

ing from diorite to monzonite in composition. Medium-grained gabbro/diorite, monzodiorite and monzonite fragments are also common, as are mafic to intermediate volcanic clasts containing variable proportions of feldspar, pyroxene and hornblende phenocrysts. Small clasts of pyroxenite, syenite and limestone were observed locally. The matrix consists mainly of feldspar with scattered mafic mineral grains. In many exposures it is difficult to distinguish the matrix from the feldspathic fragments that dominate the clast population.

Sandstone is a relatively minor component of the polyolithic breccia unit, and occurs as thin bedded to massive intervals ranging from a few centimetres to several tens of metres in thickness (Fig 6). The sandstone intervals are generally dark grey-green in colour, and weather to lighter shades of rusty-brown or greenish-brown. They consist mainly of feldspar and dark, fine-grained matrix material, but locally include a significant proportion of mafic mineral grains (mainly pyroxene). Dark grey siltstone is intercalated with fine to coarse-grained sandstone in some thin bedded intervals, and thin lenses of impure limestone occur along the eastern edge of the belt at the Nemrud skarn occurrence (von Guttenberg, 1995).



Figure 3. Volcanic breccia of the Nicola volcanoclastic succession, Highway 97 near the south boundary of the map area.



Figure 5. Epidote-altered breccia of the Nicola polyolithic breccia unit, 4 km east of Peach Lake.



Figure 4. Limestone of the Nicola volcanoclastic succession, 10 km southeast of Lac La Hache. View is to the west.



Figure 6. Thin sandstone units interbedded with conglomerate, Nicola polyolithic breccia unit, 2 km southeast of Peach Lake.

Massive sandstone intervals are generally coarse-grained, commonly contain scattered rounded to subrounded pebbles, and locally grade into matrix-supported conglomerate. The clast population of the pebbly sandstone and conglomerate is typically dominated by fine to medium-grained intrusive rocks ranging from gabbro to monzonite in composition.

Volcanic rocks were not positively identified within the polyolithic breccia unit, but it includes exposures of aphanitic to fine-grained feldspathic rock, locally with phenocrysts of feldspar and/or pyroxene, of uncertain origin. It is suspected that most of these are high level intrusions, at least in part related to the Spout Lake intrusive suite, but some could be volcanic flows.

In the area south of Spout Lake, the polyolithic breccia unit is underlain by pyroxene-rich flows and breccia units of the volcanoclastic succession across an east-dipping contact. This contact appears to be one of mixed gradation, with pyroxene porphyry breccia intercalated with polyolithic breccia over a stratigraphic interval of several hundred metres. However, the polyolithic breccia unit is overlain by pyroxene-rich breccia, sandstone and volcanic rocks assigned to the volcanoclastic succession along its southern margin. It is therefore inferred that the polyolithic breccia unit comprises a thick lens that is interleaved with the volcanoclastic succession in its upper part, as schematically shown on Figure 7. The polyolithic breccia unit has not been directly dated, but it is older than the monzodioritic stocks and dikes of the Spout Lake intrusive suite that intrude it. One of these stocks has yielded a U-Pb titanite date of 203 ± 4 Ma, and a nearby feldspar-phyric andesitic rock, interpreted to be a high level intrusion within the polyolithic breccia unit, has yielded a similar U-Pb zircon date of 203.9 ± 4.2 Ma (Whiteaker et al., 1998). These dates are Late Triassic according to the time scale of Pálffy et al. (2000). The polyolithic breccia unit is therefore inferred to be Late Triassic, because it is within the upper part of the mainly Late Triassic volcanoclastic succession, and is cut by Late Triassic intrusive rocks. Similar breccia in the area of the Mount Polley mine (unit 3 of Panteleyev et al., 1996) is considered to be Early Jurassic because it passes stratigraphically upwards into sedimentary rocks that contain Early Jurassic fossils.

RED SANDSTONE-CONGLOMERATE UNIT

The red sandstone-conglomerate unit crops out in the north-central part of the map area, north and northwest of Mount Timothy. It overlies the polyolithic breccia unit and the intervening section of pyroxene-rich rocks assigned to the volcanoclastic succession, and therefore appears to be the highest stratigraphic element of the Nicola Group exposed within the map area. The top of the unit is not exposed. It is cut by a small porphyritic monzonite plug and is unconformably overlain by Eocene volcanic rock of the Skull Hill Formation. The red sandstone-conglomerate unit consists mainly of sandstone and heterolithic conglomerate and breccia, but also includes pyroxene-phyric volcanic flows and associated flow breccia. The conglomerate and breccia are similar in composition to those of the polyolithic breccia unit, but the red sandstone-conglomerate unit is dis-

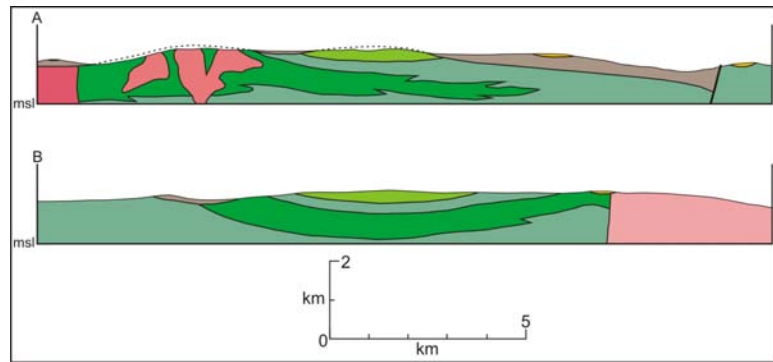


Figure 7. Schematic vertical cross sections along the lines shown in Figure 2.

tinguished by a higher proportion of sandstone and its predominant red colour.

The sandstone within the unit is fine to coarse-grained, and consists mainly of feldspar, along with variably altered mafic grains (largely pyroxene) and very fine grained, dark matrix material. The clastic feldspar grains include plagioclase and K-feldspar, and can be subhedral, broken or weakly rounded. Bedding is evident as vague planar laminations (Fig 8), or as thin, planar to gently undulating beds defined mainly by contrasting grain size in adjacent beds. The sandstone is typically red on both weathered and fresh surfaces, but grey and green units are also present, and it is not uncommon for sandstone in a single outcrop to show irregular colour variations, mainly in shades of red and green.

Conglomerate and conglomeratic sandstone are a major component of the red sandstone-conglomerate unit, and locally dominate intervals 100 m or more in thickness. The conglomerate generally has an overall red or purple colour (Fig 9), but locally displays patchy colour variations in shades of red, purple, grey and green. It is matrix-supported and very poorly sorted, with clasts commonly ranging from a few millimetres to 20 cm in size, and locally ranging up to 60 cm across. The clasts are commonly subangular to subrounded, but in places are mainly angular to subangular. They are similar to those found in the polyolithic breccia unit, consisting mainly of fine to medium-grained,



Figure 8. Laminated red sandstone of the Nicola red sandstone-conglomerate unit, 6 km northwest of Mount Timothy.



Figure 9. Conglomerate of the Nicola red sandstone-conglomerate unit, 5 km northwest of Mount Timothy.

equigranular to weakly porphyritic, feldspar-rich volcanic and plutonic rock types ranging from monzonite to diorite in composition. The medium to coarse-grained sandy matrix consists largely of feldspar, accompanied by mafic mineral grains and fine-grained matrix material. The fragmental texture is generally more conspicuous than in the polyolithic breccia unit, because the matrix tends to be more friable and recessive-weathering.

Basalt flows and related flow breccia are a relatively minor component of the red sandstone-conglomerate unit, but were noted at several different localities within the unit. The flows are commonly mottled in shades of medium to dark purple, grey and green, and weather to lighter shades of these same colours. They include 1 to 3 mm pyroxene phenocrysts that comprise 10 to 20% of the rock, and fewer and smaller feldspar phenocrysts, within a very fine grained groundmass that contains tiny feldspar laths. Irregularly shaped vesicles, up to 1 cm in size, are commonly filled with calcite and chlorite.

The compositions of the various rock types within the red sandstone-conglomerate unit are similar to those of corresponding rock types within the underlying volcanoclastic succession and polyolithic breccia unit. The main change is the predominant red to purple colour of all rock types, which may reflect a transition to more oxidizing conditions in a shallow marine or subaerial environment. The unit is undated, but is suspected to be Late Triassic and/or Early Jurassic.

Spout Lake Intrusive Suite

Intrusive rocks of predominantly monzodioritic composition that crop out in the north-central part of the map area are referred to as the Spout Lake intrusive suite. These rocks intrude the polyolithic breccia unit and adjacent rocks of the Nicola Group, and are associated with skarn and porphyry-style copper-gold occurrences. The largest intrusive body, here referred to as the Spout Lake pluton, crops out north of Peach Lake and extends beyond the northern limit of the Timothy Lake map area. Finer grained rocks of similar composition form several mappable stocks and numerous dikes that are common within an area of about 25 km² to the south and southeast of Peach Lake.

SPOUT LAKE PLUTON

The Spout Lake pluton is represented by a series of good exposures near the northern boundary of the map area, east of Spout Lake and north of Peach Lake. The pluton apparently intrudes the polyolithic breccia unit of the Nicola Group to the south, and is overlain by Eocene volcanic rocks to the east, but neither of these contacts is exposed. It extends northward beyond the limit of mapping in the current project for at least 7.5 km to the west end of Murphy Lake (unit TrJsd of Campbell, 1978).

The Spout Lake pluton is of fairly uniform composition where observed within and adjacent to the Timothy Lake map area. It comprises light grey-weathered, medium to coarse-grained, equigranular pyroxene-biotite monzodiorite, locally grading to diorite. Mafic minerals commonly form about 20% of the rock. Pyroxene is more abundant than biotite, but the latter mineral commonly forms larger, more conspicuous grains that partially enclose other minerals. Quartz may be present as a minor constituent, but does not generally form more than 1 or 2% of the rock. Narrow dikes of pink, fine to medium-grained monzonite and syenite are fairly common (Fig 10), and veins and patches of pegmatite, comprising K-feldspar with lesser amounts of plagioclase, quartz and hornblende, occur locally.

The Spout Lake pluton has not been dated, but a sample collected during the 2007 field season has been submitted to the geochronology laboratory at the University of British Columbia for U-Pb dating of zircons. It is suspected that it is of about the same age as the compositionally similar stocks south of Peach Lake, one of which has yielded a Late Triassic U-Pb titanite date (see following section).

STOCKS AND DIKES SOUTH OF PEACH LAKE

In the area south of Peach Lake, the Spout Lake intrusive suite is represented by the Peach Lake stock, five smaller stocks and plugs, and numerous dikes. Most of the stocks consist of medium grey, light brownish to pinkish grey-weathered, fine to medium-grained, equigranular monzodiorite. The monzodiorite locally grades to diorite or monzonite, but K-feldspar-epidote alteration is ubiquitous, and commonly of such intensity that primary compositions



Figure 10. Diorite cut by a monzonite dike; Spout Lake pluton, northeast of Spout Lake.

are masked. Mafic minerals typically make up 15 to 25% of the rock, and consist of clinopyroxene with lesser amounts of biotite, although biotite locally forms larger, more conspicuous grains. Magnetite, titanite and apatite are common accessory minerals. Pink, equigranular to weakly K-feldspar-phyrlic monzonite occurs mainly as dikes cutting monzodiorite, but also forms a large part of the northern tip of the stock that crops out south of the main Peach Lake stock. Crowded feldspar porphyry of monzonitic composition also makes up the small circular plug that cuts the red sandstone-conglomerate unit 4.5 km northwest of Mount Timothy. A small patch of clinopyroxenite described by Whiteaker (1996) occurs along the east margin of the stock west of the Peach Lake stock, and pyroxenite also occurs locally as xenoliths within the stock.

A poorly exposed plug of porphyritic quartz monzonite occurs in the eastern part of the Peach Lake stock, where it apparently intrudes the enclosing monzodiorite. This plug was mapped by geologists working for Amax Exploration Inc. in the early 1970s (Leary and Godfrey, 1972) and its presence is confirmed by diamond drilling at the Ann North prospect (Callaghan, 2005). The single exposure of this plug located during the 2007 mapping program comprises K-feldspar phenocrysts set in a groundmass of plagioclase laths, with 10 to 15% quartz and rare mafic grains altered to chlorite, epidote and actinolite.

Most of the stocks south of Peach Lake have irregular, sinuous contacts. Mapping of these contacts is difficult because the stocks and country rocks are commonly heavily altered with K-feldspar and epidote, which makes differentiating the stocks from compositionally similar rocks of the polyolithic breccia unit tenuous. Fragmental rocks along some contacts appear to be xenolith-rich marginal phases of the stocks. In other areas, fragmental rocks that have previously been described as intrusive breccia, such as along the south margin of the stock east of the main Peach Lake stock (Whiteaker, 1996), are here interpreted as altered country rock, comprising intrusive-clast breccia of the polyolithic breccia unit.

A sample collected from the monzodiorite stock east of the main Peach Lake stock has yielded a U-Pb titanite date of 203 ± 4 Ma (Whiteaker et al., 1998). This date was considered to be Early Jurassic by Whiteaker et al. (1998), but is Late Triassic according to the more recent time scale of Pálffy et al. (2000). Samples collected from two separate stocks during the 2007 field season have been submitted to the geochronology laboratory at the University of British Columbia for additional U-Pb dating.

A medium-grained quartz-hornblende-feldspar porphyry dike cuts the monzodiorite stock east of the main Peach Lake stock. The dike is not mineralized, but is spatially associated with areas of relatively gold-rich mineralization within the monzodiorite that it intrudes (Aurizon occurrence). The mineralogy of the dike suggests that it is not related to the Spout Lake intrusive suite. Whiteaker et al. (1998) report that zircons from a sample of this dike yielded a poorly-constrained upper intercept U-Pb date of $199 +23/-13$ Ma.

Kelly Lake Stock

The Kelly Lake stock is represented by a few scattered exposures of monzodiorite to diorite that extend from the shore of Kelly Lake northward about 800 m to 111 Mile Creek, between Spring and Chub lakes. The stock is in-

ferred to extend about 1.5 km west of Kelly Lake on the basis of diamond-drill holes cored during mineral exploration of the Spring Lake copper occurrence (Blann, 1995b). The stock intrudes breccia and sandstone of the Nicola volcanoclastic succession, although the contact is not exposed on surface, and is overlain to the east by volcanic rocks of the Skull Hill Formation.

The exposures of the Kelly Lake stock located during the present study consist mainly of grey, grey-brown-weathered, fine to medium-grained, equigranular monzodiorite and diorite. Mafic minerals make up 15 to 30% of the rock and consist mainly of clinopyroxene and biotite. Minor amounts of quartz are present locally, and titanite and apatite are conspicuous in thin section. The main phases of the stock are variably altered with K-feldspar, epidote and chlorite, and are locally cut by narrow dikes of monzodiorite to syenite. The Kelly Lake stock has not been dated, but is suspected to be of about the same age as the compositionally similar Peach Lake stocks.

Intrusive Rocks South of Timothy Lake

An intrusive body is inferred to underlie the area south of the east end of Timothy Lake, based on extensive angular rubble located in a recent logging cut 1 km northwest of the narrows between Timothy and Dempsey lakes. The rubble comprises red, fine to medium-grained syenite to monzonite with chlorite-epidote alteration along joint and fracture surfaces. Eighteen hundred metres to the south-east, on the northeast side of Dempsey Lake, a 60 m percussion-drill hole intersected diorite that might be part of the same intrusive system (PDH TY2-82-1; Gamble, 1983b). The presence of these intrusive rocks is noteworthy because of their compositional similarity to the economically-significant Spout Lake intrusive suite.

Takomkane Batholith

The Takomkane batholith is a large Late Triassic–Early Jurassic granitic pluton more than 40 km wide (Fig 1). The southwestern part of the batholith underlies much of the eastern part of the Timothy Lake map area, where it intrudes the Late Triassic Nicola Group to the west, and is locally overlain by volcanic rocks of Eocene, Miocene-Pliocene and Quaternary (?) ages. To the east, in the Canim Lake map area, the batholith has been subdivided into two units, referred to as the Boss Creek unit and the Schoolhouse Lake unit (Scharizza and Boulton, 2006a). The entire exposure belt within the Timothy Lake map area is correlated with the Schoolhouse Lake unit.

The Schoolhouse Lake unit is very homogeneous throughout its extent in the Timothy Lake map area. It consists of light grey to pinkish grey, coarse to medium-grained, hornblende-biotite granodiorite, locally grading to monzogranite. Tonalite occurs locally along the western margin of the batholith, northeast of Mount Timothy. Mafic minerals commonly make up 10 to 20% of the granodiorite, with hornblende predominating over biotite. The texture is typically porphyritic, with K-feldspar crystals up to several centimetres in size and, locally, quartz grains and aggregates up to 1 cm in size (Fig 11). Pegmatite and aplite dikes are a widespread but relatively minor component of the unit. Grey to pink quartz porphyry and quartz-feldspar porphyry dikes that locally cut the batholith and the adjacent Nicola Group may also be broadly related.



Figure 11. Granodiorite with K-feldspar phenocrysts; Takomkane batholith, northwest of Lang Lake.

The Takomkane batholith within the Timothy Lake map area has yielded a U-Pb zircon date of 193.5 ± 0.6 Ma from a sample collected at Ruth Lake (Whiteaker et al., 1998). This Early Jurassic age for the Schoolhouse Lake unit is confirmed by a U-Pb zircon date of 195.0 ± 0.4 Ma from a sample collected a short distance east of Lang Lake (Schiarizza and Macauley, 2007a).

Skull Hill Formation

Campbell and Tipper (1971) assigned Eocene volcanic rocks in the Bonaparte Lake map sheet to the Skull Hill Formation of the Kamloops Group. The most extensive exposures in the Timothy Lake map area are on and around Mount Timothy, but the formation also crops out in several areas to the south and north of the mountain, as well as in the southeast corner of the map area. The latter exposures comprise the north end of a continuous belt of Eocene rocks that Campbell and Tipper (1971) traced 70 km south to Bonaparte Lake. They recognized that Eocene rocks were also present farther to the northwest, but mapping during the current project shows that the Skull Hill Formation is much more extensive than portrayed by Campbell and Tipper (1971). Numerous small outliers of the formation in the north-central part of the map area suggest that the belt that encompasses Mount Timothy once formed a continuous blanket that extended to beyond the northern boundary of the map area.

The Skull Hill Formation unconformably overlies a number of different Mesozoic rock units within the Timothy Lake map area, including various units of the Nicola Group, the Takomkane batholith, the Spout Lake pluton, and the Kelly Lake stock. The southern boundaries of the Mount Timothy belt and the belt to the south are inferred to be controlled by east to northeast-striking faults. The formation consists mainly of andesitic to basaltic flows and associated flow breccia, but also includes dacitic flows, volcanic breccia, and rare exposures of arkosic wacke. The most common rocks are grey to brown, purplish brown-weathered andesitic flows characterized by abundant coarse plagioclase phenocrysts, and less conspicuous pyroxene and/or hornblende phenocrysts (Fig 12). Dark grey basaltic flows are also fairly common, and contain pyroxene and plagioclase phenocrysts. The andesitic and

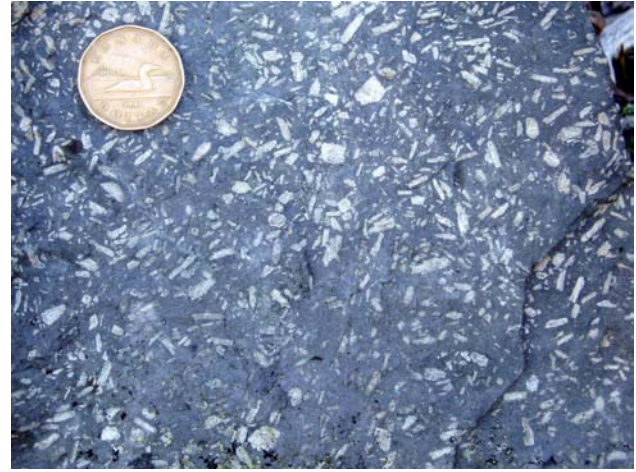


Figure 12. Plagioclase-phyric andesite of the Skull Hill Formation, south flank of Mount Timothy.

basaltic flows are commonly vesicular, and vesicles are typically filled with chalcedonic quartz or calcite. Pale grey dacitic flows are relatively rare, and were observed only in the southeastern corner of the map area, north of Bridge Creek, and in the Eocene section that crops out along the north-central boundary of the map area.

Volcanic breccia is most common on the top and south flank of Mount Timothy. It comprises purple, green and grey volcanic fragments, from less than 1 cm to more than 10 cm in size, within a friable matrix that is rich in feldspar grains. The volcanic fragments commonly contain various combinations and proportions of feldspar, pyroxene and hornblende phenocrysts. Locally, the breccia includes narrow intervals of thin-bedded sandstone to small pebble conglomerate containing volcanic-lithic grains and crystals of feldspar and mafic minerals. The breccia locally resembles that of the Nicola Group, but it shows considerably less chlorite-epidote alteration, and is clearly interbedded with the feldspar-phyric flows that characterize the Skull Hill Formation. Coarser breccia, comprising poorly sorted fragments up to 1.5 m across, within a friable, pale grey-green, feldspar-rich matrix, crops out on an isolated ridge in the southeast corner of the map area, south of Bridge Creek. External contacts were not observed, but this coarse breccia is within an area dominated by andesitic to basaltic flows that are typical of the Skull Hill Formation.

Eocene or Younger Diorite

Grey, fine to medium-grained, equigranular diorite makes up two small plugs that intrude volcanic flows and breccia of the Skull Hill Formation on the east flank of Mount Timothy. The dioritic rocks consist of plagioclase, locally with traces of K-feldspar, along with 25 to 35% mafic minerals that include hornblende, clinopyroxene and biotite. These diorite bodies have not been dated, but are inferred to be Eocene or younger because they cut rocks assigned to the Eocene Skull Hill Formation.

Chilcotin Group

The Chilcotin Group comprises flat-lying basalt flows and related rocks that cover much of the Interior Plateau of south-central British Columbia. The group ranges from

Early Miocene to Early Pleistocene in age, and is contemporaneous with the more voluminous Columbia River flood basalts of Oregon and Washington states (Mathews, 1989). The Chilcotin Group is currently the focus of a major research program at the University of British Columbia, aimed at better understanding the volcanic lithofacies and thickness variations within the group (Andrews and Russell, 2007).

The Chilcotin Group within the Timothy Lake map area is represented by two outliers near Forest Grove in the southern part of the area, by a very small outlier northeast of Peach Lake near the northern boundary of the map area, by a few exposures along the railway tracks south of Lac La Hache, and by an exposure west of Rail Lake. The latter two areas, near the western edge of the map area, are apparently part of a very extensive blanket of Chilcotin basalt flows that stretches far to the west and south. Our mapping, combined with data from exploration drillholes northeast of Rail Lake, shows that this blanket does not extend as far into the Timothy Lake area as indicated on the reconnaissance-scale map of Campbell and Tipper (1971).

The Chilcotin Group within the Timothy Lake map area consists of dark grey to blue-grey, brownish-weathered, very fine grained basalt that is variably vesicular and commonly contains pale green olivine phenocrysts 1 to 3 mm in size. The greatest thickness occurs in the outlier west of Forest Grove, where close to 100 m of basalt is exposed. The outlier north-northwest of Forest Grove has yielded a Middle to Late Miocene K-Ar whole rock date of 11.8 ± 0.5 Ma (Mathews, 1989).

Mount Timothy Basalt

Flat-lying basalt containing peridotite xenoliths occurs as five separate outliers within a north-south belt, 11 km long, which encompasses Mount Timothy (Fig 2). The basalt is grey, locally maroon, very fine grained and weakly to moderately vesicular. Red, scoriaceous basalt breccia was noted at the base of the western outlier on Mount Timothy, and also near the base of the northernmost outlier. Peridotite xenoliths, mainly spinel lherzolite, are common in all five outliers of the Mount Timothy basalt and commonly range up to 20 cm in size (Fig 13). These are locally accompanied by smaller and less common crustal



Figure 13. Basalt with lherzolite xenoliths, south flank of Mount Timothy.

xenoliths consisting mainly of medium-grained dioritic rock.

The Mount Timothy basalt, including the lherzolite xenoliths, is very similar to xenolith-bearing basalt that caps Takomkane Mountain, 30 km northeast of Mount Timothy (Schiarizza and Macauley, 2007a). The basalt on Takomkane Mountain is inferred to be Pleistocene because it rests on a glaciated surface but has been sculpted by subsequent glacial action (Sutherland Brown, 1958). We suspect that the Mount Timothy basalt is of similar age.

STRUCTURE

Outcrop scale structures within the Timothy Lake map area consist mainly of brittle faults and fractures that are more common in Mesozoic rocks than in Eocene rocks of the Skull Hill Formation. Folds of bedding were observed only rarely within the Nicola Group, and penetrative foliations occur in only a few exposures of hornfelsed and skarn-altered rocks of the Nicola Group along the margin of the Takomkane batholith.

The macroscopic structure of the Nicola Group within most of the map area is very poorly understood due to poor exposure, a lack of marker units, and the predominance of apparently non-stratified rocks. An exception is the area north of Mount Timothy, where the three mappable units of the Nicola Group outline a broad syncline with a poorly defined axial trace (Fig 7). Rocks in the core of the syncline are more or less horizontal. Those on the west limb generally dip eastward at gentle to moderate angles, although sandstone near the base of the polyolithic breccia unit south of Spout Lake is nearly vertical. Rocks on the east limb dip gently westward, but are folded through an anticlinal hinge a short distance west of the Takomkane batholith and generally dip eastward at the batholith contact.

Most of the faults mapped within the Timothy Lake area strike east to northeast and partially control the distribution of Eocene rocks. The largest of these, the Greeny Lake and Spring Lake faults, juxtapose Eocene rocks on their north side against Triassic rocks to the south, so are inferred to have a component of Eocene or younger north-side-down displacement. The Spring Lake fault may also have component of dextral strike slip, based on the apparent offset of the Takomkane batholith. Although they are faulted, Eocene rocks are essentially horizontal wherever bedding orientations were observed.

Although Eocene or younger faults are clearly present, many of the outcrop scale faults observed within Mesozoic rocks are inferred to be pre-Eocene because these structures are much more prevalent in the older rocks. Steeply dipping faults with northwest, north and northeast strikes are most common. Topographic lineaments with these orientations are also common but, with the exception of the mapped Eocene or younger faults, none have been proven to be controlled by major faults. In the Peach Lake area, northwest, northeast and east-striking structures control some of the alteration and mineralization associated with the Spout Lake intrusive suite.

MINERAL OCCURRENCES

The metallic mineral occurrences known within the Timothy Lake map area (MINFILE, 2007) are concentrated in the area south of Peach Lake, and are summarized on Fig-

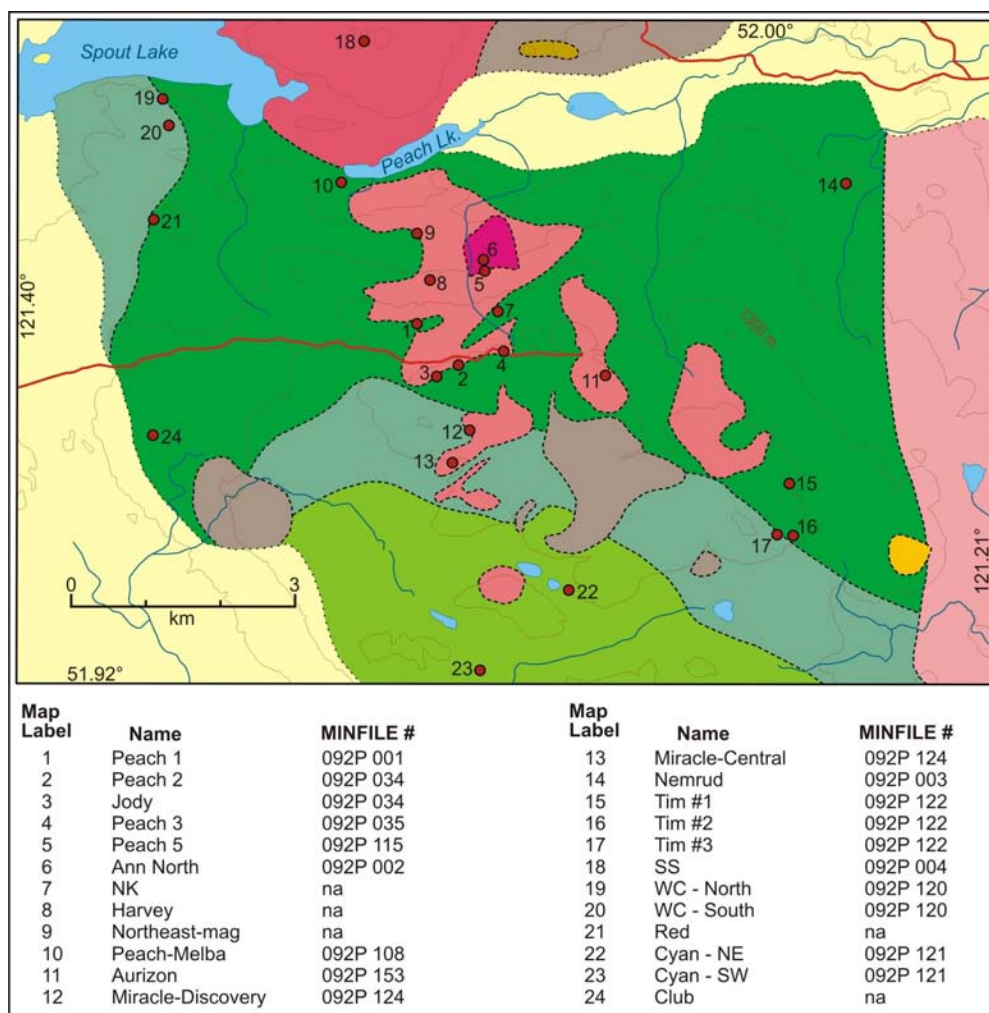


Figure 14. Geology and mineral occurrences in the Peach Lake area. See Figure 2 for legend.

ure 14. Most of these are copper-gold porphyry and skarn occurrences associated with stocks of the Spout Lake intrusive suite. Mineral occurrences scattered through other parts of the Timothy Lake map area are shown on Figure 2. These include porphyry-style copper-gold mineralization associated with the Kelly Lake stock, disseminated chalcocopyrite within the Nicola Group north of Soda Lake, molybdenum-copper showings within the Takomkane batholith, and structurally controlled polymetallic veins within the Kamloops Group west of Timothy Creek.

Occurrences in the Peach Lake area

PEACH 1 (MINFILE 092P 001)

The Peach 1 showing is located 2 km south of Peach Lake. It is the first mineral occurrence discovered in the Peach Lake area, and was explored with trenches and some short diamond-drill holes by Coranex Ltd. and Amax Exploration Ltd. between 1967 and 1972 (Janes, 1967; Sutherland Brown, 1969; Leary and Godfrey, 1972). In 1991, the trenches were remapped and sampled by Asarco Exploration Company of Canada Ltd., and an area south of the trenches was tested with 2 short percussion-drill holes (Gale, 1991).

Mineralization at the Peach 1 showing is hosted by the polyolithic breccia unit within a narrow embayment in the southern part of the Peach Lake stock. Chalcocopyrite is the main sulphide mineral. Pyrite is present in minor quantities, as are malachite, azurite and native copper. The chalcocopyrite occurs along fractures and locally as disseminations within several northeast-trending zones (Janes, 1967). Associated alteration assemblages include K-feldspar, magnetite, tourmaline and biotite. Sutherland Brown (1969) notes that the stockwork pattern within the mineralized zones is partly random, but is dominated by northward dipping fractures that strike east-northeast or west-northwest. A 12 m section sampled by Coranex Ltd. in 1967 returned 0.33% Cu and 0.576 g/t Au (Janes, 1967).

PEACH 2 (MINFILE 092P 034), JODY, AND PEACH 3 (MINFILE 092P 035)

The Peach 2 showing is located about 700 m southeast of the Peach 1 occurrence, along a northeast-trending contact zone that forms part of the southern margin of the Peach Lake stock. The mineralization was evaluated with trenches and percussion-drill holes by Amax Exploration Inc. in 1972 and by Asarco Exploration Company of Canada Ltd. in 1991 (Leary and Godfrey, 1972; Gale, 1991).

Subsequent exploration by GWR Resources Inc. included two diamond-drill holes in 1999 (Blann, 2001a), and two additional diamond-drill holes and a major trenching program in 2004 (Callaghan, 2005).

Mineralization consisting of pyrite, chalcopyrite and minor bornite occurs sporadically throughout the 150 m by 45 m area that was exposed by the recent GWR Resources Inc. trenches. Hostrocks include potassic-altered monzodiorite as well as altered breccia and related rocks of the polyolithic breccia unit. The mineralization occurs in shears, fractures and narrow veins of variable orientation, and is associated with alteration assemblages that contain K-feldspar, epidote, magnetite and locally biotite. A 28 m trench sample collected by GWR Resources Inc. in 2004 returned 0.07% Cu and 0.22 g/t Au. The highest grades encountered came from a 2 m sample that contained 0.34% Cu and 2.25 g/t Au (Callaghan, 2005).

Mineralization is also known to occur about 300 m southwest of the Peach 2 occurrence, in an area known as the Jody zone, which was explored with two trenches and five percussion-drill holes in 1991. Mineralization is within the polyolithic breccia unit a few tens of metres from the contact with the Peach Lake stock. Chalcopyrite is associated with K-feldspar-magnetite-chlorite alteration along north, northwest and west-striking fractures and faults. A sequence of six 5 m chip samples from one of the trenches returned a combined grade of 0.17% Cu and 93 ppb Au (Gale, 1991, samples 061470–061475).

The Peach 3 showing is 500 m east-northeast of the Peach 2 occurrence, where several recent trenches and scraped areas expose monzodiorite, sparsely mineralized with chalcopyrite and malachite, along the main exploration/logging road (Telegraph Corner area of Callaghan, 2005). The monzodiorite is variably altered with K-feldspar and epidote. Chalcopyrite occurs mainly as disseminated grains associated with magnetite, chlorite and pyrite along variably oriented fractures with K-feldspar haloes. The mineralization was tested with one diamond-drill hole in 1995 (von Guttenberg, 1996, hole A95-04) and two diamond-drill holes in 2004 (Callaghan, 2005, holes 04-31 and 04-32). None of these holes intersected significant mineralization — the best intersections from hole A95-04 were 0.13% Cu and 0.06 g/t Au over 4.6 m, and 1.31% Cu and 0.07 g/t Au over 1.0 m. The latter intersection includes a 30 cm thick quartz-calcite vein that contains specularite, chalcopyrite and bornite (von Guttenberg, 1996).

PEACH 5 (MINFILE 092P 115) AND ANN NORTH (MINFILE 092P 002)

The Peach 5 and Ann North occurrences are 1 500 to 1 700 m south-southeast of Peach Lake, and are associated with a small porphyritic quartz monzonite plug or dike swarm that is within the Peach Lake monzodiorite stock. The plug is very poorly exposed on surface, but was identified during exploration by Amax Exploration Inc. in 1972. The Peach 5 showing was also discovered at this time, in a trench along or near the southern margin of the stock where porphyritic quartz monzonite cuts monzodiorite. The mineralization is described as chalcopyrite in veined monzodiorite, minor disseminated chalcopyrite in the porphyritic quartz monzonite, and minor but widespread malachite along the trench (Leary and Godfrey, 1972). A small patch of subcrop at or near the remnant of this trench was located during the present field program, and comprises K-

feldspar-epidote-altered porphyritic quartz monzonite stained with malachite.

The Ann North prospect was discovered during a diamond drill program by GWR Resources Inc. in 2000, when eight of thirteen holes drilled to the north and northeast of the Peach 5 showing intersected significant mineralization. This included a 125 m intersection in hole 00-15 that returned 0.20% Cu and 0.3 g/t Au, including a 44 m interval containing 0.31% Cu and 0.41 g/t Au (Blann, 2001a). The mineralized area was further evaluated with a 13 hole, 3 536 m diamond drill program carried out by GWR Resources Inc. in 2004 and 2005. Significant mineralized zones were intersected in seven of the holes, including a 107.3 m interval in hole 04-19 that assayed 0.29% Cu and 0.33 g/t Au (Callaghan, 2005).

The main area of mineralization outlined by drilling at the Ann North prospect is centred about 150 m north of the Peach 5 showing. Mineralization is hosted mainly by potassic-altered quartz monzonite and porphyritic quartz monzonite, and occurs as a series of northeast-trending, steeply northwest-dipping lenses with widths up to 35 m and a combined strike length of more than 200 m (Callaghan, 2005). Mineralization consists of chalcopyrite and pyrite, locally with bornite, tennantite, chalcocite and native copper. Copper minerals occur as patches, disseminations, and vein and fracture-fillings, and are associated with vein and alteration assemblages that include K-feldspar, quartz, magnetite, carbonate and tourmaline.

NK ZONE

The NK zone, located about 2 200 m south of Peach Lake, is hosted in altered breccia of the polyolithic breccia unit along the southeast margin of the Peach Lake stock. The mineralization was discovered by diamond drilling carried out by GWR Resources Inc. in 1999 and 2000 (Blann, 2001a). Chalcopyrite, bornite and pyrite occur as disseminations and along fractures with variable orientations. Fracture-controlled malachite, native copper and chalcocite occur in the upper parts of drillholes. Alteration assemblages include magnetite, biotite, chlorite, epidote, albite and K-feldspar. Mineralized drill intersections are interpreted as three sub-parallel north-northeast-trending zones, 15 to 50 m wide and 100 m long, that remain open (Blann, 2001a). Notable intercepts include 89.3 m grading 0.186% Cu and 0.23 g/t Au, and 13.5 m grading 0.391% Cu and 0.24 g/t Au (Blann, 2001a).

HARVEY AND NORTHEAST-MAG ZONES

GWR Resources Inc. explored an 800 m by 500 m area in the western part of the Peach Lake stock with 2 782 m of diamond drilling in 19 holes between June 2002 and February 2004 (Barker, 2002, 2003; Callaghan, 2005). Barker (2002, 2003) referred to the southern part of this area as the Harvey zone, and called the northern part the Northeast-mag zone. Copper-gold mineralization was encountered in a number of the holes, and consists of pyrite and chalcopyrite as disseminations and fracture and vein fillings, associated with alteration minerals that include K-feldspar, epidote, magnetite and tourmaline. The host rock is mainly fine-grained K-feldspar-epidote-altered monzodiorite. Significant drill intersections include 85.2 m containing 0.25% Cu, 0.12 g/t Au and 0.77 g/t Ag from the Harvey zone (Barker, 2002), and 9 m grading 0.47% Cu and 0.46 g/t Au from the Northeast-mag zone (Barker, 2003).

About 1 km west of the Harvey zone are natural and recently trenched exposures that display chalcopyrite-malachite mineralization within both the Peach Lake stock and adjacent breccia and sandstone of the polyolithic breccia unit. Mineralization in both units is concentrated along steeply dipping, west-striking faults. Chalcopyrite mineralization within the polyolithic breccia unit is associated mainly with patches of calcite and tourmaline that are enclosed by zones of strong K-feldspar-epidote alteration. The mineralization hosted by monzodiorite of the adjacent Peach Lake stock comprises chalcopyrite and magnetite within structurally controlled zones of intense K-feldspar-epidote alteration.

PEACH-MELBA (MINFILE 092P 108)

The Peach-Melba prospect is located about 100 m southwest of the west end of Peach Lake. It is hosted by the polyolithic breccia unit of the Nicola Group a short distance south of the Spout Lake pluton and northwest of the Peach Lake stock. The occurrence is associated with a large, northwest-trending induced polarization anomaly that was tested with several drill programs by different companies between 1972 and 1994. The Peach-Melba zone was discovered when GWR Resources Inc. drilled a hole on the northeast flank of the anomaly in the spring of 1995, which yielded an intersection of 77.4 m containing 0.23% Cu and 0.23 g/t Au (Blann, 1995a, hole PL95-2). Hole PM95-01, cored later that same year, yielded a 112 m intersection grading 0.20% Cu and 0.13 g/t Au (von Guttenberg, 1996). Additional drilling within and adjacent to the zone was carried out in 1997, 2002, 2003 and 2005 (Callaghan, 2005).

The main mineralized zone at the Peach-Melba prospect trends northwest, dips steeply, and has a true width of about 80 m (von Guttenberg, 1996). Mineralization consists of disseminated and fracture controlled pyrite-chalcopyrite associated with alteration assemblages that include K-feldspar, biotite, epidote, magnetite and hematite. Host rocks include breccia and finer grained rocks of the Nicola Group as well as monzonite and syenite dikes. Pyroxene-garnet skarn, sparsely mineralized with magnetite and chalcopyrite, was intersected in drillholes east of the main mineralized zone (von Guttenberg, 1996).

AURIZON (MINFILE 092P 153)

The Aurizon occurrence is within a monzodiorite stock that crops out to the east and southeast of the Peach Lake stock. The mineralization was discovered by GWR Resources Inc. in 1994 when two diamond-drill holes were cored to test coincident induced polarization and copper in soils anomalies. One of these holes intersected copper-gold mineralization in 5 separate intervals. The best intersections, 3.8 m grading 11.41 g/t Au and 0.22% Cu, and 2.4 m grading 3.56 g/t Au and 0.47% Cu, were in quartz-calcite-chalcopyrite-veined monzodiorite along both margins of a quartz-hornblende-feldspar porphyry dike (Blann, 1995c). Three additional holes were drilled in 1995 to test for mineralization along the margins of the dike, but returned generally low and erratic gold values (von Guttenberg, 1996). More recent work by GWR Resources Inc., including part of the 2007 drill program, is targeting other portions of the Aurizon stock, which displays copper mineralization in many of the exposures examined during our 2007 field program. This mineralization consists of weakly to heavily disseminated chalcopyrite and magnetite, locally with malachite and native copper, along variably oriented fracture

surfaces within monzodiorite that is strongly altered with K-feldspar and epidote. The highest grade mineralization observed comprises clots and disseminations of chalcopyrite within a steeply dipping, northeast-striking zone of highly fractured monzodiorite veined with calcite and epidote. A grab sample from this mineralized zone, taken 1 km north of the Aurizon showing, returned 3 634 ppb Au and greater than 1% Cu.

MIRACLE (MINFILE 092P 124)

The Miracle prospect, 4 km south of Peach Lake, comprises porphyry-style Cu-Au mineralization associated with a small stock that crops out south of the Peach Lake stock. Mineralization was discovered by local prospectors in 1986, along a newly constructed logging road, and staked as the Miracle claims. The claims were optioned to GWR Resources Inc. and explored with geological mapping, trenching, geophysical and geochemical surveys and thirteen diamond-drill holes in 1987 through 1992 (White, 1987; Dunn, 1992). This work showed that Cu-Au mineralization is widespread, but did not outline any major zones with demonstrable continuity. A 2 691 m diamond drilling program in 1994 focused on an induced polarization anomaly that was outlined by a 1993 survey to the south and west of the area of previous drilling. This program outlined a northeast-trending zone of mineralization that was referred to as the Central zone (Blann, 1995d). Two additional holes were drilled on the south side of the induced polarization anomaly in 1995, but did not intersect any significant mineralization (von Guttenberg, 1996).

The Discovery showing of the Miracle prospect, currently marked by a partially caved trench, comprises altered, grey-green hornfels cut by dikes of monzodiorite and several heavily limonite-altered fault zones up to 1.5 m wide. The fault zones strike northwest and are more or less vertical, as are many of the dikes. Zones of strong K-feldspar-epidote±hematite alteration have multiple orientations, but are most common along steeply dipping, northwest to north-northwest-striking fractures and dike contacts (Fig 15). Most primary minerals have been leached from the gossanous fault zones, but traces of specularite, pyrite and chalcopyrite occur locally. Malachite occurs along fractures in the fault zones and in some



Figure 15. Potassium-feldspar-epidote-hematite alteration in a monzodiorite dike and adjacent hornfels; Discovery showing of the Miracle prospect.

of the monzodiorite dikes. A diamond-drill hole directed under the trench in 1988 included an 18 m intersection grading 0.23% Cu and 0.17 g/t Au (Blann, 1995d).

The Central zone of the Miracle prospect is several hundred metres south of the Discovery zone. It comprises mineralized drill intersections in a northeast-trending corridor about 650 m long within the southwest lobe of the stock. The mineralization is hosted by K-feldspar-altered monzodiorite, and consists of pyrite and chalcopyrite, with minor amounts of bornite and tetrahedrite, as disseminations and fracture and vein stockworks (Blann, 1995d). The best intersection is near the southwest end of the zone, where hole M94-1 cut 72 m grading 0.17% Cu and 0.21 g/t Au (Blann, 1995d).

NEMRUD (MINFILE 092P 003)

The Nemrud skarn prospect is hosted in the polyolithic breccia unit of the Nicola Group near its contact with the Takomkane batholith, about 5 km east of Peach Lake. Mineralized skarn was noted in this area by geologists working for Coranex Ltd. in the 1960s, when it was referred to as the Tim #1 showing (Janes, 1967). The main exploration work was conducted from 1993 through 1995, when the occurrence was covered by the Riley 1 claim and explored by Strathcona Mineral Services Ltd. for the Lac La Hache Joint Venture of Regional Resources Ltd. and GWR Resources Inc. The first phase of this exploration program included geological mapping, prospecting, soil, silt and rock sampling, and induced polarization and magnetometer geophysical surveys (von Guttenberg, 1994). This was followed by a program of diamond drilling that included 1 018 m in fourteen holes on the skarn occurrence, as well as 567 m in six holes to test nearby induced polarization anomalies (von Guttenberg, 1995). The results of this work, and follow-up drilling of 392 m in two holes, did not encourage further exploration of the Nemrud occurrence at that time (von Guttenberg, 1996), and no additional work has been recorded.

Outcrops of mineralized skarn on the Nemrud prospect are scattered over an area 600 m long and up to 250 m wide, along and adjacent to a north-south ridge about 400 m west of the Takomkane batholith. Mineralization comprises blebs of bornite, and rarely chalcopyrite, pyrite, native copper and malachite, within skarn-altered rock that includes garnet, diopside and epidote. Grab samples of mineralized material have returned values of up to 3.57% Cu, 82.1 ppm Ag and 1 257 ppb Au (von Guttenberg, 1994, sample 93-RCS-027). Diamond drilling indicates that mineralization is mainly within a zone that is 20 to 25 m thick, comprising intercalated lenses of skarn, impure marble, volcanic sandstone or tuff, siltstone, and possible mafic to intermediate volcanic flows (von Guttenberg, 1995). This zone is gently undulating but dips mainly to the east at shallow angles. The enclosing rocks are variably hornfelsed and skarn-altered breccia, conglomerate, sandstone and siltstone of the Nicola polyolithic breccia unit, locally cut by diorite and granodiorite dikes.

The mineralized skarn zone outlined by the initial phase of drilling on the Nemrud prospect was traced to within about 350 m of the contact with the Takomkane batholith. It has a typical average grade of 0.1% Cu, 0.03 g/t Au and 1 g/t Ag, but includes sections, 2 to 3 m long, that may carry up to 0.4% Cu, 0.1 g/t Au and 5 g/t Ag (von Guttenberg, 1995). Follow-up drilling included a 214 m hole to test the down-dip extension of the mineral-

ized zone closer to the Takomkane batholith, which was suspected to be the source of the skarn alteration and mineralization. This hole showed an eastward increase in the amount of massive skarn, but a marked decrease in copper mineralization (von Guttenberg, 1996). Subsequent determination of the lead isotope composition of a sulphide sample from the Nemrud prospect suggests that the mineralization may be related to the Spout Lake intrusive suite, represented locally by rare dioritic dikes, rather than the Takomkane batholith (Whiteaker et al., 1998).

TIM (MINFILE 092P 122)

The Tim showings comprise several occurrences of chalcopyrite-pyrite-bornite mineralization located 3.5 to 4.5 km north of Timothy Mountain. Mineralization is hosted in the volcanoclastic and red sandstone-conglomerate units of the Nicola Group, and is associated with a series of monzodiorite dikes that are part of the Spout Lake intrusive suite. Three main showings, referred to as the Tim 1, Tim 2 and Tim 3 showings, were discovered during a geological mapping program by Amax Exploration Inc. in 1972 (Leary and Allan, 1972). The area was restaked by Stallion Resources Ltd. in 1979, and explored with a program that included six short diamond-drill holes on the Tim 1 showing in 1983 (Butler, 1984). The claims were subsequently optioned by Liberty Gold Corp. and explored with VLF-EM, magnetometer, induced polarization and soil geochemical surveys in 1988 and 1989 (White, 1988; Seywerd, 1990). These surveys were followed by a 1990 program that included geological mapping, a detailed induced polarization survey, 736 m of percussion drilling in seven holes and 1 245 m of diamond drilling in twelve holes (Reynolds, 2006), although none of this work was filed for assessment credit. The claims were allowed to lapse, but the known mineral showings and anomalies were staked by P. Reynolds in 1997 as the Tam and Mat claims. These claims were optioned to GWR Resources Inc. in 2001, and explored with a program of geological mapping, soil and rock sampling and diamond drilling (Blann, 2001b). They were then optioned by Tatmar Ventures Inc., and evaluated with induced polarization, magnetometer and soil geochemical surveys in 2004 through 2006 (Reynolds, 2006).

Much of the exploration work on the Tim occurrence has been focused on the Tim 1 showing, located about 500 m southeast of the easternmost monzodiorite stock. Mineralization is associated with a monzodiorite dike that dips steeply to the northwest, and occurs within the dike itself and the country rock along its northwest margin. Mineralization consists of disseminations and fracture and vein stockworks containing pyrite, chalcopyrite and minor bornite, associated with epidote and K-feldspar (Leary and Allan, 1972). Diamond drilling carried out in 1983, 1990 and 2001 indicates that mineralization occurs in several sub-parallel, northeast-striking zones, 2 to 10 m thick, that have been traced for a strike length of 50 m and remain open (Blann, 2001b). Intercepts from the 2001 drilling program include 0.61% Cu, 0.18 g/t Au and 6.0 g/t Ag over 17.4 m in hole TAM01-1, and 0.50% Cu, 0.11 g/t Au and 3.0 g/t Ag over 5.6 m in hole TAM01-2 (Blann, 2001b).

The Tim 2 showing is located about 800 m south of the Tim 1 showing. It comprises K-feldspar-epidote-calcite-magnetite stockworks containing chalcopyrite and pyrite. This mineralization has been traced intermittently over more than 200 m within sheared rock along the southwest margin of a northwest-striking monzodiorite dike. (Leary

and Allan, 1972). The Tim 3 showing is located several hundred metres east of the Tim 2 showing. Here, chalcopyrite, pyrite and malachite are associated with epidote, K-feldspar and magnetite in fracture and vein stockworks, within and adjacent to a north to northeast-striking monzodiorite dike (Leary and Allan, 1972).

Additional scattered occurrences of chalcopyrite, malachite and native copper have been reported between and west of the main Tim showings (Leary and Allan, 1972; Blann, 2001b). Some of these occur in trenches that were excavated to test a strong IP chargeability anomaly outlined by Liberty Gold Corp in 1989, and centred about 900 m southwest of the Tim 1 showing (Seywerd, 1990). This chargeability anomaly was also tested with percussion and diamond-drill holes in 1990. According to Reynolds (2006), the drilling revealed extensive areas of pyrite, with minor chalcopyrite, bornite, native copper, molybdenite and copper oxides, within propylitic and potassic-altered Nicola breccia.

SS (MINFILE 092P 004)

The SS showings are located near the northern boundary of the map area, about 1 km northeast of the east tip of Spout Lake. They are hosted in monzodiorite of the Spout Lake pluton, and are described as shears containing bornite, chalcopyrite, magnetite, pyrite and malachite (Allen, 1968). They were covered by the SS claims in the late 1960s, which were held by Monte Cristo Mines Ltd., and explored with a soil geochemical survey (Allen, 1968) and a ground magnetometer survey (Mitchell, 1969). The showings have apparently received little attention since that time.

WC (MINFILE 092P 120)

The WC occurrence is a chalcopyrite-magnetite skarn located on the south side of Spout Lake, 2 km west of the east end of the lake. The mineralization was discovered in 1971 by Amax Exploration Inc. and covered by the WC claim group (Hodgson and DePaoli, 1972). Subsequent exploration included percussion and diamond drill programs by Amax Exploration Inc. in 1972 and 1973, and diamond drilling by Craigmont Mines Ltd. in 1974 (Rowan, 1990). During this period, the mineralization was also the focus of a study carried out at the University of Western Ontario (Winfield, 1975). The WC occurrence has received intermittent attention since the mid-1970s, including several diamond drill programs that were carried out between 1992 and 1995 (Blann, 1995a). The most recent work recorded on the occurrence was a 1 784 m, 8 hole diamond drill program carried out by GWR Resources Inc. in 2005 (Callaghan, 2005).

The WC prospect is hosted by volcanic and clastic rocks within the transition zone between the volcanoclastic succession and the polyolithic breccia unit of the Nicola Group. The host succession is dominated by volcanic and polyolithic breccia and mafic flows, but also includes intervals of massive to thin-bedded sandstone, siltstone and calcareous siltstone. These rocks are along the south margin of the Spout Lake pluton, and are cut by narrow dikes ranging from diorite to monzonite in composition. Skarn assemblages include the minerals garnet, epidote, calcite, K-feldspar, magnetite, tourmaline, clinopyroxene, actinolite, sphene and scapolite. Sulphide mineralization, comprising chalcopyrite and pyrite with subordinate bornite and covellite, occurs as stratiform lenses and fracture-controlled

zones associated with magnetite-rich skarn (Winfield, 1975; Callaghan, 2005).

Mineralization at the WC prospect occurs mainly in two zones, referred to as the North zone and the South zone. Copper-magnetite mineralization in the North zone occurs in narrow, discontinuous lenses that are roughly concordant to the northwest-striking, steeply dipping hostrock. The main zone of mineralization has been traced over a strike length of more than 400 m, and is 5 to 55 m wide. Mineralization within the zone is discontinuous, however, and copper and gold assay values tend to be low and erratic (Callaghan, 2005). Notable (oblique) intersections from the 2005 drill program include 18.4 m grading 0.60% Cu and 0.12 g/t Au, and 81.9 m grading 0.40% Cu and 0.01 g/t Au (Callaghan, 2005, hole SPL-05-01). The South zone, 150 to 200 m south of the North zone, comprises patchy skarn alteration and mineralization that has been interpreted to occur within a single gently dipping lens (Blann, 1995b) or along two narrow, parallel, north-northwest-trending fault systems (Callaghan, 2005). Notable intersections from the 2005 drill program include 32.7 m grading 0.24% Cu and 0.06 g/t Au in hole SPL-05-02, and 11.7 m grading 0.40% Cu and 0.28 g/t Au in hole SPL-05-07 (Callaghan, 2005).

RED

The Red showing, located about 2 km south of Spout Lake, comprises fracture-controlled chalcopyrite-pyrite-magnetite-malachite mineralization adjacent to a northeast-striking fault. The mineralization occurs in a small outcrop that was discovered during an exploration program on the Red property in 2005 (Blann, 2006). It is hosted by breccia that forms part of the contact zone between the Nicola volcanoclastic succession and the polyolithic breccia unit. A 1 m chip sample across the mineralized zone returned 2.54% Cu, 20.8 ppb Au and 12.8 ppm Ag (Blann, 2006, sample 151717).

CYAN (MINFILE 092P 121)

The Cyan showing, hosted by the red sandstone-conglomerate unit of the Nicola Group about 4 km northwest of Mount Timothy, comprises scattered occurrences of native copper, malachite and chalcopyrite. The area was staked as the Bear claim group in 1994, following the release of encouraging exploration results from the nearby Miracle showing (MINFILE 092P 124), and copper mineralization was discovered during a short program of reconnaissance geological mapping (Newman, 1994). It was further evaluated with geological mapping and limited soil and silt geochemistry in 1998 (Blann, 1998), but has received little attention since then.

The copper mineralization at the Cyan showing occurs as several isolated occurrences within two areas about 1 600 m apart. The northeastern area is within a series of pyroxene-phyric flows and flow breccias in the lower part of the red sandstone-conglomerate unit. It includes an exposure containing native copper as narrow fracture fillings and disseminations, an exposure of fractured malachite-stained rock 500 m to the northeast, and a narrow shear zone containing malachite, limonite and chalcopyrite 900 m northwest of the native copper exposure (Newman, 1994). A grab sample from the shear zone returned 1.67% Cu and 15 ppb Au, and a sample of the malachite-stained rock to the east returned 4 518 ppm Cu and 12 ppb Au (Blann, 1998). The second area of mineraliza-

tion, 1 600 m to the southwest, is within an area dominated by polyolithic breccia and conglomerate with local sandstone, shale and amygdaloidal flows. The main area of mineralization comprises native copper, associated with chalcedonic quartz and specularite, as vesicle fillings within an amygdaloidal flow. A grab sample of this copper mineralization returned 0.13% Cu and less than 0.03 ppm Au (Newman, 1994). A separate copper occurrence, comprising malachite-stained breccia, is located about 400 m to the north of the native copper showing (Newman, 1994).

CLUB

The Club showing is located 5 km south of Spout Lake. It comprises 10 m of intermittent malachite that was exposed in a trench excavated by Tide Resources Ltd. in 1988, during an exploration program on the Club mineral claims (White, 1989). The trench was cut through K-feldspar-epidote-altered breccia and sandstone that are here assigned to the Nicola polyolithic breccia unit. The zone of malachite was sampled in two 5 m intervals. One yielded 1 110 ppm Cu, 2.3 ppm Ag and 3 ppb Au, and the adjacent section returned 2 579 ppm Cu, 5.6 ppm Ag and 1 ppb Au (White, 1989).

Occurrences elsewhere in the Timothy Lake map area

SPRING LAKE (MINFILE 092P 114)

The Spring Lake occurrence, located in the south-central part of the map area, consists of disseminated and fracture-controlled copper mineralization within and adjacent to the Kelly Lake stock. This area was first covered by the SL claims, which were staked by Royal Canadian Ventures Ltd. in 1968 to cover a magnetic high outlined by an aeromagnetic survey (Geological Survey of Canada, 1968). The SL claims were explored with a soil geochemical survey, a ground magnetometer survey, a VLF-EM survey, and limited geological mapping in 1968 (Vollo, 1969); a mercury vapour soil geochemical survey in 1970 (Vollo, 1970), and one 67 m diamond-drill hole in 1971 (British Columbia Mineralogical Branch, 1972). The area was restaked as the Ty 1 claim by Guichon Explorco Ltd. in 1981, and covered by a soil geochemical survey (Owskiacki and Gamble, 1982) and two induced polarization surveys (Gamble, 1983a). It was again restaked in 1994, as the Spring claims of GWR Resources Inc., and explored by geological mapping, a soil geochemical survey, induced polarization and magnetometer geophysical surveys, and 1 549 m of diamond drilling in twelve holes (Blann, 1995b). Erwin Resources Ltd. conducted soil, rock and silt geochemical surveys over the area in 2003 (Thompson, 2003).

Bedrock is very poorly exposed in the area of the Spring Lake occurrence, but diamond drilling, together with some natural exposures, shows that copper mineralization is widespread, although discontinuous and generally low grade, over an area extending for about 1.5 km to both the north and west of the west end of Kelly Lake (Blann, 1995b). The mineralization occurs within the Kelly Lake stock, and in related dikes and enclosing breccia and sandstone of the Nicola volcanoclastic succession north of the stock. It consists of pyrite, chalcopyrite and bornite, and locally native copper and malachite, which occur along fractures, in narrow veins and as disseminations. Associated alteration assemblages consist mainly of K-feldspar,

epidote, chlorite and magnetite, but areas of quartz-sericite-pyrite alteration are also reported, and mineralized garnet-epidote-diopside skarn occurs within breccia north of Kelly Lake (Blann, 1995b). Diamond-drill hole S95-3, located 400 m west of Kelly Lake, cut the Kelly Lake stock and included a 21 m intersection grading 0.184% Cu, 0.03 g/t Au and 1 g/t Ag (Blann, 1995b). Diamond-drill hole S94-4, within volcanic breccia 1 500 m to the north, included a 15 m intersection that graded 0.151% Cu, 0.08 g/t Au and 1.16 g/t Ag (Blann, 1995b).

SODA LAKE (MINFILE 092P 152)

The Soda Lake occurrence is located in the southwestern part of the map area, about 1 km north of Soda Lake, and is hosted by volcanic breccia here assigned to the Nicola volcanoclastic succession. The first assessment work recorded in this area was an induced polarization survey conducted by Anaconda American Brass Ltd. in 1970 over the Whitehorse and Soda claim groups (Macrae and Cont, 1970). Most of these claims had lapsed by 1981, when R.M. Durfeld staked the Bridget 1 mineral claim to cover an area of mineralized float that he discovered while prospecting along the power transmission line (Durfeld, 1982). Subsequent prospecting, geological mapping and soil geochemical surveys led to the discovery of minor *in situ* mineralization, which Durfeld (1983) describes as pyrite and chalcopyrite, as veins and disseminations, in propylitically altered andesitic volcanics and breccias. Additional prospecting, along with soil and rock geochemical analyses, was carried out in 1996, when the area was covered by the Soda 4 claim group of Guardian Enterprises Ltd. (McCrossan, 1996b). Soil and rock samples (angular float mineralized with pyrite) returned anomalous copper values, but no subsequent work has been recorded in the area of the occurrence.

RAIL

The Rail occurrence, located about 3 km north of Rail Lake, comprises mineralization intersected in a diamond-drill hole cored to test an elongate, northwest-trending aeromagnetic anomaly in an area with no bedrock exposure. The anomaly was first staked by M.S. Morrison in 1991, and the area was surveyed with ground magnetometer surveys from 1992 to 1995, a percussion drilling program in 1996, and a VLF-EM survey in 1999 (Morrison, 1999). The percussion drilling program showed that the anomaly is underlain by a magnetite-rich microgabbro. The original claims were allowed to lapse, but the area was restaked by M.S. Morrison in 2003, and three diamond-drill holes were cored in 1995 to test a northeast-trending magnetic low, interpreted as a fault zone that offset the anomaly. The three holes intersected gabbro that is weakly mineralized with chalcopyrite and bornite in zones of potassic alteration. The best intersections returned 0.67% Cu across 25 cm and 0.27% Cu across 2 m (Morrison, 2006).

MAC (MINFILE 092P 032)

The Mac showing is located within the Takomkane batholith near its southwest margin, about 2.5 km southeast of Spring Lake. Canway Explorations Ltd. explored the area with a soil geochemical survey, two induced polarization surveys, trenching and percussion drilling from 1969 to 1974. This was followed by a small rock and soil geochemical survey carried out by Guardian Enterprises Ltd. in 1996. The known mineralization is apparently very mi-

nor, and is described as disseminations and fracture-fillings of fine-grained pyrite, chalcopyrite and molybdenite (McCrossan, 1996a).

MATH (MINFILE 092P 133)

The Math showings are located in the Takomkane batholith, about 6 km east of Timothy Lake. The area was staked by Pickands Mather and Co. in 1972 to cover an area of anomalous molybdenum values obtained in a lake sediment geochemical survey. An exploration program carried out in 1973 included geological mapping, soil and mercury vapour geochemical surveys, a magnetometer survey, and the blasting of 9 test pits. Molybdenum mineralization was exposed in two adjacent test pits. It comprises pyrite and molybdenite within a random network of quartz veinlets, hosted by intensely silicified and locally brecciated granitic rock. A 14 kg sample of mineralized material returned 0.024% Mo (Leonard and Wahl, 1973). Subsequent exploration apparently included an induced polarization survey and some drilling, but none of this work was filed for assessment purposes.

Additional exploration work in the area of the Math showing was carried out by Denison Mines Ltd. in 1980, Herb Wahl and Associates Ltd. in 1984, and Guardian Enterprises Ltd. in 1996. The 1984 exploration program outlined a zone of strong quartz-sericite-kaolin-pyrite alteration, 350 m by 400 m in size, about 1 700 m northeast of the original Math molybdenum occurrence. Anomalous Mo values of 29 to 240 ppm were obtained from propylitically altered rocks collected adjacent to this altered zone (Wahl, 1984). This peripheral zone includes an exposure of slightly silicified and chloritized granodiorite with disseminated chalcopyrite and malachite. A sample of this material returned 1 420 ppm Cu and 242 ppm Mo (Wahl, 1984).

TIMOTHY CREEK (MINFILE 092P 033)

The Timothy Creek occurrence is located on the west side of Timothy Creek, 12 km northeast of Lac La Hache. It comprises polymetallic veins within a shear zone that cuts andesitic flows and breccia of the Skull Hill Formation. The Yep claims were staked over the veins in 1972, and the claims were explored with a soil geochemical survey and rock sampling program in 1974. The highest assay from eight samples of mineralized material collected during this program was 0.30% Cu, 3.51% Pb, 6.05% Zn, 159.4 g/t Ag and 1.3 g/t Au (Fox, 1974). The mineralized structure was mapped in more detail by Reinertson (1978) after the showing had been acquired by Noranda Exploration Company Ltd. According to Reinertson the shear zone strikes 015°, dips steeply west, is up to 90 m wide, and was traced over a strike length of 725 m. Individual veins are less than 15 cm thick and vary in composition from pure galena to variable proportions of galena, chalcopyrite, sphalerite, quartz and calcite. Noranda Exploration Company Ltd. tested the vein system at depth with two angled diamond-drill holes in 1979. Although quartz-carbonate veins were intersected beneath the surface showing, they are narrow and only sparsely mineralized with disseminated galena, chalcopyrite, sphalerite and pyrite (Lewis, 1979).

SUMMARY OF MAIN CONCLUSIONS

- The Timothy Lake map area is underlain mainly by Mesozoic volcanic, sedimentary and plutonic rocks of

the Quesnel Terrane, but also includes substantial areas of Eocene volcanic rocks, small outliers of Miocene-Pliocene basalt, and several patches of Quaternary (?) basalt containing lherzolite xenoliths. Eocene volcanic rocks are much more extensive than shown on previous maps, whereas Miocene-Pliocene basalt of the Chilcotin Group is considerably less extensive.

- The Quesnel Terrane is represented mainly by the Upper Triassic Nicola Group and Early Jurassic granodiorite of the Takomkane batholith (Schoolhouse Lake unit), but also includes quartz-poor intrusive rocks of mainly monzodioritic composition. The latter intrusions are particularly abundant in the north-central part of the map area, where they are assigned to the Spout Lake intrusive suite, represented by the southern part of the Spout Lake pluton and several stocks and plugs south of Peach Lake.
- The Nicola Group in the southern part of the map area consists mainly of green pyroxene porphyry breccia and pyroxene-feldspar sandstone, which are assigned to the volcanoclastic succession and correlated with Nicola rocks previously mapped to the east and south-east. Two additional units, not recognized to the east, have been mapped in the north-central part of the map area, where they interfinger with and overlie the volcanoclastic succession. These are referred to as the polyolithic breccia unit and the red sandstone-conglomerate unit. The unique features of these units include the presence of abundant fine to medium-grained plutonic fragments (monzonite, monzodiorite, diorite, gabbro) in the conglomerate and breccia, and a predominant red colour of the sandstone and conglomerate in the upper part of the succession. These units probably correlate with unit 3 of Panteleyev et al. (1996) within the Quesnel River – Horsefly map area to the north.
- Cu-Au mineralization is concentrated in an area of 60 to 70 km² in the north-central part of the Timothy Lake map area, near Peach Lake. Mineralization occurs mostly as porphyry-style fracture and vein stockworks within and adjacent to stocks of the Spout Lake intrusive suite, but also includes several skarn occurrences. The porphyry-style mineralization comprises chalcopyrite, pyrite and locally bornite, and is associated with magnetite and K-feldspar, and locally biotite, hematite, tourmaline, chlorite and calcite, within areas of widespread K-feldspar-epidote alteration. Malachite and native copper are common throughout the mineralized belt. One of the mineralized stocks has yielded a U-Pb titanite date of 203 ± 4 Ma (Whiteaker et al., 1998), demonstrating a temporal relationship with other alkalic Cu-Au porphyry systems within central and southern Quesnel Terrane, such as Mount Polley, Afton-Ajax and Copper Mountain (Mortensen et al., 1995).
- The mineralized stocks south of Peach Lake are hosted by the polyolithic breccia unit of the Nicola Group, which is overlain by the red sandstone-conglomerate unit to the south. The spatial relationship of mineralized stocks, breccia and conglomerate units containing plutonic clasts, and red breccia and sandstone implying emergent conditions, suggests that this area is part of a relatively long-lived volcanic-plutonic centre within the Nicola arc.

ACKNOWLEDGMENTS

We thank Devin Tait and Britt Bluemel for their capable and enthusiastic assistance during fieldwork, and Kelly Schiarizza for filling in as a field assistant in the latter part of the summer. We also thank Jean and Mike Peake for their excellent hospitality at Eagle Creek, and Dave Bailey, of Bailey Geological Consultants, who led us on a field trip to examine and discuss the regional geology of the Quesnel Terrane near Morehead Lake.

REFERENCES

- Allen, A.R. (1968): Geochemical survey, Cariboo Mining Division, for Monte Cristo Mines Ltd. N.P.L.; *BC Ministry of Energy, Mines and Petroleum Resources*, Assessment Report 1 704, 15 pages.
- Andrews, G.D.M. and Russell, J.K. (2007): Mineral exploration potential beneath the Chilcotin Group (NTS 0920, P; 093A, B, C, F, G, J, K), south-central British Columbia: preliminary insights from volcanic facies analysis; *BC Ministry of Energy, Mines and Petroleum Resources*, Paper 2007-1 and *Geoscience BC*, Report 2007-1, pages 229–238.
- Barker, G.E. (2002): An assessment report on diamond drilling on the Ann 2 mineral claim (Northeast-mag zone), Clinton Mining Division, NTS 92P/14W; *BC Ministry of Energy, Mines and Petroleum Resources*, Assessment Report 27 289, 42 pages.
- Barker, G.E. (2003): An assessment report on diamond drilling on the Ann 2 mineral claim (Harvey zone), Clinton Mining Division, NTS 92P/14W; *BC Ministry of Energy, Mines and Petroleum Resources*, Assessment Report 27 017, 54 pages.
- Blann, D.E. (1995a): Geological report on the Peach Lake property, Lac La Hache, British Columbia, NTS 92P/14W, Clinton Mining Division; *BC Ministry of Energy, Mines and Petroleum Resources*, Assessment Report 23 966, 73 pages.
- Blann, D.E. (1995b): Geological report on the Spring Lake property, Lac La Hache, British Columbia, NTS 92P/14W, Clinton Mining Division; *BC Ministry of Energy, Mines and Petroleum Resources*, Assessment Report 23 965, 92 pages.
- Blann, D.E. (1995c): Diamond drilling report on the Ophir copper property, Lac La Hache, British Columbia, NTS 92P/14W; *BC Ministry of Energy, Mines and Petroleum Resources*, Assessment Report 23 975, 47 pages.
- Blann, D.E. (1995d): Geological report on the Miracle prospect, Lac La Hache, British Columbia, NTS 92P/14W; *BC Ministry of Energy, Mines and Petroleum Resources*, Assessment Report 23 976, 131 pages.
- Blann, D.E. (1998): Assessment report on the Cyan property, Cyan claim (#356334), Lac La Hache, British Columbia, NTS 92P/14W, Clinton Mining Division; *BC Ministry of Energy, Mines and Petroleum Resources*, Assessment Report 25 650, 22 pages.
- Blann, D.E. (2001a): Diamond drilling report on the Ann property, Ann 1 (208270) and Ann 2 (208271) claims, Clinton Mining Division, Lac La Hache, British Columbia, NTS 92P/14W; *BC Ministry of Energy, Mines and Petroleum Resources*, Assessment Report 26 476, 302 pages.
- Blann, D.E. (2001b): Assessment report on the Tam property, Lac La Hache, British Columbia, NTS 92P/14W/14E, Clinton Mining Division; *BC Ministry of Energy, Mines and Petroleum Resources*, Assessment Report 26 655, 62 pages.
- Blann, D.E. (2006): Geological and geochemical report on the Red property, Lac La Hache, British Columbia, UTM 92P.093/92P.094, Clinton Mining Division; *BC Ministry of Energy, Mines and Petroleum Resources*, Assessment Report 28 093, 28 pages.
- Bloodgood, M.A. (1990): Geology of the Eureka Peak and Spanish Lake map areas, British Columbia; *BC Ministry of Energy, Mines and Petroleum Resources*, Paper 1990-3, 36 pages.
- British Columbia Mineralogical Branch (1972): SL, in *Geology, exploration and mining in British Columbia, 1971*, *BC Ministry of Energy, Mines and Petroleum Resources*, page 335.
- Butler, S.P. (1984): Diamond drilling report on the Tim 2 claim, Clinton Mining Division, British Columbia, 92P/14E; *BC Ministry of Energy, Mines and Petroleum Resources*, Assessment Report 12 192, 35 pages.
- Callaghan, B. (2005): Assessment report on drilling and trenching, 2003 to 2005, on the Lac La Hache property, Clinton Mining Division, NTS 92P/14W; *BC Ministry of Energy, Mines and Petroleum Resources*, Assessment Report 28 332, 624 pages.
- Campbell, R.B. (1978): Geological map of the Quesnel Lake map area, British Columbia; *Geological Survey of Canada*, Open File 574, 1:125 000 scale.
- Campbell, R.B. and Tipper, H.W. (1971): Bonaparte Lake map area, British Columbia; *Geological Survey of Canada*, Memoir 363, 100 pages.
- Carson, J.M., Dumont, R., Potvin, J., Shives, R.B.K., Harvey, B.J.A. and Buckle, J.L. (2006a): Geophysical series, NTS 92P/14, Lac La Hache, British Columbia; *Geological Survey of Canada*, Open File 5291, 10 sheets, 1:50 000 scale.
- Carson, J.M., Dumont, R., Potvin, J., Shives, R.B.K., Harvey, B.J.A., Buckle, J.L. and Cathro, M. (2006b): Geophysical series, NTS 93A/3, 93A/2, 93A/6, 93A/7, 92P/14, Eagle (Murphy) Lake, British Columbia; *Geological Survey of Canada*, Open File 5292, 10 sheets, 1:50 000 scale.
- Carson, J.M., Dumont, R., Potvin, J., Shives, R.B.K., Harvey, B.J.A. and Buckle, J.L. (2006c): Geophysical series, NTS 93A/2, 93A/3, 92P/14, 92P/15, McKinley Creek, British Columbia; *Geological Survey of Canada*, Open File 5293, 10 sheets, 1:50 000 scale.
- Casselman, M.J., McMillan, W.J. and Newman, K.M. (1995): Highland Valley porphyry copper deposits near Kamloops, British Columbia: A review and update with emphasis on the Valley deposit; in *Porphyry Deposits of the Northwestern Cordillera of North America*, Schroeter, T.G., Editor, *Canadian Institute of Mining, Metallurgy and Petroleum*, Special Volume 46, pages 161–191.
- Colpron, M. and Price, R.A. (1995): Tectonic significance of the Kootenay terrane, southeastern Canadian Cordillera: An alternative model; *Geology*, Volume 23, pages 25–28.
- Coyle, M., Dumont, R., Potvin, J., Carson, J.M., Buckle, J.L., Shives, R.B.K. and Harvey, B.J.A. (2007): Geophysical series, Lac La Hache (southwest) 92P/14 and part of 92P/13, British Columbia - Bonaparte Lake West Geophysical Survey; *Geological Survey of Canada*, Open File 5491 and *Geoscience BC*, Map 2007-4-8, 10 sheets, 1:50 000 scale.
- Dawson, G.M. (1879): Preliminary report on the physical and geological features of the southern portion of the interior of British Columbia; in *Report of Progress, 1877-1878*, Part B, *Geological Survey of Canada*, pages 1B–187B.
- Dumont, R., Potvin, J., Carson, J.M., Harvey, B.J.A., Coyle, M., Shives, R.B.K. and Ford, K.L. (2007): Geophysical series, Lac La Hache 92P/14, British Columbia - Bonaparte Lake East Geophysical Survey; *Geological Survey of Canada*, Open File 5493 and *Geoscience BC*, Map 2007-3-6, 10 sheets, 1:50 000 scale.
- Dunn, D. St. C. (1992): Report on diamond drilling on the Miracle project, Murphy 1, Murphy 2, Murphy 3 and Murphy 4 claims, Clinton Mining Division, NTS 92P/14W; *BC Ministry of Energy, Mines and Petroleum Resources*, Assessment Report 22 603, 58 pages.
- Durfeld, R.M. (1982): Geochemical report on the Bridget 1 mineral claim, Clinton Mining Division, NTS 92P/14W; *BC*

- Ministry of Energy, Mines and Petroleum Resources, Assessment Report 10 572, 22 pages.
- Durfeld, R.M. (1983): Geochemical and geological report on the Bridget 1 mineral claim, Clinton Mining Division, NTS 92P/14W; *BC Ministry of Energy, Mines and Petroleum Resources*, Assessment Report 11 390, 17 pages.
- Ewing, T.E. (1980): Paleogene tectonic evolution of the Pacific Northwest; *Journal of Geology*, Volume 88, pages 619–638.
- Ferri, F. (1997): Nina Creek Group and Lay Range assemblage, north-central British Columbia: remnants of late Paleozoic oceanic and arc terranes; *Canadian Journal of Earth Sciences*, Volume 34, pages 854–874.
- Fox, P.E. (1974): Geochemical report on the Yep claims, Clinton Mining Division; *BC Ministry of Energy, Mines and Petroleum Resources*, Assessment Report 5067, 14 pages.
- Gale, R.E. (1991): Assessment report on the geology and drilling of the Ann 1 and 2 claims, Clinton Mining Division, B.C., 92P/14W; *BC Ministry of Energy, Mines and Petroleum Resources*, Assessment Report 21 982, Part 1, 56 pages.
- Gamble, D. (1983a): Guichon Explorco Limited, induced polarization geophysical surveys on the Ty 1 claim, Clinton Mining Division, NTS 92P/14W and E; *BC Ministry of Energy, Mines and Petroleum Resources*, Assessment Report 11 982, 68 pages.
- Gamble, D. (1983b): Guichon Explorco Limited, summary of percussion drilling and induced polarization geophysical surveys on the Ty 2 claim, Clinton Mining Division, NTS 92P/14E; *BC Ministry of Energy, Mines and Petroleum Resources*, Assessment Report 11 983, 88 pages.
- Geological Survey of Canada (1968): Aeromagnetic map, Lac La Hache, British Columbia, NTS 92P/14; *Geological Survey of Canada*, Map 5232G, 1:63 360 scale.
- Hodgson, C.J. and DePaoli, G.M. (1972): 1971 geological, geochemical and geophysical report, Spout Lake copper property, Clinton and Cariboo Mining divisions, NTS 92P/14 and 93A/3; *BC Ministry of Energy, Mines and Petroleum Resources*, Assessment Report 3690, 59 pages.
- Janes, R.H. (1967): A report on a magnetometer survey of part of the Peach north and south groups, Clinton Mining Division; *BC Ministry of Energy, Mines and Petroleum Resources*, Assessment Report 1037, 9 pages.
- Leonard, M.A., and Wahl, H.J. (1973): Pickands Mather and Co., exploration report on Math claims, 92P/14E; *BC Ministry of Energy, Mines and Petroleum Resources*, Assessment Report 4647, 40 pages.
- Leary, G.M. and Allan, J.F. (1972): 1972 geological report, Peach Lake Cu property (Coranex option; Tim claims), Clinton Mining Division, 92P/14; *BC Ministry of Energy, Mines and Petroleum Resources*, Assessment Report 4030, 13 pages.
- Leary, G.M. and Godfrey, T.J.R. (1972): 1972 geological and geochemical report, Peach Lake copper property (Coranex option), claims Peach 44, 46, 48, 59-61, 62-64, 65-68, 73-74, 77-90, 211 Fr., 212 Fr., and Pit 58-59, 67, 69-71, 92P/14, Clinton Mining Division; *BC Ministry of Energy, Mines and Petroleum Resources*, Assessment Report 3815, 61 pages.
- Lewis, T.D. (1979): Diamond drilling report on the Timothy Creek property, Clinton Mining Division; *BC Ministry of Energy, Mines and Petroleum Resources*, Assessment Report 7454, 23 pages.
- Logan, J.M. and Mihalynuk, M.G. (2005a): Regional geology and setting of the Cariboo, Bell, Springer and Northeast Porphyry Cu-Au zones at Mount Polley, south-central British Columbia; *BC Ministry of Energy, Mines and Petroleum Resources*, Paper 2005-1, pages 249–270.
- Logan, J.M. and Mihalynuk, M.G. (2005b): Porphyry Cu-Au deposits of the Iron Mask Batholith, southeastern British Columbia; *BC Ministry of Energy, Mines and Petroleum Resources*, Paper 2005-1, pages 271–290.
- Macrae, R. and Cont, T.A. (1970): A geophysical report on an induced polarization survey, Whitehorse and Soda claim groups, Clinton Mining Division, 92P/14W; *BC Ministry of Energy, Mines and Petroleum Resources*, Assessment Report 2684, 6 pages.
- Mathews, W.H. (1989): Neogene Chilcotin basalts in south-central British Columbia: geology, ages, and geomorphic history; *Canadian Journal of Earth Sciences*, Volume 26, pages 969–982.
- McCrossan, E. (1996a): SMS claim group, rock and soil geochemical report, Clinton Mining Division, NTS 92P/14E; *BC Ministry of Energy, Mines and Petroleum Resources*, Assessment Report 24 457, 19 pages.
- McCrossan, E. (1996b): Soda 4 claim group, soil and rock geochemical report, Clinton Mining Division, NTS 92P/14W; *BC Ministry of Energy, Mines and Petroleum Resources*, Assessment Report 24 521, 15 pages.
- Mitchell, J.A. (1969): Monte Cristo Mines Ltd. (N.P.L.) magnetometer survey, claims SS 1-16; 21-28, Cariboo Mining Division; *BC Ministry of Energy, Mines and Petroleum Resources*, Assessment Report 2074, 11 pages.
- MINFILE (2007): MINFILE BC mineral deposits database; *BC Ministry of Energy, Mines and Petroleum Resources*, URL <<http://www.em.gov.bc.ca/Mining/Geolosurv/Minfile/>>.
- Morrison, M.S. (1999): Geophysical assessment report on the Rail claim group, Lac La Hache area, Clinton Mining Division; *BC Ministry of Energy, Mines and Petroleum Resources*, Assessment Report 26 114, 25 pages.
- Morrison, M.S. (2006): Diamond drilling assessment report on the Rail claim group, Lac La Hache area, Clinton Mining Division; *BC Ministry of Energy, Mines and Petroleum Resources*, Assessment Report 28 221, 58 pages.
- Mortensen, J.K., Ghosh, D.K. and Ferri, F. (1995): U-Pb chronology of intrusive rocks associated with copper-gold porphyry deposits in the Canadian Cordillera; in *Porphyry Deposits of the Northwestern Cordillera of North America*, Schroeter, T.G., Editor, *Canadian Institute of Mining, Metallurgy and Petroleum*, Special Volume 46, pages 142–158.
- Mortensen, J.K., Montgomery, J.R. and Fillipone, J. (1987): U-Pb zircon, monazite and sphene ages for granitic orthogneiss of the Barkerville Terrane, east-central British Columbia; *Canadian Journal of Earth Sciences*, Volume 24, pages 1261–1266.
- Mortimer, N. (1987): The Nicola Group: Late Triassic and Early Jurassic subduction-related volcanism in British Columbia; *Canadian Journal of Earth Sciences*, Volume 24, pages 2521–2536.
- Nelson, J.L. and Bellefontaine, K.A. (1996): The geology and mineral deposits of north-central Quesnellia; Tezzeron Lake to Discovery Creek, central British Columbia; *BC Ministry of Energy, Mines and Petroleum Resources*, Bulletin 99, 112 pages.
- Newman, K.M. (1994): Summary report on reconnaissance geological mapping, Bear group, BO 1, BO 2, BO 3, Max 5 and Max 6 claims, Lac La Hache area, BC, Clinton Mining Division, NTS 92P/14W; *BC Ministry of Energy, Mines and Petroleum Resources*, Assessment Report 23 517, 23 pages.
- Owsiacki, G. and Gamble, D. (1982): Geochemical survey on the Ty 1 claims, Ty 1 grid, Clinton Mining Division, British Columbia; *BC Ministry of Energy, Mines and Petroleum Resources*, Assessment Report 10 667, 28 pages.
- Pálffy, J., Smith, P.L. and Mortensen, J.K. (2000): A U-Pb and $^{40}\text{Ar}/^{39}\text{Ar}$ time scale for the Jurassic; *Canadian Journal of Earth Sciences*, Volume 37, pages 923–944.
- Panteleyev, A., Bailey, D.G., Bloodgood, M.A. and Hancock, K.D. (1996): Geology and mineral deposits of the Quesnel River-Horsefly map area, central Quesnel Trough, British Colum-

- bia; *BC Ministry of Energy, Mines and Petroleum Resources*, Bulletin 97, 155 pages.
- Preto, V.A. (1977): The Nicola Group: Mesozoic volcanism related to rifting in southern British Columbia; in *Volcanic regimes in Canada*, W.R.A. Baragar, L.C. Coleman and J.M. Hall, Editors, *The Geological Association of Canada*, Special Paper 16, pages 39–57.
- Preto, V.A. (1979): Geology of the Nicola Group between Merritt and Princeton; *BC Ministry of Energy, Mines and Petroleum Resources*, Bulletin 69, 90 pages.
- Rees, C.J. (1987): The Intermontane-Omineca belt boundary in the Quesnel Lake area, east-central British Columbia: Tectonic implications based on geology, structure and paleomagnetism; Ph.D. thesis, *Carleton University*, 421 pages.
- Reinertson, L.C. (1978): Geological and geochemical report on the Westim, Westim 2, Westim 3, Rainbow 1, Rainbow 2, Rainbow 3 mineral claims, Clinton Mining Division; *BC Ministry of Energy, Mines and Petroleum Resources*, Assessment Report 7256, 11 pages.
- Reynolds, P. (2006): Geophysical and geochemical report on the Tam and Mat mineral claims (Tam property), Clinton Mining Division, British Columbia, NTS 092P/14; *BC Ministry of Energy, Mines and Petroleum Resources*, Assessment Report 28 729, 34 pages.
- Ross, J.V., Fillipone, J., Montgomery, J.R., Elsby, D.C. and Bloodgood, M. (1985): Geometry of a convergent zone, central British Columbia, Canada; *Tectonophysics*, Volume 119, pages 285–297.
- Rowan, L.G. (1990): A geological report on the Dora, Pee Wee and Club claims, Spout Lake, Lac La Hache area, British Columbia, Clinton Mining Division, 92P/14W; *BC Ministry of Energy, Mines and Petroleum Resources*, Assessment Report 20 621, 49 pages.
- Schiarizza, P. (1989): Structural and stratigraphic relationships between the Fennell Formation and Eagle Bay assemblage, western Omineca Belt, south-central British Columbia: Implications for Paleozoic tectonics along the paleocontinental margin of western North America; M.Sc. thesis, *University of Calgary*, 343 pages.
- Schiarizza, P. and Boulton, A. (2006a): Geology and mineral occurrences of the Quesnel Terrane, Canim Lake area (NTS 092P/15), south-central British Columbia; *BC Ministry of Energy, Mines and Petroleum Resources*, Paper 2006-1 and *Geoscience BC*, Report 2006-1, pages 163–184.
- Schiarizza, P. and Boulton, A. (2006b): Geology of the Canim Lake area, NTS 92P/15; *British Columbia Ministry of Energy, Mines and Petroleum Resources*, Open File 2006-8, 1:50 000 scale.
- Schiarizza, P. and Israel, S. (2001): Geology and mineral occurrences of the Nehalliston Plateau, south-central British Columbia (92P/7, 8, 9, 10); *BC Ministry of Energy, Mines and Petroleum Resources*, Paper 2001-1, pages 1–30.
- Schiarizza, P. and Macauley, J. (2007a): Geology and mineral occurrences of the Hendrix Lake area (NTS 093A/02), south-central British Columbia; *BC Ministry of Energy, Mines and Petroleum Resources*, Paper 2007-1 and *Geoscience BC*, Report 2007-1, pages 179–202.
- Schiarizza, P. and Macauley, J. (2007b): Geology of the Hendrix Lake area, NTS 93A/02; *British Columbia Ministry of Energy, Mines and Petroleum Resources*, Open File 2007-3, 1:50 000 scale.
- Schiarizza, P. and Preto, V.A. (1987): Geology of the Adams Plateau-Clearwater-Vavenby area; *BC Ministry of Energy, Mines and Petroleum Resources*, Paper 1987-2, 88 pages.
- Schiarizza, P., Heffernan, S. and Zuber, J. (2002a): Geology of Quesnel and Slide Mountain terranes west of Clearwater, south-central British Columbia (92P/9, 10, 15, 16); *BC Ministry of Energy, Mines and Petroleum Resources*, Paper 2002-1, pages 83–108.
- Schiarizza, P., Heffernan, S., Israel, S. and Zuber, J. (2002b): Geology of the Clearwater - Bowers Lake area, British Columbia (NTS 92P/9, 10, 15, 16); *BC Ministry of Energy, Mines and Petroleum Resources*, Open File 2002-15, 1:50 000 scale.
- Schiarizza, P., Israel, S., Heffernan, S. and Zuber, J. (2002c): Geology of the Nehalliston Plateau (92P/7, 8, 9, 10); *BC Ministry of Energy, Mines and Petroleum Resources*, Open File 2002-4, 1:50 000 scale.
- Seywerd, M.B. (1990): Liberty Gold Corp. geophysical and geochemical report on an induced polarization and soil geochemical survey on the Tim, Tim 1 and Tim 2 claims, Clinton Mining Division, NTS 92P/14; *BC Ministry of Energy, Mines and Petroleum Resources*, Assessment Report 20 095, 116 pages.
- Struik, L.C. (1988a): Crustal evolution of the eastern Canadian Cordillera; *Tectonics*, Volume 7, pages 727–747.
- Struik, L.C. (1988b): Regional imbrication within Quesnel Terrane, central British Columbia, as suggested by conodont ages; *Canadian Journal of Earth Sciences*, Volume 25, pages 1608–1617.
- Sutherland Brown, A. (1958): Boss Mountain; in *Annual Report of the Minister of Mines for 1957*, *BC Ministry of Energy, Mines and Petroleum Resources*, pages 18–22.
- Sutherland Brown, A. (1969): Peach, Tim; in *Annual Report of the Minister of Mines for 1968*; *BC Ministry of Energy, Mines and Petroleum Resources*, pages 155–159.
- Thompson, G. (2003): Geological report on the Summer property, 92P.074 and 084, Clinton Mining Division, Lac La Hache, British Columbia; *BC Ministry of Energy, Mines and Petroleum Resources*, Assessment Report 27 361, 38 pages.
- Thompson, R.I., Glombick, P., Erdmer, P., Heaman, L.M., Lemieux, Y. and Daughtry, K.L. (2006): Evolution of the ancestral Pacific margin, southern Canadian Cordillera: Insights from new geologic maps; in *Paleozoic evolution and metallogeny of pericratonic terranes at the ancient Pacific margin of North America*, Canadian and Alaskan cordillera, Colpron, M. and Nelson, J., Editors, *Geological Association of Canada*, Special Paper 45, pages 433–482.
- Travers, W.B. (1978): Overtuned Nicola and Ashcroft strata and their relations to the Cache Creek Group, southwestern Intermontane Belt, British Columbia; *Canadian Journal of Earth Sciences*, Volume 15, pages 99–116.
- Unterschutz, J.L.E., Creaser, R.A., Erdmer, P., Thompson, R.I. and Daughtry, K.L. (2002): North American margin origin of Quesnel Terrane strata in the southern Canadian Cordillera: Inferences from geochemical and Nd isotopic characteristics of Triassic metasedimentary rocks; *Geological Society of America Bulletin*, Volume 114, pages 462–475.
- Vollo, N.B. (1969): Geological, geophysical and geochemical report on the 92P/14 SL group of Royal Canadian Ventures Ltd., at Lac La Hache, B.C.; *BC Ministry of Energy, Mines and Petroleum Resources*, Assessment Report 1834, 9 pages.
- Vollo, N.B. (1970): Geochemical report on the 92P/14 SL group of Royal Canadian Ventures Ltd., at Lac La Hache, B.C.; *BC Ministry of Energy, Mines and Petroleum Resources*, Assessment Report 2378, 3 pages.
- von Guttenberg, R. (1994): Regional Resources Ltd., GWR Resources Inc., Lac La Hache Project, Report of 1993 field work, Riley claim group, Nemrud grid, Clinton and Cariboo Mining divisions, B.C., NTS 92P/14E; *BC Ministry of Energy, Mines and Petroleum Resources*, Assessment Report 23 466, 47 pages.
- von Guttenberg, R. (1995): Regional Resources Ltd., GWR Resources Inc., Lac La Hache Project, report on diamond drilling, Nemrud bornite skarn, Mike claim group, Clinton Mining Division, B.C., NTS 92P/14E; *BC Ministry of En-*

- ergy, Mines and Petroleum Resources, Assessment Report 24 139, 84 pages.
- von Guttenberg, R. (1996): Regional Resources Ltd., GWR Resources Inc., Lac La Hache Project, 1995 drill program, Cariboo and Clinton Mining divisions, B.C., NTS 92P/14, 93A/3; *BC Ministry of Energy, Mines and Petroleum Resources*, Assessment Report 25 368, 256 pages.
- Wahl, H. (1984): Exploration report on the Quantico (1709) and Tico (1752) mineral claims, Clinton Mining Division, British Columbia; *BC Ministry of Energy, Mines and Petroleum Resources*, Assessment Report 13 254, 18 pages.
- White, G.E. (1987): GWR Resources Inc. geological, geochemical and geophysical report, Miracle 2, 3, 4 and 5 claims, Clinton Mining Division, Timothy Lake area, B.C., NTS 92P/14W; *BC Ministry of Energy, Mines and Petroleum Resources*, Assessment Report 16 586, 74 pages.
- White, G.E. (1988): Liberty Gold Corp. geophysical report, Tim, Tim 1 and Tim 2 claims, Clinton Mining Division, Lac La Hache area, B.C., NTS 92P/14E; *BC Ministry of Energy, Mines and Petroleum Resources*, Assessment Report 17 960, 23 pages.
- White, G.E. (1989): Tide Resources Ltd. geochemical and geophysical report, Club 1, 2, 6 and 7 claims, Clinton Mining Division, Lac La Hache area, B.C., NTS 92P/14W; *BC Ministry of Energy, Mines and Petroleum Resources*, Assessment Report 18 589, 30 pages.
- Whiteaker, R.J. (1996): The geology, geochronology and mineralization of the Ann property: An Early Jurassic alkalic porphyry system near Lac La Hache, B.C.; unpublished B.Sc. thesis, *The University of British Columbia*, 65 pages.
- Whiteaker, R.J., Mortensen, J.K. and Friedman, R.M. (1998): U-Pb geochronology, Pb isotopic signatures and geochemistry of an Early Jurassic alkalic porphyry system near Lac La Hache, BC; *BC Ministry of Energy, Mines and Petroleum Resources*, Paper 1998-1, pages 33-1–33-13.
- Winfield, W.D.B. (1975): Volcanic, plutonic and Cu-Fe skarn rocks, Spout Lake, B.C.; M.Sc. thesis, *The University of Western Ontario*, 121 pages.

Newly Recognized White Talc-Carbonate Filler Potential of the Greenwood – Bridesville Area, British Columbia (NTS 082E), and Brief Talc Market Review

by G.J. Simandl^{1,2}

KEYWORDS: talc, calcite, dolomite, filler, exploration, development, potential market

INTRODUCTION

British Columbia has over 40 talc deposits, at least seven of which are carbonate-hosted (MacLean, 1988; Benvenuto, 1993). Most economic talc deposits in the world can be classified as either sedimentary hosted (Simandl and Paradis, 1999) or ultramafic hosted (Simandl and Ogdén, 1999).

The recently recognized Bridesville talc-carbonate deposit, in the Greenwood – Bridesville area of southern BC, is the sedimentary-hosted variety. It has a lower grade than most traditional high-grade carbonate-hosted talc deposits, such as Henderson, Conley and East deposits located in Ontario (Simandl, 1985b) and those in Montana, United States. However, a parallel may be made between the Bridesville deposit and the New Conley deposit, Ontario. White fillers containing talc, derived from the New Conley orebody (talc-bearing dolomite), were successfully marketed in the past by Canada Talc Industries Ltd. under the trademarks Dolfil and Talfil. The possibility that there is a market for ‘talc-carbonate filler’ in western North America should be investigated. If the results of the investigation are positive, the talc-carbonate zone of the Bridesville deposit may provide sellable product without need for upgrading. The need for capital cost-intensive processing (such as flotation), to achieve a marketable product, would lower the development potential of this deposit. Even if there was no market for the talc-carbonate filler, the identification of the Bridesville deposit is significant. Carbonate-hosted talc deposits typically occur in clusters. A higher grade extension of this deposit, or another higher grade carbonate-hosted deposit (characterized by high brightness and whiteness talc ore), could be discovered in southern BC.

THE TALC MARKET

The combined world production of talc and pyrophyllite is estimated at 8.3 million tonnes for 2006 (Virta, 2007). More than one third of it originates from China. Most of the world talc production is used in the paper, ceramics, plastics and paint/coating industries. The cosmetic-grade talc market is very small but talc concentrates that meet these tight specifications have a very high unit value. If pyrophyllite is eliminated from these statistics, the talc production alone is probably close to 7 million tonnes. United States’ talc markets have been declining since they attained a high of 1.05 million tonnes in 1990. In 2004, they reached a low of 857 000 tonnes, but markets are currently recovering. United States’ consumption is expected to vary within the 875 000 to 925 000 tonne range for the next few years (Virta, 2007). Canadian shipments of talc and pyrophyllite combined were estimated at 66 000 tonnes in 2005 (Dumont, 2005), though detailed breakdown by province is not available. However, Ontario, which produces talc from both sedimentary and ultramafic-hosted deposits, is the main producer.

China’s exports of high-purity, lump-talc ore may be curtailed because of the elimination of China’s export tax rebates, the implementation of new export taxes and its shrinking reserves of high-grade ores. A substantial proportion of the high-grade, Chinese, lump talc was traditionally produced from small operations by highly selective mining and hand sorting. Therefore, in the medium term, Canadian talc producers have the potential to increase their share of total market. However, in the short term, any talc producer located along the west coast of North America has to compete with Chinese exports and with talc from Madison County, Montana.

A review of the talc industry by Virta (2007) includes a discussion of the uses and value of talc products. The primary user of talc is the paper industry. A study of the paper industry market along the west coast of North America by Harris and Ionides (1994) indicates that most of the talc products used in pulp and paper, paint and plastics production are nearly monomineralic and have tighter specifications than the concentrates used in ceramic, coating or plastic filler applications. Examples of talc product specifications used in the paper industry are provided by Harris and Ionides (1994). The second most important use of talc in terms of tonnage is probably in the asphalt industry, which consumes off-colour and low-grade products. A small amount of soapstone talc is extracted but it is primarily artisanal, there is only one commercial soapstone operation near East Broughton, Quebec. There are special circumstances, other than in asphalt use, where material containing talc-carbonate mixtures may become a sellable

¹ British Columbia Ministry of Energy, Mines and Petroleum Resources, Victoria, BC

² School of Earth and Ocean Sciences, University of Victoria, Victoria, BC

This publication is also available, free of charge, as colour digital files in Adobe Acrobat® PDF format from the BC Ministry of Energy, Mines and Petroleum Resources website at http://www.em.gov.bc.ca/Mining/Geosurv/Publications/catalog/cat_fldwk.htm

product assuming that physical and chemical homogeneity of the product can be maintained over a prolonged period of time. This has been demonstrated by the successful marketing of products derived from the New Conley deposit in Ontario (see below). This possibility should be investigated in the case of the Bridesville deposit, which has a potential to supply high whiteness product.

LOCATION AND HISTORY

The newly recognized talc-carbonate deposit in BC is located south of Bridesville in southern BC (342948E, 5432972N, elevation 1080 m asl; Fig 1). P. Chaput, of Mighty White Dolomite Ltd. (Mighty White), provided the author with a sample for mineral identification. Talc and carbonate were tentatively identified as the two main constituents. P. Chaput reported that this deposit was previously considered as a source of high-purity dolomite for agricultural and environmental applications. However, the material did not pass the neutralizing tests and the project was abandoned.

A brief reconnaissance-type examination and sampling program of the excavation was undertaken by the author. This investigation confirmed the location of the occurrence, the dimension of the excavation, and the width, orientation and mineralogy of the talc-carbonate zone and host rock.

REGIONAL GEOLOGICAL SETTING

The Bridesville talc-carbonate deposit lies within the Permian and/or Triassic Anarchist Group as defined by Little (1961), consisting of greenstone, quartzite, greywacke, limestone and locally paragneiss. Tempelman-Kluit (1989) also mapped the deposit area at a scale of 1:250 000, but a more detailed map is not currently available. The Bridesville talc-carbonate deposit may be stratigraphically related to the Rock Creek dolomite mine, also called Dolo (MINFILE 082ESE200; MINFILE, 2007), which is operated by Mighty White.



Figure 1. Location of the sedimentary-hosted Bridesville talc-carbonate deposit, southern BC.

The Rock Creek dolomite mine is located approximately 5 km southeast of the community of Rock Creek. It occurs within the Permian to Carboniferous Knob Hill Group (MINFILE 082ESE200). This terminology is in line with a suggestion by Little (1983) not to use the Anarchist Group term within the Greenwood area; however, MacLean (1988) reiterates that the dolomite mined near Rock Creek is part of the Anarchist Group. Massey (2007) included the Rock Creek dolomite in the Anarchist schist but stated that the relationship between this unit and the rest of the Anarchist schist is enigmatic.

The high-quality dolomite from Rock Creek mine is similar in chemical composition and colour to the dolomite that is hosting the Bridesville talc-carbonate deposit. However, the Rock Creek dolomite contains traces of serpentine rather than traces of talc. Mafic dikes crosscutting the dolomite at Rock Creek have sharp and predictable contacts with the dolomite, although in places they are schistose. It is therefore possible that the Rock Creek and Bridesville dolomite zones are stratigraphically related, differing only in degree of deformation. The highly schistose greenstone exposed in the Bridesville excavation is a postdeformational equivalent of the mafic dikes. A detailed re-examination of the Rock Creek dolomite is justified. MacLean (1988) reports a talc-bearing zone near the base of dolomite ore. This zone was not exposed, or at least not observed, at the time of the author's brief visit to the minesite as part of an industry monitoring program in 2001.

The clarification of the exact stratigraphic relationship between the rocks hosting the Bridesville and the Rock Creek deposits is very relevant for dolomite exploration. It may be less critical for talc exploration, especially if mineralization-controlling structures are very recent relative to dolostone units (chemical composition of dolomites being equal).

DEPOSIT DESCRIPTION

The exposure of the talc-carbonate deposit is limited to the isolated quarry; no other outcrops were observed in immediate proximity of the excavation (Fig 2). The excavation is approximately 60 m in length, 20 m in width and, in places, is more than 6 m deep. The overburden in the excavation area varies from 0 to >1 m thick (Fig 3). It contains white fragments of underlying talc-bearing rock. Three main rock types are exposed within the excavation: a) talc-bearing schistose carbonate, b) greenstone and c) massive dolostone. The talc-bearing zone has a strongly developed schistosity and is exposed on the eastern wall of the excavation (Fig 3).

The talc-bearing zone is several metres thick, striking approximately north-south and dipping 20 to 40° eastwards, assuming that the orientation of the schistosity approximates that of the talc zone. Contacts of the talc zone and dolomite are wavy and they are marked by an abrupt disappearance of the schistosity. Talc accounts for approximately half of the rock within the talc-carbonate zone, based on visual estimates. The talc is concentrated along schistosity planes. Calcite is the main carbonate mineral with minor dolomite. Systematic sampling and laboratory work are needed to better constrain the talc content and relative proportion of calcite and dolomite. The talc-bearing zone is described in more detail in the next section.

The greenstone is characterized by its green colour on both fresh and weathered surfaces. The contact between the



Figure 2. View of the excavation at Bridesville talc-carbonate deposit, southern BC; looking north (truck for scale). Abbreviations: Do, dolostone; Ta-Ca, talc-carbonate zone.

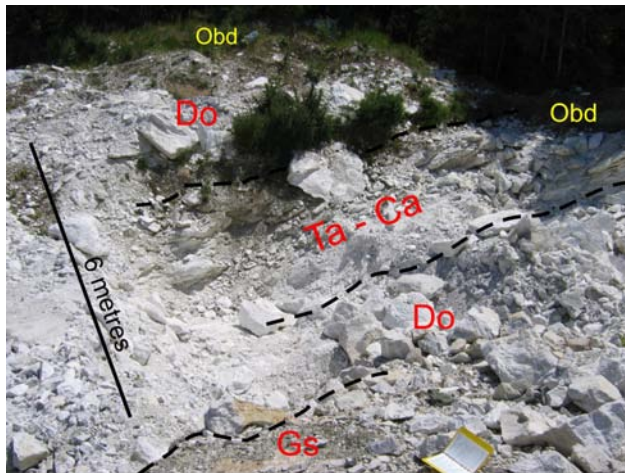


Figure 3. View of the excavation at Bridesville talc-carbonate deposit, southern BC; looking at the eastern wall (notebook for scale). Abbreviations: Ta-Ca, talc-carbonate zone; Do, dolostone; Gs, greenstone; Obd, overburden.

steeply dipping greenstone unit and the surrounding marble is sharp and highly irregular. Similarly to the talc-bearing zone, the greenstone is also characterized by a strong schistose fabric; however, it consists largely of chlorite (>60%). Carbonates, dominantly calcite, account for less than 40% of this rock. Calcite is either intergrown with chlorite or forms veinlets. Quartz forms decimetre-scale, irregularly



Figure 4. Weathered surface of dolostone showing nearly random fracturing, Bridesville talc-carbonate deposit, southern BC. Fracture pattern is enhanced by preferential weathering. Five-cent coin for scale.

distributed pods and veins constituting <5% of the exposure. Quartz is also present as fine-grained aggregates in contact with chlorite or calcite. Quartz veins and pods do not appear to extend from the greenstone into the dolostone. Sulphides (mostly pyrite) are restricted to localized zones within the greenstone and occur as disseminations, typically constituting <1% of the rock; rarely 1–3%. Talc, hematite and tentatively identified albite are trace constituents. The greenstone fabric is strongly discordant to the schistosity of the talc-bearing zone, but their intersection is not exposed within the excavation. The greenstone's protolith may have been a mafic dike or sill (such dikes and sills are visible in the dolomite quarry operated by Mighty White); however, it could have also been a lava flow, tuff or volcanic rock-derived sediment.

The dolostone, the third lithological unit within the excavation, is massive, pale grey on weathered surfaces (Fig 4) and very pale grey to white (locally mottled) on fresh surfaces. Healed fractures that are hard to discern on the fresh surface are enhanced on the weathered surface by preferential weathering. The dolostone consists predominantly of dolomite (>95%) with minor concentrations of calcite, talc and trace pyrite. Talc (<1%) is observed in veinlets in association with coarser carbonate (calcite?) within the mottled variety of dolomite. The chemical composition of the dolostone is given in Table 1.

TABLE 1. CHEMICAL COMPOSITION OF TALC-CARBONATE ZONE AND DOLOMITE FROM THE BRIDESVILLE DEPOSIT, SOUTHERN BC. THE CO₂ CONTENT WAS CALCULATED FROM TOTAL CARBON (TOT-C X 44/12 = CO₂). IN THE CASE OF THE TALC-BEARING ZONE, CO₂ IS HIGHER THAN LOSS-ON-IGNITION; THIS SHOULD NOT HAPPEN. TALC IS A HYDRATED MINERAL CONTAINING APPROXIMATELY 4.75% OF H₂O, AND THIS DISCREPANCY MAY BE ATTRIBUTED TO LOW ANALYTICAL PRECISION.

	SiO ₂	Al ₂ O ₃	Fe ₂ O ₃	MgO	CaO	Na ₂ O	K ₂ O	TiO ₂	P ₂ O ₅	MnO	Cr ₂ O ₃	LOI	TOT-C	CO ₂	TOT-S	SUM
Talc-carbonate zone	35.01	<0.03	0.13	18.58	25.62	0.01	<0.04	<0.01	0.05	0.03	<0.001	20.6	5.92	21.7	<0.01	100
Grey carbonate, dolostone (limy)	2.08	0.15	0.11	17.9	34.26	0.01	0.04	0.01	0.03	0.01	0.001	45.4	12.07	44.26	0.01	99.97
Mottled dolomite	2.46	0.05	0.07	19.45	32.57	0.01	0.04	0.01	0.03	0.01	0.001	45.3	12.38	45.39	0.01	99.97

Physical and Chemical Properties of the Talc-Bearing Zone

The talc-bearing zone is very pale grey on weathered surfaces and is characterized by its flaky texture (Fig 5), which distinguishes it from the massive dolomitic hostrock (Fig 4). It is highly schistose where exposed in the excavation, suggesting that it would be relatively easy to crush. It is snow white on the fresh surface, suggesting that the processed material will most likely be very white and bright (as required in the most demanding filler applications). The talc-bearing dolomite shows a strong planar fabric (Fig 6) and breaks easily into sheets and lenses (typically <1cm thick). However, these sheets may be paper thin within the most schistose portions of the zone. The talc-bearing zone was visually estimated to consist of 50–65% talc and 35–50% carbonate, most of which is calcite {CaCO₃} and possibly minor dolomite {CaMg(CO₃)₂}. Pyrite is present in some parts of the zone as a trace constituent. Plagioclase may be present as traces. Talc platelets are concentrated along the schistosity planes. They are oriented (elongated) parallel to the schistosity planes, suggesting that talc is predeformational, or most likely syndeformational, and that it is formed by the interaction of metasomatic/metamorphic fluids with dolomite hostrock. Neither tremolite nor chrysotile was observed within the talc-bearing zone; however, the absence of these minerals should be confirmed. The talc content and composition of the carbonate of the talc-bearing zone should be better constrained by systematic sampling and related laboratory work. Chemical composition of the talc-carbonate zone is given in Table 1.

New Conley, Henderson and View Deposits

The following section describes materials from New Conley and Henderson talc-carbonate deposits located in eastern Ontario and from the View deposit in southeast BC. These descriptions are essential to understand the similarities and differences between these deposits and the newly discovered Bridesville deposit. In the discussion section below, the parallel is drawn with the materials derived from the New Conley deposit.

The property on which the Henderson (in operation since 1896), Conley (Old Conley), New Conley and East

deposits (discovered in 1981) are located, has changed hands numerous times and is currently owned by Dynatec Corporation. It is located near Madoc, southeastern Ontario (Simandl, 1985a). In the 1970s and the early 1980s, three of these deposits were exploited by Canada Talc Ltd.

New Conley had a much lower talc content than its famous neighbour, the high-grade Henderson talc deposit (Simandl, 1982; Simandl, 1985b). Crushed material from the New Conley deposit consisted mainly of dolomite. Talc (≅10%), tremolite (≅10%), phlogopite (<10%) and antigorite (1.5%) were the remaining identified constituents (Goldberg and Wehrung, 1981). The crushed material was successfully commercialized and marketed under the names Dolfil™ and Talfil™ (Simandl, 1985a, b). Chemically, these products consisted of 20–24% MgO, 26–30% CaO, 16–18% SiO₂, 0.5–1% Al₂O₃, 0.5–1% Fe₂O₃ and 30–35% loss-on-ignition (LOI). These products were marketed as functional fillers for sealants, putties and adhesives, paint and coatings, plastics and stucco/drywall construction products. Top of the line varieties of these products were also marketed as inert carriers for commercial pesticides, fertilizers and insecticides. The raw material for this product was extracted from underground workings connected to the Conley #3 shaft, but the plans existed to start mining at the surface as well.

The main product line of Canada Talc Industries Ltd., called CANTAL™, was derived from the Henderson orebody. According to Goldberg and Wehrung (1981), in the 1970s and 1980s, this product consisted of talc (>70%), dolomite (24%), prismatic tremolite (0.2%), antigorite (2.6%) and phlogopite (1.8%). Richardson (1981) indicates that its typical chemical composition was 42–45% SiO₂, 25–28% MgO, 9–12% CaO, 2–3% Al₂O₃, 0.5–1% Fe₂O₃ and 10–12% LOI. This data is in line with the analyses of grab samples reported by Simandl (1985a).

The specifications of the main line of talc-rich products currently produced by Dynatec Corporation are still referred to as CANTAL but specifications evolved. The company's website (Dynatec Corporation, 2007a) indicates that in addition to its CANTAL™ line of products, the company produces a dolomite-rich product under the trademark DYNAFIL. The product safety sheets for DYNAFIL™ are currently identical to those of Dolfil™, as indicated by Canada Colors and Chemicals Limited's website (Canada



Figure 5. Weathered surface of the talc-bearing zone, Bridesville talc-carbonate deposit, southern BC, characterized by "flaky" texture (strong preferential planar fabric). Five-cent coin for scale.



Figure 6. Strong preferential fabric and snow white colour characterizes talc-bearing zone, Bridesville, southern BC. Hammer for scale.

Colors and Chemicals Limited, 2007) and Dynatec Corporation's website (Dynatec Corporation, 2007b). DYNAFIL™ and Dolfil™ products are reported to contain 90–93% dolomite, 3–4% calcite and 1–3% non-actinolite tremolite. Today, the raw material for DYNAFIL™ (Dolfil™'s functional equivalent) may be coming from the open pit operation rather than from underground because it differs in mineralogy from the sample analyzed by Goldberg and Wehrung (1981).

The View deposit (MINFILE 082FSE070), located approximately 30 km west of Creston, BC, is also known to contain low-grade talc, dolomite, muscovite and calcite; however, the mineralization is not white, whereas Bridesville ore is white. Here, impure talc was considered for commercial use without upgrading. It was explored and developed in 1964 (Olson, 1965). A trial shipment was extracted from this deposit in 1983 by International Marble and Stone Company Ltd. This low whiteness and low brightness material was intended as low-cost filler and dusting component in asphalt (Hora, 1984).

DISCUSSION

Similarities between the Bridesville white talc-carbonate zone and the previously described New Conley white talc-dolomite deposit near Madoc, Ontario, suggest that the recently discovered Bridesville deposit may be of economic interest. Both the New Conley and Bridesville deposits have relatively low talc contents, which could make talc-carbonate separation difficult to justify. A high-quality dolomite product is already commercially available in the Bridesville area from the Mighty White operation (Simandl et al., 2006, 2007). However, there is the possibility that the crushed or micronized white talc-carbonate ore may be sold at a premium over straight dolomite or straight high-calcium carbonate as a specialty mineral filler. A low-cost market study, aiming to identify potential buyers for the talc-carbonate product is justified. The talc content of the Bridesville zone is intermediate between ores from the New Conley and Henderson deposits. The presence of calcite (rather than dolomite) as the main carbonate within the Bridesville talc-bearing zone is a positive feature. Calcite is preferred to dolomite in most filler applications. The existing mill located at Rock Creek, currently being used to process dolomite, could possibly handle the processing of the talc-carbonate ore for filler applications (with some modifications or additions).

Carbonate-hosted talc deposits typically occur in clusters (Simandl, 1985a; Simandl and Paradis, 1999), as illustrated by spatial association of several talc-bearing deposits near Madoc, Ontario, and higher grade dolomite-hosted talc deposits may also be discovered in the Bridesville area. A descriptive model for carbonate-hosted talc deposits (Simandl and Paradis, 1999) provides leads for future exploration. However, a preliminary market study and more detailed laboratory analyses of the talc-carbonate zone are recommended before additional exploration work is carried out either to establish reserves, or to find high-grade talc deposits.

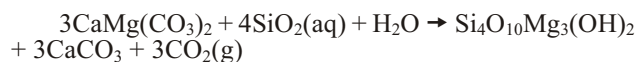
In this particular case, the laboratory work should include both physical and chemical parameters of the talc-bearing zone including detailed mineralogy, whiteness and brightness, surface area, oil adsorption and abrasion. The detailed mineralogy of several representative samples is essential, as the talc ores that do not contain acicular or fi-

brous amphiboles have a major marketing advantage over talc products that contain acicular or fibrous constituents. Products containing fibrous minerals attract intense scrutiny from environmental and health authorities worldwide.

Origin

Any hypothesis proposed to explain the origin of the Bridesville talc deposit must be in accordance with observed structural control on the talc-calcite zone and the abrupt contact of the talc-calcite zone with the dolostone. It should also be in agreement with the mineralogy of the talc-bearing zone (talc-calcite) and the mineralogy of the host rock (nearly monomineralic dolomite) and with subgreenschist or greenschist metamorphic conditions.

The following reaction explains the formation of talc {Si₄O₁₀Mg₃(OH)₂} and satisfies all of the above listed constraints:



This reaction was proposed by Page (1951) and Zwart (1954) and experimentally studied by Metz and Puhani (1970). According to the experimental work of Metz and Puhani (1970) on dolomite-quartz equilibrium, assuming the mole fraction of CO₂ (XCO₂ ≅ 0.5) and depending on the lithostatic pressure (P), talc may form at temperatures below 550°C (at P = 5 kbar) and well below 400°C (at P = 0.5 kbar). At lower XCO₂, the temperatures needed to form talc are even lower. Therefore, if a hydrothermal talc deposit is discovered in unmetamorphosed carbonate, or in carbonate that was subject to metamorphic conditions inferior to those needed to form tremolite during the prograde metamorphic phase, then the chances the talc ore is amphibole free are excellent. Amphiboles that form during the prograde phase of contact or regional metamorphism are commonly destabilized during the retrograde metamorphic phase, resulting in the formation of talc pseudomorphs after tremolite. However, the talcification of amphiboles is rarely complete. No rigorous metamorphic study has been done in the Bridesville area. Based strictly on the combination of mineral assemblages in the greenstone and marble, the rocks were most likely affected by greenschist (or subgreenschist) metamorphism. At this stage, there is no strong evidence to conclude if the Bridesville deposit was formed during the prograde or the retrograde phase of the thermal event, but talc-forming fluids were focused along a structural weakness plane. The source of heat driving the hydrothermal system may have been local or regional. If the talc-forming fluids were related to regional greenschist facies metamorphism, then sediment-hosted talc deposits in the Bridesville area could also be located along the contacts of dolostone with siliceous units (both silica and magnesia would be *in situ*, only water would be needed). Greenschist facies conditions, suggested by mineralogy of the greenstone, are also favourable for the formation of ultramafic-hosted talc deposits (Simandl and Ogden, 1999).

SUMMARY

The presence of the dolomite-hosted, talc-calcite mineralization at the Bridesville deposit is important from a talc exploration perspective. This occurrence fits the sedimentary-hosted talc deposit model (Simandl and Paradis, 1999). It can be considered as an analogue to the obscure,

yet economic, low-grade sedimentary-hosted, talc-carbonate (dolomite) New Conley deposit in Ontario.

The results of this investigation are sufficiently encouraging to recommend additional work, including a preliminary market investigation and systematic characterization of the talc-carbonate rock within the excavation to determine if a more comprehensive deposit evaluation is justified.

The Bridesville talc-carbonate deposit could be of economic interest if there is a market for white talc-carbonate filler on the west coast. The need for upgrading the Bridesville talc-bearing rock would significantly increase capital cost requirements. There is also a possibility that the Bridesville deposit has a higher-grade extension, or that additional dolomite-hosted talc deposits will be discovered in the area. Although the Greenwood – Bridesville area was prospected intensively for precious and base metals for more than a century, the documentation of this deposit demonstrates that the area is far from maturity in terms of exploration for industrial minerals.

ACKNOWLEDGMENTS

This paper benefited from improvement by Dr. Nick Massey and Tania Demchuk of BC Ministry of Energy, Mines and Petroleum Resources in Victoria, BC, and by Laura Simandl of St Michaels University School. Laura also provided photographic documentation for this project.

REFERENCES

- Benvenuto, G. (1993): Geology of several talc occurrences in Middle Cambrian dolomites, southern Rocky Mountains, British Columbia (82N1/E, 820/4W); in Geological Fieldwork 1992, *BC Ministry of Energy, Mines and Petroleum Resources*, Paper 1993-1, pages 361–379.
- Canada Colors and Chemicals Limited (2007): Material safety data sheet dolomite; *Canada Colors and Chemicals Limited*, URL <<http://www.canadacolors.com/canadacolors/docs/msds/english/395902.pdf>>, 7 pages [November 2007].
- Dumont, M. (2005): Talc and pyrophyllite; *Natural Resources Canada*, Canadian Mines Yearbook 2005, pages 54.1–54.9.
- Dynatec Corporation (2007a): Material safety data sheet, dolomite; *Dynatec Corporation*, URL <<http://www.dynatecminerals.com/en/PDF/msds-dolomite.pdf>>, 6 pages [November 2007].
- Dynatec Corporation (2007b): Technical data sheets; *Dynatec Corporation*, URL <<http://www.dynatecminerals.com/en/techdata.html>>, 1 page [November 2007].
- Goldberg, E.J. and Wehrung, J.M. (1981): Analysis of two talc samples by SEM, EDXA; consultant report to *W.R. Barnes Company Ltd.*, Waterdown, Ontario, 18 pages.
- Harris, M. and Ionides, G.N. (1994): Update of a market study for talc; *BC Ministry of Energy, Mines and Petroleum Resources*, Open File 1994-24, 63 pages.
- Hora, Z.D. (1984): British Columbia; in Industrial Minerals in Canada – A Review of Recent Developments, *Industrial Minerals*, Number 200, pages 111–117.
- Little, H.W. (1961): Kettle River (west half), British Columbia; *Geological Survey of Canada*, Map 15-1961, scale 1:253 440.
- Little, H.W. (1983): Geology of the Greenwood map area, British Columbia; *Geological Survey of Canada*, Paper 79-29, 37 pages, 1 map at 1:50 000 scale.
- MacLean, M. (1988): Talc and pyrophyllite in British Columbia; *BC Ministry of Energy, Mines and Petroleum Resources*, Open File 1988-19, 108 pages.
- Massey, N.W.D. (2007): Geology and mineral deposits of the Rock Creek area of BC (082E/2W, 082E/3E); *BC Ministry of Energy, Mines and Petroleum Resources*, Open File 2007-07, scale 1:25 000.
- Metz, P. and Puhan, D. (1970): Experimentelle Untersuchung der Metamorphose von kieselig dolomitischen Sedimenten; *Contributions to Mineralogy and Petrology*, Volume 26, pages 302–314.
- MINFILE (2007): MINFILE BC mineral deposits database; *BC Ministry of Energy, Mines and Petroleum Resources*, URL <<http://www.em.gov.bc.ca/Mining/Geolsurv/Minfile/>> [November 2007].
- Olson, P.E. (1965): View 1, 2, 3; in Minister of Mines Annual Report, *BC Ministry of Energy, Mines and Petroleum Resources*, page 278.
- Page, B.M. (1951): Talc deposits of steatite grade, Inyo County, California; *California Division of Mines*, Special Report 8, 35 pages.
- Richardson, J.A. (1981): Cantal 325, product data; *Canada Talc Industries Ltd.*, 1 page.
- Simandl, G.J. (1982): Industrial mineral potential of the unique high-grade Madoc talc deposit, Ontario; *Canadian Institute of Mining and Metallurgy*, 84th Annual General Meeting, General Program, pages 51–52.
- Simandl, G.J. (1985a): Geology and geochemistry of talc deposits in the Madoc area, Ontario; unpublished MSc thesis, *Carleton University*, 154 pages.
- Simandl, G.J. (1985b): Geology of the Henderson talc deposit, Madoc, Ontario; *Geological Association of Canada-Mineralogical Association of Canada*, Annual Meeting, Abstract, Volume 10, page A-56.
- Simandl, G.J., Irvine, M.L., Grieve, D., Lane, R., Wojdak, P., Madu, B., Webster, I., Northcote, B. and Schroeter, T. (2007): Industrial minerals in British Columbia – 2006 overview; *BC Ministry of Energy, Mines and Petroleum Resources*, Information Circular 2007-2, 12 pages.
- Simandl, G.J. and Ogden, D. (1999): Ultramafic-hosted talc-magnesite; in Selected British Columbia Mineral Deposit Profiles, Volume 3, Industrial Minerals and Gemstones, Simandl, G.J., Hora, Z.D. and Lefebure, D.V., Editors, *BC Ministry of Energy, Mines and Petroleum Resources*, pages 65–68.
- Simandl, G.J. and Paradis, S. (1999): Carbonate-hosted talc; in Selected British Columbia Mineral Deposit Profiles, Volume 3, Industrial Minerals and Gemstones, Simandl, G.J., Hora, Z.D. and Lefebure, D.V., Editors, *BC Ministry of Energy, Mines and Petroleum Resources*, pages 35–38.
- Simandl, G.J., Robinson, N.D. and Paradis, S. (2006): Dolomite in BC: geology, current producers and possible development opportunities along the west coast; in Geological Fieldwork 2005, *BC Ministry of Energy, Mines and Petroleum Resources*, Paper 2006-1, pages 197–207.
- Tempelman-Kluit, D.J. (1989): Geological map with mineral occurrences, fossil localities, radiometric ages and gravity field for Penticton map area (NTS 82E), southern British Columbia; *Geological Survey of Canada*, Open File 1969, 17 pages, 5 maps at 1:250 000 scale.
- Virta, R.L. (2007): Talc and pyrophyllite; *United States Geological Survey*, Mineral Commodity Summaries, January 2007, pages 162–163.
- Zwart, H.J. (1954): La géologie du Massif du Saint-Barthelemy, Pyrénées, France; *Ryksmuseum van Geologie en Mineralogie*, Leidse Geologische Mededelingen, Leyden, Netherlands, 228 pages.

Fireside Deposit: Diagenetic Barite in Strata of the Kechika Group, and Vein Barite Related to Rifting of the Kechika Trough, Northwestern British Columbia (NTS 094M/14)

by P.J. Wojdak

KEYWORDS: barite, Fireside mine, Kechika Trough

INTRODUCTION

Dresser Industries produced barite from the Fireside property from 1983 to 1985 for use in oil and gas exploration. After a twelve-year hiatus, mining was reactivated on a sporadic seasonal basis by Fireside Minerals Inc. from 1997 to the present. Examination by the author of new exposures during this second phase of mining has elucidated the geology of the deposit and led to a better understanding of barite vein formation.

The Fireside mine, located in NTS area 94M/14, is reached from the Alaska Highway 125 km east of Watson Lake, or 11 km west of Fireside, via a 5.5 km gravel road (Fig 1). Realignment of the Alaska Highway in the 1990s north of its former location shortened the length of the access road by 1.5 km. The property is located 5 km north of the Liard River in rolling upland of the Liard Plain, an area dotted with numerous small lakes and blanketed by glacial till. Outcrop is sparse and confined to the tops of low hills and along major streams. Decades ago, an extensive forest fire swept the Fireside district. The area is covered now with dense growth of young spruce and birch. Early exploration at Fireside included many bulldozer-cut lines with unsystematic orientations, spacings and lengths. These are regrown with a tangle of alder. Foot travel away from roads at Fireside is difficult.

History and Production

G.B. Smith of Edmonton, Alberta recorded the first four claims at Fireside in October 1963. The claims were acquired by Magnet Cove Barium Corporation in 1964, and a seismic refraction survey on the Bear, Moose and Wolf claims was filed for assessment by H.C. Bickel (1965). The earliest geological description was by J.W. McCammon (1965). He described a large stripped area and barite showings that, based on topographic and geological relationships, correspond to the Bear West and Bear East veins. A secondary barite showing 300 m to the southwest, also noted by McCammon, does not correspond to the Moose or Beaver showings and is unknown to the writer.

Dresser Minerals Inc., a subsidiary of Dresser Industries and affiliated with Magnet Cove Barium, continued to

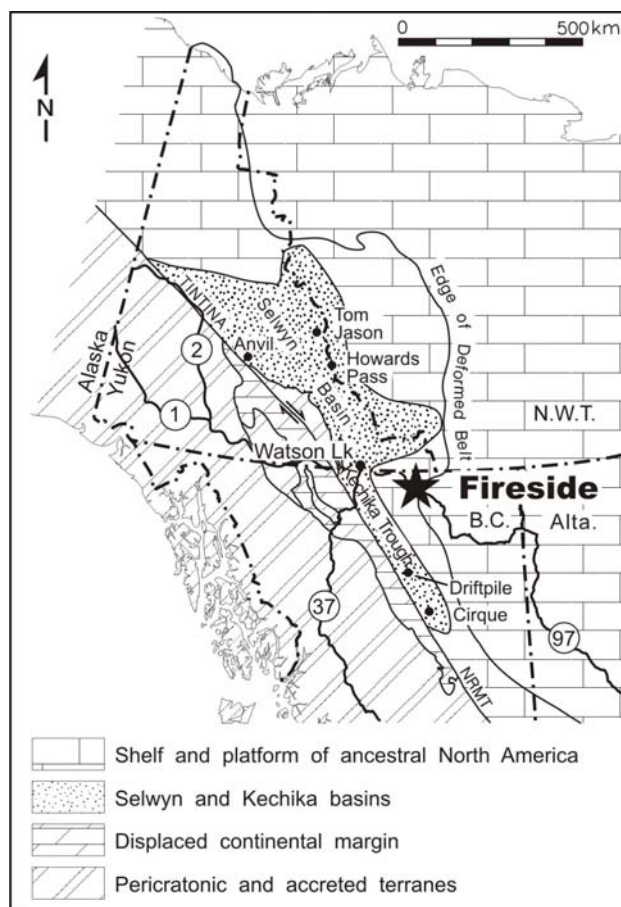


Figure 1. Regional setting of the Fireside barite deposit.

explore and develop the property (Crosby, 1971; McLeish and Baron, 1981) and began in 1984 to prepare the Moose deposit for mining. By 1986, some 70 000 t had been mined (Butrenchuk and Hancock, 1997), from which 41 071 t of barite were produced. Much of the barite was stockpiled and hauled to Watson Lake on a market basis until 1989. By 1997, the original Fireside claims had lapsed and new claims were acquired by Matovich Mining Industries Ltd. Later that year, Fireside Minerals Inc. became operator through an option agreement with Matovich and mined the Moose deposit. The Moose pit was reclaimed and, in 1998, Fireside Minerals developed Bear West. The majority of subsequent barite production has been obtained from that deposit, with a small amount coming from Bear East. An-

This publication is also available, free of charge, as colour digital files in Adobe Acrobat® PDF format from the BC Ministry of Energy, Mines and Petroleum Resources website at http://www.em.gov.bc.ca/Mining/Geosurv/Publications/catalog/cat_fldwk.htm

TABLE 1. ANNUAL PRODUCTION AT FIRESIDE BARITE MINE (1998–2007). PRODUCTION IN 2002 EXCLUDES 5000 TONNES THAT WERE MINED BUT NOT MILLED. PRODUCTION IN 2003 INCLUDES THE 5000 TONNES MINED IN 2002.

Year	Ore source	Mined (tonnes)	Barite production (tonnes)
1984 1986	Moose, minor Bear East	70000	41071
1997	Moose	15000	9000
1998	Bear West	18000	11500
1999	Bear West	36000	23000
2000		0	0
2001	Bear East & West	15000	10000
2002	Bear East	7500	1500
2003	Bear West	15000	10000
2004	Bear West	14000	9000
2005	Bear West	15000	10000
2006	Bear West	30000	12000
2007		0	4000
Total		235500	141071

Annual barite production at Fireside totals 141 071 t of barite from 235 000 t of ore (Table 1).

Mining leases 361111 and 361112 cover areas of 41.8 ha over the Moose deposit and 82.3 ha over the Bear deposit, respectively, and are owned by D.C. Allan of Red Deer Alberta. The Ram and Lynx claims that adjoin the leases are also owned by Mr. Allan.

Operations Summary — Mining, Beneficiation and Reserves

Dresser Minerals mined primarily the Moose deposit, supplemented by a small amount from Bear East. Fireside Minerals acquired the infrastructure built by Dresser Minerals. This includes a crusher, jigs and large lay-down area near the Moose deposit, plus a grinding and bagging plant in Watson Lake. Fireside Minerals contracts mining and ore hauling to Jedway Enterprises Ltd. Mining (Fig 2) is done with a track drill, a bulldozer and an excavator. Three 30 t



Figure 2. Mining in the Bear West pit, 2005.



Figure 3. Loading haul truck in the Bear West pit, 2006.

trucks transport the ore (Fig 3) on the 4.2 km haul road to a crusher at the Moose site. Crushed raw ore is upgraded by jigs that separate barite, with a specific gravity of 4.48, from lighter rock. Average mine product has a specific gravity of 4.3; a minimum of 4.2 is required to be saleable, equivalent to 90% pure barite (E.W. Craft, pers comm, 2006). The mine normally operates for three months each year, from June to August. Highway trucks are used for the 125 km trip to Watson Lake. Trucking of barite concentrate begins in mid-summer and the Watson Lake plant operates for about three months, from August to October. The operation provides temporary employment for 25 people.

The ground and bagged barite (Fig 4) is sold to the oil and gas drilling industry in northeastern British Columbia and northern Alberta and, during the 1980s, was sold for use in Alaska (S. Butrenchuk, pers comm, 1998). Barite is a component of drilling ‘mud’. It provides a high hydrostatic head that helps prevent ‘gushers’ and consequent environmental impact and oil loss. Environmental regulations require lead content of barite used in oilfield drilling to be less than 10 ppm. Fireside barite is well within the environmental standard; no galena has been found in the Bear vein and occurs rarely near the margin of the Moose vein. Fireside



Figure 4. Bagged barite at the Watson Lake plant, ready for shipment.

barite also meets American Petroleum Institute criteria for low content of soluble alkaline earth metals, such as calcium.

DJ Drilling Company Ltd. initiated exploration drilling at Fireside to guide mining by its affiliate, Jedway Enterprises Ltd. (D. Schussler, pers comm, 2005). A series of holes was drilled in the vicinity of the Moose pit in late 2005 and ten holes were drilled in the area of Bear West in early 2006, in both cases on a 30 m grid. The Bear West drillcore was used by E.W. Craft to calculate a mining reserve and to design a five-year plan for mining (Craft, 2006), to begin in 2007. Craft noted that his report is not compliant with National Instrument 43-101. He determined a 'resource' of 208 000 t, with 512 000 t of waste rock requiring removal in order to recover barite, giving a strip ratio of 2.46:1. There was no mining at the Fireside property in 2007, but barite was produced from stockpiled material.

GEOLOGICAL SETTING

The Fireside area is underlain by a sequence of siliciclastic sedimentary rocks, limestone and dolomite of Cambrian (or older) to Devonian age, deposited on the ancestral margin of North America (Souther, 1992). These strata form the Selwyn Basin in the Yukon and, in northern British Columbia, a 500 km long embayment known as the Kechika Trough. Fireside is located near the junction between the southern margin of the Selwyn Basin and the

northern end of the Kechika Trough (Fig 1). Sedimentary rocks on the Fireside property closely resemble the Kechika Group (Late Cambrian to Early Ordovician) or the overlying lower Road River Group. Ferri et al. (1999) noted the difficulty in distinguishing slate of the upper Kechika Group from overlying strata of the lower Road River Group (Ordovician to Early Silurian). The boundary between the two groups is where tan and light-coloured limy slate and siltstone of the Kechika Group are succeeded upwards by similar rocks, black in colour, of the Road River Group. Accordingly, J. Nelson (pers com., 2007) assigned Fireside strata to the Kechika Group. The upper Road River Group, not seen in the vicinity of the deposit, comprises dolomitic siltstone with minor limestone and chert of Silurian to Late Devonian age. These Paleozoic depositional basins are displaced by the Eocene Tintina fault, which cuts obliquely across the region 60 km south of Fireside.

Important sedimentary exhalative (SEDEX) zinc-lead-barite deposits occur extensively in the lower Paleozoic strata of the Selwyn Basin and Kechika Trough (Carne and Cathro, 1982; MacIntyre, 1992; Ferri et al., 1999). Barite veins are similarly widespread, crosscutting these strata.

GEOLOGY IN THE VICINITY OF THE BARITE VEINS

The vicinity of the Bear and Moose veins is underlain by thin bedded, limy siltstone and shale (Fig 5). Bedding at-

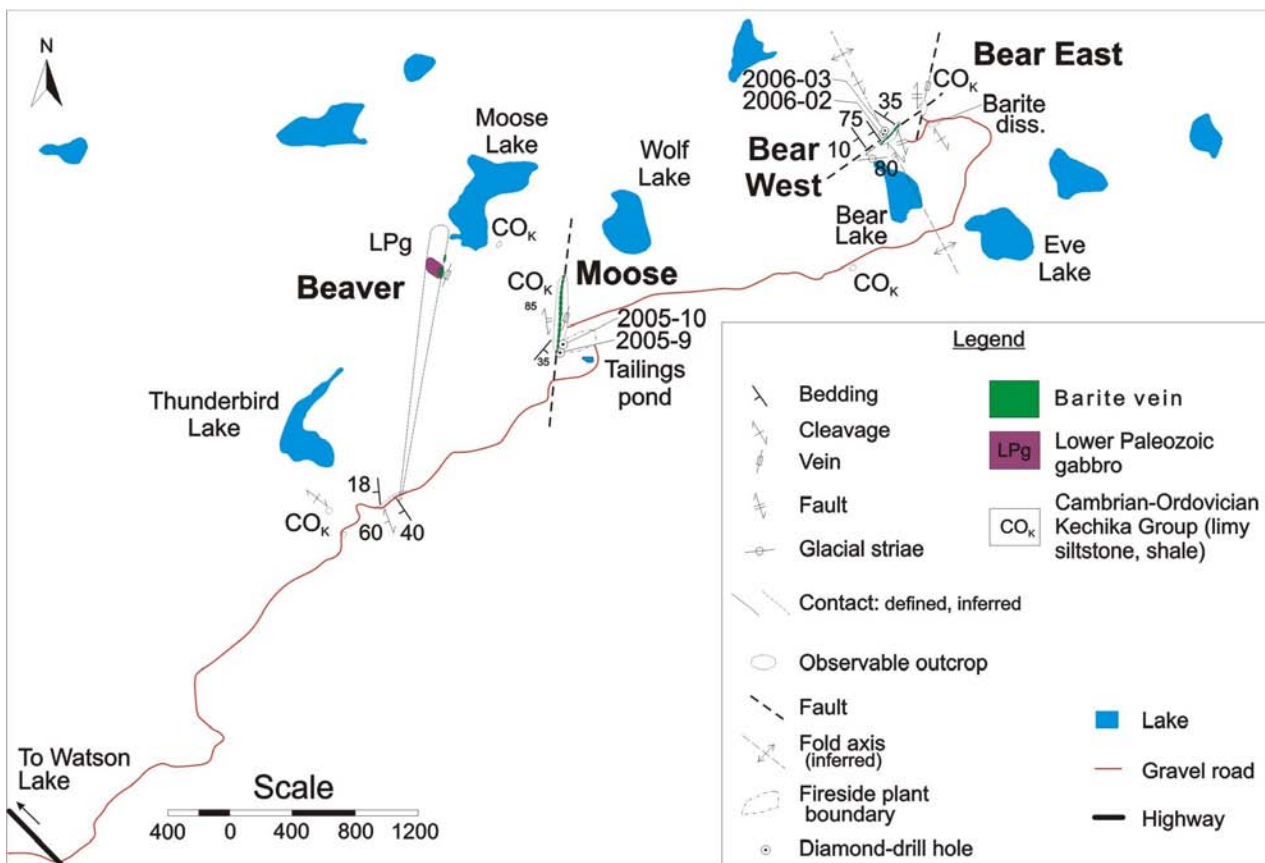


Figure 5. Geology of the Fireside barite minesite.

titudes are variable: the rocks strike northwesterly but the dip ranges from flat to moderate to the northeast and the southwest. A strong fracture cleavage is developed that commonly masks bedding. Open, upright folds about northwesterly axes are inferred from variation in bedding attitudes. Nonweathered rocks are grey, but most near-surface rocks are tan-brown to orange. Quarry exposures show that the transition between the two colours is sharp, occurring within a few centimetres, and cuts across bedding and cleavage in a complex pattern (Fig 6).

Two outcrops in the poorly exposed area near the Bear and Moose veins are particularly interesting. An outcrop where the access road crests a low rise, southeast of Thunderbird Lake, contains very well preserved worm burrows. The same outcrop contains a spotted mafic dike described in detail below. Another road outcrop, just south of the Bear East vein, contains barite as disseminated crystals 0.3 to 0.5 cm in size (Fig 7). Identification of barite was corroborated by X-ray diffraction analysis (J.A. McLeod, pers comm, 2006). The barite crystals occur preferentially in thicker siltstone beds, up to 10 cm thick, and are generally concentrated in the centre of the bed. Barite forms 5 to 20% of receptive siltstone layers and is absent from thin black mudstone layers. The long axis of individual barite crystals is randomly oriented with respect to bedding, indicating that these are not detrital barite grains. Ferri et al. (1999) described authigenic barite in calcareous slate to silty limestone horizons of the lower Road River Group.

Near the Beaver vein, a body of gabbro is fairly well exposed in outcrop over a 150 m wide area. The Beaver vein is situated at the contact between the gabbro to the west and siltstone to the east. The medium-grained gabbro consists of about 50% feldspar and 50% mafic minerals, and is altered. Feldspar, presumably plagioclase, is altered and the principal mafic mineral, pyroxene or amphibole, is indeterminate, having been replaced by chlorite and secondary amphibole. Interestingly, biotite that appears to be primary is a minor constituent. The gabbro body at the Beaver barite vein is on strike with an exposure on the access road of bedrock rubble of a spotted mafic dike. These exposures are correlated, defining a dike that trends nearly due north. The mafic unit on the access road is more strongly altered than the larger body near the Beaver vein. The spotted texture derives from clots of chlorite of indeterminate origin, either phenocrysts or amygdules. Similar altered mafic dikes occur near the Moose and Bear West veins (*see below*).

Barite Veins

The Bear West, Bear East, Moose and Beaver veins are similar in that they consist of coarse white barite with essentially no other minerals. There are differences between the veins in orientation and wallrock geology. The Bear West vein strikes east-northeast, whereas the other three trend northerly. All four veins dip subvertically. The author selectively examined core from two diamond-drill holes in the south end of the Moose zone and four holes in the Bear



Figure 6. Siltstone and shale in the north wall of the Bear Pit, showing bedding, steep fractures and irregular boundary between grey and orange rocks.



Figure 7. Barite crystals in siltstone.

zone. Locations of two of the most important drillholes in each zone are shown on Figure 5.

The Bear West vein is known in the most detail, owing to recent mine exposures. It strikes 050 to 055° and dips vertically to steeply north. On the south, the footwall is a quartz-siltstone breccia. The first stage in brecciation is orange carbonate veinlets, each typically less than a centimetre wide, that form a closely spaced subhorizontal sheeted vein network (Fig 8). These are crosscut by second-stage anastomosing silica veinlets, which grade into the breccia that characterizes the footwall of the Bear West vein. The breccia, which consists of quartz-cemented angular black siltstone fragments (Fig 9), forms a zone 8 m wide at one locality. Quartz-siltstone breccia is cut by coarsely crystalline white barite veins. Quartz and barite generally occur in separate veins, but locally they occur in banded veins in which quartz is on the margin and barite in the core

of the vein (Fig 8). Within the pit, the Bear West vein ranges from 4 to 10 m wide and splits into two branches. The north (hangingwall) of the Bear West vein is soft phyllite that is problematic to mine: too soft to blast yet too hard to rip with a bulldozer. Bear West has been mined over a 400 m length. Hole 2006-02 (Fig 5) was drilled at a dip of 45° across the Bear vein and intersected two altered igneous dikes. The barite vein has an apparent width in drillcore of 21.7 m (Fig 10) and the two dikes, 4.9 and 2.8 m in core width, are 16 and 25 m wide in the hangingwall of the vein. In hole 2006-03, the Bear vein is an impressive 29.0 m wide (in core length), with a 3 m internal block of quartz-cemented siltstone breccia near the footwall. The hangingwall comprises a 10 m wide fault zone containing a 30 cm mafic dike. Nearby drillholes show similar relationships but without a mafic dike, implying that mafic dikes fill faults in a discontinuous fashion.

The Bear East pit is about 75 m long but, due to sloughing of pit walls, the barite vein is poorly exposed. The vein strikes about 015°, almost perpendicular to Bear West. However, like Bear West, it is characterized by orange carbonate veinlets and quartz breccia on the east (footwall) margin.

Because the Moose pit is reclaimed, the Moose vein is known only from historical descriptions and from exploration core holes drilled in 2005 and 2006. Butrenchuk and Hancock (1997) described the Moose vein as a steeply dipping system within a north-trending braided fault. The barite vein strikes 005°. It pinches and swells up to 3.5 m wide, and was mined over a 400 m length. The author examined the Moose pit in 1997 before it was reclaimed. A metre-wide altered mafic dike was noted in the vein zone. Hesketh (1985), a manager of the Fireside barite mine for Dresser Canada Inc., described the Moose deposit as follows: “Mineralization appears to be directly associated and contacting with an intrusive porphyritic diorite. The intrusive is present at depth and extends, at places, to within 20 feet of the surface on both the hanging and foot walls.” The mafic intrusion was not described by Butrenchuk and Hancock (1997). Holes 2005-09 and 2005-10, collared 30 m apart, were drilled at an orientation of 272°/45° to explore for a southerly continuation of the Moose vein (Fig 5). The core is stored in the Jedway Construction Ltd. – DJ Drilling Ltd. yard in Watson Lake and only selected boxes were examined. Both drillholes intersected siltstone and argillite. A portion of a 3.4 m dike in drillhole 2005-9 is shown in Figure 11. Altered feldspar phenocrysts, chloritic ‘spots’ (probably amygdules) and bright green mariposite are visible. The dike is cut by veins of dolomite, quartz and barite. A second dike, 1 m wide, occurs a few metres deeper in the hole. Both dike/vein intercepts contain sparse clots of base metal sulphides: pyrite, chalcopyrite, sphalerite and galena. Similar altered dike and narrow barite stringers occur in drillhole 2005-10.

The Beaver vein is well exposed in an early exploration trench; no work has been done by Fireside Minerals. The vein strikes about 010°. It is 4 m wide and occurs at the sharp contact between a body of gabbro, interpreted to be a dike, and grey shale. Description of mafic-rich grit by Butrenchuk and Hancock (1997) is erroneous. The subvertically dipping barite vein can be traced about 50 m north in a series of overgrown, shallow trenches. A swamp masks exposure to the south.



Figure 8. Narrow, orange dolomite veinlets (D) cut by quartz (Q, bright white) and barite (Ba, dull white) in the Bear East pit.

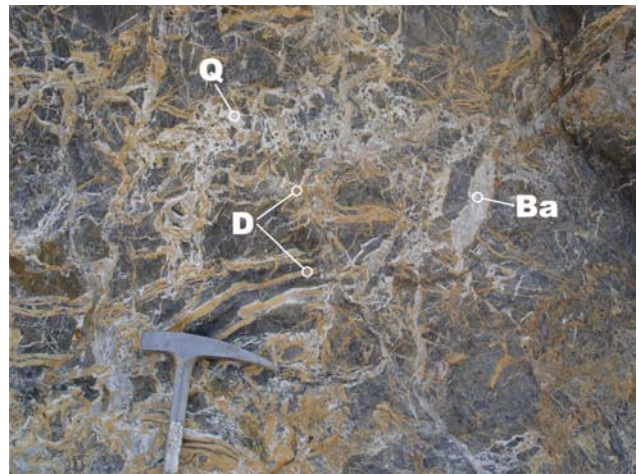


Figure 9. Quartz (Q) and barite (Ba) veins cut disrupted network of dolomite veinlets (D).



Figure 10. Barite vein intercept below the Bear West pit in diamond-drill hole 2006-02; black footwall breccia is also visible.

ORIGIN OF THE FIRESIDE BARITE DEPOSIT

Disseminated barite in siltstone described near the Bear East vein is interpreted to be diagenetic. Its characteristics are inconsistent with a detrital origin. The presence of vertical worm burrows suggests shallow water during sedimentation, possibly an intertidal environment. Following deposition but prior to lithification, siltstone beds were more permeable than the adjoining shale to infiltration of ocean water below the seabed. The Selwyn Basin – Kechika Trough is renowned for syngenetic barite deposits, particularly in Devonian rocks but also in older rocks, including the Kechika and Road River groups (Ferri et al., 1999). It is inferred that Selwyn Basin – Kechika Trough seawater was, at least episodically, enriched in barium. In-cursion of barium-enriched seawater, perhaps in a sabkha environment, might produce the observed diagenetic barite horizons. The quartz breccia that characterizes the footwall of the Bear West and Bear East veins is reminiscent of an epithermal emplacement, and is consistent with a continental shelf to subaerial environment.

Barite veins at Fireside are spatially associated with gabbro dikes. The association may be accidental, veins and dikes coincidentally occupying the same structural openings, or causative (i.e., there may be a genetic link between igneous activity and the hydrothermal veins). Significantly, the gabbro intrusions and barite veins fill northerly-trending structures, not northwesterly ones related to folding. A regional perspective may give further insight into the age and genesis of the gabbro.

Geological mapping by Ferri et al (1999) found several northerly-elongated bodies of gabbro 30 km southwest of Fireside in the Hare-Gemini Lakes area. Composition and texture closely resemble the Fireside gabbro, including the presence of biotite, a rather uncommon mineral to be found in a mafic intrusion. One hypothesis is that the gabbro dikes fill dilational structures generated during Eocene movement along the Tintina fault (J. Nelson, pers comm, 2007). However, Eocene lamprophyre dikes are generally fresh, whereas the Fireside gabbro is altered and located 60 km distant from the Tintina – northern Rocky Mountain megafault. Furthermore, as noted by Ferri et al. (1999) and previously by Gabrielse (1962), these gabbro intrusions (dikes and sills) are never found cutting rocks younger than Kechika age. Three features strongly suggest that these igneous bodies are related to inception of rifting of the Kechika Trough: 1) their mafic composition; 2) their northerly orientation; and 3) their age, which must be immediately post-Kechika and correspond to initiation of deep-water sedimentation. The evidence is not conclusive but, on balance, is persuasive that the Fireside gabbro is Paleozoic in age. If this interpretation is correct, and because Fireside is located off the axis of the trough (Fig 1), it must be located on a failed splay of the rift system.

The deduced age of the gabbro intrusions links them with regional mafic volcanism. Souther (1992) provided a compilation of the many localities in the Selwyn Basin and Kechika Trough where basalt occurs within the Kechika and Road River groups. In addition to age and stratigraphic position, similarities between these basalts and the Fireside – Gemini Lake gabbro bodies include the presence of primary biotite.



Figure 11. Altered mafic dike (D) and veined argillite (A) in diamond-drill hole 2005-09.

CONCLUSIONS AND RECOMMENDATIONS

The close association of mafic intrusions and barite veins that was observed first by Hesketh (1985) has been corroborated. The barite veins at Fireside are interpreted to have a two-stage origin. The origin of early diagenetic barite is uncertain, possibly related to prior, basin-scale enrichment in barium. The second stage involved remobilization of hydrothermal fluids generated by high-level mafic intrusions. A heat source is necessary to initiate a seafloor hydrothermal system. By the model presented in this paper, the heat source was a high-level mafic magma that resulted in intrusion of gabbro dikes and extrusion of basalt. The resultant circulation of heated seawater caused the formation of marginally younger, crosscutting barite veins at Fireside. Barite was deposited in fault zones near the apex of gabbro dikes. The sequence of mineral deposition was dolomite, then quartz and finally barite. Episodes of brecciation punctuated the mineralizing process.

Mafic magmatism is deduced to have originated during an episode of rifting of the Kechika Trough. The inferred early Paleozoic age of the gabbro dikes should be established by radiometric dating. Whole-rock and minor-element chemical analyses are prime topics for future investigation, to test for a common fingerprint between the gabbro intrusions and the Kechika – Road River basalt. Such data could indicate a common origin that is independent of radiometric dating evidence.

The occurrence of base metal sulphides in the Moose vein, though very minor, suggests a link between the Fireside barite veins and base metal – barite (SEDEX) deposits. The epithermal character of the Fireside veins is consistent with low hydrostatic pressure in a shallow-water shelf environment that is consistent with a failed rift on the continental margin. Formation of a hydrothermal fluid is attributed to high-level mafic magmatism. Considerations of the composition of the ore fluid and mechanism of barite precipitation, from both a theoretical perspective and from investigation of fluid inclusions, are additional topics worthy of further study.

Exploration potential of the Fireside district for additional barite veins is excellent. The Bear West vein is a significant source of barite, and is associated with a west-northwest fault and a very narrow mafic dike. This structure is nearly orthogonal to the northerly trend of the much larger mafic intrusions and other barite veins. Future exploration in this area should use these associations as search parameters, as they are more refined compared with early exploration models.

ACKNOWLEDGMENTS

People associated with the Fireside mine provided open access to the site and, in visits over a 10-year period, were generous with their time in describing and explaining the operation. They include Gordon Webster (President of Fireside Minerals Inc.), Keith Macleod (General Manager of Fireside Minerals), David Schussler (President of Jedway Enterprises Ltd.), Ed Craft (Mine Manager in 2006), Al Matovich and Steve Butrenchuk (Mine Manager in 1998). Frances Sharpe assisted with property and pit mapping in 2006, and expertly prepared the Fireside geology map. And, finally, this paper has benefited considerably from critical review by Jo-Anne Nelson and George Simandl, for which the author is very appreciative. Kirk Hancock kindly assisted with preparation of the figures.

REFERENCES

- Butrenchuk, S.B. and K.D. Hancock (1997): Barite in British Columbia; *BC Ministry of Energy, Mines and Petroleum Resources*, Open File 1997-16, pages 87–90.
- Bickel, H.C. (1965): Geophysical report on refraction survey, Bear, Beaver and Moose claims; *BC Ministry of Energy, Mines and Petroleum Resources*, Assessment Report 767, 8 pages.
- Carne, R.C. and Cathro, R.J. (1982): Sedimentary exhalative (Sedex) zinc-lead-silver deposits, northern Canadian Cordillera; *Canadian Institute of Mining and Metallurgy Bulletin*, Volume 75, pages 66–78.
- Craft, E.W. (2006): Fireside Minerals Ltd., pit design and production forecast; unpublished report prepared for *Fireside Minerals Ltd.*
- Crosby, R.O. (1971): Airborne geophysical survey, Wolf claim group; *BC Ministry of Energy, Mines and Petroleum Resources*, Assessment Report 2880, 2 pages.
- Ferri, F., Rees, C., Nelson, J. and Legun, A. (1999): Geology and mineral deposits of the northern Kechika Trough between Gataga River and the 60th Parallel; *BC Ministry of Energy, Mines and Petroleum Resources*, Bulletin 107, 122 pages.
- Gabrielse, H. (1962): Geology, Kechika, BC; *Geological Survey of Canada*, Preliminary Map 42-1962, scale 1:253 440.
- Hesketh, J. (1985): Fireside barite mine, Fireside BC; unpublished report prepared for *Dresser Canada Inc.*, Magcobar Minerals Division.
- MacIntyre, D.G. (1992): Geological setting and genesis of sedimentary exhalative barite and barite-sulphide deposits, Gataga district, northeastern British Columbia; *Exploration and Mining Geology*, Volume 1, Number 1, pages 1–20.
- McCammon, J.W. (1965): Bear, Moose, Beaver groups; *BC Ministry of Energy, Mines and Petroleum Resources*, Annual Report, 1965, pages 257–258.
- McLeish, C.A. and Baron, R. (1981): Fireside project, project cost estimate by Canadian Mine Services Ltd for Dresser Industries Inc.; *BC Ministry of Energy, Mines and Petroleum Resources*, Assessment Report 9052, 78 pages.
- Souther, J.G. (1992): Volcanic regimes; in *Geology of the Cordilleran Orogen in Canada*, H. Gabrielse and C.J. Yorath, Editors, Geological Survey of Canada, Geology of Canada, Number 4, pages 459–490.

